# BIOCHEMICAL PROFILING OF ADIPOCYTE METABOLISM

Thesis submitted in accordance with the requirements of the University of Liverpool for the degree of Doctor in Philosophy

Submitted by

**Kaylie Haynes**

**December 2012**

**DECLARATION**

I declare that the research reported in this thesis has been carried out by me, and any help received has been duly acknowledged. I believe that the contents of this thesis are wholly original, except where references are made. The work reported in this thesis has not been presented for any other degree.

.

Kaylie Haynes

University of Liverpool

December 2012

**ACKNOWLEDGEMENTS**

There are many people to whom I owe my gratitude, and I would sincerely like to thank everyone who has helped and supported me throughout my studies.

Firstly, I would like to thank my supervisors Dr Lucy Pickavance, Professor Phil Whitfield and Dr Alex German for providing the required resources, and also for their help and guidance throughout the practical and written part of this thesis.

A thank you also goes to Professor Ian Megson for allowing me to spend time at the department of Diabetes and Cardiovascular Science, UHI, Inverness, and also to the members of the Lipidomic Research Facility; especially Dr Ben Maskrey for his assistance with the eicosanoid analysis in this thesis, as well as general mass spectrometry help.

I am also very grateful to Professor Rob Beynon for incorporating me (and the GCT!) into the PFG when I was without mass spectrometry support, and also for all of his advice and guidance. I would also like to thank the members of PFG for making me feel welcome.

The 3T3-L1 cell culture and gene expression studies were performed in the Obesity Research Unit at the University of Liverpool, and so I would like to thank the group for theitr help and support, especially Leif Hunter for his technical advice and assistance.

A big thank you also goes to Dr Melanie Smith for her emotional support and guidance during my stay in Inverness.

I would like to say a massive thank you to all of the fellow students that I have met over the last four years in all of the groups that I have been a part of, both in Liverpool and Inverness. Firstly, thank you goes to Maz, who, after starting her PhD project on the same day as me, has now become a great friend, and been through the whole process with me. Thank you also goes to my new Scottish friends Andrew, Ben and Jenni for making my stay in Inverness more enjoyable, and enlightening me on all things Scottish! A special thank you goes to Lorna, for keeping me amused with all of our random outings, and late nights in the lab, I don't think that I would have survived without you!

Thank you also goes to my family for their love, support and encouragement. To my mum, for all of the funny times that we have shared, as well as the long-winded stories over the phone! To my dad, for all of his 'advice', I hope you are looking forward to reading this thesis! To Danny for, well, being my brother and being a source of entertainment over the years. Finally, thank you goes to my Nana, for the Saturday afternoon trips, and also for acting as a storage facility during my many moves! I love you all.

My final and biggest thank you goes to John, who has been my rock during the course of my PhD. Thank you for enduring the 400 mile distance during my stay in Inverness, and for the countless hours spent in the car, on a train, or plane coming to visit me, for which, I am eternally grateful. Thank you also for the support, and endless cups of tea, which helped to get this thesis written!

In loving memory of my handsome 'pony' Solo who brought me so much joy and happiness over the years, and is truly missed.

These studies were supported financially by a BBSRC CASE award, and Pfizer Animal Health.

**ABBREVIATIONS**

| | |
|---|---|
| **DMEM** | Dulbecco's Modified Eagle Medium |
| **24EE** | 24 hour energy expenditure |
| **AA** | arachidonic acid |
| **AC** | alternating current |
| **ACE** | angiotensin-converting enzyme |
| **ACN** | Acetonitrile |
| **ACRH** | adrenocorticotrophic hormone |
| **ADD-1/SREBP-1** | adipocyte determination- and differentiation-dependent factor-1/sterol regulatory element-binding protein-1 |
| **AF** | ammonium formate |
| **AgRP** | agouti-related protein |
| **AGT** | angiotensinogen |
| **AMPK** | AMP-activated protein kinase |
| **ARC** | arcuate nucleus |
| **as** | Antisense |
| **AT1** | angiotensin receptors type I |
| **AT2** | angiotensin receptors type 2 |
| **ATGL** | adipose triglyceride lipase |
| **ATP** | adenosine-5'-triphosphate |
| **BAT** | brown adipose tissue |
| **BMI** | body mass index |
| **BMR** | basal metabolic rate |
| **C/EBP-** | CAAT/enhancer binding proteins- |
| **cAMP** | cyclic adenosine 3', 5'-monophosphate |
| **CART** | cocaine-amphetamine–regulated transcript |
| **CCK** | Cholecystokinin |
| **cDNA** | complementary DNA |
| **CID** | collision induced dissociation |
| **CNS** | central nervous system |
| **COX** | Cyclooxygenase |
| **CRF** | corticotrophin releasing factor |
| **CS** | calf serum |
| **Ctr** | centering with no scaling |
| **CVD** | cardiovascular disease |
| **DC** | direct current |
| **DG** | Diglyceride |
| **DHA** | docosahexaenoic acid |
| **DI-MS** | direct infusion-mass spectrometry |
| **DMH** | dorsomedial nucleus |
| **DNA** | deoxyribonucleic acid |
| **DNL** | *de novo* lipogenesis |
| **dsDNA** | double-stranded DNA |
| **EDTA** | trypsin/ethylenediaminetetraacetic acid |
| **EGIR** | European Group for study of Insulin Resistance |
| **EPA** | eicosapentaenoic acid |
| **ER** | endoplasmic reticulum |
| **ESI** | electrospray ionisation |
| **EtBr** | ethidium bromide |
| **FA** | fatty acid |
| **fAd** | full length adiponectin |
| **FAM** | FAM-6-carboxyfluorescein |
| **FAS** | Fatty acid synthase |
| **FAT** | fatty acid translocase |
| **FATP** | fatty acid transport protein |
| **FDA** | food and drug administration |

| | |
|---|---|
| **FFA** | free fatty acid |
| **FIZZ** | found in inflammatory zone |
| **FRET** | fluorescence resonance energy transfer |
| **FT-ICR-MS** | fourier transform ion cyclotron resonance |
| **gAd** | globular adiponectin |
| **GAPDH** | glyceraldehyde-3-phosphate dehydrogenase |
| **GBP** | gelatine binding protein |
| **GC** | gas chromatography |
| **GH** | growth hormone |
| **GLUT4** | glucose transporter type 4 |
| **H** | Hour |
| **HDL** | high density lipoprotein |
| **HESI** | heated electrospray ionisation |
| **HIF-1** | hypoxic inducible factor-1 |
| **hMAD** | human multipotent adipose tissue-derived |
| **HMDB** | human metabolome database |
| **HMW** | high molecular weight |
| **HPLC** | high performance liquid chromatography |
| **HSL** | hormone sensitive lipase |
| **IBMX** | 3-Isobutyl-1-methylxanthine |
| **ICAM** | intercellular adhesion molecule |
| **IDF** | international Diabetes Federation |
| **IGF-1** | insulin-like growth factor-1 |
| **IL** | Interleukin |
| **IPA** | Isopropanol |
| **JAK** | janus kinase |
| **LC** | liquid chromatography |
| **LC-MS** | liquid chromatography-mass spectrometry |
| **LC-MS/MS** | liquid chromatography tandem mass spectrometry |
| **LHA** | lateral hypothalamic area |
| **LHS** | left hand side |
| **LIPID MAPS** | LIPID metabolites and pathways strategy |
| **LIT** | linear ion trap |
| **LMW** | low molecular weight |
| **LOX** | Lipoxygense |
| **LPL** | lipoprotein lipase |
| **LPS** | Lipopolysaccharide |
| **LT** | Leukotrienes |
| **LX** | Lipoxin |
| **m/z** | mass-to-charge ratio |
| **MALDI** | matrix assisted laser desorption/ionisation |
| **MCH** | melanocortin concentrating hormone |
| **MCP-1** | monocyte chemoattractant protein-1 |
| **METLIN** | metabolite and tandem MS database |
| **MG** | Monoglyceride |
| **MGL** | monoglyceride lipase |
| **MIF** | migration inhibitory factor |
| **min** | Minutes |
| **MRFA** | L-methionyl-arginyl-phenylalanyl-alanine acetate x water |
| **MRM** | multiple reaction monitoring |
| **mRNA** | messenger RNA |
| **MT** | Metallothionein |
| **MVDA** | multivariate data analysis |
| **NGF** | nerve growth factor |
| **NPY** | neuropeptide Y |
| **NSAIDs** | non-steroidal anti-inflammatory drugs |
| **NTC** | non-template control |

| | |
|---|---|
| **OLETF** | Otsuka Long-Evans Tokushima fatty |
| **PAI-1** | Plasminogen-activator inhibitor 1 |
| **Par** | Pareto scaling |
| **PC** | phosphatidylcholine |
| **PCA** | principle component analysis |
| **PCR** | polymerase chain reaction |
| **PDE3B** | phosphodiesterase 3B |
| **PE** | phosphatidylethanolamine |
| **PF** | platelet factor |
| **PG** | Prostaglandin |
| **PI** | phosphatidylinositol |
| **PI3K** | phosphoinositide 3-kinase |
| **PKA** | protein kinase A |
| **$PLA_2$** | phospholipase $A_2$ |
| **PLS** | partial least square |
| **PLS-DA** | partial least squares discriminant analysis |
| **POMC** | prepro-opiomelanocortin |
| **PPAR** | peroxisome proliferator-activated receptor |
| **ppm** | parts per million |
| **pref-1** | Pre-adipocyte factor-1 |
| **PS** | phosphatidylserine |
| **PVN** | paraventricular nucleus |
| **PYY** | peptide YY |
| **qPCR** | real time-PCR |
| **RAAS** | renin-angiotensin aldosterone system |
| **REF** | inflammatory lipids |
| **RF** | radio frequency |
| **RHS** | right hand side |
| **RIST** | radioimmunosorbent techniques |
| **RNA** | ribonucleic acid |
| **RNA pol 2** | RNA polymerase IIa |
| **RT** | retention time |
| **RT-PCR** | reverse transcription PCR |
| **S** | sense |
| **SCOUT** | Sibutramine Cardiovascular Outcomes |
| **SD** | standard deviation |
| **SDS** | sodium dodecyl sulphate |
| **sec** | seconds |
| **SM** | sphingomylelin |
| **SNS** | sympathetic nervous system |
| **sOCs** | suppressor of cytokine signalling |
| **SPE** | solid phase extraction |
| **SRC-3** | steroid receptor coactivator-3 |
| **SSA** | serum amyloid A |
| **ssDNA** | single stranded DNA |
| **STAT** | signal transducer and activator of transcription |
| **SVF** | stromal vascular fraction |
| **T2DM** | type 2 diabetes mellitus |
| **Ta** | annealing temperature |
| **TAMRA** | tetramethylrhodamine |
| **TBE** | Tris Borate-EDTA |
| **TEE** | total energy expenditure |
| **TEGF** | vascular endothelial factor |
| **TG** | Triglyceride |
| **TGF** | transforming growth factor |
| **TGH-1** | triglyceride hydrolase |
| **TIC** | total ion current |

| | |
|---|---|
| **TLC** | thin layer chromatography |
| **TNF** | tumour necrosis factor |
| **TOF** | time of flight |
| **Tx** | Thromboxane |
| **TZDs** | thiazolidinediones |
| **UCP** | uncoupling protein |
| **UHPLC** | ultra high performance liquid chromatography |
| **UV** | unit variance |
| **v,v** | volume, volume |
| **VCAM** | vascular cell adhesion molecule |
| **VEGF** | vascular endothelial growth factor |
| **VLDL** | very low density lipoprotein |
| **VMH** | ventromedial nucleus |
| **w,v** | weight, volume |
| **WAT** | white adipose tissue |
| **WC** | waist circumference |
| **WHR** | waist to hip ratio |
| **α-MSH** | α-melanocyte stimulating hormone |

**TABLE OF CONTENTS**

**LIST OF FIGURES**

**LIST OF TABLES**

**ABSTRACT**

Obesity is a worldwide health issue that has reached epidemic proportions, and is defined as increased white adipose tissue mass. This increase in adiposity is caused by either hypertrophy of existing mature adipocytes, or hyperplasia of pre-adipocytes, leading to increased adipocyte numbers. The current study used the murine 3T3-L1 pre-adipocyte cell line to explore *in vitro* the differentiation process from pre-adipocytes to mature adipocytes, termed adipogenesis. Lipidomic analyses demonstrated a shift in the predominant lipid species present; from phospholipids in the pre-adipocytes, to triglycerides in the mature adipocytes. This was expected from the morphological changes known to occur in this cell line, from fibroblastic pre-adipocytes, to spherical lipid-loaded mature adipocytes. The production of various eicosanoids was also investigated, and their concentration was greatest during the pre-adipocyte stage. This profile was also seen with arachidonic acid, a precursor in eicosanoid synthesis. These changes in lipid metabolism and eicosanoid production appeared to be linked, allowing the differentiation process and lipid accumulation to continue.

The obese state is also associated with a chronic low-grade inflammation, and so the effects of TNF-α and IL-6 intervention on adipocyte metabolism were investigated. Differences in lipid mobilisation caused by these pro-inflammatory agents were suggested due to increases or decreases observed in the concentrations of various triglyceride and fatty acid species. Increases were observed in the concentration of various detected eicosanoid species from the arachidonic acid cascade, mainly prostanoid species.

Effects of the anti-inflammatory agent dexamethasone were also investigated in mature 3T3-L1 adipocytes. It was associated with increases in the concentration of both triglyceride and fatty acid species, suggesting possible increase in lipogenesis and/or decrease in lipolysis. Increases in the production of various eicosanoid species from the arachidonic acid pathway were also observed. The majority of these species are pro-inflammatory; however, $PGE_2$ is known to have both pro-and anti-inflammatory effects, and this may help to explain these findings.

In conclusion, the work presented in this thesis has revealed how adipocyte metabolism changes in the naturally occurring stages of adipogenesis, as well as in response to pro- and anti-inflammatory intervention. Associations were observed between adipokine gene expression, lipid metabolism and eicosanoid production; however, further work is required to confirm these links by identifying the underlying mechanisms involved.

# CHAPTER 1:

## GENERAL INTRODUCTION

## 1.1. OBESITY

Obesity is a medical condition defined by the World Health Organisation (WHO) as being associated with the accumulation of excess body fat to the extent of causing adverse health effects (WHO, 2000). The disorder is thought to involve a genetic predisposition to weight gain, with twin and adoption studies showing that body mass index (BMI) is under strong genetic control. The estimated heritability of BMI ranges between 64 and 84% (Stunkard *et al*., 1986). A study involving pairs of monozygous twins born in Sweden between 1886 and 1958 and raised separately, calculated an intrapair correlation for these twins as 0.70 and 0.66 for men and women, respectively (Stunkard *et al*., 1990). A similar figure was calculated in a cohort of twins from the UK, with a heritability of 0.61 being noted (Price and Gottesman, 1991). Along with the high heritability of obesity in humans, several major genes are known to contribute to the variation in obesity related phenotypes. The current obesity epidemic is unlikely to have been caused by genetic changes alone due the relatively short time frame in which it has occurred.

### 1.1.1. Cause and prevalence of obesity

The increased fat mass, also termed adiposity, associated with obesity is precisely regulated in the process of energy homeostasis, in which food intake is matched to energy expenditure and the size of the body's energy stores (Kennedy, 1953). When excessive food intake is coupled with low levels of energy expenditure, an expansion of adipose tissue mass occurs in the body, leading to increased body weight. In periods of energy deficit, the negative energy balance would cause weight loss.

Obesity is a major worldwide health issue that has reached epidemic proportions (WHO, 2003). Even with increased knowledge of diet and exercise and growing medical awareness, the prevalence of obesity has increased by more than 75% since 1980 (Flegal *et al*., 1998). In the UK, the latest Health Survey for England (HSE) indicated that 62.8% of adults are either overweight or obese. An increase in childhood obesity was also observed, with 30.3% of girls and boys aged 2-15 being overweight or obese (HSE, 2010). If current trends continue, it is predicted that 60% of men, 50% of women and 25% of children in Britain will be obese by 2050 (Foresight Report, 2007).

### 1.1.2. Measurements of obesity

The WHO report published in 2000 was concerned with the health hazards associated with being overweight or obese, prevention of excessive weight gain and the treatment of the different degrees of obesity (WHO, 2000). One simple method to assess the weight status of an individual is the use of body mass index (BMI) which is calculated by dividing the weight in kilograms by the square of the height in metres ($kg/m^2$). The healthy range of BMI values was suggested as being between 18.5 and 24.9 $kg/m^2$, with an age-related increase in the upper limits (WHO, 2000). A study in the early 1990's highlighted that the prevalence of obesity was dependant on the shift in the distribution of the whole population, thereby concluding that total population strategies should be the focus of obesity prevention schemes. A mean population of BMI < 23 $kg/m^2$ would be necessary if the prevalence of obesity (BMI ≥ 30 $kg/m^2$) was to be minimised (Rose, 1991).

An alternative classification system for Asian populations was proposed due to their greater incidences of hypertension and diabetes (WHO, 2000). A BMI of 25 $kg/m^2$ was proposed to signify obesity, with an upper normal limit of 22.9 $kg/m^2$. The recommended BMI cut-off points for Caucasian populations are shown in Table 1.1.

**Table 1.1. Recommended BMI Cut-Off Points for Caucasians**

| BMI RANGE ($kg/m^2$) | CONDITION |
|---|---|
| **Less than 18.5** | Underweight |
| **18.5-24.9** | Normal / Ideal |
| **25-25.9** | Overweight |
| **30-40** | Obese |
| **Greater than 40** | Morbidly obese |

BMI provides a measure of overall adiposity; however, increased abdominal adiposity is a greater risk factor many obesity related diseases. A 13-year follow-up study of middle-aged men demonstrated that abdominal obesity was associated with an increased risk of stroke, myocardial infarction and premature death, and this association did not occur with measures of general obesity, such as BMI (Larsson *et al*., 1984). Due to this fact, other obesity measures are commonly used alongside BMI to signify body fat distribution, including the waist-to-hip ratio measurement (WHR) to indicate body shape, and also the waist circumference (WC), which is a simple predictor of abdominal adiposity (Lemieux *et al*., 1996; Han *et al*., 1997). The WHO report in 2000 provided WC cut-off points to predict obesity within an individual, and also their susceptibility to lipid disorders. Values of WC for the diagnosis of abdominal obesity were originally based on white Caucasians, and were 94cm for men, and 80cm for women at a BMI of 25kg/$m^2$, or 102cm for men and 88cm for women at a BMI of 30kg/$m^2$ (Lean *et al*., 1995). As with BMI, lower cut-off values for WC were implemented for non-European populations. The current waist circumference cut-off points for different ethnic groups proposed by the International Diabetes Federation (IDF) are presented in Table 1.2.

**Table 1.2. Ethnic Specific Cut-Off Points for Waist Circumference**

| ETHNIC GROUP | SEX | WAIST CIRCUMFERENCE (CM) |
|---|---|---|
| **Europids / Sub-Saharan Africans / Middle East (Arab) and Eastern Mediterranean populations** | Male<br>Female | ≥ 94<br>≥ 80 |
| **USA (ATP III values)** | Male<br>Female | ≥ 102<br>≥ 88 |
| **South Asians / Ethnic South and Central Americans** | Male<br>Female | ≥ 90<br>≥ 80 |
| **Chinese** | Male<br>Female | ≥ 90<br>≥ 80 |
| **Japanese** | Male<br>Female | ≥ 85<br>≥ 90 |

*Table adapted from* (IDF, 2005). ATP III (Adult Treatment Panel III).

### 1.1.3. Obesity as a medical condition

Excess weight is associated with an increased incidence of many co-morbidities including type 2 diabetes mellitus (T2DM), coronary heart disease, dyslipidaemia (Mokdad *et al*., 2001) and various cancers (Calle *et al*., 2003). Life-insurance studies have found that mortality rates steadily increase with rising degrees of obesity (Lew, 1985). In confirmation of this, weight loss in obese patients can improve many of the obesity related comorbidities including insulin resistance, T2DM, dyslipidaemia and hypertension (Sjostrom *et al*., 1999).

T2DM is characterised by a decline in pancreatic β-cell function and target tissue resistance to insulin (DeFronzo, 1988; Kudva and Butler, 1997; Yach *et al*., 2006), and the risk of developing diabetes directly correlates with BMI (Ayata *et al*., 2000). General obesity has also been identified as an independent risk factor for cardiovascular disease (CVD; Poirier and Eckel, 2002); however, central adiposity is more closely linked to the disease (Yusuf *et al*., 2005). Visceral adipose tissue is functionally and morphologically different from subcutaneous adipose tissue, possibly explaining the elevated risk for CVD (Peiris *et al*., 1989; Hayashi *et al*., 2004). Adipocytes found in the visceral region are less responsive to the anti-lipolytic effects of insulin and have a higher rate of fatty acid (FA) turnover when compared to subcutaneous adipocytes (Wajchenberg, 2003).

#### *1.1.3.1. The metabolic syndrome*

Obesity is connected with a number of metabolic abnormalities that are known risk factors for T2DM and CVD. A common clustering of these factors, including: insulin resistance, hyperglycaemia, hypertension, low high density lipoprotein (HDL)-cholesterol, and raised very low density lipoprotein (VLDL)-triglycerides was termed the metabolic syndrome (Reaven, 1988). A later study highlighted the need to add obesity, especially visceral obesity, as another risk factor involved in the syndrome (Lemieux *et al*., 2000). A number of expert groups have attempted to provide a definition of the metabolic syndrome. Three such definitions were provided by WHO in 1999, The European Group for study of Insulin Resistance (EGIR; Beck-Nielsen, 1999), and finally, The National Cholesterol Education Program – Third Adult Treatment Panel (NCEP ATP III) in 2001. The most recent definition for the syndrome was provided by the International Diabetes Federation (IDF) and is described in Table 1.3. The definition requires visceral adiposity with the ethnic specific WC cut-off points seen in Table 1.1, plus two additional risk factors.

**Table 1.3. The 2005 IDF definition of the metabolic syndrome**

| CRITERIA | SET VALUES |
|---|---|
| **Serum triglyceride level (mg/dL)** | >150 or specific treatment |
| **Serum high density lipoprotein cholesterol, mg/dL** | < 40 (male), <50 (female) or specific treatment |
| **Blood pressure, mmHg** | ≥130/85 |
| **Fasting plasma glucose, mg/dL** | ≥100 |
| **Albuminuria, mg/g albumin-to-creatinine ratio** | ≥30 |

*Table adapted from* IDF (2005).

### 1.1.4. Treatment of obesity

The purpose of obesity treatment is to not only decrease weight, but to reduce the risk factors of the comorbidities associated with the disease. Currently the main approach in the treatment of obesity is to combine a calorie restricted diet with increased physical activity. Many studies have demonstrated that weight loss achieved by exercise only is less effective than that attained by diet alone (Bertram *et al*., 1990; Anderssen *et al*., 1995). The use of behavioural therapy alongside the diet and exercise treatment has been shown to improve short-term weight loss and be more effective at maintaining weight (Avenell *et al*., 2004).

Pharmacotherapy has become involved in obesity management; however, the history of anti-obesity drugs has not been successful, due to their health risks outweighing possible weight loss benefits. One example is rimonabant, a cannabinoid receptor Type 1 blocker (Rinaldi-Carmona *et al*., 1994) discovered and manufactured by Sanofi-Aventis. Treatment with this drug causes weight loss, reduction in WC, and an improvement in various metabolic factors, although adverse psychiatric events were observed at daily doses of 20mg compared to a placebo (Christensen *et al*., 2007). These findings lead to the removal of this drug by the European Medicines Agency, and the Food and Drug Administration (FDA) in the USA to refuse the approval of its use.

Another anti-obesity drug to be banned was sibutramine (Knoll Laboratories / Abbott Laboratories), a selective inhibitor of the reuptake of serotonin as well as norepinephrine (Mun *et al*., 2001). It causes a reduction in food intake and also increases thermogenesis in humans (Hansen *et al*., 1998; Seagle *et al*., 1998). In one study, patients treated with

sibutramine achieved a continued weight loss of up to 15% over one year after an initial diet-induced weight loss, whereas those treated with a placebo regained the weight (Apfelbaum *et al*., 1999). In contrast to the weight loss benefits of this drug, the Sibutramine Cardiovascular Outcomes (SCOUT) trial in 2010 (James *et al*., 2010) highlighted increased risk of non-fatal myocardial infarction and stroke after long-term sibutramine treatment in patients with pre-existing cardiovascular conditions. The findings in this report prompted the removal of this drug from worldwide markets. Previously withdrawn drugs were fenfluramine (Pondimin; Wyeth) and dexfenfluramine (Redux; Wyeth) in 1997 due to increased risk of cardiac valvulopathy; and more recently, benfluorex in 2009, also due to valvulpathy risk.

The removal of sibutramine from the market meant that orlistat was the only approved prescription drug remaining for the long-term treatment of obesity. Orlistat is a lipase inhibitor, and has been shown to achieve a weight loss of approximately 10%, compared to an average 5% with a placebo drug (Sjostrom *et al*., 1998; Davidson *et al*., 1999). It was marketed as Xenical (Roche), and without prescription as Alli (GlaxoSmithKline). With only orlistat left, there was an apparent need for effective, yet safe weight-loss drugs.

Very recently (2012), the FDA has approved two new drugs to be used in conjunction with diet and exercise regimes. The first is lorcaserin, trade name Belviq (Arena Pharmaceuticals), a selective agonist of the serotonin receptor (FDA briefing, May 2012); and the second is a combination of an anorectic agent (phentermine) and the antiepileptic drug topiramate (FDA briefing, February 2012). This second medication has the trade name Qsymia and is produced by Vivus. Both lorcaserin and phentermine/topiramate are appetite suppressants, and can induce a negative energy balance. Both drugs met at least one of the two clinical weight loss criteria set by the FDA in a one year placebo controlled clinical trial, and improved cardiometabolic and anthropometric measures, such as WC and blood pressure (Colman *et al*., 2012).

A final treatment option is surgery; however, this is often only used as the last resort. Due to the increased risk of morbid obesity with premature death, the NIH consensus panel set the guidelines for surgical treatment BMI ≥40 kg/$m^2$ or ≥35 kg/$m^2$ with co-morbidities (Consensus Development Conference Panel, 1991).

Two groups of bariatric surgical techniques exist, and they are malabsorptive and restrictive procedures. The first type involves shortening the small intestine to induce a negative energy balance, and eventually, weight loss. One of the original procedures was the jejunoileal bypass, although it was associated with many long-term complications including liver failure, causing this method to no longer be used (Santry *et al*., 2005). Other malabsorptive methods are currently used, although, long-term health complications are associated with this type of surgery, including malnutrition and vitamin deficiencies (Murr *et al*., 1999).

Restrictive procedures reduce the size of the stomach leading to reduced meal size and calorie intake. One example of this type of surgery is the vertical banded gastroplasty, where the stomach is portioned to form a small pouch, thereby limiting the food passage into the bulk of the stomach (Mason, 1982).

### 1.1.5. Obesity as an inflammatory condition

The obese state is characterised by chronic low-grade systemic inflammation and is linked to the increased risk of developing CVD and T2DM in obesity (Yudkin *et al*., 1999; Festa *et al*., 2001). The circulating concentrations of various inflammatory markers and pro-inflammatory cytokines increase in the obese state (Trayhurn and Wood, 2004).

This inflammatory environment in adipose tissue occurs due to changes in the expression and secretion of the inflammatory adipokines, and also the infiltration of macrophages (Weisberg *et al*., 2003; Xu *et al*., 2003). The number of macrophages in white adipose tissue (WAT) is directly correlated with the size of adipocytes in both humans and mice, thereby possibly increasing the secretion of the pro-inflammatory cytokines, and contributing to obesity associated diseases (Weisberg *et al*., 2003; Xu *et al*., 2003; Curat *et al*., 2004). Monocyte chemoattractant protein 1 (MCP-1) is a chemokine expressed by adipocytes, and this expression is directly correlated with obesity (Christiansen *et al*., 2005). Other proteins secreted by adipocytes that contribute to the infiltration and retention of macrophages are leptin and macrophage migration inhibitory factor (MIF), the expression of which increase in obesity (Trayhurn and Wood, 2004; Skurk *et al*., 2005a). As well as an infiltration of macrophages occurring in the obese state, pre-adipocytes are capable of differentiating into macrophages (Cousin *et al*., 2001).

The inflammatory environment caused by the infiltration of macrophages into adipose tissue may contribute to the onset of the obesity-associated comorbidities (Bouloumie *et al*., 2005). The immune response observed in obesity may possibly be triggered by the development of hypoxia within the adipose tissue. As WAT mass expands during the development of obesity, adipocytes distanced from the vasculature will become hypoxic, with areas of low oxygen tension (Trayhurn and Wood, 2004). The transcription factor hypoxic inducible factor-1 (HIF-1) is a heterodimeric protein consisting of α and β sub units expressed within adipocytes (Lolmede *et al*., 2003). The β sub unit is constitutively expressed, whereas HIF-1α acts as a molecular oxygen sensor (Semenza, 2001) and is expressed in response to hypoxia (Jiang *et al*., 1996). Activation of the HIF-1 complex leads to an increase in the release of several pro-inflammatory cytokines, chemokines and angiogenic factors with the purpose of stimulating angiogenesis and increasing blood flow to the depleted areas (Trayhurn and Wood, 2004).

Endoplasmic reticulum (ER) stress has been suggested as another possible cause for the inflammatory state observed in obesity. A molecular link between ER stress, reduction in insulin sensitivity and the development of T2DM has been demonstrated (Ozcan *et al*., 2004). These proposed mechanisms for the inflammatory response are linked, as hypoxia has been shown to induce ER stress, and also the generation of ROS (Koumenis *et al.*, 2002; Carriere *et al.*, 2004).

#### *1.1.5.1. Treatment of the obesity related inflammatory co-morbidities*

A class of drugs called thiazolidinediones (TZDs) were introduced in the 1990's to treat T2DM. Three of these agents are rosiglitazone (Avandia), pioglitazone (Actos) and troglitazone (Rezulin); however, only pioglitazone is still on the market. These drugs activate the peroxisome proliferator-activated receptors (PPARs) which causes decreased insulin resistance, modified adipocyte differentiation and altered adipokine profiles; including increased adiponectin (Ghanim *et al*., 2006) and decreased IL-6 (Miles *et al*., 1997) gene expression and protein secretion. These findings support the anti-inflammatory effects of these drugs; however, they also have dangerous side effects. Rosiglitazone, for example, was withdrawn from the European market because it was linked to an increased risk of myocardial infarction and stroke.

The adrenal cortex produces a family of hormones called glucocorticoids, and they have been used historically to treat a variety of inflammatory conditions, such as asthma (Barnes, 1985). Dexamethasone is a synthetic glucocorticoid and has potent anti-inflammatory properties, as seen by its ability to inhibit the gene expression and protein secretion of the inflammatory cytokines IL-6 and IL-8 (Fain *et al*., 2005). Therefore, this agent could be of clinical interest. However, chronic dexamethasone treatment is associated with a number of side effects, including reduction of the anti-inflammatory adipokine adiponectin, and also an impairment of insulin-induced glucose uptake (Sakoda *et al*., 2000; Bazuine *et al*., 2004). Also, excessive glucocorticoid excess is the main cause of Cushing's disease, which is associated with increased visceral adiposity, glucose intolerance and hypertension (Cushing, 1912). Due to these findings, dexamethasone tends to only be used for acute treatments on inflammatory conditions in the clinical setting.

### 1.2. ADIPOSE TISSUE

The adipose organ of mammals consists of two different types of adipose tissue; brown adipose tissue (BAT) and WAT, and cells from both types can be found together in specific sites; especially the subcutaneous and visceral depots (Frontini and Cinti, 2010). Suggestions that trans-differentiation can occur between the two cell types in response to environmental changes have been put forward (Himms-Hagen *et al*., 2000; Granneman *et al*., 2005; Barbatelli *et al*., 2010). The location of WAT varies between species; however, mammals and birds have both visceral and subcutaneous WAT. In humans, WAT is found at both visceral and subcutaneous depots (Gesta *et al*., 2007). As mentioned, BAT often coexists with white adipose tissue, although it is mainly found in mammal foetuses and newborns in axillary, cervical, perirenal, and periadrenal regions (Cannon and Nedergaard, 2004), and in the past was believed to be completely lost by adulthood (Lean, 1989).

#### 1.2.1. Brown adipose tissue

Brown adipocytes are densely packed with mictochondria, which, along with the rich vascular supply of BAT, account for the brown colouration of the tissue. Lipid is stored in multiple droplets within the brown adipocyte, and they have a centrally located nucleus (Avram *et al*., 2005). In humans, BAT is found in the neonate and newborn in the interscapular region, pancreas, adrenal glands, kidneys and also perivascularly (Ricquier and Bouillaud, 2000).

#### *1.2.1.1. Function of BAT*

BAT has also been referred to as the 'hibernation gland' due to its original discovery in hibernating mammals (Cannon and Nedergaard, 2004). Its main function is to enable heat production by non-shivering thermogenesis from the metabolism of triglycerides (Au-Yong *et al.,* 2009). BAT is activated in cold conditions by the sympathetic nervous system (SNS; Cannon and Nedergaard, 2004), and can generate 300 times more heat than any other tissue (Power, 1989). Brown adipocytes exclusively express uncoupling protein (UCP)-1 (Dulloo and Samec, 2000), a 32kDa protein found in the inner mitochondrial membrane. This protein uncouples mitochondrial oxidative phosphorylation to dissipate the electrochemical gradient as heat, rather than adenosine-5'-triphosphate (ATP) synthesis (Cannon and Nedergaard, 2004). The process of UCP-1 expression is regulated by the SNS basal tone, in response to cold, diet and photoperiod (Dulloo and Samec, 2000). Increased sympathetic activity results in hypertrophic and hyperplastic expansion of BAT, as well as increased blood flow and utilisation of lipid and carbohydrate substrates for oxidative metabolism (Avram *et al.*, 2005).

BAT thermogenesis is activated after excess dietary energy intake (Klaus, 2001a), possibly acting to limit weight gain and obesity. This tissue may therefore also have a role in obesity, with a previous study suggesting an inverse correlation between BMI and BAT activity (Cypess *et al*., 2009). A study of knockout mice without BAT resulted in diet-induced obesity and T2DM (Lowell *et al*., 1993). Increased age- and diet-induced obesity has also been observed in UCP-1 deficient mice (Kontani *et al*., 2005). The activity of BAT decreases with age, which may correlate with age-related obesity (Saito *et al*, 2009).

### 1.2.2. White adipose tissue

In humans, the majority of WAT is found in major abdominal depots around the omentum, intestines, and perirenal areas, and also in subcutaneous depots in the buttocks, thighs, and abdomen (Gesta *et al*., 2007). Body fat distribution is a sexual characteristic, with woman tending to gain weight in the gluteo-femoral depot, and men in the abdominal region. The male and female type obesity are termed android and gynoid, and it has been observed that both men and women can vary between the two, with android-type obesity being a greater risk factor for obesity-related metabolic diseases (Vague, 1956). A later study demonstrated that with increasing weight gain, females under the age of 60 stored the excess fat in subcutaneous sites, whereas males of all ages and women over the age of 60 stored fat in visceral depots (Enzi *et al*., 1986).

#### *1.2.2.1. Morphology and function of WAT*

Mature adipocytes account for approximately 50% of WAT in adults, with the remaining tissue mass consisting of other cell types, including fibroblasts, pre-adipocytes and macrophages (Hausman, 1985). Developing white adipocytes contain multiple lipid droplets before these finally coalesce into a single droplet (Napolitano, 1963).

The fat storage mechanisms present in WAT lead to the view that the tissue acts as a long-term fuel reserve, with the storage and release of FAs being its main function (Trayhurn and Beattie, 2001). The discovery of leptin in 1994 changed this view, and established WAT as an endocrine organ (Zhang *et al*., 1994), supporting a wide range of roles for adipose tissue.

#### *1.2.2.2. Energy balance*

In obesity, WAT mass increases due to both hyperplasia and hypertrophy of white adipocytes (Johnson *et al*., 1971; Faust *et al*., 1978; Johnson *et al*., 1978; Lowell *et al*. 1993). This can only occur if energy intake is greater than energy expenditure, with the changes in the fat stores acting as a buffer for any imbalance (Trayhurn, 2005). Energy homeostasis may be more adept at preventing weight loss than weight gain, as seen by the obesity epidemic (Ahima *et al*., 1996 and 1999). Two pathways involved in energy homeostasis are termed anabolic and catabolic. Anabolic-effector pathways stimulate food intake and weight gain, whereas catabolic-effector pathways lead to weight loss. Both pathways are regulated such that an increase in one accompanies decreases in the other to maintain stability in the energy balance equation (Schwartz *et al*., 2000). Previous studies have demonstrated that weight loss caused by calorie restriction leads to an increase in food intake (Levitsky, 1970), and vice versa, with energy intake being suppressed by over-feeding and weight gain (Cohn and Joseph, 1962). The majority of adult mammals maintain stable body weight by closely matching their intake and expenditure (Frayn, 2003).

#### *1.2.2.3. Energy intake*

Regulation of adipose tissue stores by the brain was suggested by the 'set-point theory' in the 1950s, a negative-feedback system based around an individual's target 'set-point'. Any deviations from this set point would result in food intake adjustments (Kennedy, 1953). The brain is an important site of appetite regulation, especially the hypothalamic arcuate (ARC) nucleus, which has two opposing neuronal pathways, either the appetite stimulating anabolic pathway, or the appetite inhibiting catabolic pathway (Schwartz *et al*., 2000; Gale *et al*., 2004). Subsets of neurons in the ARC nucleus express two peptides within the anabolic

pathway. These are neuropeptide Y (NPY) and agouti-related protein (AgRP), and both stimulate food intake (Broberger *et al*., 1998; Hahn *et al*., 1998) either directly or indirectly. NPY directly signals to the paraventricular nucleus (PVN) to promote energy intake, whereas AgRP blocks the appetite-inhibiting receptors melanocortin type 3 and 4 (MC3R and MC4R) and acts indirectly to counteract the effects of α-melanocyte stimulating hormone (α-MSH), which is anorexigenic (Stanley *et al*., 2005). NPY is expressed and secreted by human adipocytes, and reduces leptin secretion which effects central appetite control (Kos *et al.*, 2007). The catabolic pathway synthesises precursor prepro-opiomelanocortin (POMC) derived α-MSH, and also expresses cocaine-amphetamine–regulated transcript (CART), which, like α-MSH, also potently reduces food intake (Elmquist *et al*., 1999).

Both pathways are influenced by peripheral hormonal signals that can cross the blood-brain barrier, such as leptin, insulin, ghrelin and peptide YY (Gale *et al*., 2004). ARC NPY/AgRP neurons are inhibited by leptin and insulin, whereas the reverse is true for the POMC/CART neurons (Schwartz *et al*., 1997; Thornton *et al*., 1997; Mizuno *et al*., 1998; Benoit *et al*., 2002). Leptin and insulin are involved in long-term regulation of food intake, lesser circulating concentrations of both cause an increase energy intake, and decrease energy expenditure (Mizuno *et al*., 1999; Benoit *et al*., 2002). Both leptin and insulin stimulate α-MSH and suppress NPY and AgRP expression in the hypothalamus, therefore activating the catabolic pathway, and inhibiting the anabolic pathway (Gale *et al*., 2004). However, direct administration of both leptin and insulin into the central nervous system (CNS) has been shown to reduce food intake and body weight in a dose-dependent manner (Chavez *et al*., 1995).

Short-term control of food intake involves neural and humoral signals from the gastrointestinal tract and liver generated in response to nutrient intake (McMinn *et al.*, 2000). One hormone involved is ghrelin, a peptide secreted from the stomach and upper intestine to stimulate food intake (Kamegai *et al*., 2000; Tschop *et al*., 2000). Central administration of ghrelin stimulates endogenous growth hormone (GH) release by binding to hypothalamic and pituitary growth hormone secretagogue receptor, which is a G-protein coupled receptor. In humans, ghrelin is involved in initiation of food consumption; a peak in plasma ghrelin concentration is observed before a meal, and decreases afterwards (Cummings *et al*., 2002; Espelund *et al.*, 2005).

Other hormones involved in short-term regulation of food intake are peptide YY (PYY) and cholecystokinin (CCK). Both are released from the intestinal tract after ingestion of food to enhance satiety. PYY inhibits NPY- and AgRP-expressing neurons to decrease food intake (Batterham *et al*., 2002). Administration of PYY significantly decreases energy intake over a 24 hour period in both lean and obese subjects (Batterham *et al*., 2003). The same study also found that the obese subjects had lower endogenous concentrations of PYY in comparison to their lean counterparts, suggesting a possible role for PYY deficiency in the pathogenesis of obesity (Batterham *et al*., 2003). The hormone CCK acts both locally on CCK-A receptors, and centrally within the hypothalamus CCK-B receptors to enhance satiety (Wilding, 2002).

#### *1.2.2.4. Energy expenditure*

Energy is expended continuously over a daily period, with the majority being accounted for by the basal metabolic rate (BMR). Changes in BMR have a major impact on total energy expenditure (TEE), and a reduced rate of energy expenditure is a known risk factor for weight gain (Ravussin *et al*., 1988). Ravussin and colleagues discovered that energy expenditure over a 24 hour period (24EE) varied between subjects according to their body size. Obese subjects had higher 24EE, and the effects of exercise were even greater on energy expenditure when compared with lean subjects. This is due to a greater tissue mass which is metabolically active, and a greater energy demand of physical activity (Ravussin *et al*., 1988). Variance in BMR can be explained by body mass (including free fat mass), age and sex (Boothby *et al*, 1936; Halliday *et al*., 1979; Bogardus *et al*., 1986). A genetic link has also been suggested with a study of twins finding that the heritability of BMR accounts for approximately 40% of the variation seen (Bouchard *et al*., 1989).

Other factors contributing to energy expenditure include physical activity and skeletal muscle metabolism. A previous study has reported an inverse relationship between slow muscle fiber types and body fatness, and suggested that muscle fiber type may be a possible cause of obesity (Wade *et al*., 1990). A final process requiring energy is thermogenesis, as described in Section 1.2.1.1.

#### *1.2.2.5. Lipid metabolism*

The major energy reserve in WAT of higher eukaryotes is in the form of triglyceride (TG). Two major processes keep this lipid pool in a constant state of flux, and they are lipogenesis and lipolysis (Figure 1.1). Lipogenesis is the synthesis of lipid whereas lipolysis refers to the breakdown of lipid, and a balance between the two determines fat accumulation. Lipogenesis acts to synthesis FAs, whereas during lipolysis TGs are hydrolysed to generate FAs and glycerol.

#### *1.2.2.6. Lipogenesis*

Lipogenesis converts excess carbohydrates into lipids for storage, and the process starts with *de novo* FA synthesis from simple sugars and this occurs in the cytoplasm of the cell. The FAs produced are then esterified with glycerol to form TGs, which are either stored in the adipocyte, or incorporated into complex structures such as lipoproteins. Lipoprotein lipase (LPL) is involved in the regulation of lipogenesis, and is the rate-limiting enzyme for importing triglyceride-derived fatty acids into adipocyte storage (Weinstock *et al*., 1997). A summary of this process is shown in Figure 1.2.

Two enzymes are important during the lipogenesis process and these are acetyl-CoA carboxylase and fatty acid synthase (FAS). Both use acetyl-CoA and malonyl-CoA derived from carbon precursors such as glucose to generate palmitate, and various lipid species can then be produced due to modification of palmitate by endogenous elongase and desaturase enzymes. The process of *de novo* lipogenesis (DNL) can produce lipid species with bioactivities distinct from those of lipids derived predominantly from the diet (Cao *et al*., 2008). DNL in liver causes increased serum TGs and intrahepatic lipid (steatosis), leading to non-alcoholic fatty liver disease and steatohepatitis (Postic and Girard *et al*., 2008). Increased liver DNL is associated with insulin resistance (Hudgins *et al*., 2011); however, the opposite is true for adipocyte DNL, with a previous study in humans finding that increased expression of lipogenic enzymes lead to enhanced insulin sensitivity, irrespective of obesity (Roberts *et al*., 2009).

Lipogenesis is very responsive to changes in diet. Polyunsaturated fatty acids (PUFA) have been shown to decrease lipogenesis by suppressing gene expression of many of the necessary enzymes, including fatty acid synthase (Jump *et al*., 1994). Carbohydrates stimulate lipolysis in both liver cells and adipocytes, leading to increased postprandial plasma TG concentration. During chronic energy deprivation, adipose tissue lipogenesis is reduced,

and this is combined with an increase in lipolysis, causing a loss of TGs from adipocytes, and eventually weight loss (Kersten, 2001). Glucose is a substrate for lipogenesis, and stimulates FA synthesis by being converted into acetyl-CoA. It can also induce the expression of the lipogenic genes, and, stimulate the release of insulin whilst inhibiting the release of glucagon from the pancreas (Kersten, 2001).

Insulin is an important hormonal factor which influences lipogenesis. It binds to its receptor on the cell surface and activates its tyrosine kinase activity, thereby inducing many effects via tyrosine phosphorylation (Lane *et al*., 1990; Nakae and Accili, 1999). Some of the effects of insulin include increased glucose uptake into the adipocyte via recruitment of glucose transporters to the plasma membrane, and also activating lipogenic and glycotic enzymes (Kersten, 2001). Leptin is also involved, as it stimulates FA oxidation and inhibits lipogenesis (Bai *et al*., 1996; Wang *et al*., 1999) to increase the release of glycerol from adipocytes (Siegrist-Kaiser *et al*., 1997). Another important hormonal factor is GH which reduces lipogenesis in adipose tissue (Goodman, 1963).

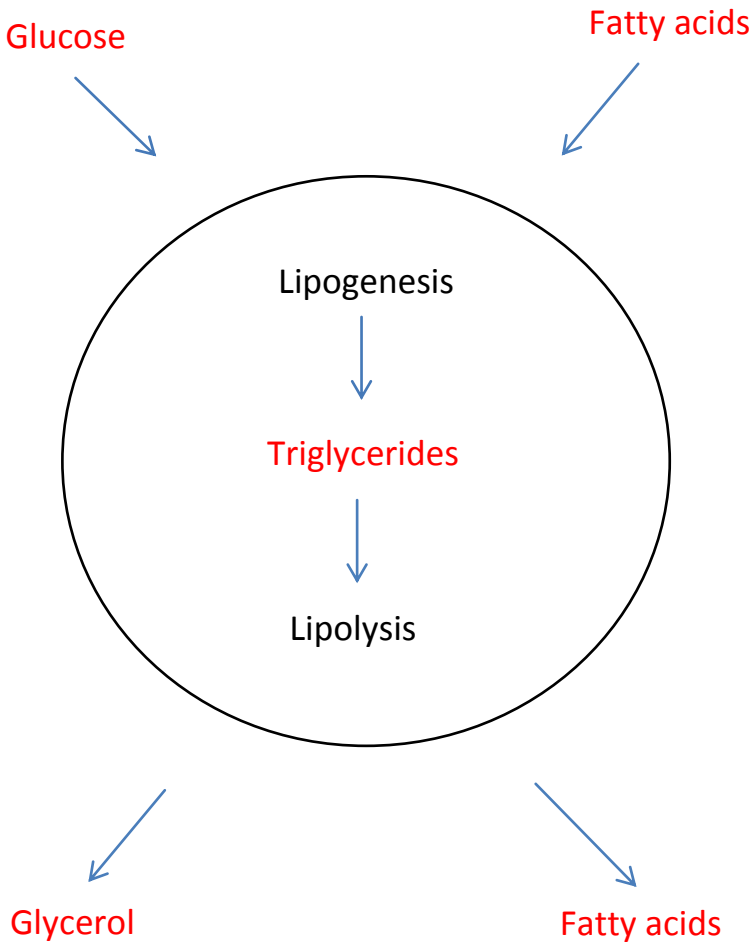


**Figure 1.1. Lipid metabolism in adipocytes**

The lipid pool within mature adipocytes is in a constant state of flux due to two processes; lipogenesis and lipolysis. Lipogenesis is the synthesis fatty acids which can be incorporated into TG structures, whereas lipolysis involves the hydrolysis of TG species into FAs and glycerol. Abbreviations used: FA, fatty acid; TG, triglyceride.

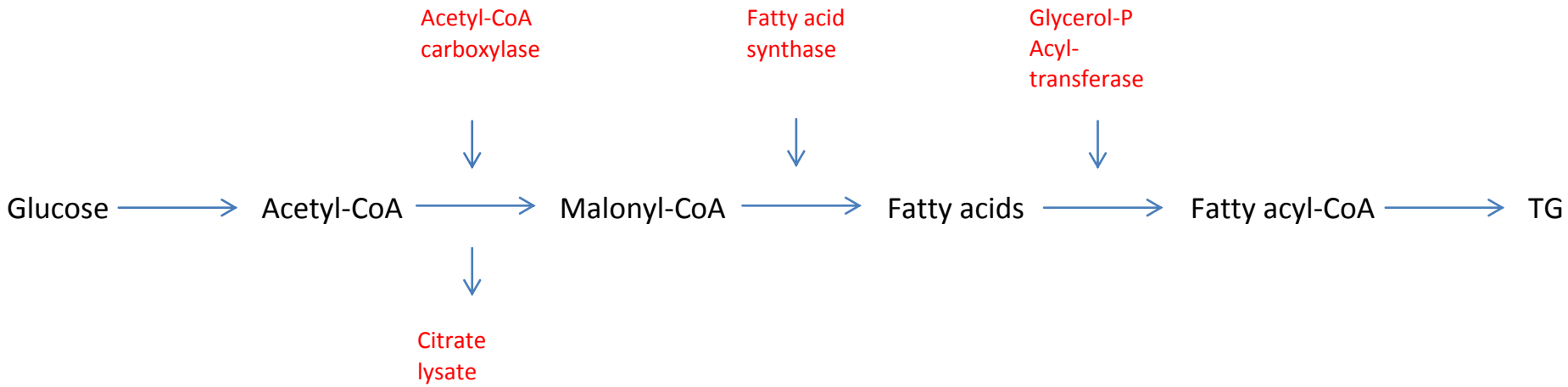


**Figure 1.2. Schematic representation of lipogenesis**

The process of lipogenesis begins with the synthesis of fatty acids, which are then esterified with glycerol to form TG. The enzymes involved in the process are shown in red. Abbreviations used: CoA, Coenzyme A; TG, triglyceride.

### *1.2.2.7. Lipolysis*

Obesity is associated with disturbances in lipolysis; an increase in the basal rate has been shown to contribute to the development of insulin resistance and also impaired responsiveness to stimulated lipolysis (Reynisdottir *et al*., 1995; Large *et al*., 1999). This is due to fact that obese individuals have a greater relative abundance of larger adipocytes, and the size of adipocytes has been directly correlated to lipolysis (Large *et al*., 1999). Lipolysis is the process by which TGs are hydrolysed to form a diglyceride (DG), and then a monoglyceride (MG), with a FA being released at each stage. This process is dependent on specific hydrolases, termed lipases (Lass *et al*., 2006; Figure 1.3). Finally, MG is hydrolysed to liberate the final FA along with glycerol.

During energy deprivation, net rates of lipolysis initially increase, leading to a greater generation of FAs and glycerol through hydrolysis of TG. These FAs are released into the vasculature and utilised as energy substrates by other organs. Longer-term fasting; however, results in the rates of lipolysis returning to baseline after initial stimulation of the process (Weber and Reidy, 2012). During periods of increased energy demand, lipolysis in adipocytes is mediated by hormone-sensitive lipase (HSL). This process is activated by the catecholamine family of hormones interacting with G protein-coupled receptors. Resistance to catecholamine-induced lipolysis occurs in the subcutaneous depot of obese adults and children (Jensen *et al*., 1989; Bougneres *et al*., 1997).

There are two types of catecholamine-binding adrenergic receptors (adrenoreceptors), α and β, both of which are expressed in white adipocytes, with the β-receptors being able to mediate lipolysis in both rats and mice (Arch *et al*., 1984) and thermogenesis in BAT (Arch *et al*., 1989). The binding of an agonist to a β subtype results in activation of cyclic adenosine 3', 5'-monophosphate (cAMP)-dependent protein kinase A (PKA) as well as an increase in adenylate cyclase activity and cAMP. Phosphorylation of HSL by PKA then occurs at several serine residues and by extracellular signal-regulated kinase (Holm *et al*., 2000). This phosphorylated HSL is then translocated from the cytoplasm of the adipocyte to the surface of the lipid droplet (Egan *et al*., 1992), where it binds to a docking protein, lipotransin (Syu and Saltiel, 1999), and to fatty acid-binding protein (Shen *et al*., 1999). PKA also phosphorylates a protein found on the surface of the lipid droplet called perilipin A, and this action changes its conformation, exposing the stored TGs to HSL action (Greenberg *et al*., 1991). This protein moves to the cytoplasm in response to lipolytic stimulation (Brasaemle *et al*., 2000).

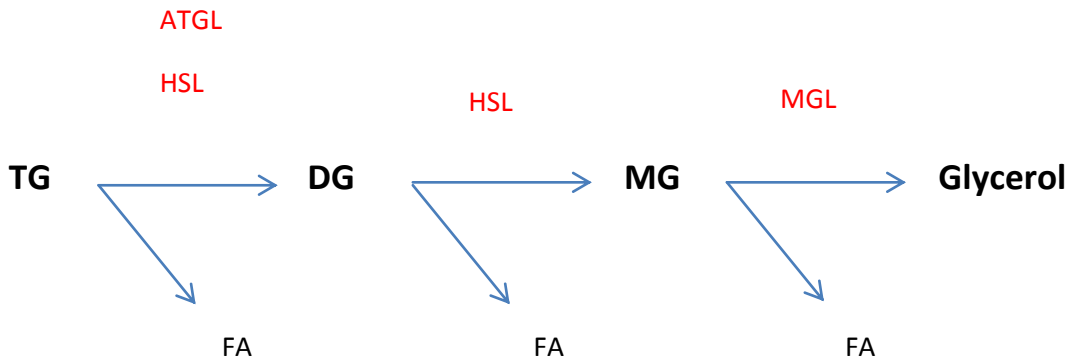


**Figure 1.3. Schematic representation of lipolysis**

Lipolysis is the process by which triglycerides are hydrolysed in a multistep process. The TG is firstly hydrolysed to a diglyceride, and then a monoglyceride, with a fatty acid being released at each stage. The enzymes involved in the process are shown in red. Abbreviations used: ATGL, adipose triglyceride lipase; DG; diglyceride; FA, fatty acid; HSL, hormone sensitive lipase; MG, monoglyceride; MGL, monoglyceride lipase; TG, triglyceride.

HSL was originally thought to be the only factor involved in lipolysis within adipocytes (Holm *et al*., 2000); however, studies with HSL-deficient mice have suggested otherwise (Osuga *et al*., 2000; Wang *et al*., 2001; Haemmerle *et al*., 2002). These mice showed a reduction in both subcutaneous and abdominal adipose depots when compared to normal littermates. Adipocytes isolated from these mice had a lack of catecholamine-induced lipolysis, although basal lipolytic activity was similar to that of normal cells, suggesting that non-HSL mediated pathways of adipocyte lipolysis exist.

A triglyceride lipase called adipose triglyceride lipase (ATGL) has recently been identified and also plays a role in lipolysis (Jenkins *et al*., 2004; Villena *et al*., 2004; Zimmermann *et al*., 2004). The study by Zimmermann and colleagues used antibodies against ATGL in the HSL-deficient mice and found that this lipase is involved during lipolysis. A low DG-hydrolase activity was observed with ATGL treatment by an approximate 20-fold increase in DG accumulation, in contrast to the lack of DG accumulation with HSL. It was calculated that almost 90% of the FAs released from ATGL treated cells came from the hydrolysis of TG in the first ester bond. In contrast, the FA release in the HSL treated cells was seen from all three ester bonds (Zimmermann *et al*., 2004). These findings suggest that both HSL and ATGL may coordinate in the breakdown of TGs.

A lipase called monoglyceride lipase (MGL) has been identified as specific to the hydrolysation of MG but not TG or DG (Tornqvist and Belfrage, 1976). Other lipases possibly involved in lipolytic activities in adipocytes include four members of the PNPLA family which have high sequence homology to ATGL, and are referred to as PNPLA 1, 3, 4 and 5 (Lake *et al*., 2005). PNPLA 3 is the closest to ATGL, although its TG hydrolase activity is much smaller (Jenkins *et al*., 2004). Two proteins from the carboxylesterase family are also involved; carboxylesterase 3, also called triglyceride hydrolase (TGH-1) and carboxylesterase ML1, also called TGH-2. TGH-1 was originally purified from mouse WAT (Soni *et al*., 2004). Both TGH-1 and TGH-2 are weak hydrolases for long chain fatty acid TGs, preferring short chain esters. They move to the ER rather than lipid droplet and this may imply that these proteins are involved in the hydrolysis of the microsomal TG pool, rather than the TG within the lipid droplet (Gilham *et al*., 2005; Okazaki *et al*., 2006).

### 1.2.3. Adipocyte differentiation and development

The increase in adiposity associated with obesity is due to either hypertrophy of existing white adipocytes, or hyperplasia of pre-adipocytes leading to an increased number of mature adipocytes (Johnson *et al*., 1971; Faust *et al*., 1978; Johnson *et al*., 1978; Lowell *et al*. 1993). In periods of excess energy intake, adipocytes increase up to a maximal size, and once reached, hyperplasia is triggered (Faust *et al*., 1978).

The adipocyte lineage is thought to be derived from an embryonic stem cell precursor with the capacity to differentiate into the mesodermal cell types of adipocytes, chondrocytes, osteoblasts, and myocytes (Konieczny and Emerson, 1984). The complex adipocyte differentiation process is called adipogenesis, and starts with the pre-adipocytes undergoing mitosis and growth arrest 24 hours after induction (Bernlohr *et al.,* 1985). After a further 24 hours, the cells complete post-confluent mitosis, and undergo another period of growth arrest, after which they are destined to become mature adipocytes (Scott *et al.,* 1982a and 1982b). Late markers of differentiation begin to be expressed at day 3 post-differentiation, and are responsible for the mature adipocyte phenotype. The cells become terminally differentiated adipocytes between days 5 and 7, with characteristic spherical morphology, and accumulation of lipid droplets (Ntambi and Kim, 2000).

Each stage of adipogenesis is characterised by the involvement of many factors, as well as the presence of specific markers, and these are summarised in Table 1.4. The induction of differentiation is triggered by two families of transcription factors; the first are the CAAT/enhancer binding proteins- (C/EBP-) α, β and δ; and these are expressed at specific times during adipogenesis (Cao *et al*., 1991). The second is the peroxisome proliferator-activated receptor (PPAR) family, made up of α, γ and δ subunits (Dreyer *et al*., 1992; Kliewer *et al*., 1994; Tontonoz *et al*., 1994). PPARγ exists as two isoforms, γ1 and γ2, formed by alternative splicing (Zhu *et al*., 1995), and N-terminal differences (Tontonoz *et al*., 1994). The γ2 isoform is greatly expressed in adipose tissue (Tontonoz *et al*., 1994).

In the early stages of adipocyte differentiation, C/EBP-β and –δ are stimulated (Lane *et al.*, 1999), and induce the expression of PPARγ. This transcription factor then induces C/EBP-α expression, which is necessary for terminal differentiation due to its proliferation inhibition effect (Tang *et al*., 2005; Wang *et al*., 2006).

Another factor involved in the differentiation process is adipocyte determination- and differentiation-dependent factor-1/sterol regulatory element-binding protein-1 (ADD-1/SREBP-1), and it is induced early on during adipogenesis to stimulate the expression of genes required for the synthesis of FAs (Kim and Spiegelman, 1996; Ericsson *et al*., 1997). This protein also induces the expression of PPARγ along with C/EBP-β and –δ. A final factor is steroid receptor coactivator-3 (SRC-3) which acts with C/EBP to control the gene expression of PPARγ and therefore has an impact on the formation of adipocytes (Louet *et al*., 2006).

Many markers are associated with each stage of the differentiation process; one example is LPL which is abundant in adipose tissue, and catalyses the hydrolysis of TGs. Its expression is considered as an early marker of adipocyte differentiation (MacDougald and Lane, 1995). Pre-adipocyte factor-1 (pref-1) is also an important differentiation marker, and its expression decreases during the process (Smas and Sul, 1993). Intermediate markers of differentiation include aP2, a fatty acid binding protein specific to adipocytes (Spiegelman and Ginty, 1983; Bernlohr *et al*., 1984). It has a role in intracellular metabolism and transport of FAs. Finally, adipocytes also express and secrete adipsin, angiotensinogen II and leptin, and all three are described as late markers of adipocyte differentiation (Jones *et al*., 1997). The activation of many of these genes, including aP2 and leptin is coordinated by both PPARγ and C/EBP-α (Spiegelman *et al*., 1993; Hollenberg *et al*., 1997).

**Table 1.4. Stages of adipocyte differentiation**

| EVENT | CELL TYPE | REGULATORY GENES | MARKERS |
|---|---|---|---|
| | Mesenchymal / pleuripotent<br>Multipotential, can differentiate into many cell types | | |
| Determination | Adipoblasts<br>Unipotential, can only differentiate into adipocytes | | LPL<br>Pref-1 |
| Commitment | Pre-adipocytes | C/EBP-β and –δ<br>ADD-1/SREBP-1<br>SRC-3 | aP2 |
| Terminal differentiation | Adipocytes<br>(lipid accumulation) | PPARγ<br>C/EBP-α | adipsin<br>angiotensinogen II<br>leptin |

*Citations present in text (Section 1.2.3).*

### *1.2.3.1. Adipocyte and adipose tissue studies*

The use of clonal cell lines has facilitated adipocyte biology research *in vitro*, with the murine 3T3-L1 and 3T3-F442A cells being the most commonly used. When pre-adipocytes from both cell lines are injected into mice, they differentiate and form fat pads that are indistinguishable from normal adipose tissue (Green and Kehinde, 1979). This finding has led to the development of both lines into well-established models for studying the conversion of pre-adipocytes into adipocytes. Both cell types can also spontaneously arrest growth at confluence and can be induced to differentiate after treatment with adipogenic compounds (Spiegelman *et al.*, 1993). The 3T3-L1 cell line is a derivative of the 3T3 mouse fibroblast cell line, developed by Green and colleagues (Green and Meuth, 1974; Green and Kehinde, 1974). It has been extensively characterised, and mimics the differentiation process seen *in vivo (*MacDougald and Lane, 1995). Like other established cell lines, 3T3-L1 adipocytes may be propagated indefinitely; however, they remain in a resting state for long periods once a confluent monolayer has formed (Todaro and Green, 1963). This period of growth arrest is essential for successful differentiation, and is achieved through contact inhibition (Chang and Polakis, 1978).

Other advantages of clonal cell-lines are that they are homogeneous, and at the same stage of differentiation, which allows a consistent response to external stimuli. They are also relatively straightforward to set up and maintain in culture. A final advantage of clonal cell-lines is that they are immortal as long as they are passaged and stored correctly; however, it is known that the ability of 3T3-L1 pre-adipocytes to differentiate into adipocytes declines with increasing passage number (Poulos *et al.,* 2010).

A limitation of clonal cell-lines is that genetic modifications have occurred to ensure the immortality of these cell-lines and this is disadvantageous as the properties of these cells may be to be different from adipocytes isolated from primary sources. Another disadvantage is that they do not allow assessment of depot-specific differences. The metabolic behaviour of adipocytes differs between depots; pre-adipocytes isolated from different areas have different adipogenic potential (Djian *et al*., 1985; Adams *et al*., 1997).

Only recently has the use of a human clonal cell-line been documented. The increase in adipose tissue mass in obesity depends on the self-renewal capacity of adipocyte progenitors, and these are present during adult life (Hauner *et al*., 1989; Spalding *et al*., 2008). These adipocyte progenitors are found in the stromal vascular fraction (SVF) of adipose tissue, along with a heterogeneous mixture of other cell types. It has been reported that subpopulations of adipocyte progenitors show stem cell properties in the SVF of human adipose tissue, and so could be an alternative source of mesenchymal stem cells (Zuk *et al*., 2002). Since then, a mesenchymal stem cell population, called human Multipotent Adipose tissue-Derived Stem cells (hMADs cells) has been isolated from human infant adipose tissue. These cells exhibit stem cell properties such as self-renewal and multipotency (Rodriguez *et al*., 2005). The multipotency of these hMADs cells was proved when previous studies found that they could differentiate into adipocytes and osteocytes; and that the differentiation into both was temporally regulated by the expression of transcription factors specific to the two lineages (Rodriguez *et al*., 2004; Elabd *et al*., 2007). Once fully differentiated, these cells display many of the features of human adipocytes *in vivo* (Rodriguez *et al.*, 2004).

Before the discovery of this cell line, the SGBS human pre-adipocyte cell strain was, and still is, commonly used. These cells derive from the subcutaneous WAT of a human infant with Simpson-Golabi-Behmel syndrome, characterised by generalised tissue overgrowth (Wabitsch *et al.*, 2001). These cells have a high capacity for adipocyte differentiation and

the mature adipocytes are functionally indistinguishable from those differentiated in primary culture (Wabitsch *et al.*, 2001). Therefore, these cells provide an almost unlimited supply of identical human pre-adipocytes, but their lack of immortality means that they cannot be called a cell-line.

Other methods used for *in vitro* study of adipocyte metabolism include primary culture and mature adipocytes. During primary culture pre-adipocytes are removed from adipose tissue and induced to differentiate into mature adipocytes, and these cells can survive in culture for between two and four weeks (Hauner *et al.*, 2001). A disadvantage to this method includes the requirement of large volumes of material due to only a small fraction of WAT being made up of pre-adipocytes. Approximately 50% of WAT is composed of mature adipocytes; the reminder of the tissue consists of numerous other cell types, including pre-adipocytes (Hausman, 1985). Finally, mature adipocytes are isolated from WAT and these cells may give the closed representation of the *in vivo* system due to the limited intervention. However mature adipocytes are fragile and can only be maintained in culture for up to 48h (Fain *et al.*, 2003).

The use of both primary culture and clonal cell-lines require a differentiation step, and *in vitro* differentiation has been shown to activate the majority of the genes present in adipose tissue *in vivo* (Spiegelman *et al.*, 1993). In culture, the pre-confluent cells resemble fibroblasts, both morphologically and biochemically (Green and Meuth, 1974; Green and Kehinde, 1975). Once confluence has been reached, the cells can be differentiated by an adipogenic cocktail. Maximal differentiation is achieved with a combination of insulin-like growth factor-1 (IGF-1), a glucocorticoid, an intracellular cAMP elevator and bovine serum (Student *et al.,* 1980). IGF-1 can be substituted for insulin in the adipogenic mixture (Smith *et al*., 1988). Both IGF-I and insulin have been shown to stimulate differentiation of pre-adipocytes through their own receptors, although greater numbers of IGF-I receptors are present on pre-adipocytes (Christoffersen *et al*., 1998). IGF-I is more potent than insulin in stimulating proliferation of pre-adipocytes, whereas insulin is more potent in promoting differentiation (Deslex *et al*., 1987; Vierck *et al*., 1996; Rajkumar *et al*., 1999). A commonly used glucocorticoid is dexamethasone, which is used to stimulate the glucocorticoid receptor pathway, and 3-isobutyl-1-methylxanthine (IBMX) increases intracellular cAMP levels by stimulating the cAMP-dependent protein kinase pathway (Rosen and Spiegelman, 2000). Dexamethasone is a powerful inductor of adipogenesis at the early stages of differentiation, but is antiadipogenic if added at later

stages of adipocyte maturation, implying that its effects are time dependent (Caprio *et al*., 2007). Bovine serum contains a variety of proteins and growth factors, and these are essential for the maintenance of cell culture systems (Student *et al*., 1980).

The *in vitro* studies are advantageous in that they can be used to identify a specific cause and effect relationship. Disadvantages include a lack of a paracrine interaction between the cultured cells and other cell types that would be present in whole adipose tissue. Also, endocrine and neural signals would be interacting with the adipocytes in a whole body system. These problems are solved with the use of *in vivo* studies, which are able to investigate the full physiological response to a stimulus.

### 1.3. ENDOCRINE FUNCTION OF WAT

Until recently, WAT was just regarded as an inactive energy store; however, it is now recognised as a major secretory organ which releases fatty acids during fasting, as well as other lipid moieties such as cholesterol, retinol, steroid hormones and prostaglandins (Trayhurn and Beattie, 2001). The discovery of leptin by the identification and sequencing of the mouse *obese* (*ob*) gene in 1994 (Zhang *et al*., 1994) firmly established WAT as an endocrine organ. Since this discovery, a wide range of hormones and proteins secreted by WAT have been identified, and these act at the autocrine, paracrine and endocrine level and collectively named 'adipokines' (Kershaw and Flier, 2004). This term is restricted to proteins secreted by adipocytes alone, as whole WAT contains other cell types than can also secrete proteins (Trayhurn and Wood, 2004). Therefore, WAT is now known to communicate with the brain and peripheral tissues via secretion of these adipokines (Trayhurn and Beattie, 2001; Ronti *et al.*, 2006). Increased adipocyte size in humans is related to dysregulated adipokine expression and secretion (Skurk *et al*., 2007).

The endocrine role of WAT is summarised in Figure 1.4 and its secretory products will be discussed in more detail in later sections.

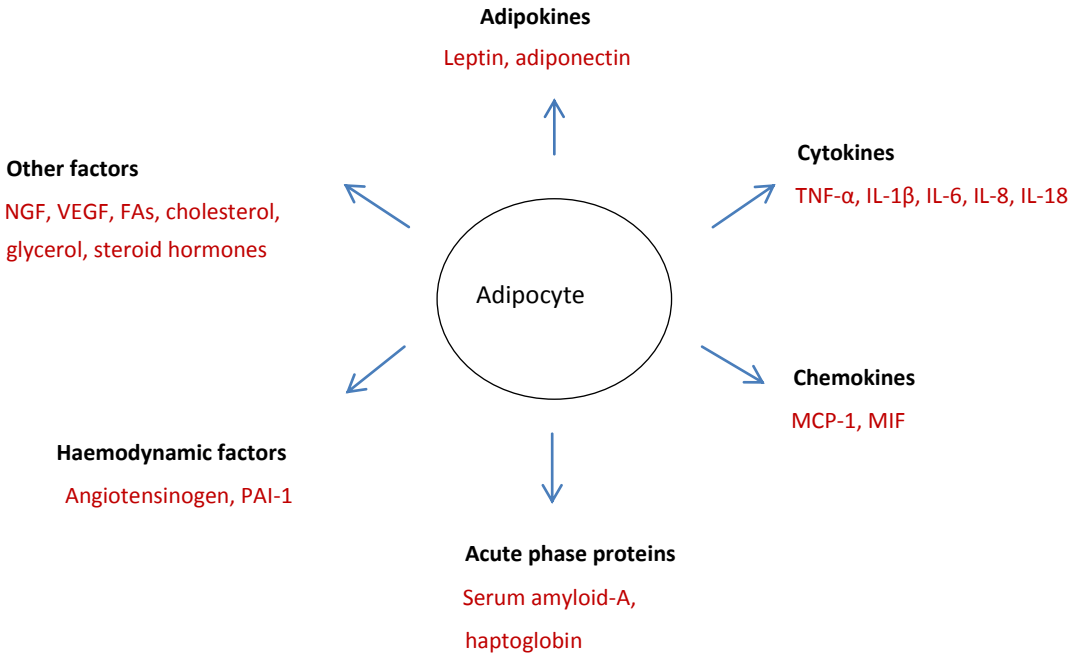


**Figure 1.4. Proteins secreted from white adipocytes**

This figure is a schematic representation of factors secreted by white adipocytes, although it is not a complete list. TNF-α, tumour necrosis factor-α; IL, interleukin; MCP-1, monocyte chemoattractant protein-1; MIF, monocyte chemoattractant protein 1; NGF, nerve growth factor; VEGF, vascular endothelial factor; FAs, fatty acids. *Adapted from* (Trayhurn and Wood, 2004; Romijn and Fliers, 2005).

### 1.3.1. Leptin

The discovery of leptin by the identification and sequencing of the mouse *obese* (*ob*) gene in 1994 (Zhang *et al*., 1994) contributed to the understanding that WAT is an active endocrine organ. Leptin (Greek *leptos*, meaning thin or small) encodes an 18-kDa protein containing a signal sequence which is cleaved to produce the mature 16-kDa hormone. It was originally identified as a satiety factor secreted by WAT in genetically obese (*ob/ob*) mice using positional cloning (Zhang *et al*., 1994). Both leptin gene expression and protein secretion are exclusive to adipocytes within WAT, although leptin is also produced in additional sites including BAT (Moinat *et al.*, 1995), placenta (Hoggard *et al.*, 1997a), skeletal muscle (Wang *et al.*, 1998), oestoblasts (Reseland *et al.*, 2001) and also stomach, mammary gland, ovarian follicles, heart, bone and possibly the brain (Trayhurn *et al*., 1999). Even though leptin synthesis occurs in multiple sites, WAT is the main source of the circulating concentrations of the hormone (Considine *et al*., 1996).

#### *1.3.1.1. Regulation of leptin expression and secretion*

Leptin is expressed and secreted from all WAT depots; however, there are variations between the sites. In humans, gene expression and secretion is greater in subcutaneous adipocytes than visceral cells (Russell *et al*., 1998; Van Harmelen *et al*., 1998). The opposite is true in rodents, with the lowest leptin gene expression occurring in subcutaneous tissue, with the epididymal and perirenal depots showing greater leptin concentration (Trayhurn *et al*., 1995).

Serum leptin displays a diurnal rhythm, with an increase during the night shortly after initiation of feeding, and a decrease during the day in both rodents (Saladin *et al*., 1995) and humans (Sinha *et al*., 1996). This diurnal rhythm of leptin is strongly associated with meal pattern (Schoeller *et al*., 1997), although plasma leptin concentration is also pulsatile, with approximately 30 pulses in a 24h period (Licinio *et al*., 1997; Sinha *et al*., 1996). Leptin gene expression responds to nutritional status, with a decrease seen during short-term starvation of rodents (Becker *et al*., 1995; Saladin *et al*., 1995) and humans (Boden *et al*., 1996; Considine *et al*., 1996) which returned to normal after re-feeding. Plasma leptin concentration declines gradually during 24-36h of fasting in both lean and obese subjects, with little or no loss of fat mass observed (Boden *et al*., 1996; Kolaczynski *et al*., 1996). Leptin acts as a signal of the size of WAT stores, and the two are directly correlated, meaning that its gene expression increases with weight gain (Maffei *et al*., 1995; Kolaczynski *et al*., 1996; Rosenbaum *et al*. 1997) and decreases with weight loss

(Maffei *et al*. 1995). A diet high in carbohydrates produces greater leptin peaks during the night when compared to a high-fat diet, without affected leptin concentration in the morning (Havel *et al*., 1999). The effect of acute cold exposure on leptin production is similar to that of short-term fasting, with reduced expression and secretion being observed; however, this can be reversed by re-warming (Trayhurn *et al*., 1995; Hardie *et al*., 1996).

Leptin gene expression and protein secretion is also controlled by a number of hormones. Therefore, it has been proposed that the SNS regulates the production of leptin via a negative feedback loop (Trayhurn *et al*., 1998). This is suggested because leptin gene expression is inhibited by administration of the catecholamines noradrenaline and adrenaline (Trayhurn *et al*., 1995). Furthermore, inhibition of noradrenaline synthesis in rodents leads to increases in both gene expression and secretion of leptin (Rayner *et al.*, 1998). The effects of SNS on leptin are mediated through β3-adrenoceptors in rodents (Gettys *et al.*, 1996; Trayhurn *et al.*, 1996) and β1 and β2 adenoreceptors in humans (Rayner and Trayhurn, 2001).

A class of drugs called thiazolidinediones (TZDs) are used to treat T2DM and have been shown to suppress both gene expression and protein secretion of leptin via activation of PPARγ (Mantzoros *et al*., 1996; Trayhurn *et al*., 1996). Numerous studies have suggested that glucocorticoids increase plasma leptin concentration as well as gene expression *in vivo*. In humans, the synthetic glucocorticoid dexamethasone increases plasma leptin concentration (Larsson and Ahren, 1996) from 9h onwards (Miell *et al*., 1996), and leptin gene expression in subcutaneous tissue after 2h (Kolaczynski *et al*., 1997). These findings were not related to insulin sensitivity; however, glucocorticoids have been shown to induce insulin resistance and hyperinsulinemia (Larsson and Ahren, 1996; Papaspyrou-Rao *et al*., 1997). A direct role of insulin in leptin regulation was demonstrated *in vitro*, with 24h of insulin treatment in human subcutaneous white adipocytes causing a 50% increase in leptin secretion, although there was no effect on its gene expression (Russell *et al*., 1998). Also, insulin is crucial for maintenance of leptin gene expression and secretion over 24h in human adipocyte culture (Wabitsch *et al*., 1996). Finally, leptin concentration increases in response to inflammatory cytokines, with an increase in leptin gene expression seen after treatment with tumour necrosis factor (TNF)-α and lipopolysaccharide (LPS); and to a lesser extent IL-6 (Sarraf *et al*., 1997).

#### *1.3.1.2. Function of leptin*

Leptin is a satiety signal and is part of a feedback loop to modulate the size of WAT mass. A direct relationship is seen between leptin concentration and body fat mass in the fed state. With the onset of starvation, a reduction in leptin concentration is observed which is disproportional to changes in adipose tissue mass (Ahima *et al*., 1996). This decrease in leptin production signals for the initiation of the adaptive response to starvation. Energy homeostasis consists of a balance between energy intake and expenditure. Leptin administration either centrally or peripherally decreases food intake and body weight, and also a mutation in the leptin gene or receptor is associated with obesity in both humans and rodents (Friedman and Halaas, 1998). As well as inhibition of food intake, leptin also influences energy expenditure. Previous studies in *ob/ob* mice found that leptin administration increased body temperature and physical activity (Pelleymounter *et al*., 1995). Another study demonstrated that body weight reduction in chronic leptin-treated animals was too great for decreased food intake alone (Levin *et al*., 1996). Therefore leptin appears to play a role in both sides of the energy balance equation (Campfield *et al.*, 1995).

Another important role of leptin is the regulation of insulin sensitivity, as demonstrated by the significant reduction of insulin-mediated glucose uptake in isolated mature human omental and subcutaneous adipocytes (Zhang *et al.*, 1999). Also, insulin sensitivity was improved in a mouse model of diabetes with localised adipose tissue loss when leptin was over-expressed (Ebihara *et al.*, 2001).

Leptin-deficient (*ob/ob*) and leptin-receptor-deficient (*db/db*) mice are characterised by obesity, as well as abnormal reproductive function, hormonal imbalances, and alterations in the hematopoietic and immune system, with similar dysfunctions being described in leptin-deficient humans (Ozata *et al*., 1999). Therefore, leptin is also involved in the reproductive system as demonstrated by causing a restoration of fertility in infertile *ob/ob* mice (Chehab *et al.*, 1996). Finally, leptin appears to be a significant modulator of both immune and inflammatory responses, including in the activation of neutrophils, macrophages and natural killer cells and lymphocyte proliferation (Otero *et al.*, 2005). It also modulates cytokine production from monocytes/macrophages; an increase in LPS-induced production of TNF-a, IL-6, and IL-12 has been reported in both murine peritoneal macrophages and human monocytes (Loffreda *et al*., 1998; Santos-Alvarez *et al*., 1999).

#### *1.3.1.3. Leptin receptor*

The leptin receptor (Ob-R) is a product of the *Lepr* gene (Tartaglia *et al.*, 1995) and due to alternative splicing, six isoforms exist in mice, and these are: Ob-Ra, c, d and f (short form); Ob-Rb (long form) and Ob-Re, a soluble form (Lee *et al*., 1996). Four isoforms of the human leptin receptor exist and are known as Ob-R5, -15, -67, and -274 (Barr *et al*., 1999). The splice variants have identical extracellular ligand binding domains, but different intracellular domains (Ahima and Osei, 2004; Koerner *et al*., 2005). The long form of the receptor is found in various tissues, including the kidney, adrenal medulla, pancreatic β-cells and adipose tissue (Emilsson *et al.*, 1997; Guan *et al.*, 1997; Hoggard *et al.*, 1997b). It is highly expressed in the hypothalamic arcuate nucleus (ARC), dorsomedial nucleus (DMH), paraventricular nucleus (PVN), ventromedial nucleus (VMH) and lateral hypothalamic area (LHA) of the central nervous system (Ahima *et al*., 2000). The hypothalamus is involved in the regulation of energy homeostasis (Trayhurn *et al.*, 1999), and the presence of the Ob-Rb protein supports the idea that this part of the brain is a target for leptin (Hakansson *et al.*, 1998). The Ob-Rb receptor regulates gene transcription via janus kinase (JAK) and signal transducer and activator of transcription (STAT) proteins (Vaisse *et al.*, 1996). Leptin also induces STAT-3 translocation and phosphorylation of both phosphoinositide 3-kinase (PI3K) and phosphodiesterase 3B (PDE3B), and this reduces cAMP levels in the hypothalamus.

The short form of the leptin receptor Ob-Ra is highly expressed in the choroid plexus and facilitates leptin transport across the blood-brain-barrier (McClain, 1998). Once in the CNS, leptin interacts with the Ob-Rb receptor, causing the expression of the appetite stimulants NPY, melanocortin concentrating hormone (MCH), AgRP and orexin-A, which are inhibited by leptin. NPY has been classified as an adipokine, as it is expressed and secreted by human adipocytes (Kos *et al.*, 2007). This adipokine decreases leptin secretion and therefore may play a role in the central control of appetite (Kos *et al.*, 2007). Alternatively, appetite suppressants such as α-MSH derived from POMC, CART and corticotrophin releasing factor (CRF) show an increased response caused by leptin (McMinn *et al.*, 2000).

### 1.3.2. Adiponectin

The production of adiponectin is exclusive to adipocytes (Ouchi *et al*., 1999) and it has the greatest circulating plasma concentration of all the adipokines (Diez and Iglesias, 2003). The circulating plasma concentration of adiponectin is significantly greater in women than in men (Arita *et al.*, 1999; Nishizawa *et al*., 2002). This protein is also known as AdipoQ, AcrP30, apM1 or gelatine binding protein- (GBP)-28 and was first described as a collagen-like molecule (Maeda *et al*., 1996); however, it is now known that adiponectin is composed of a globular and a collagenous domain. Once synthesised, adiponectin forms trimers, and these then oligomerise to form polymers consisting of between four and six trimers. Adiponectin is present in the circulation of both humans and mice in three forms; trimer, low molecular weight (LMW) hexamer and a high molecular weight (HMW) oligomer. These are also commonly termed full length adiponectin (fAd) and globular adiponectin (gAd).

#### *1.3.2.1. Regulation of adiponectin gene expression and secretion*

As opposed to leptin, plasma concentrations of adiponectin decrease in a number of dysfunctional metabolic states, including obesity (Arita *et al*., 1999), dyslipidemia (Matsubara *et al*., 2002), T2DM, and coronary artery disease (Hotta *et al*., 2000). Many factors are able to regulate adiponectin gene expression and secretion, with one being diet. Weight loss in both obese and insulin resistant individuals increased circulating adiponectin concentrations (Hotta *et al*., 2000; Yang *et al*., 2001). Gene expression of adiponectin also increases with weight loss, with a previous study demonstrating that this increased in subcutaneous WAT biopsies in humans after diet induced weight loss, and this was also coupled with increased plasma concentrations. The same reversal effect has been documented after treatment with insulin sensitising TZDs (Maeda *et al*., 2001; Combs *et al*., 2002).

Circulating concentrations of adiponectin are inversely correlated with insulin sensitivity, suggesting a role for insulin in adiponectin regulation. A previous *in vitro* study of 3T3-L1 adipocytes found that insulin acted as a negative regulator of adiponectin gene expression (Fasshauer *et al*., 2002). Certain cytokines are also suggested regulators of adiponectin production; TNF-α has been shown to decrease adiponectin gene expression and secretion in both human pre-adipocytes (Kappes *et al*., 2000) and 3T3-L1 adipocytes (Fasshauer *et al*., 2002). A reduction in both is also seen in human adipocytes after IL-6 treatment (Bruun *et al*., 2003a). Administration of anti-inflammatory drugs, such as the TDZs, is

known to increase the concentration of serum adiponectin. These drugs are therefore used to treat T2DM in humans (Ghanim *et al.*, 2006). Testosterone therapy also reduces plasma adiponectin concentrations, which may explain the differences between men and women (Nishizawa *et al*., 2002). Other proposed regulators of adiponectin production include glucocorticoids (Halleux *et al*., 2001) and beta-adrenergic agonists (Delporte *et al*., 2002; Zhang *et al*., 2002).

#### *1.3.2.2. Function of adiponectin*

Adiponectin acts to modulate a number of metabolic processes, and has anti-atherogenic (Ouchi *et al*., 1999 and 2000) and anti-inflammatory (Yokota *et al*., 2000) properties. As mentioned above, gene expression and protein secretion of this protein decreases in the obese state (Arita *et al*., 1999), as well as in CVD with increasing severity (Matsuzawa *et al*., 2004), insulin resistance and T2DM (Hotta *et al*., 2000) and finally dyslipidaemia (Matsubara *et al*., 2002). Adiponectin reduces the TG content of adipose tissue by increasing FA oxidation, and is therefore known as an insulin sensitiser (Yamauchi *et al.*, 2001). The concentration of adiponectin increases when insulin sensitivity improves, such as after weight loss or insulin-sensitising drug treatment (Yang *et al*., 2001; Matsazawa *et al*., 2004), leading to the suggestion that adiponectin plays a part in the onset of the metabolic syndrome (Matsazawa *et al*., 2004). Adiponectin also plays a role in obesity, as seen in obese mice, as it enhanced energy expenditure and prevented adipocyte differentiation (Bauche *et al.*, 2006).

Adiponectin is thought to be involved in the inflammatory response, as shown by the fact that it down-regulates the production of TNF-α (Masaki *et al*., 2004), whereas TNF-α is also known to reduce adiponectin production (Kappes *et al*., 2000). Other anti-inflammatory effects of adiponectin include inhibition of IL-6 gene expression and secretion, and an induction of the anti-inflammatory cytokines IL-1 and IL-10 receptor antagonist (Kumada *et al*., 2004; Wolf *et al*., 2004; Wulster-Radcliffe *et al*., 2004).

The protein also may have an effect on vascular structure and function. Studies in adiponectin knockout mice demonstrate vascular alterations, including thickening of the intima layer and increased production of vascular smooth muscle cells in mechanically injured arteries (Kubota *et al*., 2002), and so, adiponectin may be part of a link between atherosclerosis and obesity (Ouchi *et al*., 1999). These effects may be caused by adiponectin inhibiting intercellular adhesion molecule- (ICAM) -1 and vascular cell

adhesion molecule- (VCAM) -1 by either TNF-α or resistin (Ouchi *et al*., 1999; Kawanami *et al*., 2004). Also, over expression *in vivo* of adiponectin in apolipoprotein E-deficient mice suppresses atherosclerosis by reducing production of adhesion molecules (Okamoto *et al*., 2002). Over expression of adiponectin RNA *in vitro* resulted in greater cell proliferation and differentiation as well as increases in the expression of adipogenic genes, lipid content, and improved insulin sensitivity (Fu *et al*., 2005).

#### *1.3.2.3. Adiponectin receptor*

Two receptor forms have been cloned for adiponectin, and both are unique in distribution and affinity for the molecular forms of the protein. The two forms are AdipoR1 which has a high affinity receptor for gAd but low affinity for fAd, and AdipoR2, which shows similar affinity for both forms of adiponectin (Yamauchi *et al*., 2003). AdipoR1 is mainly expressed in skeletal muscle, whereas AdipoR2 is predominantly expressed in the liver. Therefore, both gAd and fAd have metabolic effects in skeletal muscle, and fAd alone has a greater effect on hepatic metabolic signalling (Tomas *et al*., 2002; Yamauchi *et al*., 2002 and 2003). Adiponectin mediates its insulin sensitising effects by binding to both receptors and activating 5'-AMP-activated protein kinase (AMPK), an enzyme involved in FA oxidation, and glucose metabolism in both the liver and skeletal muscle (Yamauchi *et al.*, 2002). The expression of both receptors decreases in the obese state (Kadowaki and Yamauchi, 2005), and both are expressed in human adipose tissue and isolated adipocytes, although the expression of AdipoR1 is greater than AdipoR2. T2DM and insulin treatment decreases AdipoR1 expression, but maintains that of AdipoR2 (Inukai *et al*., 2005). This may suggest that AdipoR1 expression plays a role in insulin sensitivity and secretion, as previously demonstrated in mice (Staiger *et al*., 2004) and humans (Civitarese *et al*., 2004).

### 1.3.3. Adipsin

Adipsin is a differentiation dependent serine protease, and was originally called protein 28K (Hunt *et al*., 1986). Initially this hormone was thought to be primarily expressed in adipose tissue (Cook *et al*., 1985), and mainly by adipocytes in mice and humans (White *et al*., 1992). This protein is associated with metabolic and genetic obesity in rodent models, and acts as a feed-back signal for food intake regulation (Cleary *et al*., 1980; Flier *et al*., 1987). The concentration of adipsin is reduced in obese mice models (Flier *et al*., 1987), but either increased (Napolitano *et al*., 1994), or constant in humans. Roles for adipsin in the regulation of lipolysis and lipogenesis have also been suggested (Flier *et al*., 1987).

### 1.3.4. Recent adipokine discoveries

Since the turn of the century, a number of new adipokines have been identified, and a few are mentioned here. The first is resistin, discovered in 2001, and originally found to induce insulin resistance in mice, where it was primarily expressed by adipocytes (Steppan *et al*., 2001). In humans; however, macrophages are the greatest source of resistin (Rea and Donnelly, 2004). Resistin is a member of the FIZZ (found in inflammatory zone) family of molecules, which are involved in the regulation of inflammation. Original studies demonstrated that insulin resistance was induced by resistin (FIZZ3) administration in mice (Steppan *et al*., 2001), indicating a possible link between obesity and insulin resistance. Later studies; however, have shown a decrease or no change in resistin concentration in obese mice, meaning that its true role is yet to be established (Way *et al*., 2001).

Four new adipokines were all identified around the same time, and these are visterin, visceral adipose tissue–derived serpin (vaspin), omentin 1 and retinol-binding protein 4 (RBP4). Visfatin is expressed mainly by visceral WAT, and mimics insulin action both *in vivo* and *in vitro* by binding to the insulin receptor (Fukuhara *et al*., 2005). Unlike insulin, concentration of visfatin is not affected by either fasting or feeding (Fukuhara *et al*., 2005). Visfatin gene expression appears to be mediated by many factors; it increases in response to dexamethasone, and decreases after treatment with growth hormone and TNF-α in 3T3-L1 adipocytes (Kralisch *et al*., 2005).

Vaspin is a member of the serine protease inhibitor family, and was identified in the visceral adipose tissue of Otsuka Long-Evans Tokushima fatty (OLETF) rats (Hida *et al*., 2005). This rat model shares common signs of human T2DM such as abdominal obesity, insulin resistance, hypertension, and dyslipidemia (Kawano *et al*., 1992). Administration of vaspin to obese mice improves glucose tolerance and insulin sensitivity (Hida *et al*., 2005). In humans, vaspin gene expression is detected more frequently in visceral as opposed to subcutaneous adipose tissue (Kloting *et al*., 2006).

Greater gene expression of omentin 1 is found in visceral adipose tissue in relation to subcutaneous adipose tissue. This protein was originally identified as being secreted by visceral stromal vascular cells (Kralisch *et al*., 2005; Schaffler *et al*., 2005; Yang *et al*., 2006). Omentin 1 is also found in other cell types, albeit at a lesser expression, and these

include intestinal Paneth cells (Komiya *et al*., 1998), endothelial cells and visceral adipose stromal-vascular cells (Yang *et al*., 2006). In isolated human adipocytes, omentin 1 activates the protein kinase Akt/protein kinase B to increase insulin signal transduction, and also enhances insulin-stimulated glucose transport (Yang *et al*., 2006). The secretion of this adipokine is decreased in cultured human adipocytes by D-glucose and insulin (de Souza Batista *et al*., 2007; Tan *et al*., 2008). Human plasma concentrations and gene expression of omentin 1 in versceral tissue are decreased in obesity (de Souza Batista *et al*., 2007).

Finally, RBP4 is a protein secreted by both adipocytes and the liver, and may be involved in systemic insulin resistance (Yang *et al*., 2005). Increased concentrations of the protein are associated with T2DM (Basualdo *et al*., 1997; Abahusain *et al*., 1999), and administration of RBP4 into mice impairs insulin signaling in muscle (Yang *et al*., 2005). Serum concentrations of RBP4 correlate with CVD risk factors along with insulin resistance as part of the metabolic syndrome (Reaven, 2005).

### 1.3.5. Cytokines

Cytokines have been described as a wide range of low molecular weight, pharmacologically active proteins that are secreted by a cell and have either an autocrine or paracrine effects (McDermott, 2001). Over 200 cytokine ligands have been identified; however, only a few of these have been studied in adipose tissue, particularly the interleukins (IL) and TNF-α.

#### *1.3.5.1. TNF-α*

TNF-α is a well-studied cytokine and was originally identified in the WAT of rodents, and the majority of its gene expression is found within the adipocytes (Hotamisligil *et al*., 1993; Kern *et al*., 1995; Montague *et al*., 1998). The gene expression of TNF-α is less than that of other proteins in WAT (Montague *et al*., 1998), and minimal secretion occurs from normal tissue (Crawford *et al*., 1997). In obese subjects; however, secretion of TNF-α is increased (Hotamisligil *et al*. 1997). Gene expression of TNF-α has been found to be increased in human subcutaneous WAT when compared to visceral tissue (Fain *et al*., 2004). TNF-α is also expressed by the stromovascular cells of WAT and pre-adipocytes, although its gene expression increases with the degree of differentiation (Hube and Hauner, 1999). The protein is synthesised as a 26-kDa transmembrane pro-hormone and is cleaved into a 17-kDa biologically active molecule. Both forms of TNF-α mediate its biological effects.

*1.3.5.1.1. Function of TNF-α*

TNF-α is also known as cachectin due to its original characterisation as a cachexia inducing factor (Oliff *et al*., 1987; Siegel *et al*., 1995). This condition, also known as 'wasting syndrome' is caused by a negative energy balance and is therefore on the other side of the energy equation to obesity; however, both are inflammatory conditions. TNF-α has been well documented as being an important mediator of obesity-related insulin resistance (Hotamisligil *et al.*, 1993, 1994 and 1995). It has been shown to induce serine phosphorylation of the insulin receptor, thereby inhibiting insulin signalling. Weight loss is associated with decreased production of TNF-α, and improved insulin sensitivity (Hotamisligil *et al.*, 1995). Insulin-sensitising drugs such as TZDs decrease TNF-α gene expression *in vivo* (Miles *et al.*, 1997).

The cytokine also down-regulates glucose transporter type 4 (GLUT4) in adipocytes, which causes a decrease in insulin-stimulated intracellular glucose transport (Stephens and Pekala, 1991; Stephens *et al.*, 1997). This reduction by TNF-α is coupled with an increase in HSL gene expression, therefore leading to an increase in lipolysis (Sumida *et al*., 1997). TNF-α has also been shown to inhibit the activity and gene expression of LPL (Kawakami *et al*., 1982; Semb *et al.*, 1987; Fried and Zechner, 1989; Feingold *et al*., 1992), causing an induction of insulin resistance and mobilisation of lipids (Ogawa *et al*., 1989; Hauner *et al*., 1995) from within the adipocytes. TNF-α mediates these effects by suppression of C/EBPs (Stephens and Pekala, 1991) and PPARγ (Zhang *et al*., 1996), possibly down-regulating certain adipocyte-specific proteins involved in lipogenesis (Doerrler *et al.*, 1994). These include fatty acid-binding protein, fatty acid synthase, acetyl-CoA carboxylase, glucose-6-phosphate dehydrogenase, LPL and GLUT4 (Hube and Hauner, 1999). TNF-α is also able to decrease the gene expression of β3-adrenoceptors in both white and brown adipocytes (Berkowitz *et al*., 1998; Nisoli *et al*., 2000), and these receptors are involved in sympathetically-mediated lipolysis and thermogenesis in WAT and BAT respectively (Zaasma and Nahorski, 1990; Langin *et al*., 1991; Lonnqvist *et al*., 1993). TNF-α deficient mice exhibit lower concentrations of circulating free fatty acids (FFAs) and TGs than their wild-type littermates (Uysal *et al.*, 1997), possibly implying that mediation of insulin resistance by TNF-α may occur due to increased lipolysis.

The down-regulation of the transcription factors C/EBP and PPARγ by TNF-α as mentioned above (Stephens and Pekala, 1991; Zhang *et al*., 1996) may also be involved in the inhibition of adipocyte differentiation caused by the cytokine. TNF-α also suppresses the expression of adipocyte-specific genes in fully differentiated adipocytes (Ruan *et al.*, 2002). Many of these genes, such as GLUT 4 and aP2 have binding sites for PPARγ and/or C/EBPα in their promoters, which may explain why their gene expression decreases after TNF-α treatment. TNF-α may also regulate cell size; as the cells grow, gene expression and secretion of TNF-α increases, acting to limit adipocyte size or to induce apoptosis (Hotamisligil *et al*., 1995). An induction of apoptosis by TNF-α has been seen in both pre-adipocytes and mature adipocytes (Prins *et al*., 1997). Treatment with the adipogenic and anti-inflammatory agent, dexamethasone, reverses the anti-adipogenic and apoptotic (Zhang *et al.*, 2001) effect of TNF-α.

Finally, TNF-α is a regulator of adipokine gene expression, especially inflammatory mediators. It has been shown to upregulate gene expression and secretion of leptin (Grunfeld *et al*., 1996; Kirschgessner *et al*., 1997; Berkowitz *et al*., 1998), as well as gene expression of IL-6, MCP-1, nerve growth factor (NGF), vascular endothelial growth factor (VEGF) among others in adipocytes *in vitro* (Wang *et al.*, 2005).

*1.3.5.1.2. TNF-α receptors*

TNF-α interacts with many receptors; however, the major TNF receptors active in adipose tissue are TNF-R1 and TNF-R2. Studies with knockout models have found that TNF-R1 is involved in the stimulation of lipolysis (Sethi *et al*., 2000). TNF-R2 is thought to be involved in insulin resistance (Hube and Hauner, 1999). Both receptors can be released from the cell membrane and exist in a soluble form. Membrane-bound TNF-α binds to both receptors, whereas soluble TNF-α preferably interacts with TNF-R1 (Hube and Hauner, 1999). The circulating concentration of both receptors increases in obesity (Hotamisligil *et al.*, 1997) and therefore may alter the activity of TNF-α (Sethi and Hotamisligil, 1999).

#### *1.3.5.2. Interleukins*

The interleukins (IL) are a group of cytokines who got their name from the originally identified members which were both produced by, and acted on leukocytes. The first to be discovered was IL-1, derived from macrophages (Smith *et al*., 1980). It triggers the T-helper cell to produce IL-2 along with mitogen or antigen (Farrar *et al*., 1980; Smith *et al*., 1980). IL-2 maintains the proliferative capacity of activated cells (Smith *et al*., 1983), influences antibody responses to T-dependent antigens (Leibson *et al*., 1981) and also causes maturation of cytotoxic precursor cells into effectors (Shaw *et al*., 1978; Wagner *et al*., 1980). Many interleukins have since been identified, and are known to be expressed and secreted by other cell types, including white adipocytes (Trayhurn and Wood, 2004).

IL-6 is the most extensively characterised member of the IL family. Both IL-6 and its receptor IL-6R are expressed in adipocytes and adipose tissue, with approximately a third of circulating IL-6 originating from adipose tissue (Fernandez-Real and Ricart, 2003). IL-6 circulates in various glycosylated forms of different sizes, while the receptor exists as either a membrane-bound form, or a soluble form (Fain *et al*., 2004). Depot differences in IL-6 gene expression and secretion occur, with the greatest observed in the omental depot when compared to subcutaneous tissue (Fain *et al*., 2004). Production of IL-6 is positively correlated with adiposity in humans (Fried *et al*., 1998); an increase in plasma concentration is observed in obese and insulin resistant states (Mohamed-Ali *et al*., 1997; Bastard *et al*., 2000; Vozarova *et al*., 2001), whereas weight loss leads to a decrease in circulating concentrations of IL-6 (Ziccardi *et al*., 2002; Esposito *et al*., 2003). Furthermore, increased IL-6 concentration is predictive of the development of T2DM (Pradhan *et al*., 2001) and is therefore thought to be involved in insulin resistance, as it suppresses insulin-stimulated metabolic actions in hepatocytes via the induction of suppressor of cytokine signalling- (sOCs) -3 gene expression (Senn *et al*., 2003). This has been demonstrated by the inability of insulin to suppress glucose production in the liver after IL-6 administration in mice (Kim *et al*., 2004). On the other hand, IL-6 deficiency in high-calorie fed mice causes increased hepatic insulin resistance (Matthews *et al*., 2010). However, reduced IL-6 activity in adipose tissue inhibits insulin resistance via regulation of sOCs3 expression in the liver (Sabio *et al*., 2008). Other functions of IL-6 include inhibition of adipogenesis and the stimulation of lipolysis (Path *et al*., 2001). Gene expression of IL-6 is stimulated by TNF-α (Wang *et al.*, 2005) and like TNF-α it has implications in the WAT wasting as seen in cancer cachexia (Greenberg *et al.*, 1992).

Other interleukins expressed by WAT include IL-1β, IL-18 and IL-10 (Fain *et al.*, 2004; Juge-Aubry *et al.*, 2005). IL-1β binds to the IL-1 receptor and activates the NFκB signalling pathway. It stimulates leptin secretion from human adipocytes (Flower *et al*., 2003) and also promotes leptin production in response to inflammatory stimuli in mice (Faggioni *et al*., 1998). Concentration of IL-1β increases with obesity (Um *et al.*, 2004), and this increase is a risk factor to both T2DM and the metabolic syndrome when combined with an increase in IL-6 production (Spranger *et al.*, 2003). Chronic IL-1β treatment causes insulin resistance in both human and rodent adipocytes (Lagathu *et al.*, 2006), due to decreased IRS-1 expression (Jager *et al.*, 2007). IL-18 is also a pro-inflammatory cytokine, and is expressed in both human adipose tissue and adipocytes. IL-18 gene expression is induced by LPS, TNF-α and IL-1β in these sites (Juge-Aubry *et al.*, 2005; Skurk *et al*., 2005b), whilst dexamethasone has been shown to inhibit IL-18 gene expression (Bruun *et al*., 2001). The plasma concentration of IL-18 has also been shown to increase with obesity, and decrease after weight loss (Esposito *et al.*, 2002). However, mice deficient in IL-18 or its receptor exhibit hyperphagia, insulin resistance, hyperglycaemia and obesity (Netea *et al*., 2006). Finally, IL-10 is secreted from human adipocytes and also the stromal vascular fraction of human WAT (Fain *et al*., 2004). It differs from most cytokines due to its anti-inflammatory nature. An expansion in WAT mass in both humans and mice causes increased gene expression of IL-10 (Esposito *et al*., 2003; Juge-Aubry *et al*., 2005).

### 1.3.6. Chemokines

Chemokines are low molecular weight proteins structurally similar to cytokines. Their main functions include regulation of cell trafficking and also leukocyte migration into damaged tissues. Chemokines were first discovered with the purification of secreted platelet factor- (PF) -4 (Wu *et al*., 1977). Since then, more than 50 human chemokines and 20 chemokine receptors have been identified (Zlotnik *et al.*, 1999). As previously mentioned, infiltration of macrophages is associated with obesity, causing an increase in the expression of several macrophage-specific genes (Weisberg *et al.*, 2003; Xu *et al.*, 2003). The gene expression of MCP-1, MIF and IL-8 from adipocytes is particularly important in macrophage infiltration (Gerhardt *et al.*, 2001). MCP-1 is mainly produced by macrophages and endothelial cells, and is a potent chemotactic factor for monocytes. Many previous studies have demonstrated that MCP-1 gene expression is increased with obesity. MCP-1 is also present in human adipose tissue, with increased gene expression and secretion found in the visceral depot, compared to subcutaneous WAT (Bruun *et al*., 2005). The expression of an MCP-1 transgene under the control of the *aP2* gene promoter

in adipose tissue has been found to induce macrophage infiltration into adipose tissue, insulin resistance, and increased hepatic triglyceride content in mice. The same study also found that acute disruption of MCP-1 lead to improved insulin resistance and hepatic steatosis in obese mice, and suggested that the increased MCP-1 gene expression in adipose tissue during obesity is important in the pathogenesis of insulin resistance, macrophage infiltration into adipose tissue, and hepatic steatosis (Kanda *et al*., 2006). This possible role in insulin resistance is also supported by the fact that TNF-α (known to induce insulin resistance), increases MCP-1 gene expression and secretion in human adipocytes in *vitro* (Wang *et al.*, 2005). Another function of MCP-1 within adipose tissue includes a reduction in the gene expression of adipogenic genes, leading to an inhibition of adipocyte growth and differentiation (Sartipy and Loskutoff, 2003).

MIF is also involved in macrophage infiltration into WAT, and has been demonstrated to be positively correlated with BMI in humans (Skurk *et al.*, 2005a); circulating concentration of MIF is increased in the obese state (Dandona *et al.*, 2004; Ghanim *et al.*, 2004) and decreased after weight loss (Church *et al.*, 2005). The chemokine is also expressed by pancreatic β-cells and in the presence of raised plasma concentrations of glucose, increased gene expression of MIF may be used as a marker for β-cell dysfunction (Church *et al.*, 2005).

A member of the interleukin family, IL-8, is expressed and secreted from human adipocytes *in vitro* and *in vivo.* Like the other chemokines, circulating concentrations of IL-8 correlate with adiposity, and so may be involved in obesity related comorbidities (Bruun *et al.*, 2003b).

A more recently discovered chemokine is chemerin (Wittamer *et al*., 2003), and it is expressed in both the liver and WAT (Bozaoglu *et al*., 2007; Goralski *et al*., 2007). It modulates chemotaxis, and activates dendritic cells and macrophages through G protein-coupled receptors (Cash *et al*., 2008; Zabel *et al*., 2008). Macrophage derived cysteine proteases cleave chemerin to generate potent anti-inflammatory products that inhibit the production of pro-inflammatory mediators such as TNF-α, IL-1β, and IL-6, whilst increasing the gene expression of anti-inflammatory cytokines (Cash *et al*., 2008). Chemerin is also associated with the metabolic syndrome (Bozaoglu *et al*., 2007).

### 1.3.7. Other factors

WAT also expresses and secretes a wide range of other factors. These include haemostatic and haemodynamic factors, acute phase proteins and growth factors. Haemostatic and haemodynamic factors include the renin-angiotensin aldosterone system (RAAS) and Plasminogen-activator inhibitor 1 (PAI-1). RAAS is a regulator of systemic blood pressure and renal electrolyte homeostasis (Engeli *et al*., 2000). Many of the RAAS proteins are secreted by WAT including renin, angiotensinogen (AGT), angiotensin I and II, angiotensin receptors type I (AT1) and II (AT2), and angiotensin-converting enzyme (ACE). RAS gene expression is positively correlated with adiposity in humans, and is therefore possibly involved in obesity-associated hypertension (Harte *et al.*, 2005). PAI-1 is a serine protein inhibitor, and increased concentrations are a risk factor for thrombosis (Fay, 2004). It its concentration increases with visceral obesity (Kershaw and Flier, 2004). PAI-1 deficient mice have smaller adipocytes and lower tissue triglyceride concentration than wild-type mice in response to a high-fat diet (Schafer *et al*., 2001; Ma *et al*., 2004), suggesting a role for this protein in WAT development.

Acute phase proteins are mainly secreted by the liver; however, several are expressed in and secreted from WAT. These are therefore classed as adipokines, and their circulation concentration increases in the obese state (Trayhurn and Wood, 2004). One such protein is serum amyloid A (SAA), an amyloid A precursor. It is an independent risk factor for coronary artery disease and AA amyloidosis, with its serum concentration being correlated with BMI and adiposity (Poitou *et al.*, 2005). Haptoglobin is another acute phase protein and its gene expression is known to increase during the differentiation process in both humans and mice (do Nascimento *et al.*, 2004). It binds haemoglobin to prevent kidney damage during haemolysis, and has also been demonstrated to stimulate endothelial cell differentiation and vascularisation (Cid *et al*., 1993). Another acute phase protein is metallothionein (MT), which is expressed in BAT, where it has a suggested antioxidant role (Beattie *et al*., 2000). This antioxidant role has also been suggested in WAT by protecting fatty acids from oxidative damage (Trayhurn *et al.*, 2000). The gene expression of MT occurs in all WAT depots, and is adipocyte specific (Trayhurn *et al.*, 2000).

WAT expresses and secretes various growth factors including; transforming growth factor- (TGF) -β, IGF-1, vascular endothelial factor (VEGF) and nerve growth factor (NGF). TGF-β is expressed in WAT, and mice obesity models demonstrate an increase in its gene expression (Samad *et al*., 1997). It is involved in many processes, including tissue

remodelling, wound repair, cell adhesion and migration, extracellular matrix production (Sporn *et al*., 1987), and so regulates differentiation of many cell types. IGF-1 is secreted from WAT and stimulates pre-adipocyte differentiation (Hausman *et al*., 2001). VEGF is mainly secreted by visceral WAT, and *db/db* mice have an increased plasma concentration of this growth factor (Miyazawa-Hoshimoto *et al*., 2005). NGF is a target-derived neurotrophin, and these proteins are involved in the development of the nervous system (Hennigan *et al.*, 2007). The SNS is involved in many aspects of WAT function, including lipolysis (Hales *et al*., 1978; Bartness and Bamshad, 1998) and adipokine production (Trayhurn *et al*., 1995; Rayner and Trayhurn, 2001). Therefore, neurotrophins are involved in the regulation and maintainance of sensory neurons (Vega *et al*., 2003). NGF has been shown to be expressed in mice and human WAT *in vivo* (Peeraully *et al.*, 2004), and is also secreted *in vitro* by mice and human adipocytes (Peeraully *et al.*, 2004).

### 1.4. EICOSANOIDS

Eicosanoids are local hormones that have specific effects on nearby target cells. They are produced by multiple cell types, and therefore have many functions. Their main role is as mediators of inflammation, giving the view that these signalling lipids are pro-inflammatory; however, some have anti-inflammatory roles, such as the lipoxins (Gewirtz *et al*., 2002; Serhan *et al*., 2003). Others, such as prostaglandin (PG) $E_2$, have both pro- and anti-inflammatory effects. This eicosanoid is an inhibitor of certain pro-inflammatory cytokines, including TNF-α and IL-1, as seen in monocytes and macrophages (Miles *et al*., 2002). In contrast, $PGE_2$ induces the formation of anti-inflammatory lipoxins (Levy *et al*., 2001; Vachier *et al*., 2002).

Production of eicosanoid species occurs via the oxidation of $C_{20}$ polyunsaturated fatty acids, primarily 5,8,11,14-eicosatetraenoic acid, also known as arachidonic acid (AA); but also 5,8,11,14,17-eicosatrienoic acid, commonly named eicosapentaenoic acid (EPA), and *all-cis*-docosa-4,7,10,13,16,19-hexa-enoic acid; docosahexaenoic acid (DHA; Levin *et al*., 2002; Wada *et al*., 2007). AA is a member of the omega-6 family, whereas both EPA and DHA are omega-3 fatty acids. The eicosanoid species produced by these pathways include PGs, leukotrienes (LT) and lipoxins (LX), as summarised in Figure 1.5.

The eicosanoid species investigated in this thesis are all derived from AA, and so, this pathway will be discussed in greater detail in Sections 1.4.1 to 1.5.

### 1.4.1. The arachidonic acid cascade

The classic eicosanoid family is comprised of three groups, produced via three pathways, as summarised in Figure 1.6. These are the cyclooxygenase (COX) pathway, whose products include PGs and thromboxanes (Tx); the lipoxygense (LOX) pathway which forms LTs and certain mono-, di- and tri-hydroxy acids; and finally epoxides are synthesised by the epoxygenase pathway. These pathways are often referred to as cascades, and they all need a critical oxygenase to produce a reactive intermediate, which occurs by integrating molecular oxygen into the arachidonic acid structure. These intermediates are then processed by secondary enzymes to form the biologically active eicosanoid species. All three oxygenase cascades will be discussed in more detail.

#### *1.4.1.1. The cyclooxygenase cascade*

Prostanoids are produced via the COX pathway, and are synthesised in response to cell specific stimuli. The intermediate involved in this cascade is $PGH_2$, and this is then converted into the biologically active eicosanoids, such as $PGE_2$ which utilises $PGE_2$ synthase (Helliwell *et al*., 2004). Before the conversion of $PGH_2$ into $PGE_2$, AA is released via hydrolysation of phospholipids present in the cell membrane by the enzyme phospholipase $A_2$ ($PLA_2$). After its release, AA is converted into $PGG_2$, the prostanoid precursor, and this is subsequently peroxidised to $PGH_2$. Both of these reactions are catalysed by COX. There are two COX isoforms, COX-1 located in the ER and COX-2 which acts near the nuclear envelope (Morita *et al*., 1995). COX-1 is constitutively expressed (O'Neill *et al*., 1994) and is involved in physiological functions such as platelet aggregation (Funk *et al*., 1991). The inflammatory functions of prostanoids are due to expression of COX-2 (Maier *et al*., 1990; Lee *et al*., 1992; Xie *et al*., 1992). The biologically active prostanoids are considered as $PGD_2$, $PGE_2$, $PGF_{2\alpha}$, $PGI_2$ (possibly $PGH_2$) and $TxA_2$ (Straus and Glass, 2001; Hata and Breyer, 2004). These are synthesised from the conversion enzyme substrate, $PGH_2$. These enzymes are $PGD_2$, $PGE_2$, $PGF_{2\alpha}$, prostacyclin and thromboxane synthase. Some of the biologically active prostanoids can be further converted into other products, for example, $PGE_2$ can form $PGA_2$, $PGB_2$ and $PGC_2$, while $PGI_2$ can be converted into 6-keto-$PGF_{1\alpha}$ (Straus and Glass, 2001). This more detailed COX pathway is presented in Figure 1.7.

#### *1.4.1.2. Prostanoid structure and function*

The prostanoids all share a similar structure; they are all oxygenated fatty acids composed of 20 carbon atoms and contain a cyclic ring, a *trans*-double bond between C-13 and C-14, and a hydroxyl group at C-15. The prostanoid group contains PG species, all of which contain a cyclopentane ring, and classified into types A to I due to modifications of this ring. PG types D to I exist naturally, with $PGG_2$ and $PGH_2$ being unstable intermediates (Hamberg and Samuelsson, 1973). Types A to C are produced in extraction procedures, but are prone to artefacts (Schneider *et al*., 1966). A final PG to be discovered was $PGI_2$, also called prostacyclin (Moncada *et al*., 1976), whose structure differs from the remaining PGs due to an oxygen bridge between carbons six and nine. The prostanoid group also consists of two Tx sub-groups, A (Hamberg *et al*., 1975) and B (Hamberg and Samuelsson, 1974), and both contain a cyclohexane ring. Individual prostanoids species structures are shown in Figure 1.8.

The prostanoids play a major role in the inflammatory response, especially the 2-series members derived from AA. The symptoms of acute inflammation include local reddening, heat, swelling and pain. Studies using prostanoid receptor knockout mice identified that prostanoids and their receptors mediated these symptoms. Mice deficient in IP receptor displayed a reduction in carrageenin-induced paw swelling when compared to wild-type mice (Murata *et al*., 1997). This reduction was also seen in the non-steroidal anti-inflammatory drugs (NSAIDs) treated wild-type mice. These drugs act in a similar way to aspirin by inhibiting PG biosynthesis (Vane, 1971). Therefore it was predicted that prostanoids are mediators of acute inflammation.

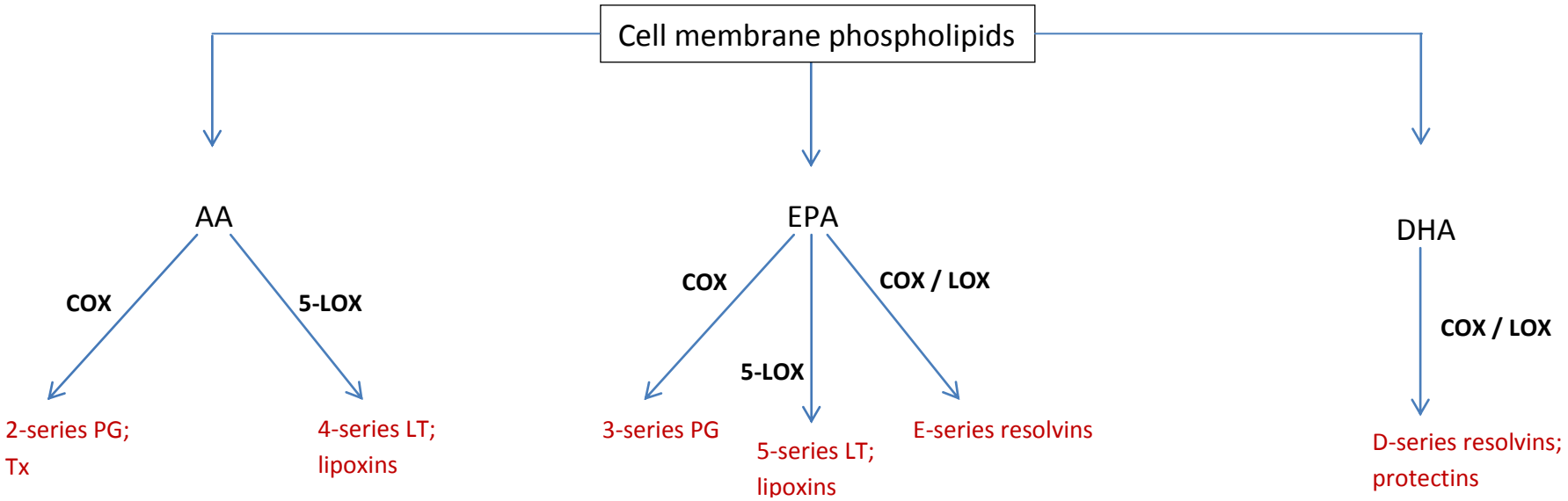


**Figure 1.5. Eicosanoid synthesis pathways**

Summary of the eicosanoid synthesis pathways including enzymes (bold) and products (red). The AA pathway is presented in more detail in future sections. The abbreviations used are: AA, arachidonic acid; EPA, eicosapentaenoic acid, DHA; docosahexaenoic acid; COX, cyclooxygenase; LOX, lipoxygenase; PG, prostaglandin; Tx, thromboxane; LT, leukotrienes. The series number relates to the number of double bonds.

Other studies using knockout mice have discovered that IP, $EP_1$, $EP_3$, and $EP_4$ prostanoid receptors are involved in perphipheral hyperalgesia, with $EP_2$ being shown to inhibit glycinergic inhibitory neurotransmission in the spinal cord, thus causing this effect (Ahmadi *et al*., 2002). The formation of both $PGE_2$ and $PGI_2$ via activation of both $EP_2$ and IP respectively has been shown to increase vascular permeability and leukocyte infiltration (Hirata *et al*., 1991). A lack of fever generations has also been observed in $EP_3$-deficient mice after administration of bacterial endotoxin (LPS) and IL-1 (Ushikubi *et al*., 1998). An induction of COX-2 is evident in inflammatory cells and tissue; however, both COX isoforms have an inflammatory role (Kennedy *et al*., 1982).

COX inhibitors (such as aspirin) are known to have physiological implications. A study in COX-2 knockout mice found that these animals developed severe nephropathy (Morham *et al*., 1995). However, another study has demonstrated a decrease in the size and number of polyps in COX-2 knockout mice with adenomatous polyposis (Oshima *et al*., 1996). Opposing effects have been noted between some of the prostanoids species, for example, $PGI_2$ is mainly synthesised by vascular endothelium and is a potent vasodilator and inhibits platelet aggregation (Moncada *et al*., 1976; Tatesson *et al*., 1977), whereas $TxA_2$ is a vasoconstrictor and aggregator of platelets (Needleman *et al*., 1976; Ellis *et al*., 1977).

As well as the pro-inflammatory functions described above, some of the 2-series prostanoids also have anti-inflammatory properties. One example is $PGD_2$ and its derivatives, as they have been shown to be involved in the resolution of inflammation in rat pleurisy (Gilroy *et al*., 1999 and 2003). More commonly associated with anti-inflammatory actions are the 1-series prostanoids derived from dihomo-c-linolenic acid (DGLA). Examples include $PGA_1$, an inductor of the anti-inflammatory cytokine IL-10 in activated monocytes and macrophages (Kim *et al*., 2008); and $PGE_1$ which improved inflammation in murine models for arthritis (Zurier and Quagliata, 1971).

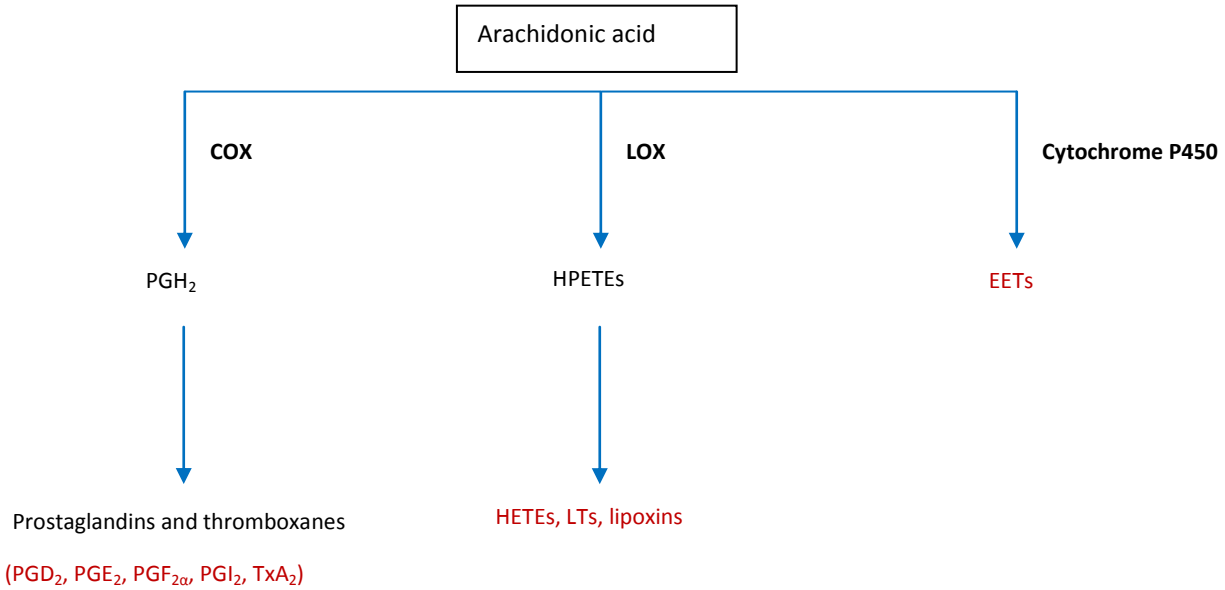




**Figure 1.6. The arachidonic acid cascade**

Summary of the eicosanoid generated pathways including enzymes (bold) and products (red). These pathways are presented in more detail in future sections. The abbreviations used are: COX, cyclo-oxygenase; PG, prostaglandin; TX, thromboxane; LOX, lipoxygenase; HPETEs, hydroperoxyeicosatetraenoic acids; HETEs, hydroxyeicosatetraenoic acids; LTs, leukotrienes; Cytochrome P450, Cytochrome P450 epoxygenase; EETs, epoxyeicosatrienoic acids.

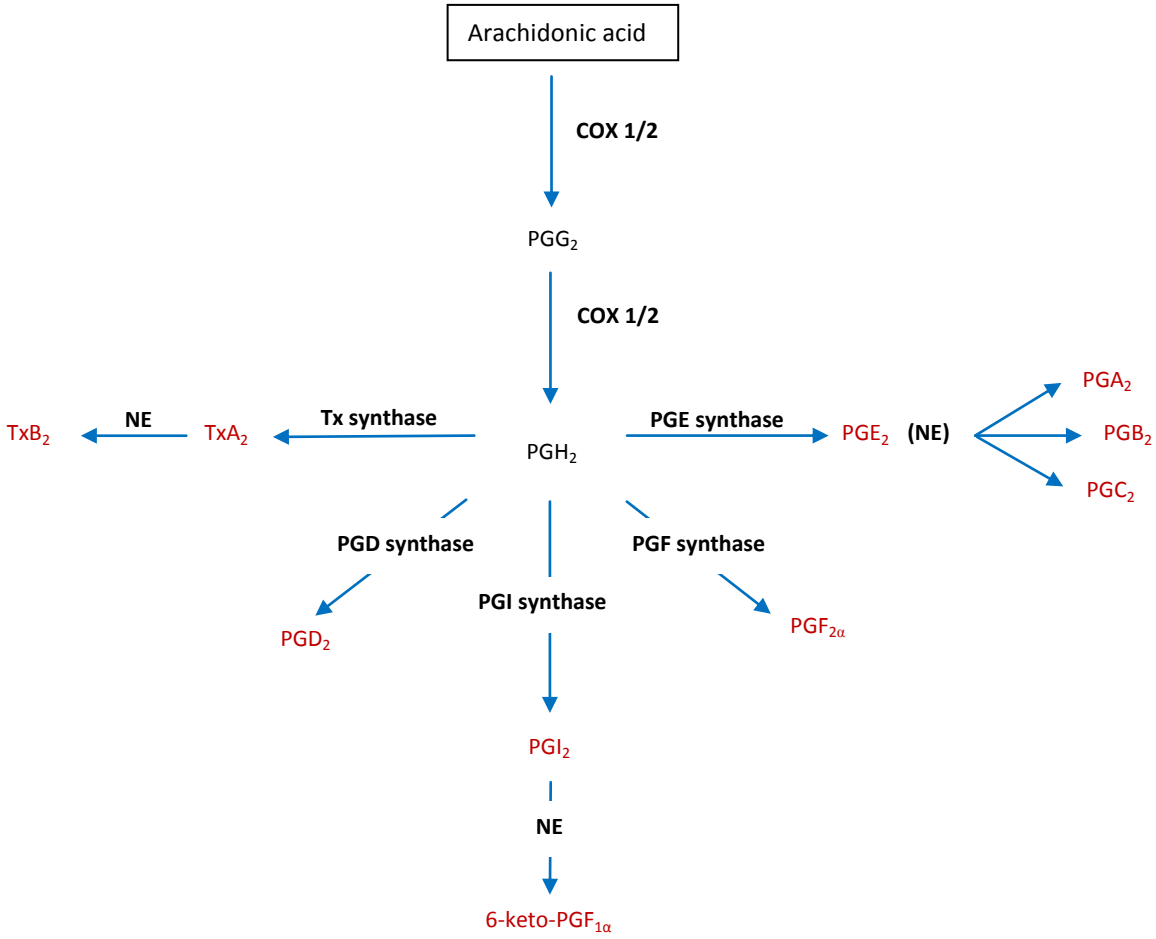


**Figure 1.7. The cyclooxygenase cascade**

This schematic representation illustrates the COX cascade, which leads to the production of various prostanoid species. The enzymes (bold) involved and the final products synthesised (red) are included in the diagram. The abbreviations used are: COX, cyclooxygenase; PG, prostaglandin; TX, thromboxane; NE, non-enzymatic.

#### *1.4.1.3. Prostanoid function in WAT*

Adipocytes have been identified as a source of prostanoid synthesis (Shillabeer *et al*., 1998). Secretion of $PGE_2$, $PGD_2$, $PGF_{2\alpha}$ and 6-keto-$PGF_{1\alpha}$ occurs from 3T3-L1 adipocytes (Borglum *et al*., 1999). In isolated human adipocytes, the secretion of $PGI_2$ and $PGE_2$ has been observed, although greater gene expression of these prostanoids is found in the stromal vascular fraction (Fain *et al*., 2002). The prostanoids have various roles within WAT, with both pre-adipocytes and mature adipocytes synthesising them to regulate their own cellular functions (Lu *et al*., 2003). This study by Lu and colleagues confirmed $PGD_2$ formation by arachidonic acid during the maturation phase of the adipocyte differentiation process, whereas the opposite was true for the production of $PGE_2$, which was more efficient in the pre-adipocyte stage in 3T3-L1 adipocytes. It was suggested that these findings reflect a switch in prostanoid generation depending on the stage of the adipocyte life cycle (Lu *et al*., 2003). Also, the greater gene expression of $PGE_2$ in pre-adipocytes may cause inhibition of adipocyte differentiation (Vassaux *et al*., 1992a and 1992b). $PGD_2$ is effective in the stimulation of triglyceride accumulation, and $PGE_2$ promotes the storage of lipids. A previous study with rat isolated adipocytes demonstrated that $PGE_2$ interacted with G-protein-linked $EP_3$ receptors to inhibit lipolysis (Strong *et al*., 1992), possibly causing the increased accumulation of triglycerides. Another action of $PGE_2$ is the stimulation of leptin release by WAT (Fain *et al*., 2000). These multiple actions of $PGE_2$ may be due to the fact that it can bind to four EP subtypes (Negishi *et al*., 1995).

A final prostanoid found in WAT is $PGF_{2\alpha}$, and this has an antiadipogenic effect (Lepak and Serrero, 1993). Therefore, the major roles of prostanoids in WAT are during adipogenesis, with the differing actions depending on specific prostanoids, and also the stage of adipocyte differentiation.

| **Prostanoid:** | **Structure:** |
|---|---|
| $TxA_2$ | 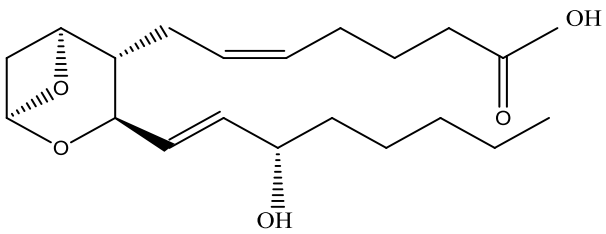 |
| $PGD_2$ | 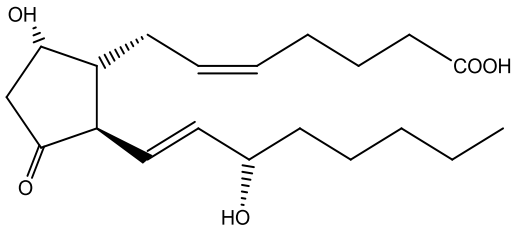 |
| $PGE_2$ | 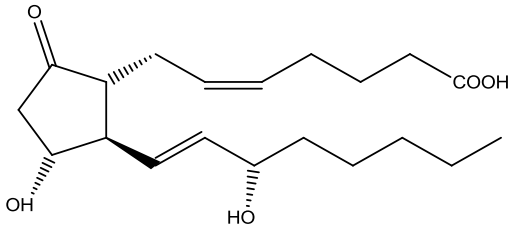 |
| $PGF_{2\alpha}$ | 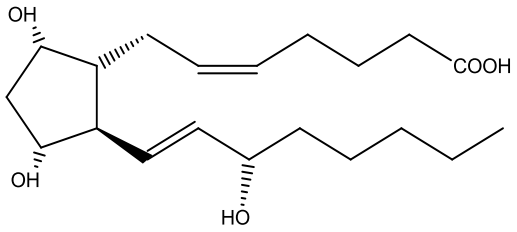 |
| $PGI_2$ | 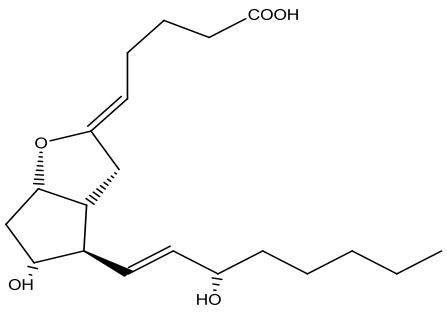 |

**Figure 1.8. Chemical structures of members of the prostanoid family**

Chemical structure of the primary prostanoids.

#### *1.4.1.4. Prostanoid receptors*

The first prostanoid receptor to be cloned was the human $TxA_2$ receptor (Hirata *et al*., 1991). Since then, eight types and subtypes of prostanoid receptors were identified in various species. The receptors are a family of rhodopsinlike seven transmembrane spanning G-protein-coupled prostanoid receptors (GPCRs). These identified receptors are all present in humans and mice, and a few have also been found in other species. They include DP, a PGD receptor; PGF receptor FP; PGI receptor IP; and TP which is the TxA receptor (Hata and Breyer, 2004). The final receptors are those for PGE, and they compose a complete receptor family, consisting of four receptors, $EP_1$ to $EP_4$ (Narumiya *et al*., 1999). Each prostanoid has its highest binding affinity to its corresponding receptor; however, cross-reactivity between the prostanoids and receptors has been observed (Breyer *et al*., 2001). Ligand-receptor interactions are responsible for the roles of the prostanoid receptors, and these interactions depend on many factors including ligand affinity, receptor expression profile and differential coupling to signal transduction pathways (Hata and Breyer, 2004). The expression of the prostanoid receptors also differs with tissue distribution. The $EP_1$ receptor is mainly found in fibroblasts, with $EP_2$ and $EP_4$ predominately observed in smooth muscle cells. The FP receptor is found in kidney cells and astrocytes, TP receptor in platelets and DP receptors in the ileum, lung, stomach, and uterus (Bos *et al*., 2004). The prostanoids may also act through intracellular targets, for example, $PGI_2$ has been suggested as a ligand for PPARα and PPARδ (Kubis and Levy, 2004; Pola *et al*., 2004).

### 1.4.2. The lipoxygenase cascade

The three lipoxygenases present in mammals aid the incorporation of molecular oxygen into AA. The name of each of the three enzymes indicates the position at which molecular oxygen is inserted, and so these are 5-, 12- or 15-lipoxygenase (LO). The first product produced from AA via these enzymes is a hydroperoxyeicosatetraenoic acid (5-, 12-, or 15-HPETE). This is then reduced to the corresponding hydroxyeicosatetraenoic acid, either 5-, 12- or 15-HETE, (Smith, 1989). The 5-LOX pathway is involved in leukotriene (LT) formation; 5-HETE is converted into $LTA_4$ due to the removal of water. This is turn can be converted into $LTB_4$ via $LTA_4$ hydrolase and the addition of water (Funk *et al*., 1987; Minami *et al*., 1987), or into $LTC_4$ by the addition of a glutahionyl group via glutathione S-transferase action (Hammarstrom *et al*., 1985). $LTC_4$ can then produce $LTD_4$ via cleavage by γ-glutamyltranspeptidase, and $LTD_4$ can be further metabolised by dipeptidase to form $LTE_2$ (Hammarstrom *et al*., 1985). The 15-LOX pathway also forms additional products. As

well as 15-HETE, 15-HPETE can be converted into epoxytetraene, and then lead to lipopoxin formation (LX) of which there are two types; $LXA_4$ and $LXB_4$. The 15-HETE product of 15-HPETE can also be further metabolised into 15-oxo-ETE. The LOX cascade is summarised in Figure 1.9, and the structures of the LOX products are shown in Figure 1.10.

#### *1.4.2.1. Functions of LOX cascade products*

The lipoxygenases catalyse the LOX cascade reactions, and are also involved in other processes. They are classified based on the position of molecular insertion in the arachidonate substrate. The LOXs have been identified in various sites; 12-LO has been characterised in mice and human platelets, 15-LO in human monocytes, 5-LO in human neutophils and 12/15-LO in murine peritoneal macrophages (Hammond and O'Donnell, 2012). The expression and secretion of 12-LO is upregulated by hyperglycemia (Kang *et al*., 2001; Chakrabarti *et al*., 2002; Laybutt *et al*., 2002) in pancreatic β-cells and mesangial cells and also by inflammatory cytokines in pancreatic β-cells (Chakrabarti *et al*., 2002) and human islets (Ma *et al*., 2010). It has a role in the development of atherosclerosis (Natarajan and Nadler, 2004; Reilly *et al*., 2004), as does 5-LO and 5-LO-activating protein (5-FLAP) which are involved in the inflammatory pathways leading to this disorder (Radmark, 2003; Osher *et al*., 2006; Back *et al*., 2007; Ferguson *et al*., 2007; Gubitosi-Klug *et al*., 2008). The formation of $LTB_4$ is enhanced by 5-FLAP, a fatty acid transport protein that specifically binds to arachidonic acid. $LTB_4$ has been shown to increase MCP-1 gene expression in human monocytes (Huang *et al*., 2004).

#### *1.4.2.2. Functions of LOX cascade products in WAT*

The LOXs also have functions within WAT. Inflammation within adipose tissue, and also insulin resistance has been shown to be implicated by 12-LO in response to a high-fat diet (Nunemaker *et al*., 2008; Sears *et al*., 2009). The gene expression and secretion of 12-LO is increased in 3T3-L1 adipocytes by free fatty acids (Bullo *et al*., 2003). Addition of 12-LO products has been shown to increase the gene expression of several cytokines in 3T3-L1 adipocytes, suggesting a possible role for 12-LO in the inflammatory pathways present within adipocytes (Chakrabarti *et al*., 2009). Both 5-LO and 5-FLAP have also been found to have roles in obesity and insulin resistance (Ferguson *et al*., 2007; Horrillo *et al*., 2010).

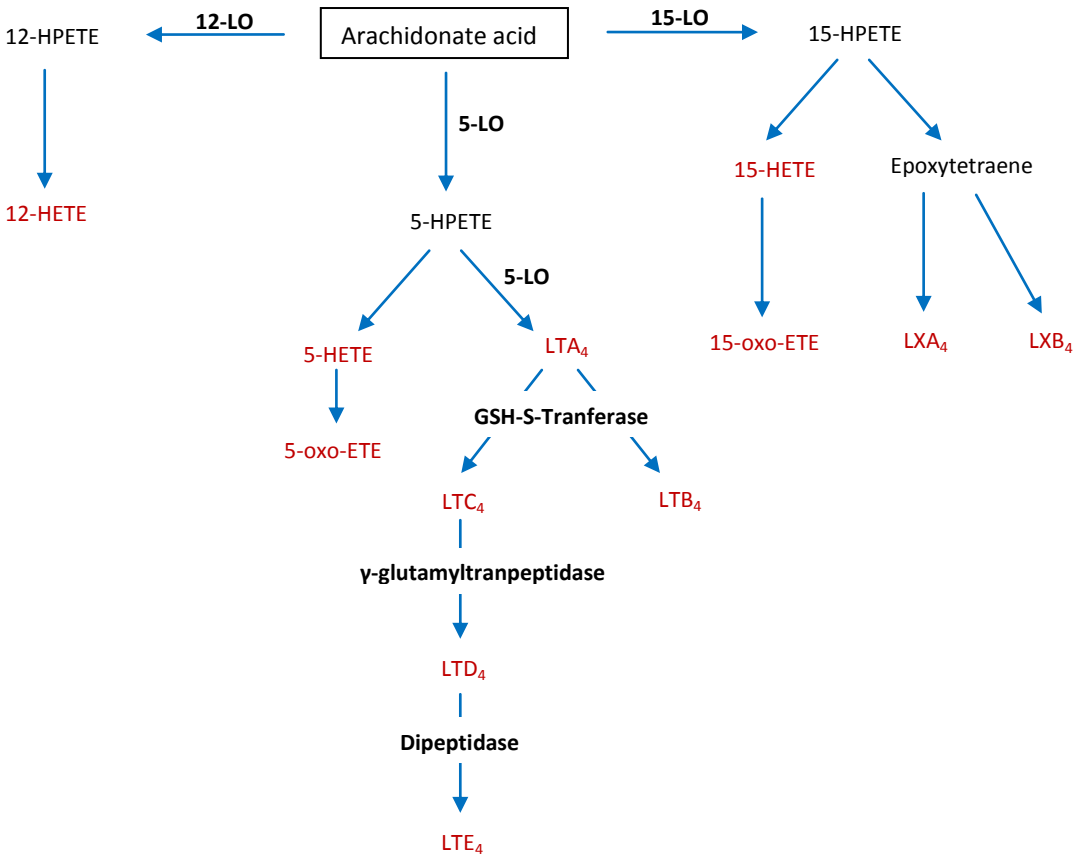


**Figure 1.9. The lipoxygenase cascade**

This schematic representation illustrates the LOX cascade, which leads to the production of HETEs, LTs and lipoxins. The enzymes (bold) and the final products (red) involved in the cascacde are included in the diagram. The abbreviations used are: LO, lipoxygenase; HPETE, hydroperoxyeicosatetraenoic acid; HETE, hydroxyeicosatetraenoic acid; LTs, leukotrienes and LX, lipoxin.

| **LOX product:** | **Structure:** |
|---|---|
| 5-HETE | 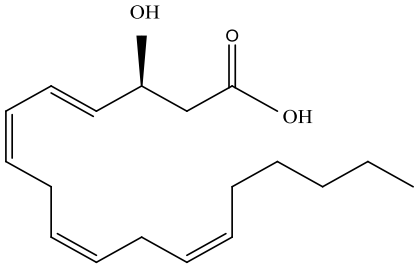 |
| 12-HETE | 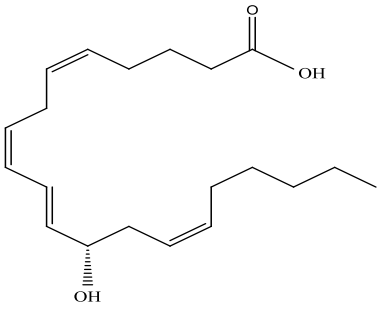 |
| 15-HETE | 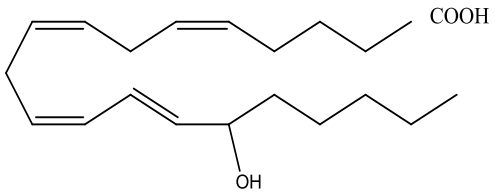 |
| $LTA_4$ | 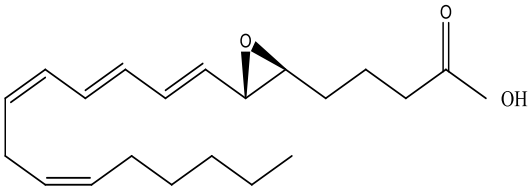 |
| $LXA_4$ | 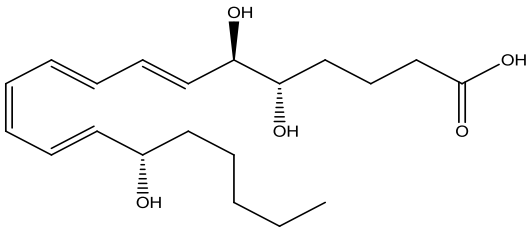 |
| $LXB_4$ | 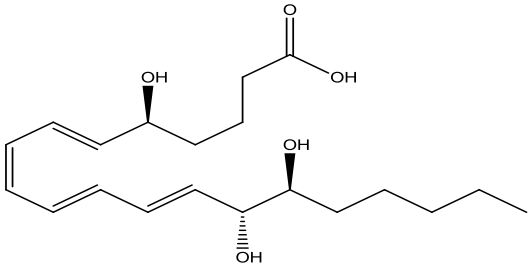 |

**Figure 1.10. Chemical structures of products from the lipoxygenase cascade**

Chemical structure of the primary LOX products

As mentioned previously, macrophage infiltration occurs in the obese state, and 12-LOX is highly expressed in macrophages. Its products have been shown to increase IL-6 and MCP-1 gene expression of cultured macrophages (Wen *et al*., 2007). Similarly, the addition of 12/15-LO products to cultured macrophages caused upregulation of TNF-α and MCP-1 gene expression in a previous study (Wen *et al*., 2008).

When directly added to 3T3-L1 adipocytes, the 12/15-LO products also up-regulated the gene expression of several cytokines, such as TNF-α, IL-6 and MCP-1, as well as down-regulating the gene expression of adiponectin (Chakrabarti *et al*., 2009). The gene expression of 5-LO has been shown to be greater in the macrophage containing SVF than in adipocytes (Chakrabarti *et al*., 2009).

As well as a role in inflammation, the 12/15-LO products may also be involved in insulin resistance, as 12/15-LO deletion in mice fed on a high-fat diet has been shown to improve glucose metabolism (Chakrabarti *et al*., 2009). Also, 12-HETE (product of 12-LO) administration in 3T3-L1 adipocytes increases JNK-1 activation, which is known to reduce insulin signalling (Okamoto *et al*., 2005). Therefore, 5-, 12- 12/15-LO may all be involved in the activation of the inflammatory response, as well as insulin signalling impairment within adipocytes.

### 1.4.3. The epoxygenase cascade

The epoxygenase pathway produces epoxyeicosatrienoic acids (EETs) from AA via cytochrome P450 (CYP) epoxygenases. The epoxygenase inserts molecular oxygen into arachidonic acid on a double bond and this double bond reduces as the epoxide forms. Epoxidation of arachidonic acid leads to four EET regioisomers which are termed 5,6-; 8,9-; 11,12- and 14,15-EET by the CYP2C and CYP2J epoxygenase enzymes (Wu *et al*., 1996). The EETs can then be hydrolysed to their corresponding dihydroxyeicosatrienoic acid (DHET) metabolites by soluble epoxide hydrolase (sEH), and these are less biologically active than EETs (Fang *et al*., 2001).

#### *1.4.3.1. Function of EETs*

One group of products of the epoxygenase cascade are the EETs, and these have effects within the vascular and renal systems (Fitzpatrick and Murphy, 1989; McGiff, 1991; Harder *et al*., 1995). Deletion of sEH has been shown to decrease blood pressure in mice (Sinal *et al*., 2000), and treatment with a sEH inhibitor has also been shown to decrease blood pressure in hypertensive rats (Yu *et al*., 2000). These EET products also have anti-inflammatory effects in the endothelium (Node *et al*., 1999), and can stimulate angiogenesis (Munzenmaier and Harder, 2000; Medhora *et al*., 2003) and prevent arterial smooth muscle migration (Sun *et al*., 2002).

#### *1.4.3.2. Function of EETs in WAT*

The EETs are thought to reduce adipocyte dysfunction (Inceoglu *et al*., 2007; De Taeye *et al*., 2010) because they can down-regulate the 2-LO and 5-LO pathways, resulting in synergism with NSAIDs and aspirin to decrease the concentration of inflammatory eicosanoids (Schmelzeret *et al*., 2006). These eicosanoids are degraded by sEH into the less active DHETs and sEH activity increases during adipocyte maturation (De Taeye *et al*., 2010), thereby decreasing the concentration of the anti-inflammatory EETs, leading to tissue inflammation. The concentration of sEH has been shown to be increased by PPARα agonists in rodents (Hammock *et al*., 1983) and PPARγ agonists can induce the activity of this enzyme in adipose tissue (De Taeye *et al*., 2010). De Taeye and colleagues also demonstrated that the gene expression and secretion of sEH did not differ in mice when fed either a normal or high-fat diet, although sEH activity was increased in the adipose tissue of obese mice (De Taeye *et al*., 2010). Therefore sEH appears to be involved in inflammation, obesity and its related comorbidities. In subjects with T2DM, single nucleotide polymorphisms in the gene that encodes sEH can lead to a greater risk of cardiovascular disease (Lee *et al*., 2006), insulin resistance (Ohtoshi *et al*., 2005) and hypertension (Burdon *et al*., 2008). Anti-inflammatory agents including the NSAIDS and aspirin appear to reduce the severity of the metabolic syndrome (van Kerckkhoven *et al*., 2000; Yuan *et al*., 2001; Renna *et al*., 2009).

### 1.5. LIPIDOMICS

The major challenge of the post-genomic era has been the global analysis of biomolecules such as proteins, lipids and carbohydrates within a cell, tissue or organism. Various strategies have evolved to aid in this research, including transcriptomics approaches to study all mRNA species present at a particular time and/or set of conditions, and proteomics techniques to monitor changes in protein expression, as well as investigate post-translational modifications. A relatively new tool is the use of metabolomics analyses, used to examine low molecular weight metabolites and observe any changes occurring in set environmental conditions (Fiehn *et al*., 2001). These metabolic profiling techniques provide a 'snapshot' of the biochemical status of a system at any one time (Hellerstein, 2003). Metabolomics has advantages over both transcriptomics and proteomics. The metabolome is further downstream than both the proteome and the transcriptome, meaning that it is more closely related to the phenotype of the cell (Barsch *et al*., 2004). Also, the metabolite profile displays any changes before they are seen in the proteome or genome, thereby making it useful in monitoring a biological response to any environmental changes (Davis and Hord, 2005).

Lipidomics is a subset of metabolomics, and this term can be used to describe the emerging field of systems-level analysis of lipids and factors that interact with them (Han and Gross, 2003; Lagarde *et al*., 2003). Initial studies in the field of lipidomics involved the use of mass spectrometry, and led to the observation of chemical properties common to lipid species (Han and Gross, 2003). Some accepted definitions commonly used in both the metabolomics and lipidomic fields are given in Table 1.5; however, variations in these definitions exist.

Two main types of lipidomic analyses exist, and they are 'global' and 'targeted', and both allow different areas of the lipidome to be analysed, as shown in Figure 1.11. Global lipidomics maps the entire spectrum of lipids and lipid molecular species in a biological system. Targeted lipidomics, on the other hand, quantifies a single, or multiple selected species. Interest in lipidomics has been driven by the wide and diverse role of lipid species in the cell (Roberts *et al*., 2008), technological advances, and the recent recognition of the role of lipids in many metabolic diseases (Gross and Han, 2007).

**Table 1.5. Lipidomic and metabolomic definitions**

| TERM | DEFINITION | REFERENCE |
|---|---|---|
| Metabolomics | The identification and quantification of all metabolites in a given biological sample | Weckwerth and Fiehn, 2002 |
| Metabonomics | The time-related multiparametric metabolic response of living systems to pathophysiological stimuli or genetic modification | Nicholson *et al*., 1999 |
| Metabolome | The metabolic composition of a cell; analogous to the genome or proteome | Lindon *et al*., 2003 |
| Lipidomics | The full characterisation of lipid molecular species and of their biological roles with respect to expression of proteins involved in lipid metabolism and function, including gene regulation | Spener *et al*., 2003 |
| Lipidome | The entire spectrum of lipids in a biological system | Seppanen-Laakso and Oresic, 2009 |

### 1.5.1. Current experimental strategies

The predominant approach for lipidomic analysis is the use of mass spectrometry (MS) techniques. These are advantageous in that they are extremely sensitive and selective, and can be used for quantitative analysis if internal standards are added to the sample mixture. The major disadvantages of MS techniques are that the majority of biological samples have to undergo extensive preparation prior to analysis, and also if a chromatography system is coupled to an MS, analysis times are increased (Dunn *et al*., 2005a and 2005b; Scalbert *et al*., 2009). Chromatography itself is a lipidomic experimental strategy which has been well adapted for the analysis of various lipid classes. Many approaches exist including thin layer chromatography (TLC), liquid chromatography (LC) and gas chromatography (GC). Various combinations of chromatography systems coupled to mass spectrometers exist, and are used in the field of lipidomics. In the current study, global lipidomic profiling methods were achieved using LC coupled to an orbitrap MS; and targeted techniques involved the use of an LC system coupled to a triple quadruple MS. Both systems are described in Section 2.9.

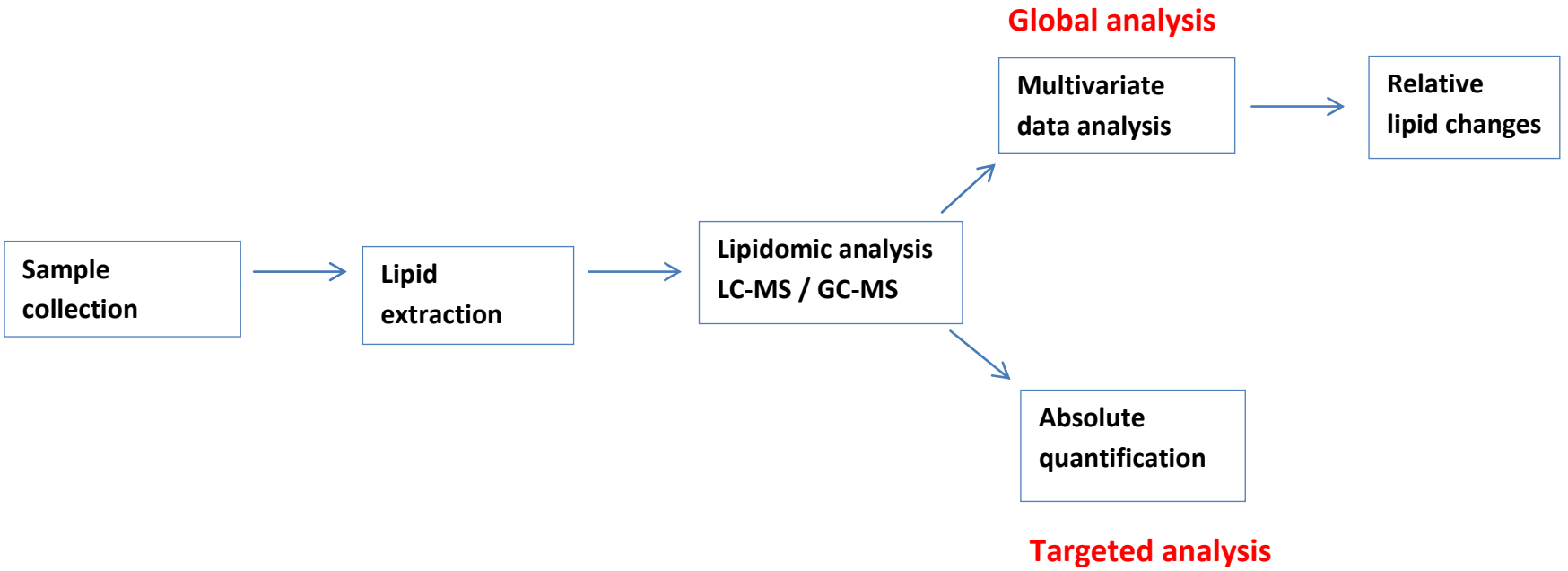


**Figure 1.11. Schematic representation of a lipidomic work flow**
Global analysis allows the whole lipidome to be profiled, although only relative changes can be observed. Absolute quantification is achieved with targeted approaches, in which a selected lipid species is extracted and analysed. Abbreviations used: GC-MS, gas chromatography-mass spectrometry; LC-MS, liquid chromatography-mass spectrometry.

Many recent lipidomic techniques have evolved, one example involves fluorescently tagging lipids to study various functions including trafficking and partitioning into specialised sub-cellular compartments and membrane domains (Mukherjee and Maxfield, 2000), and also the transbilayer movement of lipids (Kol *et al*., 2004).

### 1.6. APPLICATIONS OF LIPIDOMIC TECHNIQUES

The main advantage of lipidomic techniques is that lipid profiles produced from cells, tissues or body fluids provide a global snapshot of the lipids present in a sample, meaning that effects of environmental changes can be directly investigated. Therefore, a major application for lipidomic techniques is the identification of biomarkers in lipid related diseases. Lipidomic techniques have been previously used in the discovery of potential biomarkers in metabolic diseases such as obesity (Yetukuri *et al*., 2007; Kolak *et al*., 2007), T2DM (Han *et al*., 2007), cardiovascular disease (Brindle *et al*., 2002) and various cancers (Tung *et al*., 2008). Breast cancer is the most frequently diagnosed amongst women, and a previous study has suggested that lysophospholipids are potential biomarkers in the bloodstream (Murph *et al*., 2007). Lipidomic methods have also been applied to rat and mouse models, including Kyoto and Wistar rats of fatty liver disease (Griffin *et al*., 2007), APOE*3 Leiden transgenic mice of atherosclerosis and liver inflammation (Kleemann *et al*., 2007) and purebred male wild-type C57bl6 mice of starvation-induced hepatic steatosis (van Ginneken *et al*., 2007). These studies have uncovered a variety of lipid biomarkers by comparisons of the lipid profiles between control and diseased animals.

Another application of lipidomic techniques is in the identification of metabolic pathways and enzymes. This involves analysis of paired samples, followed by differential analysis (Forrester *et al*., 2004), including multivariate data analysis, and metabolic control analysis (Cascante *et al*., 2002). Many genetic disturbances in model animals do not cause the expected phenotype, and so inspection of lipid metabolites may help to identify the underlying metabolic pathways involved in such cases (Weckwerth *et al*., 2004).

The identification of new lipid-binding proteins may provide new opportunities in drug design and development. The previous discovery of cannabinoid receptors caused the discovery of a potent ligand for the CB1 cannabinoid receptor (Devane *et al*., 1992). As well as drug development, lipidomics may also aid in drug delivery and response.

### 1.6.1. Lipidomic analyses of adipocytes, adipose tissue, and obesity

Lipidomics-based analyses have been widely used to investigate many areas of adipocyte metabolism. Due to the fact that obesity is associated with increased adiposity, and that this can be caused by either hyperplasia of existing adipocytes, or the differentiation of pre-adipocytes; the process of adipogenesis has been investigated by various previous studies in terms of lipid metabolism. One such study use lipidomic methodologies to explore the lipid metabolism of 3T3-L1 cells during the differentiation process, and demonstrated that odd-chain fatty acids including TG and phospholipid species accumulated during adipogenesis (Su *et al*., 2004). More recently, a more complete study also explored the effects of differentiation on lipid metabolism of 3T3-L1 cells. Changes in metabolite concentrations during various stages of the differentiation process were investigated, and various mechanisms were demonstrated as implicit to the maturation of these cells, including glycolysis, and the oxidation, synthesis, and desaturation of fatty acids, among others (Roberts *et al*., 2009).

Lipidomic analyses of serum samples from human patients and animal models can be useful when exploring possible lipid profile changes between control and diseased states. A previous study used monozygotic twins to determine whether acquired obesity is associated with changes in serum lipid profiles (Pietilainen *et al*., 2007). Obesity was found to be related to an increase in the concentration of lysophosphatidylcholines, and a decrease in that of other phospholipid species known to have antioxidant properties.

A recent development in adipose tissue metabolism investigations was the discovery of a 'lipokine', first used in 2008 to describe FAs that modulate lipid metabolism via a chaperone effect (Cao *et al*., 2008). This study focused on mice deficient in the adipose tissue chaperones aP2 and mal1 (FABP4 and FABP5, respectively). Deficiency of both affects systemic metabolic regulation, and causes the mice to become resistant to all components of the metabolic syndrome (Maeda *et al*., 2005). Lipidomic analyses of these mice found increased *de novo* lipogenesis, creating adipose tissue resistance to the effects of dietary lipid exposure. The identification of an adipose tissue-derived lipid hormone led to the term lipokine, and it was C16:1n7-palmitoleate. This hormone stimulates insulin action of the muscle, and suppresses hepatosteatosis, allowing the authors to conclude that adipose tissue uses lipokines to regulate systemic metabolic homeostasis via communication with other organs (Cao *et al*., 2008).

### 1.7. AIMS OF THE THESIS

WAT is a complex secretory and endocrine organ with extensive roles in regulating appetite and energy homeostasis. Obesity and its associated diseases are linked to adipocyte dysfunction, reflected by altered gene expression, and concentrations of various lipid species. The work presented in this thesis focuses on characterising adipokine metabolism using the 3T3-L1 pre-adipocyte cell line, in terms of gene expression and the lipidome. The overall purpose was to explore the effects of differentiation, as well as the addition of various inflammatory and anti-inflammatory agents on gene expression and both global and targeted lipidomic profiles of adipoytes.

The first specific aim of the thesis was to biochemically characterise the course of differentiation using the 3T3-L1 cell line from pre-adipocyte to fully mature adipocyte. A change in the gene expression profile was predicted, with the differentiation markers leptin and adiponectin only being expressed once the differentiation process had begun. It was also predicted that a shift in the abundant lipids present would occur. As adipocytes mature, lipid accumulation is evident, and so it was predicted that the abundance of triglyceride species would increase as the adipocytes continue to mature. Once gene expression and lipidomic profiles of differentiation were established, these baseline data would act as a reference for the future aims.

The second aim was to monitor the response of these baseline cells to the inflammatory mediators TNF-α and IL-6. Obesity is linked to adipocyte dysfunction, and so it was predicted that treatment with these agents would cause both the gene expression and lipidomic profiles to differ between the control and treated cells. More specifically, the targeted lipid analysis focussed on eicosanoid synthesis, and so it was further predicted that members of this lipid species would increase with inflammatory agents, due to their role in various inflammatory conditions.

The final aim was to look at the effect of the anti-inflammatory agent dexamethasone on the metabolism on baseline adipocytes. Glucocorticoids have both lipolytic and adipogenic actions, as well as being potent anti-inflammatory agents. It was predicted that changes would be observed between the control and treated cells, although specific changes were not hypothesised due to the multiple functions of dexamethasone, and so this final aim was exploratory.

# CHAPTER 2:

## Materials and methods

## 2.1. 3T3-L1 ADIPOCYTE CELL CULTURE

Aseptic technique was essential for the prevention of infection. All work was carried out in a category II biological safety cabinet, which had been cleaned with 1% (w,v) Virkon, followed by 70% (v,v) ethanol, and everything placed into the cell culture hood was sprayed with 70% (v,v) ethanol. All media were prepared within this sterile environment and filtered through a 0.22µm filter membrane (Helena Biosciences / TPP, Tyne and Wear, UK). Excess culture medium was kept for a maximum of one week at 4$^{o}$C and preheated at 37$^{o}$C in a water bath before use. Both induction and feeding media were freshly made before use.

### 2.1.1. Reagents and suppliers

3T3-L1 pre-adipocytes, along with 1 x Dulbecco's Modified Eagle Medium (DMEM) and Calf Serum (CS) were all obtained from LGC standards (Middlesex, UK). Dexamethasone, Insulin, 3-Isobutyl-1-methylxanthine (IBMX), TRI Reagent® and trypsin/ethylenediaminetetraacetic acid (EDTA) were all purchased from Sigma-Aldrich Chemical Company (Dorset, UK). Isotonic phosphate buffered saline (PBS; pH 7.2) was from PAA Laboratories Ltd (Somerset, UK). Virkon was from Antec International Ltd (Suffolk, UK) and the ethanol used to clean the cell culture hood was obtained from Fisher Scientific (Leicestershire, UK).

#### *2.1.1.1. Medium components*

Culture medium: 1 x DMEM; 10% (v,v) CS.

Induction medium: 1 x DMEM; 10% (v,v) CS; 5µg/mL Insulin; 0.25mM dexamethasone; 0.5mM IBMX.

Both dexamethasone and IBMX stock solutions were made in 95% (v,v) ethanol, and aliquots stored at -20$^{o}$C.

Feeding medium (post-differentiation): 1 x DMEM; 10% (v,v) CS; 5µg/mL Insulin

### 2.1.2. Cell culture and maintenance

3T3-L1 cells were immediately cultured at 37$^{o}$C according to the manufacturer's protocol in an incubator with a humidified atmosphere of 5% $CO_2$/95% air. Extra frozen cell aliquots were stored at -150$^{o}$C. If cultured from frozen, the vial was removed from -150$^{o}$C storage, and thawed in a water bath set to 37$^{o}$C. The defrosting process was helped by the addition of 1mL of pre-warmed culture medium, which was gently pipetted up and down inside the cell vial. This thawed aliquot was then added to a 25mL Universal vial containing 9mL of culture medium. The cells were then centrifuged at 125 x *g* for 5 minutes (min) using a Heraeus Biofuge Pimo R (Thermo Scientific, Hemel Hempstead, UK). The supernatant was removed, and a further 1mL of culture medium was added, and pipetted up and down to break up the cell pellet. The cells were then transferred into a 25cm$^3$ flask containing 3mL of culture medium, and placed in the incubator. The medium was replaced every 48 hours (h) for as long as necessary, to ensure the survival of the cells.

#### *2.1.2.1. Cell passaging*

Greater cell numbers were generated by splitting the original 25cm$^3$ flask into four extra flasks when the cells in the original flask were approximately 70% confluent. The medium was removed, and 3mL trypsin/EDTA added to the flask. The flask was then placed in the incubator for between 1 and 2 min, to allow the detachment of cells, confirmed by microscopy. Once the cells had detached from the flask surface, 1mL of CS was added to deactivate the trypsin. The cell suspension was gently pipetted up and down to break up any clumps, and then transferred to a 25mL Universal. Four flasks containing 3mL culture medium each received 1mL of cells, and were then placed back into the incubator.

#### *2.1.2.2. Cell plating*

The cells were trypsinised as described in Section 2.1.3.1, and the cell suspension from each flask was transferred into a single universal. The required number of plates were set up with 1mL culture medium in each well, and 50µL of cells were added per well.

#### *2.1.2.3. Cell differentiation*

Once the cells had been plated out into 12-well plates, they were left to reach confluence, supported by fresh culture medium every 48h. Two days after confluence had been observed by microscopy (Leica DM IL LED inverted microscope, Leica Microsystems Ltd,

Bucks, UK), the cells were induced to differentiate by replacing the culture medium with 1mL of differentiation medium per well. The cells were kept in this medium for 72h, which was then replaced with feeding medium for a further 48h. From day 5 post-differentiation up to 24h before the cells were treated and/or harvested, they were fed with culture medium which was replaced every 48h. Differentiation into adipocytes was confirmed by the accumulation of lipid droplets.

#### *2.1.2.4. Cell and medium collection for polymerase chain reaction analysis*

The medium from each well was removed and collected into individual sterile 2mL RNase-free tubes. The cells were removed from each well by the addition of 1mL of TRI Reagent®, which was used to wash the cells to ensure removal of the maximum number of cells. The cells from each well were transferred into individual 2mL sterile RNase tubes. Both the cells and medium were stored at -80$^{o}$C until required.

#### *2.1.2.5. Cell and medium collection for lipidomic analysis*

As described in Section 2.1.2.4, the medium from each well was collected into individual sterile 2mL RNase-free tubes. Each well was then washed three times with PBS, and after the final wash, 125µL of sterile water was added to each well. A cell scraper was used to remove the cells from the bottom of each well. Two wells were combined into a sterile 0.5mL centrifuge tube, resulting in six tubes per plate, each containing 250µL of the cell suspension. Both cells and media were stored at -80$^{o}$C until required.

### 2.2. OIL RED O STAINING

Oil Red O staining is a technique used for staining neutral lipids (Lillie and Ashburn, 1943). The dye stains triglycerides red, and a counter stain of haematoxylin is used to stain the nucleus of the cell blue.

#### 2.2.1. Reagents and suppliers

1 x isotonic PBS (pH 7.2) was purchased from PAA Laboratories Ltd, and 10% Formalin was from ReAgent (Cheshire, UK). Oil Red O and Haematoxylin stains were both obtained from Sigma-Aldrich Chemical Company, and were filtered through a 0.22µm filter (Helena Biosciences / TPP, Tyne and Wear, UK) prior to use to remove any debris.

### 2.2.2. Method

After removal of medium, cells were washed twice with 1xPBS and fixed by adding 1mL of 10% (v,v) formalin solution to each well for 30 min at room temperature. The washing step was then repeated, and 1mL of Oil Red O stain was added per well, which stains the lipids. The cells were incubated on a shaking platform (Orbital shaker SSM1, Stuart, Staffordshire, UK) for 1h at room temperature. Once stained, each well was washed five times with cold water, and 1mL of haematoxylin stain was added to stain the nuclei. The plate was returned to the shaking platform for a further 5 min at room temperature, and then washed five times with hot water, and 1mL water was added. Images were captured using a Leica DM IL LED inverted microscope (Leica Microsystems).

## 2.3. TOTAL RNA EXTRACTION FROM 3T3-L1 ADIPOCYTES

### 2.3.1. Reagents and suppliers

Chloroform (HPLC grade) and Isopropanol (LC-MS grade) were obtained from Fisher Scientific. 100% molecular biology grade ethanol was from VWR (Poole, UK).

### 2.3.2. RNA extraction method

Frozen cell aliquots were thawed, and pipetted up and down inside the tube to break up clumps of cells. Once thawed, 500µL of the cell and TRI Reagent® mixture was removed into a separate centrifuge tube. The cells were pulled through a 23 gauge needle five times, and the needle was changed between different groups of cells. The samples were incubated for 5 min at room temperature, before the addition of 100µL of chloroform, and were then vigorously shaken for 15 seconds (sec). The samples were incubated at room temperature for 10 min, and then centrifuged at 20,800 x *g* 10 min at 4°C (Legend X1R, Thermo Scientific). This created three phases, a bottom red phenol phase containing protein, a white DNA interphase, and an upper colourless aqueous phase containing RNA. The upper RNA phase was transferred to a new centrifuge tube, and 35µL isopropanol was added to remove any genomic DNA which may have also been transferred. The samples were vortexed, left to stand at room temperature for 10 min, and then centrifuged at 20,800 x *g* for 10 min at 4°C. The supernatant was removed into a new tube, with the addition of 225µL isopropanol to precipitate out the RNA. The samples were once again vortexed, incubated at room temperature for 10 min, and centrifuged at 20,800 x *g* for 10 min at 4°C to produce an RNA pellet. The supernatant was carefully discarded to avoid disturbing the pellet, and 100µL of 75% (v,v) ethanol was added. The

samples were centrifuged at 20,800 x *g* for 10 min at 4°C for the final time, and the supernatant removed. The pellet was allowed to air dry for 5-10 min, and then dissolved in 20µL of autoclaved water. If the RNA samples were not being used for PCR straight away, they were stored at -80°C until required.

### 2.3.3. RNA quantification

Nucleic acids have maximal light absorbance at A260, and proteins at A280. The ratio between A260 and A280 gives an indication of the RNA purity in the sample. The optimal ratio is between 1.8 and 2.0, which indicates RNA of high purity. A ratio of 1.6 or less suggests protein contamination (increased absorbance at A280), whereas a ratio above 2.0 is indicative of genomic DNA contamination. The RNA concentration per sample was calculated automatically by the spectrophotometer using the Beer-Lambert law, (Swinehart, 1962; Ricci *et al*., 1994):

[RNA] µg/µL = A260 x extinction coefficient x dilution factor

The extinction coefficient for RNA is approximately 40, and the samples were tested undiluted. Therefore, the equation becomes: [RNA] µg/mL = A260 x 40

The RNA samples were quantified using a NanoDrop Spectrophotometer ND-1000 (Fisher Scientific). The sensor was first cleaned using 1µL distilled water, and then 1µL of sample was added. The RNA-40 programme was selected, and absorbance was measured at 260nm (A260) and 280nm (A280), with distilled water used as a blank. The RNA concentration was automatically calculated.

## 2.4. REVERSE TRANSCRIPTION

The purpose of reverse transcription is to produce single stranded DNA which is complimentary to a given mRNA template sequence (complimentary DNA; cDNA). A premix of anchored oligo-dT and random primers were used. Anchored oligo-dT primers are specifically designed to anneal at the mRNA/poly-A junction, to produce higher quality cDNA and improve the efficacy of PCR and real-time PCR for genes that are not highly expressed. Standard dT and random primers are less specific as they anneal randomly within the poly-(A) tail, or at a random point along the mRNA sequence respectively.

### 2.4.1. Reagents

Reverse transcription was completed by using an iScript cDNA synthesis kit from Bio-Rad Laboratories Ltd (Hemel Hempstead, UK), which contained the following:

(i) RNase $H^+$ iScript reverse transcriptase

(ii) Premix of RNase inhibitor and blend of oligo dT and random primers

(iii) Nuclease-free water

### 2.4.2. Method

This procedure was carried out using sterile RNase/DNase–free tubes and filter tips. All incubations were performed using a GeneAmp PCR system 2700 (Applied Biosystems, Cheshire, UK) and the manufacturer's instructions were modified. For a 10µL reaction, 0.5 µg of RNA, 2µL of 5xbuffer and 0.5µL of reverse transcriptase were added to a 0.5mL tube. This was made up to 10µL with 7.5µL nuclease-free water and vortexed. The samples were then incubated at 25$^{o}$C for 5 min to allow the primers to anneal to the RNA. This was followed by 30 min incubation at 42$^{o}$C to synthesise the cDNA and a final stage at 85$^{o}$C for 5 min to terminate the reaction. The samples were then immediately used for PCR, or stored at -80$^{o}$C.

## 2.5. Polymerase Chain Reaction

Polymerase chain reaction (PCR) was discovered by Kary Mullis (Saiki *et al*., 1985) and amplifies the cDNA of interest with the use of gene-specific primers and DNA polymerase. The process starts with a denaturation phase by incubating at 94$^{o}$C, and is followed by 20 to 40 amplification cycles. Each cycle doubles the amount of DNA synthesised from the previous cycle, and consists of three stages; denaturation, annealing and extension. Denaturation reduces the DNA double helix by dissociating the double-stranded DNA (dsDNA) into single stranded DNA (ssDNA), making the strands accessible to the primers. The annealing step enables the primers to hybridise to their complementary bases on the DNA template strand. The annealing temperature ($T_a$) is primer specific and depends on factors such as primer length. During the final extension phase, the DNA polymerase synthesises a complementary DNA strand in a 5'-3' direction, starting from the primer annealing site.

When assessing RNA expression of the gene of interest, it is compared to that of a constitutive gene that is transcribed at a constant concentration. These are termed housekeeping genes and are expressed by all cells of an organism (Butte *et al.,* 2001). Typical housekeeping genes include β-actin, glyceraldehyde-3-phosphate (GAPDH), 18S rRNA and RNA polymerase IIa (RNA pol 2). In this study, β-actin was used as the housekeeping gene for reverse-transcription PCR (RT-PCR); and three housekeeping genes, β-actin, GAPDH and RNA pol 2 were used for real time-PCR (qPCR).

### 2.5.1. Reagents and suppliers

A ReddyMix PCR Master Mix Kit: 1.1x ReddyMix was obtained from ABgene (Epsom, UK), and the sense (s) and anti-sense (as) primer mixes used (10µM) were from Eurogenetec (Hampshire, UK).

### 2.5.2. Method

This procedure was performed using sterile 0.2mL RNA/DNA-free tubes and filter tips. A master mix was prepared which contained 11.25µL of 1.1x ReddyMix, 0.25µL of primer mix and 0.5µL of ultra-pure water per sample. This master mix was vortexed, and 12µL was added to each tube, along with 0.5µL of the cDNA template, to make a final reaction volume of 12.5µL. For non-template controls (NTC), the cDNA template was replaced with ultra-pure water. After addition of all elements, the tubes were vortexed, centrifuged and then placed into the GeneAmp PCR system 2700 (Applied Biosystems) ready for the PCR reaction. A denaturation step starts the PCR program by incubating the samples at 94$^{o}$C for 2 min. This was followed by 20-35 cycles of the following:

1. 94$^{o}$C for 20 sec (denaturation)
2. 53-62$^{o}$C for 30 sec (annealing)
3. 72$^{o}$C for 30 sec (extension)

The cycle number and annealing temperature ($T_a$) is optimised for each primer pair (see Table 2.1). After the final cycle, the samples underwent a final elongation step at 72$^{o}$C for 5 min.

**Table 2.1 Sequences of the RT-PCR primers and PCR conditions**

| GENE | PRIMER SEQUENCE 5'-3' | $T_a$ (°C) | CYCLE NUMBER | PRODUCT SIZE (bp) |
|---|---|---|---|---|
| ***β-actin*** s<br>***β-actin*** as | TGCTGTCCCTGTATGCCTCT<br>AGGTCTTTACGGATGTCAACG | 60 | 23 | 463 |
| ***Leptin*** s<br>***Leptin*** as | CTGTCTTATGTTCAAGCAGTGCCTAT<br>AAGCCACCACCTCTGTGGAGTA | 62 | 34 | 394 |
| ***Adiponectin*** s<br>***Adiponectin*** as | TTAATCCTGCCCAGTCATGCCG<br>AGAACTTGCCAGTGCTGCCGTC | 62 | 34 | 430 |

*Primer sequences taken from (Dutton and Trayhurn, 2008).*

### 2.5.3. Agarose gel electrophoresis

The PCR products were identified on a 1.5% (w,v) agarose gel stained with ethidium bromide (EtBr). This binds strongly to DNA by intercalating between the bases and is fluorescent.

#### *2.5.3.1. Reagents*

The agarose used was obtained from Prepro Tech EC (London, UK), and EtBr at 5mg/mL was from Sigma-Aldrich Chemical Company. 1x Tris Borate-EDTA (TBE) buffer and the GeneRuler™ 100 bp DNA ladder (Fermentas) were from Fisher Scientific.

#### *2.5.3.2. Method*

An appropriately-sized gel casting tray was prepared by sealing both ends with autoclave tape. The agarose was weighed and placed into a 500mL conical flask containing 1x TBE and heated in a microwave, mixing occasionally, until the agarose had completely melted. Once cool, the EtBr was added and mixed, and the mixture was poured into the casting tray. The combs were placed in their slots, after being used to push any bubbles to the edges and the gel was left to set for at least 30 min. Once set, the combs and autoclave tape were removed and the gel was placed into the electrophoresis tank. The gel was completely submerged by adding 1x TBE to the tank, and then loaded with 10µL of PCR product and 2µL of the 100bp ladder in separate wells. The loaded gel was run at 105 V for 20-30 min or until the samples were at least halfway down the gel. Bands were

identified using a UV Transilluminator (2011 Macrovue™, Ultra-Violet products). The images were captured with a DC120 digital camera (Kodak) and analysed using digital Science ID 1 image analysis software (Kodak).

### 2.6. Real-time Polymerase Chain Reaction

The concentration of mRNA within a sample can be quantified using qPCR. During the reaction, fluorescence is emitted, which represents the formation of product during each PCR cycle. The fluorescence signal is directly proportional to the amount of PCR product produced, and there is an increase during the exponential phase. The earlier the fluorescence signal begins its exponential rise, the more initial template present in the sample.

#### 2.6.1. TaqMan® system

The qPCR work completed in this thesis was carried out using the TaqMan® system, which amplifies the mRNA of interest, and was first reported in 1991 (Holland *et al*., 1991). The method involves the use of two primers (forward and reverse), and a TaqMan® probe. The probe is composed of a short oligodeoxynucleotide which is labelled with two different fluorescent dyes. The 5' base has the reporter dye (FAM-6- carboxyfluorescein), and the 3' base has the quenching dye (TAMRA – 6 carboxytetrametheyrhodamine). The probe is homologous to a target sequence in the PCR amplicon, and is able to bind to it. When the probe is intact, the reporter dye is unable to emit fluorescence due to the proximity of the quencher, and energy is transferred between the two, based on the fluorescence resonance energy transfer (FRET) principle (Cardullo *et al*., 1988). The probe cleaves during the extension phase of PCR by 5' nuclease activity of Taq polymerase. This separates the reporter from the quencher dye, which ends the FRET, and allows the reporter dye to emit fluorescence (at 518nm for FAM). The amount of fluorescence increases with each cycle of PCR, and is proportional to the rate of probe cleavage. A camera within the qPCR machine measures the fluorescence spectrum and intensity, which is caused by exciting each well with a laser light source. This occurs during each PCR cycle, to generate real-time data. The increase in fluorescence (ΔR) is detected by monitoring the accumulation of PCR product (Bustin, 2002; Ayra *et al*., 2005). The reporter dye signal is normalised to a reference dye (ROX) and plotted as $\Delta R_N$. The reference dye is used to correct for differences in reaction mix volumes between wells. The principle of the TaqMan® assay is illustrated in Figure 2.1.

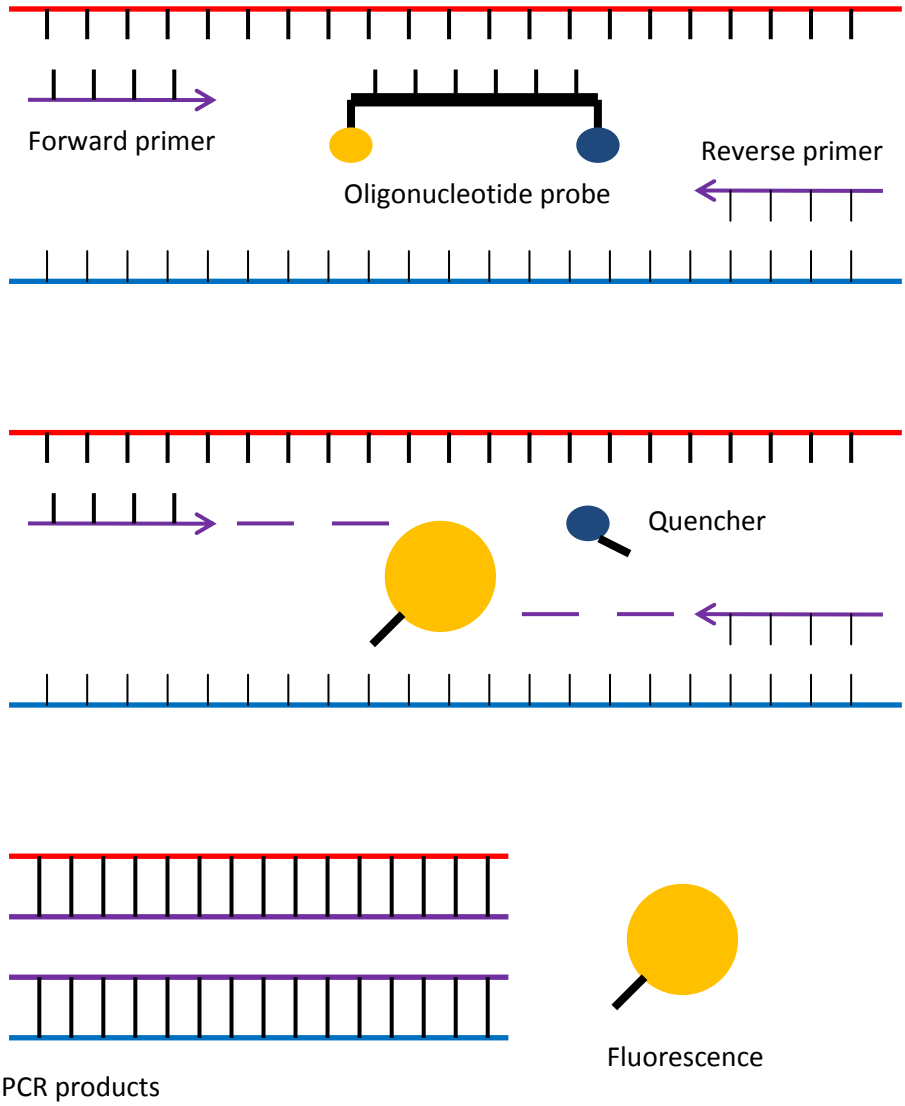


**Figure 2.1 Principle of TaqMan® assay**

This figure illustrates what happens at each TaqMan® cycle. A specific probe oligionucleotide is used which has a reporter dye (FAM) at the 5' end, and a quenching dye (TAMRA) at the 3' end. The probe anneals to its target sequence and product is amplified 5' to 3'. During this polymerisation step, the exonuclease activity of the polymerase cleaves the probe, which separates the reporter and quencher dyes, ending FRET. This allows fluorescence emission from the reporter dye to occur. The amount of fluorescence increases with each cycle of PCR, and is proportional to the rate of probe cleavage.

### 2.6.2. Preparation of a 96 well plate for real-time PCR

#### *2.6.2.1. Reagents*

A qPCR Core Kit was obtained from Eurogentec, which included: 10 x reaction buffer; 50mM magnesium chloride; 5mM dNTP mix and 5U/µL Hot Goldstar enzyme. The sense and anti-sense primers, as well as the TaqMan® probes used were also from Eurogentec.

#### *2.6.2.2. Method*

A master mix was prepared for each gene of interest, using the following components and amounts per well, as follows:

| | |
|---|---|
| 10 x reaction buffer | 1.25µL |
| 50mM magnesium chloride | 1.25µL |
| 5mM dNTP mix | 0.5µL |
| Sense primer | 0.038µL |
| Antisense primer | 0.038µL |
| TaqMan® probe | 0.063µL |
| 5U/µl Hot Goldstar enzyme | 0.0625µL |
| Ultra-pure water | 8.2985µL |

Each well of the 96 well plate received 11.5µL of the master mix. The addition of 1µL of the selected cDNA to each well completed the plate which was then sealed with an adhesive optical cover. All samples were run six times and NTCs, in which the cDNA was replaced with ultra-pure water, for each primer and probe set were also included. The plate was centrifuged using a plate spinner (BR3.11, Jouan; Thermo Scientific) for 1 min to remove bubbles and ensure that the reaction mixture was at the bottom of the well. The sequences and conditions of both the sense and antisense primers used, as well as the TaqMan® probes are detailed in Table 2.2.

**Table 2.2. Sequences and conditions of the primers and TaqMan® probes used qPCR analyses**

| GENE | PRIMER SEQUENCE 5'-3' | CONCENTRATION (nm) | PRODUCT SIZE (bp) |
|---|---|---|---|
| ***β-actin*** s | ACGGCCAGGTCATCACTATTG | 300 | 97 |
| ***β-actin*** as | CAAGAAGGAAGGCTGGAAAAG | 300 | |
| ***β-actin*** p | ACGAGCGGTTCCGATGCCCTG | 100 | |
| ***Leptin*** s | CATCTGCTGGCCTTCTCCAA | 300 | 76 |
| ***Leptin*** as | ATCCAGGCTCTCTGGCTTCTG | 300 | |
| ***Leptin*** p | AGCTGCTCCCTGCCTCAGACCAGTG | 100 | |
| ***Adiponectin*** s | GGCTCTGTGCTCCTCCATCT | 300 | 97 |
| ***Adiponectin*** as | AGAGTCGTTGACGTTATCTGCATAG | 300 | |
| ***Adiponectin*** p | CCCATACACCTGGAGCCAGACTTGGT | 100 | |
| ***IL-6*** s | ACAACCACGGCCTTCCCTACTT | 300 | 76 |
| ***IL-6*** as | CACGATTTCCCAGAGAACATGTG | 300 | |
| ***IL-6*** p | TTCACAGAGGATACCACTCCCAACAGAACCT | 100 | |
| ***TNF-α*** s | CCCAGACCCTCACACTCAGATC | 300 | 78 |
| ***TNF-α*** as | GCCACTCCAGCTGCTCCTC | 300 | |
| ***TNF-α*** p | TAGCCCACGTCGTAGCAAACCACCAAG | 100 | |

### 2.6.3. TaqMan® system real-time PCR setup

All reactions were performed on a StepOnePlus Real-Time PCR system (Applied Biosystems, Cheshire, UK). The plate was inserted into the heat block, and the cover locked into position. The reporter dye was selected as FAM and the reference dye as ROX. Amplifications started with a denaturation step by incubating at 95°C for 10 min. This was followed by 40 cycles consisting of:

(i) 95˚C for 15 sec (denaturation)
(ii) 60˚C for 60 sec (combined primer annealing and extension)

The total run time was approximately 2h. Data were automatically collected by the software and analysed once the run had completed.

### 2.6.4. Analysis of real-time PCR data

The amplification plots were displayed in log scale and the threshold was automatically set with the StepOnePlus software (Applied Biosystems). The $C_T$ values were exported as a Microsoft Excel file and the gene expression was analysed by relative quantification using the 2-ΔΔCT method (Livak and Schmittgen, 2001). Two or three housekeeping genes were used as internal standards for all qPCR experiments. All samples were normalised to either β-actin, GAPDH or RNAPolIIa, and the results were expressed as fold changes of $C_T$ values relative to controls.

#### *2.6.4.1. Statistical data analysis of qPCR data*

For qPCR data, non-parametric statistical tests have been suggested to be more robust than parametric statistical tests, irrespective of normality (Yuan *et al*., 2006). Therefore, non-parametric test were used for the analysis of qPCR data in this study, even though the data were normally distributed. The data were presented as mean ± standard deviation (SD) and the specific test used is indicted in the data chapters, for a group size of six.

## 2.7. ENZYME-LINKED IMMUNOSORBENT ASSAY FOR LEPTIN AND ADIPONECTIN PROTEIN CONCENTRATION

The Enzyme-Linked Immunosorbent Assay (ELISA) technique was based on a previous method known as radioimmunosorbent techniques (RIST), in which a radioactively labelled antigen is coupled to cellulose, along with insolubilised antibodies. The binding of the labelled antigen is competitively inhibited by unlabelled antigen (Wide and Porath, 1966). Two research groups were simultaneously involved in the development of the ELISA method, both of which labelled the antigen with an enzyme, rather than an isotope. The first group (Engvall and Perlmann, 1971) used rabbit IgG as the antigen, and this was labelled with alkaline phosphatase. The 'immunosorbent' was formed by the attachment of anti-rabbit IgG antibodies to cellulose, and the enzyme-linked antigen and unknown antigen would be reacted with it. The unknown antigen is unlabelled and competes with labelled antigen. Therefore, the enzyme attached to the immunosorbant would reduce as more of the unknown antigen was added. The second group (van Weemen and Schuurs, 1971) described a similar assay. These original ELISAs were competitive assays.

Sandwich ELISAs were used in this study to quantify the concentration of leptin and adiponectin within cell medium samples. In this method, the surface of the ELISA plate is pre-coated with a polyclonal antibody which is specific to the protein of interest. Samples are then added to the desired wells on the plate, and any specific protein present in the samples is bound by the antibody. The plate is washed to remove any unbound antibody-enzyme reagent, and an enzyme-linked antibody, specific to the primary antibody, is added. The addition of a substrate solution causes a blue colouration, and this is changed to yellow after a stop solution is added to the wells. The intensity of this colour is directly related to the concentration of protein within the sample. A schematic representation of the sandwich ELISA principle is illustrated in Figure 2.2.

In the current study, concentrations of mouse leptin and adiponectin were measured in the medium using a Mouse Leptin or Adiponectin Immunoassay kit. The sensitivity of the kits were and 22pg/mL and 0.003ng/mL for leptin and adiponectin, respectively. Any concentration less than this this was considered to be non-detectable.

### 2.7.1. Reagents

All reagents were prepared according to the manufacturer's protocol (R&D systems, Abingdon, UK) and brought to room temperature before use. The kit reagents consisted of:

(i) Mouse leptin or adiponectin kit control

- Reconstituted with 1mL distilled water

(ii) Wash buffer

- For one plate add 25mL to 600mL distilled water

(iii) Substrate solution

(iv) Mouse leptin or adiponectin standard

- Reconstitute with 2mL calibrator diluent to produce a 4000pg/mL stock solution for leptin standard
- Reconstitute with 5mL calibrator diluent to produce a 10ng/mL stock solution for adiponectin standard

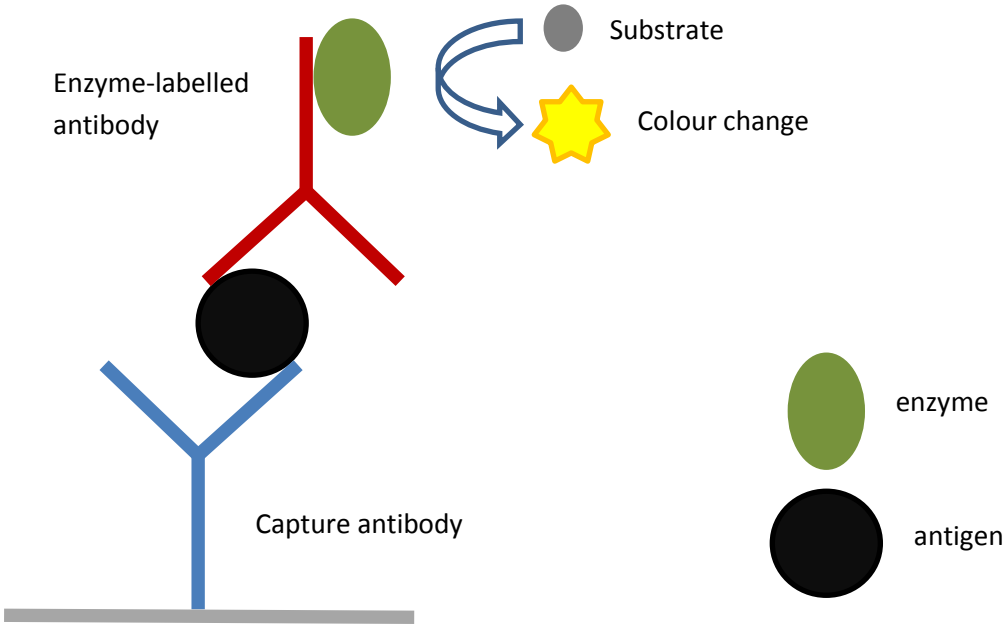


**Figure 2.2. Principle of a sandwich ELISA**

This schematic diagram represents the principle of the sandwich ELISA, which is a competitive assay. The intensity of the final colour is directly proportional to the concentration of the antigen in the sample.

### 2.7.2. Method

The reagents were brought to room temperature and prepared as described above. A two-fold serial dilution of the stock solution was prepared to produce a standard curve and give the following concentrations for leptin (ng/mL): 4000, 2000, 1000, 500, 250, 125 and 62.5. The final concentrations for the adiponectin kit (pg/mL) were as follows: 10, 5, 2.5, 1.25, 0.62, 0.31 and 0.16. Once all reagents, standard curve dilutions and samples were prepared, 50µL of Assay Diluent was added to each well, followed by 50µL of standard, control or sample and covered with an adhesive strip. A preliminary experiment, with different concentrations of leptin and adiponectin medium, indicated that undiluted samples fell within the standard curve range, and so the samples were added to the wells undiluted. Distilled water was used for the blank measurements. The plate was left to incubate for 2h at room temperature. After the incubation, each well of the plate was aspirated and washed, and this process was repeated a further four times to give a total of five washes. Once washed, 100µL of mouse leptin or adiponectin conjugate was added to each well. The plate was covered with another adhesive strip and left to incubate at room temperature for a further 2h. The aspiration and washing step was repeated, making sure the plate was washed five times. After washing, 100µL of substrate solution was added to each well and the plate was covered and protected from light for 30 min at room temperate. The addition of 100µL of stop solution to each well completed the method, and the plate was gently tapped to ensure thorough mixing. The absorbance was determined immediately using a Varioskan Flash MultiMode Reader (Thermo Scientific) at 450nm corrected to 540nm. Data were collected for each protein, analysed and a standard curve for each was generated using GraphPad Prism 5 (GraphPad software).

### 2.7.3. Statistical analysis of ELISA data

A Shapiro–Wilk W test was initially used to determine whether the sample data were normally distributed. This test suggested that they were not, and so the non-parametric Cuzick's test for trend (Cuzick, 1985) was used, and the data are presented as median ± range for a group size of three.

## 2.8. PROTEIN ASSAY (BRADFORD ASSAY)

The Bradford assay originated from the observation that Coomassie Brilliant Blue G-250 exists as either a red or blue colour. The red form changes to the blue form when the dye is bound to protein (Reisner *et al*., 1975). This causes an alteration in the light absorbance properties of the dye in the acidic environment of the reagent. The red (unbound form) maximally absorbs light with a wavelength of 465nm, and this shifts to a maximum of 595nm after the addition of protein. A direct relationship occurs between the protein concentration and absorbance of light at 595nm. This protein-dye complex was utilised in the development of the Bradford assay (Bradford, 1976), which allows measurement of the protein concentration within a sample at a wavelength of 595nm. The assay is very sensitive for the measurement of protein concentration, and is also very efficient because the binding of the dye to the protein occurs in approximately 2h. Finally the dye-protein complex remains dispersed in solution for up to 1h, meaning that this assay is easy to use, reliable and efficient in the detection of protein.

In this study, the Bradford assay was used to determine the concentration of protein in all of the cell samples. These concentration figures were then used for the normalisation of mass spectrometry data.

### 2.8.1. Reagents and suppliers

Bovine Serum Albumin (BSA) was obtained from PAA Laboratories Ltd and Coomassie Plus Protein Assay Reagent was from Thermo Scientific, and was brought up to room temperature before use.

### 2.8.2. Method

Diluted albumin standards were prepared from the BSA stock solution in the following manner:

| *Vial* | *Volume of diluent (µL)* | *Volume and source of BSA (µL)* | *BSA concentration (µg/mL)* |
|---|---|---|---|
| A | 0 | 300 from stock | 2000 |
| B | 125 | 375 from stock | 1500 |
| C | 325 | 325 from stock | 1000 |
| D | 175 | 175 from B | 750 |
| E | 325 | 325 from C | 500 |
| F | 325 | 325 from E | 250 |
| G | 325 | 325 from F | 125 |

Once the BSA dilutions had been prepared, 10µL of each standard, blank or unknown sample was added to the appropriate wells. Distilled water was used for the blank reading, and the standards, blanks and unknown samples were all assayed undiluted in triplicate. This was followed by the addition of 300µL of Coomassie reagent to each well, and the plate was mixed on an Orbital shaker SSM1 (Stuart, Staffordshire, UK) for 30 sec. The plate was removed and incubated at room temperature for 10 min away from light. After incubation, the absorbance was read at 595nm with a Varioskan Flash Multimode Reader (Fisher Scientific). The average of the blank measurements was removed from each individual standard or unknown sample, and a standard curve was created using GraphPad Prism 5 (GraphPad software).

### 2.9. MASS SPECTROMETRY ANALYSIS

Mass spectrometry (MS) is a powerful analytical tool widely used in lipid analysis. The technique involves detection of charged ionised analytes according to their mass-to-charge ratio (m/z). Initially, MS could only be used to analyse small and volatile lipids, until two soft ionisation techniques were developed. These techniques were matrix assisted laser desorption/ionisation (MALDI) and electrospray ionisation (ESI), both of which allowed generation of ions of intact biomolecules (Karas and Hillenkamp, 1988; Fenn *et al*., 1989).

A typical mass spectrometer is composed of three parts, which include an ion source, a mass analyser and a detector, as represented in Figure 2.3. Most mass spectrometers also have a way of automatically injecting the samples, such as an autosampler, and a computer to collect the data (de Hoffmann and Stroobant, 1999). There are several commonly used mass analysers in lipid research, including: Paul ion trap, linear

quadrupole, time of flight (TOF), Fourier transform ion cyclotron resonance (FT-ICR-MS) and Orbitrap. Many mass spectrometers are coupled to a chromatography system which allows the separation of a sample before it enters the mass spectrometer. Two types exist, gas chromatography (GC) and liquid chromatography (LC). If a lipid extract is introduced after chromatographic separation, the process is termed either gas-chromatography-mass spectrometry (GC-MS) or liquid chromatography-mass spectrometry (LC-MS; Houjou *et al*., 2005), depending on the type of chromatography used. The work presented in this thesis was conducted using LC-MS, and so strategies appropriate to this technique will be described in more detail.

### 2.9.1. Ionisation

The lipidomic analysis in the current study was performed using LC-MS, and the ionisation technique used was electrospray ionisation (ESI). This is a soft ionisation technique, which produces intact ions. The major principle of ESI is to transfer ions from solution into a gaseous phase before they enter the mass spectrometer.

This occurs by infusing a sample into a capillary tube, and a high voltage is applied to the tip, which, in the case of positive ion ESI, pulls a positive charge towards the liquid front. When electrostatic repulsion becomes greater than surface tension, the surface of the emerging liquid becomes charged and is dispersed into a fine spray of charged droplets (Fenn *et al*., 1989; Figure 2.4). A nebulising gas, such as nitrogen, can be applied to enhance a higher flow rate. The charged droplets present in the spray then pass down a pressure and potential gradient, and with the aid of an elevated ESI-source temperature and nitrogen, the solvent is evaporated under vacuum to produce analyte ions.

Two theories exist as to how the small droplets produce analyte ions. The first is called the “Charged Residue Model” in which the solvent evaporation continues and causes the droplet to continue decreasing in size until only the analyte ion remains (Dole *et al*., 1968). The “Ion Evaporation Mechanism” is the second theory, and it states that when the droplets become small enough, the electric field at its surface reaches a critical point (Rayleigh limit) causing it to expel a charged analyte ion from the surface of the droplet into the surrounding gas (Iribarne and Thomson, 1976).

Both positively and negatively charged ions can be produced with ESI. Polar molecules which do not contain an acidic or basic group can be charged through the formation of adducts with various ions. In positive ion mode, many adducts can be formed including $Na^+$, $K^+$, and $NH_4^+$. In negative ion mode, $Cl^-$ adducts can be produced. Therefore various ion charge states can be produced, and a few are presented in Table 2.3.

**Table 2.3. Adduct formation with ESI-MS**

| ION MODE | ADDUCT ION TYPE |
|---|---|
| Positive | [M+H]+<br>[M+Na]+<br>[M+K]+<br>[M+$NH_4$]+ |
| Negative | [M-H]-<br>[M-Cl]- |

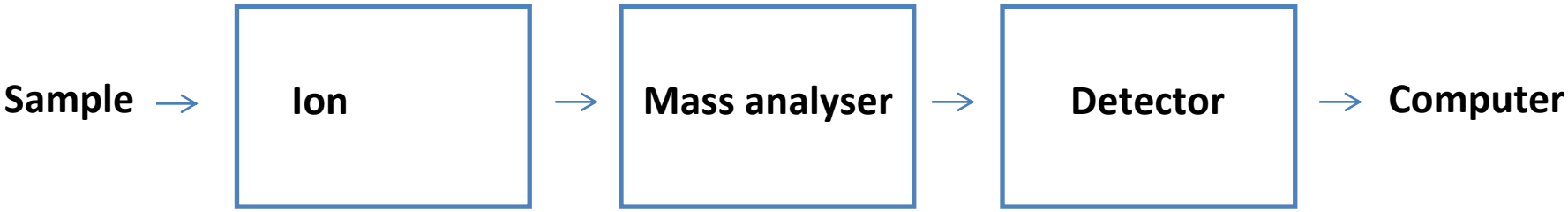




**Figure 2.3. Schematic representation of a typical mass spectrometer**

A mass spectrometer consists of three parts, including an ion source, mass analyser and a detector. A method of introducing samples and a computer to collect the data are often present.

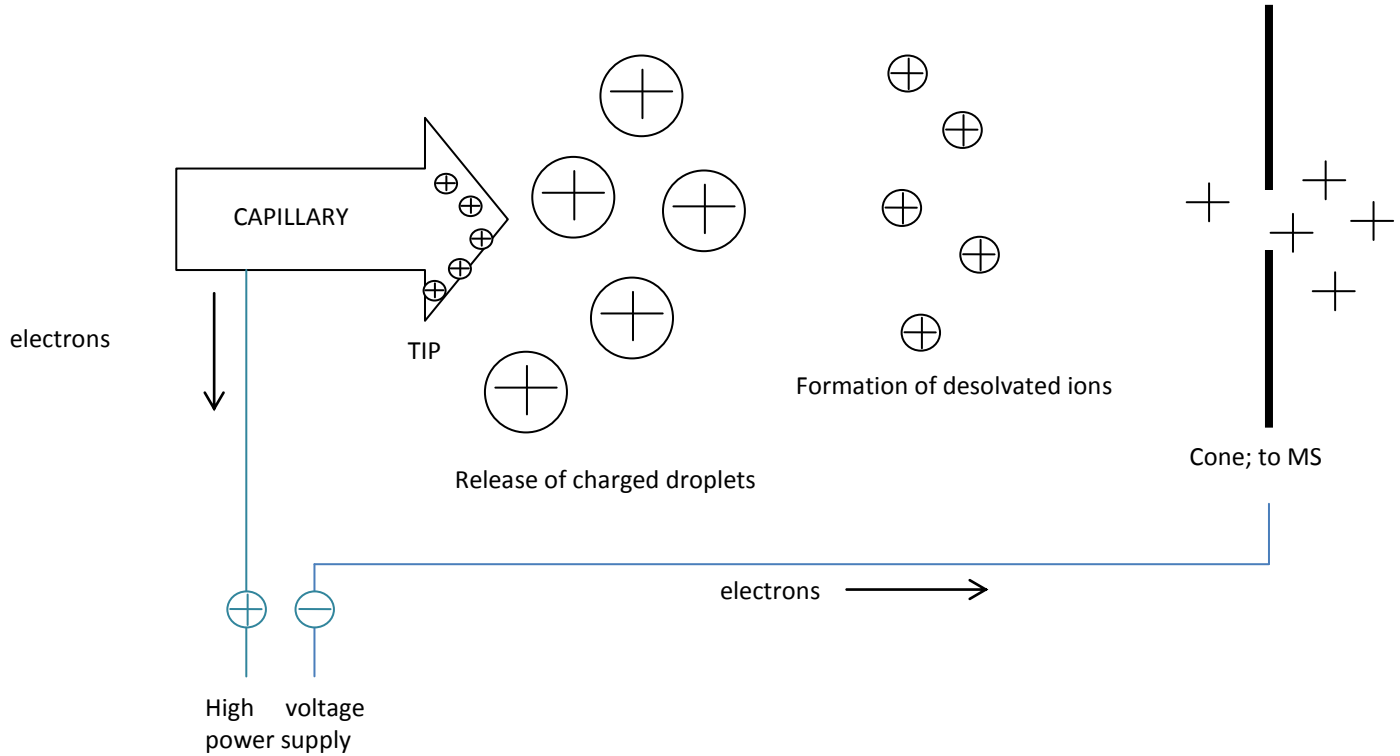


**Figure 2.4. Schematic representation of positive ion ESI**

A high voltage is applied to the capillary tip which charges the surface of the emerging liquid, releasing a fine spray of charged droplets. The solvent is removed, due to evaporation and these ions pass into the mass spectrometer.

### 2.9.2. Mass analysers

Following ionisation, the ions move to an analyser to be detected. Two mass analysers were used in the work presented in this thesis, an orbitrap for global lipidomic analysis, and a triple quadrupole mass analyser for a targeted lipidomic approach.

#### *2.9.2.1. Orbitrap*

The orbitrap was proposed by Alexander Makarov (Makarov, 2000). It is a modification of the Kingdon ion trap (Kingdon, 1923) which consists of a thin central wire and an outer cylindrical electrode. A static applied voltage results in a radial logarithmic potential between the electrodes. A modified outer electrode was later added and it included an axial quadrupole which confined the ions on the trap axis (Knight, 1981).

The external part of the orbitrap is barrel shaped and cut into two parts which are separated by a small gap, and inside is a central electrode which is spindle shaped. The ions are injected tangentially into the electric field through the space between the two parts of the external electrode. These ions are trapped in an electrostatic field (Makarov, 2000; Hardman and Makarov, 2003). This electrostatic attraction towards the central electrode is compensated by a centrifugal force, and so the ions are forced to move in complex spiral patterns (Figure 2.5). The frequency of the oscillations is inversely proportional to the square root of the m/z, and so the orbitrap can be used as a mass analyser to accurately detect the m/z of analyte ions.

The performance of a mass spectrometer is judged on characteristics including resolution (the ability to distinguish between two peaks of slightly different m/z), mass accuracy, mass range and ion dynamic range (McLuckey and Wells, 2001). The best quality of the orbitrap is the very high resolution obtained. The orbitrap resolving power is proportional to the number of oscillations of the ions, and therefore inversely proportional to the square root of m/z. The orbitrap also has high mass accuracy and dynamic range (Makarov *et al*., 2006). In the current study, an Orbitrap Exactive mass spectrometer was used, and an overiew diagram of this system is shown in Figure 2.6.

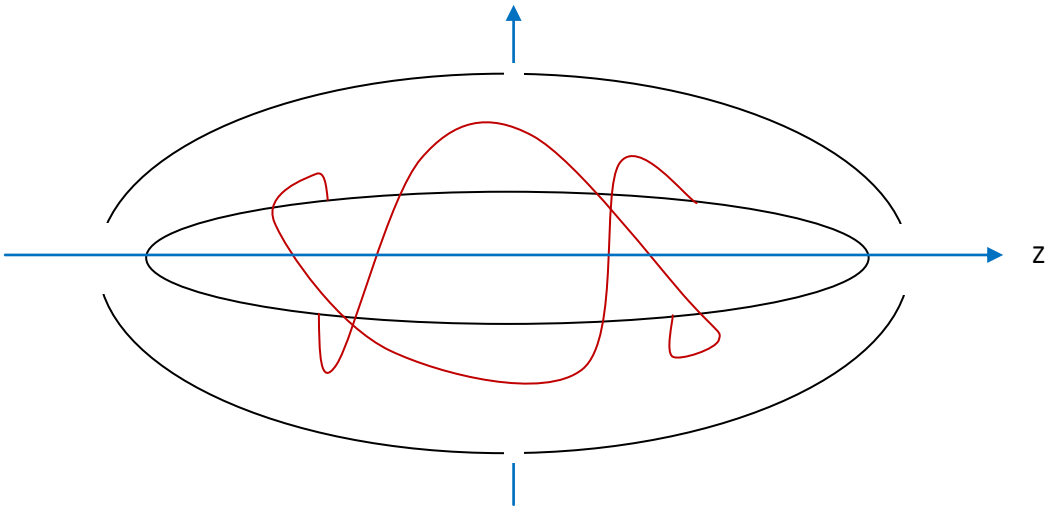


**Figure 2.5. Schematic representation of the orbitrap**

*Adapted from* de Hoffman and Stroobant, 2006. A barrel shaped outer electrode is cut into two parts separated by a small gap. The ions spiral around the central electrode while oscillating back and forth along the z-axis.

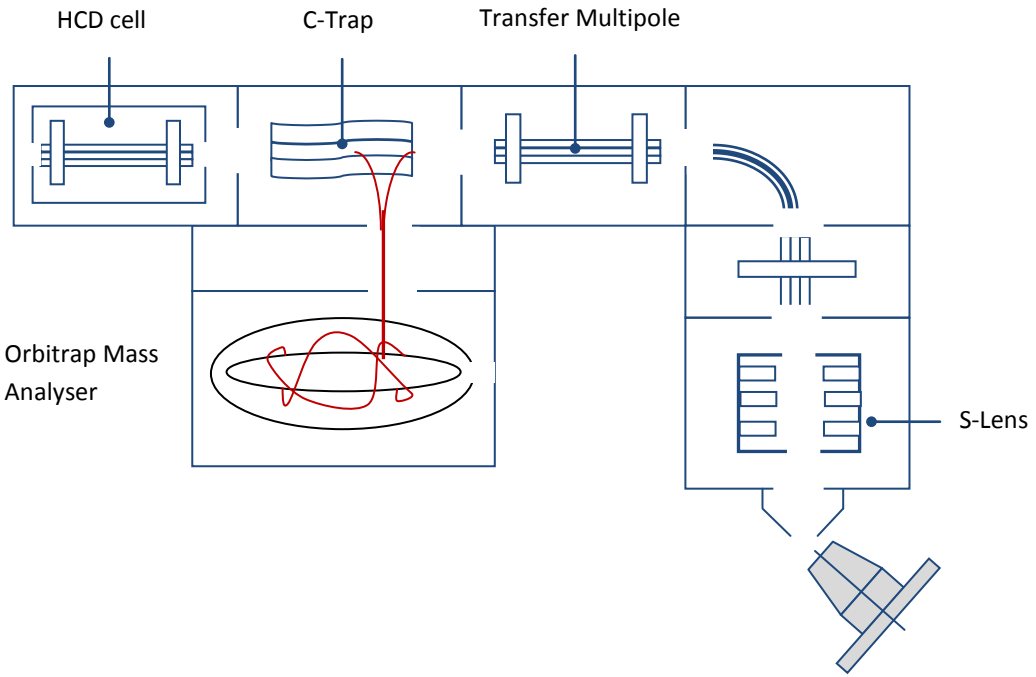


**Figure 2.6. Schematic representation of the Orbitrap Exactive**

Charged analytes are moved from the ion source to the orbitrap analyser via a series of ion optics which use a combination of direct current (DC) and radio frequency (RF) voltages, and a vacuum gradient. The ions can be held in the analyser for a selected period of time, and the ions are detected by the outer electrodes which surround the orbitrap analyser.

#### *2.9.2.2. Quadrupoles*

The quadrupole analyser uses the stability of the trajectories in oscillating electric fields to separate ions according to their m/z (Paul and Steinwedal, 1953). A quadrupole consists of four parallel rods equally spaced around a central area (Figure 2.7). Opposite rods are electronically connected, and an equal but opposite direct current (DC) voltage superimposed with a radio frequency (RF) alternating current (AC) voltage is applied to the diagonally placed pair of rods. This causes the ions to move in the z direction with an oscillatory motion in the x-y plane. The amplitude of oscillation can be controlled by altering the DC and RF voltages, and has a relationship with the m/z. The DC and RF voltages can be set so that the amplitudes of oscillation for desirable m/z are stable, allowing the ions to travel along the z-axis without hitting the quadrupole rods, and therefore reaching the detector. The oscillatory amplitudes of undesirable ions are unstable and so hit the metal rods and get neutralised, rather than reach the detector (Ho *et al*., 2003). Positive and negative fields are generated at perpendicular axes to each other by the application of opposing polarities to pairs of rods. A positive ion entering the space between the rods will be attracted towards a negative rod. If the potential changes sign before discharging itself on the rod, the ion will change direction (de Hoffman and Stroobant, 1999).

Quadrupole mass analysers are advantageous in that they are robust, economical, physically small, and easily interfaced with a wide variety of inlet systems (Ho *et al*., 2003). A series of three quadrupole analysers can be set-up in a linear fashion to form a triple quadrupole.

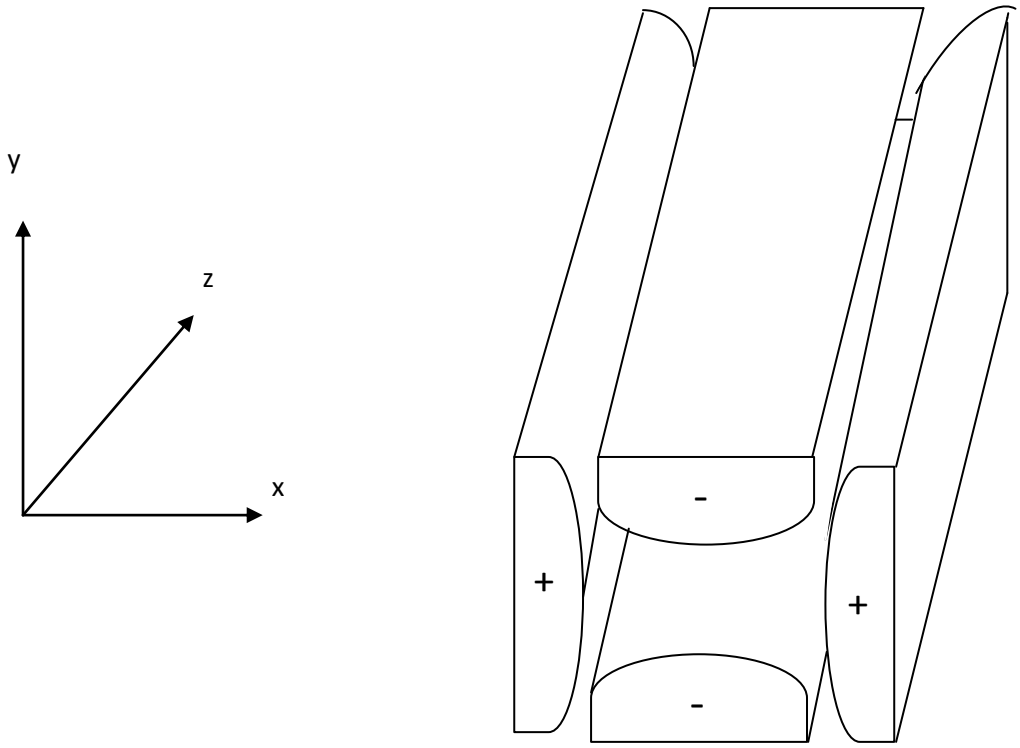


**Figure 2.7. Schematic drawing of a quadruple**

*Adapted from* de Hoffman and Stroobant, 2006. Four hyperbolic rods are equally spaced around a central area. The electrical potential of the rods are denoted by the + or – symbols. There are three major dimensions of the trajectory of the ions through the quadrupole, and these are x, y and z.

In a typical triple quadrupole system (Figure 2.8), the ions enter the first quadrupole (Q1) where specific ions (precursor ions) are mass selected. By selecting specific m/z, Q1 acts as a filter to the other ions present and so can help reduce sample purification before MS analysis. The selected ions then collide with a collision gas in Q2 causing fragmentation of the precursor ions, which is a process known as collision induced dissociation (CID). The resulting product ions are then monitored by Q3, and finally move to the detector. Both Q1 and Q3 are operated by DC and RF potentials, whereas Q2 is operated only by the RF potential (Dass, 2007). Different data acquisition modes are commonly used with this type of mass analyser and are:

- Product ion scan; a precursor ion is focussed in Q1, fragmented in Q2 and detected by scanning in Q3
- Precursor ion scan; Q3 is held to measure the occurrence of a selected fragment ion and Q1 is scanned, resulting in a spectrum of precursor ions relating to a particular product ion
- Neutral loss scan; both Q1 and Q3 are scanned to produce a spectrum of precursor ions that undergo the same neutral loss
- Multiple reaction monitoring (MRM); both Q1 and Q3 are static for a pre-determined precursor and product ion pair

These scanning modes have many applications, for example, previous studies have used precursor ion and neutral loss scanning to detect sub-sets of lipids containing a specific functional group such as phospholipids (Ekroos *et al*., 2002; Han *et al*., 2005; Han *et al*., 2006a and 2006b). These scanning acquisitions are a major advantage of a triple quadrupole mass spectrometer; however, they also have several disadvantages including low resolution, medium mass accuracy and a low duty cycle for the scanning modes (excluding MRM). Hybrid instruments now exist in which Q3 is replaced with a different analyser to try and improve the problems. When Q3 is replaced with a TOF analyser, named QTOF (Ekroos *et al*., 2002; Rainville *et al*., 2007), a good mass accuracy and resolving power can be provided for product ion, but they cannot perform precursor and neutral loss scans. Another hybrid instrument called QQ-LIT or Qtrap replaces Q3 with a linear ion trap (LIT), and this can perform precursor and neutral loss scans (Hopfgartner *et al*., 2004; Hou *et al*., 2008).

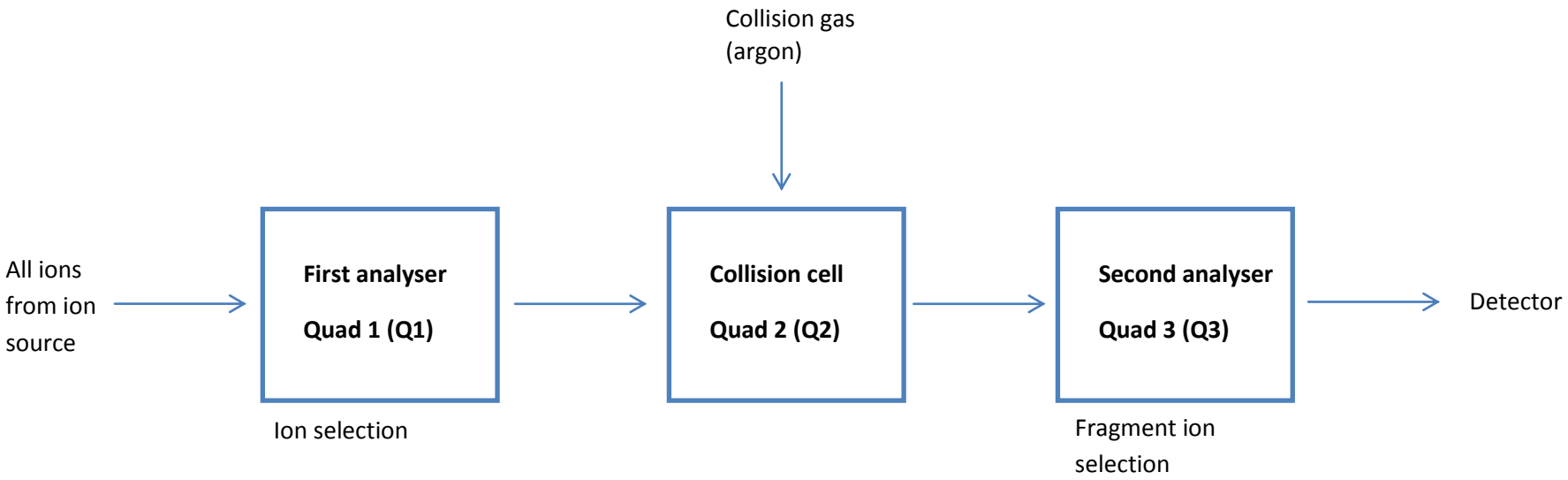


**Figure 2.8. Schematic representation of a triple quadrupole mass spectrometer**

A triple quadrupole mass spectrometer consists of three quadrupoles. The ions enter the first quadrupole (Q1) where specific ions (precursor ions) are mass selected. These then pass into Q2 where they collide with a collision gas which causes fragmentation of the precursor ions. The resulting product ions are then monitored in Q3 and detected by the detector.

### 2.9.3. Detectors

Once ions have passed through the analyser, they reach the detector, used to measure and record their m/z. Electron multipliers are the most common detector type used in mass spectrometry. This type of detector operates by a process called secondary electron emission. When an ion strikes the surface it causes the ions in the outermost area of the atom (secondary electrons) to be released from atoms in the surface layer. The number of these secondary electrons released depends on the type of primary particle, the angle it strikes the surface, and the energy and characteristic of the incident surface.

There are two basic forms of electron multipliers: the discrete-dynode electron multiplier, and the continuous-dynode electron multiplier. The discrete-dynode electron multiplier is made up of 12 to 20 dynodes that have good secondary emission properties. These dynodes are held at decreasing negative potentials by a chain of resistors. When secondary electrons from the conversion dynode strike the first dynode surface, secondary electrons are emitted, and these are then accelerated towards the next dynode. These electrons therefore strike the secondary dynode, causing the emission of even more electrons. This continues until an electric current is produced at the end of the electron multiplier (de Hoffmann and Stroobant, 1999).

A continuous-dynode electron multiplier exists in a curved tube shape and has good secondary emission properties. The walls of the tube have a standardised electric resistance. Therefore when a voltage is applied at either end of the tube, a continuous accelerating field is produced. The secondary particles emitted from the conversion dynode collide with the curved inner wall of the tube, thus producing secondary electrons. These are then accelerated towards the exit of the tube, all the while striking the wall and releasing more secondary electrons. Therefore a cascade of electrons is created until eventually a metal anode collects this stream of secondary electrons at the detector exit, allowing the current to be measured (de Hoffmann and Stroobant, 1999).

Other types of detector exist, including Faraday cups and ion-to-photon detectors. In the case of the orbitrap, the detector consists of two metal surfaces in which the ions only pass as they oscillate. This means that only a weak AC current is produced in a circuit between the electrodes.

### 2.9.4. Chromatography systems

The term chromatography refers to any technique which separates compounds based on their partition coefficient between a stationary and a mobile phase (Purnell, 1962). In terms of lipid analysis, three chromatography techniques are commonly used, and each has its own advantages. Gases and volatile substances can be separated by gas chromatography (GC), involatile chemicals and high molecular weight molecules by liquid chromatography (LC) and finally, inexpensive separations can be performed using thin layer chromatography (TLC). Both GC and LC are performed in a column which has been pre-treated with a stationary phase. Specific properties of the stationary phase, as well as the applied compounds determine how they interact with each other. These interactions vary between the different compounds, which affects the speed at which a compound passes through the column, thereby separating them. The mobile phase (gas or liquid) passes through under pressure to elute the sample from the column. The method of TLC is much simpler; the stationary phase is coated onto a glass plate, and a liquid mobile phase travels up the plate to elute the sample. The sample is present in the mobile phase and each solute is retained, with weaker held solutes eluting first, and the more strongly held eluting later to allow separation of the sample. TLC is mainly used analytically to measure the proportions of analytes present in the sample. Both GC and LC can be used alone for analytical chemistry, or be coupled to a mass spectrometer as a preparation measure to separate a sample before analysis by mass spectrometry.

The chromatography system used for the current study was LC, which can be used to separate and detect a wide range of compounds. During LC-MS analysis, the stationary phase is packed into a column, and the mobile phase is a liquid, often a mixture of solvents and water. This solvent gradient is altered over time and causes disassociation of the compounds with the stationary phase. Modern LC-MS systems allow for up to four mobile phases to be mixed together at once; however, two phases are most commonly used. This binary solvent system consists of an aqueous solvent (often referred to a solvent A) and an organic solvent (solvent B). The aqueous phase is often HPLC grade water with 0.1% acid. Many solvents are commonly used for B, including acetonitrile (ACN), methanol (MeOH) and isopropanol (IPA). These solvents may also be mixed together, along with the addition of an acid, which is added to improve chromatography, and also to provide a source of protons. Commonly used acids are formic and acetic.

Two main types of liquid chromatography are used in lipidomic LC-MS analyses, and they are normal-phase, and reverse phase. Normal phase chromatography separates analytes based on their affinity for a polar stationary phase. The column is equilibrated with a non polar solvent, and so aids the separation of analytes soluble in these non-polar solvents. The analytes associate with the polar stationary phase, and the strength of adsorption depends on the polarity of the analyte. Therefore, the analytes with the lowest polarity elute off first, while more polar compounds are retained on the column for longer (Willoughby *et al*., 2002). As the solvents in the mobile phase become more polar, the retention time (RT) of the analytes will decrease, and vice versa. The opposite is true for reverse-phase chromatography. The column has a non-polar stationary phase, and is equilibrated with polar solvents. Therefore, polar analytes elute readily, whilst less polar molecules have longer retention times.

### 2.10. LIPIDOMIC ANALYSES USED IN THE CURRENT STUDY

Three lipidomic analysis techniques were utilised in the current study to investigate lipid species present in 3T3-L1 adipocytes from both the cells themselves, and also lipids which may have been secreted by these cells into the medium. Global lipidomic approaches were used to investigate the lipidome of the 3T3-L1 cells, and a targeted approach allowed detection of various eicosanoid species which had been secreted into the cell medium. A summary of the lipidomic analyses used is shown in Figure 2.9.

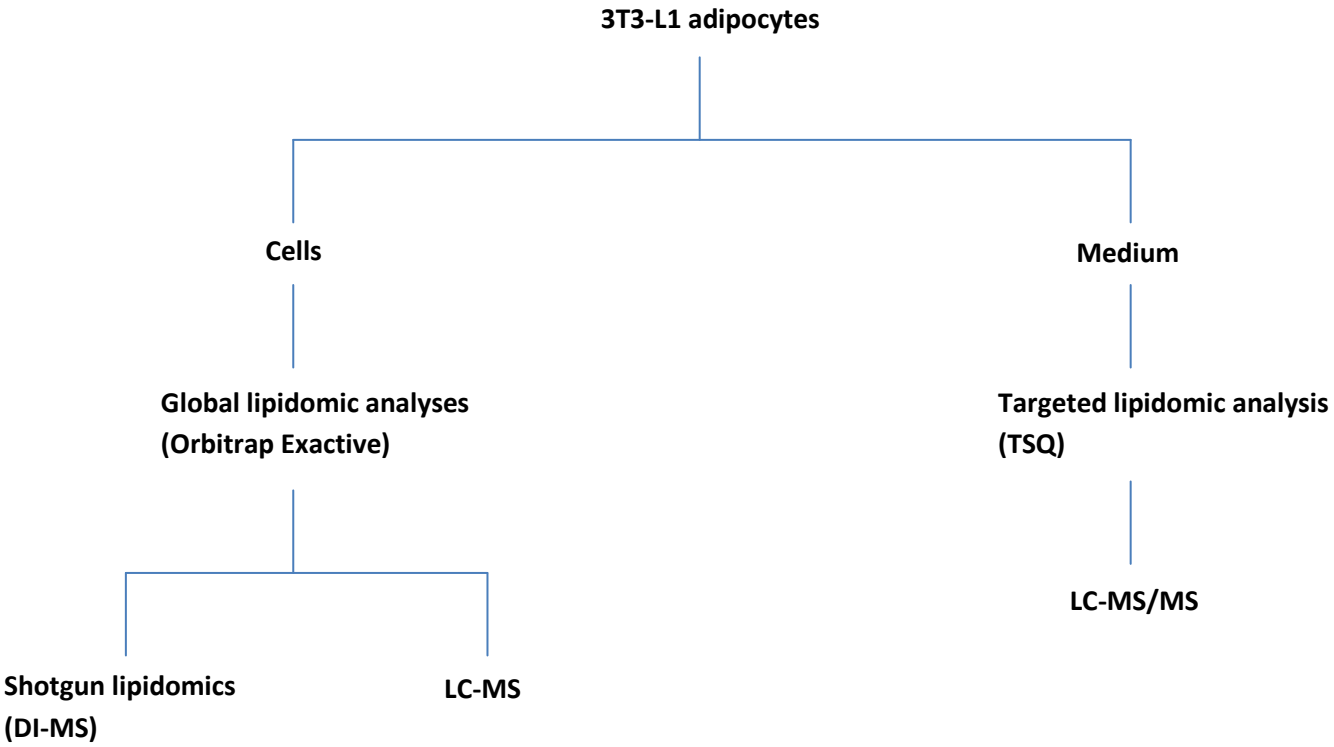


**Figure 2.9. Summary of lipidomic analyses used in the current study**

Global lipidomic analyses were used to study the lipidome of 3T3-L1 cells, and a targeted lipidomic technique was used to investigate eicosanoid secretion from the 3T3-L1 cells into the medium. Abbreviations used: DI-MS, direct infusion-mass spectrometry; LC-MS, liquid chromatography-mass spectrometry; LC-MS/MS; liquid chromatography-tandem mass spectrometry.

### 2.10.1. Global lipidomics

Lipidomics is the comprehensive understanding of the influence of all lipids, and factors that interact with them, and the term was first defined through the analysis of lipid molecular species by mass spectrometry (Han and Gross, 2003). Global lipidomics theoretically allows the identification and analysis of all lipid species present in a sample.

Two global lipidomic techniques were used in the current study. The first involved infusing the samples directly into the mass spectrometer (direct-infusion mass spectrometry), and this method has been termed 'shotgun lipidomics' (Han *et al*., 2005; Schwudke *et al*., 2006). Direct infusion-mass spectrometry (DI-MS) avoids any prior chromatographic steps, allowing a high throughput, and therefore rapid analysis of many samples. This method also provides high sensitivity and mass accuracy, as well as being simple to use (Han *et al*, 2005). There are limitations to this lipidomic analysis method, especially added difficulty in assigning identifications to lipid species due to only having the m/z to search against.

### 2.10.2. Cell preparation

There were three replicates for each sample group, and quality control (QC) samples were also prepared. Lipids were extracted from cell samples using the Folch extraction method (Folch *et al*., 1957). A 200µL aliquot of the cells collected in distilled water (described in Section 2.1.2.5) from each sample was spiked with 1 nmol of a phosphatidylcholine internal standard, 1,2-didodecanoyl-*sn*-glycero-3-phosphocholine; PC (12:0/12:0) and 1 nmol of a triacylglycerol internal standard, 1,2,3-trioctadecanoyl-sn-glycerol; TG (18:0/18:0/18:0). The internal standards were added to account for any error or variations that may occur during the sample preparation. The internal standard would undergo the same errors, and so the ratio between analyte and internal standard would remain unchanged. By adding a known volume of a known concentration, the internal standard can also be used to quantify the lipid species within the sample.

After the addition of the internal standards, the sample mixture was added to 4mL chloroform/methanol (2/1, v/v) and left to stand for 1h at room temperature. The samples were centrifuged at 1500 x *g* for 10 min (Legend X1R) and the supernatant was removed to a clean test-tube. The samples were then partitioned with 0.8mL of 0.1M KCl and centrifuged again at 1500 x *g* for 10 min. The upper aqueous phase was removed and

discarded. The lower chloroform phase was dried down under a gentle stream of nitrogen gas, and reconstituted in 600µL chloroform/methanol (2/1, v/v) and stored at -80$^{o}$C until required. Before directly infusing into the mass spectrometer, 10mM ammonium formate ($NH_4HCO_2$) was added to each sample.

**2.10.3. Calibration method**

Prior to any global lipidomic analysis, an external calibration routine was employed to reduce any instrumental drift, and to obtain accurate masses. This involved directly infusing a positive and negative calibration mixture into an Orbitrap Exactive mass spectrometer (Thermo Scientific); with a methanol wash in-between each mixture.

The positive calibration mixture consisted of caffeine; L-methionyl-arginyl-phenylalanyl-alanine acetate x water (MRFA) and Ultramark$^{TM}$ 1621, which is a commercially available mixture of fluorinated phosphazines, in an acetonitrile (ACN): MeOH: Water ($H_2O$) solution in the following percentages (%v); 50:25:25. The mixture was finalised with the addition of 1% (v) acetic acid. Stock solutions of caffeine; MRFA and Ultramark$^{TM}$ 1621 were made up firstly, to the volumes and concentrations stated below:

Caffeine: 1mL of 1mg/mL in distilled water
MRFA: 1.5mL of 166.7pmol/µL in 50:50 (%v) MeOH: $H_2O$
Ultramark$^{TM}$ 1621: 10mL of 0.1% (%v) Ultramark$^{TM}$ 1621 in ACN

The positive calibration mixture was then prepared to 10mL by firstly adding 200µL of the caffeine stock solution to a 10mL volumetric flask. To this, 100µL of the MRFA and Ultramark$^{TM}$ stock solutions were added to the flask, along with 100µL of glacial acetic acid and 5mL of ACN. The remaining volume was made up with 50:50 (%v) MeOH: $H_2O$. The negative calibration mixture was made up of the same solvent system used for the positive mixture and Ultramark$^{TM}$ 1621, as well as sodium dodecyl sulphate (SDS) and sodium taurocholate. The stock solutions were prepared to the following volumes and concentrations:

SDS: 10mL of 1nmol/µL SDS in 50:50 (%v) MeOH: $H_2O$
Sodium taurocholate: 10mL of 1nmol/µL sodium taurocholate in 50:50 (%v) MeOH: $H_2O$

Preparation of the negative ion calibration mixture began with the addition of 100µL of the SDS, sodium taurocholate and Ultramark$^{TM}$ 1621 stock solutions into a 10mL volumetric flask, along with 100µL of glacial acetic acid. As with the positive mixture, 5mL of ACN was then added and the mixture was brought up to 10mL with 50:50 (%v) MeOH: $H_2O$.

#### *2.10.3.1. Mass spectrometry parameters*

Both the positive and negative calibration mixtures were directly infused into the Orbitrap Exactive at a flow rate of 5µL/min. The intensity signal was left to stabilise for 2 min before the start of the automatic calibration, and MeOH was washed through between the mixtures for 5 min, or until the calibration mixture ions had reduced to background. Some of the settings were the same for both ionisation modes: the sheath gas was set to 5 (arbitrary units), and the vaporiser and capillary temperatures were held at 40$^{o}$C and 275$^{o}$C, respectively. The spray voltage differed between the two ionisation modes, and was set at 3kV for positive, and 2.5kV for negative. In both ionisation modes the resolution was set at 60,000 with a 2Hz scan speed. The maximum injection time was 100 milli sec (msec) and the AGC target was set at ultimate mass accuracy. The scan range analysed was between m/z 100 and 2000Da. Example spectra generated from the positive and negative calibration mixtures are shown in Figure 2.10.

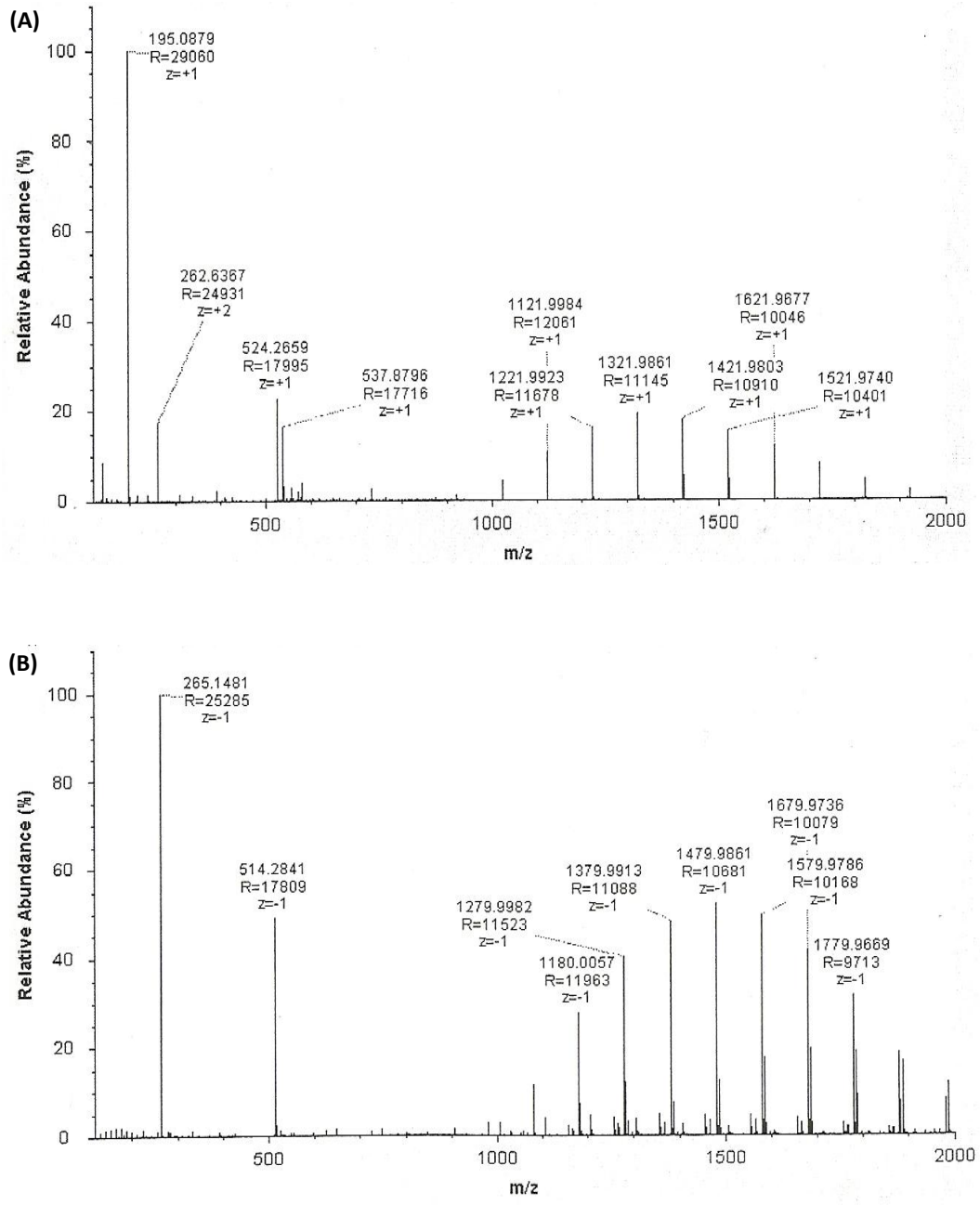


**Figure 2.10. Representative spectra of the calibration mixtures**

Representative spectra of the positive (A) and negative (B) calibration mixtures, with a mass-to-charge (m/z) range between 100 and 2000Da.

### 2.10.4. DI-MS method

Prepared 3T3-L1 adipocytes and QCs were directly infused into the Orbitrap Exactive at a flow rate of 5µL/min. A 2 min stabilisation period was employed for each sample before data were acquired for 450 scans. The samples were infused in both positive and negative ion mode, and all the settings were the same as those described in Section 2.10.3.1, with the exception of the scan range which set for m/z between 100 and 1000.

### 2.10.5. Data analysis of DI-MS global lipid profiles

A selection of abundant peaks from each experiment was selected, and quantified using the intensity of the appropriate internal standard, therefore, all TGs used TG (18:0/18:0/18:0) and all other lipid species used PC (12:0/12:0). This value was then normalised to the protein concentration of the cell lysate. The peaks were identified using their m/z with the following databases: the Human Metabolome Database (HMDB; www.hmdb.ca), LIPID Metabolites and Pathways Strategy (LIPID MAPS; www.lipidmaps.org), and the Metabolite and Tandem MS Database (METLIN; http://metlin.scripps.edu). Identifications were confident if the mass accuracy between the observed mass and the theoretical mass was less than 5 parts per million (ppm). This is calculated by the following formula:

$$ppm = \frac{\text{observed mass} - \text{theoretical mass}}{\text{theoretical mass}} \times 1{,}000{,}000$$

The concentrations of the selected lipid species from each study were presented as median ± range for a group size of three. Appropriate non-parametric tests were applied, and the specific test used is indicated in the data chapters.

### 2.10.6. Global lipidomics, LC-MS analysis

Another global lipidomic approach is the use of LC-MS. Advantages of this method include a better sensitivity than DI-MS, and the ability to detect and identify lipids based on RT and accurate mass. The major advantage of LC-MS over DI-MS; however, is that lipids in complex samples can be separated. Disadvantages include longer analysis times, and problems with sample carry over between runs, and coelution of lipids may exist (Nygren *et al*., 2011).

#### *2.10.6.1. Cell preparation*

The cell lysate samples were prepared as described in Section 2.10.2, without the addition of 10nM ammonium formate (AF).

#### *2.10.6.2. Chromatography conditions*

Lipid extracts from the cell samples and QCs were separated on a Hypersil Gold C18 1.9µm; 50mm x 2.1mm column (Thermo Scientific, Hemel Hempstead, UK). The LC conditions were adapted from a previous method (Nygren *et al*., 2011) and were the same for both positive and negative ion mode analyses. A binary solvent system was used in which mobile phase A consisted of $H_2O$ + 1% ammonium formate (AF) + 0.1% formic acid and mobile phase B of ACN/ IPA (1:1, v,v) + 1% AF + 0.1% formic acid. Analyses were performed over an 18 min gradient with a flow rate of 400µL/min. The sample tray and column were held at 4$^{o}$C and 50$^{o}$C respectively. The mobile phase gradient was as shown in Table 2.4.

**Table 2.4. Mobile phase compositions for global LC-MS analysis**

| *Time* | *% mobile phase A* | *% mobile phase B* |
|---|---|---|
| 0 | 65 | 35 |
| 2 | 20 | 80 |
| 7 | 0 | 100 |
| 14 | 0 | 100 |
| 18 | 65 | 35 |

#### *2.10.6.3. Mass spectrometry conditions*

An Accela ultra high performance liquid chromatography (UHPLC) system was coupled to an Orbitrap Exactive, which was equipped with a heated electrospray ionisation (HESI) probe. The heated capillary and HESI probe were held at 250$^{o}$C and 300$^{o}$C, respectively. The sheath gas flow was set at 50 (arbitrary units) and the auxiliary gas at 20 (arbitrary units). These conditions were constant for both positive and negative ion mode acquisitions. The spray voltage was set at 4.5kV in positive ion mode, and 2.5kV in negative ion mode. A lock mass of m/z 413.26623 was selected in positive ion mode only.

A lock mass is a compound of known mass which compensates instrumental drift. The instrument underwent a complete calibration (as described in Section 2.8.1.3) to reduce / remove instrumental drift, and improve the mass accuracy of the instrument. After calibration of the mass spectrometer, 1µM of a lyso-phosphatidylcholine standard (LPC 14:0) was directly infused in both positive and negative ion mode before every acquisition to check the chromatography conditions.

The mass spectrometer was run in high resolution mode which corresponds to a 60,000 resolution and 2 Hz scan speed. The AGC target was set at ultimate mass accuracy and the maximum injection time was 100 msec. These conditions were the same for positive and negative ion mode for a scan range between m/z 100 and 1000. Each sample set had three biological replicates which were injected once in a randomised order, with blanks and QCs being dispersed throughout the sequence run. The sample sequence was run separately in positive and negative ion modes.

**2.10.7. Analysis of global LC-MS data**

All LC-MS raw files in the current study were analysed using SIEVE v1.3 (Thermo Scientific), which is an automated label-free differential software package. It can be used for the analysis of protein, peptide and small molecule datasets. Therefore, the SIEVE experiments in this study were set up for non-differential analysis of small molecules. The workflow of these experiments consists of three stages: alignment, framing and identification. The alignment method used is called 'adaptive chromatographic alignment' and can only be applied to full datasets. This method involves pairs of full scan data being compared and separated into 'bins' of equal size. Correlations between two spectra can then be calculated, and used to construct a matrix tile. An optimal path is found in the matrix, and subsequent tiles overlap the original one. This overlapping of tiles continues until the full plane is covered, and a final alignment score can then calculated.

The next process in the SIEVE workflow is framing, which involves ordering all of the peaks above a set threshold by their intensities. Each peak relates to a frame, with the most intense peak becoming the first frame, and this continues until all of the selected peaks have been framed. The final process in the workflow is identification, and ChemSpider is the internal identification algorithm used for small molecules.

### 2.10.8. Multivariate Data Analysis

A large volume of data is produced from mass spectrometry techniques, and so the use of standard statistical techniques is not suitable. Multivariate data analysis (MVDA) allows the analysis of data relating to more than two variables from each sample. These techniques treat the data set as a group to allow the identification of values which vary from other data points.

Two main approaches are used in MVDA and they are either supervised, or unsupervised. Of the unsupervised techniques, principle component analysis (PCA) is commonly used as a tool for exploratory data analysis and for making predictive models. PCA was invented by Karl Pearson in 1901 (Pearson, 1901) and is mathematically defined as an orthogonal linear transformation. The aim of PCA is to convert data into information by analysing a dataset in an 'n' dimensional space. The data is transformed into new variables which are linear combinations of the original ones and referred to as principal components. The greatest variance of the data comes to lie on the first coordinate (called the first principal component), the second greatest variance on the second coordinate, and so on. The total number of principle components are less than or equal to the number of original variables. These new variables are uncorrelated, and so each principal component explains a different part of the information. PCA can generate a scores plot and a loadings plot. A scores plot of the first two principle components allows any clustering within a dataset to be displayed. The loadings plot provides information on any variables which contribute to the groupings of the first two principal components.

Supervised approaches, such as partial least square (PLS) analysis (Holmes and Antti, 2002; Lindon *et al*., 2003) are used to maximise separation between unknown samples after a relationship between metabolic profile and phenotype has been established. PLS projects the predicted and observed variables into a new space. Both the x (measure data) and Y (response data) are projected into a new space, and when the Y is binary, the process is called partial least squares-discriminant analysis (PLS-DA). PLS maximises the variation between X and Y by deriving latent variables. The algorithm is then applied to a dummy matrix Y which consists of an orthogonal vector unit for each class. Therefore, a

supervised technique uses an existing model from other datasets, and compares an individual dataset to it, whereas this model does not exist in unsupervised approaches.

Both supervised and unsupervised models can be improved with the correct use of scaling. Three scaling types include unit variance (UV), centering with no scaling (Ctr) and Pareto scaling (Par). The UV scaling should be used where the variables in the data are different. It gives each variable a weighting of one, and therefore an equal chance of being expressed in the model. In terms of mass spectrometry data, spectral regions containing large changes in signal amplitude will be compressed, whilst magnifying regions with less variation. A commonly used scaling type with spectral data is Ctr, in which the influence of a variable is related to its signal, and so regions of low amplitude will have little influence. A compromise between unit variance UV and Ctr scaling is Par scaling. This option allows regions of low amplitude the chance of influencing the model, but only if they show variation. This scaling type is commonly used for mass spectrometry data (Eriksson *et al*., 1999).

The fit of a model is estimated by the R2 value, and the Q2 value estimates the goodness of prediction. An R2 and Q2 value of 0.5 or greater indicates a good model, and is typical for metabolomic and lipidomic analyses.

**2.10.9. Data processing and MVDA in the current study**

After LC-MS analysis (positive and negative ion mode), the raw data files were processed using SIEVE v1.3 to produce m/z and RT pairs, along with their associated intensities. The m/z window was set at either 1 min, 30 sec or 15 sec, and the parameters used for the framing process were:

m/z minimum: 100
m/z maximum: 1000
frame time width(min): 0.25
frame m/z width (min): 0.020
RT start (min): 0
RT stop (min): 18

Lipid species were searched using the three databases mentioned in Section 2.10.5: HMDB, LIPID MAPS and METLIN, and the following adducts were included in the searches: $[M+H]^+$; $[M+K]^+$; $[M+Na]^+$ and $[M+NH_4]^+$ for positive ion, and $[M-H]^-$ for negative ion. The mass tolerance was set at 1 ppm.

After SIEVE analysis, the m/z and RT pairs, along with their intensities were manually normalised to the total ion current (TIC). Both the non-normalised and the TIC-normalised data were imported into SIMCA-P (v12, Umetrics) for MVDA by PCA and PLS. PLS was chosen due to the number of samples analysed, and also the fact that the y-variable data were continuous. Both model types were Pareto scaled and their robustness was measured using R2 and Q2 values. The corresponding loadings plots allowed identification of causes of variance within the pattern recognition models.

### 2.11. TARGETED EICOSANOID ANALYSIS

The alternative to global lipidomics is a targeted approach. Rather than all lipids present in the sample being analysed, a selected lipid class is investigated. All cell preparation and mass spectrometry conditions are designed specifically for the analysis of the chosen lipid class. In the current thesis, a targeted lipidomic analysis method was used to identify and quantify eicosanoid species secreted from 3T3-L1 adipocytes.

#### 2.11.1. Medium sample preparation

Media samples (1mL) removed from the 3T3-L1 cells were prepared by the addition of 2mL ice cold methanol and were then stored at -20$^{o}$C for 30 min. Three internal standards were added at 1ng/mL concentration per sample and they consisted of a mono-, di- and tri-hydroxy eicosanoid species. These were the deuterated forms of 15-hydroxyeicosatetraenoic acid (15(S)-HETE-$d_8$), leukotriene $B_4$ ($LTB_4$-$d_4$) and prostaglandin $E_2$ ($PGE_2$-$d_4$), respectively (Cayman Chemical, Cambridge, UK). The samples were then centrifuged at 670 x g for 10 min at 4$^{o}$C (Legend X1R, Thermo Scientific) to aid the precipitation of any protein, and the supernatant was added to 18mL distilled water. Finally, the samples were acidified to pH 3.5 with 2M HCl.

### 2.11.2. Solid phase extraction chromatography

Solid phase extraction (SPE) chromatography involves the removal of analytes from a flowing liquid sample due to retention on a solid sorbent. This is followed by the recovery of selected analytes by elution from the sorbent. This method has been greatly aided by disposable cartridges containing the solid sorbent, and the first sorbent used was bonded-phase silica. The use of SPE chromatography on commercially available bonded phase silica was first described in the clean-up of histamines from wine (Subden *et al*., 1978). The process consists of four stages (Figure 2.11). In the first, the sorbent is conditioned with solvent, to improve analyte retention and also to reduce solvent impurities passing through during elution. The solvent that is present in the sample is then passed through the conditioned column, followed by the sample itself. A number of washing steps follow, to remove any undesired sample components from the column, whilst still retaining the analytes of interest. Finally, these analytes are eluted from the column, and collected, using a suitable solvent.

#### *2.11.2.1. Solid phase extraction chromatography method*

Eicosanoid lipids were extracted from medium samples harvested from the 3T3-L1 cell culture, by SPE chromatography using C18 6cc Sep-Pak cartridges (Waters, Manchester, UK). Each cartridge was initially conditioned with 6mL methanol. This was repeated with a further 6mL of methanol, and then twice with 6mL distilled water. Once the cartridge had been conditioned, the extracted medium sample (Section 2.11.1) was applied, and allowed to run through into waste. The sample tubes were washed with 10mL distilled water, and this was also applied to the cartridge. Final drops from the cartridges were checked for a neutral pH, and the previous step was repeated if necessary until a neutral pH was achieved. The cartridge was then washed twice with 5mL hexane, and the eicosanoids eluted off with two washes of 3mL methanol into glass tubes. The eluted samples were dried down under nitrogen, and reconstituted into 100µL methanol: water (1:1; v,v). They were then stored at -80$^{o}$C until analysis.

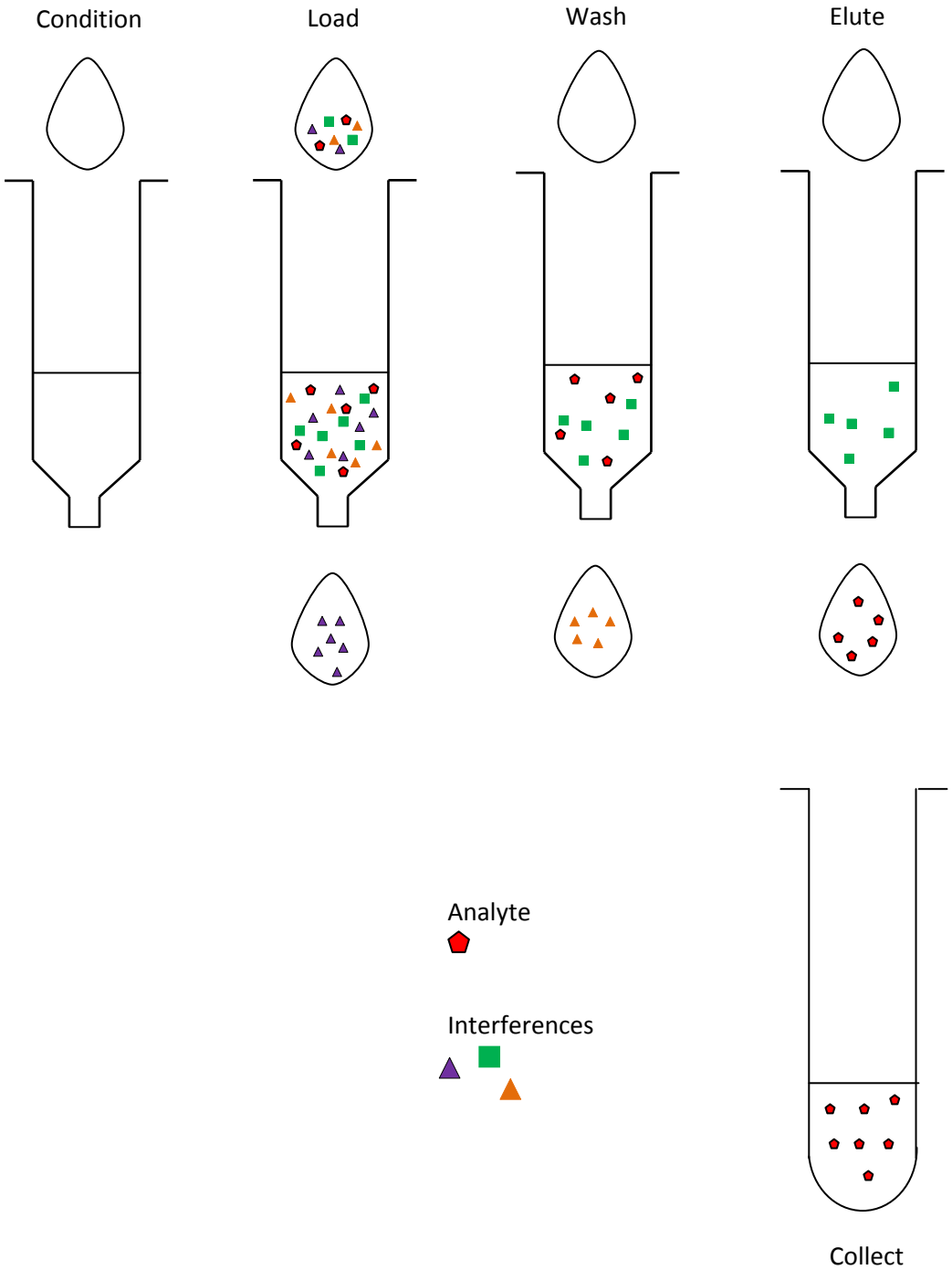


**Figure 2.11. Principles of SPE chromatography**

Schematic representation of the four stages of SPE chromatography. The first step involves conditioning the sorbent with solvent, after which, the sample is loaded onto the cartridge. This is followed by a number of washing steps to remove any undesired sample components (interferences). Finally, the analytes are eluted from the sorbent, and collected, using a suitable solvent.

### 2.11.3. LC-MS conditions

The extracted eicosanoid samples were analysed by liquid chromatography-tandem mass spectrometry (LC-MS/MS). They were analysed on a TSQ Quantum Ultra triple quadrupole mass spectrometer interfaced with a Thermo Accela UHPLC system (Thermo Scientific). The analyses were performed by Dr Benjamin Maskrey (Lipidomics Research Facility, University of the Highlands and Islands). A standard mix was run in triplicate alongside unknown samples at the following concentrations to produce a standard curve: 25, 50, 100, 200, 400 and 800 pg/mL. The standards in the mix are presented in Table 2.6.

#### *2.11.3.1. Chromatography conditions*

The eicosanoids were separated using a Hypersil Gold C18 3µm; 50mm x 2.1mm column (Thermo Scientific). The solvent gradient utilised two mobile phases with A being $H_2O$ + 10% MeOH + 0.02% Acetic acid, and B consisting of MeOH + 0.02% Acetic acid. Separations were completed over 25 min, with a flow rate of 300µL/min. The sample tray and column were held at 4$^{o}$C and 30$^{o}$C respectively. The mobile phase gradient is shown in Table 2.5:

**Table 2.5. Mobile phase gradient for targeted eicosanoid analysis by LC-MS/MS**

| *Time* | *% A* | *% B* |
|---|---|---|
| 0 | 55 | 45 |
| 10 | 40 | 60 |
| 18 | 0 | 100 |
| 21 | 0 | 100 |
| 21.1 | 55 | 45 |
| 25 | 55 | 45 |

#### *2.11.3.2. MS conditions*

The LC-MS/MS run occurred in negative ion mode, with a voltage of 2.5kV. The capillary and vaporiser temperatures were set at 250$^{o}$C and 350$^{o}$C, respectively. The sheath gas was held at 60 (arbitrary units) and the auxiliary gas at 10 (arbitrary units). A divert valve was set to go to waste for the first 90 sec, and the last 7 min, and was switched to go to the detector between these times. The collision gas used in Q2 was argon, at a pressure of 1.5mTorr. Individual eicosanoids were monitored in the multiple reaction monitoring (MRM) mode using specific precursor to product ion m/z transitions. The collision energies were optimised for each individual eicosanoid by direct infusion. The MRM transitions and respective collision energies used for eicosanoid identification are presented in Table 2.6.

Each sample set had three biological replicates which were injected once in a randomised order, with blanks and QCs being dispersed throughout the sequence run.

### 2.11.4. Quantitative data analysis of eicosanoid profiles

LCQuan v2.6 (Xcalibur, Thermo Scientific) was used to produce a standard curve for each eicosanoid present in the standard mix. These standard curves were used to automatically calculate the quantity of the eicosanoids in the unknown samples. Any concentration below the lowest standard curve point (25pg/mL) was considered to be non-detectable. An example standard curve is shown in Figure 2.12.

The intensities of the eicosanoid species present in the samples were related to the intensity of the appropriate internal standard. This was then normalised to the protein concentration of the cell.

### 2.11.5. Statistical analysis of targeted lipidomic data

A Shapiro-Wilk W test was first used to determine the normality of the data, and all targeted eicosanoid data were not normally distributed. Therefore, non-parametric tests were used, and the results presented as median ± range for a group size of three. The specific non-parametric test utilised for each experiment is indicated in the data chapters.

**Table 2.6 MRM transitions and CE used for eicosanoid identification**

| Compound | Precursor | Product | CE |
|---|---|---|---|
| ***Internal standards:*** | | | |
| 15(S)-HETE-d8 | 327.2 | 226.2 | 16 |
| $LTB_4$-$d_4$ | 339.2 | 197.2 | 17 |
| $PGE_2$-$d_4$ | 355.2 | 193.2 | 21 |
| ***Mono-hydroxy:*** | | | |
| 5-OxoETE | 317.2 | 203.2 | 23 |
| 15(S)-HETE | 319.2 | 175.3 | 17 |
| 5-HETE | 319.2 | 115.2 | 18 |
| 12(S)-HETE | 319.2 | 179.3 | 16 |
| 20-HETE | 319.2 | 245.2 | 17 |
| 5, 6 EET | 319.2 | 191.3 | 15 |
| 8, 9 EET | 319.2 | 151.2 | 15 |
| 14, 15 EET | 319.2 | 175.3 | 17 |
| 14, 15 dHET | 337.2 | 207.2 | 19 |
| ***Di-hydroxy:*** | | | |
| $LTB_4$ | 335.2 | 195.1 | 18 |
| ***Tri-hydroxy:*** | | | |
| 6-keto $PGF_{1\alpha}$ | 369.2 | 245.1 | 28 |
| Thromboxane $B_2$ | 369.2 | 169.2 | 20 |
| 20-OH $LTB_4$ | 351.2 | 195.2 | 20 |
| 11β-$PGF_{2\alpha}$ | 353.2 | 193.2 | 27 |
| $PGF_{2\alpha}$ | 353.2 | 193.2 | 27 |
| $PGD_2$ | 351.2 | 233.2 | 16 |
| $PGE_2$ | 351.2 | 189.2 | 22 |

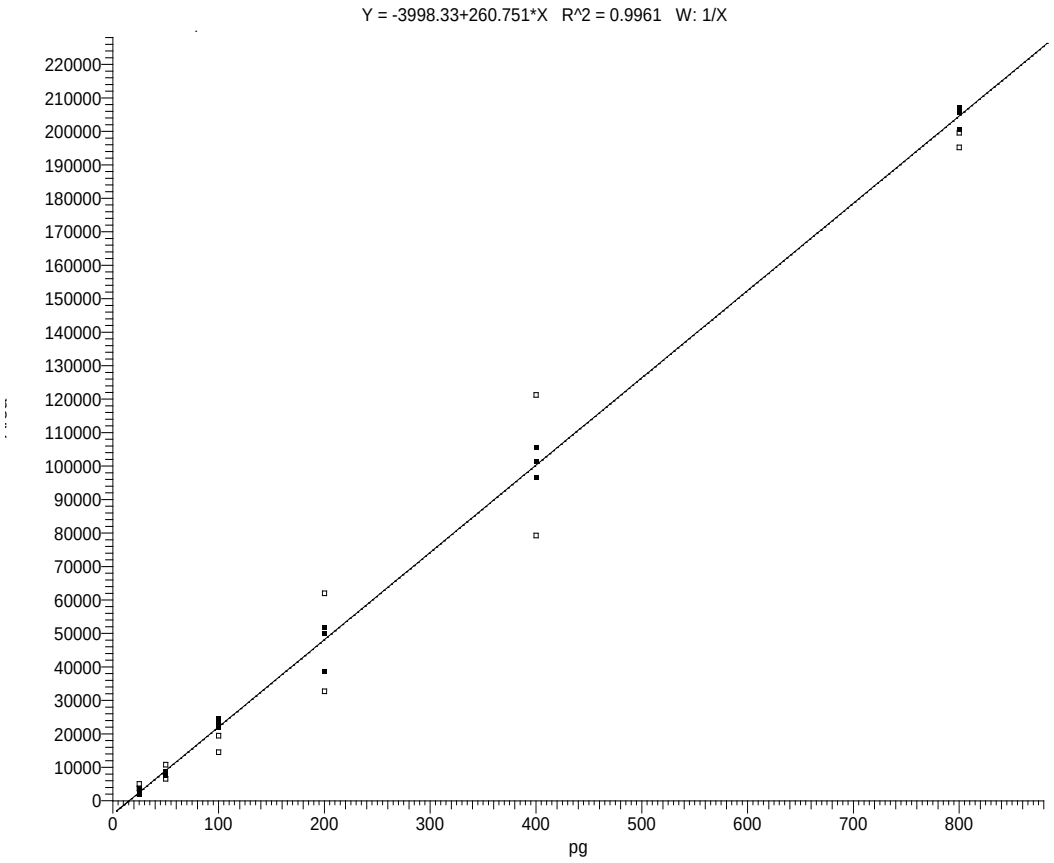


**Figure 2.12. Eicosanoid standard curve**

This figure illustrates a typical standard curve generated by the dilution of each eicosanoid present in the standard mix. The software produced a standard curve of the concentration of the eicosanoid compared to the area of the peak. A line of best was automatically plotted and used to calculate the eicosanoid concentration in each sample based on its peak area.

# CHAPTER 3

## Validation of a model of adipogenesis: Application of lipidomic analyses to this model

### 3.1. INTRODUCTION

A major role of white adipose tissue (WAT) is the storage of triglycerides (TG). An increase in TG storage is caused by a positive energy balance, which if left to continue would lead to increased adiposity, and eventually obesity. The increase in WAT mass is due to hypertrophy of mature white adipocytes, and/or hyperplasia, with hypertrophy often occurring first (Johnson *et al*., 1971; Faust *et al*., 1978; Johnson *et al*., 1978). Hypertrophy is a complex process which increases the number of mature adipocytes by the differentiation of pre-adipocytes, and is also termed adipogenesis. A detailed account of adipogenesis is outlined in Section 1.2.3, and a summary of the factors involved, and differentiation markers expressed are presented in Table 1.3.

Research into adipocyte development has been facilitated by the use of clonal cell lines, including two commonly used murine cell lines, 3T3-L1 and 3T3-F442A. The work described in this thesis has been completed using the 3T3-L1 cell line, which is a derivative of the 3T3 mouse fibroblast cell line, developed by Green and colleagues (Green and Meuth, 1974; Green and Kehinde, 1975). This cell line was chosen because it has been extensively characterised.

The process of adipogenesis is complex, involving many factors and the expression of differentiation markers. Two late markers of differentiation are the adipokines leptin and adiponectin, and the gene expression and secretion of both has been thoroughly documented. As described in Section 1.3.1, leptin is primarily expressed in and secreted by adipocytes, and plasma concentrations of this protein are positively correlated with adiposity in both humans, and rats (Maffei *et al*., 1995; Considine *et al*., 1996). In terms of adipocyte differentiation, a previous study has demonstrated that leptin gene expression was present in differentiated 3T3-L1 adipocytes from day three onwards, and this gene expression increased as the adipocytes became fully mature. Leptin gene expression; however, was not present in the pre-adipocyte stage (MacDougald *et al*., 1995). The study also found that the leptin gene expression in adipocytes was much less than that present in WAT, suggesting that WAT may have access to factors which upregulate the gene expression of leptin.

Adiponectin is exclusively produced by mature adipocytes (Ouchi *et al*., 1999) and, like leptin, not during the pre-adipocyte stage. However, unlike leptin, circulating concentrations of adiponectin are decreased in obesity (Arita *et al*., 1999). A previous study found adiponectin to be involved in pre-adipocyte proliferation and differentiation, as well as lipid accumulation in mature adipocytes, with over-expression of the protein augmenting these processes (Fu *et al*., 2005). The gene expression of various markers of differentiation were measured in response to an over-expression of adiponectin, and during differentiation, a prolonged gene expression of both PPARγ and C/EBPα occurred (Fu *et al*., 2005). The ADD1/SREBP1c gene also appears to have a role in adipocyte differentiation, with a previous study demonstrating that the expression of this gene increases as cultured pre-adipocytes begin differentiation (Kim and Spiegelman, 1996). Over-expression of adiponectin in 3T3-L1 cells lead to an increase in the gene expression of ADD1/SREBP1c (Fu *et al*., 2005), indicating a role for adiponectin in adipogenesis.

The major process involved in adipogenesis is TG accumulation, and shortly after the development of the 3T3-L1 murine pre-adipocyte cell line, these cells were used to monitor lipid accumulation during differentiation (Mackall *et al*., 1976). TG accumulation was detected from as early as three days after confluence and, by day 14, over 80% of the cells had lipid droplets, seen by Oil Red O staining. Six days after confluence *de novo* lipogenesis (DNL) also increased, leading to the conclusion that the increase in TG accumulation was associated with increased DNL (Mackall *et al*., 1976). Lipogenesis involves the processes of FA synthesis, and their esterification with glycerol to form TGs. Before the formation of TGs, elongation or desaturation of FAs is necessary, and both of these events induce lipogenesis in mice (Sampath *et al*., 2007).

Another metabolic pathway involved in adipogenesis is that of eicosanoid production (Madsen *et al*., 2003). A previous study has found that the certain products of the cyclooxygenase (COX) pathway play a role in adipocyte differentiation. Prostaglandin (PG)$D_2$ was shown to be formed during the maturation phase, as was $PGE_2$, although greater formation of this eicosanoid occurred in pre-adipocytes. Finally, $PGF_{2\alpha}$ had an opposing effect; it was seen to inhibit differentiation by reducing triglyceride accumulation (Lu *et al*., 2003).

### 3.1.2. Aims of the current study

The work described in this chapter aimed to investigate lipid metabolism processes occurring within the 3T3-L1 cell-line and monitor any changes over the course of differentiation. The first specific aim was to validate the 3T3-L1 cell-line as a model of adipogenesis. A wealth of previous work has demonstrated both morphological changes (Green and Kehinde, 1974) and also differences in the gene expression of the adipokines leptin and adiponectin (MacDougald *et al*., 1995; Ouchi *et al*., 1999) occurring during the differentiation process. It was predicted that similar findings would be observed in the current study, thereby acting as a validation for the correct behaviour of these cells.

Once validated, the second part of the current study focussed on using lipidomic analyses to investigate lipid metabolism during adipogenesis. The second specific aim was to determine whether the differentiation process caused altered global lipidomic profiles of 3T3-L1 adipocytes, particularly in terms of identifying individual lipid species present at each stage, and monitoring any changes in their concentration.

The final specific aim of the current study was to examine whether 3T3-L1 cells produced arachidonic acid (AA)-derived eicosanoid species, and if so, observe whether the concentrations of these eicosanoids changed over the course of differentiation.

## 3.2 MATERIALS AND METHODS

### 3.2.1. Cell culture

3T3-L1 cells were cultured at 37$^{o}$C in a humidified atmosphere of 5%$CO_2$ / 95% air, as previously described in Section 2.1.3. The compositions of all media are outlined in Section 2.1.2. The cells were harvested as described in Section 2.1.3 on the following days post-differentiation: 0-10, 12, 15, 18, 20, 22 and 25. In the current study, the time-course of differentiation was extended until day 25, with the aim to determine whether these cells just continue to mature and accumulate lipid, or adopt a different phenotype. The cells were synchronised by starving of CS for 24 hours (h) before collection and therefore feeding with DMEM alone. Both the cells and medium were collected and stored at -80$^{o}$C until needed.

### 3.2.2. Oil Red O and haematoxylin staining

One well per plate was stained with Oil Red O and haematoxylin, as described in Section 2.2.2, and images of the different time points were captured.

### 3.2.3 Reverse transcription PCR and Real-time PCR

Total RNA was extracted from harvested cells using TRI Reagent® as described in Section 2.4.2. The genes investigated in this study were leptin and adiponectin, with a group size of six.

### 3.2.4. Enzyme-linked Immunosorbent Assay

Leptin and adiponectin protein concentrations were analysed in the harvested cell culture medium using an Enzyme-linked Immunosorbent Assay (ELISA) kit specific to each, as described in Section 2.7.2. The standards were assayed in duplicate, and each time point had a group size of three. The optical density was read at 450nm.

### 3.2.5. Global lipidomics

#### *3.2.5.1. Cell preparation*

Lipids were extracted from cell samples using the Folch extraction method (Folch *et al*., 1957) as described in Section 2.10.2, and the lower chloroform phase was dried down under nitrogen, and reconstituted in 600µL chloroform / methanol (2/1, v/v). Three biological replicates were prepared for each sample, and 10mM of ammonium formate was added to each sample before direct infusion-mass spectrometry (DI-MS) analysis, but not liquid chromatography-mass spectrometry (LC-MS) analysis.

#### *3.2.5.2. DI-MS method*

The lipid extracts were directly infused into an Orbitrap Exactive mass spectrometer in both positive and negative ion mode as described in Section 2.10.4. One technical replicate of each sample, along with quality control (QC) samples were analysed. Selected lipid peaks were quantified using an appropriate internal standard, either: 1,2-didodecanoyl-*sn*-glycero-3-phosphocholine, PC (12:0/12:0); or, 1,2,3-trioctadecanoyl-sn-glycerol, TG (18:0/18:0/18:0), both of which were added at 1nmol concentration. These had a mass-to-charge ratio (m/z) of 622.4436 and 908.8629, respectively in positive ion mode. These values were then normalised to the protein concentration of the cell samples. Various databases were used to identify lipid species, including the Human Metabolome Database (HMDB; www.hmdb.ca), LIPID Metabolites and Pathways Strategy (LIPID MAPS; www.lipidmaps.org), and the Metabolite and Tandem MS Database (METLIN; http://metlin.scripps.edu). Confident identifications were assumed when the mass error was within 5 parts per million (ppm), and all mentioned identifications are within this error, unless stated.

#### *3.2.5.3. LC-MS method*

Lipid extracts were analysed by liquid chromatography-mass spectrometry (LC-MS) as described in Sections 2.10.6.2 and 2.10.6.3. Three biological replicates were analysed per time point, with one technical replicate each, along with three quality control (QC) samples.

#### *3.2.5.4. LC-MS data processing and multivariate data analysis*

All LC-MS raw files were processed using SIEVE v1.3 to produce m/z, retention time (RT) and intensity values. Three different RT windows were investigated, 1 minute (min), 30 seconds (sec) and 15 sec. Lipids were identified using the databases mentioned above in either positive or negative ion mode, with the parameter for confident identifications being 5ppm.

The RT and m/z pairs, along with their associated intensities, were manually normalised to the total ion current (TIC) intensity. Both the non- and TIC-normalised datasets were then imported into SIMCA-P v12 for multivariate data analysis, including the unsupervised principal component analysis (PCA), and supervised partial least squares (PLS). PLS was chosen due to the number of samples, and the fact that the y-variables are continuous. All models were Pareto scaled and both the scores and loadings plot were analysed.

### 3.2.6. Targeted eicosanoid analysis

Solid phase extraction chromatography was used to extract eicosanoid lipids from the 3T3-L1 medium samples (Section 2.9.3.1). The extracted eicosanoid samples were then analysed by LC-MS/MS as outlined in Sections 2.11.1 and 2.11.2.1. Individual eicosanoids were identified using specific precursor-to-product ion m/z transitions, as detailed in Table 2.3 (Chapter 2).

### 3.2.7. Statistical analysis

A Shapiro-Wilk W test was used to determine whether the samples were normally distributed. All mass spectrometry data (direct infusion and eicosanoid) were not normally distributed. For qPCR analyses, even though the data were normally distributed, a non-parametric test was used. It has been suggested that qPCR statistical analyses should be undertaken using non-parametric tests (Yuan *et al*., 2006). Therefore, all data in this study were analysed using the non-parametric Cuzick's test for trend (Cuzick, 1985). The data were presented as mean values ± SD for the normally distributed qPCR data, and as median ± range for non-normally distributed mass spectrometry data. The group size is mentioned in the figure captions, and a *P*-value of $< 0.05$ was considered statistically significant.

## 3.3. RESULTS – PART A; VALIDATION OF THE 3T3-L1 PRE-ADIPOCYTE CELL LINE ADIPOGENESIS MODEL

### 3.3.1. Morphological changes during adipocyte differentiation

The most obvious change that occurred during the differentiation process from pre-adipocyte to adipocyte was morphological. At induction, the cells had a fibroblast-like appearance and as differentiation continued, they began to accumulate lipid droplets. By terminal differentiation, the cells had taken on the characteristic spherical appearance of a mature adipocyte. Oil Red O stained images of 3T3-L1 cells across a full time course from day 0 to day 25 post-differentiation are presented in Figure 3.1. Lipid droplets were noticeable at day 5 post-differentiation, and continued to be accumulated until day 25.

### 3.3.2. Gene expression and secretion of leptin and adiponectin during adipogenesis

The presence or absence of leptin and adiponectin gene expression was determined by reverse transcription-PCR (RT-PCR; Figure 3.2). Both were compared to β-actin (A), which was expressed throughout the course of differentiation, as would be expected of a housekeeping gene. Leptin was detected from day 4, and adiponectin from day 1 post-differentiation (B and C, respectively). The PCR cycle numbers were 25, 32 and 26 for β-actin, leptin and adiponectin, respectively.

The gene expression of both leptin and adiponectin was then quantified by real-time PCR (qPCR) as illustrated in Figures 3.3 and 3.4, respectively. Three housekeeping (HK) genes were used: β-actin, GAPDH and RNApol2 and the gene expression of leptin with all three is represented in Figure 3.3. Both β-actin and GAPDH (A and B, respectively) produced similar profiles, although the relative fold changes were greater with GAPDH. A very different profile was associated with RNApol2 (C); however, some similarities existed. A trend of leptin gene expression was observed with all HK genes ($P$<0.0001 for all; 2 sided); as the day post-differentiation increased, so did leptin gene expression. This was true until the end of the time course where a decrease in leptin gene expression was observed with all HK genes, especially at day 25 post-differentiation. The fold changes associated with the use of RNApol2 as the HK genes were approximately three, and 25 times greater than GAPDH and β-actin, respectively.

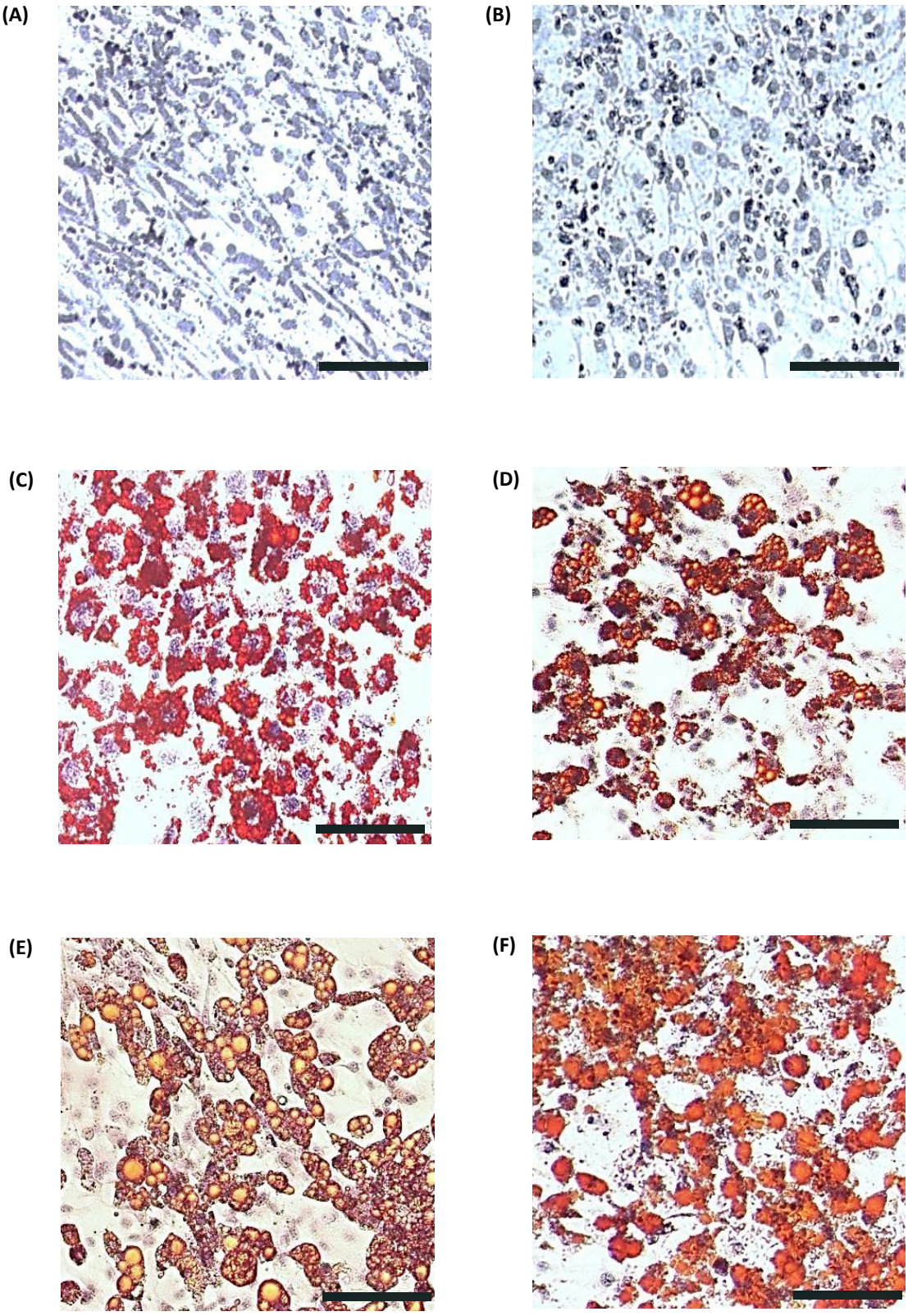


**Figure 3.1 Morphological changes during adipogenesis of 3T3-L1 cells**
Representative images of Oil Red O stained 3T3-L1 cells during the course of differentiation. The images represent cells induced to differentiate at day 0, and cultured at the following times post-differentiation; (A) 0 (B) 5 (C) 10 (D) 15 (E) 20 and (F) 25. A clear change is seen from a fibroblast pre-adipocyte at day 0, to spherical, lipid loaded mature adipocytes from day 10 onwards, with lipid accumulation continuing until day 25. The scale bars represent 100µm.

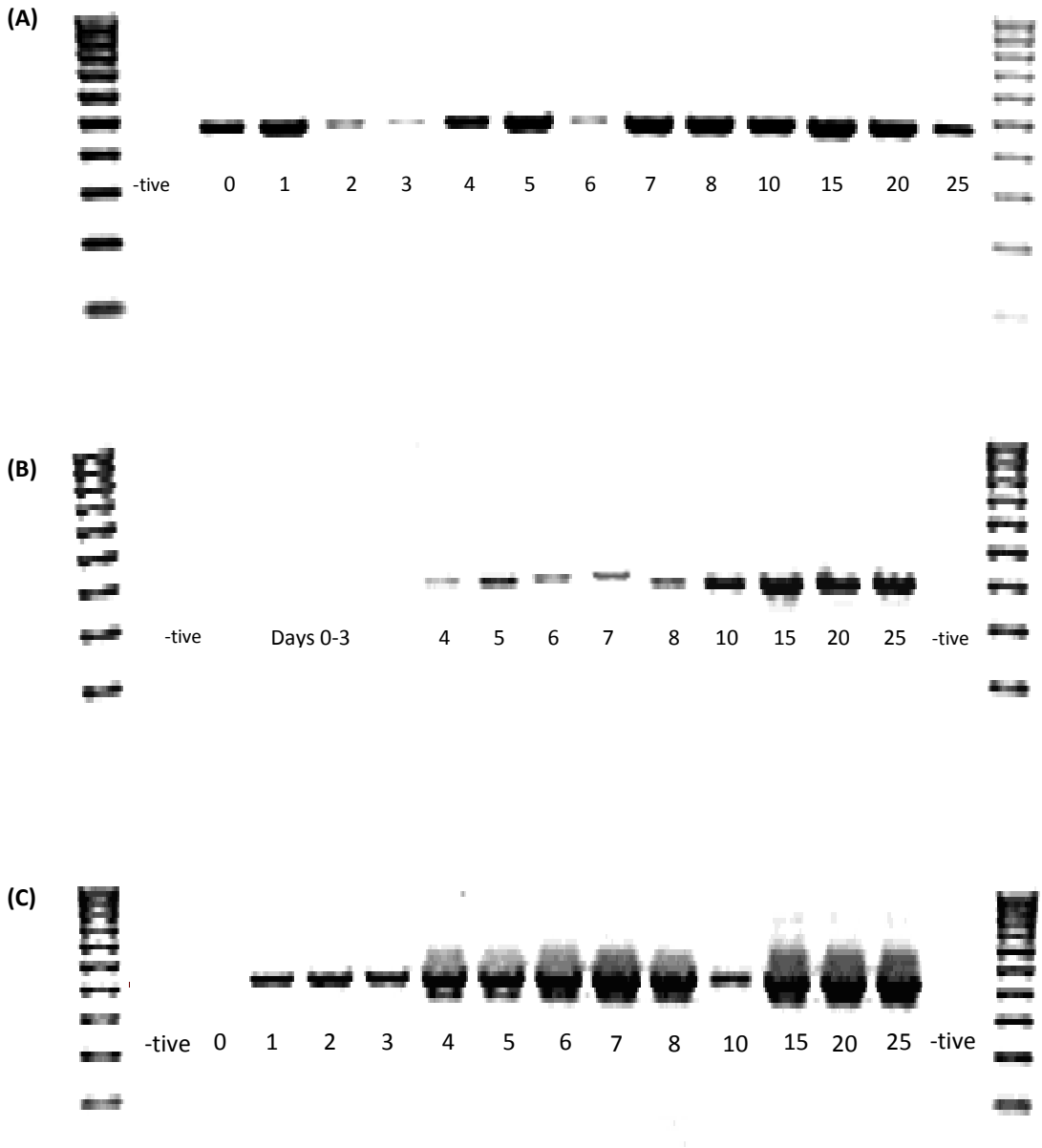


**Figure 3.2. Gene expression of leptin and adiponectin in 3T3-L1 cells during adipogenesis**
Representative RT-PCR gels of 3T3-L1 adipocytes collected at various time points after the induction of differentiation into adipocytes (days 0-8, 10, 15, 20, 25). Total RNA was extracted and gene expression of β-actin (A), leptin (B) and adiponectin (C) was determined using mouse specific primers. A negative control was run alongside the samples, which contained only the PCR mix (labelled as –tive). The gene expression of β-actin was seen throughout the whole time course, whereas that of leptin and adiponectin only occurred from day 4 and day 1 post-differentiation onwards, respectively. Amplification cycle numbers were: β-actin, 25; leptin, 32 and adiponectin, 26.

Adiponectin gene expression profiles are shown in Figure 3.4 and they appeared to vary depending on the HK gene was used. As with leptin gene expression, the use of RNApol2 (C) greatly altered the profile of adiponectin gene expression over the time course, and produced the greatest fold changes, with an approximate 9 fold, and 7 fold increase when compared to the profiles of β-actin and GAPDH (A and B, respectively). All HK genes; however, also produced a trend in adiponectin gene expression ($P$<0.0001 for all; 2 sided).

The secretion of both leptin and adiponectin was detected in cell culture medium from the differentiated adipocytes using an ELISA kit specific to each protein. The evolution of their secretion by 3T3-L1 cells is shown in Figure 3.5 (A and B for leptin and adiponectin, respectively). As expected from the qPCR data, a trend was also observed in the secretion of both proteins ($P$<0.001 for both; 2 sided), in that they were only secreted once the adipocytes had begun the terminal differentiation process and, after an initial increase, their secretion declined as the cells continued to mature. Adiponectin was secreted at much greater concentrations, roughly 1000 times that of leptin at their peak (units of measurement in ng/mL *vs.* pg/mL).

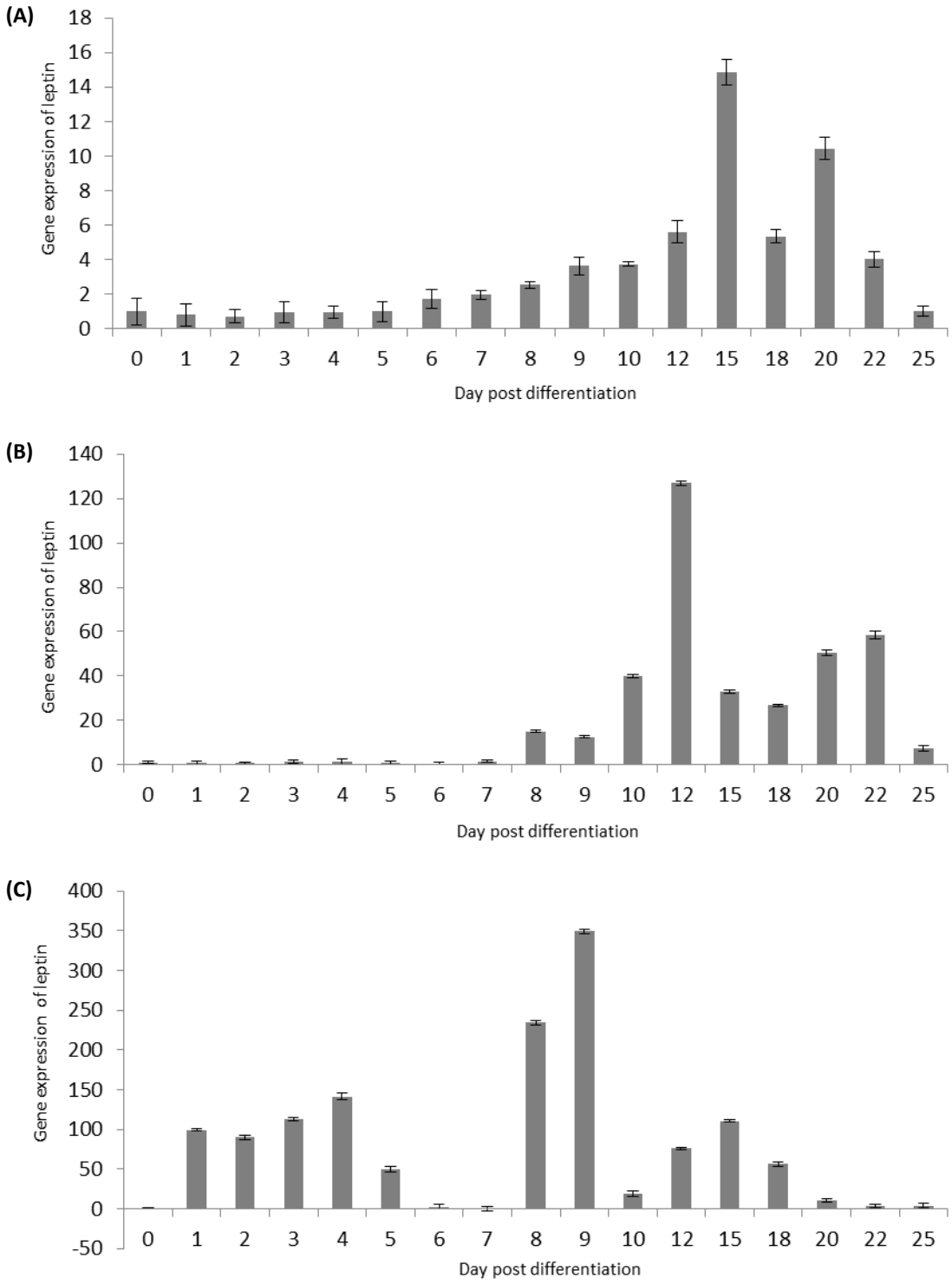


**Figure 3.3. Gene expression of leptin in 3T3-L1 cells during adipogenesis** 3T3-L1 adipocytes were collected on the following days post differentiation: 0-10, 12, 15, 18, 20, 22, and 25. For all, total RNA was extracted, and leptin expression investigated and normalised to day 0 by qPCR, using (A) β-actin, (B) GAPDH, and (C) RNApol2 as the housekeeping gene. For each time point, n=6, with results represented as mean ± SD. An increase in leptin gene expression was seen from approximately day 8 post-differentiation with the use of both β-actin and GAPDH as the housekeeping gene. The leptin gene expression profile was different when RNApol2 was used as the housekeeping gene, with an increase in leptin gene expression occurring from day 1. A 2-sided Cuzick's test for trend was applied, and a trend in leptin gene expression was observed with all three housekeeping genes ($P$<0.0001 for all).

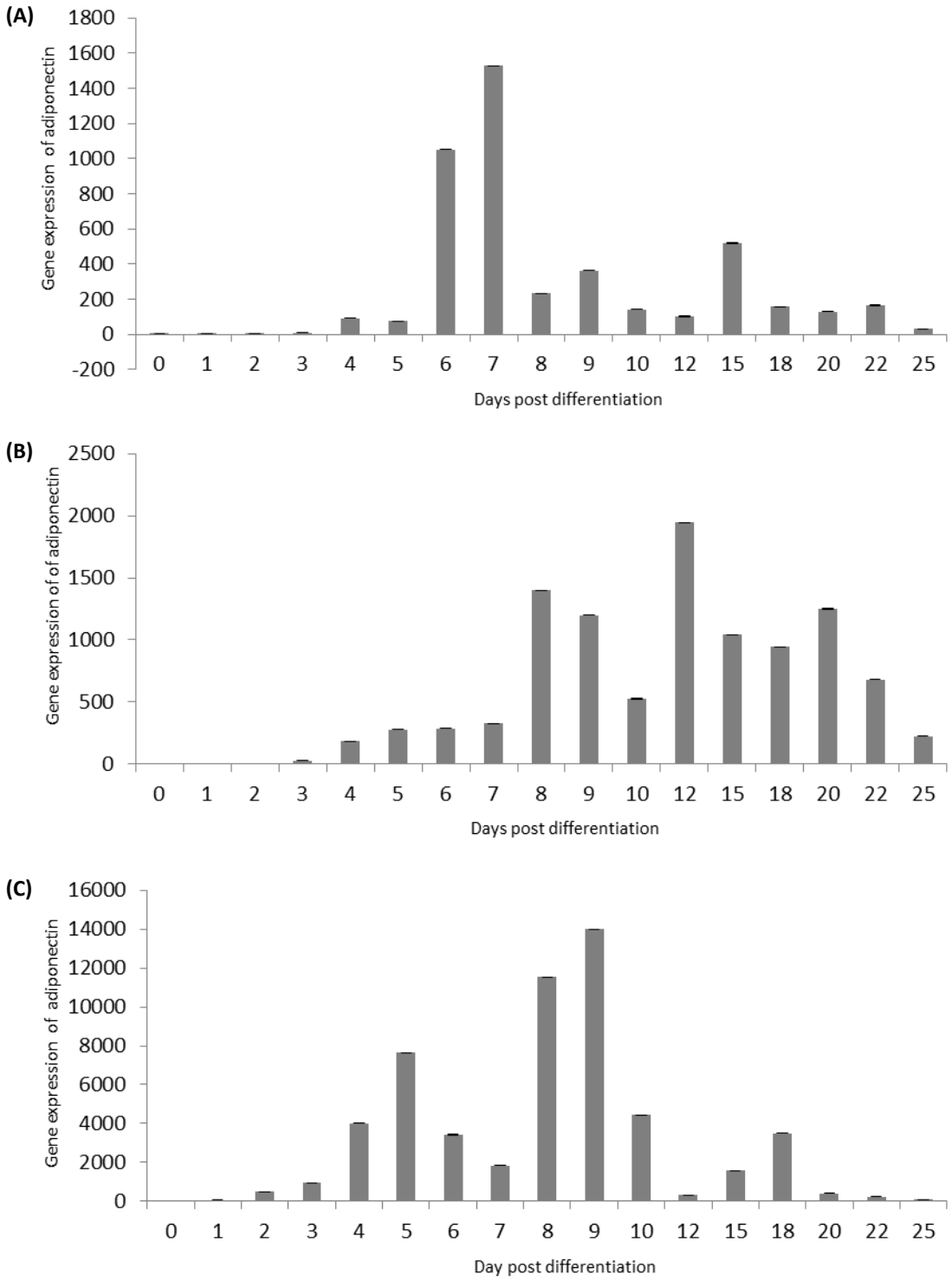


**Figure 3.4. Gene expression of adiponectin in 3T3-L1 cells during adipogenesis** 3T3-L1 adipocytes were collected on the following days post differentiation: 0-10, 12, 15, 18, 20, 22, and 25. For all, total RNA was extracted, and adiponectin expression investigated and normalised to day 0 by qPCR, using (A) β-actin, (B) GAPDH, and (C) RNApol2 as the housekeeping gene. For each time point, n=6, with results represented as mean ± SD. An increase in adiponectin gene expression was seen from approximately day 4 post-differentiation with the use of all three housekeeping genes. A 2-sided Cuzick's test for trend was applied, and a trend in adiponectin gene expression was observed with all three housekeeping genes ($P$<0.0001 for all).

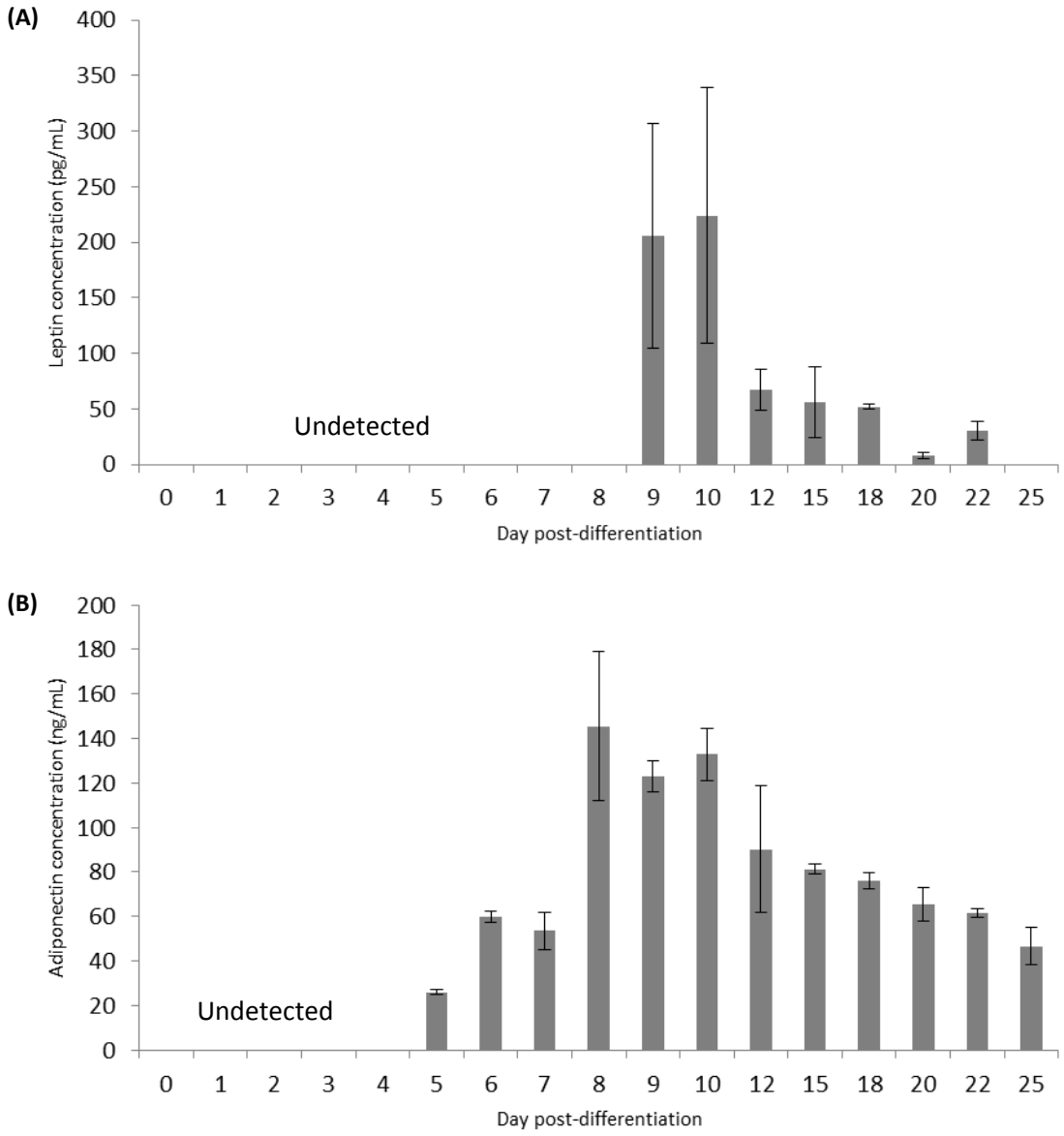


**Figure 3.5. Protein secretion of leptin and adiponectin from 3T3-L1 cells during adipogenesis** The protein levels of both leptin (A in pg/mL) adiponectin (B in ng/mL) over the course of differentiation were determined using a mouse ELISA kit specific for each. The results show actual concentrations present in the medium at each time point. Results are represented as medium ± range for a group size of three at each time point. Secretion of leptin was detected from day 9 post-differentiation, whereas this occurred at the earlier time point of day 5 for adiponectin secretion. A decrease in protein secretion was seen from day 12 post-differentiation until the end of the time course for both leptin and adiponectin. A 2-sided Cuzick's test for trend found a trend for both proteins ($P < 0.0001$ for both).

## 3.4. RESULTS – PART B; LIPIDOMIC ANALYSIS OF THE 3T3-L1 MODEL OF ADIPOGENESIS

### 3.4.1. DI-MS analysis

The time course of the global lipid profiles of 3T3-L1 adipocytes from the day of induction (day 0) to day 25 post-differentiation were analysed by DI-MS in both positive (Figure 3.6) and negative (Figure 3.7) ion modes. Both figures show representative spectra of days 0, 5, 10, 15 and 25 post-differentiation.

#### *3.4.1.1. Positive ion DI-MS analysis*

In positive ion mode, an obvious change in the lipid profile of the 3T3-L1 cells was seen over the course of differentiation. At day 0, only a few lipid species were present, and the most abundant had m/z between 700 and 850. These lipids were identified as either phospholipid or sphingomyelin (SM) species. From day 5 post-differentiation until the end of the time course, there was an increase in the number of lipid species present. The most abundant were seen with m/z between 500 and 600, and also 750-900Da. The majority of these lipid species were identified as either phospholipids or TGs.

Identifications of lipid species based on their m/z in positive ion mode are presented in Table 3.1. The top ten abundant lipid species at day 0 (A), and day 25 (B) are shown. At day 0, these were all phosphatidylcholine (PC) species, including: PC (32:0), (34:2), (34:1), (36:4), (36:3), (36:2), (38:4), with the one exception being SM (34:1). The two internal standards, PC (12:0/12:0) and TG (18:0/18:0/18:0) were also present. By day 25, the most abundant lipid species present were all TG species, and they were: TG (46:1), (47:2), (47:1), (48:2), (48:1), (49:2), (49:1), (50:3), (50:2). One diglyceride (DG) identification was also suggested, which was DG (31:3); however, its mass accuracy (ppm=65.487) fell outside of the set parameter of 5ppm, and so this was not certain.

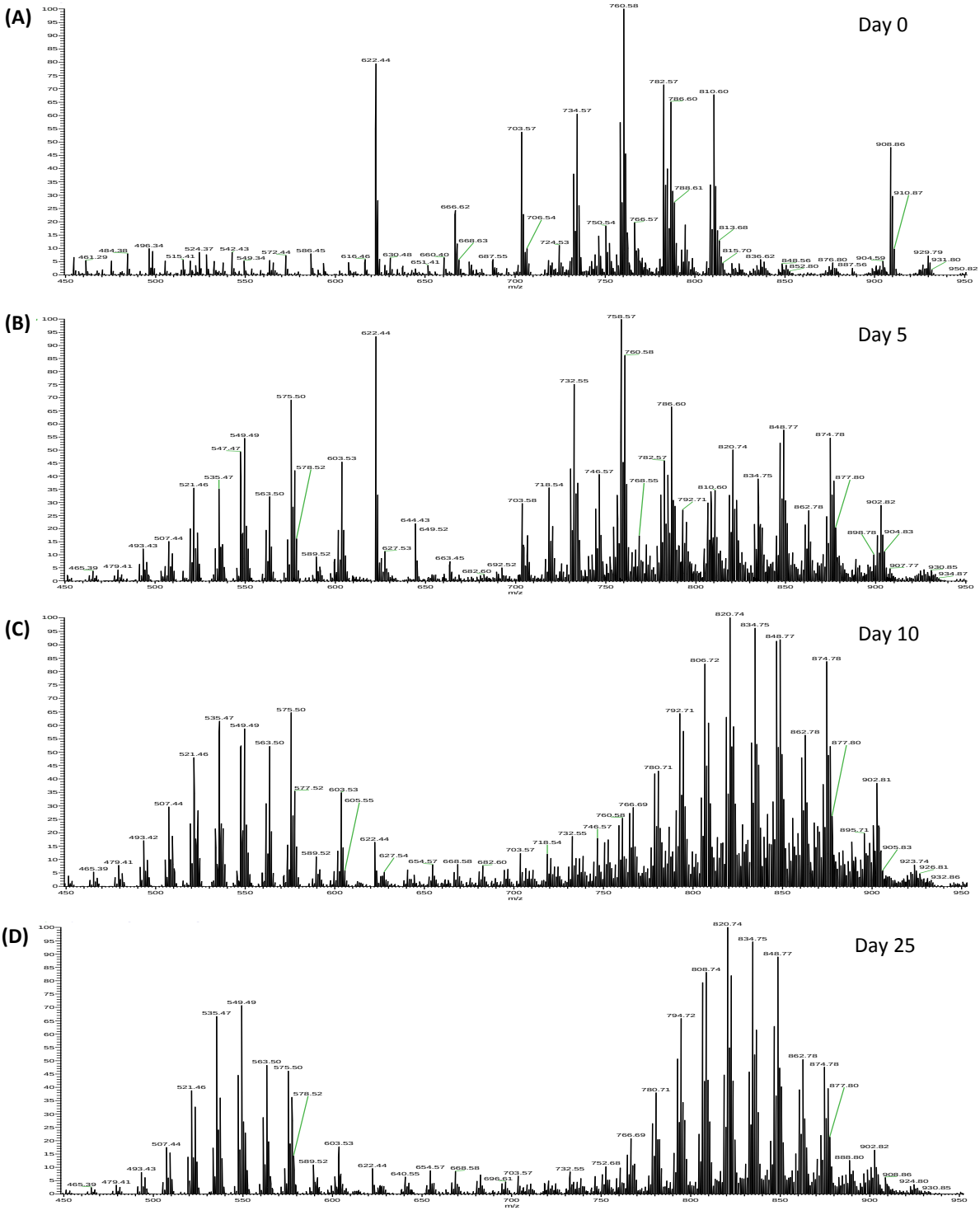


**Figure 3.6. Positive ion DI-MS analysis of 3T3-L1 cells during adipogenesis** Representative spectra of 3T3-L1 adipocytes were induced at day 0, and harvested at the following time points post-differentiation: 0 (A); 5 (B); 10 (C); 15 (D) and 25 (E). Lipids were extracted from the cell samples using a Folch extraction. The lower phase was dried down under nitrogen and reconstituted in 600µL chloroform/methanol (2/1, v/v). A 150µL aliquot was removed and had 10mM ammonium formate added to it. The samples were then directly infused into an Orbitrap Exactive mass spectrometer at a flow rate of 5µL/min for 90 sec (450 scans) in positive ion mode. The m/z range analysed was between 100 and 1000Da, and the current figure represents m/z between 450 and 950Da. A clear shift in the global lipid profiles was seen, with a few peaks with m/z between 700 and 850Da being observed at day 0. In the remaining time points, more peaks were present, and these were mainly seen at m/z 400-500 and 750-900Da.

| Calculated mass | Theoretical mass | Δ Mass accuracy (ppm) | Ion | Elemental composition | Identification |
|---|---|---|---|---|---|
| ***(A) Day 0*** | | | | | |
| 622.4436 | 622.4442 | -0.964 | $[M+H]^+$ | $C_{32}H_{64}NO_8P$ | PC (24:0) |
| 703.5744 | 703.5748 | 0.569 | $[M+H]^+$ | $C_{39}H_{79}N2O_6P$ | SM (34:1) |
| 734.5685 | 734.5694 | 1.225 | $[M+H]^+$ | $C_{40}H_{80}NO_8P$ | PC (32:0) |
| 758.5686 | 758.5694 | 1.055 | $[M+H]^+$ | $C_{42}H_{80}NO_8P$ | PC (34:2) |
| 760.5843 | 760.5850 | 0.920 | $[M+H]^+$ | $C_{42}H_{82}NO_8P$ | PC (34:1) |
| 782. 5683 | 782.5694 | 1.406 | $[M+H]^+$ | $C_{44}H_{80}NO_8P$ | PC (36:4) |
| 784. 5826 | 784.5851 | -3.186 | $[M+H]^+$ | $C_{44}H_{82}NO_8P$ | PC (36:3) |
| 786.5997 | 786.6007 | 1.271 | $[M+H]^+$ | $C_{44}H_{84}NO_8P$ | PC (36:2) |
| 810.5991 | 810.6007 | 1.974 | $[M+H]^+$ | $C_{46}H_{84}NO_8P$ | PC (38:4) |
| 908.8629 | 908.8641 | -1.320 | $[M+NH_4]^+$ | $C_{57}H_{110}O_6$ | TG (54:0) |

***(B) Day 25***

| | | | | | |
|---|---|---|---|---|---|
| 549.4872 | 549.4513 | 65.487 | $[M+NH_4]^+$ | $C_{34}H_{60}O_5$ | DG (31:3) |
| 794.7225 | 794.7232 | -0.881 | $[M+NH_4]^+$ | $C_{49}H_{92}O_6$ | TG (46:1) |
| 806.7233 | 806.7232 | 0.124 | $[M+NH_4]^+$ | $C_{50}H_{92}O_6$ | TG (47:2) |
| 808.7378 | 808.7388 | 1.484 | $[M+NH_4]^+$ | $C_{50}H_{94}O_6$ | TG (47:1) |
| 820.7379 | 820.7389 | 1.097 | $[M+NH_4]^+$ | $C_{51}H_{94}O_6$ | TG (48:2) |
| 822.7532 | 822.7545 | 1.580 | $[M+NH_4]^+$ | $C_{51}H_{96}O_6$ | TG (48:1) |
| 834.7583 | 834.7545 | 4.552 | $[M+NH_4]^+$ | $C_{52}H_{96}O_6$ | TG (49:2) |
| 836.7682 | 836.7702 | 1.767 | $[M+NH_4]^+$ | $C_{52}H_{98}O_6$ | TG (49:1) |
| 846.7536 | 846.7545 | 1.063 | $[M+NH_4]^+$ | $C_{53}H_{96}O_6$ | TG (50:3) |
| 848.7686 | 848.7701 | -1.767 | $[M+NH_4]^+$ | $C_{53}H_{98}O_6$ | TG (50:2) |

**Table 3.1. Identifications of selected positive ions from 3T3-L1 cells at day 0 and 25 post-differentiation**

Abbreviations used: DG, diglyceride; PC, phosphatidylcholine; SM, sphingomyelin; TG, triglyceride

These identified lipid species from Table 3.1 were quantified using the relevant internal standard, either PC (12:0/12:0) with m/z 622.4436 or TG (18:0/18:0/18:0) at m/z 908.8629, and then normalised to the protein content of the sample. The top two concentrated species from day 0 and the top three from day 25 post-differentiation were chosen, and presented graphically in Figure 3.7. The two selected from day 0 had m/z 760.5843 and 782.5683, and were identified as PC (34:1) and PC (36:4), respectively. Their concentration was greatest between days 0 and 2 post-differentiation. By day 3, their concentration decreased and remained at a lesser concentration in the rest of the time points ($P$<0.01 for both; 2-sided). At day 7, three TG species (48:2, 49:2 and 50:2) were the most concentrated in the samples, and their concentration continued to increase throughout the remainder of the time course ($P$<0.0001 for all; 2 sided).

#### *3.4.1.2. Negative ion DI-MS analysis*

The number of lipid species detected in negative ion mode (Figure 3.8) was less than that in positive ion mode, and fewer changes were observed across the course of differentiation. At day 0, the most abundant lipid species present had m/z between 250 and 350Da, in particular 311.17, 325.18 and 339.19. These peaks were thought to relate to linear alkylbenzenesulfonates (Andreu and Pico, 2004), which are commonly used as surfactants in detergents, and therefore contaminants. Due to this, these ions were excluded from all data analysis.

The profiles for days 5, 10 and 15 post-differentiation were all the same in regards to the m/z of the top three most abundant species, which were: 253.2175, 281.2488 and 303.2331. These were identified as the fatty acids C16:1, C18:1 and C20:4, respectively. At day 25, these three lipids were still present, along with another species with m/z 301.2176, which was the most concentrated at this time point, and identified as C20:5.

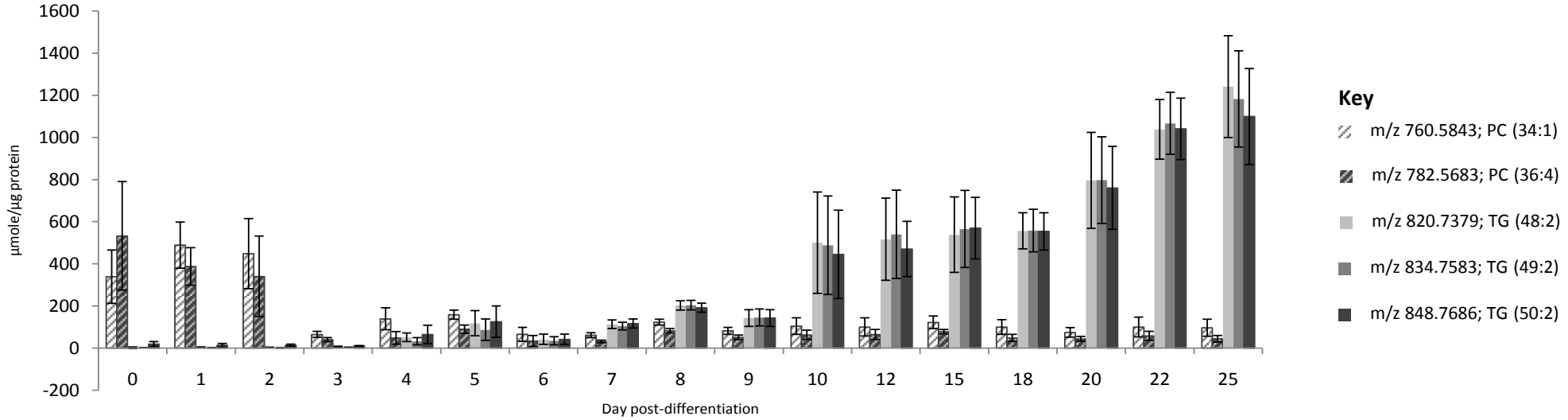




**Figure 3.7. Concentration of individual lipid species during adipogenesis of 3T3-L1 cells from positive ion DI-MS analysis**
3T3-L1 cells were induced to differentiate at day 0, and harvested at the following time points: 0-10, 12, 15, 18, 20, 22 and 25. Lipids were extracted from the cell samples using a Folch extraction. The lower phase was dried down under nitrogen and reconstituted in 600µL chloroform/methanol (2/1, v/v). A 150µL aliquot was removed and had 10mM ammonium formate added to it. The samples were then directly infused into an Orbitrap Exactive mass spectrometer at a flow rate of 5µL/min for 90 sec (450 scans) in positive ion mode.

The selected phospholipid species were quantified using the PC internal standard, PC (12:0/12:0) with m/z 622.4443; and TG species using TG (18:0/18:0/18:0) at m/z 908.86. The selected lipids are shown in the key, and for each time point, n=3, with results represented as median ± range. The concentration of the two phospholipid species was the greatest in the pre-adipocytes (days 0-6 post-differentiation). By day 7, the three triglycerides were the most concentrated. A Cuzick's 2-sided trend test was applied to each lipid species over the time course, and $P$=0.0009 and 0.0024 for PC (34:1) and PC (36:4), respectively. For the TG species, $P$<0.0001 for all.

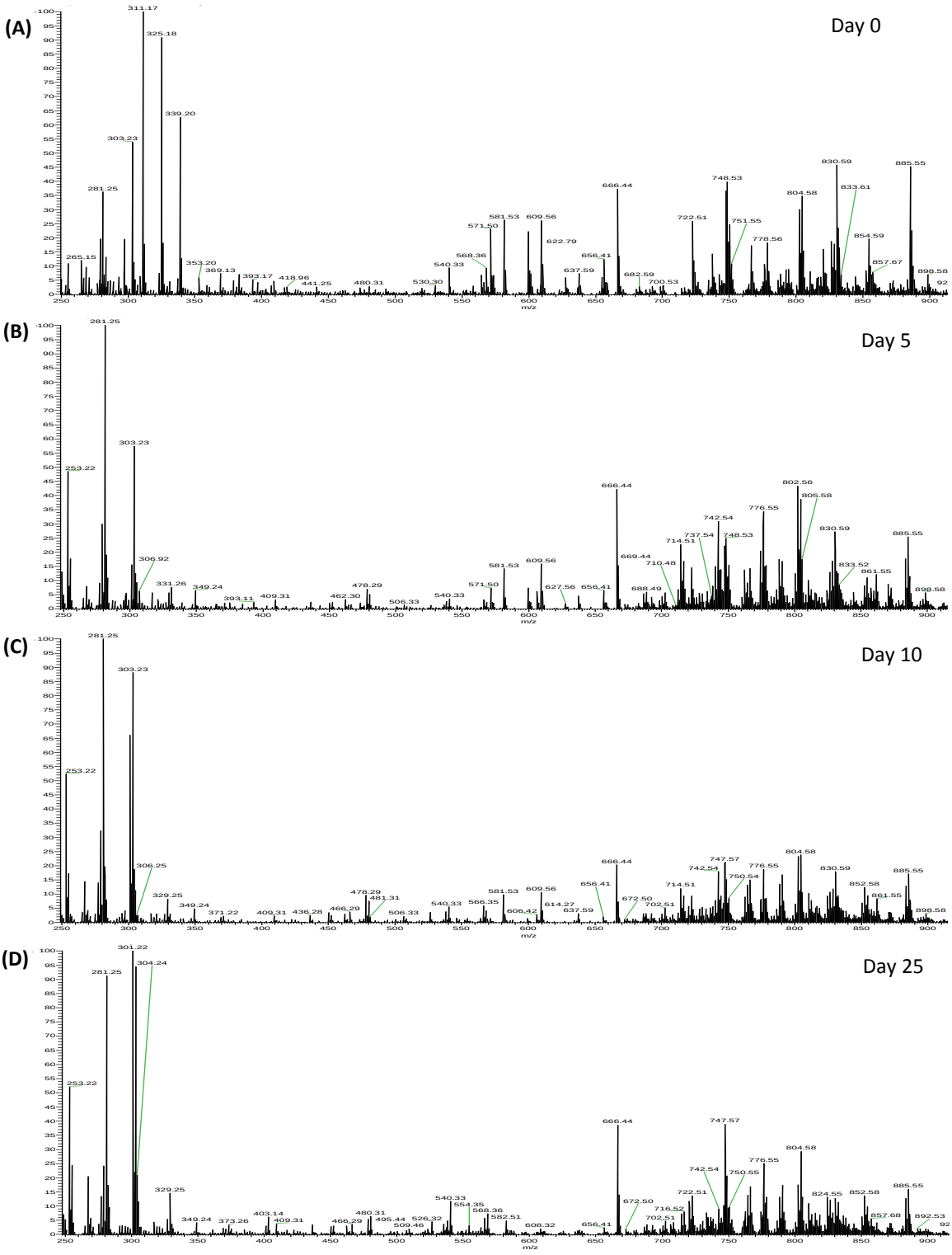


**Figure 3.8. Negative ion DI-MS analysis of 3T3-L1 cells during adipogenesis** Representative spectra of 3T3-L1 adipocytes were induced at day 0, and harvested at the following time points post-differentiation: 0 (A), 7 (B), 15 (C) and 25 (D). Lipids were extracted from the cell samples using a Folch extraction. The lower phase was dried down under nitrogen and reconstituted in 600µL chloroform/methanol (2/1, v/v). A 150µL aliquot was removed and had 10mM ammonium formate added to it. The samples were then directly infused into an Orbitrap Exactive mass spectrometer at a flow rate of 5µL/min for 90 sec (450 scans) in negative ion mode. The m/z range analysed was from 100-1000Da, and the current figure represents 200 to 900Da. The most abundant ions present in all spectra (not including the contaminant peaks) had m/z 281.2488 and 303.2331.

The identifications of these and other lipid species are presented in Table 3.2. As with positive ion mode, the top ten abundant peaks from day 0 (A) and day 25 (B) post-differentiation are presented. At day 0, the lipids present were mainly phospholipids, including phosphatidylcholine (PC), phosphatidylethanolamine (PE), phosphatidylglycerol, phosphatidylinositol (PI) and phosphatidylserine (PS) species. At day 25, the majority were fatty acids, with one PS species and four of the species present in the top 10 at day 0 were also seen in this final time point.

These species were quantified using the internal standard PC (12:0/12:0) with m/z 666.4443, and then normalised to the protein content of the sample. Five of the most concentrated lipid species present in all time points were selected, and presented graphically in Figure 3.9. These chosen lipid species had m/z 281.2488, 303.2331, 747.5673, 804.5769 and 885.5515, and were identified as C18:1, C20:4, phosphatidylglycerol (O-35:1)/(P-35:0), PC (38:6) and PI (38:4), respectively. All were confident identifications, with the exception of phosphatidylglycerol (O-35:1)/(P-35:0) and PC (38:6) due to their mass accuracy being outside the set parameter (ppm=16.989 and 27.344, respectively). The concentration of the fatty acids C18:1 and C20:4 fluctuated throughout the time course, whereas that of phosphatidylglycerol (O-35:1)/ (P-35:0), PC (38:6) and PI (38:4) decreased from day 3 post-differentiation until the end of the time course, with this trend being significant in the last two ($P$<0.001 for both).

| Calculated mass | Theoretical mass | Δ Mass accuracy (ppm) | Ion | Elemental composition | Identification |
|---|---|---|---|---|---|
| ***(A) Day 0*** | | | | | |
| 281.2488 | 281.2486 | 0.711 | $[M-H]^-$ | $C_{18}H_{34}O_2$ | C18:1 |
| 303.2331 | 303.2330 | 0.330 | $[M-H]^-$ | $C_{20}H_{32}O_2$ | C20:4 |
| 722.5145 | 722.5130 | 2.076 | $[M-H]^-$ | $C_{41}H_{74}NO_7P$ | PC (P-36:4)<br>PC (O-36:5) |
| 747.5673 | 747.5546 | 16.989 | $[M-H]^-$ | $C_{41}H_{81}O_9P$ | phosphatidylglycerol (O-35:1)<br>phosphatidylglycerol (P-35:0) |
| 748.5313 | 748.5287 | 3.473 | $[M-H]^-$ | $C_{43}H_{76}NO_7P$ | PE (P-38:5)<br>PE (O-37:6) |
| 750.5442 | 750.5079 | 48.367 | $[M-H]^-$ | $C_4H_{74}NO_8P$ | PC (34:5) |
| 802.5618 | 802.5392 | 28.161 | $[M-H]^-$ | $C_{46}H_{78}NO_8P$ | PC (38:7) |
| 804.5769 | 804.5549 | 27.344 | $[M-H]^-$ | $C_{46}H_{80}NO_8P$ | PC (38:6) |
| 830.5933 | 830.5917 | 1.926 | $[M-H]^-$ | $C_{45}HNO_{10}P$ | PS (39:1) |
| 885.5515 | 885.5499 | 1.807 | $[M-H]^-$ | $C_{47}H_{83}O_{13}P$ | PI (38:4) |

***(A) Day 25***

| | | | | | |
|---|---|---|---|---|---|
| 253.2175 | 253.2173 | 0.790 | $[M-H]^-$ | $C_{16}H_{30}O_2$ | C16:1 |
| 255.2332 | 255.2330 | 0.783 | $[M-H]^-$ | $C_{16}H_{32}O_2$ | C16:0 |
| 267.2330 | 267.2330 | 1.123 | $[M-H]^-$ | $C_{17}H_{32}O_2$ | C17:1 |
| 279.2330 | 279.2330 | 0 | $[M-H]^-$ | $C_{18}H_{32}O_2$ | C18:2 |
| 301.2176 | 301.2173 | 0.996 | $[M-H]^-$ | $C_{20}H_{30}O_2$ | C20:5 |
| 776.5477 | 776.5447 | 3.863 | $[M-H]^-$ | $C_{41}H_{80}NO_{10}P$ | PS (35:0) |



**Table 3.2. Identifications of selected negative ions from 3T3-L1 cells at day 0 and 25 post-differentiation**

Abbreviations used: DG, diglyceride; PC, phosphatidylcholine; PE, phosphatidylethanolamine; PI, phosphatidylinositol; PS, phoshatidylserine; ppm, parts per million

Underlined species are present in both day 0 and 25.

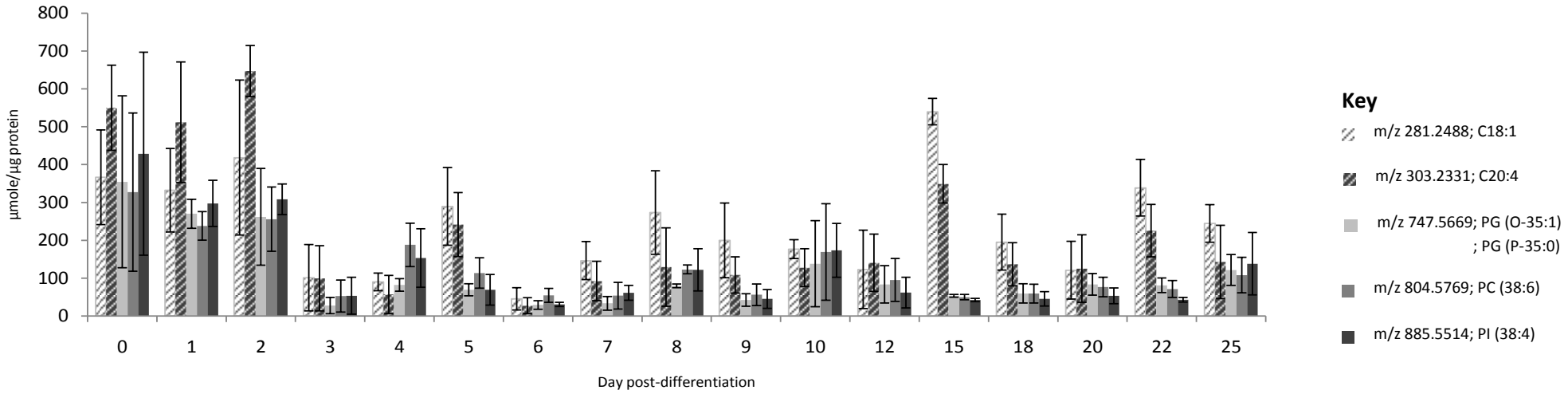


**Figure 3.9. Concentration of individual lipid species during adipogenesis of 3T3-L1 cells from negative ion DI-MS analysis**
3T3-L1 cells were induced to differentiate at day 0, and harvested at the following time points: 0-10, 12, 15, 18, 20, 22 and 25. Lipids were extracted from the cell samples using a Folch extraction. The lower phase was dried down under nitrogen and reconstituted in 600µL chloroform/methanol (2/1, v/v). A 150µL aliquot was removed and had 10mM ammonium formate added to it. The samples were then directly infused into an Orbitrap Exactive mass spectrometer at a flow rate of 5µL/min for 90 sec (450 scans) in negative ion mode.

The selected species were quantified using the internal standard, PC (12:0/12:0) with m/z 666.4443; and then to the protein concentration of the cell sample. The selected lipids are shown in the key. The fatty acids C18:1 and C20:4 were the most concentrated species present at each time point, and this fluctuated over the course of differentiation. The concentration of the remaining lipids decreased from day 3 post-differentiation onwards. A Cuzick's 2-sided trend test was applied to each lipid species, and the trend seen in PC (38:6) and PI (38:4) was significant ($P$<0.001 for both). For this figure only, PG represents phosphatidylglycerol.

### 3.4.2. Positive ion LC-MS analysis

Representative chromatograms of days 0, 5, 10 and 25 post-differentiation are shown in Figure 3.10. A few peaks were identified on the day 0 chromatogram, and these all had a retention time (RT) between 5 and 8 min. The lipid profiles in the chromatograms from day 5 post-differentiation onwards were all similar, with a greater number of peaks being observed. All of these peaks were in the RT region between 5 and 9.5 min. At day 25 post-differentiation, the relative abundance of peaks with RT between 4.5 and 6.5 min decreased. The most abundant ions associated with these chromatographic peaks are identified in Table 3.3. The majority had a mass accuracy that was much greater than 5ppm, and so were not confident identifications.

Multivariate data analysis (MVDA) was used to analyse the positive ion LC-MS data, starting with principal component analysis (PCA). The PCA scores plots of principal component 1 *vs.* principal component 2 for the raw data (not normalised) and that which had been normalised to the TIC are presented in Figure 3.11. Three RT windows were investigated, as indicated in the figure. The sample data were interpreted as being split into three main groups with all RT windows, and these were: days 0-2, 3-12 and 15-25. In all PCA plots, the QCs were located either on, or outside of the ellipse, which is based on Hotelling's $T^2$ 95% tolerance, and observations outside of this ellipse are considered to be outliers. Tighter clustering of the data points was observed with all RT windows when the data were normalised to the TIC before MVDA. When the RT window was set at 1 min, the R2 and Q2 of the models were: 0.773 and 0.635 for the non-normalised data; and 0.778 and 0.64, for the TIC-normalised data, respectively. With the 30 sec RT window, the R2 and Q2 were: 0.767 and 0.604; and 0.738 and 0.582 for the non- and TIC-normalised data, respectively. Finally, when the RT window was narrowed to 15 sec, these values were: 0.694 and 0.527 for the non-normalised data, and for the TIC-normalised data they were 0.677 and 0.503, respectively.

Loadings plots were also produced for all of the PCA plots, and were labelled by m/z, as seen in Figure 3.12. The plots were all similar, and various points were possible causes of variance between the chromatograms due to their distance from the origin. Out of these points, those that could be identified were all located on the left hand side (LHS) of the origin, and were all PC species, with one SM. The individual identifications are presented in Table 3.4. When these points underwent trend analysis; the abundance of all species increased until between day 5 and 7 post-differentiation, where it then either plateaued, or gradually decreased until the end of the time course.

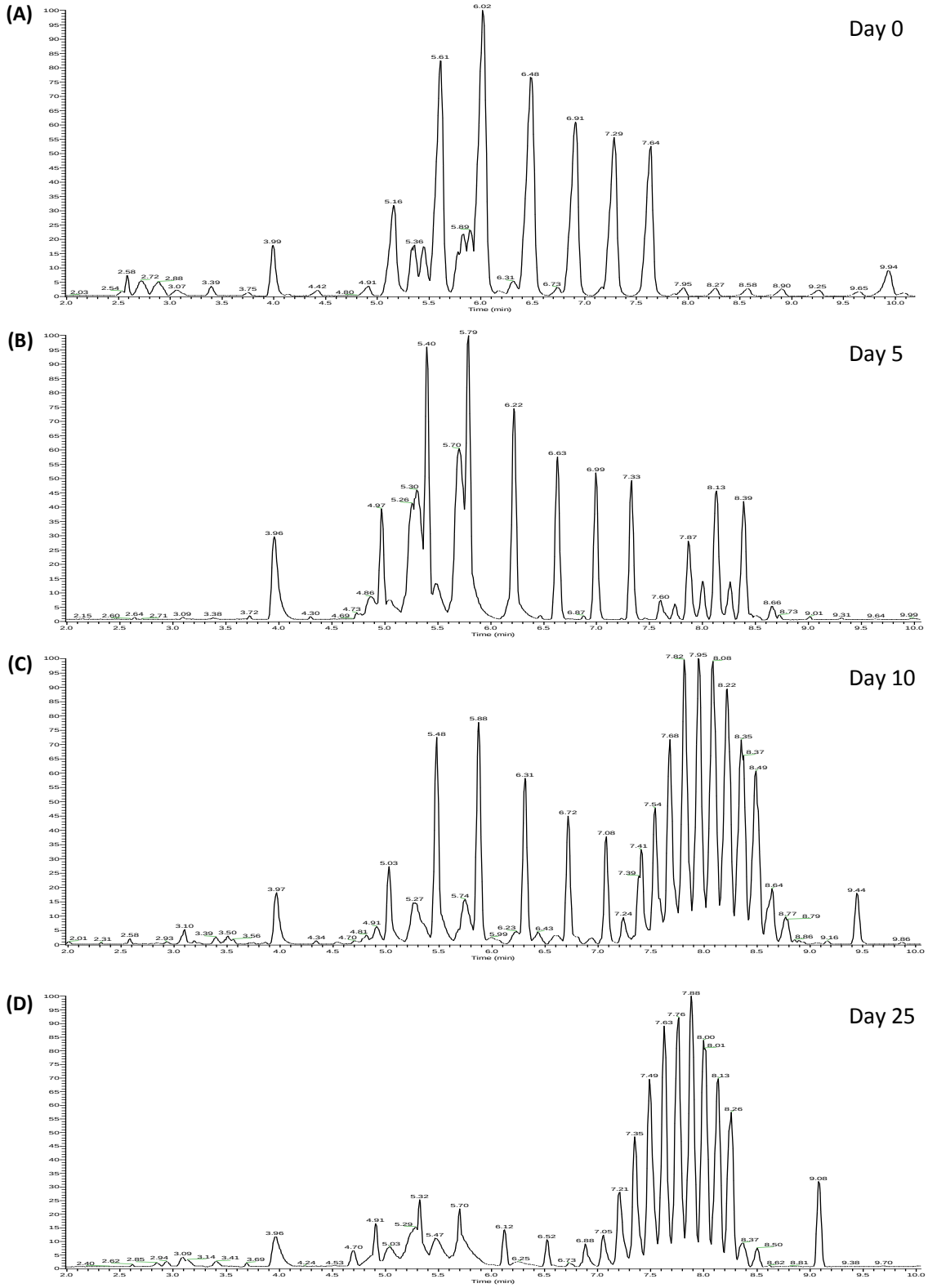


**Figure 3.10. Positive ion LC-MS analysis of 3T3-L1 cells during adipogenesis** Representative chromatograms of 3T3-L1 adipocytes, which had been induced at day 0 and harvested at the following time points post-differentiation: 0 (A); 5 (B); 10 (C); 15(D) and 25 (E). Lipids were extracted from the cell samples using a Folch extraction. The lower phase was dried down under nitrogen and reconstituted in 600µL chloroform/methanol (2/1, v/v). The samples were analysed by LC-MS in positive ion mode over 18 min for a scan range of 100 – 1000 m/z. The presented chromatograms show RT between 2 and 10 min. An increase in the abundance of lipids with RT between 7 and 8.5 min was seen at the following time points: 10, 15 and 25.

| Retention time (min) | Ion mass | Theoretical mass | Δ Mass accuracy (ppm) | Ion | Empirical composition | Identification |
|---|---|---|---|---|---|---|
| ***Day 0*** | | | | | | |
| 5.36 | 703.5745 | 703.5748 | -0.426 | $[M+H]^+$ | $C_{39}H_{79}N_2O_2P$ | SM (34:1) |
| 5.43 | 758.5694 | 758.5694 | 0 | $[M+H]^+$ | $C_{42}H_{80}NO_8P$ | PC (34:2) |
| 5.61 | 610.1841 | 610.1681 | 26.222 | $[M+H]^+$ | $C_{31}H_{29}O_{13}$ | |
| 5.80 | 760.5843 | 760.5850 | -0.920 | $[M+H]^+$ | $C_{42}H_{82}NO_8P$ | PC (34:1) |
| 6.02 | 684.2031 | 684.2134 | -15.054 | [M+H]+ | $C_{30}H_{38}NO_{17}$ | |
| 6.49 | 758.2222 | 758.2264 | -5.539 | $[M+H]^+$ | $C_{33}H_{41}O_{20}$ | |
| 6.91 | 832.2401 | 832.2420 | -2.283 | $[M+H]^+$ | $C_{39}H_{43}O_{20}$ | |
| 7.28 | 906.2610 | | | | | |
| 7.64 | 980.2786 | | | | | |
| 9.94 | 908.8651 | 908.8640 | 1.210 | $[M+NH_4]^+$ | $C_{57}H_{110}O_6$ | TG (54:0) |
| ***Day 25*** | | | | | | |
| 5.32 | 610.1833 | 610.1681 | 24.911 | $[M+H]^+$ | $C_{31}H_{29}O_{13}$ | |
| 5.70 | 684.2025 | 684.2134 | -15.931 | [M+H]+ | $C_{30}H_{38}NO_{17}$ | |
| 6.12 | 758.225 | 758.2264 | -5.144 | $[M+H]^+$ | $C_{33}H_{41}O_{20}$ | |
| 6.52 | 832.2403 | 832.2420 | -2.043 | $[M+H]^+$ | $C_{39}H_{43}O_{20}$ | |
| 6.88 | 906.2597 | | | | | |

| | | | | | | |
|---|---|---|---|---|---|---|
| 7.05 | 776.6769 | 776.6768 | 0.129 | [M+NH4]+ | $C_{48}H_{86}O_6$ | TG (45:3) |
| 7.21 | 790.6920 | 790.6919 | 0.126 | [M+NH4]+ | $C_{49}H_{88}O_6$ | TG (46:3) |
| 7.36 | 778.6920 | 778.6919 | 0.128 | [M+NH4]+ | $C_{48}H_{88}O_6$ | TG (45:2) |
| 7.49 | 792.7076 | 792.7076 | 0 | [M+NH4]+ | $C_{49}H_{90}O_6$ | TG (46:2) |
| 7.63 | 806.7228 | 806.7232 | -0.496 | [M+NH4]+ | $C_{50}H_{92}O_6$ | TG (47:2) |
| 7.76 | 820.7385 | 820.7389 | -0.487 | $[M+NH_4]^+$ | $C_{51}H_{98}O_6$ | TG (48:2) |
| 7.88 | 834.7541 | 834.7545 | -0.479 | $[M+NH_4]^+$ | $C_{52}H_{96}O_6$ | TG (49:2) |
| 8.00 | 848.7694 | 848.7701 | -0.825 | $[M+NH_4]^+$ | $C_{53}H_{98}O_6$ | TG (50:2) |
| 8.12 | 862.7851 | 862.7858 | -0.811 | $[M+NH_4]^+$ | $C_{54}H_{100}O_6$ | TG (51:2) |
| 8.25 | 876.8011 | 876.8014 | -0.342 | $[M+NH_4]^+$ | $C_{55}H_{102}O_6$ | TG (52:2) |
| 8.35 | 890.8167 | 890.8171 | -0.449 | $[M+NH_4]^+$ | $C_{56}H_{104}O_6$ | TG (53:2) |
| 8.50 | 904.8323 | 904.8327 | -0.442 | $[M+NH_4]^+$ | $C_{57}H_{106}O_6$ | TG (54:2) |
| 9.08 | 908.8654 | 908.8640 | | $[M+NH_4]^+$ | $C_{57}H_{110}O_6$ | TG (54:0) |

**Table 3.3. Retention times and associated abundant ion mass of each major chromatographic peak from positive ion LC-MS analysis of 3T3-L1 cells during adipogenesis**

Red highlight indicates internal standard

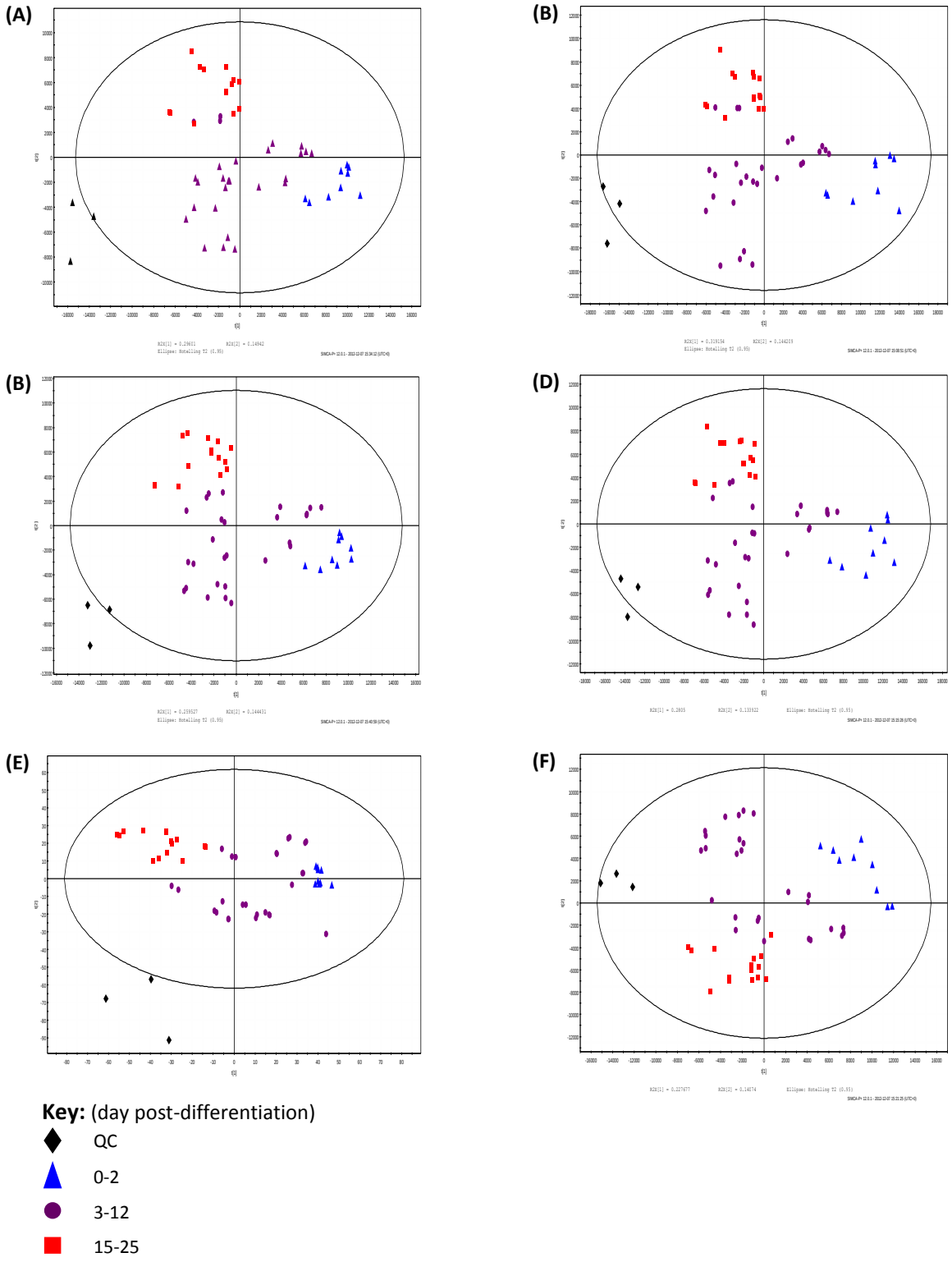


**Figure 3.11. PCA scores plots representing positive ion LC-MS analysis of 3T3-L1 cells during adipogenesis**

3T3-L1 adipocytes were induced to differentiate at day 0, and harvested at the following days post-differentiation: 0-10, 12, 15, 18, 20, 22 and 25. Lipids were extracted using a Folch extraction, and the lower phase was analysed by LC-MS in positive ion mode, and the data was processed using SIEVE. The data represented here have been Pareto scaled, and the RT window was set at either 1min, 30sec or 15sec. Either the raw data or data which were normalised to the total ion current were analysed. Each time point consisted of three biological replicates. The panels represent: 1min RT window, no-norm (A); 1min RT window, TIC norm (B); 30sec RT window, no-norm (C); 30sec RT window, TIC-norm (D); 15sec RT window, no-norm (E) and 15sec RT window, TIC-norm (F).

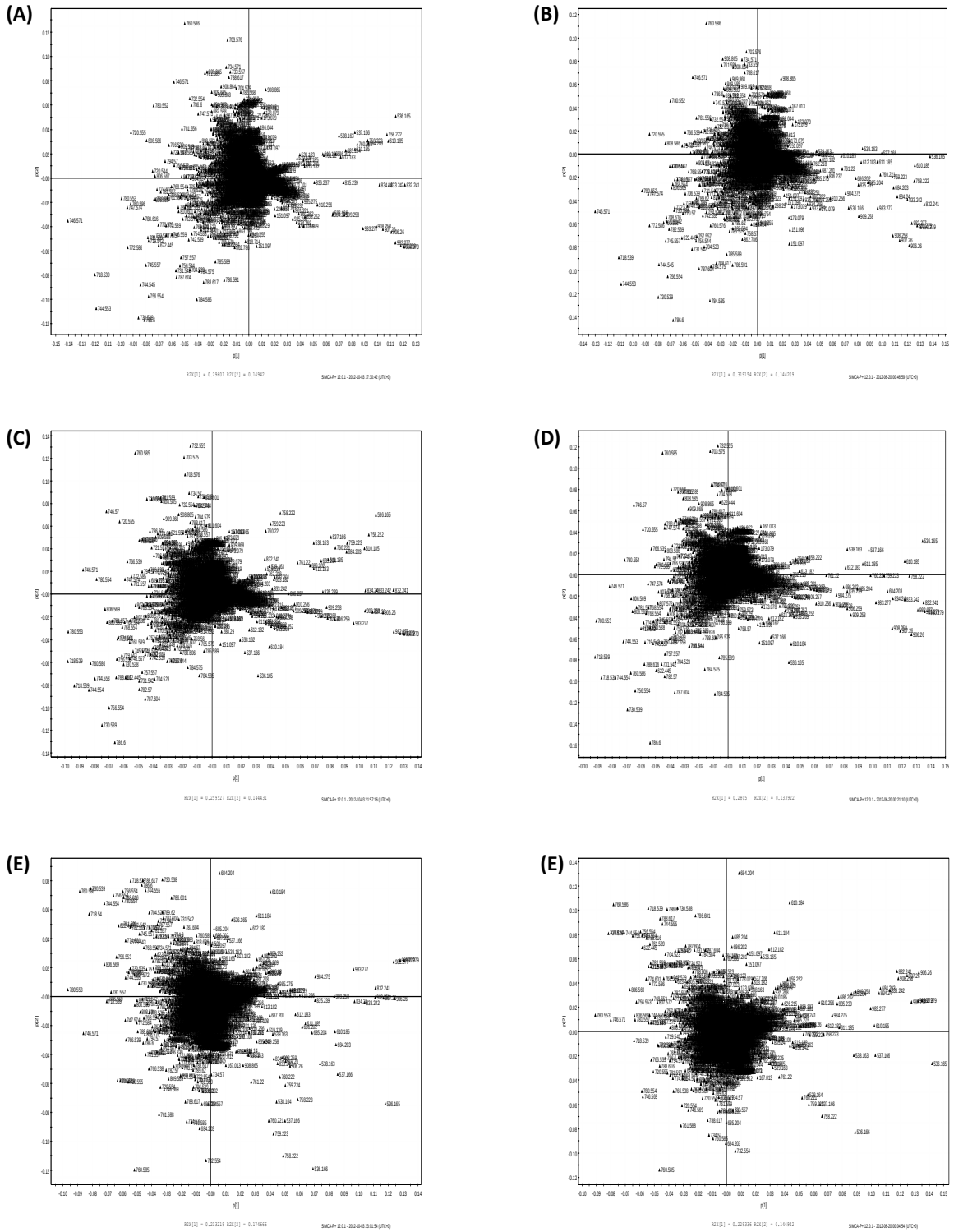


**Figure 3.12. PCA loadings plots representing positive ion LC-MS analysis of 3T3-L1 cells during adipogenesis**

3T3-L1 adipocytes were induced to differentiate at day 0, and harvested at the following days post-differentiation: 0-10, 12, 15, 18, 20, 22 and 25. Lipids were extracted using a Folch extraction, and the lower phase was analysed by LC-MS in positive ion mode. Before multivariate data analysis, the data was processed using SIEVE. The data represented here have been Pareto scaled, and the RT window was set at either 1min, 30sec or 15sec. Either the raw data or data which were normalised to the total ion current were analysed. Each time point consisted of three biological replicates. The panels represent: 1min RT window, no-norm (A); 1min RT window, TIC-norm (B); 30sec RT window, no-norm (C); 30sec RT window, TIC-norm (D); 15sec RT window, no-norm (E) and 15sec RT window, TIC-norm.

| Calculated mass | Theoretical mass | Δ Mass accuracy (ppm) | Ion | Elemental composition | Identification |
|---|---|---|---|---|---|
| 703.5750 | 703.5748 | 0.284 | $[M+H]^+$ | $C_{39}H_{79}N_2O_6P$ | SM (34:1) |
| 718.5390 | 718.5381 | 1.253 | $[M+H]^+$ | $C_{39}H_{76}NO_8P$ | PC (31:1) |
| 720.5650 | 720.5538 | 15.544 | $[M+H]^+$ | $C_{39}H_{78}NO_8P$ | PC (31:0) |
| 732.5550 | 732.5538 | 1.638 | $[M+H]^+$ | $C_{40}H_{78}NO_8P$ | PC (32:1) |
| 744.5530 | 744.5538 | -1.074 | $[M+H]^+$ | $C_{41}H_{78}NO_8P$ | PC (33:2) |
| 746.5700 | 746.5694 | 0.804 | $[M+H]^+$ | $C_{41}H_{80}NO_8P$ | PC (33:1) |
| 760.5850 | 760.5850 | 0 | $[M+H]^+$ | $C_{42}H_{82}NO_8P$ | PC (34:1) |
| 756. 5540 | 756.5538 | 0.264 | $[M+H]^+$ | $C_{42}H_{78}NO_8P$ | PC (34:4) |
| 786.6000 | 786.6007 | -0.890 | $[M+H]^+$ | $C_{44}H_{84}NO_8P$ | PC (36:2) |
| 786.5997 | 786.6007 | -1.271 | $[M+H]^+$ | $C_{44}H_{84}NO_8P$ | PC (36:2) |

**Table 3.4. Lipid species identified as causes of variance from positive ion PCA and PLS loadings plots**

The next step involved a supervised technique called partial least squares (PLS). The scores plots of the models for all three RT windows are presented in Figure 3.13. As with the PCA data in Figure 3.11, all PLS plots were seen to have three major groupings of data points. These groupings were much clearer than those in the PCA models, especially with the 15 sec RT window, as the data points were clustered tightly within the groups, and gaps were seen on the plot between the three groups. The QCs were still situated outside of the 95% tolerance region for all plots in the figure. For the 1 min RT window, the R2X, R2Y and Q2 values were: 0.502, 0.925 and 0.849 for the non-normalised data, and 0.529, 0.912 and 0.85 for the TIC-normalised data, respectively.

At the 30sec RT window, the TIC-normalised model (D) had one point situated outside of the 95% tolerance region, and so may be considered an outlier. This point related to one of the day 22 post-differentiation samples. The R2X, R2Y and Q2 for the 30sec RT window data were: 0.578, 0.982 and 0.9 for the non-normalised data, and for the TIC-normalised data these were: 0.498, 0.963 and 0.897. For the 15 sec RT window dataset, these values were: 0.471, 0.968 and 0.833 for the non-normalised data, and 0.498, 0.963 and 0.897 for the TIC-normalised data, respectively.

The loadings plots for the positive ion PLS models are shown in Figure 3.14. The points of interest were comparable between the different RT windows, and normalisation conditions, and were also similar to those seen in the PCA loadings plots. The individual identifications of the points of interest are, therefore, also found in Table 3.4 and, as mentioned above, were all phospholipid species. Although they were located in different areas of the loadings plots for each model, trend analysis showed that the relative abundance of these species behaved in a similar manner to those seen with PCA analysis. An increase was observed from at least day 12 post-differentiation which, after a continued increase for a few time points in some species, either plateaued or slightly decreased towards the end of the time course.

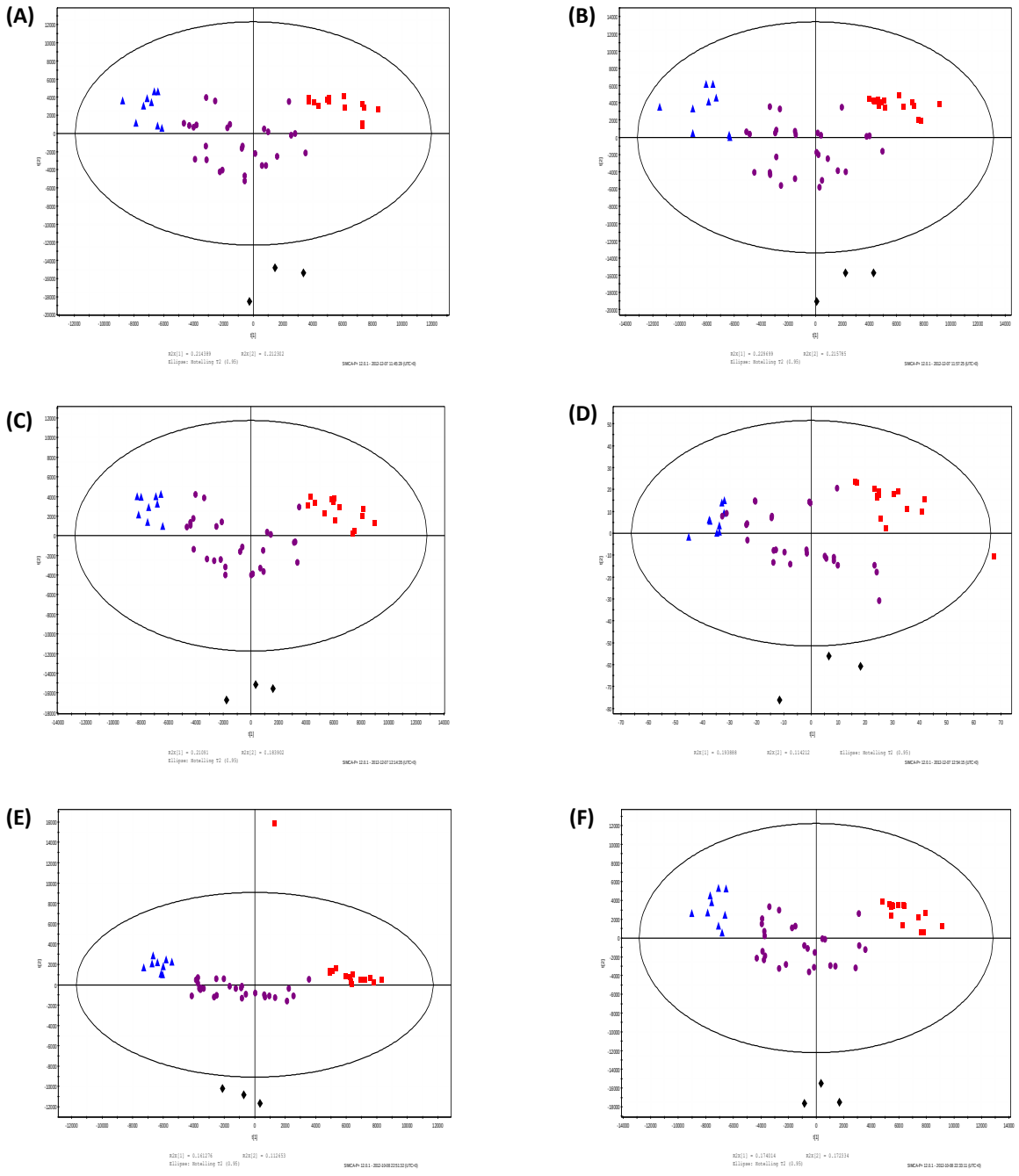


**Figure 3.13. PLS scores plots representing positive ion LC-MS analysis of 3T3-L1 cells during adipogenesis**

3T3-L1 adipocytes were induced to differentiate at day 0, and harvested at the following days post-differentiation: 0-10, 12, 15, 18, 20, 22 and 25. Lipids were extracted using a Folch extraction, and the lower phase was analysed by LC-MS in positive ion mode. Before multivariate data analysis, the data was processed using SIEVE. The data represented here have been Pareto scaled, and the RT window was set at either 1min, 30sec or 15sec. Either the raw data or that normalised to the total ion current were analysed. Each time point consisted of three biological replicates. The panels represent: 1min RT window, no-norm (A); 1min RT window, TIC norm (B); 30sec RT window, no-norm (C); 30sec RT window, TIC-norm (D); 15sec RT window, no-norm (E) and 15sec RT window, TIC-norm.

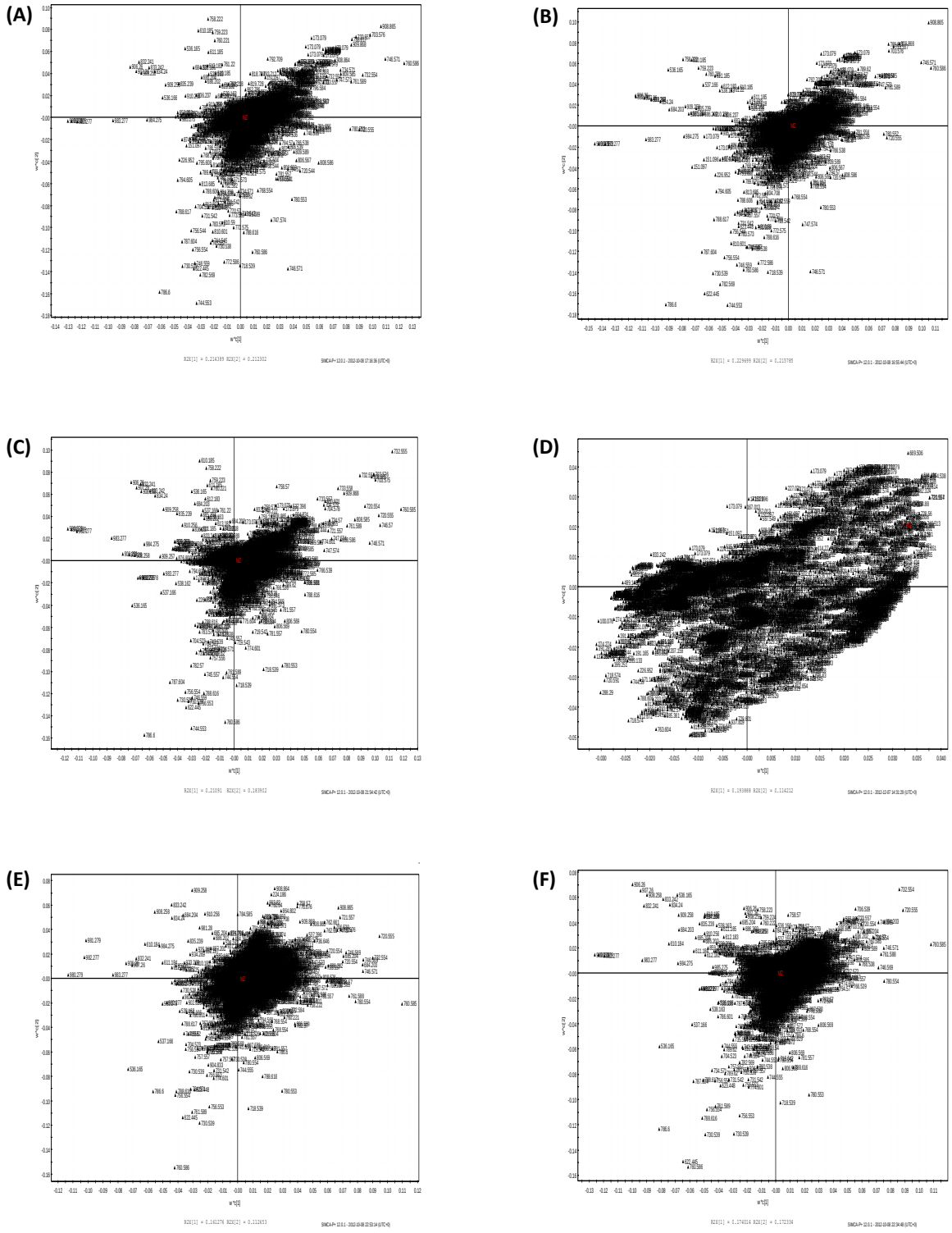


**Figure 3.14. PLS loadings plots representing positive ion LC-MS analysis of 3T3-L1 cells during adipogenesis**

3T3-L1 adipocytes were induced to differentiate at day 0, and harvested at the following days post-differentiation: 0-10, 12, 15, 18, 20, 22 and 25. Lipids were extracted using a Folch extraction, and the lower phase was analysed by LC-MS in positive ion mode. Before multivariate data analysis, the data was processed using SIEVE. The data represented here have been Pareto scaled, and the RT window was set at either 1min, 30sec or 15sec. Either the raw data or data which were normalised to the total ion current were analysed. Each time point consisted of three biological replicates. The panels represent: 1min RT window, no-norm (A); 1min RT window, TIC norm (B); 30sec RT window, no-norm (C); 30sec RT window, TIC-norm (D); 15sec RT window, no-norm (E) and 15sec RT window, TIC-norm (F).

### 3.4.3. Negative ion LC-MS analysis

Representative chromatograms of days 0, 5, 10 and 25 post-differentiation from negative ion LC-MS analysis are shown in Figure 3.15. Fewer peaks were observed in these chromatograms when compared to those from positive ion analyses. The most abundant ion associated with the chromatographic peaks at day 0 (A) and day 25 (B) post-differentiation are identified in Table 3.5. The majority of these had a mass accuracy much greater than 5ppm, and so these identifications were not confident ones.

The three RT windows which were analysed with positive ion mode data above were also used to investigate data acquired in negative ion mode. As before, the datasets were first analysed by PCA, and the scores plots of the non- and TIC-normalised data for all RT windows are presented in Figure 3.16. The sample data in all of the plots present in the figure were interpreted as forming two groups, and these were: days 0-6, and days 7-25 post-differentiation. Some overlap was observed between these two groups with the two larger RT windows (1 min and 30 sec). The QCs were located inside of the tolerance regions in all plots. Slight differences were observed between the non- and TIC-normalised data, for example, in the 1 min RT window models, a point relating to a day 25 post-differentiation sample was located outside of the 95% tolerance region with the TIC-normalised dataset (B). With the 30 sec RT window models, the non-normalised data (D) also mirrored (B) in the fact that one of the day 25 replicates was located outside of the 95% tolerance region. This point moved inside of the tolerance region when the data were TIC-normalised (C) prior to PCA analysis.

The R2 and Q2 were calculated for all models, and for the 1 min RT window, these were: 0.989 and 0.970; and 0.987 and 0.965 for non- and TIC-normalised data, respectively. When the RT window was set to 30 sec, the R2 and Q2 for the non-normalised dataset were: 0.991 and 0.973, and for the TIC-normalised dataset they were: 0.986 and 0.959, respectively. When narrowed to 15 sec, the R2 and Q2 for these models were 0.963 and 0.934 for non-normalised data, and 0.974 and 0.942 for TIC-normalised data, respectively.

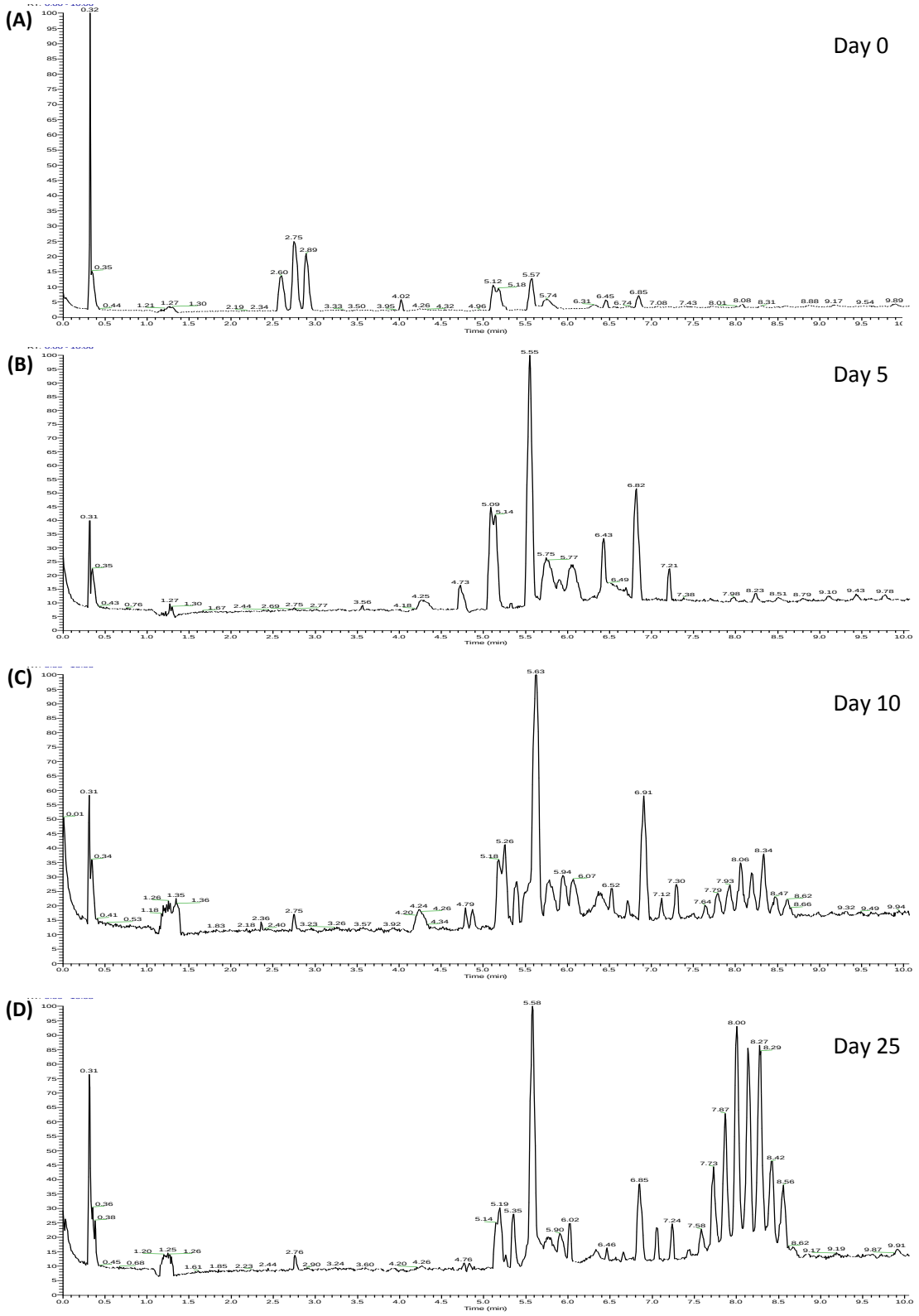


**Figure 3.15. Negative ion LC-MS analysis of 3T3-L1 cells during adipogenesis** Representative chromatograms of 3T3-L1 adipocytes, which were induced at day 0 and harvested at the following time points post-differentiation: 0 (A), 7 (B), 15 (C) and 25 (D). Lipids were extracted from the cell samples using a Folch extraction. The lower phase was dried down under nitrogen and reconstituted in 600µL chloroform/methanol (2/1, v/v). The samples were analysed by LC-MS in negative ion mode over 18 min for a scan range of m/z 100 – 1000Da. An increase in the abundance of species with RT between 5 and 7.5 min was seen from day 5 post-differentiation onwards, and from day 10, the abundance of lipids with RT between 7.5 and 9 min also increased.

| Retention time (min) | Ion mass | Theoretical mass | Δ Mass accuracy (ppm) | Ion | Empirical composition | | Identification |
|---|---|---|---|---|---|---|---|
| ***Day 0*** | | | | | | | |
| 2.60 | 311.1686 | | | | | | |
| 2.75 | 325.1837 | | | | | | |
| 2.89 | 339.1996 | | | | | | |
| 4.02 | 564.3447 | 564.3671 | -39.691 | [M-H]- | $C_{28}H_{56}NO_8P$ | | PC (20:0) |
| 5.12 | 885.5524 | 885.5499 | 2.823 | [M-H]- | $C_{47}H_{83}O_{13}P$ | | PI (38:4) |
| 5.58 | 572.4824 | 572.5303 | -83.664 | [M-H]- | $C_{35}H_{63}D_5O_5$ | | DG (32:0) |
| 5.70 | 748.5302 | 748.5498 | -26.184 | [M-H]- | $C_{40}H_{80}NO_9P$ | | |
| 6.45 | 680.6120 | | | | | | |
| 6.85 | 682.5999 | | | | | | |
| 8.06 | 158.9750 | 159.0299 | -345.218 | [M-H]- | $C_6H_8O_5$ | | |
| 9.54 | 112.9849 | 113.0608 | -671.320 | [M-H]- | $C_6H_{10}O_2$ | | |

| | | | | | | |
|---|---|---|---|---|---|---|
| ***Day 25*** | | | | | | |
| 5.14 | 885.5503 | 885.5499 | 0.4517 | [M-H]- | $C_{47}H_{83}O_{13}P$ | PI (38:4) |
| 5.36 | 558.4661 | | | | | |
| 5.59 | 572.4808 | 572.5303 | -86.458 | [M-H]- | $C_{35}H_{63}D_5O_5$ | DG (32:0) |
| 5.72 | 748.5382 | 748.5134 | 33.132 | [M-H]- | $C_{39}H_{76}NO_{10}P$ | PC (33:0) |
| 6.85 | 656.5549 | 656.6242 | -105.540 | [M-H]- | $C_{41}H_{75}D_5O_5$ | DG (38:0) |
| 7.05 | 670.5987 | 670.5264 | 107.826 | [M-H]- | $C_{38}H_{73}NO_8$ | |
| 7.23 | 684.6792 | 684.6555 | 34.616 | [M-H]- | $C_{43}H_{79}D_5O_5$ | DG (40:0) |

**Table 3.5. Retention times and the associated abundant ion mass of each major chromatographic peak from negative ion LC-MS analysis of 3T3-L1 cells during adipogenesis**

The loadings plots relating to these PCA plots are presented in Figure 3.17. Points of interest were similar between all loadings plots. The majority of the points identified were phospholipid species, and trend analysis revealed that a large increase in their abundance was seen at day 1 post-differentiation, which then steadily decreased until day 7 where it plateaued for the remainder of the time course. Individual identifications of these points are shown in Table 3.6.

The supervised PLS analysis was also employed on the negative ion data with all three RT windows, and this is presented in Figure 3.18. The grouping of points on these plots varied depending on the RT window and normalisation conditions. When the RT window was set to 1 min, three groups were apparent in the data which had not been normalised (A). These groups corresponded to the QCs which were located either on the edge, or outside of the 95% tolerance region, and then day 0-6 and 7-25 post-differentiation. There was some overlap between the groups, with three points representing day 4 post-differentiation samples being present in the day 7-25 group. After these data were normalised to the TIC (B), the PLS plot looked slightly different, with two definite groups being produced, which were days 0-6 and 7-25 post-differentiation. The QCs had moved from the tolerance region, and were situated within the days 7-25 group. The overlap of day four samples was still seen. The R2X, R2Y and Q2 for the 1 min RT window model were: 0.908, 0.967 and 0.849; and 0.939, 0.977 and 0.954 for non- and TIC-normalised data respectively.

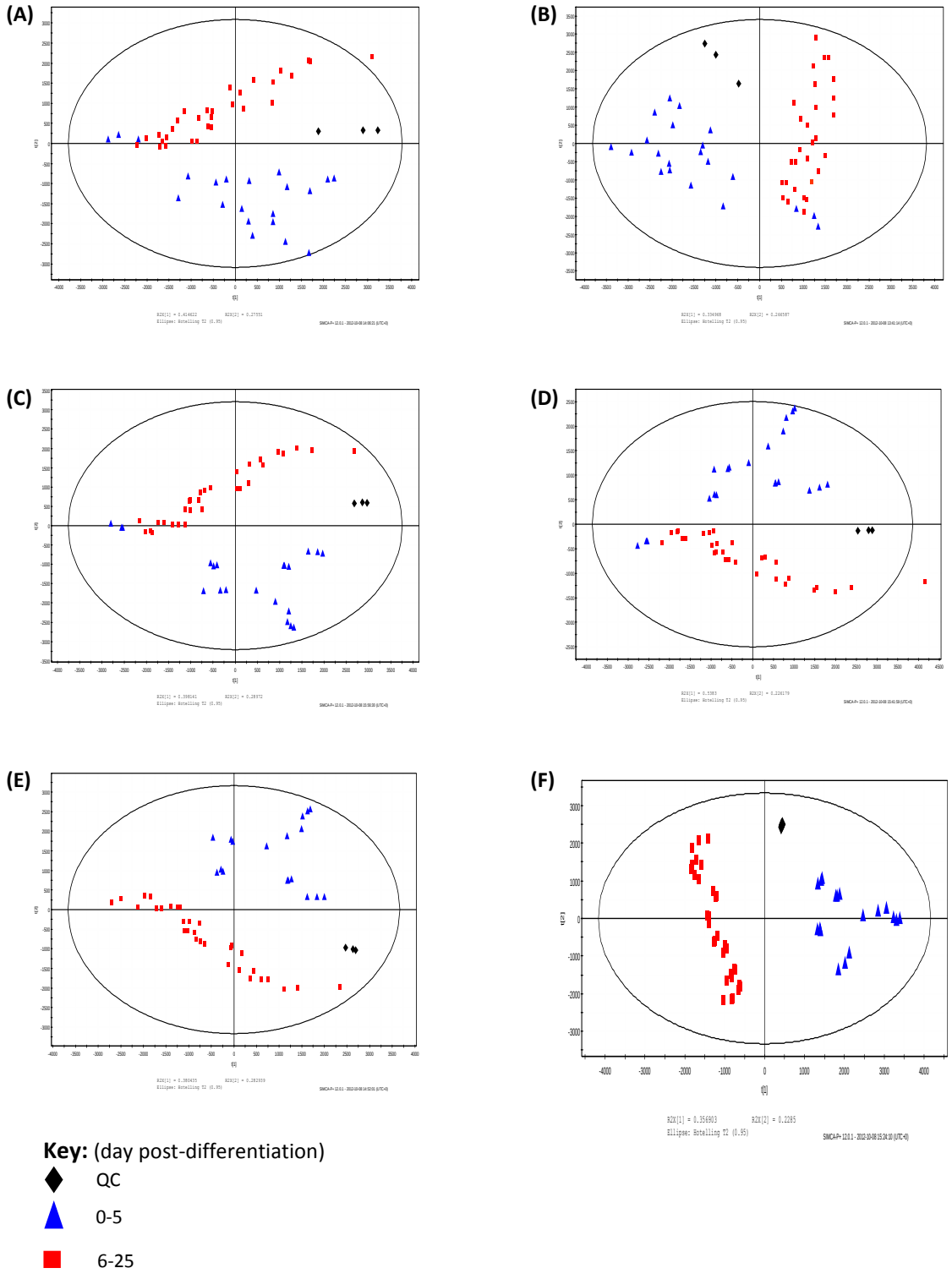


**Figure 3.16. PCA scores plots representing negative ion LC-MS analysis of 3T3-L1 cells during adipogenesis**

3T3-L1 adipocytes were induced to differentiate at day 0, and harvested at the following days post-differentiation: 0-10, 12, 15, 18, 20, 22 and 25. Lipids were extracted using a Folch extraction, and the lower phase analysed by LC-MS in negative ion mode. Before multivariate data analysis, the data was processed using SIEVE. The data represented here have been Pareto scaled, and the RT window was set at either 1min, 30sec or 15sec. Either the raw data or data which were normalised to the total ion current were analysed. Each time point consisted of three biological replicates. The panels represent: 1min RT window, no-norm (A); 1min RT window, TIC norm (B); 30sec RT window, no-norm (C); 30sec RT window, TIC-norm (D); 15sec RT window, no-norm (E) and 15sec RT window, TIC-norm (F).

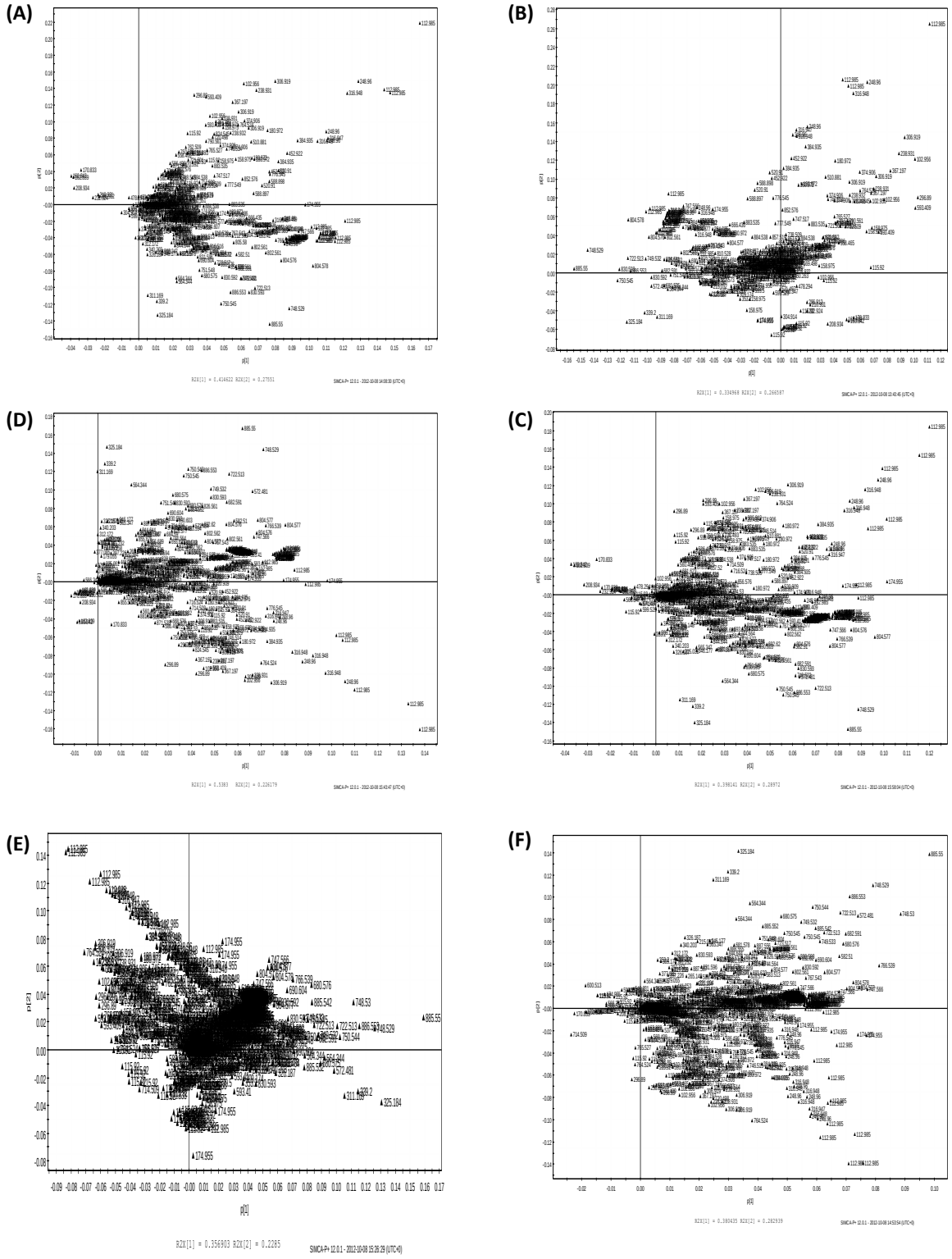


**Figure 3.17. PCA loadings plots representing negative ion LC-MS analysis of 3T3-L1 cells during adipogenesis**

3T3-L1 adipocytes were induced to differentiate at day 0, and harvested at the following days post-differentiation: 0-10, 12, 15, 18, 20, 22 and 25. Lipids were extracted using a Folch extraction, and the lower phase was analysed by LC-MS in negative ion mode. Before multivariate data analysis, the data was processed using SIEVE. The data represented here have been Pareto scaled, and the RT window was set at either 1min, 30sec or 15sec. Either the raw data or data which were normalised to the total ion current were analysed. Each time point consisted of three biological replicates. The panels represent: 1min RT window, no-norm (A); 1min RT window, TIC norm (B); 30sec RT window, no-norm (C); 30sec RT window, TIC-norm (D); 15sec RT window, no-norm (E) and 15sec RT window, TIC-norm.

With the 30 sec RT window, the PLS plots were similar for both non-normalised (C) data, and data which had been normalised to the TIC (D). These plots were interpreted as having three groups: the QCs which were located outside of the 95% tolerance region; and then day 0-6; and 7-25 post-differentiation. As with the 1 min data, an overlap was observed, with the day four samples being present in the day 7-25 group. Both plots also showed one sample from the 7-25 group outside of the 95% tolerance region, and this was identified as one of the day 25 samples. The R2X, R2Y and Q2 for these models were 0.938, 0.969 and 0.946 for non-normalised data; and 0.913, 0.976 and 0.948 for TIC-normalised data, respectively.

The final RT window was set at 15 sec, and when the data were not normalised before analysis (E), three groups were found. These were: QCs, day 0-6, and day 7-25 post-differentiation. The QCs were located close to the day 7-25 group, and one replicate from the day 25 samples was still found outside of the 95% tolerance region. Another group of samples were also found outside this region, and these points related to day one post-differentiation samples. The overlap between the sample groups had now disappeared, and a clear separation was observed between them. Once the data had been normalised to the TIC (F), the groupings remained the same, although the day one samples were now inside the tolerance region. Clear separation between the sample groups was also seen, and the clustering within groups was tighter than that seen in the non-normalised data. The R2X, R2Y and Q2 for these models were: 0.892, 0.982 and 0.957; and 0.766, 0.976 and 0.963 for non- and TIC-normalised data, respectively.

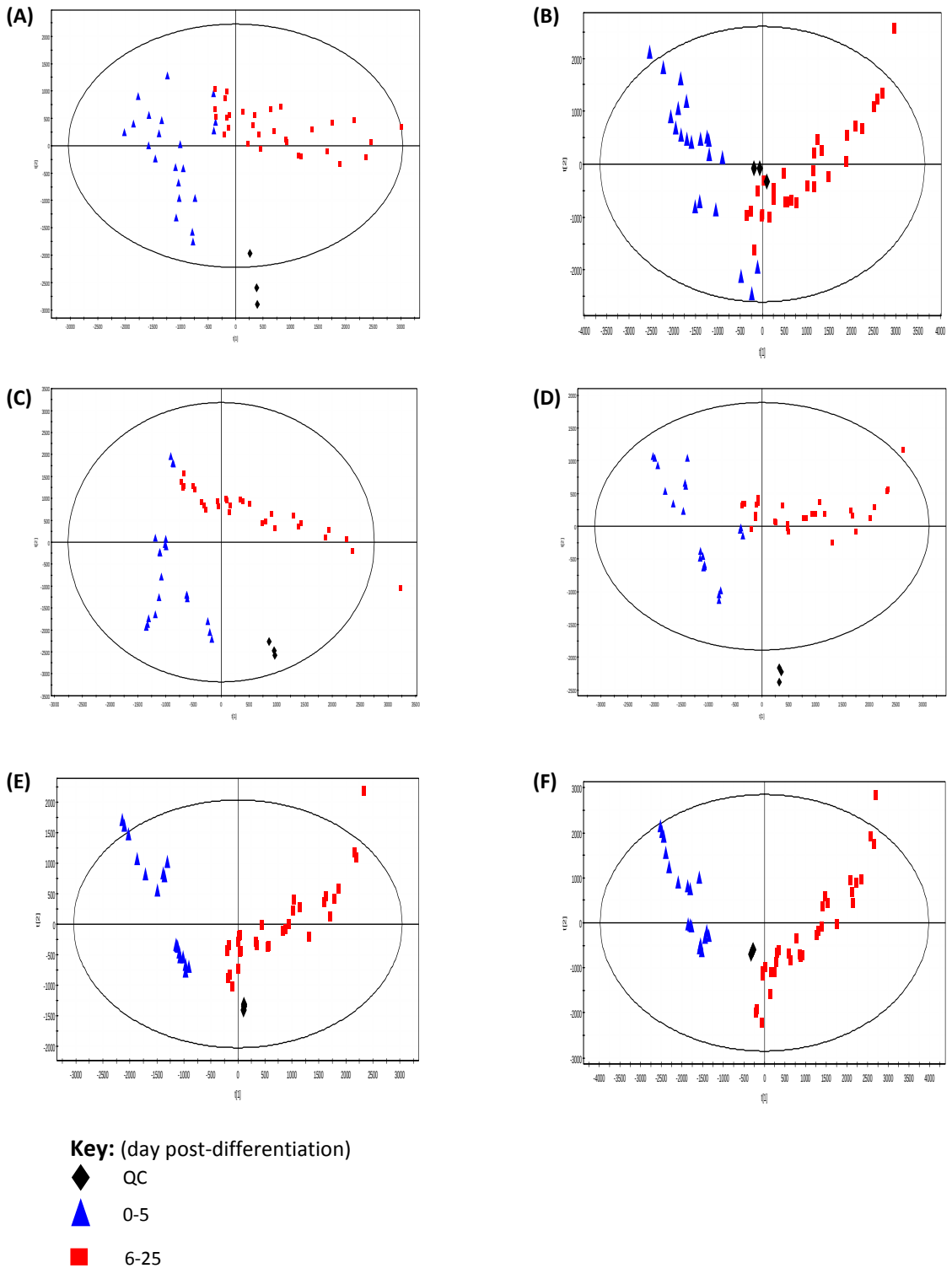


**Figure 3.18. PLS scores plots representing negative ion LC-MS analysis of 3T3-L1 cells during adipogenesis**

3T3-L1 adipocytes were induced to differentiate at day 0, and harvested at the following days post-differentiation: 0-10, 12, 15, 18, 20, 22 and 25. Lipids were extracted using a Folch extraction, and the lower phase was analysed by LC-MS in negative ion mode. Before multivariate data analysis, the data was processed using SIEVE. The data represented have been Pareto scaled, and the RT window was set at either 1min, 30sec or 15sec. Either the raw data or data which were normalised to the total ion current were analysed. Each time point consisted of three biological replicates. The panels represent: 1min RT window, no-norm (A); 1min RT window, TIC norm (B); 30sec RT window, no-norm (C); 30sec RT window, TIC-norm (D); 15sec RT window, no-norm (E) and 15sec RT window, TIC-norm.

The PLS loadings plots relating to these scores plots are presented in Figure 3.19, and are labelled according to their m/z. Although the plots in the figure looked different from each other, the majority of the relevant masses are the same, and are also the same as those observed in the PCA loadings plots, and so are also presented in Table 3.6. These selected points were mainly phospholipid species, and once trend analysis was employed, it was evident that their abundance over the time course changed in various ways. The abundance of the phospholipids with m/z 722.5130, 748.5313 and 885.5515 initially increased at day 1 post-differentiation, and remained so until day 4. At day 4, their abundance sharply decreased and stayed low for the remainder of the time course. These were identified as PE (P-36:4) / PE (O-36:5), PE (P-38:5) / PE (O-37:6) and PI (38:4), respectively. The abundance of another phospholipid with m/z 830.5933 fluctuated until day 6 post-differentiation, where it decreased and stabilised over the rest of the time course. This was identified as PS (39:1).

After comparing non-normalised and TIC normalised datasets from both PCA and PLS models, for both ion modes, the models were auto-transformed; however, no changes were observed, and so these data are not shown.

### 3.4.4. Eicosanoid analysis by LC-MS/MS

A targeted lipidomic approach was employed to analyse the secretion of eicosanoid species from 3T3-L1 cells over the course of differentiation. Only seven eicosanoids were detectable in the 3T3-L1 cell media samples. These were: Prostaglandin (PG)$D_2$, $PGE_2$, $PGF_{2\alpha}$, thromboxane (Tx) $B_2$, 11β-$PGF_{2\alpha}$, 6-keto $PGF_{1\alpha}$ and 15-HETE.

The concentration of these eicosanoids showed a trend over the course of differentiation ($P$<0.03 for all; 2 sided), with the exception of 6-keto $PGF_{1\alpha}$, as presented in Figures 3.20 and 3.21. The greatest concentrations of all seven eicosanoids were observed between days 0 and 1 post-differentiation. By day 2, the concentration of these species had decreased, and this continued until the end of the time course, with some fluctuation.

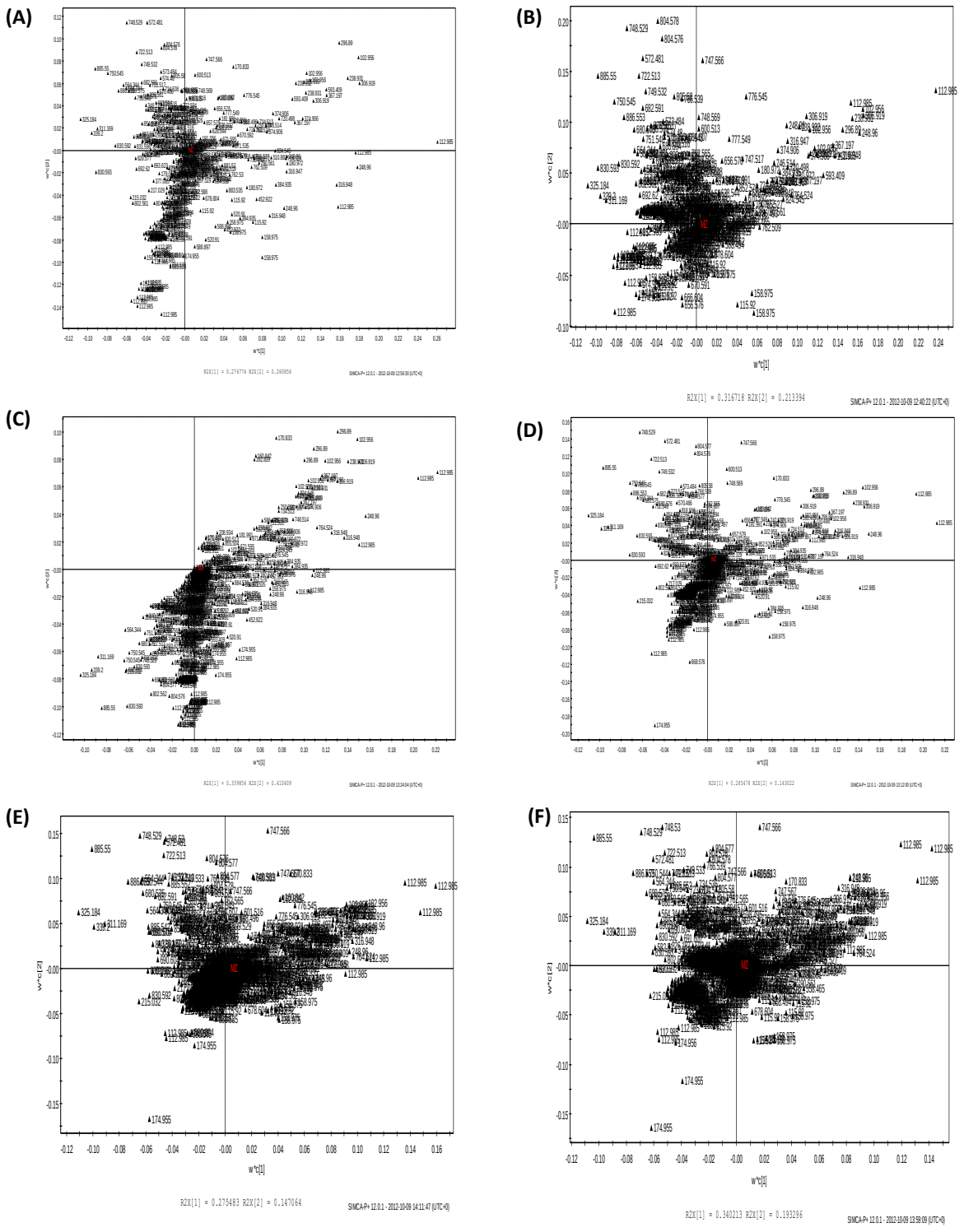


**Figure 3.19. PLS loadings plots representing negative ion LC-MS analysis of 3T3-L1 cells during adipogenesis**

3T3-L1 adipocytes were induced to differentiate at day 0, and harvested at the following days post-differentiation: 0-10, 12, 15, 18, 20, 22 and 25. Lipids were extracted using a Folch extraction, and the lower phase was analysed by LC-MS in negative ion mode. Before multivariate data analysis, the data was processed using SIEVE. The data represented here have been Pareto scaled, and the RT window was set at either 1min, 30sec or 15sec. Either the raw data or data which were normalised to the total ion current were analysed. Each time point consisted of three biological replicates. The panels represent: 1min RT window, no-norm (A); 1min RT window, TIC norm (B); 30sec RT window, no-norm (C); 30sec RT window, TIC-norm (D); 15sec RT window, no-norm (E) and 15sec RT window, TIC-norm.

| Calculated mass | Theoretical mass | Δ Mass accuracy (ppm) | Ion | Elemental composition | Identification |
|---|---|---|---|---|---|
| 722.513 | 722.5130 | 0 | $[M-H]^-$ | $C_{41}H_{74}NO_7P$ | PE (P-36:4) |
| | | | | | PE (O-36:5) |
| 748.5313 | 748.5287 | 3.473 | $[M-H]^-$ | $C_{43}H_{76}NO_7P$ | PE (P-38:5) |
| | | | | | PE (O-37:6) |
| 749.532 | 749.5338 | -2.401 | $[M-H]^-$ | $C_{40}H_{79}O_{10}P$ | PC (34:0) |
| 750.553 | 750.5443 | 11.592 | $[M-H]^-$ | $C_{43}H_{78}NO_7P$ | PE (P-38:4) |
| | | | | | PE (O-38:5) |
| 764.524 | 764.5236 | 0.523 | $[M-H]^-$ | $C_{43}H_{76}NO_8P$ | PC (35:5) |
| 766.539 | 766.5392 | -0.261 | $[M-H]^-$ | $C_{43}H_{78}NO_8P$ | PC (35:4) |
| 804.577 | 804.5549 | 27.469 | $[M-H]^-$ | $C_{46}H_{80}NO_8P$ | PC (38:6) |
| 830.5933 | 830.5917 | 1.926 | $[M-H]^-$ | $C_{45}H_{86}NO_{10}P$ | PS (39:1) |
| 885.5515 | 885.5499 | 1.807 | $[M-H]^-$ | $C_{47}H_{83}O_{13}P$ | PI (38:4) |
| 886.553 | 886.5604 | -8.347 | $[M-H]^-$ | $C_{50}H_{82}NO_{10}P$ | PS (44:8) |

**Table 3.6. Lipid species identified as causes of variance from negative ion loadings plots**

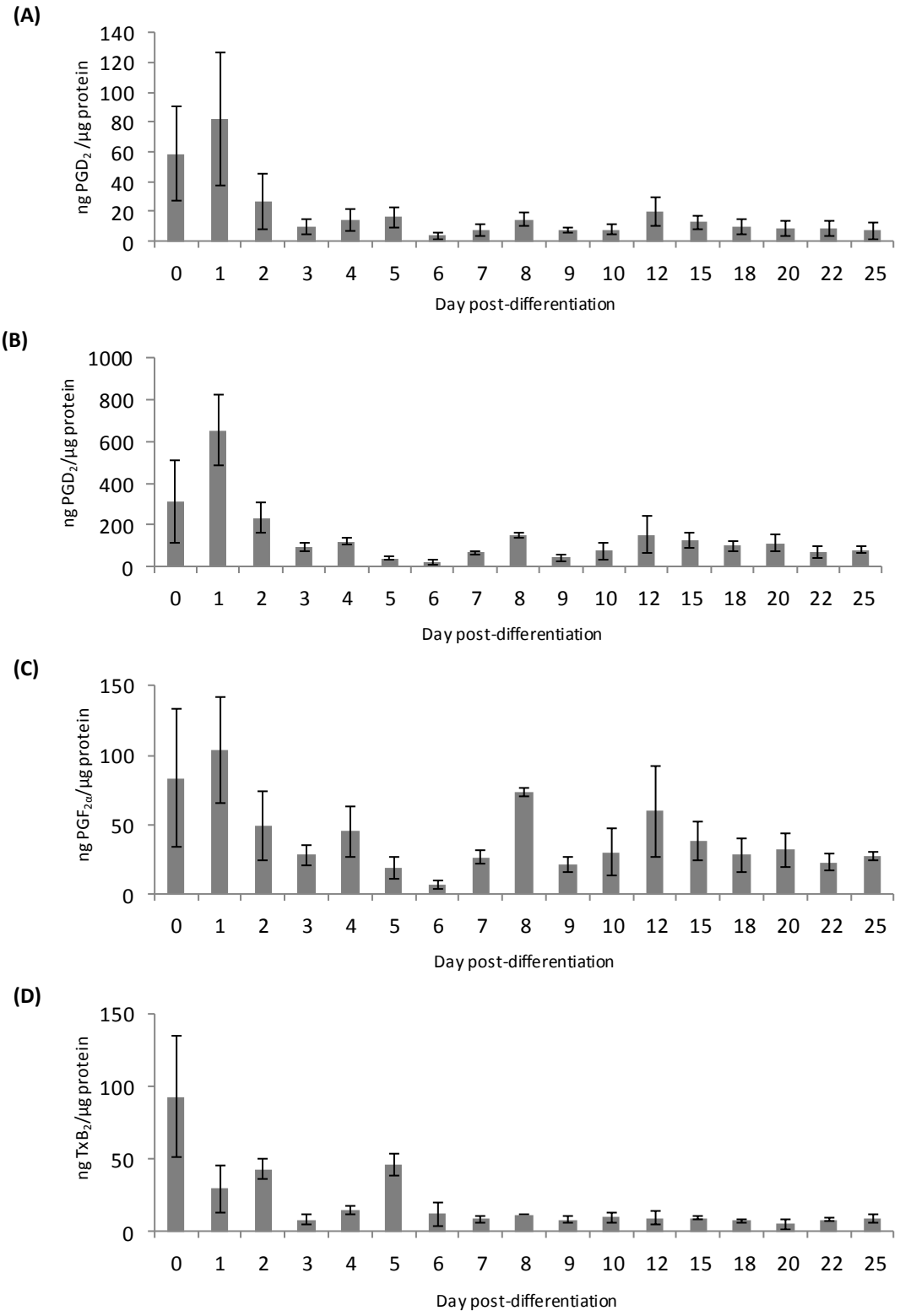


**Figure 3.20. Secretion of eicosanoid lipids by 3T3-L1 cells during adipogenesis**

Eicosanoids were extracted from 3T3-L1 cell culture medium by solid phase extraction chromatography for the following days post-differentiation: 0-10, 12, 15, 18, 20, 22 and 25. The extracted samples were analysed by LC-MS/MS in negative ion mode, and individual eicosanoids were monitored using specific precursor to product ion m/z transitions. Selected eicosanoids were quantified using relevant internal standards (either 15S-HETE-$d_8$, $LTB_4$-$d_4$ or $PGE_2$-$d_4$) and then normalised to the protein concentration of the cell sample. Results are presented as median ± range, for a group size of 3. The selected eicosanoids are $PGD_2$ (A), $PGE_2$ (B), $PGF_{2\alpha}$ (C) and $TxB_2$ (D). A 2-sided Cuzick's test for trend was applied, and a trend was observed in the secretion of all eicosanoids ($P$<0.03 for all).

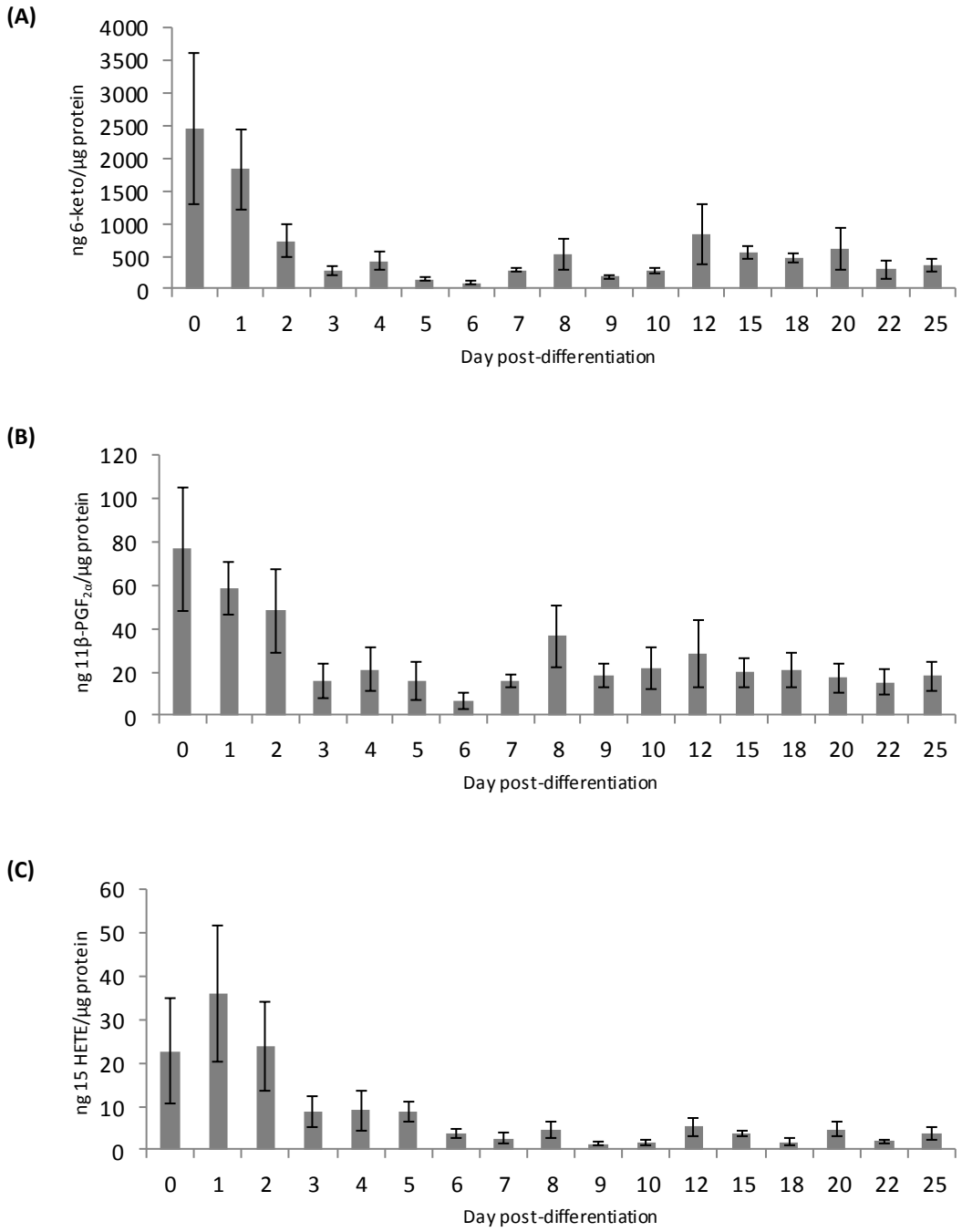


**Figure 3.21. Secretion of eicosanoid lipids by 3T3-L1 cells during adipogenesis**
Eicosanoids were extracted from 3T3-L1 cell culture medium samples by solid phase extraction chromatography for the following days post-differentiation: 0-10, 12, 15, 18, 20, 22 and 25. The extracted samples were analysed by LC-MS/MS in negative ion mode, and individual eicosanoids were monitored using specific precursor to product ion m/z transitions. Selected eicosanoids were quantified using relevant internal standards (either 15S-HETE-$d_8$, $LTB_4$-$d_4$ or $PGE_2$-$d_4$) and then normalised to the protein concentration of the cell sample. Results are presented as medium ± range, for a group size of 3. The selected eicosanoids are 11β-$PGF_{2\alpha}$ (A), 6-keto $PGF_{1\alpha}$ (B) and 15-HETE (C). A 2-sided Cuzick's test for trend was applied, and a trend was observed in the secretion of all eicosanoids, with exception of 6-keto ($P$<0.03 for all).

## 3.5. DISCUSSION

An increase in adiposity is observed in the obese state, which is caused by hypertrophy of mature white adipocytes, and/or adipogenesis of pre-adipocytes (Johnson *et al*., 1971; Faust *et al*., 1978; Johnson *et al*., 1978). This process was explored in the current study *in vitro*, using the established 3T3-L1 cell line and a combination of morphological, transcriptional and lipidomic analyses were used to investigate specific areas of adipogenesis. The 3T3-L1 cell line was validated histologically, and by the expression of key adipokines by comparison with previous studies. Once validated, this model was then used to explore lipid profile changes associated with adipocyte differentiation.

### 3.5.1. Validation of the 3T3-L1 cell line

During adipogenesis, the 3T3-L1 cells start to accumulate lipids in the form of droplets, and change from a fibroblast appearance, to a spherical one (Green and Meuth, 1974; Green and Kehinde, 1976). These morphological changes were evident in the current study. By successfully inducing pre-adipocytes to differentiate into fully mature adipocytes, as proved by the accumulation of lipid droplets, the 3T3-L1 pre-adipocyte cell line was considered a suitable model for the analysis of adipogenesis.

To validate this cell culture system further, the gene expression and secretion of the differentiation dependent proteins leptin and adiponectin were profiled. The gene expression of leptin (MacDougald *et al*., 1995) and adiponectin (Ouchi *et al*., 1999) only occurs after the induction of adipogenesis. These findings were replicated in the current study, as RT-PCR and qPCR, and ELISA analyses only detected gene expression and secretion of these proteins after the differentiation process had been initiated.

For qPCR analyses, a normalisation step is required to correct for sample to sample errors. A common normalisation method is to use an internal control, or housekeeping gene, whose expression should remain stable between cells or tissues, and environmental conditions (Dheda *et al.*, 2004; Radonic *et al*., 2004). Many of the well-used housekeeping genes have shown varying levels of expression between tissues, and so are unsuitable for use as a control. One way to counteract this is to use a number of housekeepers for each

experimental condition (Schmid *et al*., 2003). For that reason, three housekeeping genes were used in the current study. Both β-actin and GAPDH produced similar profiles for both adipokines, suggesting little variability between them, whereas RNApol2 produced a different profile for both leptin and adiponectin. On inspection of the raw data it was noted that there was a great degree of variability in the $C_T$ values for RNApol2 between samples. This suggests that RNApol2 was not an adequate housekeeping gene, and so it was decided to remove it from future qPCR analyses.

### 3.5.2. Changes in global lipid profiles during adipogenesis

Changes across the course of differentiation were also observed with global lipidomic techniques. Both DI-MS and LC-MS analyses were undertaken in positive and negative ion modes to maximise the coverage of the lipidome within the 3T3-L1 adipocytes. Positive ion DI-MS analysis showed a shift in the abundant lipids present from phospholipids (mainly PCs) to TGs over the course of differentiation. It has been documented that an increase in odd-chain FAs, mainly in the form of TG, occurs as 3T3-L1 cells differentiate (Su *et al*., 2004). A previous study found that FAs could be generated during 3T3-L1 metabolism by the utilisation of glucose. Once synthesised, they were either Δ9 desaturated, or underwent α-oxidation to produce odd-chain FAs (Roberts *et al*., 2009). However, this α-oxidation only occurred after differentiation, and pre-adipocytes contain minute concentrations of odd chain FAs, which increase after differentiation (Su *et al*., 2004). The synthesis of unsaturated FAs is catalysed by the enzyme stearoyl-CoA desaturase 1 (SCD1). The gene encoding this enzyme is differentiation-dependent, and has been isolated from 3T3-L1 pre-adipocytes (Ntambi *et al*., 1988).

With the negative ion DI-MS data in this study, the most abundant lipid present in the 3T3-L1 cells from approximately day 3 post-differentiation onwards was the monounsaturated long-chain FA C18:1, identified as oleic acid. A very recent study found that oleic acid is involved in the proliferation of 3T3-L1 pre-adipocytes. When post confluent pre-adipocytes were exposed to low concentrations of oleate, an increase in the division and proliferation of these cells was observed; however, no effects were seen at a greater concentration. In mature 3T3-L1 adipocytes, as the concentration of oleate increased, the number of viable cells decreased due to apoptosis and necrosis, suggesting that this FA has cytotoxic effects in mature adipocytes (Rohana *et al*., 2011).

Principal component analysis and partial least squares analysis were used to analyse both positive and negative LC-MS data. Three RT window values selected at the pre-processing stage were tested in the current study for each of the models. As the RT window narrowed, the clustering of groups became tighter, showing greater separation between early and late time points during the process of adipogenesis. This may be because as the RT window narrows, more frames are created, providing a more thorough representation of the chromatogram. A reduction in R2 and Q2 for PCA, and R2X, R2Y and Q2 for PLS models occurred as the RT window decreased; however, these values were above 0.5 in all models, which indicates a good fit and good predictability. It was, therefore, decided that, for further PCA and PLS analyses, the RT window would be set at 15 sec.

Variation in the abundance of various lipid species was observed over the course of differentiation in the loadings plots. The majority of the selected points were phospholipid species, and the abundance of those identified in positive ion mode increased from as early as day 5 post-differentiation. Those identified in negative ion mode showed an initial increase in abundance between days 0 and 3, followed by a decrease until the end of the time course. Therefore, opposing actions occurred in the abundance of the phospholipid species identified. A previous study has demonstrated that phospholipid content of cultured 3T3-L1 adipocytes was approximately 8-fold greater than that of pre-adipocytes, and the majority of these lipids present were PC and PE species. This increase in the phospholipids, along with TG species and cellular protein was observed from day 3 post-differentiation onwards (Kasturi and Wakil, 1983). The authors of this study suggested that the increase in phospholipid and protein content observed during the differentiation process may be due to a requirement for membrane synthesis and assembly.

The decrease in phospholipid species abundance from the negative ion datasets were seen from approximately day 4 post-differentiation, which may explain why samples from this time point were situated closer to the day 7-25 group rather than the day 0-6 group in the majority of PCA and PLS models.

### 3.5.3. Changes in eicosanoid secretion during adipogenesis

A change in the production of AA-derived eicosanoid species by these cells was also observed as the 3T3-L1 cells began the differentiation process. Only members of the prostanoid family, which consists of PG and Tx species produced via the cyclooxygenase pathway, were detectable in the media samples of the differentiating cells, with the exception of 15-HETE. It is known that adipocytes can synthesise prostanoids, with the secretion of $PGE_2$, 6-keto-$PGF_{1\alpha}$, $PGF_{2\alpha}$ and 15d-$PGJ_2$ by 3T3-L1 adipocytes being documented (Borglum *et al*., 1999). A previous study demonstrated that 3T3-L1 adipocytes produce different concentrations of prostanoids depending on their life cycle. The formation of $PGD_2$ occurred during the maturation phase, whereas $PGE_2$ was more efficiently produced by pre-adipocytes (Lu *et al*., 2003). $PGE_2$ negatively modulates cAMP production and lipolysis in both human and rat adipocytes, via interaction with specific receptors, which could explain the increased accumulation of TG (Strong *et al*., 1992; Vassaux *et al*., 1992b). In contrast, $PGF_{2\alpha}$ inhibits adipocyte differentiation (Miller *et al*., 1996; Vassaux *et al*., 1994). The data presented in the current study agree with these findings, $PGD_2$, $PGE_2$ and $PGF_{2\alpha}$ were all detectable in the medium from both pre- and fully mature adipocytes. For all profiles, a transient increase occurred, followed by a gradual decline. Seeing as $PGF_{2\alpha}$ inhibits adipocyte differentiation, this decrease could explain the continual accumulation of lipid droplets. An initial increase of $PGE_2$ suggests more efficient production by pre-adipocytes, and although concentration decreases over the time course, it is still detectable in mature adipocytes, which may help inhibit lipolysis. Finally, $PGD_2$ was detectable across the course of differentiation, possibly aiding maturation of these cells.

The AA-derived non-prostanoid 15-HETE was also detected, and this eicosanoid is a product of the lipoxygenase pathway, and has been suggested to derive from leukocyte-12/15-LO when it reacts with saturated fatty acids (Chakrabarti *et al*., 2009). A role in adipocyte differentiation has been suggested as the inhibition of 12/15-LO prevents 3T3-L1 cells differentiating into mature adipocytes (Madsen *et al*., 2003). Even though the present study shows a decrease in 15-HETE secretion from day 4 post-differentiation onwards, it is still detectable throughout the time course, and so may play a part in adipocyte differentiation.

### 3.5.4. Limitations and future directions

A few limitations were present in the current study, which related to the global lipidomic analyses. The first was the fact that with the direct infusion data, only the mass-to-charge ratio could be used to search the lipid databases for identification of the lipid species. With the LC-MS data, the retention time was also used alongside the mass-to-charge ratio, thereby providing extra information to aid in the identification of lipid species. By only having exact mass data, fatty acid compositions could not be assigned to the phospholipid or triglyceride species. For example, PC 16:0/18:1 could also be PC 18:1/16:0, or PC 16:1/18:0 etc. and it is impossible to determine which one is correct with only m/z. Therefore, in the current study, this phosphatidylcholine species would be named PC (34:1). A final limitation was the slight shift in retention time observed in some of the global LC-MS chromatograms. These shifts could have been occurred due to many reasons, one of which is fluctuations in temperature. In the current study, the mobile phases had to be remade occasionally, due to the quantity of samples, and so slight variations in mobile phase composition may have been the cause. Ideally, all samples would have been run with the same mobile phases (A and B) for all samples, to help eliminate these shifts.

### 5.3.5. Conclusions and future work

The work presented in this chapter demonstrated that as 3T3-L1 cells were differentiated from pre-adipocytes to fully mature adipocytes, changes in lipid metabolism occurred. Individual lipid species were identified, and positive ion analyses showed a change from the presence of predominantly phospholipid species in the pre-adipocytes, to mainly triglycerides in the mature adipocytes. Analysis of selected individual species also found that the concentration of TG (48:2) and TG (50:2) became greater than that of PC (34:1) and PC (36:4) at day 7 post-differentiation, and continued to increase throughout the remainder of the time course. This was expected due to the continual accumulation of lipid droplets which is characteristic of this cell line during the differentiation process.

Various AA-derived eicosanoid species were secreted by the 3T3-L1 cells in the current study, and their concentrations were greatest at the stage of pre-adipocyte and early differentiation. Of interest were the prostanoids $PGE_2$ and $PGF_{2\alpha}$ because they are known to have contrasting actions, with $PGE_2$ reducing lipolysis in human and rat adipocytes (Strong *et al*., 1992; Vassaux *et al*., 1992b) and $PGF_{2\alpha}$ inhibiting adipocyte differentiation (Miller *et al*., 1996; Vassaux *et al*., 1994). These eicosanoids are produced from AA (Piomelli, 1993), which is released from membrane phospholipids. This fatty acid was identified in the current study

(C20:4), and its concentration was seen to decrease in the later time points. This may also play a role in the decreased concentration of all detected eicosanoid species observed after differentiation in the current study.

Therefore, it was concluded from the current study that the individual lipid metabolism processes investigated could possibly to be linked. Maturation from a pre-adipocyte to an adipocyte led to a lipid profile change from mainly phospholipid species, to predominantly triglycerides. This switch caused a decrease in arachidonic acid, and therefore eicosanoid production by the cells further on in the differentiation process. A decrease in the concentration of certain eicosanoids allows the continuation of lipid accumulation associated with adipogenesis, for example $PGF_{2\alpha}$ which inhibits the process, and would allow the accumulation of TG species, as identified by morphological changes, and also the change in lipid profiles.

Various extra experiments would improve these conclusions. One example would be to investigate the gene expression of SCD1 which is expressed in adipocytes in a differentiation dependent manner (Ntambi *et al*., 1988), and aids the synthesis of unsaturated FAs. It would be interesting to observe how the gene expression of SCD1 changes, in relation to the shift in lipid species observed in the current study.

Various genes are involved in the induction of adipogenesis, including PPARγ, C/EBPα and ADD1/SREBP1c. It would be of interest, therefore, to monitor the gene expression of these factors, also to see if their expression profiles correlate to the findings in the current study.

# CHAPTER 4:

## Effect of inflammatory agents on 3T3-L1 adipocyte metabolism

## 4.1. INTRODUCTION

Obesity is characterised by chronic low-grade systemic inflammation (Yudkin *et al*., 1999; Festa *et al*., 2001), and changes in the gene expression and protein secretion of a number of adipokines and cytokines have been linked to this inflammatory state (Trayhurn and Wood, 2004). One example is TNF-α, the production of which increases in rodent models of obesity (Hotamisligil *et al.*, 1993). This cytokine acts in both an autocrine and paracrine way to influence its own expression, as well as a number of other processes, including the production and inhibition of several adipokines and cytokines. For example, TNF-α treatment of human adipocytes caused conflicting effects of the gene expression of various adipokines and cytokines, with an increase in that of IL-6 as well as itself being observed. No effect on leptin gene expression was seen, whereas that of adiponectin decreased (Wang *et al.*, 2005).

The cytokine IL-6 also has an autocrine effect on its own gene expression and protein secretion in murine adipocytes, and is capable of inducing insulin resistance in these cells (Lagathu *et al.,* 2003). Conflicting reports about the effect of IL-6 on leptin expression exist, with a previous study finding that IL-6 decreases leptin expression in rodent adipocyte models (Granowitz, 1997). In contrast, reports in human adipose tissue have shown that IL-6 either increased or had no effect on leptin gene expression, depending on the experimental conditions used (Bruun *et al*., 2002; Tujillo *et al*., 2004). Adiponectin expression has been shown to be inhibited by IL-6 (Fasshauer *et al*., 2003b).

There is increasing evidence demonstrating that TNF-α is involved in the dysfunction of normal lipid metabolism, as seen in TNF-α deficient mice which have decreased circulating free fatty acids (FFA) and triglycerides (TG) compared to their wild-type littermates (Uysal *et al*., 1997; Ventre *et al*., 1997). The addition of TNF-α to 3T3-L1 adipocytes stimulates lipolysis (Kawakami *et al*., 1987). And a similar finding was observed in primary rat epididymal adipocytes, where the addition of TNF-α caused an increase in lipolysis, although no change was seen in the concentration of hormone-sensitive lipase (Green *et al*., 1994). TNF-α is an important mediator of obesity-related insulin resistance (Hotamisligil *et al.*, 1993; 1994 and 1995). Stimulation of lipolysis leads to an increase in the concentration of FFA, and so, the insulin-resistant state caused by TNF-α may be due to increased lipolysis (Miles *et al*., 1997; Peraldi *et al*., 1997).

A role for IL-6 in lipid metabolism has also been suggested, with a previous study demonstrating that it decreases the activity of lipoprotein lipase (LPL) in the 3T3-L1 cell-line (Greenberg *et al*., 1992). This finding was also supported in obese human patients, who demonstrated decreased LPL activity and increased rates of spontaneous or basal lipolysis after IL-6 treatment (Trujillo *et al*., 2004). A previous *in vitro* study demonstrated that IL-6 impaired insulin signalling in 3T3-L1 and human adipocytes (Rotter *et al*., 2003).

The inflammatory state associated with obesity also has an effect on the production of various eicosanoid species. Treatment with TNF-α is known to decrease lipoprotein lipase LPL synthesis and inhibit adipocyte differentiation. Increased gene expression and protein secretion of COX-2 has been observed in response to TNF-α treatment of pre-adipocytes (Xu *et al*., 2007); whereas COX-2 inhibitors have been shown to reverse the inhibition of differentiation induced by TNF-α (Yan *et al*., 2003). Coupled to this is the fact that TNF-α also stimulates the formation of $PGE_2$ in various cell types (Dayer *et al*., 1985; Bachwich *et al*., 1986; Lehmmann *et al*., 1988), which itself also causes inhibition of adipocyte differentiation (Vassaux *et al*., 1992b).

### 4.1.2. Aims of the current study

Previous studies have shown that the inflammatory state associated with obesity causes normal lipid metabolism processes within the adipocyte to become dysregulated. Therefore, the purpose of the current study was to explore the effects of the inflammatory agents TNF-α and IL-6 on the normal function of 3T3-L1 adipocytes. These cells were treated at day 10 post-differentiation with either TNF-α or IL-6 at three concentrations for either 2, or 24 hours (h).

The first specific aim was to quantify the gene expression of leptin, adiponectin, IL-6 and TNF-α in both the control day 10 adipocytes, and also in those which had been treated with the inflammatory agents. It was predicted that normal adipokine gene expression would be affected, specifically the gene expression of leptin, TNF-α and IL-6 would increase in the treated cells when compared to the control cells, whereas the gene expression of adiponectin would decrease. This prediction was based on previous findings after treatment with TNF-α (Wang *et al*., 2005) and IL-6 (Granowitz, 1997; Bruun *et al*., 2002; Fasshauer *et al*., 2003b; Lagathu *et al*., 2003; Tujillo *et al*., 2004).

The second aim was to produce global lipid profiles of these adipocytes. It was predicted that the majority of the lipid species present would be both phospholipid and triglyceride species; however, the abundance of these species would change after treatment with TNF-α and IL-6, causing a lipid profile change.

After global lipid profiles were produced, the final aim was to monitor any changes in the concentration of detected eicosanoid species secreted by these adipocytes, and it was hypothesised that the concentration of any detected species would increase in the cells treated with the inflammatory agents when compared to the controls.

## 4.2 MATERIALS AND METHODS

### 4.2.1. Cell culture

3T3-L1 adipocytes were cultured at 37°C in a humidified atmosphere of 5%$CO_2$ / 95% air as previously described in Section 2.1.3. All media protocols are listed in Section 2.1.2. The cells were induced to differentiate at day 0, and all treatments occurred at day 10 post-differentiation. The adipocytes were starved of calf serum (CS) for 24 hours (h) before treatment, by feeding with DMEM alone. After 24h, the cells were treated with CS-free medium containing either mouse recombinant TNF-α or IL-6 at the following concentrations: 5, 25 and 50 ng/mL. The control cells had the CS-free incubation medium renewed. The cells were harvested at two and 24h post-treatment, along with the medium, and both were stored at -80°C until needed.

### 4.2.2. Real time PCR

Total RNA was extracted from cultured cells using TRI Reagent® as described in Section 2.4.2. Gene expression was quantified by real-time PCR (qPCR) as described in Sections 2.6.2.2 and 2.6.3. The genes investigated in this chapter were leptin, adiponectin, TNF-α and IL-6.

### 4.2.3. Global lipidomic analysis

#### *4.2.3.1. Cell preparation*

Lipids were extracted from cell and quality control (QC) samples using the Folch extraction method (Folch *et al*., 1957) as described in Section 2.10.2, and the lower chloroform phase was dried down under nitrogen, and reconstituted in 600µL chloroform / methanol (2/1, v/v). Ammonium formate (10mM) was added to the direct infusion-mass spectrometry (DI-MS) analysis samples, but not the liquid chromatography-mass spectrometry (LC-MS) samples.

#### *4.2.3.2. DI-MS method*

The lipid extracts were directly infused into an Orbitrap Exactive mass spectrometer in both positive and negative ion mode as described in Section 2.10.4. Selected lipid peaks were quantified using an appropriate internal standard, either 1,2-didodecanoyl-*sn*-glycero-3-phosphocholine, PC 12:0/12:0, or, 1,2,3-trioctadecanoyl-sn-glycerol TG 18:0/18:0/18:0, and then normalised to the protein concentration of the cell samples. Three databases were used to identify the lipid species based on their mass-to-charge ratio (m/z), and they were: the Human Metabolome Database (HMDB; www.hmdb.ca), LIPID Metabolites and Pathways Strategy (LIPID MAPS; www.lipidmaps.org), and the Metabolite and Tandem MS Database (METLIN; http://metlin.scripps.edu). Confident identifications were assumed when the mass accuracy was within 5 parts per million (ppm), and unless stated, all discussed lipid species were within this parameter.

#### *4.2.3.3. LC-MS method*

Lipid extracts were analysed by LC-MS as described in Sections 2.10.6.2 and 2.10.6.3. All LC-MS raw files were processed using SIEVE to produce m/z, retention time (RT) and intensity values. The RT window was set to 15 seconds (sec). Lipids were identified with the databases mentioned above in either positive or negative ion mode.

#### *4.2.3.4. Multivariate data analysis of LC-MS data*

The RT and m/z pairs, along with their intensities were normalised to the total ion current (TIC) intensity. The multivariate data analysis (MVDA) package SIMCA-P (v12) was used for principal component analysis (PCA) and partial least squares (PLS) analysis of the normalised and non-normalised datasets, and all models were Pareto scaled.

### 4.2.4. Targeted eicosanoid analysis

Eicosanoids were extracted from 3T3-L1 medium samples using solid phase extraction chromatography, as described in Section 2.11.1 and 2.11.2.1. Once the eicosanoids had been eluted, they were dried down under a gentle stream of nitrogen and reconstituted in 100µL $H_20$:MeOH (1:1, v:v). The samples were then analysed by LC-MS/MS using a TSQ Quantum Ultra triple quadrupole mass spectrometer, as described in Section 2.11.3. Identification of the eicosanoid species was achieved by using specific precursor-to-product ion m/z transitions, which are shown in Table 2.3 (Chapter 2).

### 4.2.5. Statistical analysis

All statistical analyses were completed using StatsDirect. To determine the normality of the sample data, a Shapiro-Wilk W test was used. All of the mass spectrometry data were not normally distributed, and so the non-parametric Friedman's two-way analysis of variance test was used followed by an all pairwise comparisons (Conover) post-hoc test to identify differences between groups. Statistical analysis of qPCR data is often completed using non-parametric tests irrespective of normality (Yuan *et al*., 2006), and so the Friedman's two-way analysis of variance test was also used for all qPCR analyses. Normally distributed data were presented as mean values ± SD, whereas data which were not normally distributed were presented as median ± range. The group size used is indicated in the figure captions, and a *P*-value of $< 0.05$ was considered statistically significant.

## 4.3. RESULTS

### 4.3.1. Gene expression of leptin and adiponectin

The gene expression of four genes was monitored in response to either IL-6 or TNF-α, and these were leptin, adiponectin, IL-6 and TNF-α. After 2h of TNF-α treatment (Figure 4.1), a direct relationship was seen between TNF-α treatment concentration and leptin gene expression, although the increase was only significant at the greatest concentration (50ng/mL; *P*=0.014 *vs.* control; Figure 4.2A). The inverse relationship was observed at the 24h treatment time (*P*<0.05 *vs.* control for all). A significant decrease in adiponectin gene expression was seen at both time points for the 25 and 50ng/mL TNF-α treatment concentrations (*P*<0.001 *vs.* control; Figure 4.2B). A significant increase in IL-6 gene expression was seen at the greatest treatment concentration (50ng/mL) after 2h of TNF-α treatment (*P*=0.008) and this profile was similar after 24h of treatment, although the gene expression was significant for all concentrations (*P*<0.01 *vs.* control for all; Figure 4.1C). TNF-α gene expression was undetermined in the majority of the TNF-α treatment concentrations at both time points, and so was not presented in the figure.

After 2h of IL-6 treatment (Figure 4.2), an increase was seen in leptin gene expression (A) which became significant at 25 and 50 ng/mL (*P*=0.032 *vs.* control for both), and an increase was also observed after 24h of treatment (*P*<0.001 *vs.* control for all concentrations). No significant changes were observed in the gene expression of adiponectin at the 2h treatment time; however, after 24h of treatment a decrease was observed at the two greater concentrations (*P*<0.001 *vs.* control for both 25 and 50ng/mL; Figure 4.2B). IL-6 treatment caused an increase in its own expression after 2h (*P*=0.007 and *P*<0.001 *vs*. control for 25 and 50ng/mL, respectively). A similar increase was also seen after 24h of IL-6 treatment (*P*=0.013 and *P*<0.001 *vs.* control for 5 and 50ng/mL, respectively; Figure 4.2C). The gene expression of TNF-α increased after 2h of IL-6 treatment at 50ng/mL (*P*<0.001 *vs.* control; Figure 4.2D). At the 24h IL-6 treatment time, an increase in the gene expression of TNF-α was seen at two of the concentrations (*P*<0.001 *vs.* control for 5 and 50ng/mL, respectively).

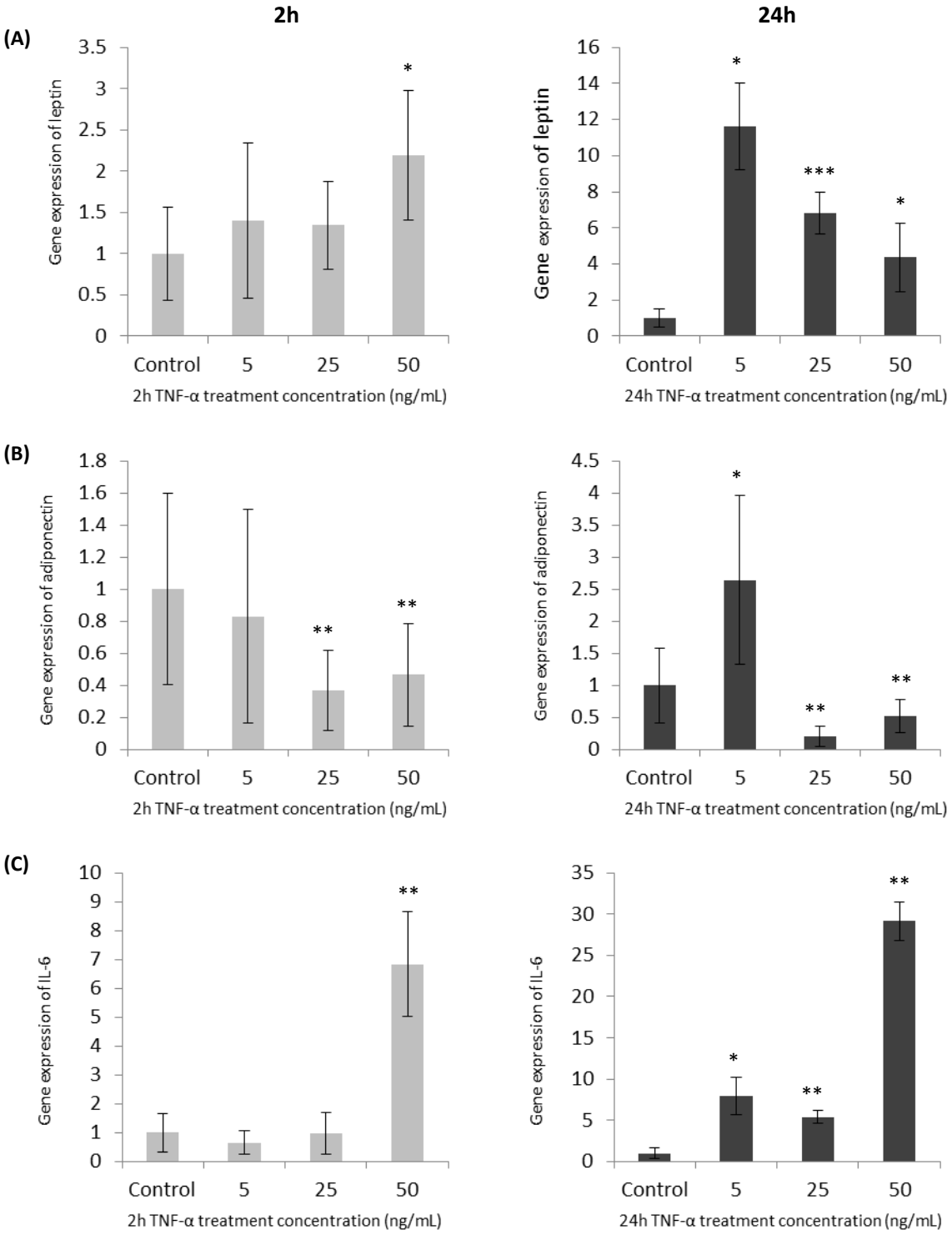


**Figure 4.1. Adipokine gene expression of TNF-α treated 3T3-L1 adipocytes**

Differentiated 3T3-L1 adipocytes at day 10 post-differentiation were pre-incubated with CS-free medium for 24h, and then treated with mouse recombinant TNF-α for 2 and 24h. The concentration of TNF-α treatments were 5, 25 and 50ng/mL. Adipokine gene expression was quantified by qPCR and normalised to GAPDH relative to the control group. Results are represented as means ± SD for a group size of 6. The adipokines quantified were leptin (A), adiponectin (B), and IL-6 (C). Significant increases were observed in the gene expression of leptin and IL-6, whereas adiponectin gene expression was seen to significantly decrease with TNF-α treatment. Statistical significance from the control cells is represented by *$P$<0.05; **$P$<0.01 and *** $P$<0.001.

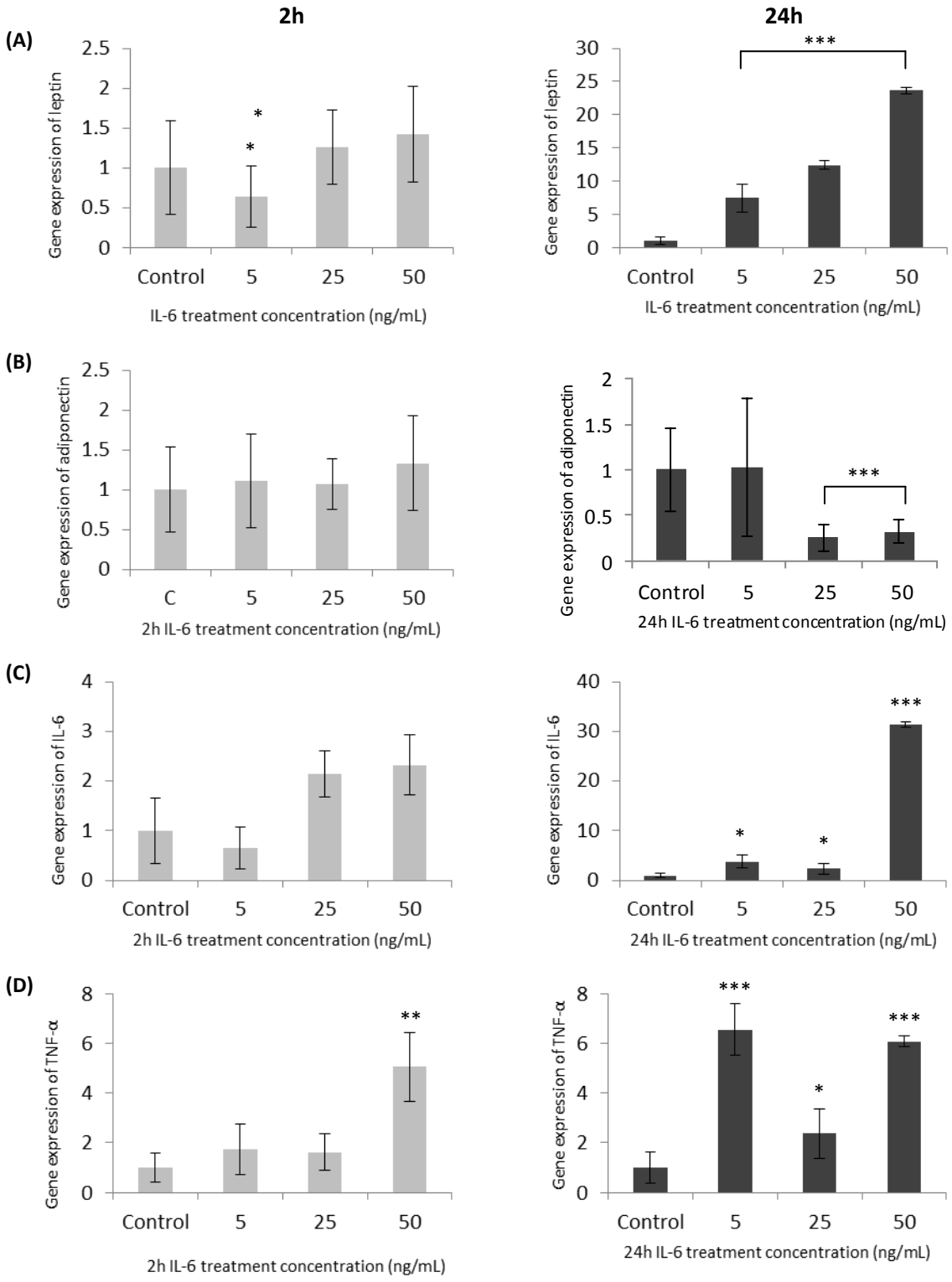


**Figure 4.2. Adipokine gene expression of IL-6 treated 3T3-L1 adipocytes**

Differentiated 3T3-L1 adipocytes at day 10 post-differentiation were pre-incubated with CS-free medium for 24 hours, and then treated with mouse recombinant IL-6 for 2 and 24 hours. The concentration of IL-6 treatments were 5, 25 and 50ng/mL. Adipokine gene expression was quantified by qPCR and normalised to GAPDH relative to the control group. Results are represented as means ± SD for a group size of 6. The adipokines quantified were leptin (A), adiponectin (B), IL-6 (C) and TNF-α (D). The gene expression of leptin, IL-6 and TNF-α increased after 24h of IL-6 treatment, whereas adiponectin gene expression decreased. Statistical significance from the control cells is represented by * $P<0.05$; ** $P<0.01$ and *** $P<0.001$.

### 4.3.2. Positive ion mode DI-MS analysis

#### *4.3.2.1. TNF-α treatment*

Representative positive ion spectra of control cells and those treated with 50ng/mL TNF-α at 24h, are presented in Figure 4.3 (A and B, respectively). Differences were observed in these global lipid profiles between the control and treated cells at both time points. More peaks were present between m/z 700 and 900Da in the control cells when compared to the TNF-α treated samples. The abundance of all peaks seemed to decrease in the treated samples, as seen by the increase in the peaks with m/z 622.4432 and 908.8631, which relate to the internal standards.

The ten most abundant peaks from the global lipid profiles of the control cells, and the top ten from the TNF-α treated samples from Figure 4.3 were identified, and are presented in Table 4.1. In the control cells (A), the lipids identified were all either phosphatidylcholine (PC), diglyceride (DG), or triglyceride (TG) species. In the TNF-α treated cells, the top ten abundant peaks were different from those seen in the controls, with exception of the peak with m/z 575.50. The majority of the remaining lipids were either DG or TG species. There were also two phospholipid species present. The majority of these species had a mass accuracy much greater than 5ppm, and so were not considered to be confident identifications.

The lipid species identified in Table 4.1 were quantified using the relevant internal standard, either PC (12:0/12:0) or TG (18:0/18:0/18:0), with m/z 622.4432 or 908.8631, respectively. They were then normalised to the protein content of the sample. After this stage, the top four lipid species from the control cells, and all TNF-α treatments at both 2h (A) and 24h (B) were represented graphically in Figure 4.4. These species had m/z 575.5023, 603.5342, 846.7528 and 874.7845, and were identified as DG (33:4); DG (35:4); TG (50:3) and TG (52:3). After 2h of TNF-α treatment, no changes in the concentration of these lipids was observed, with the exception of DG (35:4) which decreased ($P$=0.005 and P<0.001 *vs.* control for 5 and 50ng/mL, respectively). The concentration of this lipid species also decreased after 24h of TNF-α treatment ($P$=0.0134 and $P$<0.001 *vs.* control for 5 and 25ng/mL, respectively). The remaining lipids all behaved in the same way, with a decrease in their concentration at 5 and 25ng/mL, followed by an increase at the greatest treatment concentration ($P$=0.05 for all).

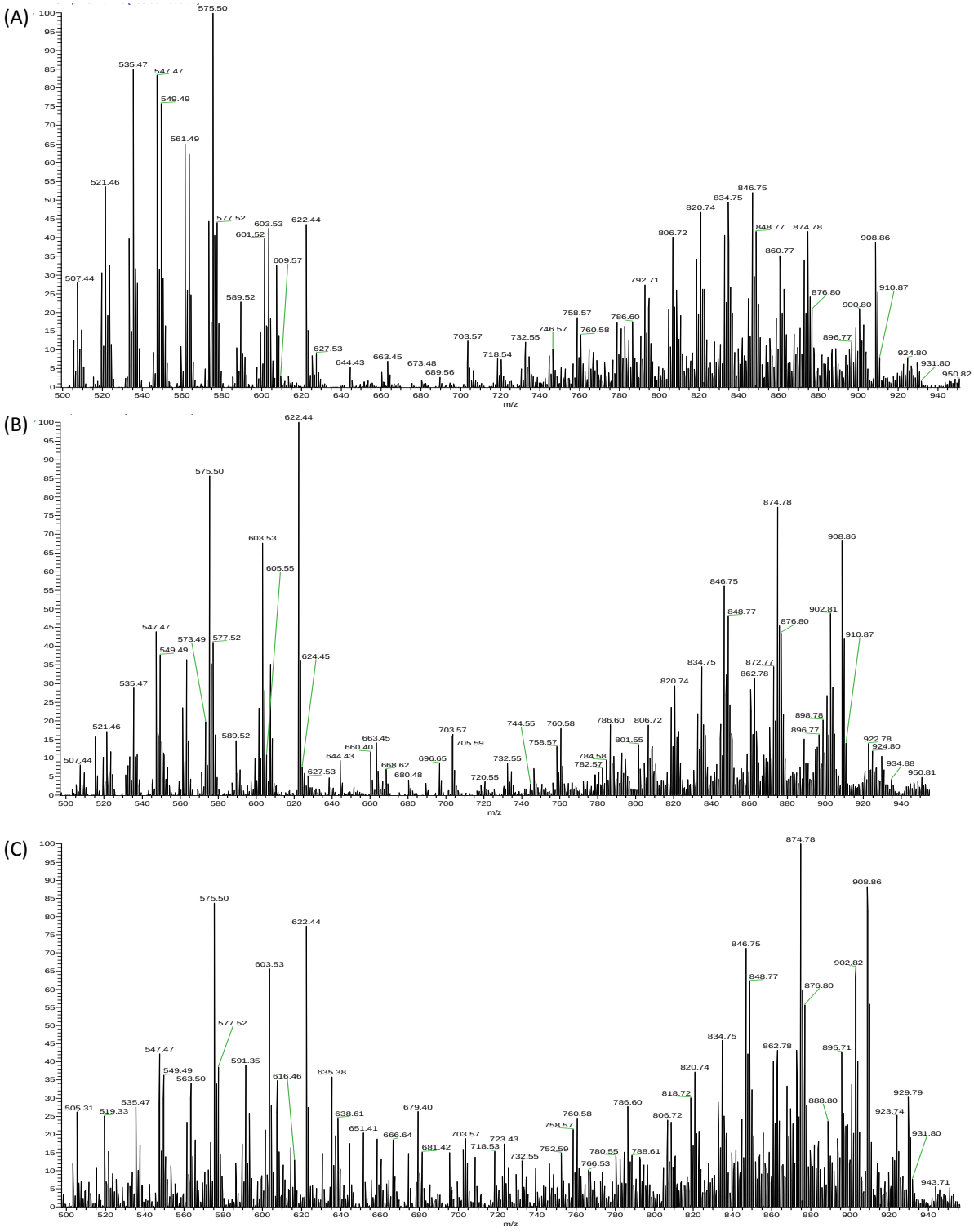


**Figure 4.3. Positive ion DI-MS analysis of TNF-α and IL-6 treated 3T3-L1 adipocytes** Representative spectra of differentiated 3T3-L1 adipocytes at day 10 post-differentiation which were pre-incubated with CS-free medium for 24h, and then treated with mouse recombinant TNF-α or IL-6 for 2 and 24h. The treatments represented are: control 24h (A); 50ng/mL TNF-α 24h (B) and 50ng/mL IL-6 24h (C). Lipids were extracted from the cell samples using a Folch extraction. The lower phase was dried down under nitrogen and reconstituted in 600µL chloroform/methanol (2/1, v/v). A 150µL aliquot was removed and had 10mM ammonium formate added to it. The samples were then directly infused into an Orbitrap Exactive mass spectrometer at a flow rate of 5µL/min for 90 seconds (450 scans) in positive ion mode. The m/z range represented is between 500 and 950Da. A greater relative abundance of peaks with m/z 622.44, 874.78 and 908.86 were observed in the treated cells compared to the controls.

| Calculated mass | Theoretical mass | Δ Mass accuracy (ppm) | Ion | Elemental composition | Identification |
|---|---|---|---|---|---|
| ***(A) Control*** | | | | | |
| 535.4715 | 535.4387 | 61.258 | $[M+H]^+$ | $C_{33}H_{58}O_5$ | DG (30:3) |
| 547.4713 | | | | | |
| 549.4868 | 549.4513 | 64.610 | $[M+H]^+$ | $C_{34}H_{60}O_5$ | DG (31:3) |
| 563.5025 | 563.4670 | 63.003 | $[M+H]^+$ | $C_{35}H_{62}O_5$ | DG (32:3) |
| 575.5023 | 575.4670 | 61.341 | $[M+H]^+$ | $C_{36}H_{62}O_5$ | DG (33:4) |
| 834.7528 | 834.7545 | -2.037 | $[M+NH_4]^+$ | $C_{52}H_{96}O_6$ | TG (49:2) |
| 841.6669 | 841.6429 | 28.516 | $[M+NH_4]^+$ | $C_{47}H_{86}NO_8P$ | PC (39:4) |
| 855.6821 | 855.6586 | 27.464 | $[M+NH_4]^+$ | $C_{48}H_{88}NO_8P$ | PC (40:4) |
| 867.6822 | 867.6586 | 27.200 | $[M+NH_4]^+$ | $C_{49}H_{88}NO_8P$ | PC (41:5) |
| 895.7122 | 895.7263 | -15.741 | $[M+NH_4]^+$ | $C_{52}H_{96}NO_7P$ | PC (O-44:5) |

***(B) Extra identifications from TNF-α treatment at 50ng/mL***

| | | | | | |
|---|---|---|---|---|---|
| 603.5342 | 603.4994 | 57.664 | $[M+H]^+$ | $C_{38}H_{66}O_5$ | DG (35:4) |
| 607.5654 | 607.5296 | 58.927 | $[M+H]^+$ | $C_{38}H_{70}O_5$ | DG (35:2) |
| 622.4432 | 622.4442 | -1.607 | $[M+H]^+$ | $C_{32}H_{64}NO_8P$ | PC (24:0) |
| 663.4535 | 663.4708 | -26.075 | $[M+H]^+$ | $C_{34}H_{63}O_{10}P$ | PG (28:2) |
| 846.7528 | 846.7545 | -2.008 | $[M+NH_4]^+$ | $C_{53}H_{96}O_6$ | TG (50:3) |
| 848.7686 | 848.7701 | -1.767 | $[M+NH_4]^+$ | $C_{53}H_{98}O_6$ | TG (50:2) |
| 874.7845 | 874.7858 | -1.486 | $[M+NH_4]^+$ | $C_{55}H_{104}NO_6$ | TG (52:3) |
| 902.8155 | 902.8171 | -1.772 | $[M+NH_4]^+$ | $C_{57}H_{104}O_6$ | TG (52:2) |
| 908.8631 | 908.8641 | -1.100 | $[M+NH_4]^+$ | $C_{57}H_{110}O_6$ | TG (54:0) |

**Table 4.1. Identifications of selected positive ions from control and TNF-α treated 3T3-L1 adipocytes**

Abbreviations used: DG, diglyceride; PC, phosphatidylcholine; TG, triglyceride; ppm, parts per million

Underlined masses are present in both control and TNF-α treated cells, and those highlighted in red represent the internal standards



183

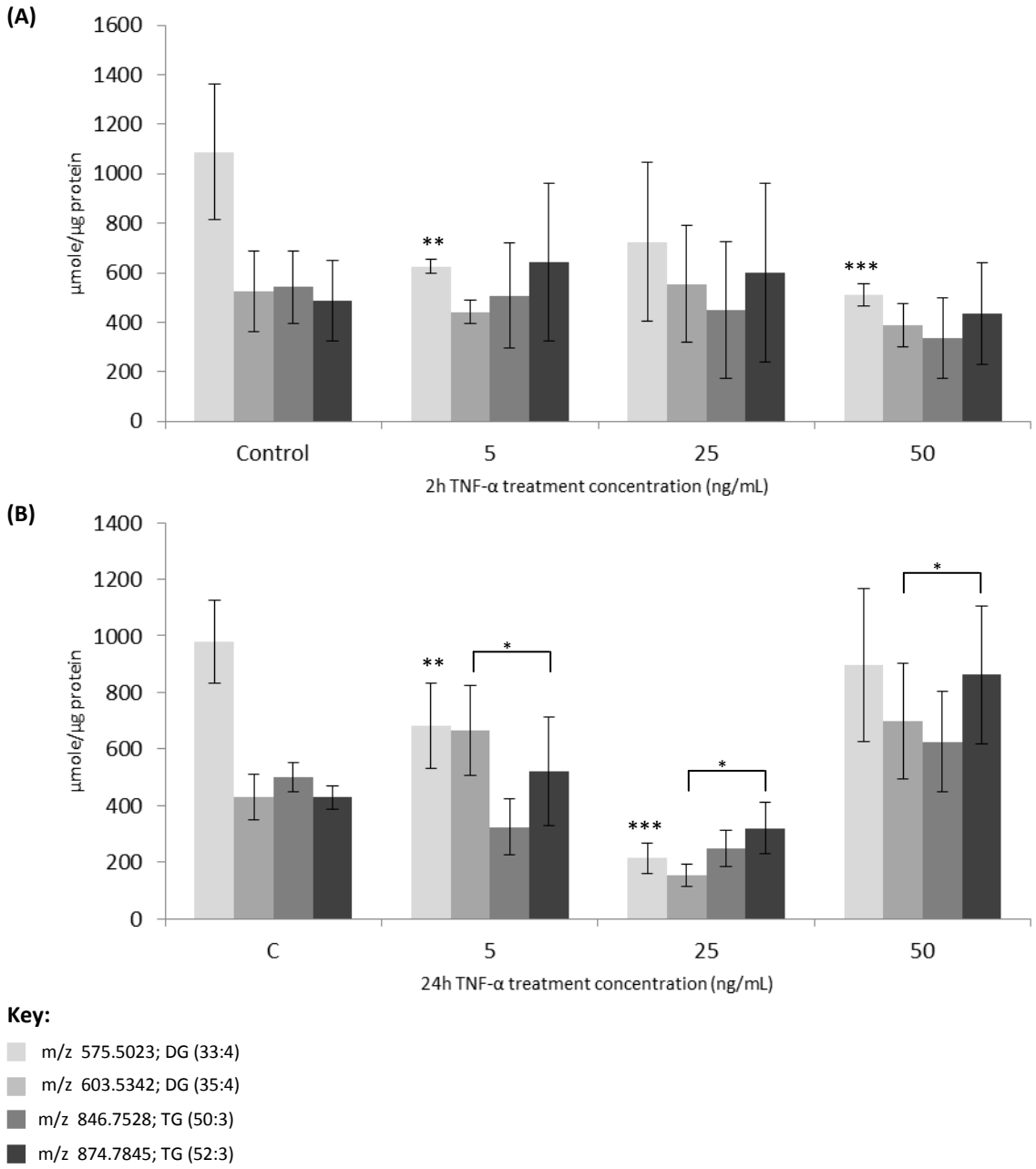


**Figure 4.4. Individual lipid concentrations from positive ion DI-MS analysis of TNF-α treated 3T3-L1 adipocytes**

Differentiated 3T3-L1 adipocytes at day 10 post-differentiation were pre-incubated with CS-free medium for 24 hours, and then treated with mouse recombinant TNF-α for 2 and 24h at the following concentrations: 5, 25 and 50ng/mL. Lipids were extracted from the cell samples using a Folch extraction, and the lower phase was dried down under nitrogen and reconstituted in 600µL chloroform/methanol (2/1, v/v). A 150µL aliquot was removed and had 10mM ammonium formate added to it. The samples were then directly infused into an Orbitrap Exactive mass spectrometer at a flow rate of 5µL/min for 90 seconds (450 scans) in positive ion mode. The raw data intensities were normalised to that of the relevant internal standard which were PC (12:0/12:0) or TG (18:0/18:0/18:0), and had m/z 622.44 and 908.86, respectively. They were then normlaised to the protein concentration of the cell sample.

The top four normalised lipids are presented in this figure, and identified in the key. For each time point, n=3, with results represented as median ± range. A decrease was seen in the concentration of DG (33:4) after 2h, and decreases were seen all species after 24h at 5 and 25ng/mL, whereas an increase was observed at the greatest TNF-α treatment concentration. Statistical significance from the control cells is represented by **P*<0.05; ***P*<0.01 and ****P*<0.001.

#### *4.3.2.2. IL-6 treatment*

Representative spectra of IL-6 treated cells were also produced, and a representive spectrum of 3T3-L1 cells treated with 50ng/mL IL-6 for 24h is shown in Figure 4.3C. As with the TNF-α treated cells, the abundant lipid species present had m/z between 500-650Da; and also 800-950Da. The abundance of peaks with m/z 622.4432 and 908.8631 increased in the IL-6 treated cells compared to the controls, and these peaks correspond to the internal standards, suggesting a decrease in the abundance of sample lipid species.

The top ten most abundant peaks from the lipid profiles of the control cells, and those treated with 50ng/mL IL-6 from Figure 4.3C were identified, and are presented in Table 4.2. The majority of these identified lipids were either DG or TG species, and were mostly the same in both the control and IL-6 treated cells. As with the lipid species from the TNF-α treated samples shown in Table 4.1, approximately half of these lipids had a mass accuracy much greater than 5ppm, and so were not confident identifications.

The changes in the top four normalised abundant lipids in response to IL-6 treatment are shown in Figure 4.5. As with the Figure 4.4, these species were identified as DG (33:4); DG (35:4); TG (50:3) and TG (52:3). After 2h of IL-6 treatment, no changes in the concentration of these lipids was observed, with the exception of DG (35:4) and TG (52:3) which increased at the greatest concentration (50ng/mL; *P*=0.0231 and 0.0465, respectively *vs.* control). The concentration of DG (35:4) also increased after 24h of TNF-α treatment (*P*=0.0231 and 0.0408 *vs*. control for 25 and 50ng/mL, respectively). An increase was also seen in the concentration of TG (52:3) after 24h of TNF-α treatment at 5 and 25ng/mL (*P*=0.0231 and 0.0408 *vs.* control, respectively). The concentration of the remaining lipid species did not change with any of the three treatment concentrations after 24h.

| Calculated mass | Theoretical mass | Δ Mass accuracy (ppm) | Ion | Elemental composition | Identification |
|---|---|---|---|---|---|
| ***(A) Control*** | | | | | |
| 547.4710 | | | | | |
| 575.5023 | 575.4670 | 61.341 | $[M+H]^+$ | $C_{36}H_{62}O_5$ | DG (33:4) |
| 603.5334 | 603.4994 | 56.338 | $[M+H]^+$ | $C_{38}H_{66}O_5$ | DG (35:4) |
| 820.7366 | 820.7389 | -2.802 | $[M+NH_4]^+$ | $C_{51}H_{94}O_6$ | TG (48:2) |
| 834.7520 | 834.7545 | -2.995 | $[M+NH_4]^+$ | $C_{52}H_{96}O_6$ | TG (49:2) |
| 846.7524 | 846.7545 | -2.480 | $[M+NH_4]^+$ | $C_{53}H_{96}O_6$ | TG (50:3) |
| 847.7578 | 847.7749 | -20.170 | $[M+H]^+$ | $C_{54}H_{102}O_6$ | TG (51:1) |
| 848.7670 | 848.7701 | -3.652 | $[M+NH_4]^+$ | $C_{53}H_{98}O_6$ | TG (50:2) |
| 874.7833 | 874.7858 | -2.858 | $[M+NH_4]^+$ | $C_{55}H_{104}NO_6$ | TG (52:3) |
| 902.8141 | 902.8171 | -3.323 | $[M+NH_4]^+$ | $C_{57}H_{104}O_6$ | TG (52:2) |

***(B) Extra identifications from IL-6 treatment at 50ng/mL***

| | | | | | |
|---|---|---|---|---|---|
| 563.5021 | 563.4670 | 62.293 | $[M+H]^+$ | $C_{35}H_{62}O_5$ | DG (32:3) |
| 867.6825 | 867.6586 | 27.545 | $[M+NH_4]^+$ | $C_{49}H_{88}NO_8P$ | PC (41:5) |
| 895.7124 | 895.7263 | -15.518 | $[M+NH_4]^+$ | $C_{52}H_{96}NO_7P$ | PC (O-44:5) |

**Table 4.2. Identifications of selected positive ions from control and IL-6 treated 3T3-L1 adipocytes**

Abbreviations used: DG, diglyceride; PC, phosphatidylcholine; TG, triglyceride; ppm, parts per million

Underlined masses are present in both control and IL-6 treated cells

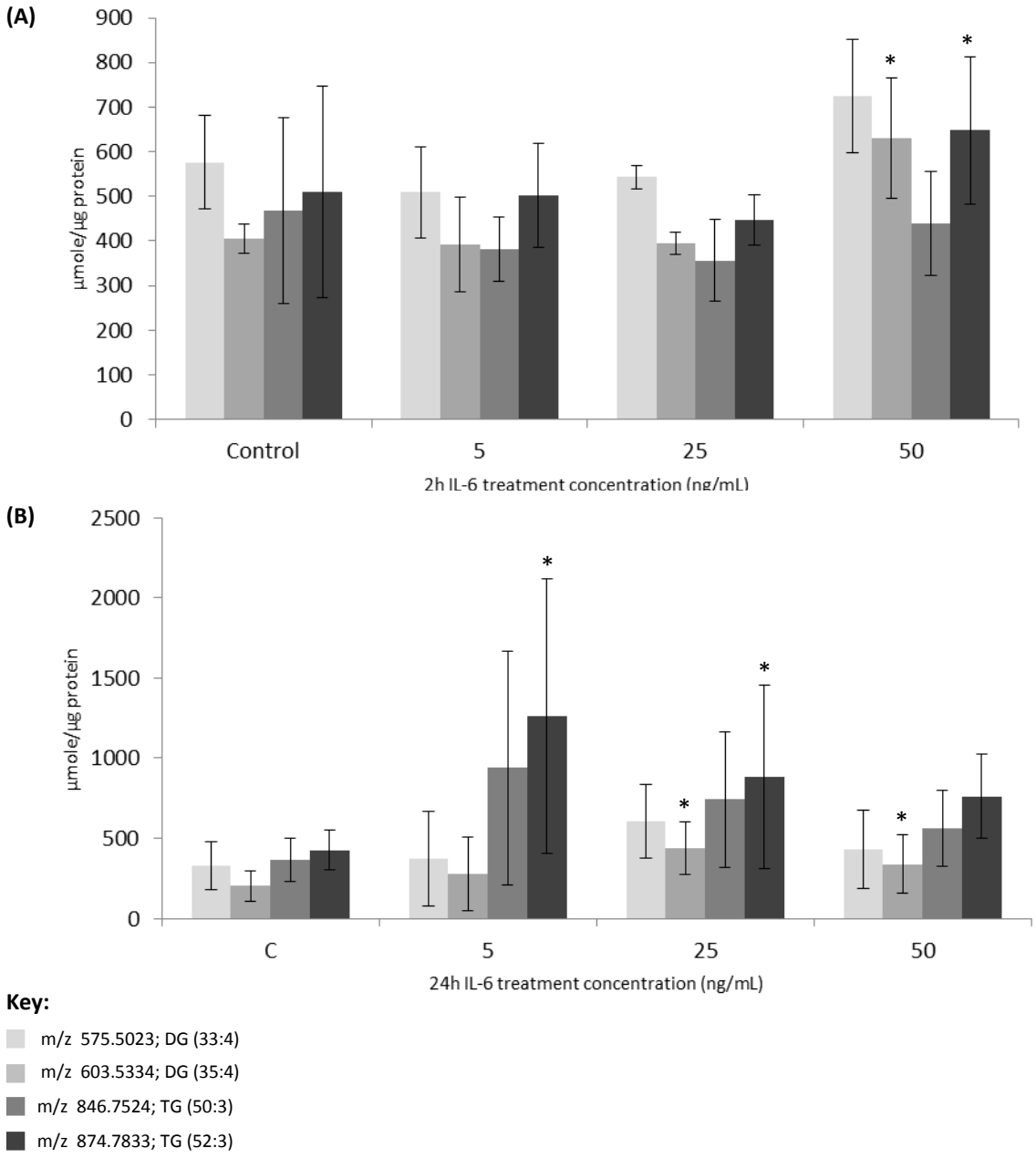


**Figure 4.5. Individual lipid concentrations from positive ion DI-MS analysis of IL-6 treated 3T3-L1 adipocytes**

Differentiated 3T3-L1 adipocytes at day 10 post-differentiation were pre-incubated with CS-free medium for 24h, and then treated with mouse recombinant IL-6 for 2 and 24h. The concentration of the inflammatory agents were 5, 25 and 50ng/mL. Lipids were extracted from the cell samples using a Folch extraction. The lower phase was dried down under nitrogen and reconstituted in 600µL chloroform/methanol (2/1, v/v). A 150µL aliquot was removed and 10mM ammonium formate was added to it. The samples were then directly infused into an Orbitrap Exactive mass spectrometer at a flow rate of 5µL/min for 90 seconds (450 scans) in positive ion mode. The raw data intensities were normalised to that of the relevant internal standard (PC 12:0/12:0 or TG 18:0/18:0/18:0), and had m/z 622.44 and 908.86, respectively. They were then normalised to the protein concentration of the cell sample.

The top four normalised lipids are presented in this figure. An increase in the concentration of DG (35:4) and TG (52:3) was seen after 2h of IL-6 treatment at 50ng/mL. Increases were also seen in the concentration of these lipids after 24h. For each time point, n=3, with results represented as median ± range. Statistical significance from the control cells is represented by *$P$<0.05; **$P$<0.01 and *** $P$<0.001.

### 4.3.3. Negative ion mode DI-MS analysis

#### *4.3.3.1. TNF-α treatment*

Representative negative ion spectra of control cells, along with cells treated with 50ng/mL TNF-α, are presented in Figure 4.6 (A and B, respectively). The global lipid profile relating to cells which had been treated with TNF-α for 24h looked different to the others in the figure. The abundance of all lipids present in this profile (B) appeared to have decreased, as seen by the increase in the peak relating to the internal standard (m/z 666.4364). The most abundant peak present in the control cells had m/z 564.3461, whereas this changed in the TNF-α treated cells to two peaks with m/z 281.2552 and 666.4364 (internal standard).

The top ten peaks from the global lipid profiles of the control cells, and the top ten from the TNF-α treated cells seen in Figures 4.7 were identified, and are presented in Table 4.2. Many of the abundant lipid species from the treated cells were not present in the global lipid profile of the control cells, and so these lipids are identified in Table 4.2(B). All of the identified lipid species in both the control and treated cells were either fatty acids or phospholipid species (Table 4.2A). All identified lipid species were normalised to the internal standard (m/z 666.4364) and then to the protein content of the cell. The five most concentrated from both the control, and TNF-α treated cells are graphically represented in Figure 4.8.

These five lipid species had m/z 253.2179, 255.2336, 281.2492, 283.2648 and 564.3461, and were identified as C16:1, C16:0, C18:1, C18:0 and PC (20:0). All identifications were considered to be good matches, with the exception of PC (20:0) due to its mass error (-37.210) falling outside of the set parameter of 5ppm. Therefore this was a tentative identification. At the 2h time point (Figure 4.8A); PC (20:0) had the greatest concentration in the control cells, and this switched to C18:1 in all of the TNF-α treated samples, with the concentration of PC (20:0) decreasing with all of the treatment concentrations ($P$=0.05 *vs.* control for all). The concentration of remaining selected lipids all decreased at the 5ng/mL TNF-α treatment ($P$<0.05 for all). No changes were observed at 25ng/mL, and at the greatest TNF-α treatment, a decrease was seen in the concentration of C16:0 and C18:0 ($P$=0.05 and 0.005 *vs.* control, respectively).

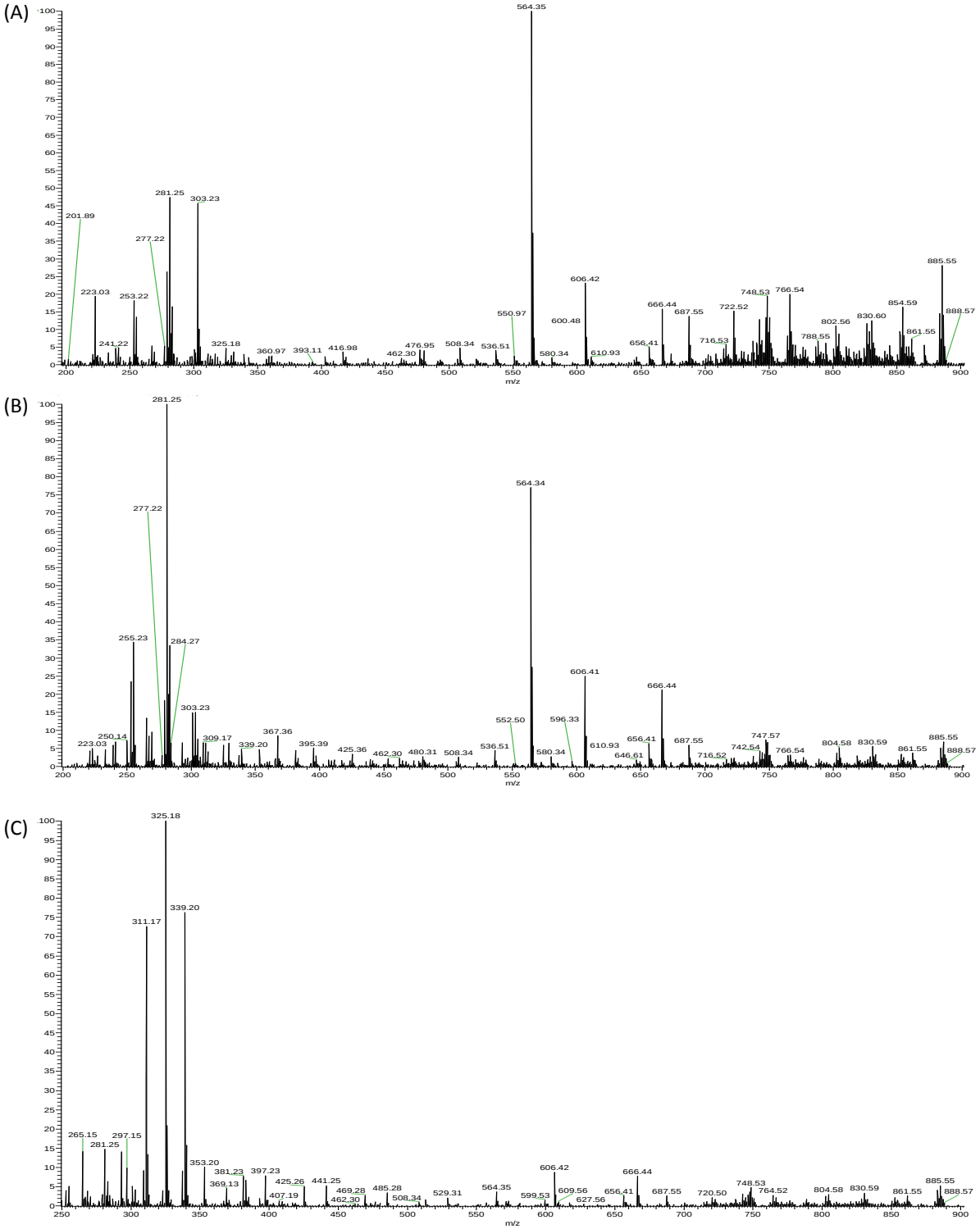


**Figure 4.6. Negative ion DI-MS analysis of TNF-α and IL-6 treated 3T3-L1 adipocytes** Representative spectra of differentiated 3T3-L1 adipocytes at day 10 post-differentiation which were pre-incubated with CS-free medium for 24h, and then treated with mouse recombinant TNF-α or IL-6 for 24h. The treatments represented are: control 24h (A); 50ng/mL TNF-α 24h (B) and 50ng/mL IL-6 24h (D). Lipids were extracted from the cell samples using a Folch extraction. The lower phase was dried down under nitrogen and reconstituted in 600µL chloroform/methanol (2/1, v/v). A 150µL aliquot was removed and had 10mM ammonium formate added to it. The samples were then directly infused into an Orbitrap Exactive mass spectrometer at a flow rate of 5µL/min for 90 seconds (450 scans) in negative ion mode. The m/z range represented is between 200 and 900Da. An increase in the abundance of the peak with m/z 281.25 is observed in (B), whereas in (C), the abundance of three peaks has greatly increased, and these have m/z 311.17, 325.18 and 339.20.

| Calculated mass | Theoretical mass | Δ Mass accuracy (ppm) | Ion | Elemental composition | Identification |
|---|---|---|---|---|---|
| ***(A) Control*** | | | | | |
| 253.2179 | 253.2173 | 2.370 | $[M-H]^-$ | $C_{16}H_{30}O_2$ | C16:1 |
| 255.2336 | 255.2330 | 2.351 | $[M-H]^-$ | $C_{16}H_{32}O_2$ | C16:0 |
| 279.2337 | 279.2330 | 2.507 | $[M-H]^-$ | $C_{18}H_{32}O_2$ | C16:2 |
| 281.2492 | 281.2486 | 2.133 | $[M-H]^-$ | $C_{18}H_{34}O_2$ | C18:1 |
| 283.2648 | 283.2643 | 1.765 | $[M-H]^-$ | $C_{18}H_{36}O_2$ | C18:0 |
| 303.2336 | 303.2330 | 1.979 | $[M-H]^-$ | $C_{20}H_{32}O_2$ | C20:4 |
| 564.3461 | 564.3671 | -37.210 | $[M-H]^-$ | $C_{28}H_{56}NO_8P$ | PC (20:0) |
| 565.3491 | 565.3511 | -3.538 | $[M-H]^-$ | $C_{28}H_{55}O_9P$ | Lyso-phosphatidylglycerol (22:1) |
| 606.4164 | 606.3984 | 29.683 | $[M-H]^-$ | $C_{31}H_{59}NO_8P$ | PE (26:1) |
| 885.5517 | 885.5499 | 2.033 | $[M-H]^-$ | $C_{47}H_{83}O_{13}P$ | PI (38:4) |
| ***(B) Extra identifications from TNF-α treatment at 50ng/mL*** | | | | | |
| 301.2174 | 301.2173 | 0.332 | $[M-H]^-$ | $C_{20}H_{30}O_2$ | C20:5 |
| 666.4364 | | | | | |

**Table 4.3. Identifications of selected negative ions from control and TNF-α treated 3T3-L1 adipocytes**

Abbreviations used: PC, phosphatidylcholine; PE, phosphatidylethanolamine; PG, phosphatidylglycerol; PI, phosphatidylinositol; ppm, parts per million

Underlined masses are present in both control and IL-6 treated cells, and those highlighted in red represent the internal standard

After 24h (Figure 4.7B) differences were observed in the concentrations of the various lipid species depending on the treatment conditions. The concentration of C16:1 decreased at the 5 and 25ng/mL treatment, and then increased at the greatest TNF-α treatment concentration (*P*=0.05 *vs.* control for all). The species C16:0 had an increase in its concentration at the least, and greatest TNF-α treatment, and a decrease at 25ng/mL (*P*=0.05 *vs.* control for all). A decrease in the concentration of C18:1 at 25ng/mL, followed by an increase at 50ng/mL was also observed (*P*=0.013 and 0.005 *vs.* control, respectively). The concentration of C18:0 increased after TNF-α treatment at both 5, and 50ng/mL (*P*<0.01 *vs.* control for both). Finally, the concentration of PC (20:0) decreased at the 25ng/mL TNF-α treatment (*P*=0.017 *vs.* control).

#### *4.3.3.2. IL-6 treatment*

A representative spectrum of cells treated with 50ng/mL IL-6 for 24h is presented in Figure 4.6C. A gross change was observed between the control and IL-6 treatment profiles. The most abundant peaks present in the control profiles had m/z 281.2488 and 564.3479; whereas in the control cells, the abundant peaks had m/z 311.17, 325.18 and 339.20. These last three peaks were thought to be contamination, relating to linear alkylbenzenesulfonates (Andreu and Pico, 2004), which are commonly used as surfactants in detergents. Therefore, the peaks with m/z 311.17, 325.18 and 339.20 were excluded from all data analysis.

The top ten most abundant peaks from these profiles were also identified, and are presented in Table 4.4. The majority of abundant peaks were present in both the control and treated cells, and related to fatty acids, or phospholipid species, with one sphingomylelin (SM) species also being present. The selected lipids were then quantified as before, and the effect of IL-6 treatment on the concentration of the top four species was investigated, as seen in Figure 4.8. These four lipid species had m/z 281.2488, 564.3479, 747.5664 and 830.5933, and were identified as C18:1, PC (20:0), a phosphatidylglycerol species (P-35:0) and a phosphatidylserine (PS) species (39:1), respectively. The identifications for m/z 564.3479 and 747.5664 were only tentative due to their mass error (-34.202 and 15.785, respectively).

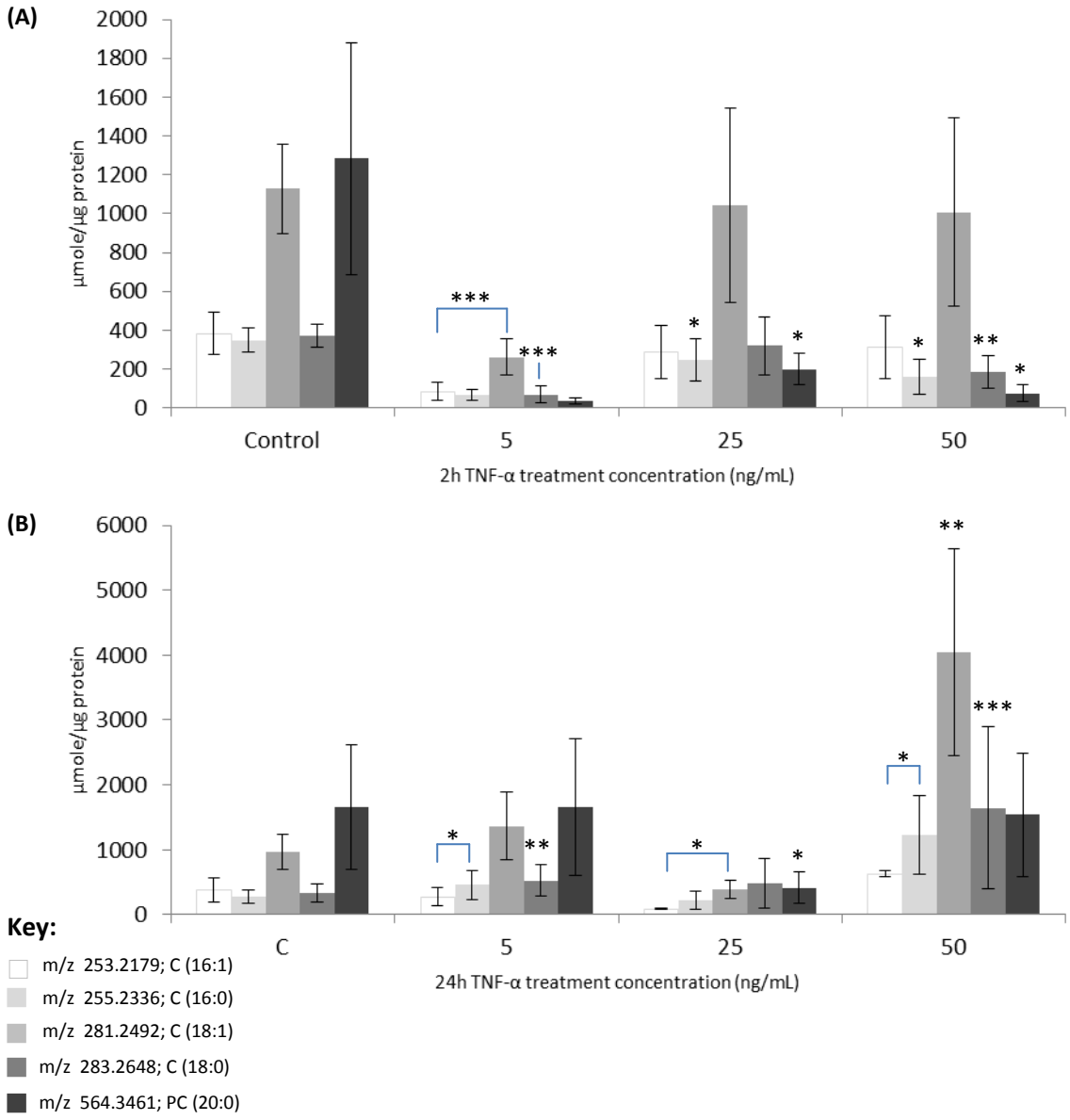


**Figure 4.7. Individual lipid concentrations from negative ion DI-MS analysis of TNF-α treated 3T3-L1 adipocytes**

Differentiated 3T3-L1 adipocytes at day 10 post-differentiation were pre-incubated with CS-free medium for 24 hours, and then treated with mouse recombinant TNF-α for 2 and 24 hours at the following concentrations: 5, 25 and 50ng/mL. Lipids were extracted from the cell samples using a Folch extraction. The lower phase was dried down under nitrogen and reconstituted in 600µL chloroform/methanol (2/1, v/v). A 150µL aliquot was removed and had 10mM ammonium formate added to it. The samples were then directly infused into an Orbitrap Exactive mass spectrometer at a flow rate of 5µL/min for 90 seconds (450 scans) in negative ion mode. The raw data intensities were normalised to that of the relevant internal standard (PC 12:0/12:0; m/z 666.4434) and then to the protein concentration of the cell sample.

The top five normalised lipids are presented in this figure, and are identified in the key. For each time point, n=3, with results represented as median ± range. Decreases in the concentration of these lipid species were observed with 5ng/mL TNF-α treatment after both 2 and 24h, and this decrease was also seen at the 25ng/mL treatment concentration after 24h. Statistical significance from the control cells is represented by *$P$<0.05; **$P$<0.01 and ***$P$<0.001.

| Calculated mass | Theoretical mass | Δ Mass accuracy (ppm) | Ion | Elemental composition | Identification |
|---|---|---|---|---|---|
| ***(A) Control*** | | | | | |
| 281.2488 | 281.2486 | 0.711 | $[M-H]^-$ | $C_{18}H_{34}O_2$ | C18:1 |
| 564.3479 | 564.3671 | -34.202 | $[M-H]^-$ | $C_{28}H_{56}NO_8P$ | PC (20:0) |
| 666.4363 | | | | | |
| 747.5664 | 747.5546 | 15.785 | $[M-H]^-$ | $C_{41}H_{81}O_9P$ | PG (P-35:0) |
| 748.5323 | 748.5287 | 4.809 | $[M-H]^-$ | $C_{43}H_{76}NO_7P$ | PE (P-38:5) |
| | | | | | PE (O-37:6) |
| 802.5617 | 802.5604 | 1.620 | $[M-H]^-$ | $C_{43}H_{82}NO_{10}P$ | PS (37:1) |
| 804.5763 | 804.5549 | 26.599 | $[M-H]^-$ | $C_{46}H_{80}NO_8P$ | PC (38:6) |
| 830.5933 | 830.5917 | 1.926 | $[M-H]^-$ | $C_{45}H_{86}NO_{10}P$ | PS (39:1) |
| 883.5355 | 883.5342 | 1.471 | $[M-H]^-$ | $C_{47}H_{81}O_{13}P$ | PI (38:5) |
| 885.5506 | 885.5499 | 0.790 | $[M-H]^-$ | $C_{47}H_{83}O_{13}P$ | PI (38:4) |

***(B) Extra identifications from IL-6 treatment at 50ng/mL***

| | | | | | |
|---|---|---|---|---|---|
| 687.5469 | 687.5933 | -67.482 | $[M-H]^-$ | $C_{38}H_{77}N_2O_6P$ | SM (d33:1) |
| 742.5414 | 742.5392 | 2.963 | $[M-H]^-$ | $C_{41}H_{78}NO_8P$ | PC (33:2) |
| 746.5158 | 746.5705 | -73.268 | $[M-H]^-$ | $C_{41}H_{82}NO_8P$ | PC (33:0) |
| 764.5222 | 764.5236 | -1.831 | $[M-H]^-$ | $C_{43}H_{76}NO_8P$ | PC (35:5) |

**Table 4.4. Identifications of selected negative ions from control and IL-6 treated 3T3-L1 adipocytes**

Abbreviations used: PC, phosphatidylcholine; PE, phosphatidylethanolamine; PG, phosphatidylglycerol; PI, phosphatidylinositol; PS, phosphatidylserine; SM, sphingomyelin; ppm, parts per million

Underlined masses are present in both control and IL-6 treated cells, and those highlighted in red represent the internal standard



195

At the 2h time point (Figure 4.8A); the lipids with the greatest concentrations in the control samples were C18:1 and PC (20:0), and the concentration of both decreased at the 5ng/mL IL-6 treatment concentrations ($P$=0.05 or less *vs.* control for both). Opposite actions were observed in the concentration of these two species at the greatest treatment (50ng/mL), with that of C18:1 increasing ($P$=0.01 *vs.* control) and the concentration of PC (20:0) decreasing ($P$=0.05 *vs.* control). An increase in the concentration of both phosphatidylglycerol (P-35:0) and PS (39:1) was seen 5 and 50ng/mL IL-6 treatment ($P$<0.01 *vs.* control for all). After 24h of IL-6 treatment, no changes were observed in the concentration of C18:1 in any of the IL-6 treated samples, whereas the concentration of PC (20:0) was seen to decrease with all IL-6 treatments ($P$=0.05 *vs.* control for all). Both phosphatidlyglycerol (P-35:0) and PS (39:1) behaved in the same way, with an increase in their concentration occurring at both 5 and 50ng/mL IL-6 treatment ($P$=0.049 *vs.* control for all). After 24h (Figure 4.8B) the most concentrated lipids seen in the control samples were also C18:1 and PC (20:0). The concentration of these lipids decreased in the treatment samples, although this decrease was only significant for PC (20:0) ($P$<0.05 *vs.* control for all IL-6 treatment concentrations).

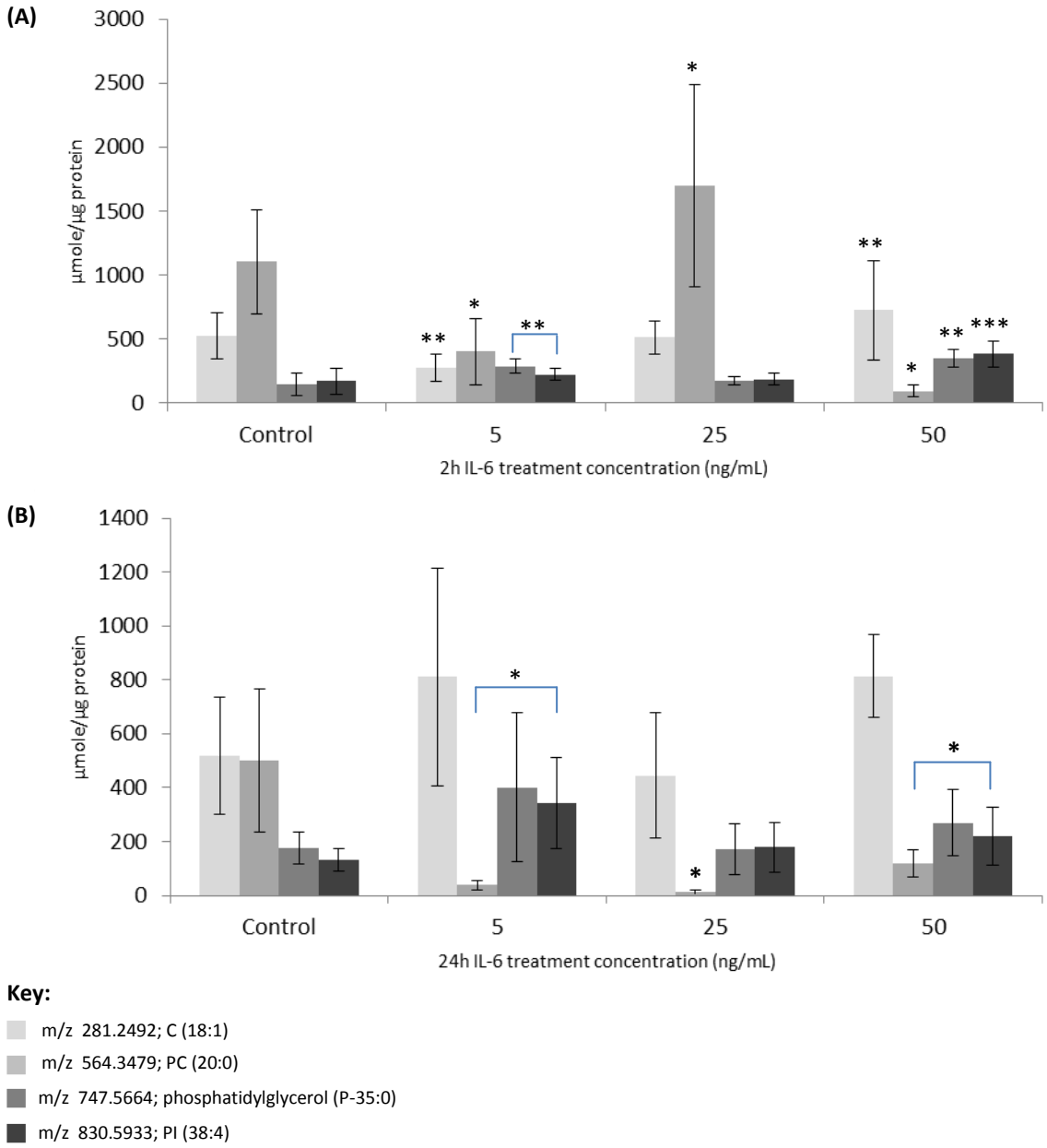


**Figure 4.8. Individual lipid concentrations from negative ion DI-MS analysis of IL-6 treated 3T3-L1 adipocytes**

Differentiated 3T3-L1 adipocytes at day 10 post-differentiation were pre-incubated with CS-free medium for 24h, and were then treated with mouse recombinant IL-6 for 2 and 24h. The concentration of inflammatory agents were 5, 25 and 50ng/mL. Lipids were extracted from the cell samples using a Folch extraction. The lower phase was dried down under nitrogen and reconstituted in 600µL chloroform/methanol (2/1, v/v). A 150µL aliquot was removed and had 10mM ammonium formate added to it. The samples were then directly infused into an Orbitrap Exactive mass spectrometer at 5µL/min for 90 seconds (450 scans) in negative ion mode. The raw data intensities were normalised to that of the relevant internal standard (PC 12:0/12:0; m/z 666.44), and then to the protein concentration of the cell sample.

The top four normalised lipids are presented in this figure. For each time point, n=3, with results represented as median ± range. Flucuations in the concentration of these species were observed after 2h of IL-6 treatment, and after 24h, a significant decrease was seen in the concentration of PC (20:0) with all treatment concentrations, whereas the concentration of PG (P-35:0) and PS (39:1) significantly increased at 5, and 50ng/mL IL-6 treatment concentrations. Statistical significance from the control cells is represented by *$P$<0.05; **$P$<0.01 and ***$P$<0.001.

### 4.3.4. Positive ion LC-MS analysis

#### *4.3.4.1. TNF-α treatment*

Representative positive ion chromatograms of control cells, and those treated with 50ng/mL TNF-α for 2 or 24h, are presented in Figure 4.9. The global lipid profiles between the control and TNF-α treated cells appeared similar; however, the abundance of peaks present between RT 7.5 and 8.5 min increased in the treated samples. The most abundant ion associated with each chromatographic peak is identified in Table 4.5. The majority of ions were unable to be identified; however, those that could were all TG species.

Multivariate data analyses were employed on the positive ion LC-MS data, starting with principal component analysis (PCA). The PCA scores and loadings plots from the TNF-α treated cells are presented in Figure 4.10. The data, which have not been normalised, were analysed first, and this model had an R2 and Q2 of 0.709 and 0.307, respectively. The PCA scores plot (A) showed no obvious groupings, with the QCs being integrated in with the samples; however, one replicate of the samples relating to 2h of TNF-α treatment at 25ng/mL was situated outside of the 95% tolerance limit. The points seen in the loadings plot (C) did not group together around the origin, and so no points of possible variance were identified.

Next, the data were normalised to the total ion current (TIC), and the scores plot (B) was interpreted as having two groups; one contained the 24h 50ng/mL TNF-α treated samples, and also one replicate of the 25ng/mL treated cells, also at the 24h time point. The remaining samples were all clustered together in the second group, and the R2 and Q2 for this model were 0.698 and 0.463 respectively. The majority of points seen as possible causes of variance on the loadings plot (D) were located on the left hand side (LHS) of the origin. The majority were unable to be confidently identified; however, trend analysis of these points showed that the profile of their abundance were similar throughout with all TNF-α treatments; for example, the variance of points relating to m/z 684.204-687.201; 758.223-761.223 and 832.242-834.241 increased with all of the 24h treatments. The points corresponding to m/z 610.183-162.182 showed an increase in variance in the 24h control samples, which then decreased back to the original variance.

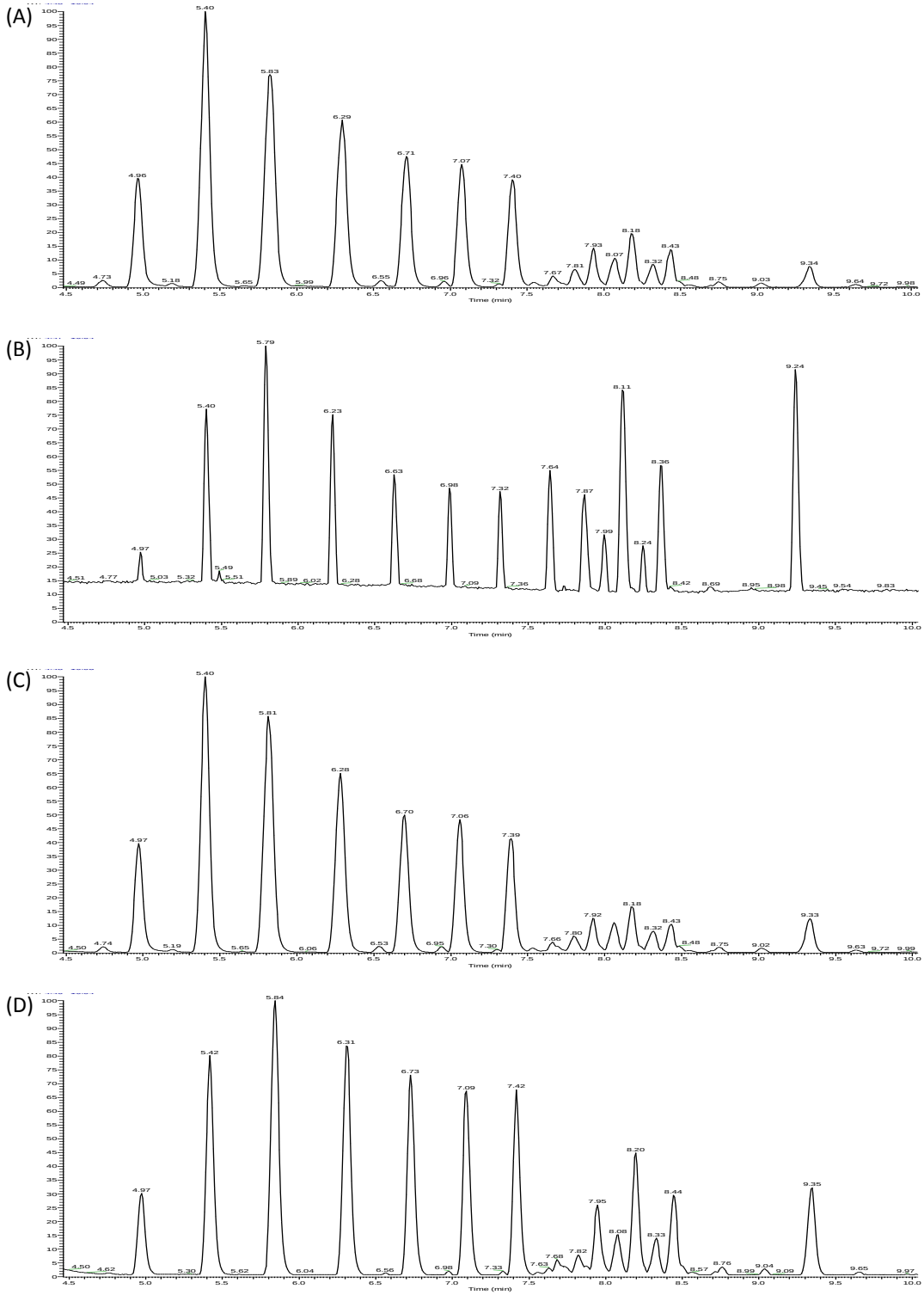


**Figure 4.9. Positive ion LC-MS analysis of TNF-α treated 3T3-L1 adipocytes** Representative chromatograms of differentiated 3T3-L1 adipocytes at day 10 post-differentiation which were pre-incubated with CS-free medium for 24h, and then treated with mouse recombinant TNF-α for 2 and 24h. The treatments represented are: control 2h (A); 50ng/mL 2h (B); control 24h (C); and 50ng/mL 24h (D). Lipids were extracted from the cell samples using a Folch extraction. The lower phase was dried down under nitrogen and reconstituted in 600µL chloroform/methanol (2/1, v/v). The lipids were then separated over 18 min by LC-MS. Increases in the abundance of lipids present between retention time 7.5 and 8.5min was observed in the TNF-α treated samples when compared to the control cells.

| Retention time (min) | Ion mass | Theoretical mass | Δ Mass accuracy (ppm) | Ion | Empirical composition | Identification |
|---|---|---|---|---|---|---|
| | | **PEAKS BEFORE 7.55MIN WERE NOT IDENTIFIABLE** | | | | |
| 7.55 | 804.7072 | 804.7076 | -0.497 | $[M+NH_4]^+$ | $C_{50}H_{90}O_6$ | TG (47:0) |
| 7.69 | 818.7225 | 818.7232 | -0.855 | $[M+H]^+$ | $C_{51}H_{92}O_8$ | TG (48:3) |
| 7.81 | 832.7382 | 832.7545 | -19.574 | $[M+NH_4]^+$ | $C_{52}H_{94}O_6$ | TG (49:3) |
| 7.93 | 846.7549 | 846.7545 | 0.472 | $[M+NH_4]^+$ | $C_{53}H_{96}O_6$ | TG (50:3) |
| 8.06 | 834.7548 | 834.7545 | 0.359 | $[M+NH_4]^+$ | $C_{52}H_{96}O_6$ | TG (49:2) |
| 8.19 | 874.7851 | 874.7858 | -0.800 | $[M+NH_4]^+$ | $C_{55}H_{104}NO_6$ | TG (52:3) |
| 8.31 | 862.7853 | 862.7858 | -0.580 | $[M+NH_4]^+$ | $C_{54}H_{100}O_6$ | TG (51:2) |
| 8.44 | 902.8159 | 902.8171 | -1.329 | $[M+NH_4]^+$ | $C_{57}H_{104}O_6$ | TG (52:2) |
| 8.75 | 904.8325 | 904.8327 | -0.221 | $[M+NH_4]^+$ | $C_{57}H_{106}O_6$ | TG (54:2) |
| 9.33 | 908.8633 | 908.8640 | -0.770 | $[M+NH_4]^+$ | $C_{57}H_{110}O_6$ | TG (54:0) |

**Table 4.5. Retention times and their associated abundant mass of each major peak present in the positive ion LC-MS chromatograms of TNF-α and IL-6 treated 3T3-L1 adipocytes**

Abbreviations used: TG, triglyceride; ppm, parts per million

Red highlight indicates internal standard

One identifiable point on the plot was located on the RHS of the origin, and represented m/z 758.570. This was identified as PC (34:1), and its variance saw a transient increase after 2h of 5ng/mL TNF-α concentration, which then decreased at 25ng/mL TNF-α treatment (2h) and then a plateau was observed throughout the remaining treatments.

After PCA, both datasets also underwent partial least squares (PLS) analysis, and the scores and loadings plots for these models are presented in Figure 4.11. Both scores plots showed similar groupings to those seen in the PCA model scores plots; with two groups seen with the non-normalised data (A) and no obvious groupings observed in the TIC-normalised data (B). The R2X, R2Y and Q2 for the non-normalised model were 0.494, 0.787 and 0.572, respectively. For the TIC-normalised model, these were; 0.818, 0.97 and 0.68, respectively. The loadings plot for the non-normalised data (C) showed that the points at distance from the origin were the same as those found in the PCA scores plot. The only identified point had m/z 758.570 and, therefore, was PC (34:1). The trend analysis of this point found that its abundance increased with 2h TNF-α treatment at 5ng/mL, and then decreased at the 25ng/mL concentration (2h time point), and then plateaued with the rest of the treatments. This exact variance pattern of PC (34:1) was also observed in the loadings plot of the TIC-normalised data (D).

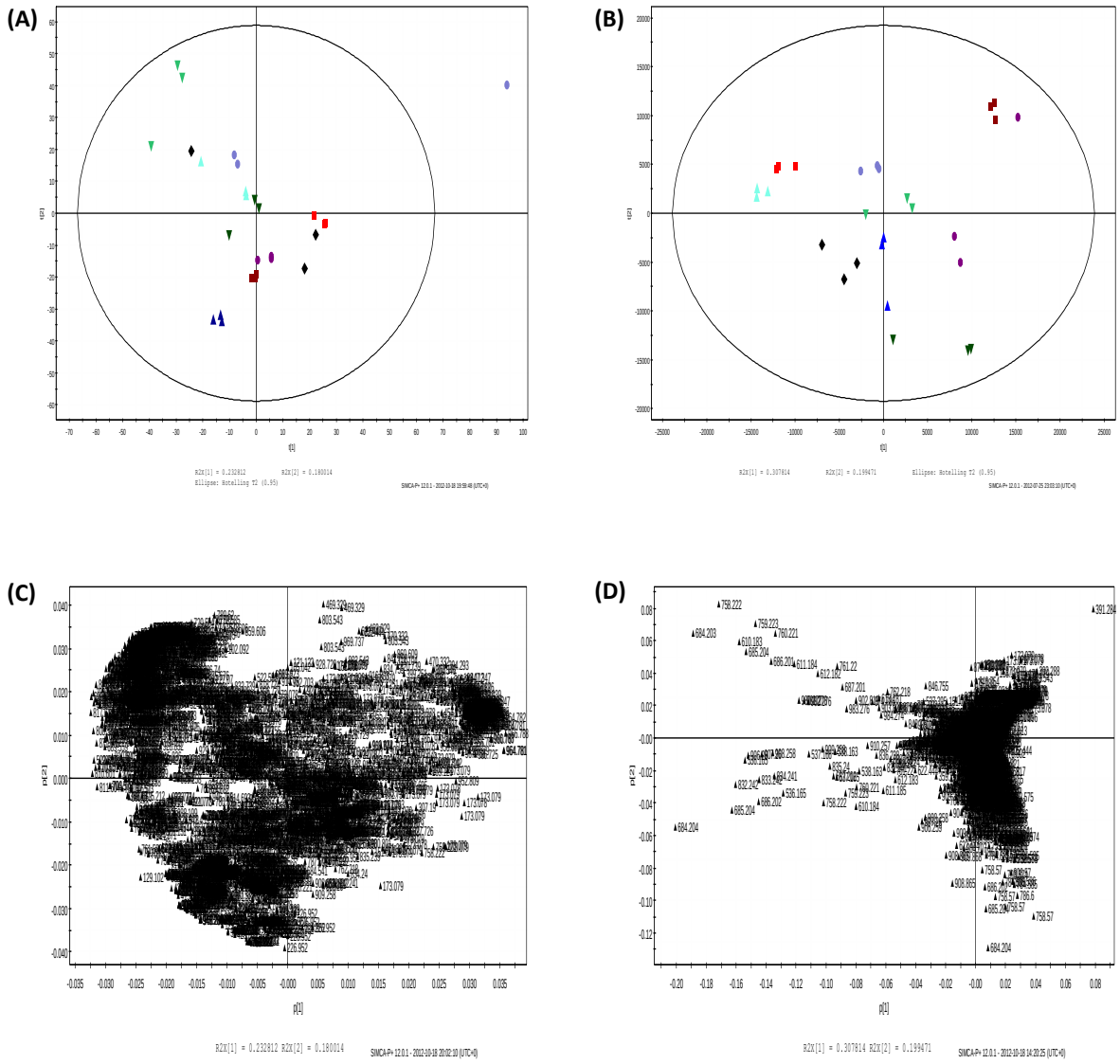


**Figure 4.10. PCA scores and loadings plots representing positive ion LC-MS analysis of TNF-α treated 3T3-L1 adipocytes**

3T3-L1 adipocytes at day 10 post-differentiation were pre-incubated with CS-free medium for 24h, and then treated with mouse recombinant TNF-α for 2 and 24h at the following concentrations: 5, 25 and 50ng/mL. Lipids were extracted using a Folch extraction, and the lower phase was analysed by LC-MS in positive ion mode. Before multivariate data analysis, the data were processed using SIEVE. The data represented here have been Pareto scaled, and the RT window was set at 15sec. Either the raw data, or data which were normalised to the total ion current were analysed. Each time point consisted of three biological replicates. The panels represent: no norm, scores plot (A); TIC norm, scores plot (B); no norm, loadings plot (C); and TIC norm, loadings plot (D). No obvious groupings were observed in either scores plot.

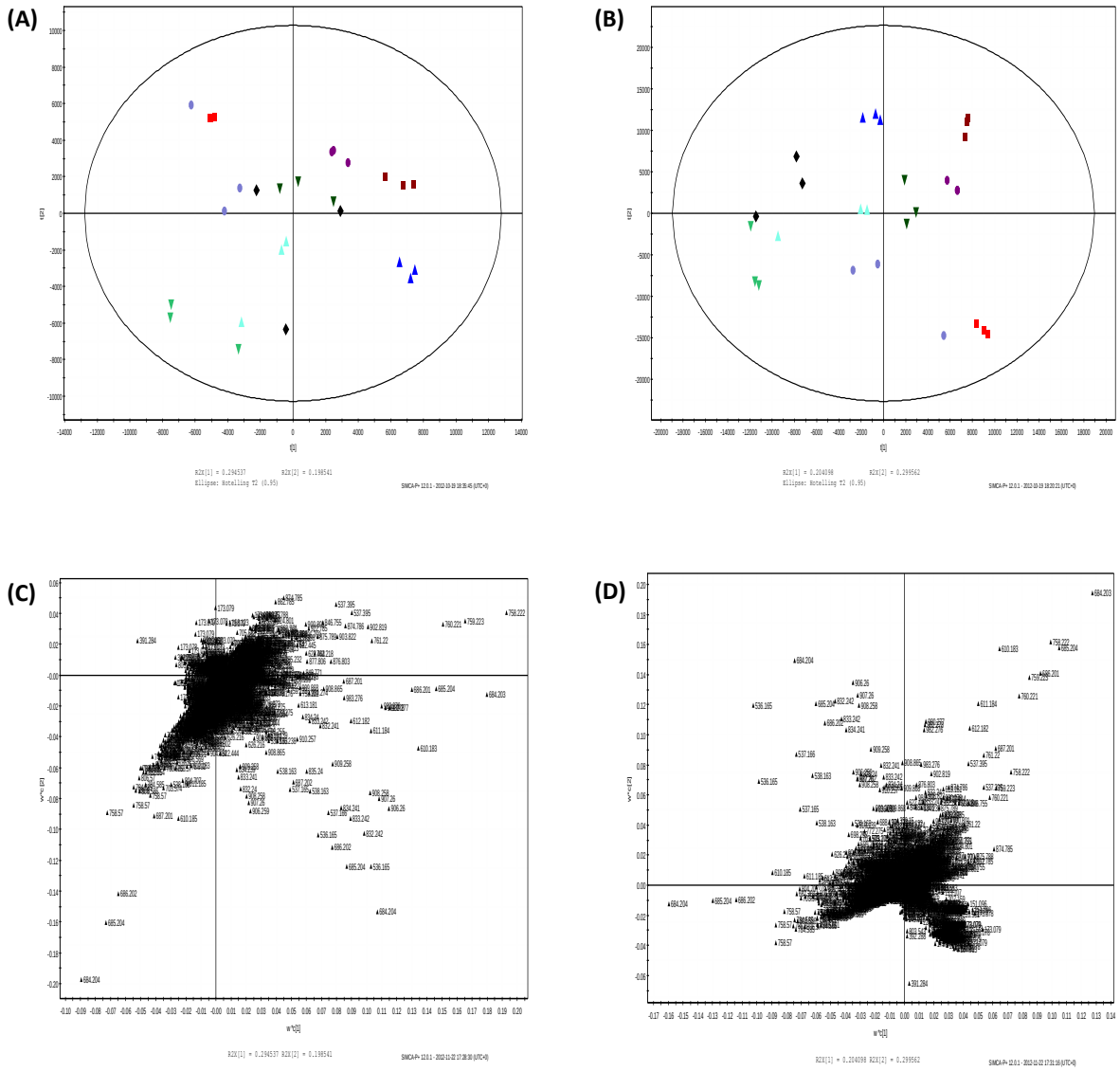


**Figure 4.11. PLS scores and loadings plots representing positive ion LC-MS analysis of TNFα treated 3T3-L1 adipocytes**

3T3-L1 adipocytes at day 10 post-differentiation were pre-incubated with CS-free medium for 24h, and then treated with mouse recombinant TNF-α for 2 and 24h at the following concentrations: 5, 25 and 50ng/mL. Lipids were extracted using a Folch extraction, and the lower phase was analysed by LC-MS in positive ion mode. Before multivariate data analysis, the data were processed using SIEVE. The data represented here have been Pareto scaled, and the RT window was set at 15sec. Either the raw data, or data which were normalised to the total ion current were analysed. Each time point consisted of three biological replicates. The panels represent: no normalisation, scores plot (A); TIC normalisation, scores plot (B); no normalisation, loadings plot (C); and TIC normalisation, loadings plot (D). No obvious groupings were seen with either model.

#### *4.3.4.2. IL-6 treatment*

Similar chromatograms were produced for the 3T3-L1 adipocytes which had been treated with IL-6, as seen in Figure 4.12. These global lipid profiles between the control and IL-6 treated cells appeared similar; however, the peaks present between RT 7.5 and 8.5 min decreased in the 2h 50ng/mL treated cells compared to the control samples, and vice versa with the 24h IL-6 treated cells (50ng/mL). These chromatograms were also similar to those seen with the TNF-α treated adipocytes, and so the abundant ions associated with each peak are the same as those in Table 4.5.

Samples treated with IL-6 were analysed by PCA, and the scores and loadings plots are presented in Figure 4.13, and the scores plot of the non-normalised data model (A) was interpreted as having three groups, which were: QCs; 25 and 50ng/mL (24h); and all other samples. The R2 and Q2 for this model were 0.736 and 0.46, respectively. The points situated on the RHS of the loadings plot (Figure 4.20C) for this model were not confidently identified; however, the variance of all of species decreased in the 25 and 50ng/mL (24h) treatment samples. On the LHS of the origin, one point with m/z 537.395 was given a tentative identification of PC (18:2), and another point with m/z 902.816 was identified as TG (54:3). The variance of both increased in the 25 and 50ng/mL samples. These findings were replicated when the data were normalised to the TIC, as represented by (D) and the R2 and Q2 for this model were 0.736 and 0.435, respectively.

The PLS models of these data were also similar to each other, with the PLS scores plots showing that the samples clustered into two groups, as seen in Figure 4.14. One group contained samples treated with IL-6 at either 25 or 50ng/mL for 24h. The rest of the samples formed a second group, with the QCs located within this group. The R2X, R2Y and Q2 for these models were 0.494, 0.737, and 0.572 for the non-normalised data (C); and for the TIC-normalised (D) data they were 0.481, 0.78 and 0.556, respectively. The variance of the unidentified points on the LHS of the origin of the loadings plots (C and D) decreased in both the 25 and 50ng/mL (24h) IL-6 treated samples. The points identified as PC (18:2) and TG (54:3) were positioned on the RHS of the origin. Another point with m/z 173.079 was also found in this location, and a tentative identification was applied to it, which was a FA with the formula $C_8H_{12}O_4$. The variance of all three increased in the 25 and 50ng/mL (24h) IL-6 treated samples.

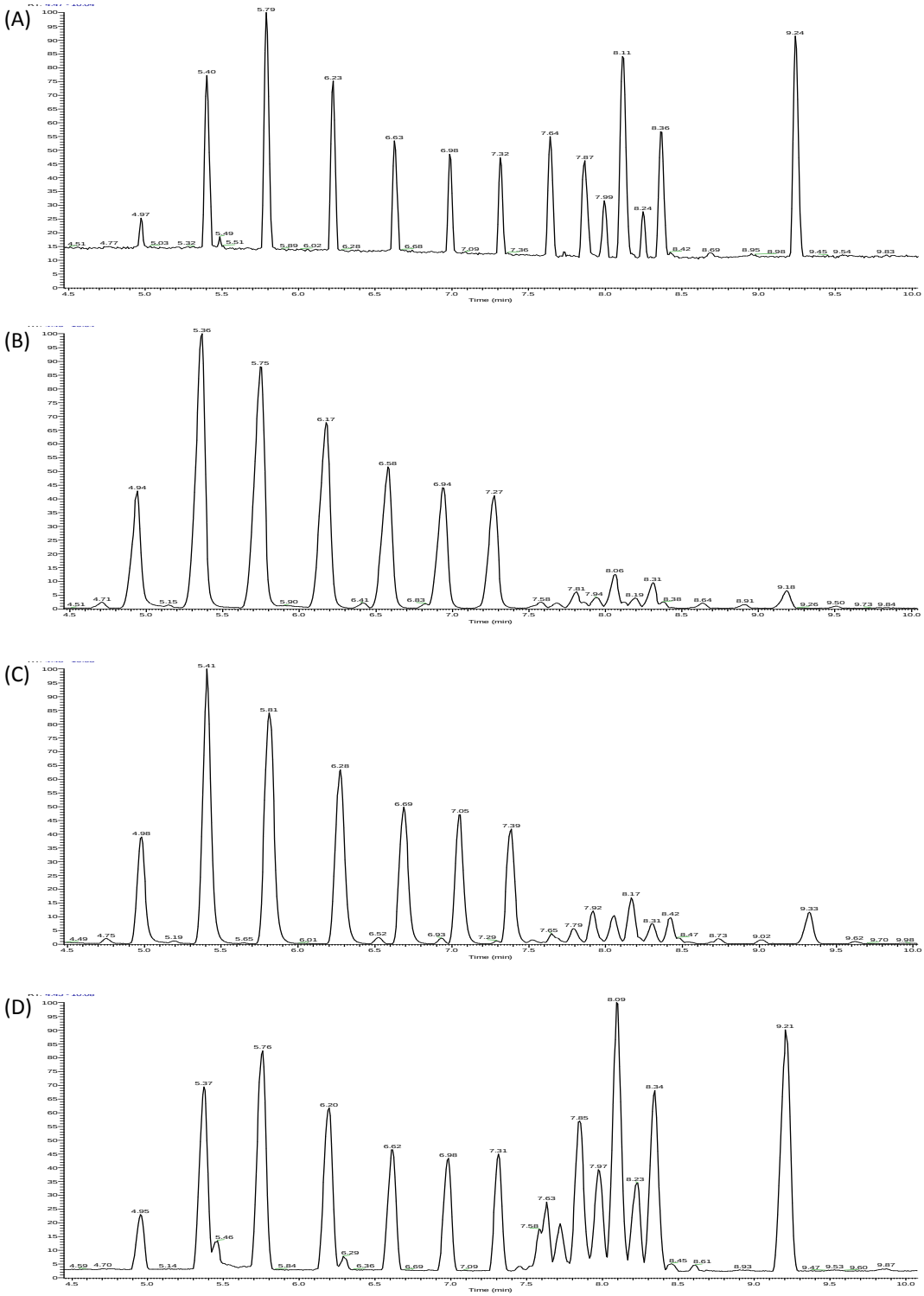


**Figure 4.12. Positive ion LC-MS analysis of IL-6 treated 3T3-L1 adipocytes** Representative chromatograms of differentiated 3T3-L1 adipocytes at day 10 post-differentiation which were pre-incubated with CS-free medium for 24h, and then treated with mouse recombinant IL-6 for 2 and 24h. The treatments represented are: control 2h (A); 50ng/mL 2h (B); control 24h (C); and 50ng/mL 24h (D). Lipids were extracted from the cell samples using a Folch extraction. The lower phase was dried down under nitrogen and reconstituted in 600µL chloroform/methanol (2/1, v/v). The lipids were then separated over 18 min by LC-MS. A decrease was observed in the abundance of all species after 24h of IL-6 treatment at 50ng/mL as seen by the increase in abundance of the peak at retention time 9.21 which corresponds to the internal standard TG (18:0/ 18:0/ 18:0) with m/z 908.8633.

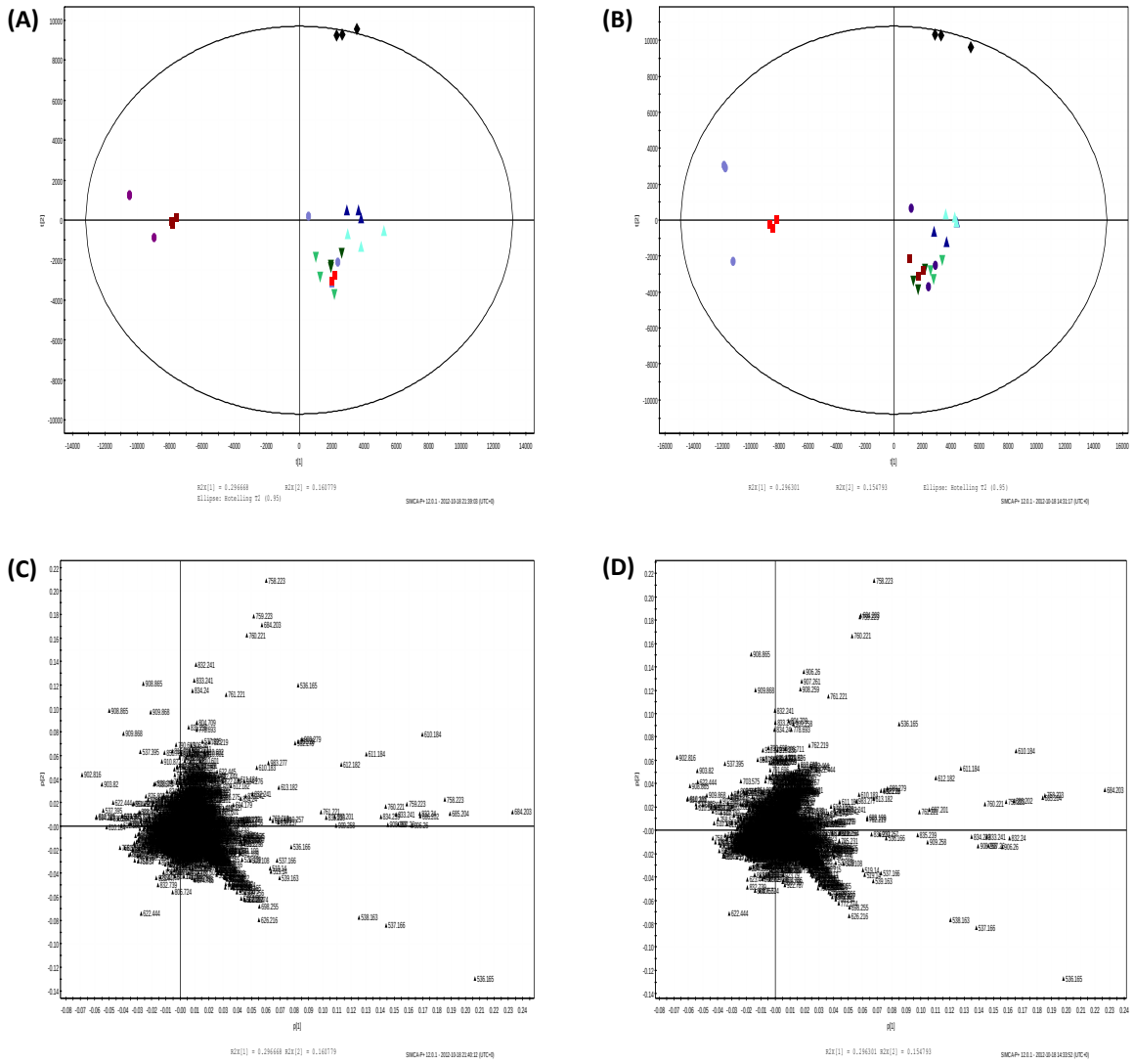


**Figure 4.13. PCA loadings and scores plots representing positive ion LC-MS analysis of IL-6 treated 3T3-L1 adipocytes**

3T3-L1 adipocytes at day 10 post-differentiation were pre-incubated with CS-free medium for 24h, and then treated with mouse recombinant IL-6 for 2 and 24h at the following concentrations: 5, 25 and 50ng/mL. Lipids were extracted using a Folch extraction, and the lower phase was analysed by LC-MS in positive ion mode. Before multivariate data analysis, the data were processed using SIEVE. The data represented here have been Pareto scaled, and the RT window was set at 15 seconds. Either the raw data, or data which were normalised to the total ion current were analysed. Each time point consisted of three biological replicates. The panels represent: no normalisation, scores plot (A); TIC normalisation, scores plot (B); no normalisation, loadings plot (C); and TIC normalisation, loadings plot (D). With both models, a clear separation was seen between the QCs and the experimental samples. With the non-normalised model (A), a group consisting of 25 and 50ng/mL IL-6 treated samples after 24h was clustered away from the other samples; whereas in the TIC-normalised model, this separated group contained 2h IL-6 treated samples at 25 and 50ng/mL.

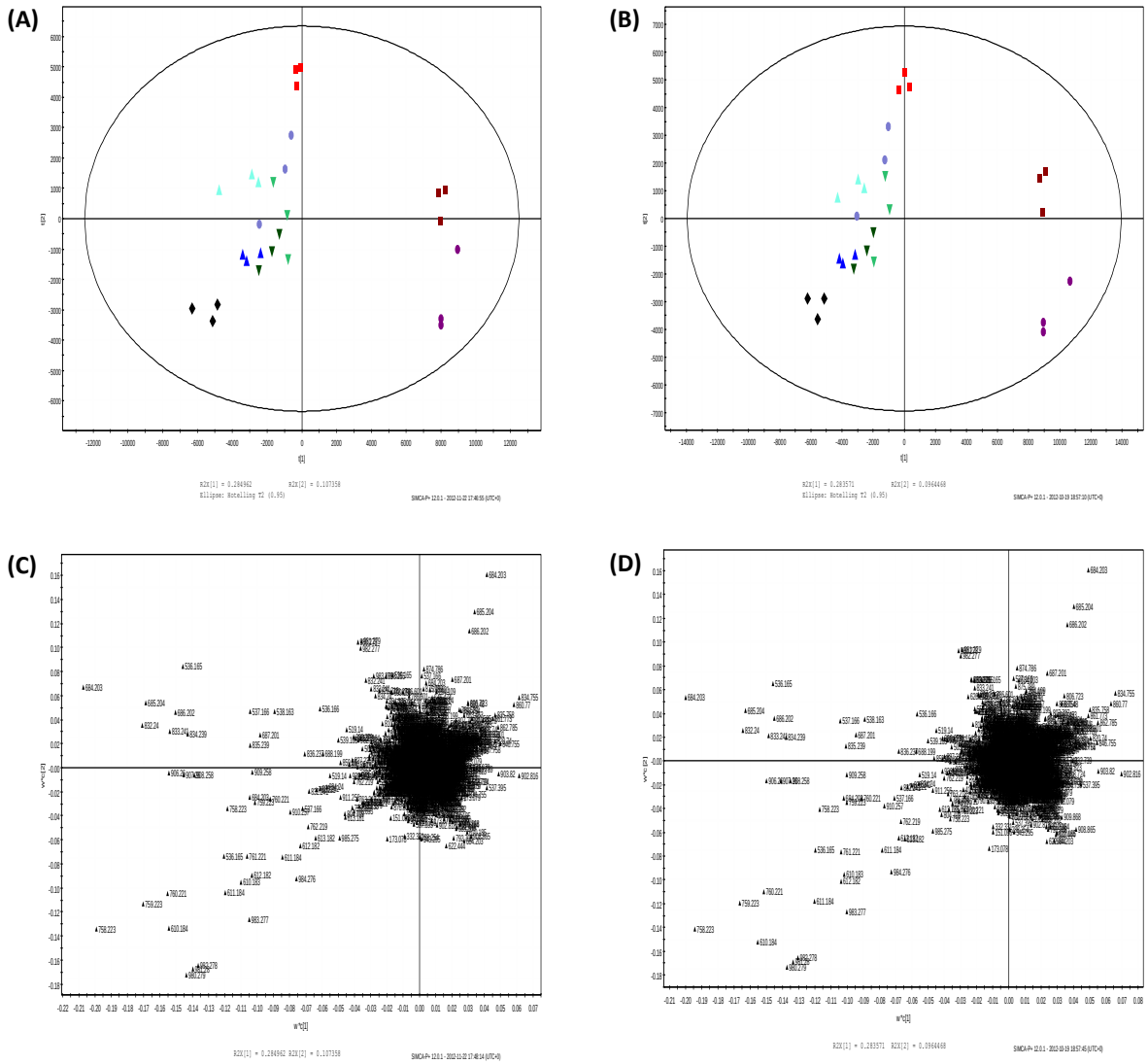


**Figure 4.14. PLS scores and loadings plots representing positive ion LC-MS analysis of IL-6 treated 3T3-L1 adipocytes**

3T3-L1 adipocytes at day 10 post-differentiation were pre-incubated with CS-free medium for 24h, and then treated with mouse recombinant IL-6 for 2 and 24h at the following concentrations: 5, 25 and 50ng/mL. Lipids were extracted using a Folch extraction, and the lower phase was analysed by LC-MS in positive ion mode. Before multivariate data analysis, the data were processed using SIEVE. The data represented here have been Pareto scaled, and the RT window was set at 15 seconds. Either the raw data, or data which were normalised to the total ion current were analysed. Each time point consisted of three biological replicates. The panels represent: no normalisation, scores plot (A); TIC normalisation, scores plot (B); no normalisation, loadings plot (C); and TIC normalisation, loadings plot (D). Both PLS plots demonstrate a separation in the samples, with a group relating to cells which had been treated with IL-6 for 24h at 25 and 50ng/mL being situated away from the remaining samples.

### 4.3.5. Negative ion mode LC-MS analysis

#### *4.3.5.1. TNF-α treatment*

Representative negative ion chromatograms of control cells and those treated with 50ng/mL TNF-α for 2 and 24h are presented in Figure 4.15. Fewer peaks were present than seen in the positive ion chromatograms. The most abundant peak present in the 2h control cells had a retention time (RT) of 4 min, and this changed to RT 2.45, 2.65 and 2.79 min in all other chromatograms in the figure. The most abundant ion associated with each chromatographic peak is identified in Table 4.6. Only one ion was identifiable, which had a RT of approximately 4 min. However, the mass error for this species (-37.564) fell outside of the set parameter of 5ppm, and so this identification was only tentative.

Negative ion LC-MS data of TNF-α treated cells were also analysed using PCA and PLS. The PCA scores and loadings plots are shown in Figure 4.16, and for the non-normalised data (A), the samples were clustered into four groups: QCs; controls (2 and 24h); 5ng 24h and all other treatments. The R2 and Q2 for this dataset were 0.978 and 0.911. Two points were identified on the loadings plot (B) and were situated away from the origin on the RHS. These points had m/z 564.345 (ppm=-37.564) and 885.553 and were identified as PC (20:0) and PI (38:4), respectively. Two other points were situated in the same area of the loadings plot and had m/z 346.177 and 582.511; however, no identifications were obtained for these species. Trend analysis of the identified species, demonstrated a decrease in variance of PC (20:0) in all of the samples, except for those acting as a control at the 2h time point. A decrease in the variance of PI (38:4) was also seen; although this decrease only occurred from the 50ng/mL (2h) through to 25ng/mL (24h) samples.

The PCA plot of the TIC-normalised data (B) showed three groups, which were: QCs, controls (2 and 24h); all treated samples. The R2 and Q2 for this model were 0.981 and 0.909, respectively. The loadings plot for this model (D) was similar to that of the non-normalised data model; with the identifiable points PC (20:0) and PI (38:4) being located on the RHS of the origin, and the variance of these phospholipid species acting in the same way.

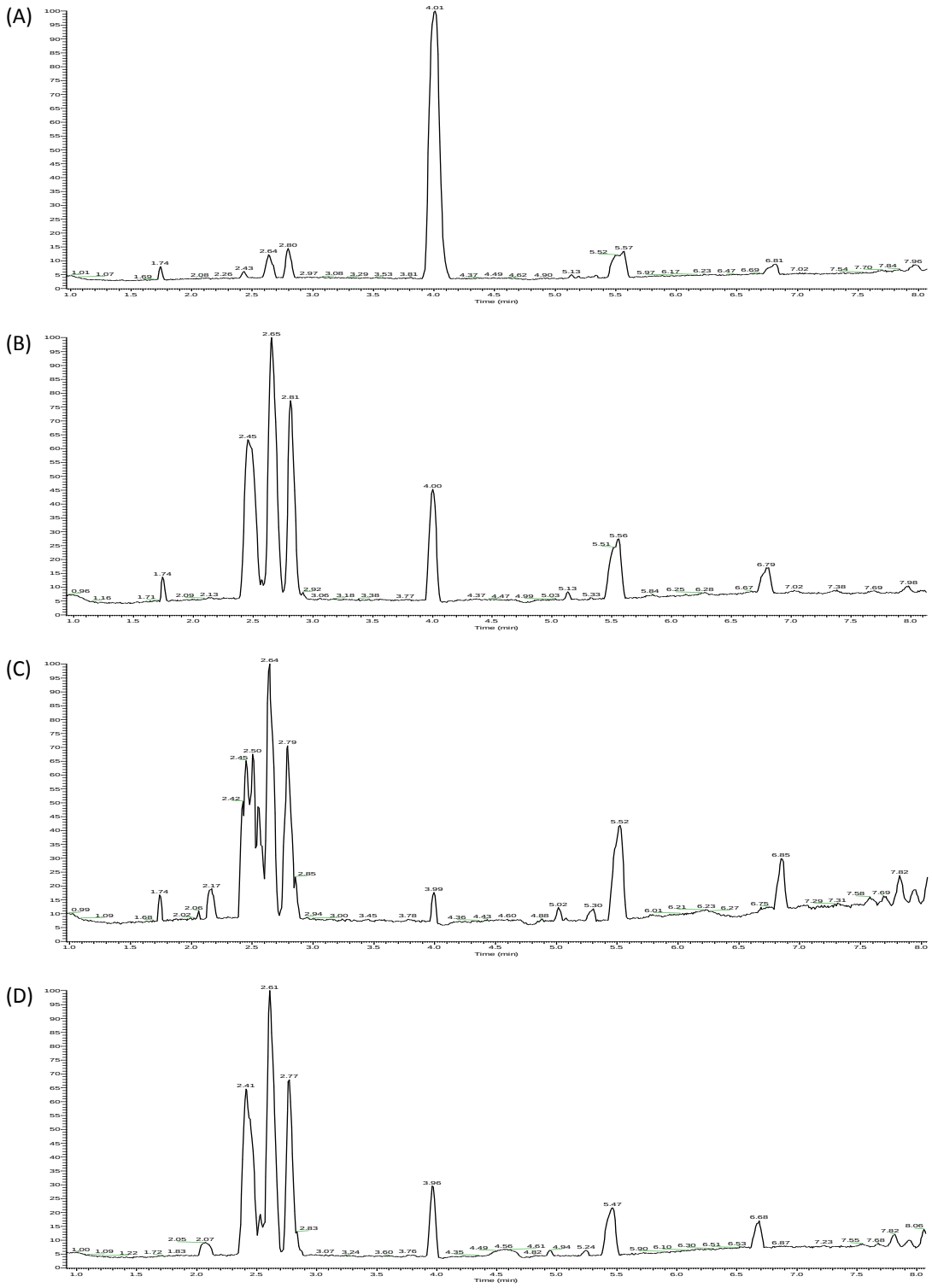


**Figure 4.15. Negative ion LC-MS analysis of TNF-α treated 3T3-L1 adipocytes** Representative chromatograms of differentiated 3T3-L1 adipocytes at day 10 post-differentiation which were pre-incubated with CS-free medium for 24h, and then treated with mouse recombinant TNF-α for 2 and 24h. The treatments represented are: control 2h (A); 50ng/mL 2h (B); control 24h (C); and 50ng/mL 24h (D). Lipids were extracted from the cell samples using a Folch extraction. The lower phase was dried down under nitrogen and reconstituted in 600µL chloroform/methanol (2/1, v/v). The lipids were then separated over 18 min by LC-MS. A change in the lipid profiles was observed, with peaks in the retention time region between 2 and 3min being the most abundant in panels (B)-(D).

| Retention time (min) | Ion mass | Theoretical mass | Δ Mass error (ppm) | Ion | Empirical composition | | Identification |
|---|---|---|---|---|---|---|---|
| 1.74 | 317.0209 | | | | | | |
| 2.65 | 325.1852 | | | | | | |
| 2.81 | 339.2007 | | | | | | |
| 4.00 (20:0) | 564.3459 | 564.3671 | -37.564 | [M-H]- | $C_{28}H_{56}NO_8P$ | | PC |
| 5.55 | 582.5119 | | | | | | |
| 6.79 | 692.6212 | | | | | | |



**Table 4.6. Retention times and their associated abundant mass of each major peak present in the negative ion LC-MS chromatograms of TNF-δ treated adipocytes**

Abbreviations used: PC, phosphatidylcholine; ppm, parts per million

PLS analysis of the non-normalised and TIC-normalised data, were very similar, and both produced five possible groups on the PLS scores plot (Figure 4.17 A and B, respectively), which were interpreted as being: control 2h, control 24h, QCs, 5ng 24h, and all other treated samples. The R2X, R2Y and Q2 for the non-normalised model were 0.954, 0.979 and 0.927, respectively. For the TIC-normalised model, these were 0.961, 0.989 and 0.966, respectively. The phospholipid species PC (20:0), as well as the unidentified point with m/z 346.177 were located on the LHS of both loadings plots (C and D), and the abundance of these species decreased in all of the samples, except the control cells at 2h.

#### *4.3.5.2. IL-6 treatment*

Negative ion chromatograms from the IL-6 treated cells are presented in Figure 4.18. The change in global lipid profiles between the control and IL-6 treated cells were the same as those seen in the TNF-α treated cells, with a peak at RT 4 min being the most abundant in the 2h control samples. This changed to three peaks with RT 2.45, 2.65 and 2.79 being the most abundant in the remaining samples. The most abundant ion associated with each peak were the same as those for the TNF-α treated cells, and so are also presented in Table 4.6.

The PCA scores plot, for non-normalised data relating to the cells treated with IL-6 are presented in Figure 4.19A. Three groups were interpreted on the plot, with one containing 25ng/mL (24h) and two replicates of the 50ng/mL (24h) samples; another consisting of control (2h) cells and the QCs; and the final group was made up of the remaining samples. The R2 and Q2 for this model were 0.944 and 0.841, respectively. Three points with m/z 311.17, 325.18 and 339.20 were situated on the RHS of the origin in the PCA loadings plot (Figure 4.32), and the variance of all three increased in the 25 and 50ng/mL treated samples at both two, and 24h. As mentioned above, these were believed to represent contamination, and so their pattern of variance was not considered in the interpretation of this model. For this reason, these points will not be mentioned again in the remaining plots. Points representing PC (20:0) and the unidentified species with m/z 346.177 were found on the RHS of the origin, and the variance of these lipid species decreased with all of the IL-6 treatment concentrations.

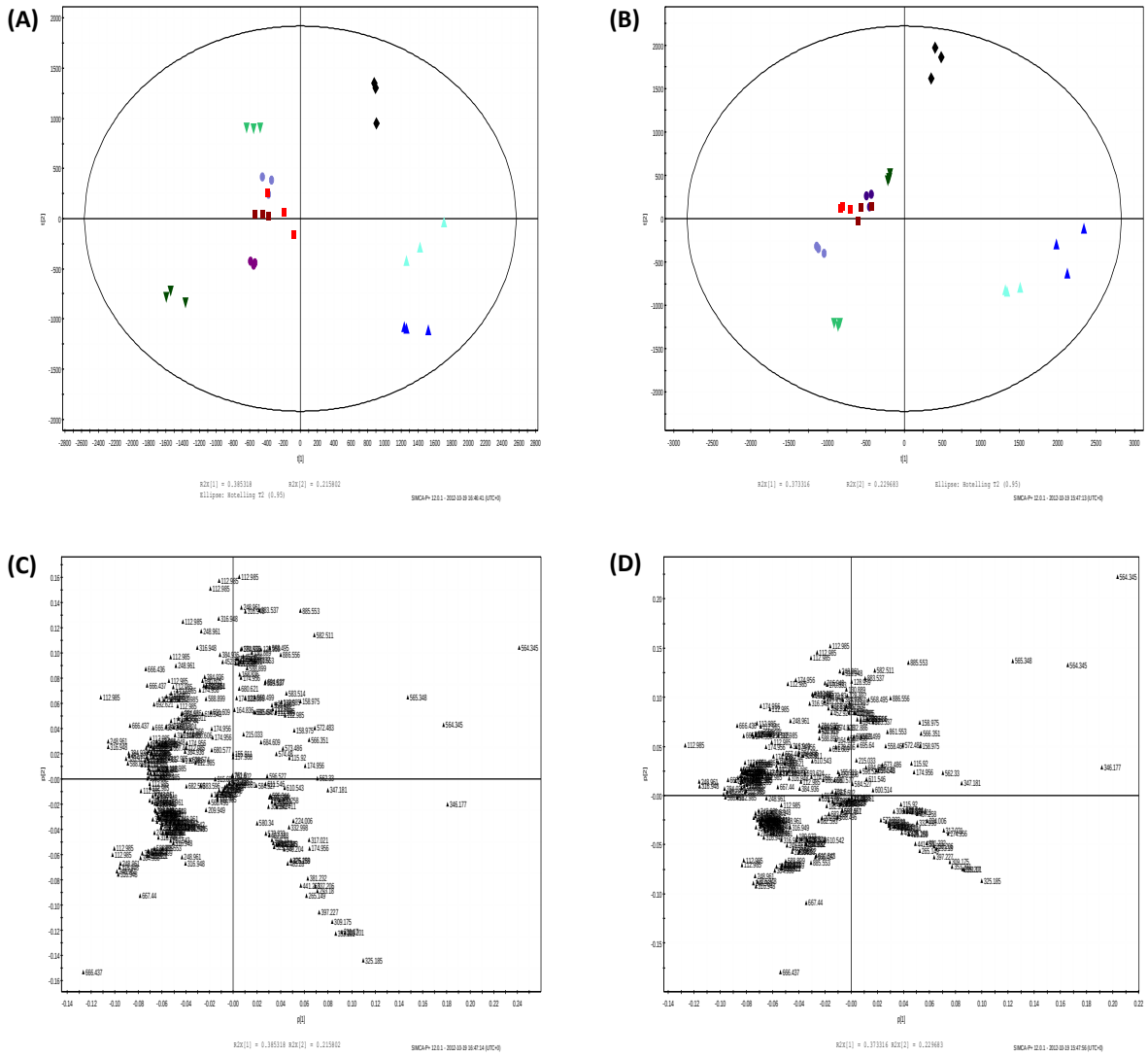


**Figure 4.16. PCA scores and loadings plots representing negative ion LC-MS analysis of TNF-α treated 3T3-L1 adipocytes**

3T3-L1 adipocytes at day 10 post-differentiation were pre-incubated with CS-free medium for 24h, and then treated with mouse recombinant TNF-α for 2 and 24h at the following concentrations: 5, 25 and 50ng/mL. Lipids were extracted using a Folch extraction, and the lower phase was analysed by LC-MS in negative ion mode. Before multivariate data analysis, the data were processed using SIEVE. The data represented here have been Pareto scaled, and the RT window was set at 15 seconds. Either the raw data, or data which were normalised to the total ion current were analysed. Each time point consisted of three biological replicates. The panels represent: no normalisation, scores plot (A); TIC normalisation, scores plot (B); no normalisation, loadings plot (C); and TIC normalisation, loadings plot (D). Both models showed a clear separation between the QCs, control and treated samples.

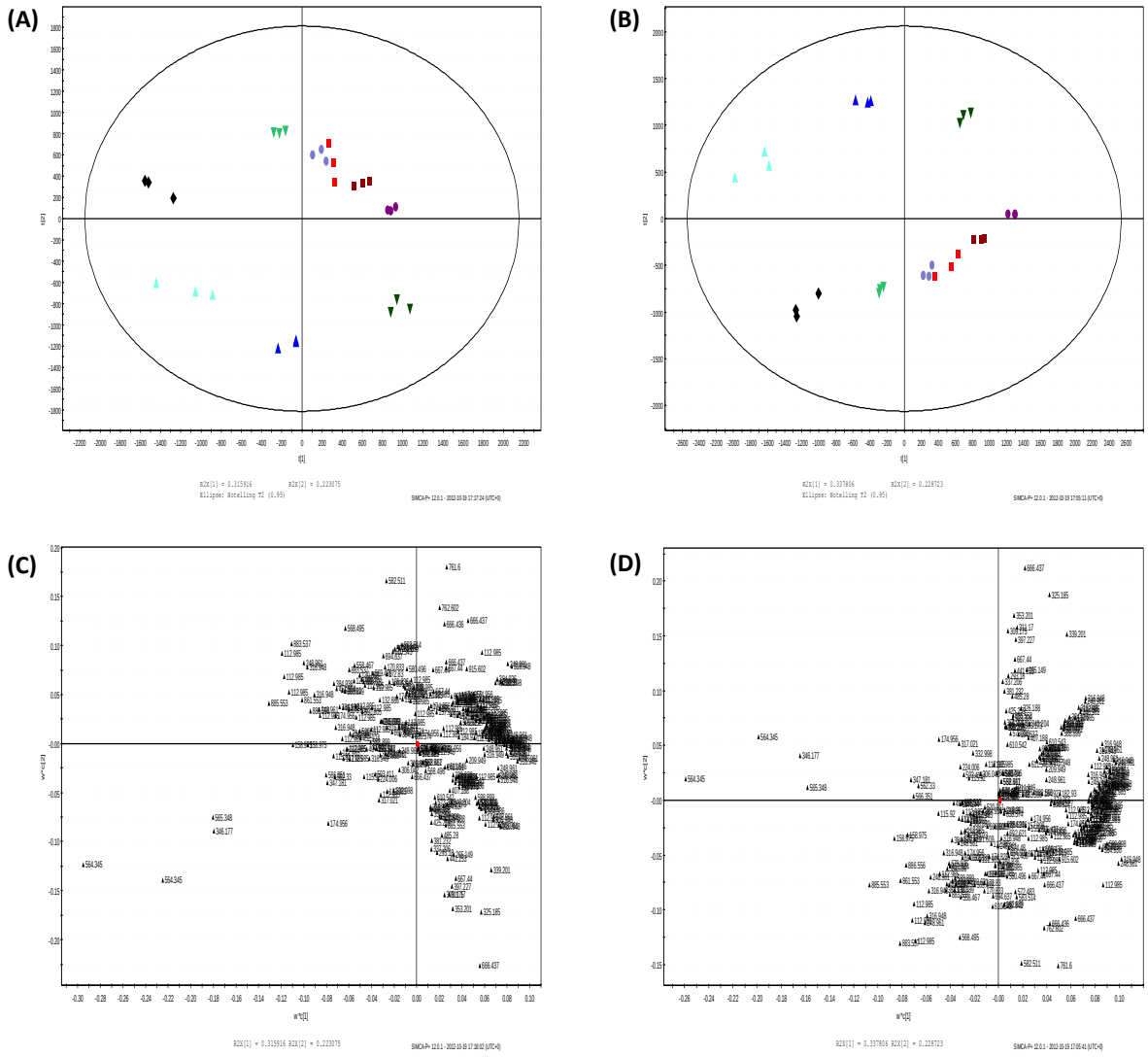


**Figure 4.17. PLS scores and loadings plots representing negative ion LC-MS analysis of TNF-α treated 3T3-L1 adipocytes**

3T3-L1 adipocytes at day 10 post-differentiation were pre-incubated with CS-free medium for 24h, and then treated with mouse recombinant TNF-α for 2 and 24h at the following concentrations: 5, 25 and 50ng/mL. Lipids were extracted using a Folch extraction, and the lower phase was analysed by LC-MS in negative ion mode. Before multivariate data analysis, the data were processed using SIEVE. The data represented here have been Pareto scaled, and the RT window was set at 15 seconds. Either the raw data, or data which were normalised to the total ion current were analysed. Each time point consisted of three biological replicates. The panels represent: no normalisation, scores plot (A); TIC normalisation, scores plot (B); no normalisation, loadings plot (C); and TIC normalisation, loadings plot (D). Both models showed a clear separation between the QCs, control and treated samples.

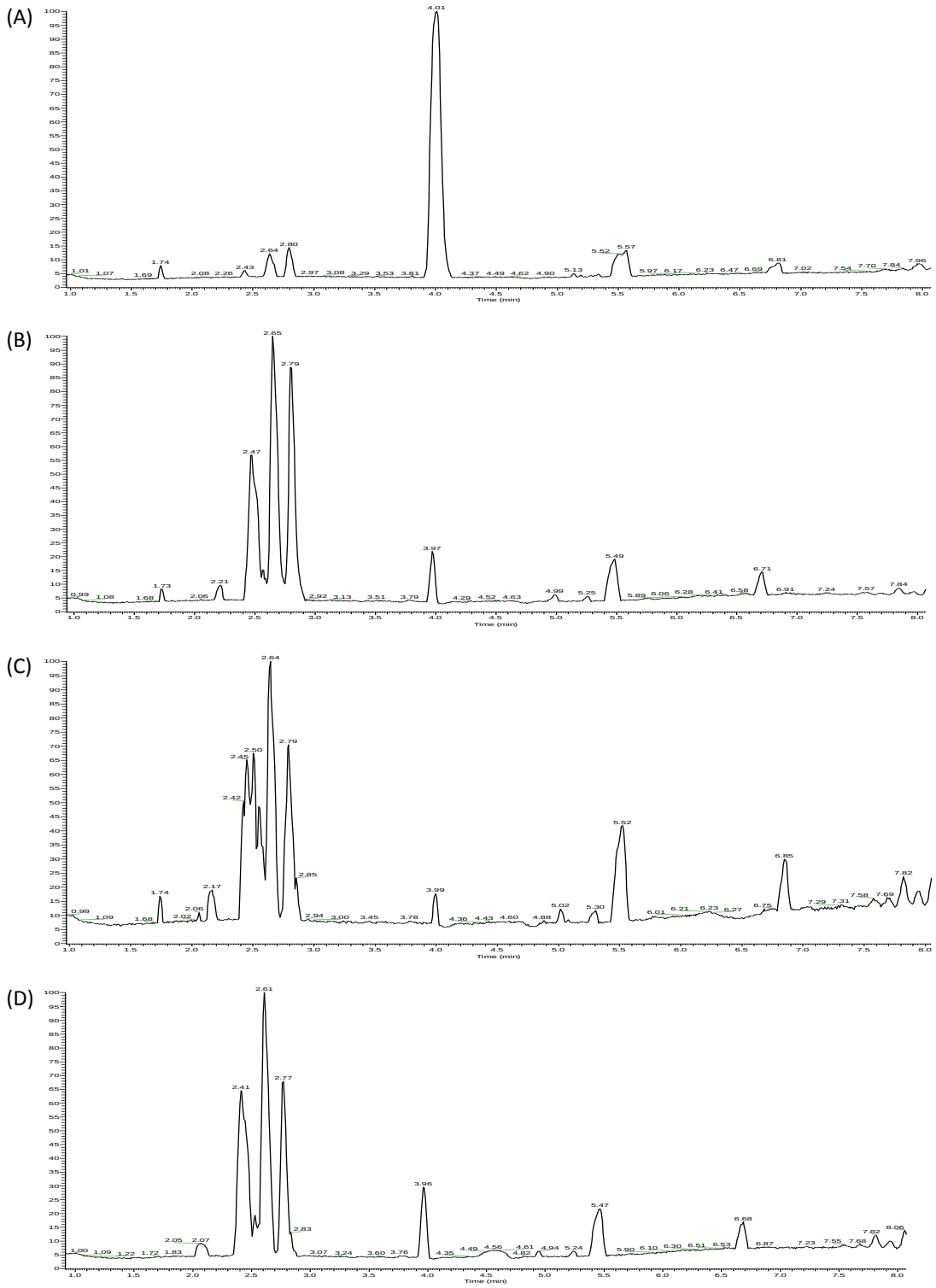


**Figure 4.18. Negative ion LC-MS analysis of IL-6 treated 3T3-L1 adipocytes** Representative chromatograms of differentiated 3T3-L1 adipocytes at day 10 post-differentiation which were pre-incubated with CS-free medium for 24h, and then treated with mouse recombinant TNF-α for 2 or 24h. The treatments represented are: control 2h (A); 50ng/mL 2h (B); control 24h (C); and 50ng/mL 24h (D). Lipids were extracted from the cell samples using a Folch extraction. The lower phase was dried down under nitrogen and reconstituted in 600µL chloroform/methanol (2/1, v/v). The lipids were then separated over 18 min by LC-MS. A change in the lipid profiles was observed, with peaks in the retention time region between 2 and 3min being the most abundant in panels (B)-(D).

The groupings present in the PCA scores plot differed when the data were normalised to the TIC before analysis (Figure 4.19B). All samples clustered into three groups, with the first consisting of cells treated with IL-6 for 24h at both 25 and 50ng/mL. The rest of the samples clustered together in a second group, with exception of the QCs, which formed the final grouping outside of the 95% tolerance limit. The R2 and Q2 for this model were 0.97 and 0.91, respectively. The PCA loadings plot for this model (D) found points representing PC (20:0) and m/z 346.177 on the RHS of the origin. A trend analysis on these points found that their variance decreased in all IL-6 treated samples in comparison to the controls at both 2 and 24h. Another point with m/z 174.956 was also found in this area, and its variance increased in the 24h treated samples.

PLS analysis was also undertaken on both datasets, and the PLS scores and loadings plots are shown in Figure 4.20, and the PLS model representing the non-normalised data (A) showed two groups. The first consisted of the following: two replicates 25ng/mL (2h), 50ng/mL (2h) and both 25 and 50ng/mL (24h). The rest of the samples, including the QCs, clustered together to form the second group. The R2X, R2Y and Q2 for this model were 0.651, 0.868 and 0.785, respectively. The loadings plot for this model (B) showed that the points corresponding to the phospholipid PC (20:0) and the unidentified species (m/z 346.177) were found on the RHS of the origin. A trend analysis was performed on these points, which demonstrated that the variance of both species decreased with all IL-6 treatments, when compared to the controls.

After the data were normalised to the TIC, a difference was observed in the PLS scores plot (B). Three groups were interpreted: the first contained the QCs; and the second consisted of the control cells (both time points), 5ng/mL (2 and 24h), and one replicate from the 25ng/mL (2h) sample set. The final group was made up of the remaining samples. The R2X, R2Y and Q2 were 0.745, 0.838 and 0.774, respectively. The loadings for this model had points relating to PC (20:0) and m/z 346.177 on the RHS of the origin, and their variance decreased in all of the IL-6 treated cells.

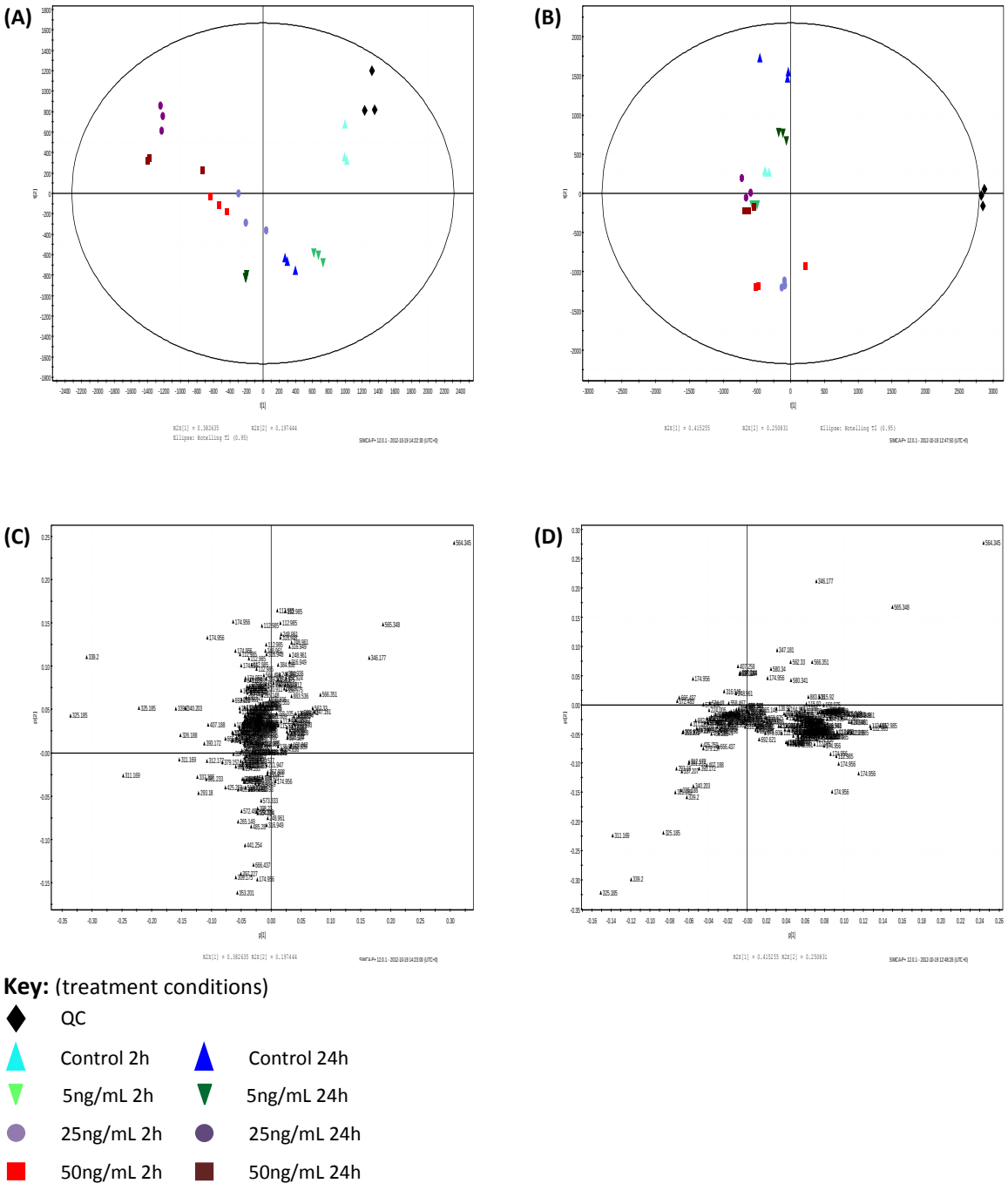


**Figure 4.19. PCA scores and loadings plots representing negative ion LC-MS analysis of IL-6 treated 3T3-L1 adipocytes**

3T3-L1 adipocytes at day 10 post-differentiation were pre-incubated with CS-free medium for 24h, and then treated with mouse recombinant IL-6 for 2 and 24h at the following concentrations: 5, 25 and 50ng/mL. Lipids were extracted using a Folch extraction, and the lower phase was analysed by LC-MS in negative ion mode. Before multivariate data analysis, the data were processed using SIEVE. The data represented here have been Pareto scaled, and the RT window was set at 15 seconds. Either the raw data, or data which were normalised to the total ion current were analysed. Each time point consisted of three biological replicates. The panels represent: no normalisation, scores plot (A); TIC normalisation, scores plot (B); no normalisation, loadings plot (C); and TIC normalisation, loadings plot (D). Two groups were formed in the non-normalised scores plot (A), with one containing the QCs and 2h control samples, and the remaining samples forming the other group. With the TIC-normalised dataset (B), the control and treated samples formed one group, and the QCs were located outside of the 95% tolerance region.

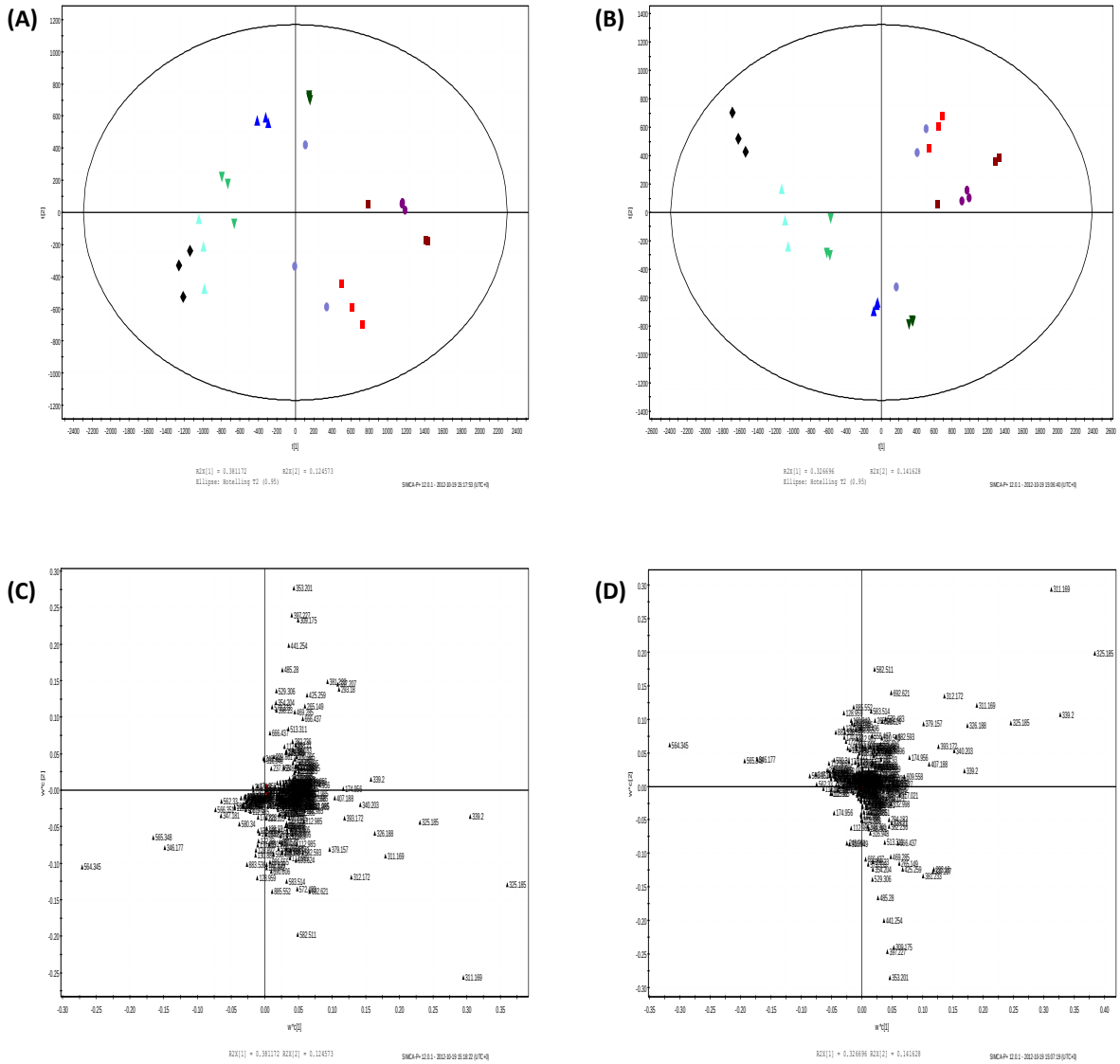


**Figure 4.20. PLS scores and loadings plots representing negative ion LC-MS analysis of IL-6 treated 3T3-L1 adipocytes**

3T3-L1 adipocytes at day 10 post-differentiation were pre-incubated with CS-free medium for 24h, and then treated with mouse recombinant IL-6 for 2 and 24h at the following concentrations: 5, 25 and 50ng/mL. Lipids were extracted using a Folch extraction, and the lower phase was analysed by LC-MS in negative ion mode. Before multivariate data analysis, the data were processed using SIEVE. The data represented here have been Pareto scaled, and the RT window was set at 15 seconds. Either the raw data, or data which were normalised to the total ion current were analysed. Each time point consisted of three biological replicates. The panels represent: no normalisation, scores plot (A); TIC normalisation, scores plot (B); no normalisation, loadings plot (C); and TIC normalisation, loadings plot (D). Both scores plots were identified as having two groups, with the first containing the QCS, along with the control cells and those treated with IL-6 at 5ng/mL at both timepoints. The second group consisted of the 25 and 50ng/mL IL-6 treated samples after both 2 and 24h.

**4.4. Eicosanoid analysis by LC-MS**

Eicosanoids secreted from 3T3-L1 adipocytes treated with either TNF-α or IL-6 were analysed by targeted LC-MS in negative ion mode. Only five were detectable in the medium samples of both treatments and they were: $PGD_2$, $PGE_2$, $PGF_{2\alpha}$, 6-keto $PGF_{2\alpha}$ (6-keto) and 20-OH $LTB_4$ (20-OH).

The changes in concentration of these eicosanoids in response to the different treatment concentrations of TNF-α at both time points are presented in Figure 4.21. All five eicosanoids produced similar profiles with both inflammatory agents. No significant changes in the concentration of the eicosanoid species were observed after 2h of TNF-α treatment, with the exception of an increase in the concentration of $PGD_2$ and $PGF_{2\alpha}$ at the 25ng/mL TNF-α treatment (*P*=0.067 and 0.047 *vs.* control, respectively). At the 24h treatment time point, a direct relationship occurred between the TNF-α treatment concentration, and the concentration of the detected eicosanoids. A significant increase was seen in the concentration of both and 20-OH (E) at the greatest TNF-α treatment concentration (50ng/mL; *P*=0.005 *vs.* control). The concentrations of the remaining eicosanoids, $PGD_2$ (A), $PGE_2$ (B), $PGF_{2\alpha}$ (C) and 6-keto (D) significantly increased at all of the TNF-α treatment concentrations (*P*=0.05 or less *vs*. control for all).

Different concentration profiles of the eicosanoids were seen after IL-6 treatment, as shown in Figure 4.24. Significant increases were observed after 2h of IL-6 treatment at the least, and greatest IL-6 treatment concentrations (5 and 50ng/mL; *P*=0.05 or less *vs.* control for all). A significant decrease in the concentration of all five eicosanoid species occurred at the 25ng/mL IL-6 treatment (*P*=0.05 or less *vs.* control for all). After 24h of IL-6 treatment, the concentration of all detected eicosanoid species significantly increased with all IL-6 treatment concentrations (*P*=0.05 or less *vs.* control for all). The only exception was $PGE_2$, whose concentration did not change with the least concentrated IL-6 treatment.

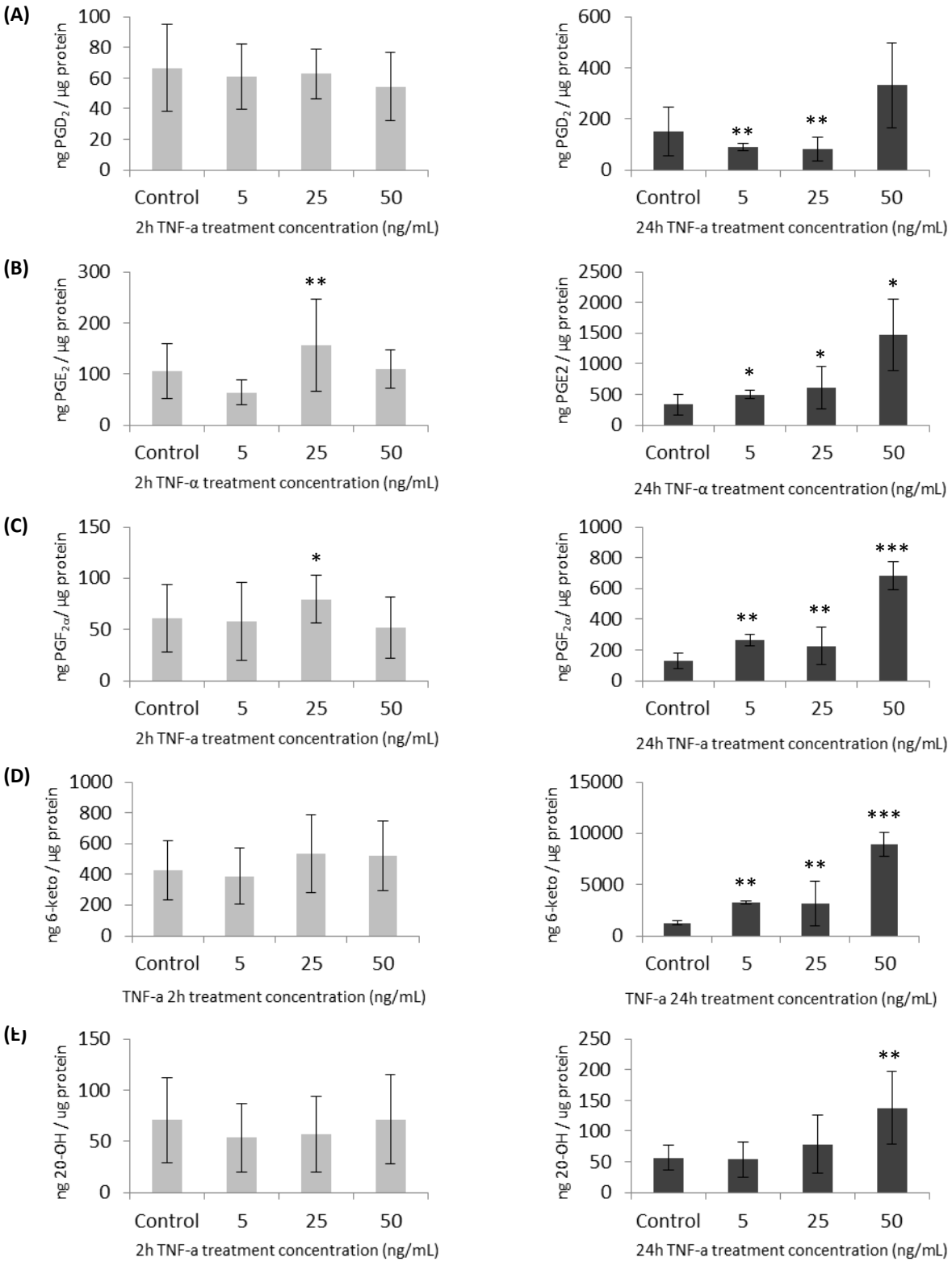


**Figure 4.21. Secretion of eicosanoids by TNF-α treated 3T3-L1 adipocytes**

Differentiated 3T3-L1 adipocytes at day 10 post-differentiation were pre-incubated with CS-free medium for 24h, and were then treated with mouse recombinant TNF-α for 2 or 24h. The concentration of TNF-α treatments used were 5, 25 and 50ng/mL. Eicosanoids were extracted from cell culture medium by solid phase extraction chromatography and were analysed by LC-MS/MS in negative ion mode. Detected eicosanoids are represented as median ± range, with a group size of 3, and are $PGD_2$ (A); $PGE_2$ (B); $PGF_{2\alpha}$ (C); 6-keto $PGF_{1\alpha}$ (D); and 20-OH $LTB_4$ (E). Increases were observed in the concentration of all eicosanoid species after 24h of TNF-α treatment. Statistical significance from the control cells is represented by **P*<0.05; ***P*<0.01 and ****P*<0.001.

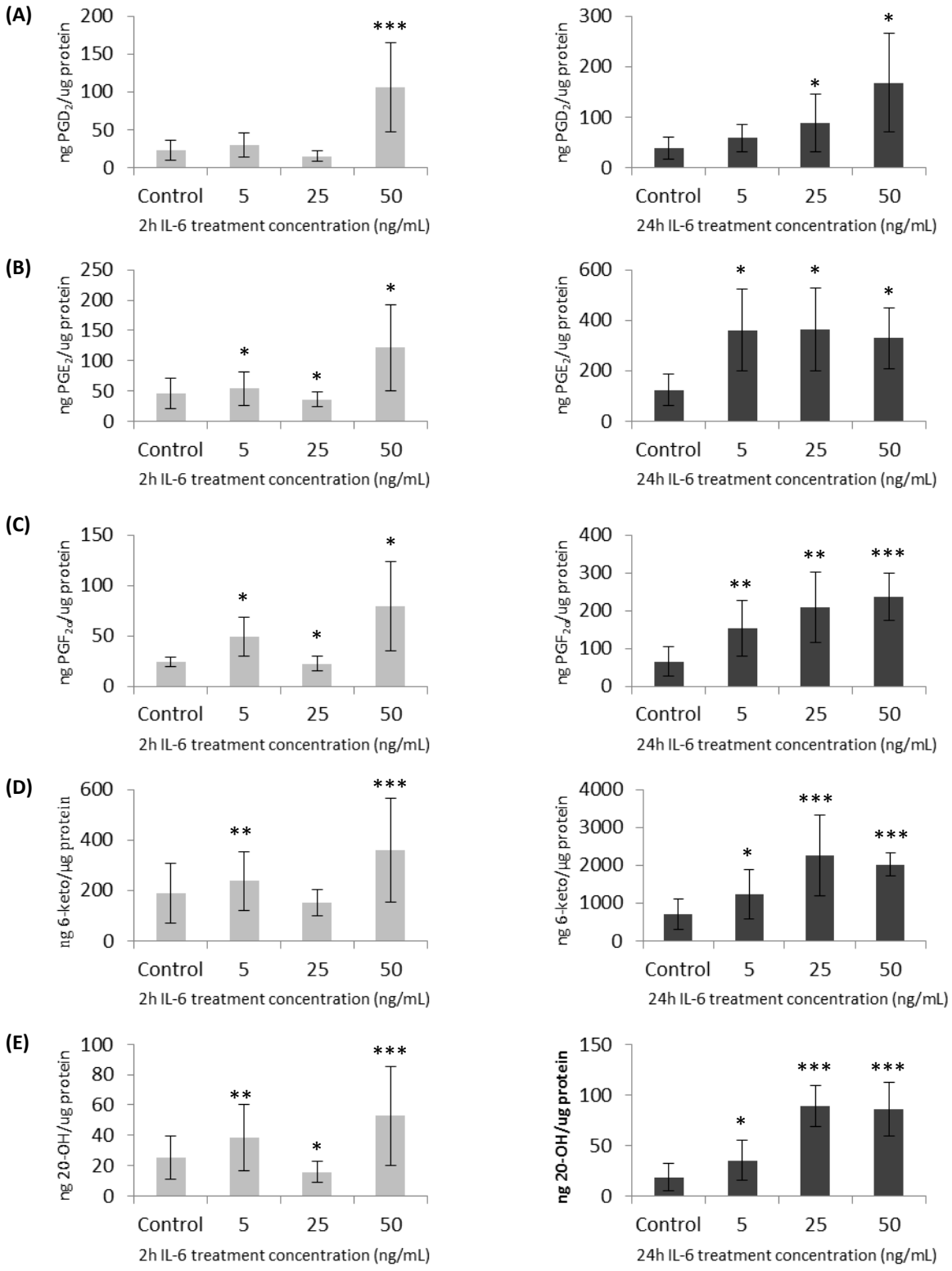


**Figure 4.22. Secretion of eicosanoid lipids by IL-6 treated 3T3-L1 adipocytes**

Differentiated 3T3-L1 adipocytes at day 10 post-differentiation were pre-incubated with CS-free medium for 24h, and were then treated with mouse recombinant IL-6 for 2 or 24h. The concentration of IL-6 treatments used were 5, 25 and 50ng/mL. Eicosanoids were extracted from cell culture medium by solid phase extraction chromatography and were analysed by LC-MS/MS in negative ion mode. Detected eicosanoids are represented as median ± range, with a group size of 3, and are $PGD_2$ (A); $PGE_2$ (B); $PGF_{2\alpha}$ (C); 6-keto $PGF_{1\alpha}$ (D); and 20-OH $LTB_4$ (E). The concentration of all eicosanoid species increased after 24h of IL-6 treatment. Statistical significance from the control cells is represented by **P*<0.05; ***P*<0.01 and ****P*<0.001.

## 4.5. DISCUSSION

This chapter has used the 3T3-L1 adipocyte model characterised in Chapter 3 to study the effect of the pro-inflammatory agents IL-6 and TNF-α on adipokine gene expression of 3T3-L1 adipocytes, as well as their global lipid profiles and the production of eicosanoids. The purpose of this work was to investigate the effect of these inflammatory mediators on the lipid metabolism of 3T3-L1 adipocytes.

### 4.5.1. Effect of inflammatory mediators on adipokine expression

Adipocytes were treated with either TNF-α or IL-6 to investigate whether these inflammatory agents had an effect on the normal expression of several adipokines within the adipocytes. A previous time-course study demonstrated that an effect by TNF-α treatment at a concentration of 25ng/mL was detectable on adipokine and cytokine gene expression and protein secretion in human adipocytes from 2h (Wang *et al.*, 2005). Therefore, a 2h treatment time was selected in this study to monitor whether the effect of acute TNF-α treatment could be replicated with the 3T3-L1 adipocyte model. A 24h treatment time was also studied, to examine longer term effects of TNF-α treatment. Extra TNF-α treatment concentrations were included in the present work, to study the effect of a lesser (5ng/mL) and a greater (50ng/mL) treatment dose. The treatment of mature 3T3-L1 adipocytes with increasing concentrations of TNF-α in this study lead to an overall increase in leptin, and IL-6 expression, and a decrease in the expression of adiponectin, and these changes became more apparent at the greatest concentration, and the longer treatment time. These findings agree with previous studies, for example, leptin gene expression of cultured adipocytes has been shown to be inhibited by chronic TNF-α treatment after a transient rise (Kirchgessner *et al*., 1997; Yamaguchi *et al*., 1998). TNF-α treatment also decreases adiponectin gene expression and protein secretion in both human pre-adipocytes (Kappes and Loffler, 2000) and 3T3-L1 adipocytes (Fasshauer *et al*., 2002), as well as increase IL-6 gene expression (Wang *et al.*, 2005).

The effect of IL-6 treatment on 3T3-L1 adipocyte metabolism was also studied with the same conditions as above, and gene expression and protein secretion of IL-6 occurs in adipocytes (Mohamed-Ali *et al*., 1997). In the current study, treatment of 3T3-L1 adipocytes with IL-6 caused the upregulation of its own gene expression, as well as that of leptin and TNF-α. In contrast, adiponectin expression decreased with IL-6 treatment. As with the TNF-α treatment, these effects were greater with the 24h treatment.

These findings agree with previous work, which demonstrate that treatment with IL-6 lead to an autocrine effect on its own secretion in murine cells (Fasshauer *et al*., 2003a; Lagathu *et al.,* 2003). Leptin gene expression increases in human adipocytes after IL-6 treatment (Tujillo *et al*., 2004), and adiponectin expression is inhibited by IL-6 (Fasshauer *et al*., 2003b).

The purpose of this section of work was to validate the expected response of 3T3-L1 adipocytes to both TNF-α and IL-6 treatment, and, overall, the findings in the current study agreed with the well-documented changes seen in adipokine gene expression in the inflammatory state. By replicating previous findings, it was proved that the dysfunction of adipokine gene expression seen in the 3T3-L1 adipocytes in the current work was as expected. Therefore, this model of adipocyte inflammation was suitable for lipidomic analyses.

**4.5.2. Effect of inflammatory mediators on global lipid profiles**

In WAT, excess energy intake results in the storage of TG, and this TG pool is constantly changing due to the metabolic processes lipolysis and lipogenesis. Alterations in the lipid metabolism of adipocytes are associated with obesity, such as increased basal lipolysis (Reynisdottir *et al*., 1995). Lipolysis is the process by which stored TG are hydrolysed to release FAs in times of energy demand. The gene expression and protein secretion of TNF-α and IL-6 (among others) are known to increase in the obese state (Wang *et al.*, 2005), and so may be involved in the changes observed in lipid metabolism. Increased gene expression and protein secretion of TNF-α is observed in obesity, along with increased basal lipolysis (Prins *et al*., 1997; Ryden *et al*., 2004). Previous studies have demonstrated that TNF-α deficient mice had decreased concentrations of circulating free fatty acids (FFA) and TGs than wild-type controls (Uysal *et al*., 1997; Ventre *et al*., 1997). Treatment of 3T3-L1 adipocytes with TNF-α suppresses lipoprotein lipase (LPL) activity, and stimulates lipolysis (Kawakami *et al*., 1982 and 1987). This cytokine also decreases the gene expression of FA transport protein (FATP) and translocase (FAT) in adipose tissue (Memon *et al*., 1988).

IL-6 may also have an effect on lipid metabolism, as suggested by previous *in vitro* and *in vivo* experiments. A previous study has shown that IL-6 increases lipolysis in human mammary adipocytes (Path *et al*., 2001). Administration of IL-6 reduced LPL activity in the adipose tissue of mice, and also within 3T3-L1 adipocytes (Greenberg *et al*., 1992).

When administered intravenously into rats, IL-6 caused an increase in the serum concentration of TGs and FAs, which occurred in a dose-dependent manner (Nonogaki *et al*., 1995).

Therefore, one major effect of both TNF-α and IL-6 in terms of lipid metabolism is an increase in lipolysis, and obesity is associated with increased basal lipolysis (Reynisdottir *et al*., 1995). In the current study, positive ion DI-MS analysis found that the concentration of two DG and two TG species either decreased, or remained constant in 3T3-L1 adipocytes after treatment with TNF-α, when compared to control cells. This decrease in the concentration of these species within the TNF-α treated cells may suggest increased lipolysis. Treatment with IL-6 showed an increase in the concentration of the DG and TG species after 24h of treatment; however, this increase declined as the concentration of IL-6 treatment increased (three concentrations were investigated; 5, 25 and 50ng/mL). This may suggest that more chronic IL-6 treatment is necessary for increased rates of lipolysis to be observed.

The gene expression data present in the current study have shown that TNF-α is stimulated by IL-6, and vice-versa is also true (Wang *et al.*, 2005). As described above, both have been shown to increase basal lipolysis. This observed increase with both TNF-α and IL-6 treatment may, therefore, be a direct effect of each agent, or a cumulative effect of the two. The adipokine leptin also plays a role in the altered lipolysis seen in dysregulated adipocytes. Treatment of lean mice adipocytes with leptin stimulates lipolytic activity, and this observation was even greater after leptin treatment in adipocytes from leptin resistant *ob*/*ob* mice (Fruhbeck *et al*., 1997). In the current study, leptin gene expression increased after both TNF-α and IL-6 treatment, and so this increase in leptin gene expression may also be involved in the changes observed in the DG/TG concentrations after treatment with the inflammatory agents.

Clearer separations were observed in the IL-6 treated cells than the TNF-α treated cells with multivariate data analysis of positive ion mode data. In all of the PCA and PLS plots presented, points representing 24h of IL-6 treatment at concentrations of 25 and 50ng/mL, were grouped away from the rest of the samples. Of the identifiable points from the loadings plots, one was TG (54:3), and the abundance of this lipid species was increased with the all IL-6 treatment concentrations. This ties in with the DG/TG species identified by DI-MS analysis of these treatments, and so the concentration of these lipid species increase with the greater IL-6 concentrations at the longer treatment time (24h).

This may suggest that basal lipolysis has not increased in these cells. In negative ion mode, various grouping combinations were observed for both TNF-α and IL-6 treated cells, but, overall, a clear separation was observed between the control and treated cells. The abundance of the phospholipid PC (20:0) decreased between the control and treated groups. This matched the negative DI-MS analysis data, where the concentration of this lipid decreased in both the TNF-α and IL-6 treated cells.

The increase in lipolysis observed in dysregulated adipocytes may be seen as advantageous, as the outcome would be a decrease in TG accumulation within the adipocyte. However, hydrolysis of TG leads to an increase in FFAs which has been linked to insulin resistance, T2DM and the metabolic syndrome (Randle *et al*., 1963). In the current study it has been suggested that increased basal lipolysis was observed in TNF-α treatment due to the decreased concentration of various DG/TG and also of PC (20:0). TNF-α is known to be an important mediator of obesity-related insulin resistance (Hotamisligil *et al.*, 1993; 1994 and 1995). It down-regulates the gene expression of glucose transporter type 4 (GLUT4) in adipocytes, causing a decrease in insulin-stimulated intracellular glucose transport (Stephens and Pekala, 1992). This is coupled with an increase in the gene expression of hormone sensitive lipase (HSL), which causes increased lipolysis (Sumida *et al*., 1997). Therefore, increased basal lipolysis may be involved in the insulin resistance caused by TNF-α.

IL-6 treatment in the current study caused increased concentrations of various individual DG/TG species after 24h of treatment, and so it was thought that increased basal lipolysis had not occurred. A previous study observed an increase in lipolysis after 24 to 48h of IL-6 treatment in human adipocytes (Trujillo *et al*., 2004), therefore, more chronic treatment with IL-6 may be needed to observe the decrease in DG / TG concentrations as seen with TNF-α treatment.

### 4.5.3. Effect of inflammatory mediators on eicosanoid production

Changes in the concentration of eicosanoid species were expected in the 3T3-L1 adipocytes after treatment with both TNF-α and IL-6, especially because dysfunction of normal adipocyte function had already been observed in both the gene expression of several adipokines and also the global lipid profiles of these cells. As with the eicosanoid species detected produced by the differentiating 3T3-L1 adipocytes in Chapter 3, only a minority of the eicosanoids present in the standard mix were detectable in the inflammatory mediator treated cells, and these were all prostanoids. As described in Chapter 3, the prostanoids are known to have a vital role in modulating differentiation and maturation of adipocytes (Shillabeer *et al*., 1998). These prostanoids can also act as lipid mediators of metabolic abnormalities, with both $PGE_2$ and $PGI_2$ being known to induce adipocyte dysfunction (Kim and Moustaid-Moussa, 2000).

In the current study, an increase in the concentration of the five detectable eicosanoid species was observed with TNF-α treatment, and these eicosanoids were: $PGD_2$, $PGE_2$, $PGF_{2\alpha}$, 6-keto $PGF_{1\alpha}$ and 20-OH $LTB_4$. TNF-α stimulates $PGE_2$ and $PGD_2$ synthesis in several cell types (Dayer *et al*., 1985). Both are involved in the synthesis and storage of TG, and inhibition of lipolysis (Strong *et al*., 1992). A direct relationship was observed between the concentration of $PGE_2$ and TNF-α treatment concentration, implying that greater TNF-α concentrations can further increase $PGE_2$ production.

Given that $PGE_2$ is a potent inhibitor of TNF-α (Miles *et al*., 2002), this may explain why gene expression of TNF-α was not detectable with the highest TNF-α treatment concentration in the current study. However, a previous study in human adipocytes demonstrated that acute TNF-α treatment had a substantial effect on its own expression (Wang *et al*., 2005). This contradicts the findings in this thesis; however, it was undertaken with human adipocytes with a TNF-α treatment concentration of 25ng/mL, and so may not be comparable. The gene expression of TNF-α was seen in the treated 3T3-L1 adipocytes in the present study at 25ng/mL (data not shown), meaning that TNF-α concentration greater than this may have an inhibitory effect on its own expression, possibly caused by an increase in $PGE_2$ synthesis.

$PGE_2$ may also have an effect on the adipokine changes seen in obesity as a previous study has demonstrated that $PGE_2$ increases leptin production in primary culture of mouse adipose tissue (Fain *et al*., 2000). Increased circulating concentrations of leptin are known to increase lipolysis (Lonnqvist *et al*., 1995). In the current study, leptin gene expression in the 3T3-L1 adipocytes increased after treatment with both TNF-α and IL-6, and so this increase may have

been caused by the increase in $PGE_2$ concentration. One way to test this hypothesis would be to block $PGE_2$ formation with the use of a cyclooxygenase (COX) inhibitor and observe the effect on leptin gene expression.

Arachidonate and FA products regulate lipolysis within adipocytes, and these are released by phospholipase $A_2$. An adipose tissue specific group XVI phospholipase $A_2$ enzyme has been characterised in mouse WAT (Duncan *et al*., 2008), and it acts at the sn2 position of phosphatidylcholine acyl chains. The observed decrease of PC (20:0) in the current study could be due to increased lipolysis, which would therefore require increased arachidonate release from the phospholipids.

Another prostanoid which significantly increased with TNF-α treatment in this study was $PGF_{2\alpha}$. This is known to stimulate expression of TNF-α in both pre- and mature adipocytes, and both TNF-α (Torti *et al*., 1985) and $PGF_{2\alpha}$ (Miller *et al*., 1996) inhibit adipocyte differentiation. A significant increase in $PGF_{2\alpha}$ concentration was observed in this study, which would lead to dysregulation of the normal adipocyte function. This increase in the concentration of $PGF_{2\alpha}$ may further increase TNF-α gene expression and protein secretion, which in turn could stimulate greater $PGE_2$ production and induce the dysfunction of the adipocyte.

In the current study, the treatment of 3T3-L1 adipocytes with IL-6 also significantly increased the concentrations of all five eicosanoid species at the higher concentrations after 24h, and also at 2h for $PGE_2$ and $PGF_{2\alpha}$. This may imply that treatment with IL-6 has the same effects on prostanoid synthesis. IL-6 is known to increase TNF-α gene expression and protein secretion; therefore, another explanation for the similarities may be that the effects of IL-6 treatment on eicosanoids may in fact be due to the increased TNF-α synthesis. Both $PGE_2$ and $PGD_2$ inhibit lipolysis (Strong *et al*., 1992), and so the increases in the concentration of these prostanoids may explain the increase in the concentration of three TG species from both DI-MS and LC-MS analyses present after IL-6 treatment of 3T3-L1 adipocytes.

### 4.5.4. Limitations

The major limitation of the current study was the lack of successful lipid species identifications in the PCA and PLS loadings plots. With those that could be identified, exact fatty acid compositions could not be assigned, and so they were represented as the total fatty acid composition; for example PC (34:1) could be PC (16:0/18:1) or PC (18:1/16:0). The points that could not be identified were possibly part of the 'background noise' ions from the LC-MS analysis. All PCA and PLS models in the current study were Pareto scaled, and this means that areas on the chromatogram with lesser amplitude can influence the model if they show variation. This scaling method is commonly used for mass spectrometry data (Eriksson *et al*., 1999). If the unidentified points did represent noise ions, then another scaling method may be more appropriate. One example would be centering with no scaling (Ctr) in which regions of less amplitude would have little influence because the influence of a variable is related to its signal.

Another problem was the possible contamination seen in the negative ion mass spectrometry analyses. In some of the spectra acquired from both DI-MS and LC-MS analyses, three peaks with m/z 311.17, 325.18 and 339.20 were present. These were thought to be linear alkylbenzenesulfonates (Andreu and Pico, 2004), which are found in detergents. These peaks were excluded from data analysis; however, their presence in the samples was evident in the PCA and PLS loadings plots.

### 4.5.5. Conclusions and future work

Obesity is characterised by chronic low-grade inflammation (Yudkin *et al*., 1999; Festa *et al*., 2001). The work in this chapter used the 3T3-L1 adipocyte model to study the effect of the pro-inflammatory agents IL-6 and TNF-α on adipokine gene expression, as well as global lipid profiles and the production of eicosanoids. An increase in the gene expression of leptin and IL-6 was observed in these treated cells, along with a decrease in adiponectin expression. Adiponectin has an anti-inflammatory action (Ouchi *et al*., 2000) and so its decrease further supports the inflammation state of these adipocytes.

Global lipidomic analyses identified a decrease in the concentration of several DG and TG species after treatment with TNF-α and so it was suggested that an increase in lipolysis was occurring in these cells. Conflicting findings were seen after IL-6 treatment, with the concentration of TG/DG species increasing. A previous study demonstrated that IL-6

treatment increased lipolysis in human adipocytes after 48h of treatment (Trujillo *et al*., 2004), and so the 24h treatment in this study may not have been long enough to replicate the effect of TNF-α treatment.

Increases in the concentration of $PGD_2$, $PGD_2$ and $PGF_{2\alpha}$ were observed after the 3T3-L1 adipocytes were treated with TNF-α and IL-6. Both $PGE_2$ and $PGD_2$ increase the production and storage of TG, and inhibit lipolysis (Strong *et al*., 1992); whereas $PGF_{2\alpha}$ is known to inhibit differentiation. As well as having a role in lipid metabolism, $PGE_2$ also increases leptin production in mouse adipose tissue (Fain *et al*., 2000). In the current study, leptin gene expression was increased after treatment with both TNF-α and IL-6. Therefore, increased $PGE_2$ concentration in the present work may increase leptin gene expression, which in turn increases lipolysis. Increased concentrations of these prostanoid species in response to treatment with the inflammatory agents may be associated with disturbances in normal lipid metabolism within the adipocyte.

Overall, the findings in this chapter have proved that treatment with inflammatory agents causes dysfunction of the normal metabolism of 3T3-L1 adipocytes. Disturbances in adipokine gene expression, global lipid profiles and eicosanoid secretion patterns were observed, and seemed to be linked. The main disturbance suggested was an increase in lipolysis. The result of lipolysis is increased hydrolysis of TG which would lead to decreased TG storage and also increased concentrations of FFAs, which have serious implications for health, as they are associated with insulin resistance and T2DM (Randle *et al*., 1963; Bays *et al*., 2004; Poynten *et al*., 2005), and also increased risk of cardiovascular disease (Carlsson *et al*., 2000; Pirro *et al*., 2002).

The current work has provided a model for abnormal adipocyte function in relation to inflammation. Increased lipolysis appears to be occurring in the TNF-α treated cells; however, this has only been based on the evidence of decreased concentrations of TG/DG species. More thorough investigations are needed for definite proof, and a simple way to monitor lipolysis is by measuring glycerol release into the medium (Bradley and Kaslow, 1989). Also, it would be interesting to investigate the gene expression of LPL, as it is known to be suppressed by TNF-α (Kawakami *et al*., 1982; Price *et al*., 1986; Kawakami *et al*., 1987) and IL-6 (Greenberg *et al*., 1992), and is related to increased lipolysis.

# Chapter 5

## Effect of dexamethasone treatment on 3T3-L1 adipocyte metabolism

## 5.1. INTRODUCTION

The results described in Chapter 4 demonstrated that 3T3-L1 adipocytes are responsive to the effects of the inflammatory mediators, TNF-α and IL-6. This current study was designed to determine whether similar or opposing effects would be observed in response to an anti-inflammatory agent. Dexamethasone was chosen because as well as being an anti-inflammatory agent, it is also a component of the differentiation cocktail used to differentiate 3T3-L1 pre-adipocytes (Rubin *et al*., 1978), and therefore has adipogenic properties.

Dexamethasone is a synthetic member of the glucocorticoid class of steroid drugs, and is a potent anti-inflammatory agent, as observed by its effects on the gene expression of several inflammatory adipokines. For example, dexamethasone treatment of human omental adipose tissue explants inhibits the gene expression and protein secretion of IL-6 and IL-8 (Fain *et al*., 2005). It is also an adipogenic agent, and is involved in the adipogenesis of 3T3-L1 adipocytes (Rubin *et al*., 1978), as well as other pre-adipocyte cell lines (Chapman *et al*., 1984; Grigoriadis *et al*., 1988; Gaillard *et al*., 1991).

Glucocorticoids are hormones produced by the adrenal cortex, and are adaptive in activating the cardiovascular system in response to a physical stressor by increasing blood pressure and cardiac output (Fisher, 1990). However, chronic glucocorticoid treatment is maladaptive and associated with an increase in the concentration of circulating free fatty acids (FFAs) and insulin resistance in humans (Divertie *et al*., 1991; Djurhuus *et al*., 2002 and 2004) and rodents (Severino *et al*., 2002). Two potential mechanisms have been suggested for insulin-resistance caused by glucocorticoid treatment; a decrease in insulin binding to cells, and also inhibition of glucose transport (Czech and Fain, 1972; Olefsky, 1975; Olefsky *et al*., 1975).

Excessive glucocorticoid treatment is known to affect lipid metabolism by increasing the gene expression of adipose triglyceride lipase (ATGL) and hormone sensitive lipase (HSL), which in turn increase lipolysis (Fain and Saperstein, 1970; Slavin *et al*., 1994; Xu *et al*., 2009; Campbell *et al*., 2011). Increased lipolysis leads to lipid loss, as seen in an *in vivo* rodent study, whereby chronic glucocorticoid treatment induced weight loss (Elliot *et al*., 1971). In contrast, chronic glucocorticoid excess is the main cause of Cushing's syndrome (hyperadrenocorticism), which is characterised by increased adiposity, particularly in the visceral region (Cushing, 1912). The classical central fat accumulation observed in Cushing's syndrome is associated with glucose intolerance and hypertension, and so the clinical features of this disease are similar to the metabolic syndrome (Reaven and Hoffman, 1987).

### 5.1.2. Aims and objectives

Previous studies have found that the glucocorticoids have lipolytic and adipogenic actions which vary according to various factors including the agent used, dose and length of treatment and the experimental model used (Masuzaki *et al*., 2001; Andrews *et al*., 2002; Kershaw *et al*., 2005; Xu *et al*., 2009). Therefore, the purpose of the work presented in the current study was to explore the effect of dexamethasone treatment on the normal function of 3T3-L1 adipocytes. These cells were treated at day 10 post-differentiation with dexamethasone at two concentrations for either two, or 24 hours (h).

The first specific aim was to measure the gene expression of leptin, adiponectin, IL-6 and TNF-α in both the control day 10 adipocytes, and those which had been treated with dexamethasone. It was hypothesised that the expression of these genes would alter when compared to control adipocytes; specifically leptin gene expression would increase after dexamethasone treatment, whereas the gene expression of adiponectin, IL-6 and TNF-α would decrease, as seen in previous studies (Bradley and Cheatham, 1999; Fasshauer *et al*., 2002 and 2003).

After the gene expression profiles had been monitored, the second aim was to produce global lipid profiles of these adipocytes. It was predicted that both phospholipid and triglyceride species would be the major components of the global lipid profiles, but also that the abundance of these lipid species would be altered by dexamethasone intervention.

The final aim was to detect arachidonic acid (AA)-derived eicosanoid species secreted by these adipocytes, and to monitor their concentration in both the control and dexamethasone treated cells.

## 5.2 Materials and Methods

### 5.2.1. Cell culture

3T3-L1 adipocytes were cultured in a humidified atmosphere of 5%$CO_2$ / 95% air at 37$^{o}$C as previously described in Section 2.1.3. All media protocols are listed in Section 2.1.2. The cells were induced to differentiate at day 0, and all treatments occurred at day 10 post-differentiation. Before treatment, the adipocytes were starved of calf serum (CS) for 24 hours (h), by feeding with DMEM alone. After 24h, the cells were treated with CS-free medium containing 2 or 20nM dexamethasone, and the control cells had the CS-free incubation medium renewed. The cells were harvested at 2 and 24h post-treatment, along with the medium, and both were stored at -80$^{o}$C until required.

### 5.2.2. Reverse transcription PCR

The gene expression of leptin, adiponectin, TNF-α and IL-6 were quantified using qPCR, as described in Sections 2.3 and 2.6.

### 5.2.3. Global lipidomic analysis

#### *5.3.2.1. Cell preparation*

A Folch extraction was used to extract lipids from cell and quality control (QC) samples (Folch *et al*., 1957) as described in Section 2.9.1.1. The lower phase was dried down under a stream of nitrogen, and reconstituted into 600µL chloroform/methanol (2,1; v,v). The direct infusion-mass spectrometry (DI-MS) samples had 10mM ammonium formate added to them, but not the liquid chromatography-mass spectrometry (LC-MS) samples

#### *5.2.3.1. DI-MS analysis*

The reconstituted samples analysed by DI-MS using an Orbitrap Exactive mass spectrometer, with one technical replicate per sample, and analysed in both positive and negative ion mode as described in Section 2.9.1.2.

Abundant peaks from both the control and treated cell samples were quantified using the relevant internal standard, which were added at 1nmol concentration, and had a mass-to-charge ratio (m/z) of either 622.4443, or 908.8651 in positive ion mode. These related to:

1,2-didodecanoyl-*sn*-glycero-3-phosphocholine, PC (12:0/12:0); or 1,2,3-trioctadecanoyl-*sn*-glycerol, TG (18:0/18:0/18:0), respectively. The samples were then normalised to the protein concentration of the cell samples. The lipids were identified according to their m/z using the following databases: the Human Metabolome Database (HMDB; www.hmdb.ca), LIPID Metabolites and Pathways Strategy (LIPID MAPS; www.lipidmaps.org), and the Metabolite and Tandem MS Database (METLIN; http://metlin.scripps.edu). If the mass accuracy was within 5 parts per million (ppm), a confident identification was assumed, and all mentioned identifications are within this limit, unless stated.

#### *5.2.3.2. LC-MS analysis*

The lipid extracts were also analysed by LC-MS using a binary solvent system to separate the samples over 18 minutes (min) as described in Sections 2.9.2.2 and 2.9.2.3.

#### *5.2.3.4. LC-MS data processing and multivariate data analysis*

All LC-MS chromatograms were processed using SIEVE (v1.3) to produce m/z and retention time (RT) frames. The retention time window was set to 15 seconds (s). These frames, along with their related intensities were manually normalised to the total ion current (TIC) of the chromatogram. As with the DI-MS data, the lipids were identified using three databases: HMDB, LIPID MAPS and METLIN in both positive and negative ion modes.

The RT and m/z pairs, along with their intensities, were manually normalised the total ion current (TIC) intensity. Both the non-normalised and TIC-normalised data sets were then imported into SIMCA-P (v12) for multivariate data analysis (MVDA), starting the unsupervised principal component analysis (PCA). A supervised technique was then used, and due to the number of sample groups, as well as the fact that the y-variable data were continuous, partial least squares (PLS) analysis was chosen. All models were Pareto scaled.

### 5.2.4. Targeted eicosanoid analysis

Solid phase extraction chromatography was used to extract eicosanoids from 3T3-L1 medium samples, and is described in Section 2.9.3.1. After the eicosanoids had been eluted, the samples were dried down under nitrogen and reconstituted in 100µL $H_20$: MeOH (1:1, v: v), before being analysed by LC-MS/MS as outlined in Sections 2.9.3.2.1 and 2.9.3.2.2. Individual eicosanoids were identified using specific precursor-to-product ion m/z transitions, as detailed in Table 2.3 (Chapter 2).

### 5.2.5. Statistical analysis

For qPCR analyses, all data were analysed using the non-parametric Friedman's two-way analysis of variance test, followed by a pairwise comparisons (Conver) post-hoc test. The Friedman's two-way analysis of variance test was chosen, even though the data were normally distributed, because it has been suggested that non-parametric tests should be used when analysing qPCR data (Yuan *et al*., 2006). For the mass spectrometry data, a Shapiro-Wilk W test was used to determine their normality, and all were not normally distributed. Therefore, the non-parametric Friedman's two-way analysis of variance test was used followed by an all pairwise comparisons (Conover) post-hoc test to identify differences between groups. All of the statistical tests were performed using the software package StatsDirect. Normally distributed data were presented as mean values ± SD, and non-normally distributed data as median values ± range. The group size is indicated in the figures, and a *P*-value of less than or equal to 0.05 was considered to be statistically significant.

## 5.3. RESULTS

### 5.3.1. Effects of dexamethasone on adipokine gene expression

The gene expression profiles of leptin, adiponectin and IL-6 from 3T3-L1 adipocytes which had been treated with dexamethasone are presented in Figure 5.1. When dexamethasone was added to the medium at 2 and 20nM for 2h, there were no significant changes observed in leptin gene expression (A). When these concentrations of dexamethasone were added to the medium for 24h, leptin gene expression significantly increased ($P$<0.001 for both treatment concentrations). No significant changes were observed in adiponectin gene expression when dexamethasone was added to the medium at 2nM. When dexamethasone was added to the medium at 20nM, a significant increase in adiponectin gene expression was seen after 2h ($P$=0.044; Figure 5.1B), with a significant decrease occurring after 24h of treatment ($P$<0.001; Figure 5.1B). The gene expression of IL-6 showed no significant differences when compared to the control cells after 2h of dexamethasone treatment at either concentration (C). After 24h of treatment, IL-6 gene expression significantly decreased at both 2 and 20nM ($P$<0.001 for both concentrations; Figure 5.1C).

The gene expression of TNF-α was below the detection limit in all of the dexamethasone treated samples, and so is not presented.

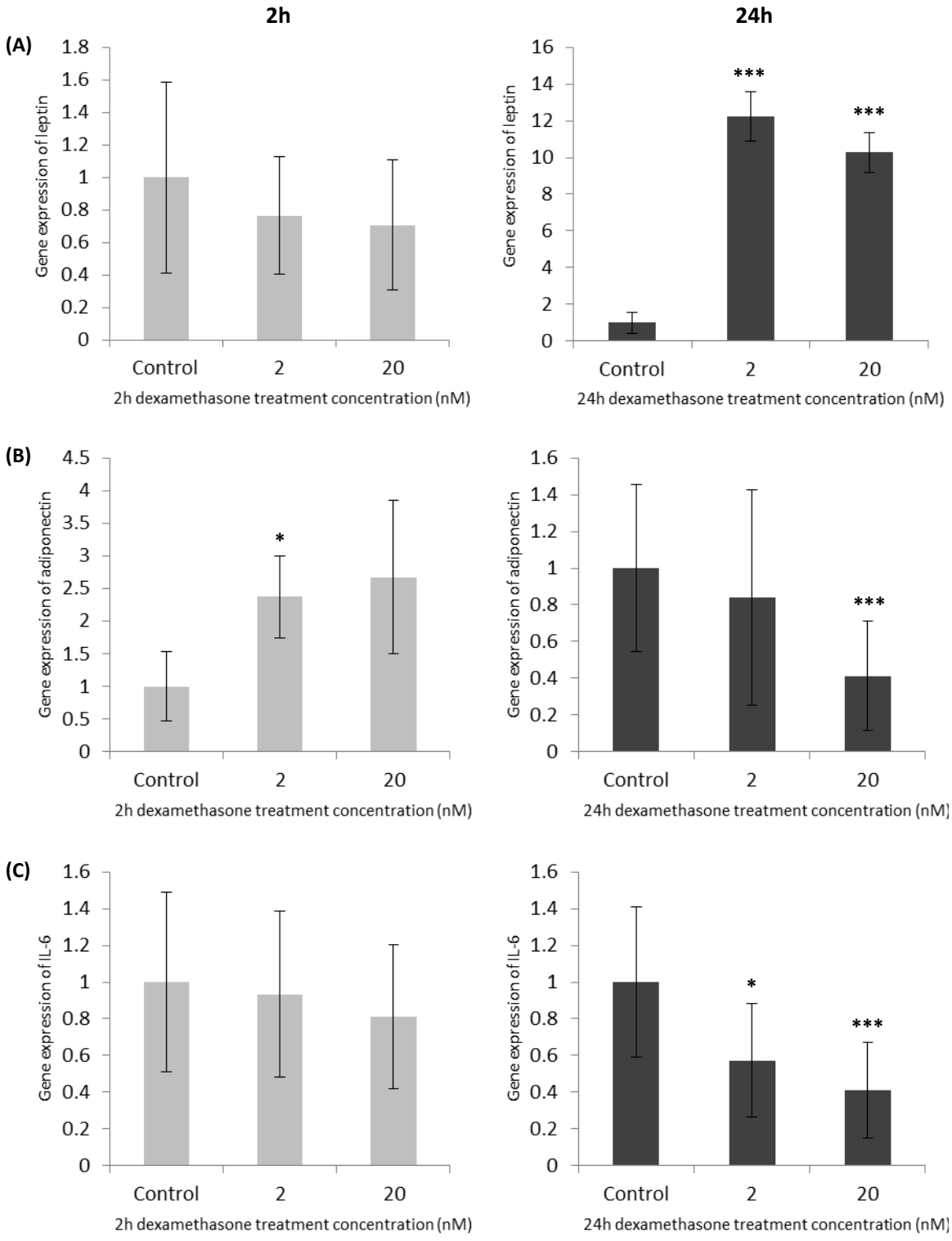


**Figure 5.1. Adipokine gene expression of dexamethasone treated 3T3-L1 adipocytes**

3T3-L1 adipocytes at day 10 post-differentiation were pre-incubated with CS-free medium for 24h, and then treated with dexamethasone for 2 or 24h. The concentration of dexamethasone treatments used were: 2 and 20nM. Adipokine gene expression was quantified by qPCR and normalised to GAPDH relative to the control group. Results are represented as means ± SD for a group size of 6. The adipokines quantified were leptin (A), adiponectin (B) and IL-6 (C). The data show a significant increase in leptin gene expression, and significant decreases in the gene expression for both adiponectin and IL-6 at the 24h treatment time. Statistical significance of each treatment group compared to the control group is represented by *$P$<0.05; **$P$<0.01 and *** $P$<0.001 *vs.* control.

### 5.3.2. Positive ion mode DI-MS analysis

Representative spectra of control cells, and cells treated with 20nM dexamethasone for 2 or 24h in positive ion mode are shown in Figure 5.2. These spectra show similar lipid profiles between the control and dexamethasone treated cells at both 2 and 24h. A decrease in the overall lipid abundance was noted in the 20nM dexamethasone treated cells when compared to the control cells, as seen by the increase in abundance of the peaks with m/z 622.4443 and 908.8651 (internal standards; PC 12:0/12:0 and TG 18:0/18:0/18:0, respectively).

A greater number of the peaks in the positive ion spectra were able to be identified compared to those in Chapter 4, and so the top 20 peaks from the global lipid profiles in Figure 5.2 were identified, and are presented in Table 5.1. All of the abundant selected lipid species from the control cells (A), as well as the majority of the dexamethasone treated cells were either diglyceride (DG) or triglyceride (TG) species. Three lipid species were identified as being within the top 20 abundant peaks in the treated cells (B), and not in the control cells. Of the three, two were the phosphatidylcholine (PC) species (36:2) and (38:4), and the third was TG (54:4).

The lipid species identified in Table 5.1 were normalised to the intensity of the relevant internal standard, either PC (12:0/12:0) with m/z 622.4443 or TG (18:0/18:0/18:0) at m/z 908.8651, and then to the protein content of the sample. After this stage, the top three lipid species from both dexamethasone treatment concentrations after 2h (A) and 24h (B) were represented graphically in Figure 5.3. When 2nM of dexamethasone was added into the medium for 2h and 24h, an increase was seen in the concentration of two TG species with m/z 846.7528 and 874.7837, which were identified as TG (50:3) and TG (52:3) ($P$=0.05 *vs.* control for all).

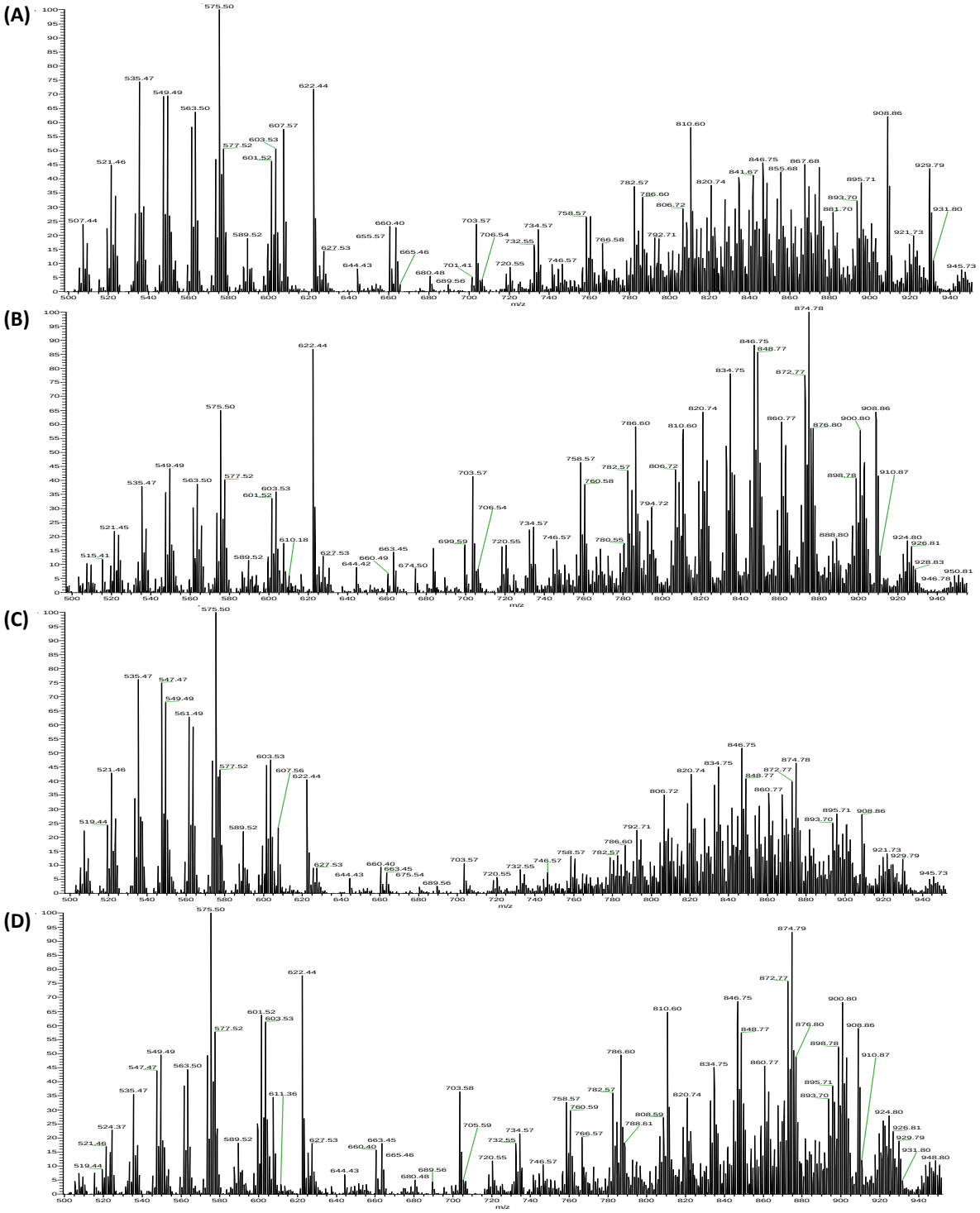


**Figure 5.2. Positive ion DI-MS analysis of dexamethasone treated 3T3-L1 adipocytes**

Representative spectra of differentiated 3T3-L1 adipocytes at day 10 post-differentiation which were pre-incubated with CS-free medium for 24h, and then treated with dexamethasone for 2 and 24h. The treatments represented are: control 2h (A), 20nM 2h (B), control 24h (C) and 20nM 24h (D). Lipids were extracted from the cell samples using a Folch extraction, and the lower phase was dried down under nitrogen and reconstituted in 600µL chloroform/methanol (2/1, v/v). A 150µL aliquot was removed and had 10mM ammonium formate added to it. The samples were then directly infused into an Orbitrap Exactive mass spectrometer at a flow rate of 5µL/min for 90 seconds (450 scans) in positive ion mode. The mass range analysed was between 100 and 1000Da, and that represented in the figure is between 500 and 950Da. An increase was observed in the lipid species with m/z between 750 and 900Da in the dexamethasone treated samples. However, an increase was observed in the intensity of the internal standard peaks (m/z 622.44 and 908.86) which suggests a decrease in the abundance of all lipid species.

| Calculated mass | Theoretical mass | Δ Mass accuracy (ppm) | Ion | Elemental composition | Identification |
|---|---|---|---|---|---|
| ***(A) Control*** | | | | | |
| 535.4715 | 535.4387 | 61.258 | $[M+H]^+$ | $C_{33}H_{58}O_5$ | DG (30:3) |
| 547.4715 | 547.4513 | 36.898 | $[M+H]^+$ | $C_{34}H_{60}O_5$ | DG (31:3) |
| 563.5024 | 563.4670 | 62.825 | $[M+H]^+$ | $C_{35}H_{62}O_5$ | DG (32:3) |
| 575.5021 | 575.4670 | 60.994 | $[M+H]^+$ | $C_{36}H_{62}O_5$ | DG (33:4) |
| 577.5177 | 577.4826 | 60.781 | $[M+H]^+$ | $C_{36}H_{64}O_5$ | DG (33:3) |
| 603.5337 | 603.4994 | 56.835 | $[M+H]^+$ | $C_{38}H_{68}O_5$ | DG (35:4) |
| 806.7219 | 806.7232 | -1.611 | $[M+NH_4]^+$ | $C_{50}H_{92}O_6$ | TG (47:2) |
| 820.7370 | 820.7389 | -2.315 | $[M+NH_4]^+$ | $C_{51}H_{94}O_6$ | TG (48:2) |
| 832.7379 | 832.7389 | -1.200 | $[M+NH_4]^+$ | $C_{52}H_{94}O_6$ | TG (49:3) |
| 834.7527 | 834.7545 | -2.156 | $[M+NH_4]^+$ | $C_{52}H_{96}O_6$ | TG (49:2) |
| 846.7528 | 846.7545 | -2.008 | $[M+NH_4]^+$ | $C_{53}H_{96}O_6$ | TG (50:3) |
| 847.7566 | 847.7749 | -21.586 | $[M+H]^+$ | $C_{54}H_{102}O_6$ | TG (51:1) |
| 848.7674 | 848.7701 | -3.181 | $[M+NH_4]^+$ | $C_{53}H_{98}O_6$ | TG (50:2) |
| 860.7686 | 860.7701 | -1.743 | $[M+NH_4]^+$ | $C_{54}H_{98}O_6$ | TG (51:3) |
| 862.7836 | 862.7858 | -2.550 | $[M+NH_4]^+$ | $C_{54}H_{100}O_6$ | TG (51:2) |

| | | | | | |
|---|---|---|---|---|---|
| 872.7683 | 872.7701 | -2.062 | $[M+NH_4]^+$ | $C_{55}H_{98}O_6$ | TG (52:4) |
| 874.7837 | 874.7858 | -2.401 | $[M+NH_4]^+$ | $C_{55}H_{100}O_6$ | TG (52:3) |
| 875.7877 | 875.8062 | -21.123 | $[M+H]^+$ | $C_{56}H_{106}O_6$ | TG (53:1) |
| 876.7972 | 876.8014 | -4.790 | $[M+NH_4]^+$ | $C_{55}H_{102}O_6$ | TG (52:2) |
| 902.8147 | 902.8171 | -2.658 | $[M+NH_4]^+$ | $C_{57}H_{104}O_6$ | TG (54:3) |

***(B) Extra identifications from 20nM dexamethasone treatment***

| | | | | | |
|---|---|---|---|---|---|
| 786.5998 | 786.6007 | -1.144 | $[M+H]^+$ | $C_{44}H_{84}NO_8P$ | PC (36:2) |
| 810.6003 | 810.6007 | -0.493 | $[M+H]^+$ | $C_{46}H_{84}NO_8P$ | PC (38:4) |
| 900.7994 | 900.8015 | -2.331 | $[M+NH_4]^+$ | $C_{57}H_{102}O_6$ | TG (54:4) |

**Table 5.1. Identifications of selected positive ions from control and dexamethasone treated 3T3-L1 adipocytes**

Abbreviations used: DG, diglyceride; PC, phosphatidylcholine; TG, triglyceride; ppm, parts per million

Underlined masses are present in both control and dexamethasone treated cells.

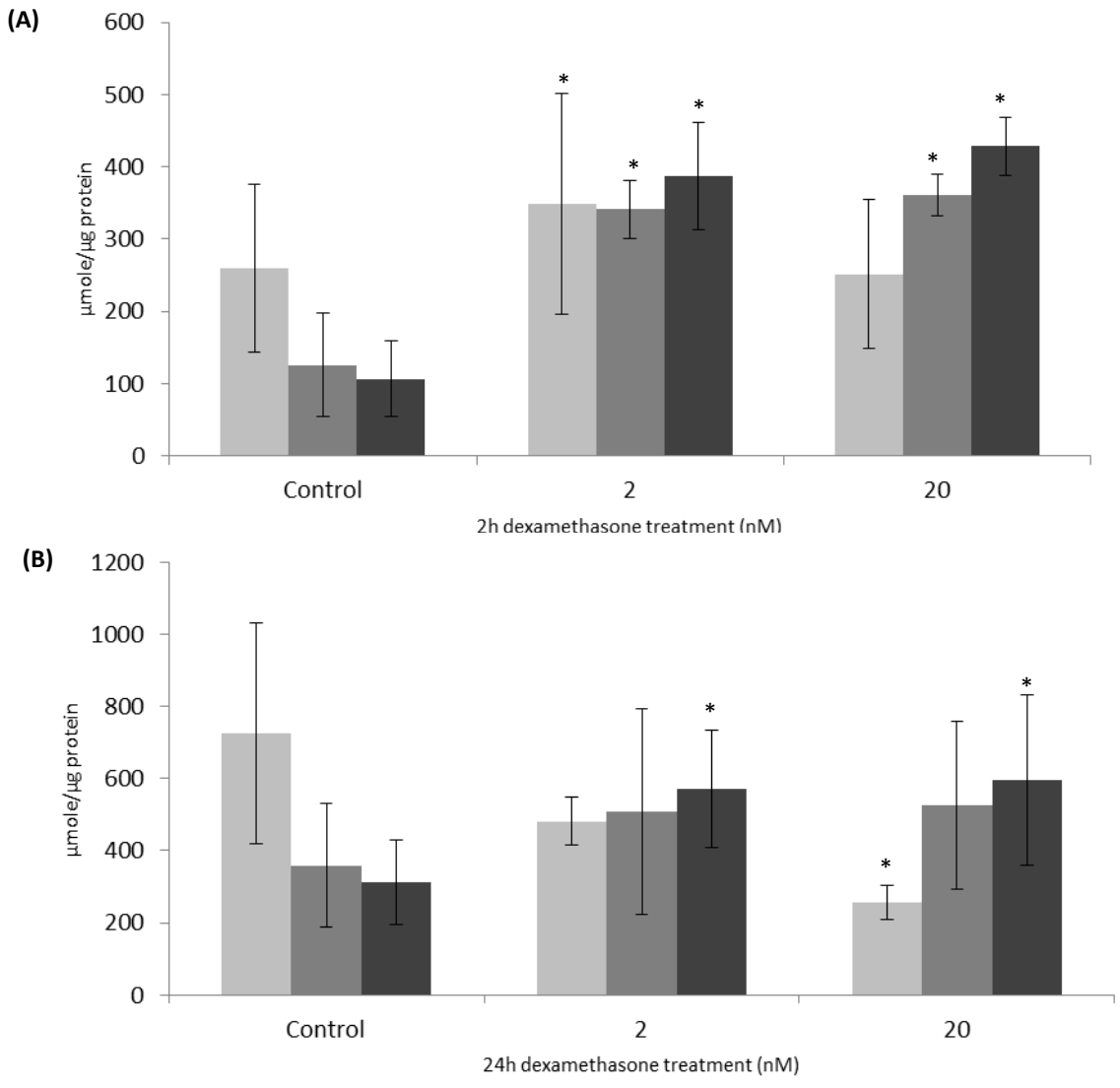


**Figure 5.3. Individual lipid concentrations from positive ion DI-MS analysis of dexamethasone treated 3T3-L1 adipocytes**

3T3-L1 adipocytes at day 10 post-differentiation were pre-incubated with CS-free medium for 24h, and then treated with dexamethasone for 2 or 24h. The concentration of dexamethasone treatments used were 2 and 20nM. Lipids were extracted from the cell samples using a Folch extraction, and the lower phase was dried down under nitrogen and reconstituted in 600µL chloroform/methanol (2/1, v/v). A 150µL aliquot was removed and had 10mM ammonium formate added to it. The samples were then directly infused into an Orbitrap Exactive mass spectrometer at a flow rate of 5µL/min for 90s (450 scans) in positive ion mode.

Selected abundant lipids are shown in the key and were quantified using a relevant internal standard, either PC (12:0/12:0) or TG (18:0/18:0/18:0), with m/z 622.4443 and 908.8651, respectively. They were then normalised to the protein concentration of the cell sample. For each time point, n=3, and the results are presented as median ± range. The data show a significant increase in the two TG species with both dexamethasone treatment concentrations after 2h. An increase in the concentration of TG (52:3) was also seen after 24h. Statistical significance of each treatment group compared to the control group is represented by *$P$=0.05 or less.

An increase was also observed in the concentration of the lipid species with m/z 575.5021, which was tentatively identified as DG (33:4), due to its mass accuracy being outside of the parameter set in Section 5.2.3.2 (ppm=60.994; *P*=0.047 *vs.* control). After 24h of 2nM dexamethasone treatment (B), the concentration of TG (52:3) increased (*P*=0.047 *vs.* control). The concentration of this TG species also increased with the greatest dexamethasone treatment, along with that of DG (33:4) (*P*=0.024 *vs.* control for both).

### 5.3.3. Negative ion DI-MS analysis

Representative negative ion mode spectra of control, and 20nM dexamethasone treated cells after 2 or 24h are shown in Figure 5.4. The most abundant peak in the 2h control cells had m/z 564.3457, and this changed to either 281.2583 or 303.2334 in the remaining spectra.

The top 20 peaks from these spectra were identified, and are presented in Table 5.2. All of the lipid species in both (A) and (B) were either fatty acid (FA) or phospholipids, with the exception of one diglyceride species. Many phospholipids were represented including, phosphatidylcholine (PC); phosphatidylethanolamine (PE); phoshatidylglycerol; phosphatidylinositol (PI) and phosphatidylserine (PS) species.

The lipid species from Table 5.2 were quantified using the internal standard, PC (12:0/12:0) with m/z 666.4443, and then normalised to the protein content of the sample. The three most concentrated lipid species from both dexamethasone treatment concentrations after 2h (A) and 24h (B) are presented graphically in Figure 5.5. These selected lipid species had m/z 281.2483, 303.2334, and 564.3457, and the first two were identified as C18:1 and C20:4, respectively. The final species was tentatively identified as PC (20:0) due to its mass accuracy (ppm=-37.919). After 2h of dexamethasone treatment, an increased concentration of the two FAs was seen with the 2nM treatment concentration (*P*=0.024 *vs.* control for both). When dexamethasone was added for 24h, an increase was observed in the concentration of all lipid species at the 2nM concentration (*P*=0.05 or less *vs.* control for all). At the 20nM dexamethasone treatment concentration, an increase was seen in the concentration of C20:4 (*P*=0.05 *vs.* control).

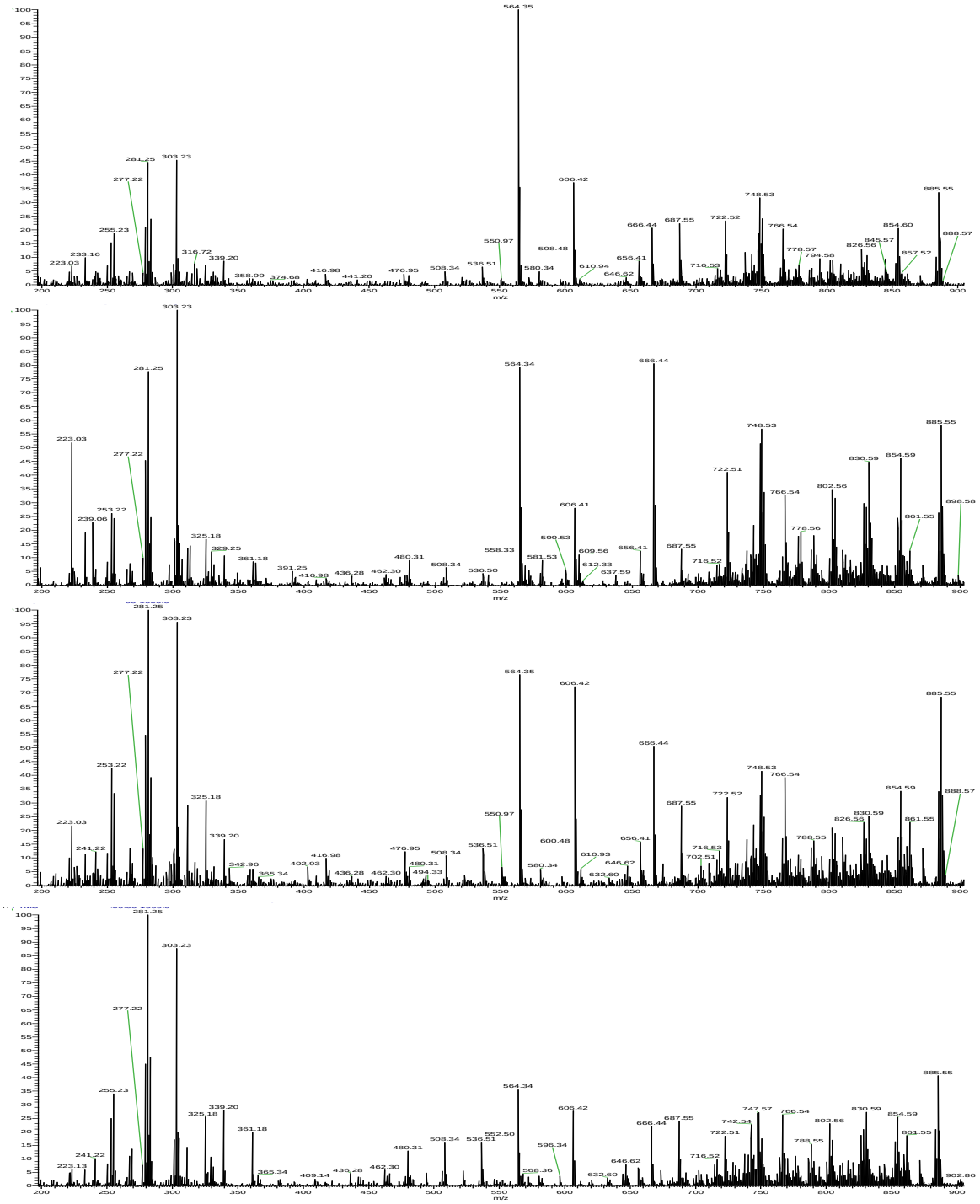

**Figure 5.4. Negative ion DI-MS analysis of dexamethasone treated 3T3-L1 adipocytes**

Representative spectra of differentiated 3T3-L1 adipocytes at day 10 post-differentiation which were pre-incubated with CS-free medium for 24h, and then treated with dexamethasone for 2 and 24h. The treatments represented are: control 2h (A), 20nM 2h (B), control 24h (C) and 20nM 24h (D). Lipids were extracted from the cell samples using a Folch extraction, and the lower phase was dried down under nitrogen and reconstituted in 600µL chloroform/methanol (2/1, v/v). A 150µL aliquot was removed and had 10mM ammonium formate added to it. The samples were then directly infused into an Orbitrap Exactive mass spectrometer at a flow rate of 5µL/min for 90 seconds (450 scans) in negative ion mode. The mass range analysed was between 100 and 1000Da, and that represented in the figure is between 200 and 900Da. No gross changes were observed between the chromatograms of the control and dexamethasone treated cells.

| Calculated mass | Theoretical mass | Δ Mass accuracy (ppm) | Ion | Elemental composition | Identification |
|---|---|---|---|---|---|
| *(A) Control* | | | | | |
| 253.2178 | 253.2173 | 1.975 | $[M-H]^-$ | $C_{16}H_{30}O_2$ | C16:1 |
| 255.2327 | 255.2330 | -1.175 | $[M-H]^-$ | $C_{16}H_{32}O_2$ | C16:0 |
| 279.2328 | 279.2330 | -0.716 | $[M-H]^-$ | $C_{18}H_{32}O_2$ | C16:2 |
| 281.2483 | 281.2486 | -1.067 | $[M-H]^-$ | $C_{18}H_{34}O_2$ | C18:1 |
| 283.2648 | 283.2643 | 1.765 | $[M-H]^-$ | $C_{18}H_{36}O_2$ | C18:0 |
| 303.2334 | 303.2330 | 1.319 | $[M-H]^-$ | $C_{20}H_{32}O_2$ | C20:4 |
| 564.3457 | 564.3671 | -37.919 | $[M-H]^-$ | $C_{28}H_{56}NO_8P$ | PC (20:0) |
| 565.3487 | 565.3511 | -4.245 | $[M-H]^-$ | $C_{28}H_{55}O_9P$ | Lyso-PG (22:1) |
| 606.4159 | 606.4140 | 3.133 | $[M-H]^-$ | $C_{31}H_{61}NO_8P$ | PE (26:0) |
| 687.5740 | 687.5933 | -28.069 | $[M-H]^-$ | $C_{44}H_{80}O_5$ | DG (41:3) |
| 722.5156 | 722.4766 | 53.981 | $[M-H]^-$ | $C_{40}H_{70}NO_8P$ | PC (32:5) |
| 742.5418 | 742.5392 | 3.501 | $[M-H]^-$ | $C_{41}H_{78}NO_8P$ | PC (33:2) |
| 747.5677 | 747.5546 | 17.524 | $[M-H]^-$ | $C_{41}H_{81}O_9P$ | PG (P-35:0) |
| 748.5321 | 748.5287 | 4.542 | $[M-H]^-$ | $C_{43}H_{76}NO_7P$ | PE (O-38:6) / PE (P-38:6) |
| 750.5473 | 750.5443 | 3.997 | $[M-H]^-$ | $C_{43}H_{78}NO_7P$ | PE (P-38:4) / PE (O-38:5) |
| 766.5437 | 766.5392 | 5.871 | $[M-H]^-$ | $C_{43}H_{78}NO_8P$ | PC (35:4) |

| | | | | | |
|---|---|---|---|---|---|
| 802.5630 | 802.5604 | 3.239 | $[M-H]^-$ | $C_{43}H_{82}NO_{10}P$ | PS (37:1) |
| 804.5766 | 804.5760 | 0.756 | $[M-H]^-$ | $C_{43}H_{84}NO_{10}P$ | PS (37:0) |
| 826.5620 | 826.5390 | 27.827 | $[M-H]^-$ | $C_{48}H_{78}NO_8P$ | PC (40:9) |
| 830.5946 | 830.5917 | 3.491 | $[M-H]^-$ | $C_{45}H_{86}NO_{10}P$ | PS (39:1) |
| 854.5941 | 854.5917 | 2.808 | $[M-H]^-$ | $C_{47}H_{86}NO_{10}P$ | PS (41:3) |
| 883.5368 | 883.5342 | 2.943 | $[M-H]^-$ | $C_{47}H_{81}O_{13}P$ | PI (38:5) |
| 885.5518 | 885.5499 | 2.146 | $[M-H]^-$ | $C_{47}H_{83}O_{13}P$ | PI (38:4) |
| 886.5561 | 886.5604 | -4.850 | $[M-H]^-$ | $C_{50}H_{81}NO_{10}P$ | PS(44:8) |

***(B) Extra identifications from 20nM dexamethasone treatment***

| | | | | | |
|---|---|---|---|---|---|
| 361.1823 | 361.1748 | 20.766 | $[M-H]^-$ | $C_{18}H_{35}BrO_2$ | Halogenated FA |
| 861.5507 | 861.5499 | 0.929 | $[M-H]^-$ | $C_{45}H_{83}O_{13}P$ | PI (36:2) |

**Table 5.2. Identifications of selected negative ions from control and dexamethasone treated 3T3-L1 adipocytes**

Abbreviations used: DG, diglyceride; FA, fatty acid; PC, phosphatidylcholine; PE, phosphatidylethanolamine; PG, phosphatidylglycerol; PI, phosphatidylinositol; PS, phosphatidylserine; ppm, parts per million

Underlined masses are present in both control and dexamethasone treated cells.

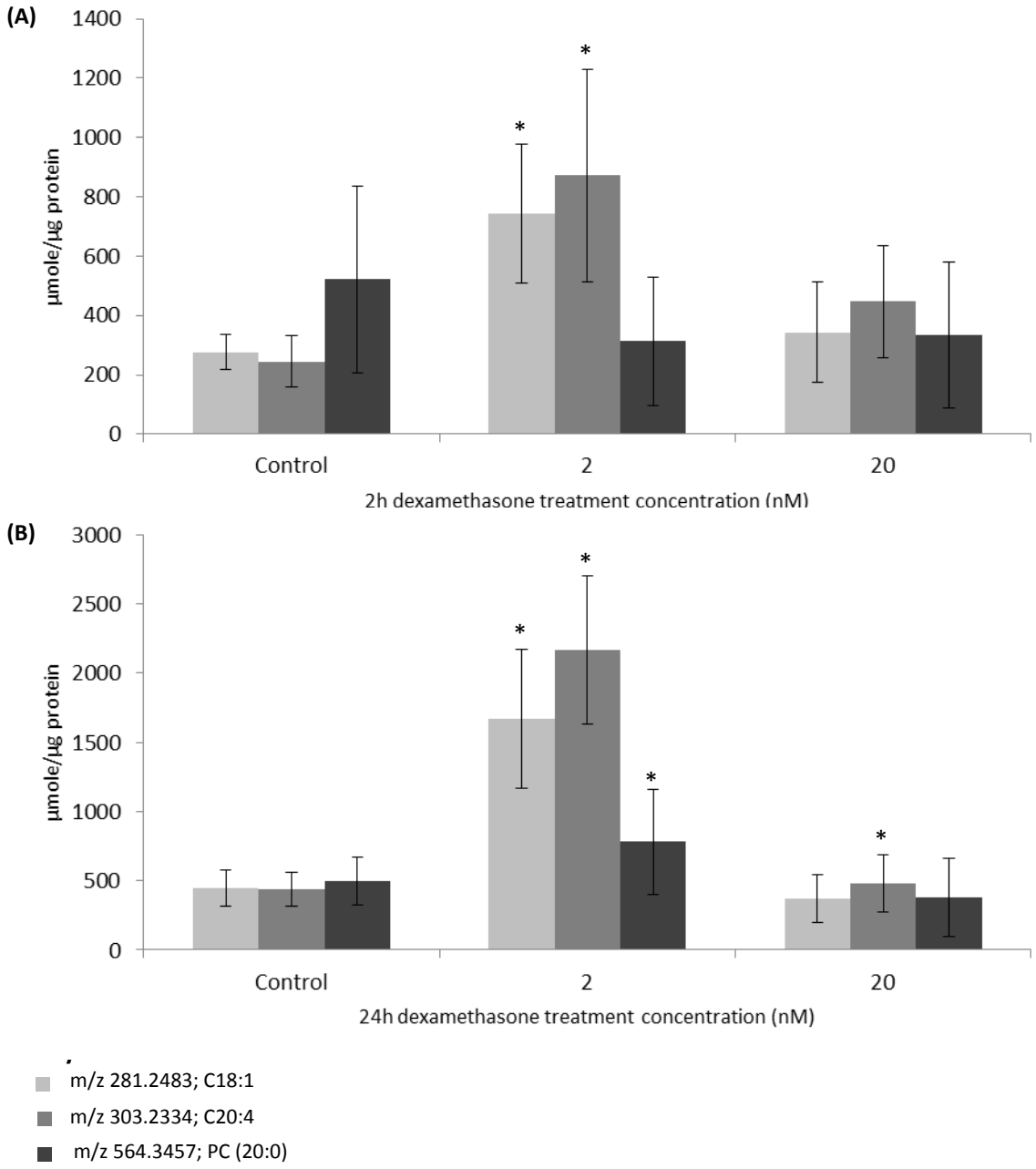


**Figure 5.5. Individual lipid concentrations from negative ion DI-MS analysis of dexamethasone treated 3T3-L1 adipocytes**

3T3-L1 adipocytes at day 10 post-differentiation were pre-incubated with CS-free medium for 24h, and then treated with dexamethasone for 2 or 24h. The concentration of dexamethasone treatments used were 2 and 20nM. Lipids were extracted from the cell samples using a Folch extraction, and the lower phase was dried down under nitrogen and reconstituted in 600µL chloroform/methanol (2/1, v/v). A 150µL aliquot was removed and had 10mM ammonium formate added to it. The samples were then directly infused into an Orbitrap Exactive mass spectrometer at a flow rate of 5µL/min for 90 seconds (450 scans) in negative ion mode.

Selected abundant lipids are shown in the key and were quantified using the relevant internal standard, PC (12:0/12:0) with m/z 666.4443. They were then normalised to the protein concentration of the cell sample. For each time point, n=3, and the results are presented as median ± range. The data show an increase in the concentration of the C18:1 and C20:4 at 2nM dexamethasone treatment concentration at both 2 and 24h. An increase in the concentration of PC(20:0) was also observed with 2nM dexamethasone treatment at 2nM, and C20:4 with 20nM after 24h of treatment. Statistical significance of each treatment group compared to the control group is represented by *$P$=0.05 or less.

### 5.3.4. Positive ion LC-MS analysis

Representative chromatograms of control adipocytes, along with those which had been treated with dexamethasone for 2 or 24h at 20nM are shown in Figure 5.6. When compared to the 2h control cells (A), a decrease in the abundance of ions with retention time (RT) between 7.5 and 8.5 min was observed in the adipocytes which had been treated with dexamethasone for 2h (B), as seen by the increase in the peak with RT 9.25 min, which represents the ion with m/z 908.8651, which is the internal standard TG (18:0/18:0/18:0). The peaks in this RT range increased in the 24h dexamethasone treated adipocytes (D) in comparison to the 24h control cells (D). The most abundant ion associated with each chromatographic peak seen in this figure is identified in Table 5.3. These abundant ions were only identifiable from a RT of 7.60min, and all ions from this time onwards were identified as TG species.

Multivariate data analysis was undertaken on these LC-MS data, starting with principal component analysis (PCA) of the raw data (no normalisation), as seen in Figure 5.7. The PCA scores (principal component 1 *vs.* principal component 2) plot is shown in Figure 5.9A and was interpreted as having three groups: QCs; control cells (both time points) and all dexamethasone treated samples. The R2 and Q2 for this model were 0.854 and 0.691, respectively. The loadings plot is presented in (B) and showed many points which were distant from the origin, although only a few were able to be confidently identified according to the search parameters outlined in Section 5.2.3.2. All of the identifiable masses were positioned on the left hand side (LHS) of the origin. The first of these had m/z 876.803 and was identified as TG (52:2). Trend analysis of this point showed that its concentration increased after 24h dexamethasone treatment at 20nM. The point representing m/z 902.816 was identified as TG (54:3) and its concentration increased after 24h of dexamethasone treatment at both 2 and 20nM. Finally, two points labelled as m/z 862.786 and 874.786 were identified as the TG species 51:2 and 52:3, respectively. Trend analysis of these points demonstrated an increase in their concentration in all of the dexamethasone treated cells when compared to the control cells.

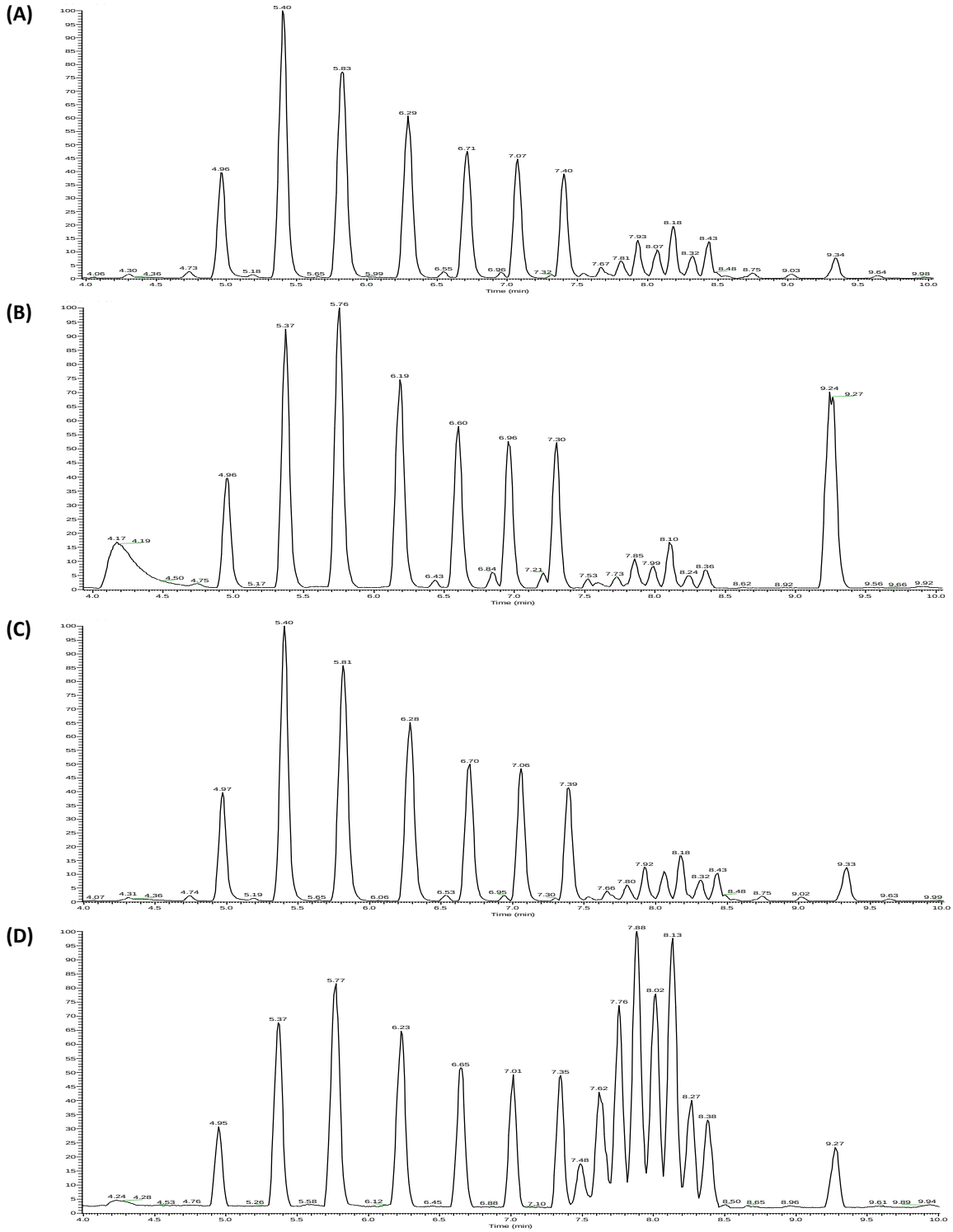


**Figure 5.6. Positive ion LC-MS analysis of dexamethasone treated 3T3-L1 adipocytes**

Representative chromatograms of differentiated 3T3-L1 adipocytes at day 10 post-differentiation which were pre-incubated with CS-free medium for 24 hours, and then treated with dexamethasone for 2 and 24h. The treatments represented are: control 2h (A), 20nM 2h (B), control 24h (C) and 20nM 24h (D). Lipids were extracted from the cell samples using a Folch extraction. The lower phase was dried down under nitrogen and reconstituted in 600µL chloroform/methanol (2/1, v/v). A 150µL aliquot was removed and had 10mM ammonium formate added to it. The lipids were then separated over 18 min by LC-MS in positive ion mode. The 2h dexamethasone treated cells show an increase in the peak with RT between 9 and 9.5 min. After 24h of dexamethasone treatment, an increase was seen in the abundance of peaks with RT between 7.5 and 8.5 min.

| Retention time (min) | Ion mass | Theoretical mass | Δ Mass accuracy (ppm) | Ion | Empirical composition | Identification |
|---|---|---|---|---|---|---|
| 7.60 | 844.7388 | 844.7389 | -0.811 | $[M+NH_4]^+$ | $C_{53}H_{94}O_6$ | TG (50:4) |
| 7.72 | 832.7407 | 832.7389 | -1.200 | $[M+NH_4]^+$ | $C_{52}H_{94}O_6$ | TG (49:3) |
| 7.85 | 846.7549 | 846.7545 | 0.472 | $[M+NH_4]^+$ | $C_{53}H_{96}O_6$ | TG (50:3) |
| 7.98 | 860.7704 | 860.7701 | 0.349 | $[M+NH_4]^+$ | $C_{54}H_{98}O_6$ | TG (51:3) |
| 8.11 | 874.7858 | 874.7858 | 0 | $[M+NH_4]+$ | $C_{55}H_{104}NO_6$ | TG (52:3) |
| 8.24 | 862.7865 | 862.7858 | 0.811 | $[M+NH_4]^+$ | $C_{54}H_{100}O_6$ | TG (51:2) |
| 8.36 | 902.8119 | 902.8171 | -5.760 | $[M+NH_4]^+$ | $C_{57}H_{104}O_6$ | TG (54:3) |
| 9.25 | 908.8651 | 908.8640 | 1.210 | $[M+NH_4]^+$ | $C_{57}H_{110}O_6$ | TG (54:0) |

**Table 5.3. Retention times and their associated abundant mass of each major peak present in the positive ion LC-MS chromatograms of dexamethasone treated adipocytes**

Red highlight indicates internal standard

The data were then manually normalised to the total ion current (TIC), and the scores plot is shown in Figure 5.7C. As with the non-normalised data, three groups were present on the plot which related to the QCs, all control samples and the treated cells. The loadings plot is presented in (D) and demonstrates points that could be responsible for the variance between samples, although none of these could be confidently identified. The R2 and Q2 for this model were 0.876 and 0.744, respectively.

After PCA, both datasets had the supervised partial least squares (PLS) analysis applied to them, as seen in Figure 5.8. The samples in the PLS scores plot for the non-normalised data (A) still clustered into three groups, although they differed from those seen in the PCA plot (Figure 5.9A). One group contained the QCs and the control cells from both time points. The dexamethasone treated samples were then split into two groups, the first consisting of the 2h treatments (2 and 20nM) and the second contained the 24h treatments (2 and 20nM). The R2X, R2Y and Q2 for this model were 0.890, 0.969 and 0.885, respectively. The PLS loadings plot identified points which were distant from the origin, and of those that could be identified, the first had m/z 862.786 (TG 51:2) and was seen to increase after 2h dexamethasone treatment. A point with m/z 876.803 was identified as TG (52:2), and trend analysis of this point showed that the concentration of this lipid increased in cells treated with 20nM dexamethasone for 24h. The final point represented m/z 902.816, TG (54:3), and its concentration increased after 24h of dexamethasone treatment (2 and 24h). All three points were situated on the top right hand side (RHS) of the origin.

The PLS scores plot of the TIC-normalised dataset is presented in Figure 5.8B. The groupings seen were the same as those in A: QCs and control cells (2 and 24h), dexamethasone treated 2h, and dexamethasone treated 24h. Out of all points with possible responsibility for the variance between the samples in the PLS loadings plot (D), the identifiable points were labelled with m/z 862.786, 876.803 and 902.816 which were identified as the TG species 51:1, 52:2 and 52:2, respectively. Trend analysis of these points showed that the concentration of TG (51:2) increased in the 2h dexamethasone treated samples (both time points). The concentrations of the TG species 52:2 and 54:3 increased after 24h of dexamethasone treatment, at 20nM and 2 and 20nM, respectively. The R2X, R2Y and Q2 for this model were 0.873, 0.968 and 0.878.

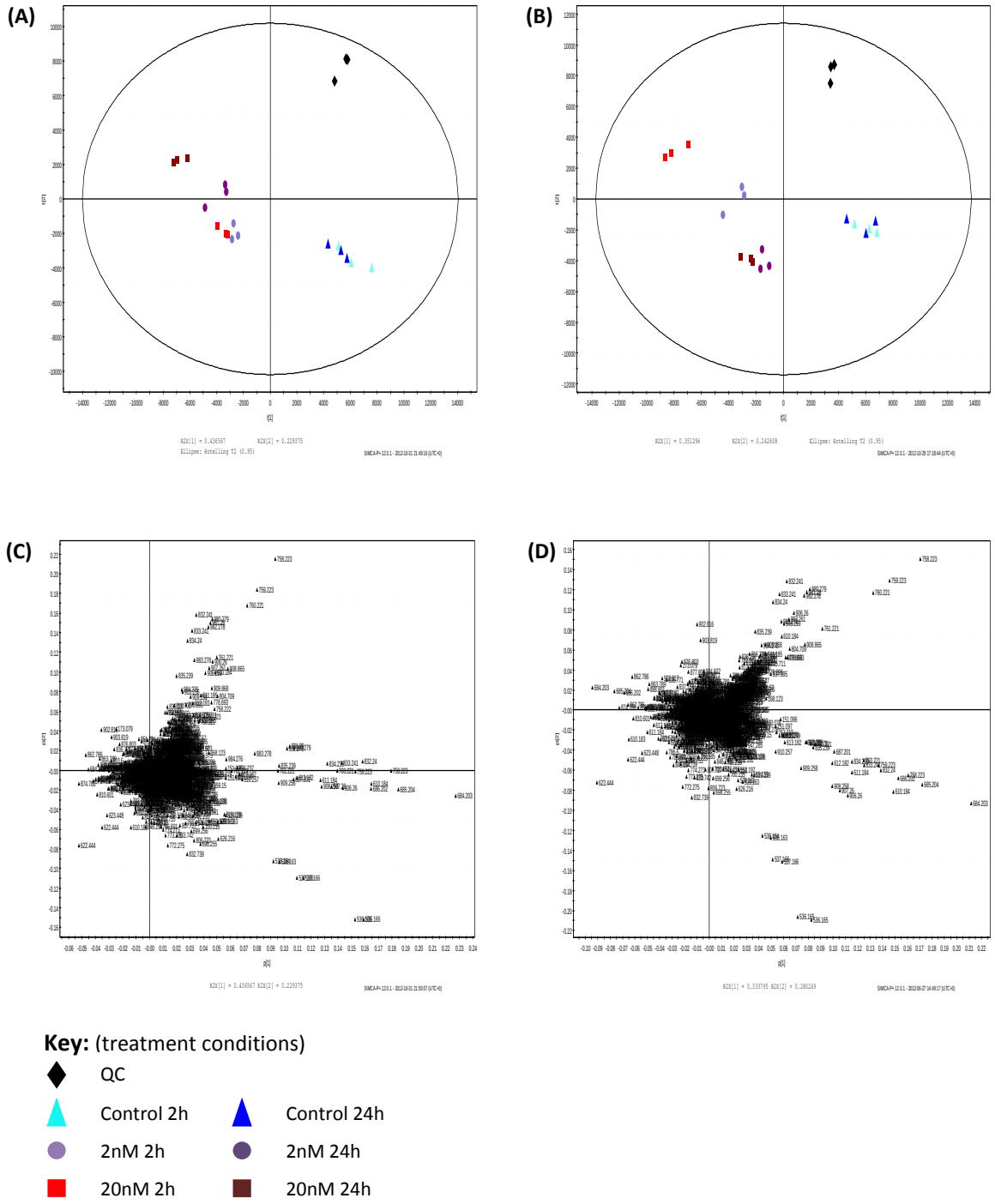


**Figure 5.7. PCA scores and loadings plots representing positive ion LC-MS analysis of dexamethasone treated 3T3-L1 adipocytes**

3T3-L1 adipocytes at day 10 post-differentiation were pre-incubated with CS-free medium for 24h, and were then treated with dexamethasone for 2 or 24h. The concentration of dexamethasone treatments used were 2 and 20nM. Lipids were extracted from the cell samples using a Folch extraction, and the lower phase was dried down under nitrogen and reconstituted in 600µL chloroform/methanol (2/1, v/v). These samples were analysed by LC-MS in positive ion mode. Panels A and B represent the PCA scores plot for non- and TIC-normalised data, respectively and these plots show a clear separation between the control and dexamethasone treated cells. Panels C and D show the PCA loadings plots for the non- and TIC-normalised data, respectively, and are labelled according to the m/z.

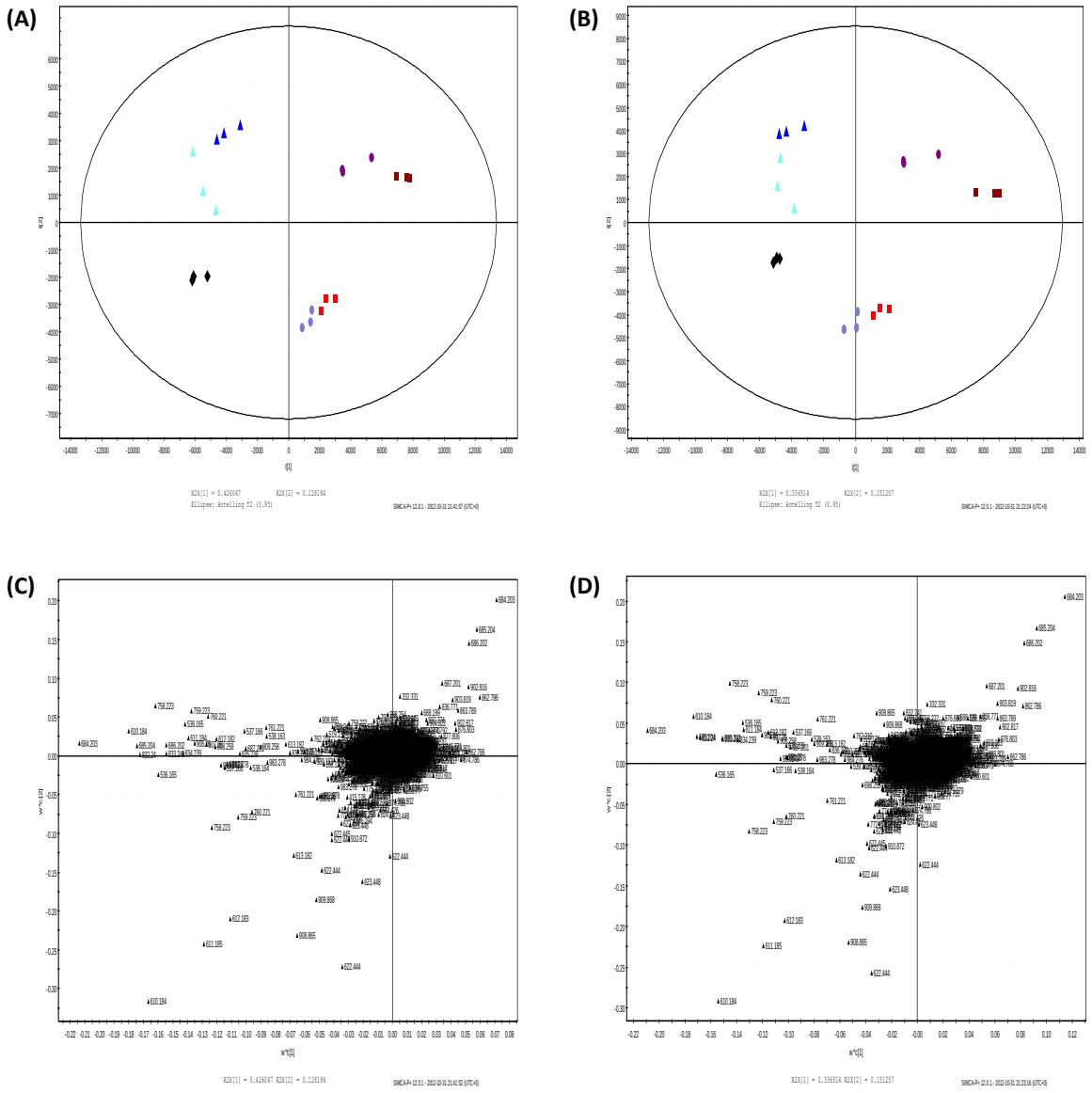


**Figure 5.8. PLS scores and loadings plots representing positive ion LC-MS analysis of dexamethasone treated 3T3-L1 adipocytes**

3T3-L1 adipocytes at day 10 post-differentiation were pre-incubated with CS-free medium for 24h, and then treated with dexamethasone for 2 or 24h. The concentration of dexamethasone treatments used were 2 and 20nM. Lipids were extracted from the cell samples using a Folch extraction, and the lower phase was dried down under nitrogen and reconstituted in 600µL chloroform/methanol (2/1, v/v). These samples were analysed by LC-MS in positive ion mode. Panels A and B represent the PLS scores plot for non- and TIC-normalised data, respectively and these plots show a clear separation between the control and dexamethasone treated cells. The treated cells were also split into two groups, consisting of the 2h and 24h treated samples. Panels C and D show the PCA loadings plots for the non- and TIC-normalised data, respectively, and are labelled according to the m/z.

### 5.3.5. Negative ion LC-MS analysis

Representative negative ion chromatograms of control adipocytes, and those which had been treated with 20nM dexamethasone at both 2 and 24h are shown in Figure 5.9. Fewer peaks were present in these chromatograms than those of the positive ion LC-MS analysis. The abundance of peaks in this figure with RT between 2.5 and 3min decreased in the treated cells when compared to the control cells at both time points. The most abundant peak in the treated cells, as well as 24h control adipocytes had a RT of approximately 4min.The most abundant ion associated with each major chromatographic peak seen in Figure 5.9 is identified in Table 5.4. The only identifiable peak in the control samples had m/z 564.3547 which was tentatively identified as PC (20:0) due to its mass accuracy (ppm=-38.345) being greater than 5 parts per million (ppm). This PC species was also present in adipocytes which had been treated with 20nM dexamethasone for 24h (B), along with PI (38:4) and DG (32:2).

Multivariate data analysis was also employed on the negative ion LC-MS data. The PCA scores plot for the negative ion non-normalised dataset is shown in Figure 5.10A. The data were interpreted as clustering into four groups, the first of which containing the QC samples. The control cells were split into two groups, representing 2 and 24h. The final group consisted of all dexamethasone treated samples. The R2 and Q2 for this model were 0.939 and 0.853, respectively. The PCA loadings plot (C) showed points relating to m/z 546.345 and 565.345 distant from the origin on its RHS. The m/z 564.345 was tentatively identified as the phospholipid species (20:0), due to its mass error being outside of the search parameters (ppm = -37.919). The m/z 565.345 was more confidently identified as lyso-phosphatidylglycerol (22:1). Trend analysis of these points found that their concentrations increased in all of the dexamethasone treatments when compared to the control cells.

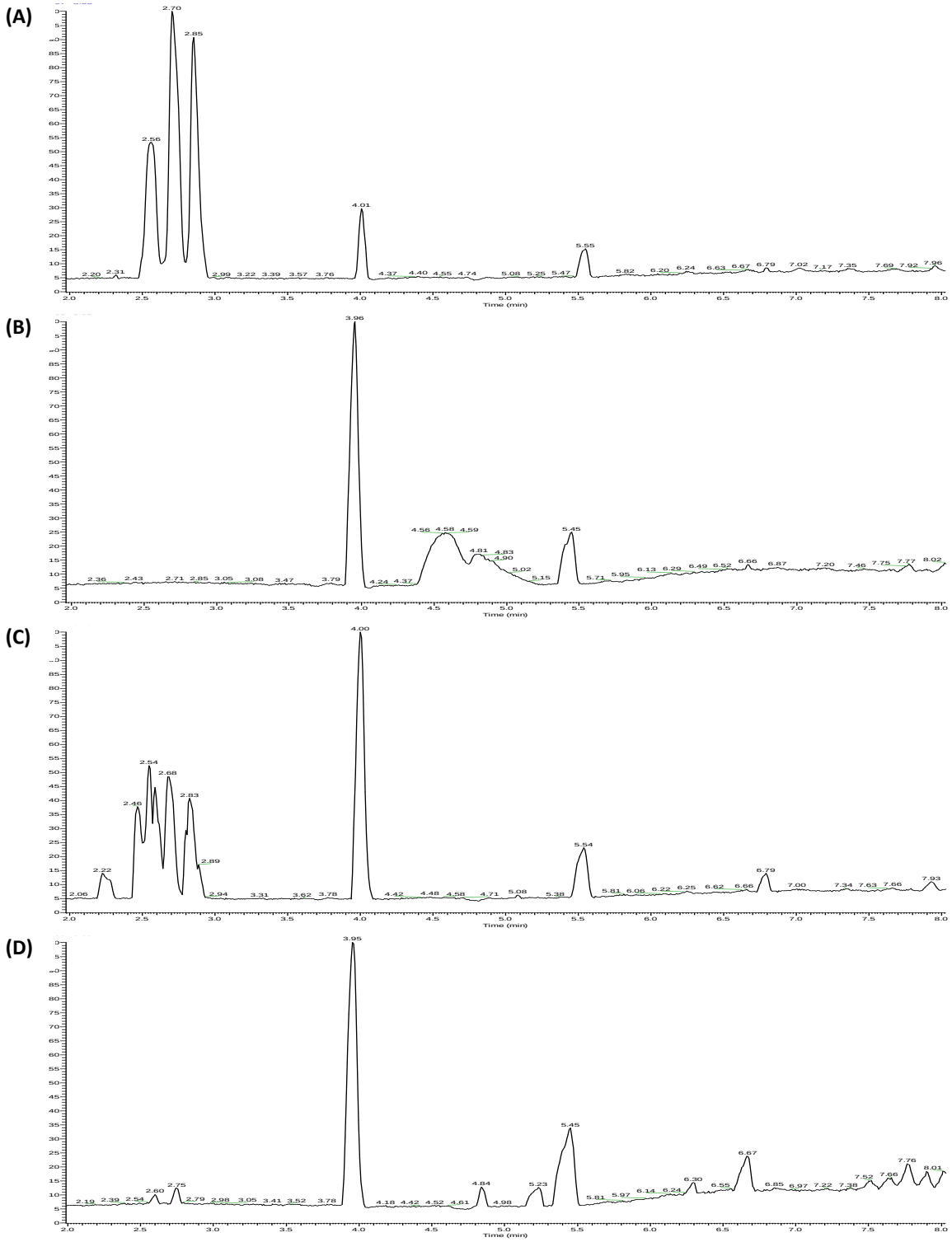


**Figure 5.9. Negative ion LC-MS analysis of dexamethasone treated 3T3-L1 adipocytes**

Representative chromatograms of differentiated 3T3-L1 adipocytes at day 10 post-differentiation which were pre-incubated with CS-free medium for 24h, and then treated with dexamethasone for 2 and 24h. The treatments represented are: control 2h (A), 20nM 2h (B), control 24h (C) and 20nM 24h (D). Lipids were extracted from the cell samples using a Folch extraction. The lower phase was dried down under nitrogen and reconstituted in 600µL chloroform/methanol (2/1, v/v). A 150µL aliquot was removed and had 10mM ammonium formate added to it. The lipids were then separated over 18 min by LC-MS in negative ion mode. The chromatograms show a decrease in the abundance of peaks between RT 2.5 and 3 min in the dexamethasone treated cells when compared to the control samples.

| Retention time (min) | Ion mass | Theoretical mass | Δ Mass accuracy (ppm) | Ion | Empirical composition | Idenification |
|---|---|---|---|---|---|---|
| ***(A) Control 24h*** | | | | | | |
| 2.46 | 309.1750 | 309.1708 | 13.584 | $[M-H]^-$ | $C_{17}H_{26}O_5$ | |
| 2.54 | 353.2010 | 353.1970 | 85.511 | $[M-H]^-$ | $C_{19}H_{29}O_6$ | |
| 4.00 | 564.3451 | 564.3671 | -38.345 | $[M-H]^-$ | $C_{28}H_{56}NO_8P$ | PC (20:0) |
| **(B)** ***20nM, 24h*** | | | | | | |
| 3.95 | 564.3449 | 564.3671 | -39.336 | $[M-H]^-$ | $C_{28}H_{56}NO_8P$ | PC (20:0) |
| 4.84 | 885.5529 | 885.5499 | 3.388 | $[M-H]^-$ | $C_{47}H_{83}O_{13}P$ | PI (38:4) |
| 5.23 | 568.4954 | 568.4990 | -6.332 | $[M-H]^-$ | $C_{35}H_{59}D_5O_5$ | DG (32:2) |

**Table 5.4. Retention times and their associated abundant mass of each major major peak present in the negative ion LC-MS chromatograms of dexamethasone treated adipocytes**

Abbreviations used: DG, diglyceride; PC, phosphatidylcholine; PI, phosphatidylinositol; ppm, parts per million

The TIC-normalised dataset was also analysed by PCA, and the R2 and Q2 for this model were 0.948 and 0.871, respectively. The PCA scores plot is presented in (B) and shows the data forming four groups, which were; QCs, control 2h, control 24h and all dexamethasone treated samples (2 and 24h). The PCA loadings plot (D) is similar to that presented in (B); with trend analysis of the points labelled as m/z 564.35 and 565.35 showing an increase in their relative abundance after all dexamethasone treatment combinations. These points were also positioned on the RHS of the origin, and identified as PC (20:0) and lyso-PG (22:1), respectively.

After PCA, the non- and TIC-normalised negative ion datasets underwent PLS analysis. The PLS scores plot of the non-normalised data is represented in Figure 5.11 (A). Four groups were identified which were: control 2h and QCs; control 24h; 20nM dexamethasone treatment after 2h; all remaining dexamethasone treated cells (2nM 2 and 24h, and 20nM 24h). The R2X, R2Y and Q2 for this model were 0.976, 0.990 and 0.951, respectively. The PLS loadings plot for this model was able to identify more points of variation than the PCA loadings plots seen in Figure 5.10 C and D. On the RHS of the origin, points corresponding to m/z 564.35 and 565.35 (PC 20:0 and lyso-PG 22:1, respectively) were situated, and trend analysis of these points showed an increase in the concentration of these lipid species in all of the dexamethasone treated samples.

The PLS model for the TIC-normalised had R2X, R2Y and Q2 of 0.958, 0.993 and 0.961, respectively. The scores plot for this model is shown in Figure 5.11B, and was interpreted as having four groups, with the first containing the QCs and the second consisting of the control samples from both time points. The dexamethasone treated adipocytes were seen to cluster into two groups, the first being cells treated with 20nM dexamethasione for 2h and the second group being made up of the remaining treatments (2nM 2 and 24h, and 20nM 24h). The PLS loadings plot is presented in (D), and the identifiable points on the RHS of the origin had m/z 564.35, 565.35, which were identified as PC (20:0), lyso-phosphatidylglycerol (22:1), respectively. Trend analysis of these three points showed that the concentration of these lipid species increased with all dexamethasone treatment combinations. Identifiable points on the LHS of the origin were labelled with m/z 885.55 and 886.56, and were identified as PI (38:4) and PS (44:8), correspondingly.

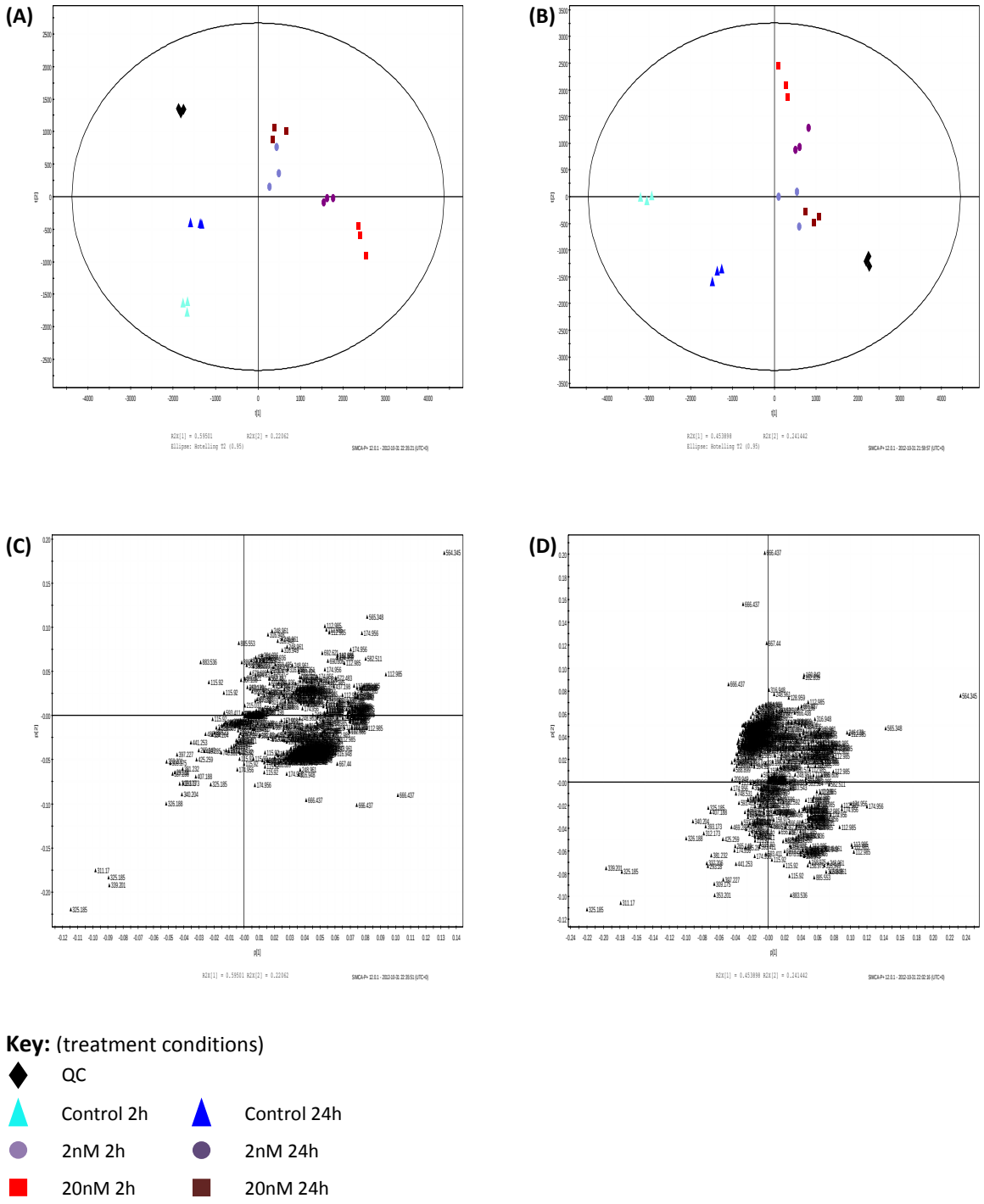


**Figure 5.10. PCA scores and loadings plots representing negative ion LC-MS analysis of dexamethasone treated 3T3-L1 adipocytes**

3T3-L1 adipocytes at day 10 post-differentiation were pre-incubated with CS-free medium for 24h, and were then treated with dexamethasone for 2 or 24h. The concentration of dexamethasone treatments used were 2 and 20nM. Lipids were extracted from the cell samples using a Folch extraction, and the lower phase was dried down under nitrogen and reconstituted in 600µL chloroform/methanol (2/1, v/v). These samples were analysed by LC-MS in negative ion mode. Panels A and B represent the PCA scores plot for non- and TIC-normalised data, respectively and these plots show a clear separation between the control and dexamethasone treated cells. Panels C and D show the PCA loadings plots for the non- and TIC-normalised data, respectively, and are labelled according to the m/z.

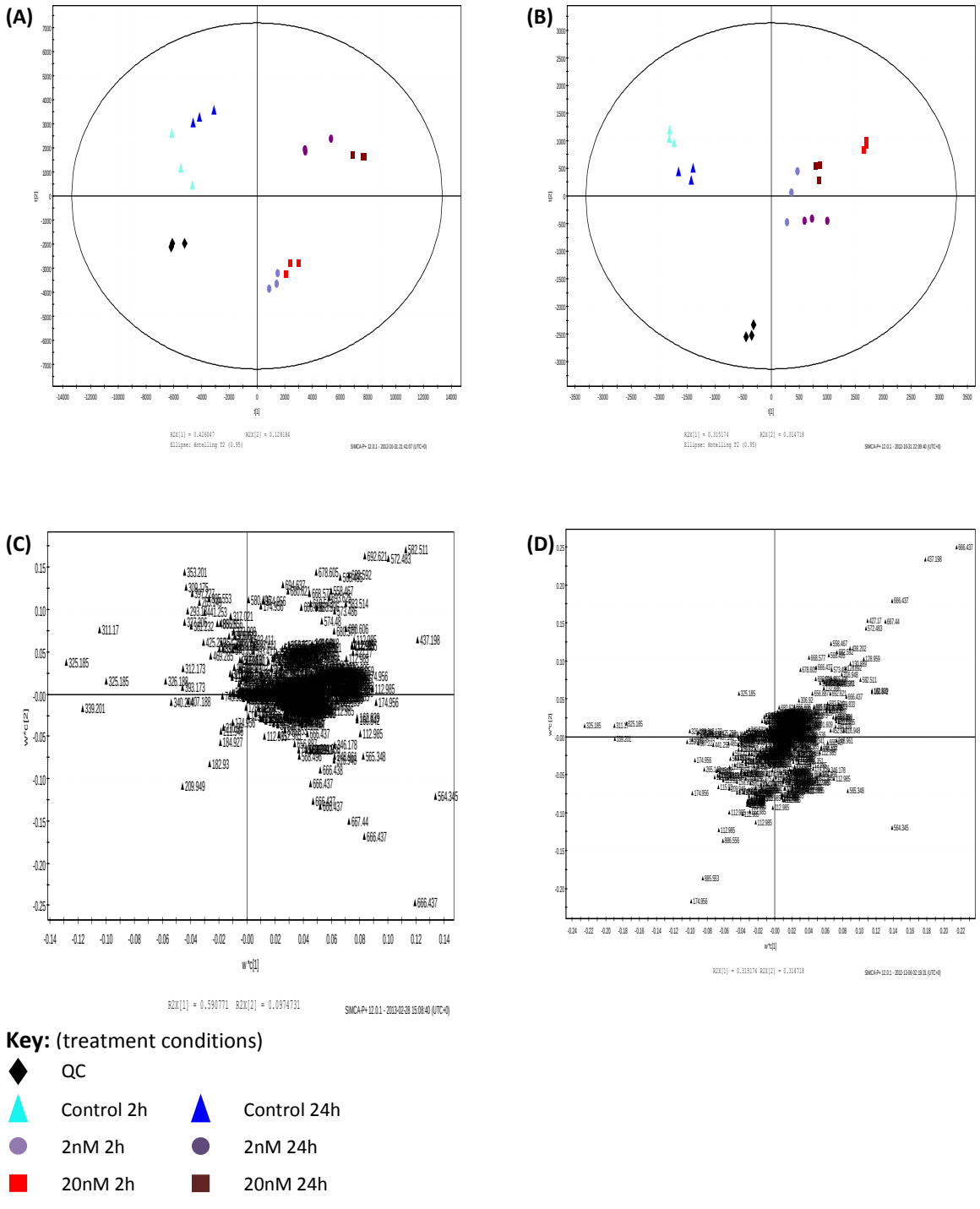


**Figure 5.11. PLS scores and loadings plots representing negative ion LC-MS analysis of dexamethasone treated 3T3-L1 adipocytes**

3T3-L1 adipocytes at day 10 post-differentiation were pre-incubated with CS-free medium for 24h, and were then treated with dexamethasone for 2 or 24h. The concentration of dexamethasone treatments used were 2 and 20nM. Lipids were extracted from the cell samples using a Folch extraction, and the lower phase was dried down under nitrogen and reconstituted in 600µL chloroform/methanol (2/1, v/v). These samples were analysed by LC-MS in negative ion mode. Panels A and B represent the PLS scores plot for non- and TIC-normalised data, respectively and these plots show a clear separation between the control and dexamethasone treated cells. Panels C and D show the PCA loadings plots for the non- and TIC-normalised data, respectively, and are labelled according to the m/z.

Trend analysis of these points demonstrated that the concentrations of these lipid species fluctuated after 2h of dexamethasone treatment, with an increase being seen with the 2nM treatment, and then a decrease when this was increased to 20nM. Finally, the unidentified points with m/z 311.17, 325.18 and 339.20 were also found on this area of the plot, and their concentration decreased in all of the dexamethasone treated samples.

### 5.3.4. Eicosanoid analysis by LC-MS

AA-derived eicosanoids secreted from 3T3-L1 adipocytes treated with dexamethasone were analysed by targeted LC-MS in negative ion mode. The changes in the detected eicosanoid species in response to dexamethasone treatment are presented in Figures 5.12 and 5.13. Only seven eicosanoids were detectable in the medium samples of all control and treated cells and the detected eicosanoid species were $PGD_2$, $PGE_2$, $PGF_{2\alpha}$, 6-keto $PGF_{2\alpha}$ (6-keto) and 20-OH $LTB_4$ (20-OH), 15-HETE and 20-HETE. The concentration of all eicosanoids increased significantly after 2h of dexamethasone treatment at both concentrations ($P$<0.05 *vs.* control for all). This significant increase was also seen after 24h of dexamethasone treatment at both concentrations, for all eicosanoid species ($P$<0.05 for all). The one exception was 20-OH which only significantly increased at the 2nM dexamethasone treatment concentration for both time points ($P$=0.047 and 0.024 *vs.* control for 2 and 24h, respectively).

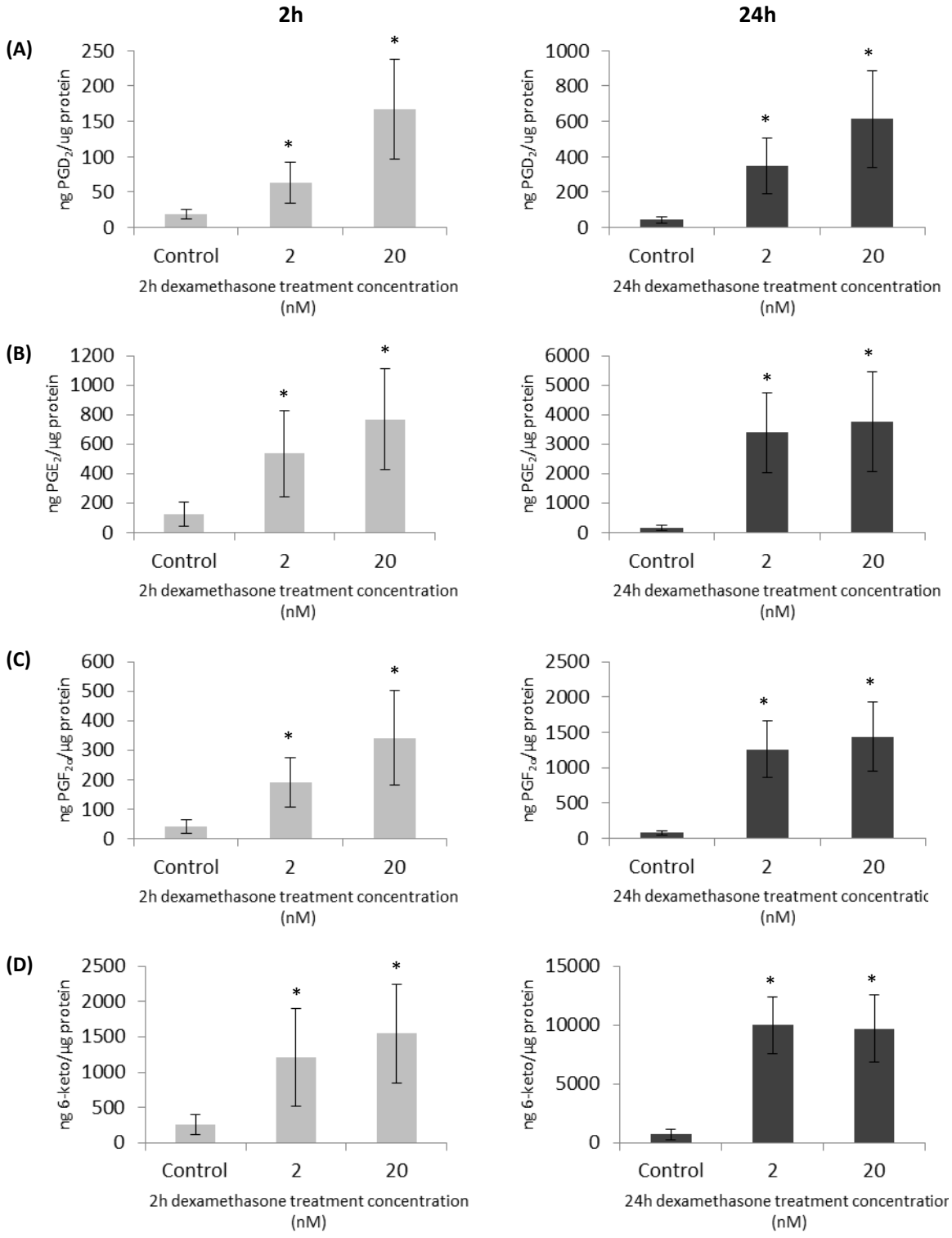


**Figure 5.12. Secretion of eicosanoid lipids from dexamethasone treated 3T3-L1 adipocytes**
Differentiated 3T3-L1 adipocytes at day 10 post-differentiation were pre-incubated with CS-free medium for 24h and were then treated with dexamethasone for 2 and 24h. The concentrations of dexamethasone treatments used were 2 and 20 nM. Eicosanoids were extracted from cell culture medium by solid phase extraction chromatography and were analysed by LC-MS/MS in negative ion mode. Detected eicosanoids are represented as median ± range, with a group size of 3 and are $PGD_2$ (A), $PGE_2$ (B), $PGF_{2\alpha}$ (C) and 6-keto $PGF_{1\alpha}$ (D). Statistical significance of each eicosanoid is represented by **P*<0.05 *vs.* control. The data show an increase in eicosanoid secretion in the treated groups compared to the control groups at both time points.

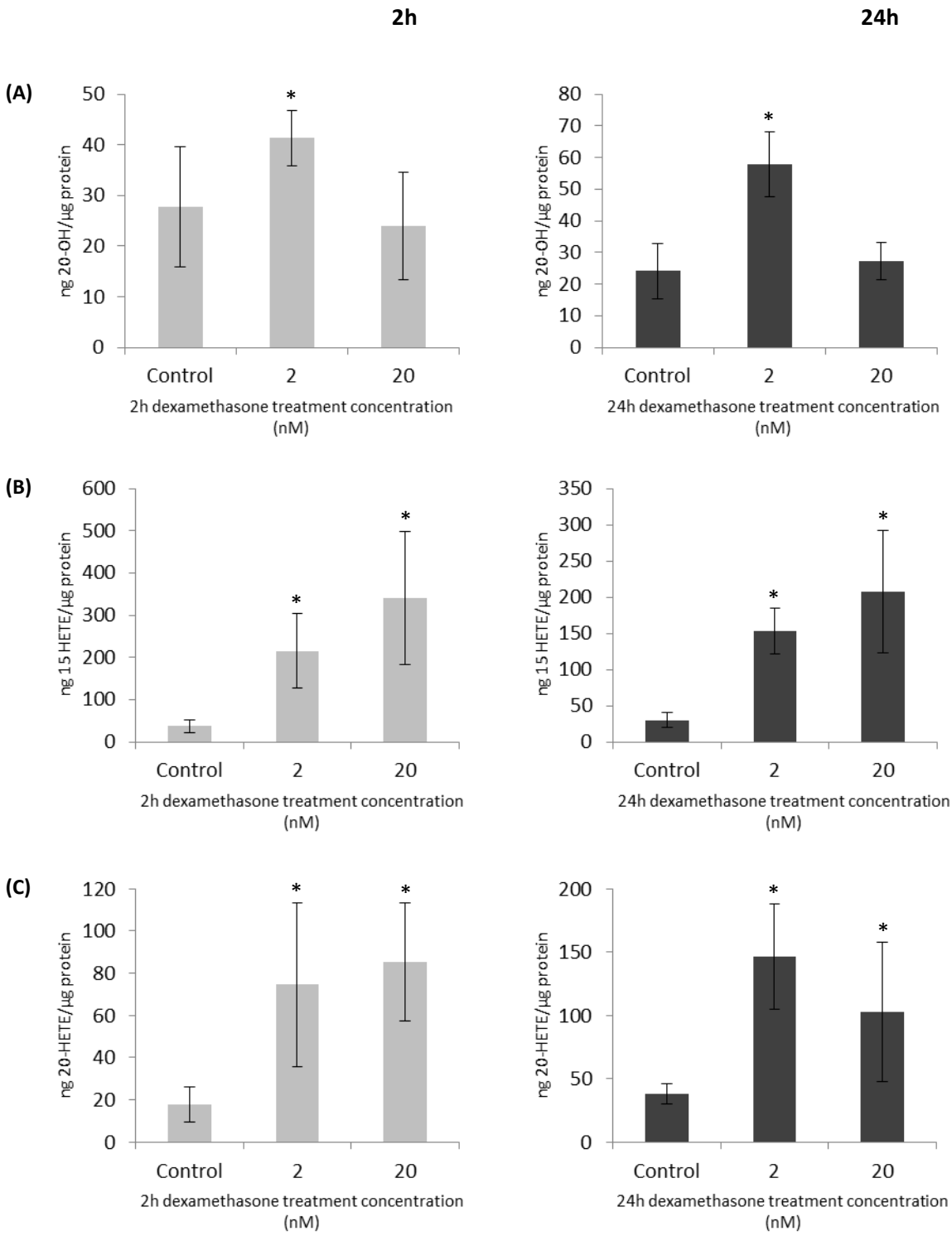


**Figure 5.13. Secretion of eicosanoid lipids by dexamethasone treated 3T3-L1 adipocytes**
Differentiated 3T3-L1 adipocytes at day 10 post-differentiation were pre-incubated with CS-free medium for 24h, and were then treated with dexamethasone for 2 and 24h. The concentrations of dexamethasone treatments used were 2 and 20 nM. Eicosanoids were extracted from cell culture medium by solid phase extraction chromatography and were analysed by LC-MS/MS in negative ion mode. Detected eicosanoids are represented as median ± range with a group size of 3. The detected eicosanoids are 20-OH $LTB_4$ (A), 15-HETE (B), and 20-HETE (C). Statistical significance of each eicosanoid is represented by *$P$<0.05 *vs.* control. A significant increase was seen in the dexamethasone treated cells with all conditions. One exception was 20-OH which only significantly increased with the 2nM treatment and both timepoints.

## 5.4. DISCUSSION

This chapter has used the 3T3-L1 adipocyte model to study the effect of the glucocorticoid dexamethasone on the metabolism of these cells in terms of the gene expression of several adipokines, as well as global lipid profiles and the production of eicosanoids by mature adipocytes. The results indicate that normal adipocyte function is significantly influenced by dexamethasone.

### 5.4.1. Effect of dexamethasone treatment on adipokine gene expression

Adipocytes were treated with dexamethasone to determine its effect on the normal expression of several adipokines. It was expected, from previous findings that the gene expression of leptin would decrease, whereas that of adiponectin, IL-6 and TNF-$\alpha$ would increase (Bradley and Cheatham, 1999; Fasshauer *et al*., 2002 and 2003). Similar findings were found in the current study, with leptin gene expression significantly increasing after 24h of dexamethasone treatment at both concentrations (2 and 20nM). Dexamethasone is a synthetic glucocorticoid, which increases leptin gene expression and protein expression, as seen in a previous study in rat adipocytes after 2h of treatment (Bradley and Cheatham, 1999). The current study saw no significant change after 2h of dexamethasone treatment; however, Bradley and Cheatham used a treatment concentration of 100nM, whereas the current study investigated lesser concentrations. Another study with 3T3-L1 adipocytes demonstrated that leptin gene expression was marginally inhibited (not significantly) by dexamethasone, and this did not vary between the three treatment concentrations used which were 10, 100 and 1000nM (Rentsch and Chiesi, 1996). The dexamethasone treatment time in this study was not stated.

Glucocorticoids are known to cause insulin resistance *in vivo* and a previous study using 3T3-L1 adipocytes found that chronic dexamethasone treatment impaired insulin-induced glucose uptake (Sakoda *et al.,* 2000; Bazuine *et al.,* 2004). These hormones inhibit the gene expression of adiponectin (Fasshauer *et al*., 2002), as seen in the current study after 24h of dexamethasone treatment at 20nM. Adiponectin is suppressed in insulin resistant and obese states (Hu *et al*, 1996b; Hotta *et al*., 2000; Weyer *et al*., 2001), and various hormones and agents may promote insulin resistance by inhibition of this protein. These previous findings, as well as those from the current study, indicate that one mechanism by which glucocorticoids impair insulin sensitivity could be hypoadiponectinemia.

As well as a significant decrease in adiponectin gene expression, the current study also demonstrated an inhibition in the gene expression of IL-6 after 24h of dexamethasone treatment (at both 2 and 20nM). This supports the idea that this agent is anti-inflammatory, and its suppressive effect on the gene expression of IL-6 has also been observed elsewhere (Fasshauer *et al*., 2003).

### 5.4.2. Effect of dexamethasone treatment on global lipid profiles

The increase in adiposity as seen in obesity is a consequence of both hyperplasia and hypertrophy (Hausman *et al*., 2001). The balance of these processes is important to determine the size of mature adipocytes and also adipose tissue mass (Gathercole *et al*., 2011). Lipid accumulation is a result of increased fatty acid uptake and lipogenesis, whereas lipolysis causes lipid loss (Gathercole *et al*., 2011). Glucocorticoids have been reported to have both lipolytic and adipogenic actions in many studies, and these actions depend on many factors including the concentration and duration of treatment, as well as the experimental model and specific glucocorticoid used (Masuzaki *et al*., 2001; Andrews *et al*., 2002; Kershaw *et al*., 2006; Xu *et al*., 2009). Previous studies both *in vivo* and *in vitro* have demonstrated stimulation of lipolysis by glucocorticoids, caused by action on hormone sensitive lipase (HSL) in both in rats and humans (Slavin *et al*., 1994; Djurhuus *et al*., 2002). On the other hand, prolonged exposure to glucocorticoids is known to promote adiposity, and this is seen in patients receiving treatment with synthetic glucocorticoids for various inflammatory conditions (Wei *et al*., 2004).

In the current study, dexamethasone treatment did have an effect on lipid metabolism, as seen with the DI-MS analysis. The concentration of two triglyceride (TG) species significantly increased after 2h of dexamethasone treatment when compared to the control cells. These were TG (50:3) and (52:3), and the concentration of TG (50:3) also significantly increased after 24h of dexamethasone treatment. Glucocorticoids can act to increase adipose tissue mass, with an increase in visceral adiposity being particularly associated with glucocorticoid treatment (Masuzaki *et al*., 2001; Bujalska *et al*., 2008; Pantoja *et al*., 2008), possibly by increasing adipogenesis of pre-adipocytes. The increased concentration of two TG species after 2nM of dexamethasone treatment observed in the current study may be indicative of dexamethasone acting to decrease lipolysis, and therefore eventually causing TG accumulation.

On the other hand, the concentration of FAs, identified as C18:1 and C20:4, significantly increased with the least concentrated dexamethasone treatment, after both 2 and 24h. When the concentration was increased to 20nM; however, C18:1 decreased after 24h of treatment. These findings may suggest an increase in lipolysis, which results in increased free fatty acids. Another possibility is that dexamethasone is acting to increase lipogenesis, which would result in increased FA uptake, and TG accumulation. This process involves either the re-esterification of FFAs with glycerol, or *de novo* lipogenesis (DNL), and a previous study in over-fed human subjects found that 40% of the increases in fat mass were due to DNL (Lammert *et al*., 2000). Glucocorticoids in combination with insulin treatment cause increased lipogenesis in subcutaneous adipocytes (Oh *et al*., 2005). Whereas, a very recent study has demonstrated that dexamethasone treatment alone led to a decrease in lipogenesis in the Chub-S7 transformed human subcutaneous pre-adipocyte cell line, which originated from an obese female.

Therefore, the glucocorticoids appear to have differing actions on lipid metabolism, as seen in the current study. The positive ion DI-MS analysis suggests that TG accumulation is occurring following dexamethasone treatment, which could be caused by a decrease in lipolysis. The opposite effect was implied by negative ion DI-MS analysis, in which the concentration of the fatty acids C18:1 and C20:4 significantly increased at 2nM dexamethasone treatment at both time points, suggesting that an increase in lipolysis was present, which would cause lipid loss. These effects appear to be conflicting; however, both support the fact that the general consequence of glucocorticoid treatment is an increase in adiposity and circulating free fatty acids, which in turn has negative effects on insulin sensitivity and energy metabolism (Campbell *et al*., 2011). The greatest changes in these species were observed at the 2nM dexamethasone treatment dose, possibly suggesting that the effects of dexamethasone treatment are dose dependent.

Clear separations were observed between the control and dexamethasone treated samples in the PCA and scores plots for both positive and negative ion mode datasets. In the positive data plots, variations were observed in the concentration of certain TG species, including those with m/z 862.79, 874.79, 876.80 and 902.82, which were identified as TG (51:2), (52:3), (52:2) and (54:3), respectively. The concentrations of these lipid species increased in various combinations of the dexamethasone treatments, and these agree with the DI-MS data and therefore suggest a decrease in lipolysis, leading to lipid accumulation in the dexamethasone treated cells. The points of interest in the negative ion models related to phospholipid

species, which were PC (20:0) and lyso-phosphatidylglycerol (22:1), and their concentration increased in the dexamethasone treated cells when compared to the control cells. These phospholipid species may be the source of the fatty acids which were detected by negative ion DI-MS analysis, and seen to increase in the dexamethasone treated cells.

A supervised partial least squares (PLS) model was also used. Both positive and negative ion scores plots showed the same separation between control and dexamethasone treated cells as seen in the PCA plots; however, separation was also observed within the treated samples, with one group containing the 2h dexamethasone treated samples, and the other consisting of cells which had been treated with dexamethasone for 24h. The DI-MS analysis found that the treatment concentration seemed to be more influential in the effect of dexamethasone treatment on 3T3-L1 adipocytes; however, LC-MS analysis suggests that the length of treatment is important. These findings agree with the fact that the actions of glucorticoids depend on many factors, including the agent and model type use, and the length and concentration of treatment (Masuzaki *et al*., 2001; Andrews *et al*., 2002; Kershaw *et al*., 2006; Xu *et al*., 2009).

**5.4.3. Effect of dexamethasone treatment on eicosanoid production**

Glucocorticoids are potent anti-inflammatory agents, and early studies found that they can suppress the formation of eicosanoids (Moncada *et al*., 1976) and also inhibit the release of AA (Hong and Levine, 1976). These drugs enhance the synthesis of a family of proteins called lipocortins, which are thought to inhibit phospholipase $A_2$ activity, therefore preventing the availability of AA, and decreasing eicosanoid synthesis (Di Rosa *et al*., 1984). However, studies with other inflammatory models have shown inconsistencies with this mechanism (Calignano *et al*., 1985; Foster and McCormick, 1985), suggesting that the effect of glucorticoids varies depending on the model used.

In the current study, dexamethasone treatment caused a significant increase in the concentration of many AA-derived eicosanoid species, including the prostanoids $PGD_2$, $PGE_2$ and $PGF_{2\alpha}$. Glucocorticoid drugs are known to decrease eicosanoid synthesis (Di Rosa *et al*., 1984), which conflicts with the findings described in the present work.

Recently; however, it has been suggested that a number of prostanoid species also have anti-inflammatory actions. One example is $PGE_2$, which inhibits the production TNF-α and IL-1 (Miles *et al*., 2002), and also induces 15-lipoxygenase, leading to an increase in the formation

of anti-inflammatory lipoxins (Levy *et al*., 2001; Vachier *et al*., 2002). This may help to explain why dexamethasone treatment caused increased concentrations of various prostanoid species.

The global lipidomic analyses described in this current study provided some suggestion of an increase in lipolysis in the 3T3-L1 adipocytes after dexamethasone treatment. Although the main source of eicosanoids are the membrane phospholipids (Flower and Blackwell, 1976), prostaglandins can also be synthesised from AA released from TG. A previous study using isolated fat cells has shown that during lipolysis, the TGs released sufficient AA to account for the prostaglandins formed (Christ and Nugteren, 1970). Negative ion DI-MS analysis as described in Section 5.3.2.2 demonstrated that one of the most abundant lipid species was identified as C20:4, which is AA. The concentration of this lipid species significantly increased after 2nM of dexamethasone treatment. This may suggest that lipolysis had increased in these cells, and more AA was released from the TGs, therefore increasing the concentration of the detected eicosanoid species in the cell medium samples.

**5.4.4. Limitations**

The major limitation of the current study was the possible representation of noise peaks in the PCA and PLS plot analyses, as many of the points present in these plots were unidentifiable when searching the LIPID MAPS database with the exact mass. The scaling method chosen in the current study was Pareto, because it is the method is commonly used for mass spectrometry data (Eriksson *et al*., 1999); however, it allows regions of the chromatogram with lesser amplitude to influence the model if variation is observed. The application of an alternative scaling method may eliminate these points, for example, the use of centring with no scaling (Ctr) is influenced by a variable based on its signal, and therefore regions of less amplitude would have little influence on the model. Another limitation was the slight retention time (RT) shifts seen with some of the global LC-MS chromatograms. RT shifts are caused by various factors, including temperature, mobile phase composition and day-to-day drift. Ideally, all samples would be run on the same day, with the same mobile phase compositions. A final limitation was the inability of assigning the exact fatty acid compositions with the exact mass alone.

### 5.4.5. Conclusions and future work

The current study has shown that the glucocorticoid dexamethasone has potent effects on both adipokine expression and lipid metabolism of 3T3-L1 adipocytes. The first part of this study demonstrated dysfunction of adipokine gene expression, specifically significant increases in leptin gene expression, and decreases in the gene expression of both adiponectin and IL-6. These findings replicated those found in other studies, whilst the decrease in the inflammatory cytokine IL-6 supports the idea that dexamethasone is an anti-inflammatory agent. Dexamethasone treatment of normal adipocytes also caused disturbances in lipid metabolism, with both activation and inhibition of lipolysis being observed. These opposing actions could eventually lead to an increase in TG accumulation and therefore adiposity, and also an increase in circulating FFAs, both of which cause insulin resistance and disrupted energy metabolism (Campbell *et al*., 2011). Dexamethasone treatment also caused an increase in the production of a number of eicosanoids, particularly prostanoid species. The increase in the concentration of two TG species was coupled with an increase in C20:4, which may be the cause of the eicosanoid profiles observed after dexamethasone treatment. Therefore this glucocorticoid has anti-inflammatory properties, but also may be involved in the increase of eicosanoid production from basal 3T3-L1 adipocytes (no prior induction of lipolysis) via an increase in AA (C20:4).

The current work has provided a model for studying the effect of dexamethasone on the normal function of 3T3-L1 adipocytes. Opposing lipolytic effects have been suggested to occurring in the dexamethasone treated cells; however, this is only based on observed increases and decreases in the concentration of TG and FA species. Therefore more definite proof is needed to ascertain whether lipolysis is being affected by dexamethasone. One way could be to investigate the gene expression of ATGL and HSL. An increase in the gene expression of both cause an increase in lipolysis, as seen after excessive glucocorticoid treatment (Fain and Saperstein, 1970; Slavin *et al*., 1994; Xu *et al*., 2009; Campbell *et al*., 2011). Another extension to the current study would be to use LC-MS/MS techniques to fully identify selected lipid species, as this would allow the discovery of the fatty acid composition of phospholipid and triglyceride species.

# CHAPTER 6:

## General Discussion and Future Perspectives

### 6.1. SUMMARY

Adipocytes become dysfunctional in the obese state, causing an inflammatory environment (Yudkin *et al*., 1999; Festa *et al*., 2001) which may contribute to the increased risk of developing obesity-associated comorbidities. Changes in normal adipocyte function are seen in altered gene expression and protein secretion profiles of many adipokines, cytokines and chemokines (Trayhurn and Wood, 2004). Disturbances in lipid metabolism are also connected with obesity, such as changes in the basal rates of lipolysis, which are directly correlated with adipocyte size (Large *et al*., 1999).

The overall purpose of the project was to characterise adipocyte metabolism in terms of gene expression of the adipokines leptin and adiponectin, and also the pro-inflammatory cytokines TNF-α and IL-6, as well as lipid metabolism in response to different environmental factors. The first specific aim was to investigate these mechanisms during adipogenesis, and on the whole, this aim was achieved. The current study demonstrated that the metabolic processes of lipolysis and eicosanoid production were both affected by the differentiation process, resulting in the accumulation of TG lipid droplets.

The second aim was to investigate these lipid metabolism processes in adipocytes treated with the inflammatory mediators, TNF-α and IL-6. Both caused disruptions in the normal metabolism of the adipocyte, involving changes in lipolysis, and eicosanoid production. A link to the gene expression of leptin was also considered, although further investigations would be needed to prove this.

The final aim was to study the effect of dexamethasone on the metabolism of adipocytes. The current study suggested both activation and inhibition of lipolysis after treatment with dexamethasone, although, as before, further investigations are required for confirmation. Increases were seen in the concentration of a variety of eicosanoid species, which differs from previous findings. Early studies demonstrated that glucocorticoids (including dexamethasone) are anti-inflammatory agents, and act by suppressing the formation of eicosanoid species (Moncada *et al*., 1976). A suggested explanation for this conflict is presented in Section 6.5.

The following discussion summarises the current findings and explores ways to address gaps in this work and to expand the field.

### 6.2. ADIPOCYTE METABOLISM DURING ADIPOGENESIS

Obesity is partly characterised by increased adiposity, which is caused by an imbalance in energy homeostasis, leading to increased storage of triglyceride (TG)s within white adipose tissue, and eventually causing an expansion of adipose tissue mass within the body. Two processes are involved in the increased adiposity observed in the obese state. These are hypertrophy of mature adipocytes, and adipogenesis of pre-adipocytes (Johnson *et al*., 1971; Faust *et al*., 1978; Johnson *et al*., 1978).

The first study described in this thesis used the well-established 3T3-L1 pre-adipocyte cell-line (Green and Meuth, 1974; Green and Kehinde, 1975) to explore the lipid metabolism of adipocytes during adipogenesis *in vitro*. The validity of this cell culture was confirmed by morphological changes, in which lipid droplets were clearly formed after the induction of differentiation, and continued to accumulate over the remainder of the time course. Gene expression and protein secretion of leptin and adiponectin were profiled, and agreed with previous findings. Both leptin (MacDougald *et al*., 1995) and adiponectin (Ouchi *et al*., 1999) are differentiation-dependent genes, and their gene expression and protein secretion were only detectable after the induction of differentiation in the current study. This section of work was necessary to authenticate this model of adipogenesis before further analyses, and by replicating previous findings, it was concluded that this had been successfully achieved. This qPCR validation stage was undertaken for all 3T3-L1 experiments, and so will not be mentioned in subsequent sections.

However, rather than simply repeating previous work, the current study extended the course of differentiation past days 10-15, which are commonly used end points for this type of study, to day 25. The aim was to investigate whether the phenotype of very mature adipocytes would remain similar to those at day 10-15 post-differentiation, or become characteristically different. The current study demonstrated morphologically that these adipocytes continued to accumulate lipid droplets up to day 25 post-differentiation. From approximately day 10 onwards, the gene expression and protein secretion of both leptin and adiponectin began to decrease, which continued until the end of the time course. This may suggest that the gene expression and secretion of these adipokines become dysfunctional as the adipocytes become larger and accumulate more lipids. Alternatively, it might simply be that 3T3-L1 adipocytes become difficult to maintain in culture past a certain length of time.

After validation of the model, lipidomic analyses were undertaken to monitor any changes in lipid metabolism occurring over the course of differentiation. The major finding in the

current study was that the lipid composition of the pre-adipocytes consisted of mainly phospholipid species. By day 10 post-differentiation, this profile had changed, and diglyceride (DG) and TG species were predominantly present. This was expected from the morphology of the cells, as lipid droplets were observed from day 5 post-differentiation, and these increased in size and number as the cells matured. During adipogenesis, the development of these lipid droplets is overseen by adipogenic transcription factors such as peroxisome proliferator-activated receptor gamma (PPARγ; Schoonjans *et al*., 1996), and this acts to regulate adipogenesis and maintain the phenotype of the mature adipocyte (Rosen *et al*., 1999; Tamori *et al*., 2002). Lipoprotein lipase (LPL), adipose triglyceride lipase (ATGL) and hormone sensitive lipase (HSL; Zimmermann *et al*., 2004) are also involved in these processes within the mature adipocyte. AGTL is induced during adipogenesis, and is greatly expressed in mature adipocytes where it is situated close to the lipid droplets and causes lipolysis (Jenkins *et al*., 2004; Villena *et al*., 2004; Zimmermann *et al*., 2004; Kershaw *et al*., 2005; Smirnova *et al*., 2006).

Another identifiable fatty acid (FA) was C20:4, arachidonic acid (AA), and its concentration also decreased at the later time points, again suggesting changes in the phenotype of the very mature adipocyte. AA is released from membrane phospholipids, and is a precursor in the synthesis of eicosanoids (Piomelli, 1993). Various eicosanoid species were secreted by the 3T3-L1 cells in the current study, and their concentrations were the greatest during the pre-adipocyte stage. Exogenous FAs are required for the differentiation of 3T3-L1 pre-adipocytes, and this process is dependent on PPARγ (Barak *et al*., 1999; Rosen *et al*., 1999). The first identified high-affinity ligand for PPARγ was a derivative of $PGJ_2$ (Forman *et al*., 1995), and other PG derivatives can also induce adipogenesis (Forman *et al*., 1995; Kliewer *et al*., 1995). Many eicosanoid species are involved in adipocyte differentiation, including the prostaglandins (PG) from the COX pathway, although these species have conflicting actions. One COX product is $PGI_2$, and it promotes adipogenesis (Negrel *et al*., 1989; Aubert *et al*., 1996). Another is $PGE_2$, and it is more efficiently produced by pre-adipocytes as seen in the current study, and elsewhere (Lu *et al*., 2004). It acts to down-regulate cAMP production and lipolysis in both human and rat adipocytes, therefore allowing continued TG accumulation (Strong *et al*., 1992; Vassaux *et al*., 1992). In contrast, $PGF_{2\alpha}$ inhibits adipocyte differentiation (Miller *et al*., 1996; Vassaux *et al*., 1994), and this is thought to occur due to the inactivation of PPARγ (Hu *et al*., 1996a). Eicosanoids are also synthesised via the LOX and P450 epoxygenase pathways. A previous study found that inhibition of the LOX pathway

prevented 3T3-L1 pre-adipocytes from differentiating, and this was resolved by the addition of the PPAR*γ* agonist, rosiglitazone (Madsen *et al*., 2003).

### 6.3. Effect of inflammatory agents on lipid metabolism of 3T3-L1 adipocytes

Obesity is characterised by chronic low-grade inflammation (Yudkin *et al*., 1999; Festa *et al*., 2001), and so investigations into the effect of the pro-inflammatory agents TNF-α and IL-6, were carried out (Chapter 4).

Increased rates of lipolysis were suggested by the treatment of 3T3-L1 adipocytes with TNF-α for 24h, as decreases in DG/TG species, and an increase in selected FAs, were observed in these cells. This agrees with previous findings, as TNF-α increases adipocyte lipolysis, resulting in an increase of free fatty acids (FFA). In cultured adipocytes, this increase is observed after approximately 6h of TNF-α treatment, with maximum rates occurring by 12-24h (Kawakami *et al*., 1987; Feingold *et al*., 1992; Green *et al*., 1994; Hauner *et al*., 1995). These FAs can then accumulate in other tissue depots, such as those in muscle and liver, and contribute to dyslipidaemia and insulin resistance (Bays *et al*., 2004).

A few mechanisms underlying the involvement of TNF-α in these conditions have been proposed, one of which is that the cytokine decreases the gene expression of the perilipins (Rosenbaum and Greenberg, 1998; Souza *et al*., 1998). These are phosphoproteins found on the surface of lipid droplets in adipocytes (Greenberg *et al*., 1991; Blanchette-Mackie *et al*., 1995), and are thought to protect against lipolysis (Souza *et al*., 1998). This decrease in the gene expression of the perilipins is thought to occur via the cAMP-dependent protein kinase A (PKA) pathway. Increased intracellular cAMP activates PKA, leading to phosphorylation of HSL and perilipin and increases in the rates of lipolysis (Miyoshi *et al*., 2006). TNF-α also induces members of the mitogen-activated protein kinase (MAPK) family, including extracellular signal-regulated kinase (ERK), c-Jun $NH_2$-terminal kinase (JNK) and p38 kinase. They act by phosphorylating downstream transcription factors, regulating the expression of lipolysis-related genes; for example, both the ERK and JNK pathways are activated by TNF-α at concentrations that stimulate lipolysis (Souza *et al*., 2003). The JNK pathway is thought to have effects on the gene expression of the perilipins (Souza *et al*., 2003; Ryden *et al*., 2004), whereas, the ERK pathway regulates lipolysis by increasing the activity of HSL (Greenberg *et al*., 2001).

In the current study, 24h of IL-6 intervention caused increased concentrations of various individual DG and TG species, suggesting that an increase in the rate of lipolysis had not occurred. Previous studies; however, demonstrate that IL-6 is involved in the regulation of lipolysis, and has a role in insulin resistance, as seen in 3T3-L1 adipocytes (Lagathu *et al.,* 2003). Investigations involving human mammary, and 3T3-L1 adipocytes, have shown increased lipolysis after 24h of IL-6 treatment (Path *et al*., 2001; Petersen *et al*., 2005). Two *in vivo* studies using human subjects concluded that IL-6 is a lipolytic agent. The first demonstrated that infusion of human recombinant IL-6 into healthy individuals increased lipolysis and fat oxidation in the absence of changes in other lipolytic hormones (catecholamines, glucagon, and insulin; van Hall *et al*., 2003). The second showed an increase in the release of glycerol after IL-6 infusion (Lyngso *et al*., 2002). Finally, another *in vivo* study with IL-6 knockout mice also suggested a role for IL-6 in lipid metabolism. These mice display rapid body fat gain in comparison to wild types, and have increased energy intake. Fat mass decreased in these mice after administration of IL-6, without an observed effect on energy intake, and these changes were not seen in the wild-type controls (Wallenius *et al*., 2002). Although the studies in human mammary and 3T3-L1 adipocytes mentioned above demonstrated increased lipolysis after 24h of IL-6 treatment, in humans IL-6 treatment only increased rates of lipolysis after 48h (Trujillo *et al*., 2004), and so, if the treatment time in the current study was increased, these effects may have occurred.

Similar mechanisms to those underpinning the actions of TNF-α on lipolysis have been suggested for those of IL-6. Treatment with both inflammatory agents only caused increases in lipolysis after approximately 6h onwards (Kawakami *et al*., 1987; Feingold *et al*., 1992; Green *et al*., 1994; Hauner *et al*., 1995; van Hall *et al*., 2003). Definite lipolytic hormones, such as adrenaline, work instantaneously, and FA metabolism normalises when they are removed. Therefore, the effect of TNF-α and IL-6 on lipolysis may be indirect by inducing changes in other lipolytic factors (van Hall *et al*., 2003).

### 6.4. EFFECT OF DEXAMETHASONE ON LIPID METABOLISM OF 3T3-L1 ADIPOCYTES

Treatment of 3T3-L1 adipocytes with dexamethasone in the current study seemed to decrease lipolysis, and/or increase the rates of lipogenesis, as seen by increases in both TG and FA concentrations. Dexamethasone is a synthetic glucocorticoid, and these hormones have dual roles, the first being lipolytic, with a number of studies demonstrating an increase in the release of FFAs after glucocorticoid treatment, both *in vivo* and *in vitro* (Slavin *et al*., 1994; Xu *et al*., 2009). However, excessive glucocorticoid treatment is associated with increased visceral adiposity, as seen in Cushing's disease (Cushing, 1912; Masuzaki *et al*., 2001; Bujalska *et al*., 2008; Pantoja *et al*., 2008), and this may be caused by either an increase in adipogenesis, a reduction in lipolysis, or a combination of the two (Ottosson *et al*., 2000). Glucocorticoids are essential for the differentiation of pre-adipocytes (Hauner *et al*, 1987; Hauner, 1990). A previous study using corticosterone demonstrated these two actions of the agent, with increases in basal lipolysis being observed. It was proposed that this action occurred due to the observed increases in the gene expression of ATGL. An increase in adipogenesis was also observed in this study, leading the authors to conclude that corticosterone regulates adipose tissue metabolism by stimulating adipogenesis of pre-adipocytes, and increasing lipolysis in the mature adipocytes (Campbell *et al*., 2011).

Specifically, both direct and indirect effects of dexamethasone on lipid metabolism have been reported. An early study demonstrated that 24h of dexamethasone treatment increased glycerol release from adipocytes (Slavin *et al*., 1994). In agreement with these findings, another study demonstrated a dose-dependent lipolytic action occurring at a concentration of 1nM, which became more pronounced at 10-100nM (Xu *et al*., 2009). Alterations in lipolysis are also affected by the length of treatment. Studies using short-term dexamethasone treatment of 6h or less observed only slight increases in lipolysis (Fain *et al*., 1963 and 1965; Goodman, 1970). Similar findings were found in the current study, as changes in lipid metabolism were more pronounced after 24h of treatment, and this effect has been observed elsewhere (Slavin *et al*., 1994; Xu *et al*., 2009).

Proposed mechanisms for dexamethasone-induced lipolysis are similar to those of TNF-α / IL-6 induced lipolysis, including increased intracellular cAMP leading to PKA activation (Miyoshi *et al*., 2006). Other mechanisms include phosphorylation (Sztalryd *et al*., 2003; He *et al*., 2006) or down-regulation of perilipin (Ren *et al*., 2006; Zu *et al*., 2008), and increased gene expression of HSL and ATGL (Fain and Saperstein, 1970; Slavin *et al*., 1994; Xu *et al*., 2009; Campbell *et al*., 2011).

### 6.5. Effect of pro- and anti-inflammatory agents on eicosanoid production by 3T3-L1 adipocytes

An increase in the concentration of various eicosanoid species was observed in the current study after treatment with both the inflammatory mediators TNF-α and IL-6, and also the anti-inflammatory agent, dexamethasone. Eicosanoids are key mediators of inflammation; however, some species have anti-inflammatory properties, or have both pro- and anti-inflammatory actions. One example is $PGE_{2,}$ which is thought to be both pro-and anti-inflammatory, which may explain why the concentration of this prostanoid (among others) increased with all of the treatments presented in this thesis. Anti-inflammatory actions of $PGE_2$ include inhibition of the production of pro-inflammatory cytokines (Miles *et al*., 2002), and also 5-lipoxygenase, which in turn decreases the production of series four leukotrienes (Levy *et al*., 2001). This prostanoid also induces 15-lipoxygenase, leading to an increase in the formation of anti-inflammatory lipoxins (Levy *et al*., 2001; Vachier *et al*., 2002).

### 6.6. Improvements to the work presented in the thesis

One limitation was the difficulty in confidently determining the FA composition of the phospholipid and DG/TG species identified, and it would be of interest to overcome thisThis could be achieved with the use of tandem mass spectrometry (MS/MS). By fragmenting an individual lipid, peaks representing its related FAs would be present in the spectrum, thereby allowing the FA composition to be determined. Prior work would be necessary to optimise the collision energy to each lipid species for favourable fragmentation.

During direct-infusion analyses, various phospholipid species were identified, although only a phosphatidylcholine internal standard was added. Ideally, an internal standard would be useed for each group present in the samples, to allow for more accurate calculation of the concentration of sample lipids.

Finally, changes in lipolysis were suggested in the adipocytes in response to the different treatments; however, this was only based on observations of changes in the concentration of selected TG species. More detailed investigations are required for confirmation. One commonly used method is to determine the glycerol content of the medium (Bradley and Kaslow, 1989; Viswanadha and Londos, 2006). Lipolysis is the process by which TG species are hydrolysed to yield FAs and glycerol, and so, in theory, a direct relationship would occur between the concentration of glycerol detected, and the rate of lipolysis.

### 6.7. FUTURE PERSPECTIVES

The work presented in this thesis has provided a foundation for future studies, some of which have been described above, as they help to complete outlined experiments. The effect of the inflammatory agents TNF-α and IL-6 were investigated (Chapter 4), and other mediators could be studied in the first instance, to provide a greater understanding of the effect of inflammation on the lipid metabolism processes occurring in 3T3-L1 adipocytes. Some examples include other members of the interleukin family, such as IL-18, a pro-inflammatory cytokine, the concentration of which increases with obesity, and decreases after weight loss (Esposito *et al.*, 2002). Therefore, it is predicted that the profile of the gene expression of those investigated in the current study (leptin, adiponectin, TNF-α and IL-6) would be similar after treatment with other inflammatory agents, such as IL-18, than those seen after treatment with both TNF-α and IL-6 in the present work. More specifically, it is predicted that the gene expression of leptin, TNF-α and IL-6 would increase, whereas that of adiponectin would decrease.

The inflammatory environment present in the adipose tissue during obesity is associated with the infiltration of macrophages (Weisberg et al., 2003; Xu *et al*., 2003). Macrophages are a potent source of the increased pro-inflammatory cytokines observed in obesity, and these proteins are able to induce an inflammatory response within the adipocyte, and cause insulin resistance (Suganami *et al*., 2005; Permana *et al*., 2006). Therefore, it would be interesting to study the presence of macrophages, in terms of how they influence lipid metabolism of 3T3-L1 adipocytes. This could be achieved by co-culture of adipocytes and macrophages, either directly by growing both cell types in the same well, or indirectly by treating 3T3-L1 adipocytes with medium previously used to feed the macrophage cell line.

A recent example using direct co-culture of 3T3-L1 adipocytes and C2D or primary peritoneal mouse macrophages demonstrated that these two cell types communicate, and are involved in the onset of insulin resistance (Xie *et al*., 2010). The presence of adipocytes increased the production of macrophage pro-inflammatory cytokines, which can induce insulin resistance in adipocytes by down-regulating the gene expression of glucose transport type 4 (GLUT4) and inhibiting adipocyte differentiation, with IL-6 having a key role in this process (Xie *et al*., 2010).

In comparison, a recent indirect co-culture study with human pre-adipocytes investigated the effects of macrophage-derived factors on the gene expression and secretion of matrix metalloproteinases (MMP)s by these cells (Gao and Bing, 2011). Adipocytes and adipose tissue express and secrete a number of MMPs, including MMP1 and MMP3 (Maquoi *et al*., 2002; Chavey *et al*., 2003; Kawamura *et al*., 2008), both of which degrade extracellular matrix (ECM) proteins (Chavey *et al*., 2003), and ECM remodelling is known to occur as adipose tissue mass expands (Halberg *et al*., 2009; Khan *et al*., 2009). Macrophage-derived factors induce the production of MMP1 and MMP3 by human pre-adipocytes, possibly suggesting a role in the ECM remodelling associated with obesity, as well as the gene expression of chemokines and pro-inflammatory cytokines, including IL-6 (Gao and Bing, 2011). Both co-culture experiments described here found increased gene expression and protein secretion of IL-6. This was observed after treatment with pro-inflammatory mediators in the current study, and IL-6 treatment led to an increase in the concentration of various DG / TG species, suggesting that an increase in the rate of lipolysis had not occurred in these 3T3-L1 adipocytes in the timeframe presented. It would be interesting, therefore, to observe whether this result would be replicated in 3T3-L1 adipocytes co-cultured (either directly or indirectly) with a macrophage cell line. It is likely that the inflammatory environment created by co-culture with macrophages would lead to increased rates of lipolysis.

Another proposed cause of the inflammatory environment seen in the obese state is hypoxia. The original hypothesis suggested that the production of inflammation-related adipokines associated with obesity is a response to clusters of adipocytes becoming distant from vasculature, and therefore hypoxic. The induced inflammatory response acts to stimulate angiogenesis and increase blood flow (Trayhurn and Wood, 2004). A recent study found that hypoxia inhibited insulin action in 3T3-L1 adipocytes, leading to increased lipolysis and cell death (Yin *et al*., 2009). Measuring the concentration of various individual DG/TG species in response to hypoxic conditions would, therefore, provide further information on the effect of hypoxia on adipocyte lipid metabolism. Due to the inflammatory environment associated with hypoxia, it would also be of interest to investigate this condition on the effects of eicosanoid production from adipocytes, and an increase in the concentration of various pro-inflammatory species such as the 2-series prostaglandins is likely.

The effect of the anti-inflammatory agent dexamethasone was also studied, and further work could incorporate the addition of other such agents to these cells' environments, especially because glucocorticoids (and presumably other anti-inflammatory agents) cause different lipolytic and adipogenic actions depending on the dose and length of treatment, and the experimental model and agent used (Masuzaki *et al*., 2001; Kershaw *et al*., 2006; Xu *et al*., 2009). Of particular interest would be drugs used for the treatment of obesity and its associated co-morbidities, such as the thiazolidinediones (TZDs), especially pioglitazone. Both pioglitazone (Actos) and rosiglitazone (trade name Avandia, GlaxoSmithKline) came to market in the 1990s as anti-diabetic drugs; however, rosiglitazone has since been withdrawn due to its links with increased risk of myocardial infarction. Chronic pioglitazone treatment increases FA and glycerol release and suppression of FA re-esterification, as seen in epididymal adipose tissue from hypertensive rats fed a high-sucrose diet (Pravenec *et al*., 2008). Replicating this study in cultured adipocytes would give a better understanding of the effect of this drug on lipid metabolism, and it is expected that an increase in the rate of lipolysis will be observed. The increased concentration of FFAs associated with lipolysis is known to be involved in the development of insulin resistance (Reynisdottir *et al*., 1995; Large *et al*., 1999), and so the efficiency of this drug may be questioned, or other side effects may be discovered.

Before pharmaceutical treatments, a calorie-controlled diet and exercise programme is often used first to treat obesity. A relatively new idea is the use of nutraceuticals, which are foods that provide health benefits. In the case of obesity, treatment with omega 3-poly unsaturated fatty acids (PUFA) could be an option, as they have been shown to reduce body fat and reduce weight gain in rats, as well as decrease the concentration of circulating TGs (Belzung *et al.,* 1993; Hainault *et al*., 1993; Ruzickova *et al*., 2004). More recently, two PUFAs with anti-inflammatory properties, namely eicosapentaenoic acid (EPA) and docosahexaenoic acid (DHA) (Chapkin *et al*., 2009), have been shown to exhibit anti-obesity effects in mice (Ruzickova *et al*., 2004). Both FAs prevent the development of obesity in rodents fed with high-fat (Storlien *et al*., 1987; Gonzalez-Periz *et al*., 2009) or high-sucrose (Ghafoorunissa *et al*., 2005) diets. Similar effects were replicated in human studies; however, the FAs had no effect on insulin sensitivity in T2DM subjects (Rivellese *et al*., 1996; Kabir *et al*., 2007). Addition of these FAs to 3T3-L1 adipocytes could provide an insight into their effects on lipid metabolism, and possibly support their use as a preliminary treatment for obesity. Attention should be drawn to their effect on the production of eicosanoid species from these cells, since both EPA and DHA are precursors of eicosanoid synthesis, and those produced are less

inflammatory than AA-derived species. Increased EPA and DHA intake causes greater incorporation of these FAs into membrane phospholipids, rather than AA, and so it is predicted that the production of AA-derived eicosanoids would decrease in adipocytes treated with either EPA or DHA, as seen previously with $PGE_2$ secretion from 3T3-L1 adipocytes (Wortman *et al*., 2009).

Possible links between eicosanoid production and lipid metabolism have been suggesting with some of the treatments used in the current study. Investigating the effect of various PGs on the lipid metabolism of 3T3-L1 adipocytes, and vice-versa, would provide more information about these two pathways, and may help to confirm a link between them. If established, a further step would be to repeat this work in the adipocyte / macrophage co-culture system described above to explore whether the link between lipid metabolism and eicosanoid synthesis is affected by macrophages.

One of the major findings presented in this thesis, is that treatment of 3T3-L1 adipocytes with selected pro- and anti-inflammatory agents effects the concentration of various DG, TG and FA species, suggesting alterations in the rates of lipolysis. This process may be of pharmacological interest, as increased rates lead to reduced TG accumulation, and eventually weight loss. However, increased serum concentrations of FFAs also occur, leading to dyslipidemia and insulin resistance (Reynisdottir *et al*., 1995; Large *et al*., 1999), which would have to be addressed.

### 6.8. CONCLUDING REMARKS

In conclusion, the work presented in this thesis has revealed how adipocyte metabolism changes with the naturally occurring stages of adipogenesis, as well as treatment with pro- and anti-inflammatory agents. Associations were observed between adipokine gene expression, lipid metabolism and eicosanoid production; however, further work is required to confirm these links by identifying the underlying mechanisms involved.

# REFERENCES

Abahusain, MA; Wright, J; Dickerson, JW; de Vol, EB (1999). Retinol, alpha-tocopherol and carotenoids in diabetes. *European Journal of Clinical Nutrition* **53**: 630-5.

Adams, M; Montague, CT; Prins, JB; Holder, JC; Smith, SA; Sanders, L; Digby, JE; Sewter, CP; Lazar, MA; Chatterjee, KK and O-Rahilly, S (1997). Activators of peroxisome proliferator-activated receptor ɣ have depot-specific effects on human preadipocyte differentiation. *The Journal of Clinical Investigation* **100**: 3149–3153.

Ahima, RS and Osei, SY (2004). Leptin signaling. *Physiology and Behavior* **81**: 223-241.

Ahima, RS; Kelly, J; Elmquist, JK; Flier, JS (1999). Distinct physiologic and neuronal responses to decreased leptin and mild hyperleptinemia. *Endocrinology* **140**: 4923–4931.

Ahima, RS; Prabakaran, D; Mantzoros, C; Qu, D; Lowell, B; Flier-Maratos, E; Flier, JS (1996). Role of leptin in the neuroendocrine response to fasting. *Nature* **382**: 250–252.

Ahima, RS; Saper, CB; Flier, JS and Elmquist, JK (2000). Leptin regulation of neuroendocrine systems. *Frontiers in Neuroendocrinology* **21**: 263-307.

Ahmadi, S; Lippross, S; Neuhuber, WL and Zeilhofer, HU (2002). PGE2 selectively blocks inhibitory glycinergic neurotransmission onto rat superficial dorsal horn neurons. *Nature Neuroscience* **5**: 34–40.

Anderssen, S; Holme, I; Urdal, P and Hjermann, I (1995). Diet and exercise intervention have favourable effects on blood pressure in mild hypertensives: the Oslo Diet and Exercise Study (ODES). *Blood Pressure* **4**: 343–349.

Andreu, V and Pico, Y (2004). Determination of linear alkylbenzenesulfonates and their degradation products in soils by liquid chromatography-electrospray-ion trap multiple-stage mass spectrometry. *Analytical Chemistry* **76**: 2878-2885.

Andrews, RC; Herlihy, O; Livingstone, DEW; Andrew, R and Walker, BR (2002). Abnormal cortisol metabolism and tissue sensitivity to cortisol in patients with glucose intolerance. *The Journal of Clinical Endocrinology and Metabolism* **87**: 5587 –5593.

Apfelbaum, M; Vague, P; Ziegler, O; Hanotin, C; Thomas, F and Leutenegger, E (1999). Long-term maintenance of weight loss after a very low-calorie diet: a randomized blinded trial of the efficacy and tolerability of sibutramine. *The American Journal of Medicine* **106**: 179–184.

Arch JR (1989). The brown adipocyte beta-adrenoceptor. *Proceedings of the Nutrition Society* **48**: 215-223.

Arch, JR; Ainsworth, AT; Cawthorne, MA; Piercy, V; Sennitt, MV; Thody, VE; Wilson, C and Wilson, S (1984). Atypical beta-adrenoceptor on brown adipocytes as target for anti-obesity drugs. *Nature* **309**: 163-165.

Arita, Y; Kihara, S; Ouchi, N; Takahashi, M; Maeda, K; Miyagawa, J; Hotta, K; Shimomura, I; Nakamura, T; Miyaoka, K; Kuriyama, H; Nishida, M; Yamashita, S; Okubo, K; Matsubara, K; Muraguchi, M; Ohmoto, Y; Funahashi, T and Matsuzawa, Y (1999). Paradoxical decrease of an adipose-specific protein, adiponectin, in obesity. *Biochemical and Biophysical Research Communications* **257**: 79-83.

Arya, M; Shergill, IS; Williamson, M; Gommersall, L; Arya, N and Patel, HR (2005). Basic principles of real-time quantitative PCR. *Expert Review of Molecular Diagnostics* **5**: 209–219.

Aubert, J; Ailhaud, G and Negrel, R (1996). Evidence for a novel regulatory pathway activated by (carba)prostacyclin in preadipose and adipose cells. *Federation of European Biochemical Societies Letters* **397**: 117–121.

Au-Yong, ITH; Thorn, N; Ganatra, R; Perkins, AC and Symonds, ME (2009). Brown Adipose Tissue and Seasonal Variation in Humans. *Diabetes* **58**: 2583-2587.

Avenell, A; Brown, TJ; Mcgee, MA; Campbell, MK; Grant, AM; Broom, J; Jung, RT and Smith, WCS (2004). What interventions should we add to weight reducing diets in adults with obesity? A systematic review of randomized controlled trials of adding drug therapy, exercise, behaviour therapy or combinations of these interventions. *Journal of Human Nutrition and Dietetics* **17**: 293–316.

Avram, AS; Avram, MM and James, WD (2005) Subcutaneous fat in normal and diseased states: 2. Anatomy and physiology of white and brown adipose tissue. *Journal of the American Academy of Dermatology* **53**: 671-683.

Ayata, E; Yumuk, V; Gurbu, U; Izmir, S; Samanci, T; Osar, Z; Damci, T; Ozyazar, M and Gorpe, U (2000) Obesity: A heavy burden on type 2 diabetes mellitus. *Diabetes Research and Clinical Practice Journal* **50**: 123-123.

Bachwich, PR; Chensue, SW; Larrick, JW and Kunkel, SL (1986). Tumor necrosis factor a stimulates interleukin-1 and prostaglandin-E2 production in resting macrophages. *Biochemical and Biophysical Research Communications* **136**: 94–101.

Back, M; Sultan, A; Ovchinnikova and O; Hansson, GK (2007). 5-Lipoxygenase-activating protein: a potential link between innate and adaptive immunity in atherosclerosis and adipose tissue inflammation. *Circulation Research* **100**: 946–949.

Bai, Y; Zhang, S; Kim, KS; Lee, JK and Kim, KH (1996). Obese gene expression alters the ability of 30A5 preadipocytes to respond to lipogenic hormones. *The Journal of Biological Chemistry* **271**: 13939-13942.

Baillie, R; Takada, R; Nakamura, M and Clarke, S (1999). Coordinate induction of peroxisomal acyl-CoA oxidase and UCP-3 by dietary fish oil: a mechanism for decreased body fat deposition. *Prostaglandins, Leukotrienes and Essential Fatty Acids* **60**: 351-356.

Barak, Y; Nelson, MC; Ong, ES; Jones, YZ; Ruiz-Lozano, P; Chien, KR; Koder, A and Evans, RM (1999). PPAR gamma is required for placental, cardiac, and adipose tissue development. *Molecular Cell* **4**: 585–595.

Barbatelli, G; Murano, I; Madsen, L; Hao, Q; Jimenez, M; Kristiansen, K; Giacobino, JP: De Matteis, R and Cinti, S (2010). The emergence of cold-induced brown adipocytes in mouse white fat depots is determined predominantly by white to brown adipocyte transdifferentiation. *American Journal of Physiology - Endocrinology and Metabolism* **298**: E1244-1253.

Barnes, PJ (1985). Inhaled glucocorticoids for asthma. *The New England Journal of Medicine* 332**:** 868–875.

Barr, VA; Lane, K; and Taylor, SI (1999). Subcellular localization and internalization of the four human leptin receptor isoforms. *The Journal of Biological Chemistry* **274**: 21416-21424.

Barsch, A; Patschkowski, T and Niehaus, K (2004). Comprehensive metabolite profiling of Sinorhizobium meliloti using gas chromatography–mass spectrometry. *Functional and Integrative Genomics* **4**: 219–230.

Bartness, TJ and Bamshad, M (1998). Innervation of mammalian white adipose tissue: implications for the regulation of total body fat. *American Journal of Physiology - Endocrinology and Metabolism* **275**: R1399-1411.

Bastard, JP; Jardel, C; Bruckert, E; Blondy, P; Capeau, J; Laville, M; Vidal, H and Hainque, B (2000). Elevated levels of interleukin 6 are reduced in serum and subcutaneous adipose tissue of obese women after weight loss. *The Journal of Clinincal Endocrinology and Metabolism* **85**: 3338-3342.

Basualdo, CG; Wein, EE and Basu, TK (1997). Vitamin A (retinol) status of first nation adults with non-insulin-dependent diabetes mellitus. *Journal of the American College of Nutrition* **16**: 39-45.

Batterham, RL; Cohen, MA; Ellis, SM; Le Roux, CW; Withers, DJ; Frost, GS; Ghatei, MA and Bloom, SR (2003). Inhibition of food intake in obese subjects by peptide YY3–36. *The New England Journal of Medicine* **349**: 941–948.

Batterham, RL; Cowley, MA; Small, CJ; Herzog, H; Cohen, MA; Dakin, CL; Wren, AM; Brynes, AE; Low, MJ; Ghatei, MA; Cone, RD and Bloom, SR (2002). Gut hormone PYY(3–36) physiologically inhibits food intake. *Nature* **418**: 650–654.

Bauche, IB; Ait, E; Mkadem, S; Rezsohazy, R; Funahashi, T; Maeda, N and Miranda, LM (2006). Adiponectin downregulates its own production and the expression of its AdipoR2 in transgenic mice. *Biochemical and Biophysical Research Communications* **345**: 1414-1424.

Bays, H; Mandarino, L and DeFronzo, RA (2004). Role of the adipocyte, free fatty acids, and ectopic fat in pathogenesis of type 2 diabetes mellitus: peroxisomal proliferator-activated receptor agonists provide a rational therapeutic approach.*The Journal of CLinical Endocrinology and Metabolism* **89**: 463–478.

Bazuine, M; Carlotti, F; Tafrechi, RS; Hoeben, RC and Maassen, JA (2004). Mitogenactivated protein kinase (MAPK) phosphatase-1 and -4 attenuate p38 MAPK during dexamethasone-induced insulin resistance in 3T3–L1 adipocytes. *Molecular Endocrinolgy* **18**: 1697–1707.

Beattie, JH; Wood, AM; Trayhurn, P; Jasani, B; Vincent, A; McCormack, G and West, AK (2000). Metallothionein is expressed in adipocytes of brown fat and is induced by catecholamines and zinc. *American Journal of Physiology - Regulatory, Integregrative and Comparative Physiology* **278**: R1082-1089

Becker, DJ; Ongemba, LN; Brichard, V; Henquin, JC and Brichard, SM (1995). Diet- and diabetes-induced changes of ob gene expression in rat adipose tissue. *Federation of European Biochemical Societies Letters* **371**: 324–328.

Beck-Nielsen H on behalf of EGIR (1999). General characteristics of the insulin resistance syndrome.

Belzung, F; Raclot, T and Groscolas, R (1993). Fish oil n-3 fatty acids selectively limit the hypertrophy of abdominal fat depots in growing rats fed high-fat diets. *The Americal Journal of Physiology* **264**: 1111-1118.

Benoit, SC; Air, EL; Coolen, LM; Strauss, R; Jackman, A; Clegg, DJ; Seeley, RJ and Woods, SC (2002). The catabolic action of insulin in the brain Is mediated by melanocortins. *The Journal of Neuroscience* **22**: 9048-9052.

Berkowitz, DE; Brown, D; Lee, KM; Emala, C; Palmer, D; An, Y and Breslow, M (1998). Endotoxin-induced alteration in the expression of leptin and beta3-adrenergic receptor in adipose tissue. *American Journal of Physiology* **274**: E992–E997.

Bernlohr, DA; Angus, CW; Lane, MD; Bolanowski, MA and Kelly, TJ Jr. (1984). Expression of specific mRNAs during adipose differentiation: identification of an mRNA encoding a homologue of myelin P2 protein. *Proceedings of the National Academy of Sciences USA* **81**: 5468-72.

Bernlohr, DA; Bolanowski, MA; Kelly, TJ and Lane, MD (1985). Evidence for an increase in transcription of specific mRNAs during differentiation of 3T3-L1 preadipocytes. *The Journal of Biological Chemistry* **260**: 5563-5567.

Bertram, SR; Venter, I and Stewart, RI (1990). Weight loss in obese women-exercise v. dietary education. *South African Medical Journal* **78**:15–18.

Blanchette-Mackie, EJ; Dwyer, NK; Barber, T; Coxey, RA; Takeda, T; Rondinone, CM; Theodorakis, JL;

Greenberg, AS and Londos C (1995). Perilipin is located on the surface layer of intracellular lipid droplets in adipocytes. *The Journal of Lipid Research* **36**: 1211–1226.

Boden, G; Chen, X; Mozzoli, M and Ryan, I (1996). Effect of fasting on serum leptin in normal human subjects. *The Journal of Clinical Endocrinology and Metabolism* **81**: 3419–3423.

Bogardus, C; Lillioia, S; Ravussin, E; Abbot, W; Zawadzki, JK; Young, A; Knowler, WC; Jacobowitz, R and Moll, P (1986). Familial dependence of the resting metabolic rate. *The New England Journal of Medicine* **315**: 96-100.

Boothby, WM; Berkson, J and Dunn, HL (1936). Studies of the energy metabolism of normal individuals: a standard for basal metabolism, with a nomogram for clinical application. *American Journal of Physiology***16**: 468-484

Borglum, JD; Pedersen, SB; Ailhaud, G; Negrel, R and Richelsen, B (1999). Differential expression of prostaglandin receptor mRNAs during adipose cell differentiation. *Prostaglandins and Other Lipid Mediators Journal* **57**: 305-317.

Bos, CL; Richel, DJ; Ritsema, T; Peppelenbosch, MP and Versteeg, HH (2004). Prostanoids and prostanoid receptors in signal transduction. *The International Journal of Biochemistry and Cell Biology* **36**: 1187-1205.

Bouchard, C; Tremblay, A; Nadeau, JP; Despres, JP; Theriault, G; Boulay, MR; Lortie, G; Leblanc, C and Fournier, F (1989). Genetic effect in resting and exercise metabolic rates. *Metabolism* **38**: 364-370

Bougneres, P; Stunff, CL; Pecqueur, C; Pinglier, E; Adnot, P;Ricquier, D (1997). *In vivo* resistance of lipolysis to epinephrine: a new feature of childhood onset obesity. *The Journal of Clinical Investigation* **99**: 2568 –2573.

Bouloumie, A; Curat, CA; Sengenes, C; Lolmede, K; Miranville, A and Busse, R (2005). Role of macrophage tissue infiltration in metabolic diseases. *Current Opinion in Clinical Nutrition and Metabolic Care* **8**: 347-354.

Bozaoglu, K; Bolton, K; McMillan, J; Zimmet, P; Jowett, J; Collier, G; Walder, K and Segal, D (2007). Chemerin is a novel adipokine associated with obesity and metabolic syndrome. *Endocrinology* **148**: 4687–4694.

Bradford, MM (1976). A rapid and sensitive method for the quantification of microgram quantities of protein utilizing the principle of protein-dye binding. *Analytical biochemistry* **72**: 248-254.

Bradley, DC and Kaslow, HR (1989). Radiometric assays for glycerol, glucose, and glycogen. *Analytical Biochemistry* **180**: 11–16.

Bradley, RL and Cheatham, B (1999). Regulation of ob gene expression and leptin secretion by insulin and dexamethasone in rat adipocytes. *Diabetes* **48**: 272-278.

Brasaemle, DL; Levin, DM; Adler-Wailes, DC and Londos, C (2000). The lipolytic stimulation of 3T3-L1 adipocytes romotes the translocation of hormone-sensitive lipase to the surfaces of lipid storage droplets. *Biochimica et Biophysica Acta* **1483**: 251–262, 2000.

Bray, GA (2004). How do we get fat? An epidemiologic and metabolic approach. *Clinics in Dermatology* **22**: 281-288.

Breyer, RM; Bagdassarian, CK; Myers, SA and Breyer, MD (2001). Prostanoid receptors: Subtypes and signaling. *Annual Review of Pharmacology and Toxicology* **41**: 661–690.

Brindle, JT; Antti, H; Holmes, E; Tranter, G; Nicholson, JK; Bethell, HWL; Clarke, S; Schofiedl, PM; McKilligin, E; Mosedale, DE and Grainger, DJ (2002). Rapid and non-invasive diagnosis of the presence

and severity of coronary heart disease using 1H-NMR-based metabonomics. *Nature Medicine* **8**: 1439-1444.

Broberger, C; Johansen, J; Johansson, C; Schalling, M and Hokfelt, T (1998). The neuropeptide Y/agouti gene-related protein (AGRP) brain circuitry in normal, anorectic, and monosodium glutamate-treated mice. *Proceedings of the National Academy of Sciences USA* **95**: 15043–15048.

Bruun, JM; Lihn, AS; Pedersen, SB and Richelsen, B (2005). Monocyte chemoattractant protein-1 release is higher in visceral than subcutaneous human adipose tissue (AT): implication of macrophages resident in the AT. The *Journal of Clinical Endocrinology and Metabolism* **90**: 2282-2289.

Bruun, JM; Lihn, AS; Verdich, C; Pedersen, SB; Toubro, S; Astrup, A and Richelsen, B (2003a) Regulation of adiponectin by adipose tissue-derived cytokines: *in vivo* and *in vitro* investigations in humans. *American Journal of Physiology - Endocrinology and Metabolism* **285**: E527-533.

Bruun, JM; Pedersen, SB and Richelsen, B (2001). Regulation of interleukin 8 production and gene expression in human adipose tissue *in vitro*. The *Journal of Clinical Endocrinology and Metabolism* **86**: 1267-1273.

Bruun, JM; Pedersen, SB; Kristensen, K and Richelsen, B (2002). Effects of pro-inflammatory cytokines and chemokines on leptin production in human adipose tissue *in vitro*. *Molecular and Cellular Endocrinology* **190**: 91–99.

Bruun, JM; Verdich, C; Toubro, S; Astrup, A and Richelsen, B (2003b) Association between measures of insulin sensitivity and circulating levels of interleukin-8, interleukin-6 and tumor necrosis factor-alpha. Effect of weight loss in obese men. *European Journal of Endocrinology* **148**: 535-542.

Bujalska, IJ; Gathercole, LL; Tomlinson, JW; Darimont, C; Ermolieff, J; Fanjul, AN; Rejto, PA and Stewart, PM (2008). A novel selective 11beta-hydroxysteroid dehydrogenase type 1 inhibitor prevents human adipogenesis. *Journal of Endocrinology* **197**: 297–307.

Bullo, M; Garcia-Lorda, P; Megias, I and Salas-Salvado, J (2003). Systemic inflammation, adipose tissue tumor necrosis factor, and leptin expression. *Obesity Research* **11**: 525-531.

Burdon, KP; Lehtinen, AB; Langefeld, CD; Carr, JJ; Rich, SS; Freedman, BI; Herrington, D and Bowden, DW (2008). Genetic analysis of the soluble epoxide hydrolase gene, EPHX2, in subclinical cardiovascular disease in the Diabetes Heart Study. *Diabetes and Vascular Disease Research* **5**: 128–134.

Bustin SA (2002). Quantification of mRNA using real-time reverse transcription PCR (RT-PCR): trends and problems. *Journal of Molecular Biology* **29:** 23-39.

Butte, AJ; Dzau, VJ and Glueck, SB (2001). Further defining housekeeping, or "maintenance," genes focus on "a compendium of gene expression in normal human tissues. *Physiological Genomics* **7**: 95–99.

Calignano, A; Carnuccio, R; Di Rosa, M; Lalenti, A and Moncada, S (1985). The anti-inflammatory effect of glucocorticoid-induced phospholipase inhibitory proteins. *Agents and Actions* **16**: 60-62.

Calle, EE; Rodriguez, C; Walker-Thurmond, K and Thun MJ (2003). Overweight, obesity, and mortality from cancer in a prospectively studied cohort of U.S. adults. *The New England Journal of Medicine* **348**: 1625-1638.

Campbell, JE; Peckett, AJ; D'souza, AM; Hawke, TJ and Riddell, MC (2011). Adipogenic and lipolytic effects of chronic glucocorticoid exposure. *American Journal of Physiology - Cell Physiology* **300**: C198–C209.

Campfield, LA; Smith, FJ; Guisez, Y; Devos, R and Burn, P (1995). Recombinant mouse OB protein: evidence for a peripheral signal linking adiposity and central neural networks. *Science* **269**: 546-549.

Cannon, B and Nedergaard, J (2004). Brown adipose tissue: function and significance. *Physiological Reviews* **84**: 277-359.

Cao, H; Gerhold, K; Mayers, JR; Wiest, MM; Watkins, SM and Hotamisligil, GS (2008). Identification of a lipokine, a lipid hormone linking adipose tissue to systemic metabolism. *Cell* **134**: 933 – 944.

Cao, Z; Umek, RM and McKnight, SL (1991). Regulated expression of three C/EBP isoforms during adipose conversion of 3T3-L1 cells. *Genes and Development* **5**: 1538–1552.

Caprio, M; Fève, B; Claës, A; Viengchareun, S; Lombès, M; Zennaro, MC. (2007) Pivotal role of the mineralocorticoid receptor in corticosteroid-induced adipogenesis. Federation of American Socities for Experimental Biology **21**(9): 2185-94.

Cardullo, RA; Agrawal, S; Flores, C; Zamecnik, PC and Wolf, DE (1988). Detection of nucleic acid hybridization by nonradioactive fluoresence resonance energy transfer. *Proceedings of the National Academcy of Sciences USA* **85**: 8790-8794.

Carlsson, M; Wessman, Y; Almgren, P and Groop, L (2000). High levels of nonesterified fatty acids are associated with increased familial risk of cardiovascular disease. *Arteriosclerosis, Thrombosis, and Vascular Biology Biol* **20**: 1588–1594.

Carriere, A; Carmona, MC; Fernandez, Y; Rigoulet, M; Wenger, RH; Penicaud, L and Casteilla, L (2004) Mitochondrial reactive oxygen species control the transcription factor CHOP-10/GADD153 and adipocyte differentiation: a mechanism for hypoxia-dependent effect. *The Journal of Biological Chemistry* **279**: 40462-40469.

Cascante, M; Boros, LG; Comin-Anduix, B; de Atauri, P; Centelles, JJ and Lee, PW (2002). Metabolic control analysis in drug discovery and disease. *Nature Biotechnology* **20**: 243-249.

Cash, JL; Hart, R; Russ, A; Dixon, JP; Colledge, WH; Doran, J; Hendrick, AG; Carlton, MB and Greaves, DR (2008). Synthetic chemerin derived peptides suppress inflammation through ChemR23. *Journal of Experimental Medicine* **205**: 767–775.

Chakrabarti, SK; Cole, BK; Wen, Y; Keller, SR and Nadler, JL (2009). 12/15-Lipoxygenase products induce inflammation and impair insulin signaling in 3T3-L1 adipocytes. *Obesity (Silver Spring)* **17**: 1657–1663.

Chakrabarti, SK; James, JC; Mirmira, RG (2002). Quantitative assessment of gene targeting *in vitro* and *in vivo* by the pancreatic transcription factor, Pdx1. Importance of chromatin structure in directing promoter binding. *The Journal of Biological Chemistry* **277**: 13286–13293.

Chang, TH and Polakis, SE (1978) Differentiation of 3T3-L1 fibroblasts to adipocytes. Effect of insulin and indomethacin on the levels of insulin receptors. *The Journal of Biological Chemistry* **253**: 4693-4696.

Chapkin, RS; Kim, W; Lupton, JR and McMurray, DN (2009). Dietary docosahexaenoic and eicosapentaenoic acid: Emerging mediators of inflammation. *Prostaglandins, Leukotrienes and Essential Fatty Acids* **81**: 187-191.

Chapman, AB; Knight, DM; Dieckmann, BS and Ringold, GM (1984). Analysis of gene expression during differentiation of adipogenic cells in culture and hormonal control of the developmental program. *The Journal of Biological Chemistry* **259**: 15548-15555.

Chavey, C; Mari, B; Monthouel, MN; Bonnafous, S; Anglard, P; Van Obberghen, E and Tartare-Deckert, S (2003). Matrix metalloproteinases are differentially expressed in adipose tissue during obesity and modulate adipocyte differentiation. *The Journal of Biological Chemistry* **278**: 11888–11896.

Chavez, M; Seeley, RJ and Woods, SC (1995). A comparison between effects of intraventricular insulin and intraperitoneal lithium chloride on three measures sensitive to emetic agents. *Behavioural*

*Neuroscience* **109**: 547–550.

Chehab, FF; Lim, ME and Lu, R (1996) Correction of the sterility defect in homozygous obese female mice by treatment with the human recombinant leptin. *Nature Genetics* **12**: 318-320.

Christ, EJ and Nugteren DH (1970). The biosynthesis and possible function of prostaglandins in adipose tissue. *Biochimica et Biophysica Acta.* **218**: 296-307.

Christensen, R; Kristensen, PK; Bartels, EM; Bliddal, H and Astrup, A (2007). Efficacy and safety of the weight-loss drug rimonabant: a meta-analysis of randomised trials. *Lancet* **370**: 1760-1713.

Christiansen, T; Richelsen, B and Bruun, JM (2005). Monocyte chemoattractant protein-1 is produced in isolated adipocytes, associated with adiposity and reduced after weight loss in morbid obese subjects. *International Journal of Obesity* **29**: 146–150.

Christoffersen, CT; Tornqvist, H; Vlahos, CJ; Bucchini, D; Jami, J; De Meyts, P and Joshi, RL (1998). Insulin and insulin like growth factor-I receptor mediated differentiation of 3T3-F442A cells into adipocytes: effect of PI 3-kinase inhibition. Biochemical *and Biophysical Research Communications* **246**: 426–430.

Church, TS; Willis, MS; Priest, EL; Lamonte, MJ; Earnest, CP; Wilkinson, WJ; Wilson, DA and Giroir, BP (2005) Obesity, macrophage migration inhibitory factor, and weight loss. *International Journal of Obesity and Related Metabolic Disorders* **29**: 675-681.

Cid, MC; Grant, DS; Hoffman, GS; Auerbach, R; Fauci, AS and Kleinman, HK (1993). Identification of haptoglobin as an angiogenic factor in sera from patients with systemic vasculitis. *The Journal of Clinical Investigation* **91:** 977-985.

Civitarese, AE; Jenkinson, CP; Richardson, D; Bajaj, M; Cusi, K; Kashyap, S; Berria, R; Belfort, R; DeFronzo, RA; Mandarino, L andRavussin, E (2004). Adiponectin receptors gene expression and insulin sensitivity in non-diabetic Mexican Americans with or without a family history of Type 2 diabetes. *Diabetologia* **47**: 816-820.

Cleary, MP; Vasselli, JR and Greenwood, MRC (1980). Development of obesity in Zucker obese (fa/fa) rat in absence of hyperphagia. *American Journal of Physiology* **238**: E284-E292.

Cohn, C and Joseph, D (1962). Influence of body weight and body fat on appetite of “normal” lean and obese rats. *Yale Journal of Biology and Medicine* **34**: 598-607.

Colman, E; Golden, J; Roberts, M; Egan, A; Weaver, J and Rosebraugh, C (2012). The FDA’s assessment of two drugs for chronic weight management. *The New England Journal of Medicine* **367**: 1577-1579

Combs, TP; Wagner, JA; Berger, J; Doebber, T; Wang, WJ; Zhang, BB; Tanen, M; Berg, AH; O’Rahilly, S; Savage, DB; Chatterjee, K; Weiss, S; Larson, PJ; Gottesdiener, KM; Gertz, BJ; Charron, MJ; Scherer, PE and Moller, DE (2002). Induction of adipocyte complement-related protein of 30 kilodaltons by PPARgamma agonists: a potential mechanism of insulin sensitization. *Endocrinology* **143**: 998–1007.

Consensus Development Conference Panel (1991). Gastrointestinal surgery for severe obesity. *Annuals of Internal Medicine* **115**: 956 –961.

Considine, RV; Sinha, MK; Heiman, ML; Kriauciunas, A; Stephens, TW; Nyce, MR; Ohannesian, JP; Marco, CC; McKee, LJ; Bauer, TL; and Caro, MD (1996). Serum immunoreactive-leptin concentrations in normal-weight and obese humans. The *New England Journal of Medicine* **334**: 292-295.

Cook, KS; Groves, DL; Min, HY and Spiegelman, BM (1985). A developmentally regulated mRNA from 3T3 adipocytes encodes a novel serine protease homologue. *Proceedings of the National Academy of Sciences USA* **82**: 6480-6484.

Cousin, B; Andre, M; Casteilla, L and Penicaud, L (2001). Altered macrophage-like functions of preadipocytes in inflammation and genetic obesity. *Journal of Cellular Physiology* **186**: 380-386.

Crawford, EK; Ensor, JE; Kalvakolanu, I and Hasday, JD (1997). The role of 3' poly(A) tail metabolism in tumor necrosis factor-alpha regulation. *The Journal of Biological Chemistry* **272**: 21120.21127.

Cummings, DE; Weigle, DS; Frayo, RS; Breen, PA; Ma, MK; Dellinger, EP and Purnell, JQ (2002). Plasma ghrelin levels after diet-induced weight loss or gastric bypass surgery. *The New England Journal of Medicine* **346**: 1623–1630.

Curat, CA; Miranville, A; Sengenes, C; Diehl, M; Tonus, C; Busse, R and Bouloumie, A (2004). From blood monocytes to adipose tissue-resident macrophages: induction of diapedesis by human mature adipocytes. *Diabetes* **53**: 1285–1292.

Cushing, H (1912). **The Pituitary Body and its Disorders**. Philadelphia, PA: J.B.Lippincott Co.

Cuzick, J (1985). A Wilcoxon-Type Test for Trend. *Statistics in Medicine* **4**: 87-89.

Cypess, AM; Lehman, S; Williams, G; Tal, I; Rodman, D; Goldfine, AB; Kuo, FC; Palmer, EL; Tseng, YH; Doria, A; Kolodny, GM and Kahn, CR (2009). Identification and importance of brown adipose tissue in adult humans. *The New England Journal of Medicine* **360**:1509–1517.

Czech, MP and Fain, JN (1972). Antagonism of insulin action on glucose metabolism in white fat cells by dexamethasone. *Endocrinology* **91**: 518-522.

Dandona, P; Aljada, A; Ghanim, H; Mohanty, P; Tripathy, C; Hofmeyer, D and Chaudhuri, A (2004) Increased plasma concentration of macrophage migration inhibitory factor (MIF) and MIF mRNA in mononuclear cells in the obese and the suppressive action of metformin. *The Journal of Clinical Endocrinology and Metabolism* **89**: 5043-5047.

Dass, C (2007). **Fundamentals of Contemporary Mass Spectrometry**. Hoboken, NJ: Wiley-interscience.

Davidson, MH; Hauptman, J; DiGirolamo, M; Foreyt, JP; Halsted, CH; Heber, D; Heimburger, DC; Luens, CP; Robbins, DC; Chung, J and Heymsfield, SB (1999). Weight control and risk factor reduction in obese subjects treated for 2 years with orlistat: a randomized controlled trial. *The Journal of the American Medical Association* **281**:235–242.

Davis, CD and Hord, NG (2005). Nutritional 'omics' technologies for elucidating the role(s) of bioactive food components in colon cancer prevention. *Journal of Nutrition* **135**: 2694–2697.

Dayer, JM; Beutler, A and Cerami, A (1985). Cachectin,tumor necrosis factor stimulates collagenase and prostaglandin E2 production by human synovial cells and dermal fibroblasts. *The Journal of Experimental Medicine* **162**: 2163-2168.

de Hoffman, E and Stroobant, V (2007). **Mass Spectrometry: principles and application**. 3rd ed. West Sussex: John Wiley and Sons Ltd.

de Souza Batista, CM; Yang, RZ; Lee, MJ; Glynn, NM; Yu, DZ; Pray, J; Ndubuizu, K; Patil, S; Schwartz, A; Kligman, M; Fried, SK; Gong, DW; Shuldiner, AR; Pollin, TI and McLenithan, JC (2007). Omentin plasma levels and gene expression are decreased in obesity. *Diabetes* **56**: 1655-1661.

De Taeye, BM; Morisseau, C; Coyle, J; Covington, JW; Luria, A; Yang, J; Murphy, SB; Friedman, DB; Hammock, BB and Vaughan, DE (2010). Expression and regulation of soluble epoxide hydrolase in adipose tissue. *Obesity (Silver Spring)* **18**: 489–498.

DeFronzo, RA (1988). Lilly Lecture 1987: the triumvirate: cell, muscle, liver: a collusion responsible for NIDDM. *Diabetes* **37**:667–687.

Delporte, ML; Funahashi, T; Takahashi, M; Matsuzawa, Y and Brichard, SM (2002). Pre- and post-translational negative effect of β-adrenoceptor agonists on adiponectin secretion: *in vitro* and *in vivo* studies. *Biochemical Journal* **367**: 677-85.
Deslex, S; Negrel, R and Ailhaud, G (1997). Development of a chemically defined serum-free medium for differentiation of rat adipose precursor cells. *Experimental Cell Research* **168**: 15–30.

Devane, WA; Hanus, L; Breuer, A; Pertwee, RG; Stevenson, LA; Griffin, G; Gibson, D; Mandelbaum, A; Etinger, A; Mechoulam, R (1992). Isolation and structure of a brain constituent that binds to the cannabinoid receptor. Science **258**: 1946-9.

Dheda, K; Huggett, JF; Bustin, SA; Johnson, MA; Rook, G and Zumla, A (2004). Validation of housekeeping genes for normalizing RNA expression in real-time PCR. *Bio Techniques* **37**: 112-119.

Di Rosa, M; Flower, RJ; Hirata, F; Parente, L and Russo-Marie, F (1984). Nomenclature announcement. Anti-phospholipase proteins. *Prostaglandins* **28**: 441-442.

Diez, JJ and Iglesias, P (2003). The role of the novel adipocyte-derived hormone adiponectin in human disease. *European Journal of Endocrinology* **148**: 293-300.

Divertie, GD; Jensen, MD and Miles, JM (1991). Stimulation of lipolysis in humans by physiological hypercortisolemia. *Diabetes* **40**: 1228–1232.

Djian, P; Roncari, DAK and Hollenberg, CH (1985). Adipocyte precursor clones vary in capacity for differentiation. *Metabolism* **34**: 880–883.

Djurhuus, CB; Gravholt, CH; Nielsen, S; Mengel, A; Christiansen, JS; Schmitz, OE and Moller, N (2002). Effects of cortisol on lipolysis and regional interstitial glycerol levels in humans. *American Journal of Physiology - Endocrinology and Metabolism* **283**: E172–E177.

Djurhuus, CB; Gravholt, CH; Nielsen, S; Pedersen, SB; Moller, N and Schmitz, O (2004). Additive effects of cortisol and growth hormone on regional and systemic lipolysis in humans. *American Journal of Physiology - Endocrinology and Metabolism* **286**: E488–E494.

do Nascimento, CO; Hunter, L and Trayhurn, P (2004) Regulation of haptoglobin gene expression in 3T3-L1 adipocytes by cytokines, catecholamines, and PPARgamma. *Biochemical and Biophysical Research Communications* **313**: 702-708.

Doerrler, W; Feingold, KR and Grunfeld C (1994) Cytokines induce catabolic effects in cultured adipocytes by multiple mechanisms. *Cytokine* **6**: 478-484.

Dole, M; Mack, LL; Hines, RL; Mobley, RC; Ferguson, LD and Alice MB (1968). Molecular Beams of Macroions. *Journal of Chemical Physics* **49**: 2240–2249.

Dreyer, C; Krey, G; Keller, H; Givel, F; Helftenbein, G and Wahli, W (1992). Control of the peroxisomal beta-oxidation pathway by a novel family of nuclear hormone receptors. *Cell* **68**: 879-887.

Dulloo, AG and Samec, S (2000) Uncoupling Proteins: Do They Have a Role in Body Weight Regulation? *News in Physiological Sciences* **15**: 313-318.

Duncan, RE; Sarkadi-Nagy, E; Jaworski, K; Ahmadian, M and Sul, HS (2008). Identification and functional characterization of adipose-specific phospholipase A2 (AdPLA). *The Journal of Biological Chemistry* **283**: 25428-25436.

Dunn, WB and Ellis, DI (2005). Metabolomics: current analytical platforms and methodologies. *TrAC: Trends Analytical Chemistry* **24**: 285-294.

Dunn, WB; Bailey, NJC and Johnson, HE (2005). Measuring the metabolome: current analytical technologies. *Analyst* **130**: 606-625.

Ebihara, K; Ogawa, Y; Masuzaki, H; Shintani, M; Miyanaga, F; Aizawa-Abe, M; Hayashi, T; Hosoda, K; Inoue, G; Yoshimasa, Y; Gavrilova, O; Reitman, ML and Nakao, K (2001) Transgenic overexpression of leptin rescues insulin resistance and diabetes in a mouse model of lipoatrophic diabetes. *Diabetes* **50**: 1440-1448.

Egan, JJ; Greenberg, AS; Chang, MK; Wek, SA; Moos, MC Jr. and Londos, C (1992). Mechanism of hormone-stimulated lipolysis in adipocytes: translocation of hormone-sensitive lipase to the lipid storage droplet. *Proceedings of the National Academcy of Sciences USA***89**: 8537–8541.

Ekroos, K; Chernushevich, IV; Simons, K and Shevchenko, A (2002). Quantitative profiling of phospholipids by multiple precursor ion scanning on a hybrid quadrupole time-of-flight mass spectrometer. *Analytical Chemistry* **74**: 941–949.

Elabd, C; Chiellini, C; Massoudi, A; Cochet, O; Zaragosi, LE; Trojani, C; Michiels, JF; Weiss, P; Carle, G; Rochet, N; Dechesne, CA; Ailhaud, G; Dani, C and Amri, EZ (2007). Human adipose tissue-derived multipotent stem cells differentiate *in vitro* and invivo into osteocyte-like cells. *Biochemical and Biophysical Research Communications* **361**: 342-348.

Elliott, P; Peters, RF and White, AM (1971). A study of the relationship between glucocorticoid-induced weight loss in rats and the activity of skeletal-muscle and cardiac-muscle ribosomes *in vitro*. *The Biochemical Journal* **125**: 106–107.

Ellis, EF; Nies, AS and Oates, JA (1977). Cerebral arterial smooth muscle contraction by thromboxane A2. *Stroke* **8**: 80-483.

Elmquist, JK; Elias, CF and Saper, CB (1999). From lesions to leptin: hypothalamic control of food intake and body weight (Review). *Neuron* **22**: 221–232.

Emilsson, V; Liu, YL; Cawthorne, MA; Morton, NM and Davenport, M (1997). Expression of the functional leptin receptor mRNA in pancreatic islets and direct inhibitory action of leptin on insulin secretion. *Diabetes* **46**: 313-316.

Engeli, S; Negrel, R and Sharma, AM (2000). Physiology and pathophysiology of the adipose tissue renin-angiotensin system. *Hypertension* **35**: 1270-1277.

Engvall, E and Perlmann, P (1971). Enzyme linked immunosorbent assay (ELISA). Quantitative assay of immunoglobulin G. *Immunochemistry* **8**: 871-874.

Enzi, G; Gasparo, M; Biondetti, PR; Fiore, D; Semisa, M and Zurio, F (1986). Subcutaneous and visceral fat distribution according to sex, age, and overweight, evaluated by computed tomography. *American Journal of Clinical Nutrition* **44**:739-746.

Ericsson, J; Jackson, SM; Kim, JB; Spiegelman, BM and Edwards, PA (1997). Identification of glycerol-3-phosphate acyl-transferase as an adipocyte determination and differentiation factor 1- and sterol regulatory element-binding protein-responsive gene. *The Journal of Biological Chemistry* **272**: 7298-7305.

Eriksson, L; Johansson, E; Kettaneh-Wold, N and Wold S (1999). Introduction to multi- and megavariate data analysis using projection methods (PCA/PLS). Umetrics AB, Umea, Sweden.

Espelund, U; Hansen, TK; Hojlund, K; Beck-Nielsen, H; Clausen, JT; Hansen, BS; Orskov, H; Jorgensen, JO and Frystyk, J (2005). Fasting unmasks a strong inverse association between ghrelin and cortisol in serum: Studies in Obese and Normal-Weight Subjects. *The Journal of Clinical Endocrinology and Metabolism* **90**: 741-746.

Esposito, K; Pontillo, A; Ciotola, M; Di Palo, C; Grella, E; Nicoletti, G and Giugliano, D (2002). Weight loss reduces interleukin-18 levels in obese women. *The Journal of Clinical Endocrinology and Metabolism* **87**: 3864-3866.
Esposito, K; Pontillo, A; Giugliano, F; Giugliano, G; Marfella, R; Nicoletti, G and Giugliano, D (2003). Association of low interleukin-10 levels with the metabolic syndrome in obese women. *The Journal of Clinical Endocrinology and Metabolism* **88**: 1055-1058.

Faggioni, R; Fantuzzi, G; Fuller, J; Dinarello, CA; Feingold, KR and Grunfeld, C (1998). IL-1 beta mediates leptin induction during inflammation. *American Journal of Physiology* **274**: R204-208.

Fain, JN and Saperstein, R (1970). The involvement of RNA synthesis and cyclic AMP in the activation of fat cell lipolysis by growth hormone and glucocorticoids. *Hormone and Metabolic Research* **2 suppl 2**: 20-27.

Fain, JN; Bahouth, SW and Madan, AK (2005). Involvement of multiple signaling pathways in the post-bariatric induction of IL-6 and IL-8 mRNA and release in human visceral adipose tissue. *Biochemical Pharmacology* **69**: 1315-1324.

Fain, JN; Cheema, PS; Bahouth, SW and Lloyd Hiler, M (2003). Resistin release by human adipose tissue explants in primary culture. *Biochemical and Biophysical Research Communications* **300**: 674-678.

Fain, JN; Kanu, A; Bahouth, SW; Cowan, GS Jr.; Hiler, ML and Leffler, CW (2002). Comparison of PGE2, prostacyclin and leptin release by human adipocytes versus explants of adipose tissue in primary culture. *Prostaglandins, Leukotrienes and Essential Fatty Acids* **67**: 467-473.

Fain, JN; Kovacev, VP and Scow, RO (1965). Effect of growth hormone and dexamethasone on lipolysis and metabolism in isolated fat cells of the rat. *The Journal of Biological Chemistry* **240**: 3522–3529.

Fain, JN; Leffler, CW; Bahouth, SW; Rice, AM and Rivkees, SA (2000). Regulation of leptin release and lipolysis by PGE2 in rat adipose tissue. *Prostaglandins and Other Lipid Mediators* **62**: 343-350.

Fain, JN; Madan, AK; Hiler, ML; Cheema, P and Bahouth, SW (2004). Comparison of the release of adipokines by adipose tissue, adipose tissue matrix, and adipocytes from visceral and subcutaneous abdominal adipose tissues of obese humans. *Endocrinology* **145**: 2273-2282.

Fain, JN; Scow, RO and Chernick, SS (1963). Effects of glucocorticoids on metabolism of adipose tissue *in vitro*. *The Journal of Biological Chemistry* **238**: 54–58.

Fang, X; Kaduce, TL; Weintraub, NL; Harmon, S; Teesch, LM; Morisseau, C; Thompson, DA; Hammock, BD and Spector, AA (2001). Pathways of epoxyeicosatrienoic acid metabolism in endothelial cells. Implications for the vascular effects of soluble epoxide hydrolase inhibition. *The Journal of Biological Chemistry* **276**: 14867–14874.

Farrar, JJ; Mizel, SB; Fuller-Farrar, J; Farrar, WL and Hilfiker, ML (1980). Macrophage-independent activation of helper T cells. I. Production of interleukin 2. *The Journal of Immunology* **125**: 793-798.

Fasshauer, M; Klein, J; Lossner, U and Paschke, R (2003a) Interleukin (IL)-6 mRNA expression is stimulated by insulin, isoproterenol, tumour necrosis factor alpha, growth hormone, and IL-6 in 3T3-L1 adipocytes. *Hormone and Metabolic Research* **35**: 147-152.

Fasshauer, M; Klein, J; Neumann, S; Eszlinger, M and Paschke, R (2002) Hormonal regulation of adiponectin gene expression in 3T3-L1 adipocytes. *Biochemical and Biophysical Research Communications* **290**: 1084-1089.

Fasshauer, M; Kralisch, S; Klier, M; Lossner, U; Bluher, M; Klein, J and Paschke, R (2003b) Adiponectin gene expression and secretion is inhibited by interleukin-6 in 3T3-L1 adipocytes. *Biochemical and Biophysical Research Communications* **301**: 1045-1050.

Faust, IM; Johnson, PR; Stern, JS and Hirsch, J (1978). Diet-induced adipocyte number increase in adult rats: a new model of obesity. *American Journal of Physiolody* **235**: E279-286.
Faust, IM; Johnson, PR; Stern, JS and Hirsch, J (1978). Diet-induced adipocyte number increase in adult rats: a new model of obesity. *American Journal of physiology* 235: E279–E286.

Fay WP (2004). Plasminogen activator inhibitor 1, fibrin, and the vascular response to injury. *Trends in Cardiovascular Medicine* **14**: 196-202.

FDA briefing information: meeting of the Endocrinologic and Metabolic Drugs Advisory Committee, February 22, 2012.

FDA briefing information: meeting of the Endocrinologic and Metabolic Drugs Advisory Committee, May 10, 2012.

Feingold, KR; Doerrler, W; Dinarello, CA; Fiers, W and Grunfeld, C (1992). Stimulation of lipolysis in cultured fat cells by tumor necrosis factor, interleukin-1, and the interferons is blocked by inhibition of prostaglandin synthesis. *Endocrinology* **130**: 10-16.

Fenn, JB; Mann, M; Meng, CK; Wong, SF and Whitehouse, CM (1989). Electrospray ionization 2. for mass spectrometry of large biomolecules. *Science* **246**: 64–71.

Ferguson, AD; McKeever, BM; Xu, S; Wisniewski, D; Miller, DK; Yamin, TT; Spencer, RH; Chu, L; Ujjainwalla, F; Cunningham, BR; Evans, JF and Becker, JW (2007). Crystal structure of inhibitor-bound human 5-lipoxygenase-activating protein. *Science* **317**: 510–512.

Fernandez-Real, JM and Ricart, W (2003). Insulin resistance and chronic cardiovascular inflammatory syndrome. *Endocrine Reviews* **24**: 278-301.

Festa, A; D'Agostino Jr, R; Williams, K; Karter, AJ; Mayer-Davis, EJ; Tracy, RP and Haffner, SM (2001). The relation of body fat mass and distribution to markers of chronic inflammation. *International Journal of Obesity* **25**: 1407–1415.

Fiehn, O; Kloska, S and Altmannn, T (2001). Integrated studies on plant biology using multiparallel techniques. *Current Opinion in Biotechnology* **12**: 82–86.

Fisher, L (1990). *Stress and cardiovascular physiology in animals.* In: Brown, M; Koob, G and Rivier, C (eds) **Stress: Neurobiology and Neuroendocrinology.** New York: Marcel Dekker pp 463–474.

Fitzpatrick, FA and Murphy, RC (1989). Cytochrome P-450 metabolism of arachidonic acid: formation and biological actions of "epoxygenase"-derived eicosanoids. *Pharmacological Reviews* **40**: 229-241.

Flegal, KM; Carroll, MD; Kuczmarski, RJ and Johnson, CL (1998). Overweight and obesity in the United States: prevalence and trends, 1960-1994. *International Journal of Obesity and Related Metabolic Disorders* **21**: 39-47.

Flier, JS; Cook, KS; Usher, P and Spiegelman, BM (1987). Severely impaired adipsin expression in genetic and acquired obesity. *Science* **237**: 405-408.

Flower, L; Gray, R; Pinkney, J and Mohamed-Ali, V (2003). Stimulation of interleukin-6 release by interleukin-1beta from isolated human adipocytes. *Cytokine* **21**: 32-37.

Flower, RJ and Blackwell, GJ (1976). The importance of phospholipase-A2 in prostaglandin biosynthesis. *Biochemical Pharmacology* **25**: 285-291.

Folch, J; Lees, M and Sloane-Stanley, GH (1957). A simple method for the isolation and purification of total lipids from animal tissues. *The Journal of Biological Chemistry* **226**: 497–509.

Foresight (2007). Tackling Obesities: Future Choices. Government Office for Science.

Forman, BM; Tontonoz, P; Chen, J; Brun, RP; Spiegelman, BM and Evans, RM (1995). 15-Deoxy-delta 12, 14-prostaglandin J2 is a ligand for the adipocyte determination factor PPAR gamma. *Cell* **83**: 803–812

Forrester, JS; Milne, SB; Ivanova, PT and Brown, HA (2004). Computational lipidomics: a multiplexed analysis of dynamic changes in membrane lipid composition during signal transduction. *Molecular Pharmacology* **65**: 813–821.

Foster, SJ and McCormick, ME (1985). The mechanism of the anti-inflammatory activity of glucocorticosteroids. *Agents and Actions* **16**: 58-59.

Frayn KN (2003). **Metabolic Regulation: A Human Perspective.** 2nd ed: Blackwell Publishing.

Fried, SK and Zechner, R (1989) Cachectin/tumor necrosis factor decreases human adipose tissue lipoprotein lipase mRNA levels, synthesis, and activity. *The Journal of Lipid Research* **30**: 1917-1923.

Fried, SK; Bunkin, DA and Greenberg, AS (1998). Omental and subcutaneous adipose tissues of obese subjects release interleukin-6: depot difference and regulation by glucocorticoid. *The Journal of Clinical Endocrinology and Metabolism* **83**: 847-850.

Friedman, JM and Halaas, JL (1998). Leptin and the regulation of body weight in mammals. *Nature* **395**: 763-770.

Frontini, A and Cinti, S (2010). Distribution and development of brown adipocytes in the murine and human adipose organ. *Cell Metabolism* **11**: 253-256.

Fruhbeck, G; Aguado, M and Martinez, JA (1997). *In vitro* lipolytic effect of leptin on mouse adipocytes: evidence for a possible autocrine/paracrine role of leptin. *Biochemical and Biophysical Research Communications* **240** : 590 –594.

Fu, Y; Luo, N; Klein, RL and Garvey, WT (2005). Adiponectin promotes adipocyte differentiation, insulin sensitivity, and lipid accumulation. *Journal of Lipid Research* **46**: 1369-1379.

Fukuhara, A; Matsuda, M; Nishizawa, M; Segawa, K; Tanaka, M; Kishimoto, K; Matsuki, Y; Murakami, M; Ichisaka, T; Murakami, H; Watanabe, E; Takagi, T; Akiyoshi, M; Ohtsubo, T; Kihara, S; Yamashita, S; Makishima, M; Funahashi, T, Yamanaka, S; Hiramatsu, R; Matsuzawa, Y and Shimomura, I (2005). Visfatin: a protein secreted by visceral fat that mimics the effects of insulin. *Science* **307**: 426-430.

Funk, CD; Funk, LB; Kennedy, ME; Pong, AS and Fitzgerald, GA (1991). Human platelet/erythroleukemia cell prostaglandin G/H synthase: cDNA cloning, expression, and gene chromosomal assignment. *The Journal of the Federation of American Societies for Experimental Biology* **5**: 2304–2312.

Funk, CD; Radmark, O; Fu, JY; Matsumoto, T; Jornvall, H; Shimizu, T and Samuelsson, B (1987). Molecular cloning and amino acid sequence of leukotriene A4 hydrolase. *Proceedings of the National Academy of Sciences USA* **84**: 6677–6681.

Gaillard, DM; Wabitsch, BP and Negrel, R (1991). Control of terminal differentiation of adipose precursor cells by glucocorticoids. *The Journal of Lipid Research* **32**: 569–579.

Gale, SM; Castracane, VD and Mantzoros, CS (2004). Energy homeostasis, obesity and eating disorders: recent advances in endocrinology. *Journal of Nutrition* **134**:, 295–298.

Gao, D and Bing, C (2011). Macrophage-induced expression and release of matrix metalloproteinase 1 and 3 by human preadipocytes is mediated by IL-1b via activation of MAPK signalling. *Journal of Cellular Physiology* **226** :2869-2880.

Gathercole, LL; Morgan, SA; Bujalska, IJ; Hauton, D; Stewart, PM and Tomlinson, JW (2011). Regulation of lipogenesis by glucocorticoids and insulin in human adipose tissue. *PLoS ONE* **6**: e26223.

Gerhardt, CC; Romero, IA; Cancello, R; Camoin, L and Strosberg, AD (2001). Chemokines control fat accumulation and leptin secretion by cultured human adipocytes. *Molecular and Cellular Endocrinology Journal* **175**: 81-92.

Gesta, S; Tseng, Y-H and Kahn, CR (2007). Developmental Origin of Fat: Tracking Obesity to Its source. *Cell* **131**: 242-256.

Gettys, TW; Harkness, P and Watson, PM (1996) The beta 3-adrenergic receptor inhibits insulin-stimulated leptin secretion from isolated rat adipocytes. *Endocrinology* **137**: 4054-4057.

Gewirtz, AT; Collier-Hyams, LS; Young, AN; Kucharzik, T; Guilford, WJ; Parkinson, JF; Williams, IR; Neish, AS and Madara, JL (2002). Lipoxin a4 analogs attenuate induction of intestinal epithelial proinflammatory gene expression and reduce the severity of dextran sodium sulfate-induced colitis. *The Journal of Immunology* **168**: 5260–5267.

Ghafoorunissa; Ibrahim, A and Natarajan, S (2005). Substituting dietary linoleic acid with alpha-linolenic acid improves insulin sensitivity in sucrose fed rats. *Biochimica et Biophysica Acta* **1733**: 67-75.

Ghanim, H; Aljada, A; Hofmeyer, D; Syed, T; Mohanty, P and Dandona, P (2004). Circulating mononuclear cells in the obese are in a proinflammatory state. *Circulation* **110**: 1564-1571.

Ghanim, H; Dhindsa, S; Aljada, A; Chaudhuri, A; Viswanathan, P and Dandona, P (2006). Low-dose rosiglitazone exerts an antiinflammatory effect with an increase in adiponectin independently of free fatty acid fall and insulin sensitization in obese type 2 diabetics. *The Journal of Clinical Endocrinology and Metabolism* **91**: 3553-3558.

Gilham, D; Alam, M; Gao, W; Vance, DE and Lehner, R (2005). Triacylglycerol hydrolase is localized to the endoplasmic reticulum by an unusual retrieval sequence where it participates in VLDL assembly without utilizing VLDL lipids as substrates. *Molecular Biology of the Cell* **16**: 984–996.

Gilroy, DW; Colville-Nash, PR; McMaster, S; Sawatzky, DA; Willoughby, DA and Lawrence, T (2003). Inducible cyclooxygenase-derived 15-deoxyΔ12−14PGJ2 brings about acute inflammatory resolution in rat pleurisy by inducing neutrophil and macrophage apoptosis. *The Journal of the Federation of American Societies for Experimental Biology* **17**: 2269–2271.

Gilroy, DW; Colville-Nash, PR; Willis, D; Chivers, J; Paul-Clark, MJ and Willoughby, DA (1999). Inducible cyclooxygenase may have anti-inflammatory properties. *Nature Medicine* **5**: 698-701.

Gonzalez-Periz, A; Horrillo, R; Ferre, N; Gronert, K; Dong, B; Moran-Salvador, E; Titos, E; Martinez-Clemente, M; Lopez-Parra, M; Arroyo, V and Claria, J (2009). Obesity-induced insulin resistance and hepatic steatosis are alleviated by omega-3 fatty acids: a role for resolvins and protectins. *The Journal of the Federation of American Societies for Experimental Biology* **23**: 1946–1957.

Goodman, HM (1963). Effects of chronic growth hormone treatment on lipogenesis by rat adipose tissue. *Endocrinolgy* **72**: 95-99.

Goodman, HM (1970). Permissive effects of hormones on lypolysis. *Endocrinology* **86**: 1064–1074

Goralski, KB; McCarthy, TC; Hanniman, EA; Zabel, BA; Butcher, EC; Parlee, SD; Muruganandan, S and Sinal, CJ (2007). Chemerin, a novel adipokine that regulates adipogenesis and adipocyte metabolism. *The Journal of Biological Chemistry* **282**: 28175–28188.

Granneman, JG; Li, P; Zhu, Z and Lu, Y (2005). Metabolic and cellular plasticity in white adipose tissue I: effects of beta3-adrenergic receptor activation. *American Journal of Physiology - Endocrinology and*

*Metabolis*. **289**: E608-616.

Granowitz, EV (1997). Transforming growth factor-beta enhances and pro-inflammatory cytokines inhibit ob gene expression in 3T3-L1 adipocytes. *Biochemical and Biophysical Research Communications* **240**: 382-385.

Green, A; Dobias, SB; Walters, DJ and Brasier, AR (1994). Tumor necrosis factor increases the rate of lipolysis in primary cultures of adipocytes without altering levels of hormone-sensitive lipase. *Endocrinology* **134**: 2581–2588.

Green, H and Kehinde, O (1974). An established pre-adipose cell line and its differentiation in culture. *Cell* **1**: 113-116.

Green, H and Kehinde, O (1975). An established pre-adipose cell line and its differentiation in culture. II. Factors affecting the adipose conversion *Cell* **5**: 19-27.

Green, H and Meuth, M (1974). An established pre-adipose cell line and its differentiation in culture. *Cell* **3**: 127-133.

Greenberg, AS; Egan, JJ; Wirk, S; Garty, N; Blanchette-Mackie, EJ and Londos, C (1991). Perilipin, a major hormonally regulated adipocyte-specific phosphoprotein associated with the periphery of lipid storage droplet. *The Journal of Biological Chemistry* **266**: 11341–11346.

Greenberg, AS; Nordan, RP; McIntosh, J; Calvo, JC; Scow,RO and Jablons, D (1992). Interleukin 6 reduces lipoprotein lipase activity in adipose tissue of mice *in vivo* and in 3T3-L1 adipocytes: a possible role for interleukin 6 in cancer cachexia. *Cancer Research* **52**: 4113-4116.

Greenberg, AS; Shen, WJ; Muliro, K; Patel, S; Souza, SC; Roth, RA and Kraerner, FB (2001). Stimulation of lipolysis and hormone-sensitive lipase via the extracellular signal-regulated kinase pathway. *The Journal of Biological Chemistry* **276**: 45456-45461.

Griffin, JL; Scott, J and Nicholson, JK (2007). The influence of pharmacogenetics on fatty liver disease in the wistar and kyoto rats: a combined transcriptomic and metabonomic study. *Journal of Proteome Research* **6**: 54–61.

Grigoriadis, AE; Heersche, JNM and Aubin, JE (1988). Differentiation of muscle, fat, cartilage and bone from progenitor cells present in a bone-derived clonal cell population: effect of dexamethasone. *The Journal of Cell Biology* **106**: 2139-2151.

Gross, RW and Han, X (2007). Lipidomics in diabetes and the metabolic syndrome. *Methods in Enzymology* **433**: 73-90.

Grunfeld, C; Zhao, J; Fuller, J; Pollack, A; Moser, A; Friedman, JE and Feingold, KR (1996). Endotoxin and cytokines induce expression of leptin, the ob gene product, in hamsters. *The Journal of Clinical Investigation* **97**: 2152-2157.

Guan, XM; Hess, JF; Yu, H; Hey, PJ and van der Ploeg, LH (1997). Differential expression of mRNA for leptin receptor isoforms in the rat brain. *Molecular and Cell Endocrinology Journal* **133**: 1-7.

Gubitosi-Klug, RA; Talahalli, R; Du, Y; Nadler, JL and Kern, TS (2008). 5-Lipoxygenase, but not 12/15-lipoxygenase, contributes to degeneration of retinal capillaries in a mouse model of diabetic retinopathy. *Diabetes* **57**: 1387–1393.

Haemmerle, G; Zimmermann, R; Hayn, M; Theussl, C; Waeg, G; Wagner, E; Sattler, W; Magin, TM; Wagner, EF and Zechner, R (2002). Hormone sensitive lipase deficiency in mice causes diglyceride accumulation in adipose tissue, muscle, and testis. *The Journal of Biological Chemistry* **277**: 4806–4815.

Hahn, TM; Breininger, JF; Baskin, DG and Schwartz, MW (1998). Coexpression of Agrp and NPY in fasting-activated hypothalamic neurons. *Nature Neuroscience* **1**: 271–272.

Hainault, I; Carolotti, M; Hajduch, E; Guichard, C and Lavau, M (1993). Fish oil in a high lard diet prevents obesity, hyperlipidemia, and adipocyte insulin resistance in rats. *Annals of the New York Academy of Sciences* **683**: 98-101.

Hakansson, ML; Brown, H; Ghilardi, N; Skoda, RC and Meister, B (1998). Leptin receptor immunoreactivity in chemically defined target neurons of the hypothalamus. *The Journal of Neuroscience* **18**: 559-572.

Halberg, N; Khan, T; Trujillo, ME; Wernstedt-Asterholm, I; Attie, AD; Sherwani, S; Wang, ZV; Landskroner-Eiger, S; Dineen, S; Magalang, UJ; Brekken, RA; Scherer, PE (2009). Hypoxia-inducible factor 1alpha induces fibrosis and insulin resistance in white adipose tissue. *Molecular and Cellular Biology* **29**: 4467–4483.

Hales, CN; Luzio, JP and Siddle, K (1978). Hormonal control of adipose-tissue lipolysis. *Biochemical Society Symposia*, 97-135.

Halleux, CM; Takahashi, M; Delporte, ML; Detry, R; Funahashi, T; Matsuzawa, Y and Brichard, SM (2001). Secretion of adiponectin and regulation of apM1 gene expression in human visceral adipose tissue. *Biochemical and Biophysical Research Communications* **288**: 1102-1107

Halliday, D; Heap, R; Stalley, SF; Warwick, P; Altman, DG and Garrow, JS (1979). Resting metabolic rate, weight, surface area and body composition in obese women. *International Journal of Obesity* **3**: l-6.

Hamberg, M and Samuelsson, B (1973). Detection and isolation of an endoperoxide intermediate in prostaglandin biosynthesis. *Proceedings of the National Academy of Sciences USA* **70**: 899-903.

Hamberg, M and Samuelsson, B (1974). Prostagland endoperoxides. novel transformations of arachidonic acid in human platelets. *Proceedings of the National Academy of Sciences USA* **71**: 3400

Hamberg, M; Svensson, J and Samuelsson, B (1975). Thromboxanes: A new group of biologically active compounds derived from prostaglandin endoperoxides. *Proceedings of the National Academy of Sciences* **72**: 2994-2998.

Hammarstrom, S; Orning, L and Bernstrom, K (1985). Metabolism of leukotrienes. *Molecular and Cellular Biochemistry* **69**: 7-16.

Hammock, BD and Ota, K (1983). Differential induction of cytosolic epoxide hydrolase, microsomal epoxide hydrolase, and glutathione S-transferase activities. *Toxicology and Applied Pharmacolgy* **71**: 254–265.

Hammond, VJ and O'Donnell, VB (2012). Esterified eicosanoids: Generation, characterization and function. *Biochimica et Biophysics Acta* **1818**: 2403-2412.

Han, TS; McNeill, G; Seidell, JC and Lean, ME (1997). Predicting intra-abdominal fatness from anthropometric measures: the influence of stature. *International Journal of Obesity and Related Metabolic Disorders* **21**: 587-593.

Han, X and Gross, RW (2003). Global analyses of cellular lipidomes directly from crude extracts of biological samples by ESI mass spectrometry: a bridge to lipidomics. *Journal of Lipid Research* **44**: 1071-1079.

Han, X; Yang, J; Yang, K; Zhao, Z; Abendschein, DR and Gross RW (May 2007). Alterations in myocardial cardiolipin content and composition occur at the very earliest stages of diabetes: a shotgun lipidomics study. *Biochemistry* **46**: 6417–6428.

Han, X; Yang, K; Cheng, H; Fikes, KN and Gross (2005). Shotgun lipidomics of phosphoethanolamine-containing lipids in biological samples after one-step in situ derivatization. *Journal of Lipid Research* **46**: 1548–1560.

Han, X; Yang, K; Yang, J; Cheng, H and Gross, RW (2006). Shotgun lipidomics of cardiolipin molecular species in lipid extracts of biological samples. *Journal of Lipid Research* **47**: 864–879.

Han, X; Yang, K; Yang, J; Fikes, KN; Cheng, H and Gross RW (2006a). Factors influencing the electrospray intrasource separation and selective ionization of glycerophospholipids. *Journal of the American Society for Mass Spectrometry* **17**: 264–274.

Hansen, D; Toubro, S; Stock, MJ; Macdonald, IA and Astrup, A (1998). Thermogenic effects of sibutramine in humans. *The American Journal of Clinical Nutrition* **68**: 1180-1186.

Harder, DR; Campbell, WB and Roman, RJ (1995). Role of cytochrome P–450 enzymes and metabolites of arachidonic acid in the control of vascular tone. *Journal of vascular Research* **32**: 79-92.

Hardie, LJ; Rayner, DV; Holmes, S and Trayhurn, P (1996). Circulating leptin levels are modulated by fasting, cold exposure and insulin administration in lean but not Zucker (fa/fa) rats as measured by ELISA. *Biochemical and Biophysical Research Communications* **223**: 660-665.

Hardman, M and Makarov, A (2003). Interfacing the orbitrap mass analyzer to an electrospray ion source. *Analytical Chemistry* **75**: 1699–1705.

Harte, A; McTernan, P; Chetty, R; Coppack, S; Katz, J; Smith, S and Kumar, S (2005). Insulin-mediated upregulation of the renin angiotensin system in human subcutaneous adipocytes is reduced by rosiglitazone. *Circulation* **111**: 1954-1961.

Hata, AN and Breyer, RM (2004). Pharmacology and signaling of prostaglandin receptors: multiple roles in inflammation and immune modulation. Pharmacology and Therapeutics **103**: 147-166.

Hauner, H (1990). Complete adipose differentiation of 3T3 L1 cells in a chemically defined medium: comparison to serum-containing culture conditions. *Endocrinology* **127**: 865–872.

Hauner, H; Entenmann, G; Wabitsch, M; Gaillard, D; Ailhaud, G; Negrel, R and Pfeiffer, EF (1989). Promoting effect of glucocorticoids on the differentiation of human adipocyte precursor cells cultured in a chemically defined medium. *The Journal of Clinical Investigation* **84**: 1663-1670.

Hauner, H; Petruschke, T; Russ, M and Eckel, J (1995). Effects of tumour necrosis factor alpha (TNF) on glucose transport and lipid metabolism of newly-differentiated human fat cells in cell culture. *Diabetologia* **38**: 764.771.

Hauner, H; Schmid, P and Pfeiffer, EF (1987). Glucocorticoids and insulin promote the differentiation of human adipocyte precursor cells into fat cells. *The Journal of Clinical Endocrinology and Metabolism* **64**: 832–835.

Hauner, H; Skurk, T and Wabitsch, M (2001). Cultures of human adipose precursor cells. *Methods in Molecular Biology* **155**: 239-247.

Hausman GJ (1985). Anatomical and enzyme histochemical differentiation of adipose tissue. *International Journal of Obesity* **9 Suppl 1:** 1-6.

Hausman, DB; DiGirolamo, M; Bartness, TJ; Hausman, GJ and Martin, RJ (2001). The biology of white adipocyte proliferation. *Obesity Reviews* **2**: 239-254.

Havel, PJ; Townsend, R; Chaump, L and Teff, K (1999). High-fat meals reduce 24-h circulating leptin concentrations in women. *Diabetes* **48**: 334-41.

Hayashi, T; Boyko, EJ; Leonetti, DL; McNeely, MJ; Newell-Morris, L; Kahn, SE and Fujimoto, WY (2004). Visceral adiposity is an independent predictor of incident hypertension in Japanese Americans. *Annuals of Internal Medicine.* **140**: 992-1000

Health Survey for England, 2010. National Obesity Observatory; www.noo.org.uk

Hellerstein, MK (2003). *In vivo* measurement of fluxes through metabolic pathways: the missing link in functional genomics and pharmaceutical research. *Annual Review of Nitrition* **23**: 379–402.

Helliwell, RJA; Adams, LF and Mitchell, MD (2004). Prostaglandin synthases: recent developments and a novel hypothesis. *Prostaglandins, Leukotrienes and Essential Fatty Acids* **70**: 101–113.

Hennigan, A; O'Callaghan, RM and Kelly, AM (2007). Neurotrophins and their receptors: role in plasticity, neurodegeneration and neuroprotection. *Biochemical Society Transactions* **35**: 424–427.

Hida, K; Wada, J; Eguchi, J; Zhang, H; Baba, M; Seida, A; Hashimoto, I; Okada, T; Yasuhara, A; Nakatsuka, A; Shikata, K; Hourai, S; Futami, J; Watanabe, E; Matsuki, Y; Hiramatsu, R; Akagi, S; Makino, H and Kanwar, YS (2005). Visceral adipose tissue-derived serine protease inhibitor: a unique insulin-sensitizing adipocytokine in obesity. *Proceedings of the National Institute of Sciences USA* **102**: 10610 –10615.

Himms-Hagen, J; Melnyk, A; Zingaretti, MC; Ceresi, E; Barbatelli, G and Cinti, S (2000). Multilocular fat cells in WAT of CL-316243-treated rats derive directly from white adipocytes. *American Journal of Physiology - Cell Physiology* **279**: C670-681.

Hirata, M; Hayashi, Y; Ushikubi, F; Yokota, Y; Kageyama, R; Nakanishi, S and Narumiya, S (1991). Cloning and expression of cDNA for a human thromboxane A2 receptor. *Nature* **349**: 617–620.

Ho, CS; Lam, NHM; Cheung, RCK; Law, LK; Lit, LCW; Suen, MWM and Tai, HL (2003). Electrospray ionisation mass spectrometry: principal and clinical applications. *The Clinical Biochemist Reviews* **24**: 3-12.

Hoggard, N; Hunter, L; Duncan, JS; Williams, LM; Trayhurn, P and Mercer, JG (1997a). Leptin and leptin receptor mRNA and protein expression in the murine fetus and placenta. *Proceedings of the National Academy of Sciences USA* **94**: 11073-11078.

Hoggard, N; Mercer, JG; Rayner, DV; Moar, K; Trayhurn, P and Williams, LM (1997b). Localization of leptin receptor mRNA splice variants in murine peripheral tissues by RT-PCR and in situ hybridization. *Biochemical and Biophysical Research Communications* **232**: 383-387.

Holland, PM; Abramson, RD; Watson, R and Gelfand, DH (1991). Detection of specific polymerase chain reaction product by utilizing the 5′ to 3′ exonuclease activity of Thermus aquaticus DNA polymerase. *Proceedings of the National Academy of Sciences USA* **88**: 7276–7280.

Hollenberg, AN; Susulic, VS; Madura, JP; Zhang, B; Moller, DE; Tontonoz, P; Sarraf, P; Spiegelman, BM and Lowell, BB (1997). Functional antagonism between CCAAT/Enhancer binding protein-alpha and peroxisome proliferator-ctivated receptor-gamma on the leptin promoter. *The Journal of Biological Chemistry* **272**: 5283-5290.

Holm, C; Osterlund, T; Laurell, H and Contreras, JA (2000). Molecular mechanisms regulating hormone-sensitive lipase and lipolysis. *Annual Reviews* **20**: 365-393.

Holmes, E and Antti, H (2002). Chemometric contributions to the evolution of metabonomics: mathematical solutions to characterising and interpreting complex biological NMR spectra. *Analyst* **127**:

1549–1557.

Hong, SCL and Levine, L (1976). Inhibition of arachidonic acid release from cells as the biochemical action of anti-inflammatory corticosteroids (prostaglandins/phospholipids/anti-inflammation/serum). *Proceedings of the National Academy of Sciences USA* **73**: 1730-1734.

Hopfgartner, G; Varesio, E; Tschappat, V, Grivet, C; Bourgogne, E and Leuthold, LA (2004). Triple quadrupole linear ion trap mass spectrometer for the analysis of small molecules and macromolecules. *Journal of Mass spectrometry* **39**: 845–855.

Horrillo, R; González-Périz, A; Martínez-Clemente, M; López-Parra, M; Ferré, N; Titos, E; Morán-Salvador, E; Deulofeu, R; Arroyo, V; Clària, J (2010). 5-lipoxygenase activating protein signals adipose tissue inflammation and lipid dysfunction in experimental obesity. *The Journal of Immunology* **184**: 3978–3987.

Hotamisligil, GS; Arner, P; Atkinson, RL and Spiegelman, BM (1997). Differential regulation of the p80 tumor necrosis factor receptor in human obesity and insulin resistance. *Diabetes* **46**: 451-455.

Hotamisligil, GS; Arner, P; Caro, JF; Atkinson, RL and Spiegelman, BM (1995). Increased adipose tissue expression of tumor necrosis factor-alpha in human obesity and insulin resistance. *The Journal of Clinical Investigation* **95**: 2409-2415.

Hotamisligil, GS; Murray, DL; Choy, LN and Spiegelman, BM (1994). Tumor necrosis factor alpha inhibits signaling from the insulin receptor. *Proceedings of the National Academy of Sciences USA* **91**: 4854-4858.

Hotamisligil, GS; Shargill, NS and Spiegelman, BM (1993). Adipose expression of tumor necrosis factor-alpha: direct role in obesity-linked insulin resistance. *Science* **259**: 87-91.

Hotta, K; Funahashi, T; Arita, Y; Takahashi, M; Matsuda, M; Okamoto, Y; Iwahashi, H; Kuriyama, H; Ouchi, N; Maeda, K; Nishida, M; Kihara, S; Sakai, N; Nakajima, T; Hasegawa, K; Muraguchi, M; Ohmoto, Y; Nakamura, T; Yamashita, S; Hanafusa, T and Matsuzawa Y (2000). Plasma concentrations of a novel, adipose-specific protein, adiponectin, in type 2 diabetic patients. *Arteriosclerosis, Thrombosis, and Vascular Biology* **20:** 1595-1599.

Hou, W; Zhou, H; Elism, F; Bennett, SAL and Figeys, D (2008). Technological developments in lipidomics. *Briefings in Function Genomics and Proteomics* **7**: 395-409

Houjou, T; Yamatani, K; Imagawa, M; Shimizu, T and Taguchi, R (2005). A shotgun tandem mass spectrometric analysis of phospholipids with normal-phase and/or reverse-phase liquid chromatography/electrospray ionization mass spectrometry. *Rapid Communications in Mass Spectrometry* **19**: 654–666.

Hu, E; Kim, JB; Sarraf, P and Spiegelman, BM (1996). Inhibition of adipogenesis through MAP kinase-mediated phosphorylation of PPARgamma. *Science* **274**: 2100–2103.

Hu, E; Liang, P and Spiegelman BM (1996b). AdipoQ is a novel adipose-specific gene dysregulated in obesity. *The Journal of Biological Chemistry* **271**: 10697–10703.

Huang, L; Zhao, A; Wong, F; Ayala, JM; Struthers, M; Ujjainwalla, F; Wright, SD; Springer, MS; Evans, J and Cui, J (2004). Leukotriene B4 strongly increases monocyte chemoattractant protein-1 in human monocytes. *Arteriosclerosis, Thrombosis, and Vascular Biology* **24**: 1748–1749.

Hube, F and Hauner, H (1999). The role of TNF-α in human adipose tissue: prevention of weight gain at the expense of insulin resistance? *Hormone and Metabolic Research* **31**: 626-631.

Hudgins, LC; Parker, TS; Levine, DM and Hellerstein, MK (2011). A dual sugar challenge test for lipogenic sensitivity to dietary fructose. *The Journal of Clinical Endocrinology & Metabolism* **96**: 861 – 868.

Hunt, CR; Ro, JH; Dobson, DE; Min, HY and Spiegelman, BM (1986). Adipocyte P2 gene: developmental expression and homology of 5'-flanking sequences among fat cell-specific genes. **83**: 3786-3790.

IDF Clinical Guidelines Task Force (2005). Global guideline for Type 2 diabetes. Brussels: International Diabetes Federation.

Inceoglu, B; Schmelzer, Kr; Morisseau, C; Jinks, SL and Hammock, BD (2007). Soluble epoxide hydrolase inhibition reveals novel biological functions of epoxyeicosatrienoic acids (EETs). *Prostaglandins and Other Lipid Mediators* **82**: 42–49.

Inukai, K; Nakashima, Y; Watanabe, M; Takata, N; Sawa, T; Kurihara, S; Awata, T and Katayama, S (2005). Regulation of adiponectin receptor gene expression in diabetic mice. *American Journal of Physiology - Endocrinology and Metabolism* **288**: E876-882.

Iribarne, JV and Thomson, BA (1976). On the evaporation of small ions from charged droplets. *Chemical Physics* **64**: 2287-2294.

Jager, J; Gremeaux, T; Cormont, M; Le Marchand-Brustel, Y and Tanti, JF (2007). Interleukin-1beta-induced insulin resistance in adipocytes through down-regulation of insulin receptor substrate-1 expression. *Endocrinology* **148**: 241-251.

James, WP; Caterson, ID; Coutinho, W; Finer, N; Van Gaal, LF; Maggioni, AP; Torp-Pedersen, C; Sharma, AM; Shepherd, GM; Rode, RA; Renz, CL and SCOUT Investigators (2010). Effect of sibutramine on cardiovascular outcomes in overweight and obese subjects. *The New England Journal of Medicine* **3**: 905-917.

Jenkins, CM; Mancuso, DJ; Yan, W; Sims, HF; Gibson, B and Gross, RW (2004). Identification, cloning, expression, and purification of three novel human calcium-independent phospholipase A2 family members possessing triacylglycerol lipase and acylglycerol transacylase activities. *The Journal of Biological Chemistry* **279**: 48968–48975.

Jensen, MD; Haymond, MW; Rizza, RA; Cryer, PE and Miles, JM (1989). Influence of body fat distribution on free fatty acid metabolism in obesity. *The Journal of Clinical Investigation* **83**: 1168 –1173.

Johnson, PR; Stern, JS; Greenwood, MRC and Hirsch, J (1978). Adipose tissue hyperplasia and hyperinsulinemia in Zucker obese female rats: a developmental study. *Metabolism* **27**: 1941–1954.

Johnson, PR; Zucker, LM; Cruce, JAF and Hirsch, J (1971). Cellularity of adipose depots in the genetically obese Zucker rat. *The Journal of Lipid Research* **12**: 706–714.

Jones, BH; Standridge, MK and Moustaid, N (1997). Angiotensin II increases lipogenesis in 3T3-L1 and human adipose cells. *Endocrinology* **138**: 1512-1519.

Juge-Aubry, CE; Somm, E; Pernin, A; Alizadeh, N; Giusti, V; Dayer, JM and Meier, CA (2005). Adipose tissue is a regulated source of interleukin-10. *Cytokine* **29**: 270-274.

Jump, DB; Clarke, SD; Thelen, A and Liimatta, M (1994). Coordinate regulation of glycolytic and lipogenic gene expression by polyunsaturated fatty acids. *The Journal of Lipid Research* 35: 1076-1084.

Kabir, M; Skurnik, G; Naour, N; Pechtner, V; Meugnier, E; Rome, S; Quignard-Boulange, A; Vidal, H; Slama, G; Clement, K; Guerre-Millo, M and Rizkalla, S (2007). Treatment for 2 mo with n-3 polyunsaturated fatty acids reduces adiposity and some atherogenic factors but does not improve insulin sensitivity in women with type 2 diabetes: A randomized controlled study. *The American Journal of Clinical Nutrition* **86**: 1670-1679.

Kadowaki, T and Yamauchi, T (2005). Adiponectin and adiponectin receptors. *Endocrine Reviews* **26**: 439-451.

Kamegai, J; Tamura, H; Shimizu, T; Ishii, S; Sugihara, H and Wakabayashi, I (2000). Central effect of ghrelin, an endogenous growth hormone secretagogue, on hypothalamic peptide gene expression. *Endocrinology* **141**: 4797–4800.

Kanda, H; Sanshiro, T; Yoshikazu, T; Kotani, K; Hiasa, K; Kitazawa, R; Kitazawa, S; Miyaci, H; Maeda, S; Egashira and Kasuga, M (2006). MCP-1 contributes to macrophage infiltration into adipose tissue, insulin resistance, and hepatic steatosis in obesity. *The Journal of Clinical Investigation* **116**: 1494-1505.

Kang, SW; Adler, SG; Nast, CC; LaPage, J; Gu, JL; Nadler, JL and Natarajan, R (2001). 12-lipoxygenase is increased in glucose-stimulated mesangial cells and in experimental diabetic nephropathy. *Kidney International* **59**: 1354–1362.

Kappes, A and Loffler, G (2000). Influences of ionomycin, dibutyryl-cycloAMP and tumour necrosis factor-alpha on intracellular amount and secretion of apM1 in differentiating primary human preadipocytes. *Hormone and Metabolic research* **32**: 548-554.

Karas M, Hillenkamp F (1988). Laser desorption ionization of proteins with molecular masses exceeding 10,000 daltons. *Analytical Chemistry* **60**: 2299–2301.

Kasturi, R and Wakil, SJ (1983). Increased synthesis and accumulation of phospholipids during differentiation of 3T3-L1 cells into adipocytes. *The Journal of Biological Chemistry* **25**8: 3559-3564.

Kawakami, M; Murase, T; Ogawa, H; Ishibashi, S; Mori, N; Takaku, F and Shibata, S (1987). Human recombinant TNF suppresses lipoprotein lipase activity and stimulates lipolysis in 3T3-L1 cells. *Journal of Biochemistry* **101**: 331-338.

Kawakami, M; Pekala, PH; Lane, DM and Cerami, A (1982). Lipoprotein lipase suppression in 3T3-L1 cells by an endotoxin induced mediator from exudate cells. *Proceedings of the National Academy of Sciences USA* **79**: 912-916.

Kawamura, T; Murakami, K; Bujo, H; Unoki, H; Jiang, M; Nakayama, T and Saito, Y (2008). Matrix metalloproteinase-3 enhances the free fatty acids-induced VEGF expression in adipocytes through toll-like receptor 2. *Experimental Biology and Medicine* **233**: 1213–1221.

Kawanami, D; Maemura, K; Takeda, N; Harada, T; Nojiri, T; Imai, Y; manabe, I; Utsunomiya, K and Nagai, R (2004). Direct reciprocal effects of resistin and adiponectin on vascular endothelial cells: a new insight into adipocytokine-endothelial cell interactions. *Biochemical and Biophysical Research Communications* **314**: 415-419.

Kawano, K; Hirashima, T; Mori, S; Saitoh, Y; Kurosumi, M and Natori, T (1992). Spontaneous long-term hyperglycemic rat with diabetic complications: Otsuka Long-Evans Tokushima fatty (OLETF) strain. *Diabetes* **41**: 1422–1428.

Kennedy, GC (1953). The role of depot fat in the hypothalamic control of food intake in the rat. *Proceedings of the Royal Society B: Biological Sciences* **140**: 578-596.

Kennedy, I; Coleman, RA; Humphrey, PP; Levy, GP; and Lumley, P (1982). Studies on the characterisation of prostanoid receptors: a proposed classification. *Prostaglandins* **24**: 667– 689.

Kern, PA; Saghizadeh, M; Ong, JM; Bosch, RJ; Deem, R and Simsolo, RB (1995). The expression of tumor necrosis factor in human adipose tissue. Regulation by obesity, weight loss, and relationship to lipoprotein lipase. *The Journal of Clinical Investigation* **95**: 2111-2119.

Kershaw, EE and Flier, JS (2004). Adipose tissue as an endocrine organ. *The Journal of Clinical Endocrinology and Metabolism* **89**: 2548-2556.

Kershaw, EE; Hamm, JK; Verhagen, LA; Peroni, O; Katic, M and Flier, JS (2006). Adipose triglyceride lipase: function, regulation by insulin, and comparison with adiponutrin. *Diabetes* **55**: 148–157.

Kershaw, EE; Morton, NM; Dhillon, H; Ramage, L; Seckl, JR and Flier, JS (2005). Adipocyte-specific glucocorticoid inactivation protects against diet-induced obesity. *Diabetes* **54**: 1023-1031.

Kershaw; EE and Flier, JS (2004). Adipose tissue as an endocrine organ. *The Journal of Clinical Endocrinology and Metabolism* **89**: 2548-2556.

Kersten, S (2001). Mechanisms of nutritional and hormonal regulation of lipogenesis. *EMBO reports* **2**: 282-286.

Khan, T; Muise, ES; Iyengar, P; Wang, ZV; Chandalia, M; Abate, N; Zhang, BB; Bonaldo, P; Chua, S and Scherer, PE (2009). Metabolic dysregulation and adipose tissue fibrosis: Role of collagen VI. *Molecular and Cellular Biology* **29**: 1575–1591.

Kim, HJ; Higashimori, T; Park, SO; Choi, H; Jianying, D; Kim, YJ; Noh, HL; Cho, YR; Cline, G; Kim, YB and Kim, JK (2004). Differential effects of interleukin-6 and -10 on skeletal muscle and liver insulin action *in vivo*. *Diabetes* **53**: 1060–1067.

Kim, HY; Kim, JR and Kim, HS (2008). Upregulation of lipopolysaccharide-induced interleukin-10 by prostaglandin A1 in mouse peritoneal macrophages. *Journal of Microbiology and Biotechnology* **18**: 1170-1178.

Kim, S and Moustaid-Moussa, N (2000). Secretory, endocrine and autocrine/paracrine function of the adipocyte. Journal of Nutrition 130: 3110–3115.

Kim, JB and Spiegelman, BM (1996). ADD1/SREBP1 promotes adipocyte differentiation and gene expression linked to fatty acid metabolism. *Genes and Development* **10**: 1096-1107.

Kingdon, KH (1923). A method for the neutralization of electron space charge by positive ionization at very low gas pressures. *Physical Review* **21**: 408–418.

Kirchgessner, TG; Uysal, KT; Wiesbrock, SM; Marino, MW and Hotamisligil, GS (1997). Tumor necrosis factor-alpha contributes to obesity-related hyperleptinemia by regulating leptin release from adipocytes. *The Journal of Clinical Investigation* **100**: 2777-2782.

Klaus S (2001b). **Overview: Biological Significance of Fat and Adipose Tissues.** 1st ed. Texas: Eurekah.com / Landes Bioscience.

Klaus, S (2001a). **Brown Adipocyte Differentiation and Function in Energy Metabolism**. 1st ed. Texas: Eurekah.com / Landes Bioscience.

Kleemann, R; Verschuren, L; van Erk, MJ; Nikolsky, Cnubben, NH; Verheij, ER; Smilde, AK; Hendriks, HF; Zadelaar, S; Smith, GJ; Kaznacheev, V; Nikolskaya, T; Melnikov, A; Hurt-Camejo, E; van der Greef, J and B. van Ommen, Kooistra, T (2007). Atherosclerosis and liver inflammation induced by increased dietary cholesterol intake: a combined transcriptomics and metabolomics analysis. *Genome Biology* **8**: R200.

Kliewer, SA; Forman, BM; Blumberg, B; Ong, E.S; Borgmeyer, U; Mangelsdorf, D.J; Umesono, K and

Evans, RM (1994). Differential expression and activation of a family of murine peroxisome proliferator-activated receptors. *Proceedings of the National Academy of Sciences USA* **91**: 7355–7359.

Kliewer, SA; Lenhard, JM; Willson, TM; Patel, I; Morris, DC and Lehmann, JM (1995). A prostaglandin J2 metabolite binds peroxisome proliferator-activated receptor gamma and promotes adipocyte differentiation. *Cell* **83**: 813–819.

Kloting, N; Berndt, J; Kralisch, S; Kovacs, P; Fasshauer, M; Schon, MR; Stumvoll, M and Bluher M (2006). Vaspin gene expression in human adipose tissue: association with obesity and type 2 diabetes. *Biochemical and Biophysical Research Communications* **339**: 430–436.

Knight, RD (1981). Storage of ions from laser-produced plasmas. *Applied Physics Letters* **38**: 221–223.

Koerner, A; Kratzsch, J and Kiess, W (2005). Adipocytokines: leptin--the classical, resistin--the controversical, adiponectin--the promising, and more to come. *Best Practice and Research Clinical Endocrinology and Metabolism* **19**: 525-546.

Kol, MA; de Kroon, AI; Killian, JA and de Kruijff, KB (2004). Transbilayer movement of phospholipids in biogenic membranes. *Biochemistry* **43**: 2673–2681.

Kolaczynski, JW; Goldstein, BJ and Considine, RV (1997). Dexamethasone, OB gene, and leptin in humans; effect of exogenous hyperinsulinemia. *Journal of Clinical Endocrinology and Metabolism* **82**: 3895-3897.

Kolaczynski, JW; Ohannesian, JP; Considine, RV; Marco, CC and Caro, JF (1996). Response of leptin to short-term and prolonged overfeeding in humans. *The Journal of Clinical Endocrinology and Metabolism* **81**: 4162-4165.

Kolak, M; Westerbacka, J; Velagapudi, V; Wagsater, D; Yetukuri, L; Makkonen, J; Rissanen, A; Häkkinen, AM; Lindell, M; Bergholm, R; Hamsten, A; Eriksson, P; Fisher, RM; Oresic, M and Yki-Järvinen, H (2007). Adipose tissue inflammation and increased ceramide content characterize subjects with high liver fat content independent of obesity. *Diabetes* **56**: 1960-1968.

Komiya, T; Tanigawa, Y and Hirohashi, S (1998). Cloning of the novel gene intelectin, which is expressed in intestinal Paneth cells in mice. *Biochemical and Biophysical Research Communications* **251**: 759 –762.

Konieczny, SF and Emerson, CP Jr (1984). 5-Azacytidine induction of stable mesodermal stem cell lineages from 10T1/2 cells: evidence for regulatory genes controlling determination. *Cell* **38**: 791-800.

Kontani, Y; Wang, Y; Kimura, K; Inokuma, KI; Saito, M; Suzuki-Miura, T; Wang, Z; Sato, Y; Mori, N and Yamashita, H. UCP1 deficiency increases susceptibility to diet-induced obesity with age. *Aging cell* **4**: 147-155.

Kos ,K; Harte, A; James, S; Snead, DR; O'Hare, JP; McTernan, PG and Kumar, S (2007). Secretion of Neuropeptide Y (NPY) in human adipose tissue and its role in maintenance of adipose tissue mass. *American Journal of Physiology - Endocrinology and Metabolism* **293**: E1335-E1340.

Koumenis, C; Naczki, C; Koritzinsky, M; Rastani, S; Diehl, A; Sonenberg, N; Koromilas, A and Wouters, BG (2002). Regulation of protein synthesis by hypoxia via activation of the endoplasmic reticulum kinase PERK and phosphorylation of the translation initiation factor eIF2alpha. *Molecular and Cellular Biology* **22**: 7405-7416.

Kralisch, S; Klein, J; Lossner, U; Bluher, M; Paschke, R; Stumvoll, M and Fasshauer, M (2005). Hormonal regulation of the novel adipocytokine visfatin in 3T3-L1 adipocytes. *Journal of Endocrinology* **185**: R1-8.

Kubis, N and Levy, BI (2004). Angiogenic effect of prostaglandin I 2 in relation with its effect on PPAR nuclear receptors. The *International Journal of Biochemistry and Cell Biology* **36**: 1187-1205.

Kubota, N; Terauchi, Y; Yamauchi, T; Kubota, T; Moroi, M; Matsui, J; Eto, K; Yamashita, T; Kamon, J; Satoh, H; Yano, W; Froguel, P; Nagai, R; Kimura, S; Kadowaki, T and Noda, T (2002). Disruption of adiponectin causes insulin resistance and neointimal formation. *The Journal of Biological Chemistry* **277**: 25863–25866.

Kudva, YC and Butler, PC (1997). Insulin secretion in type-2 diabetes mellitus. **Clinical Research in Diabetes and Obesity. Volume 2: Diabetes and Obesity**. Draznin B, Rizza R, Eds. Totowa, NJ, Humana Press, 1997, p.119–136.

Kumada, M; Kihara, S; Ouchi, N; Kobayashi, H; Okamoto, Y; Ohashi, K; Maeda, K; Nagaretani, H; Kishida, K; Maeda, N; Nagasawa, A; Funahashi, T and Matsuzawa, Y (2004). Adiponectin specifically increased tissue inhibitor of metalloprotenase-1 through interleukin-10 expression in human macrophages. *Circulation* **109**: 2046-2049.

Lagarde, M; Geloen, A; Record, M; Vance, D and Spener, F (2003). Lipidomics is emerging. *Biochimica et Biophysica Acta* **1634**: 61 (2003).

Lagathu, C; Bastard, JP; Auclair, M; Maachi, M; Capeau, J and Caron, M (2003). Chronic interleukin-6 (IL-6) treatment increased IL-6 secretion and induced insulin resistance in adipocyte: prevention by rosiglitazone. *Biochemical and Biophysical Research Communications* **311**: 372–379.

Lagathu, C; Yvan-Charvet, L; Bastard, JP; Maachi, M; Quignard-Boulange, A; Capeau, J and Caron, M (2006). Long-term treatment with interleukin-1beta induces insulin resistance in murine and human adipocytes. *Diabetologia* **49**: 2162-2173.

Lake, AC; Sun, Y; Li, JL; Kim, JE; Johnson, JW and Li, D (2005). Expression, regulation, and triglyceride hydrolase activity of adiponutrin family members. *The Journal of Lipid Research* **46**: 2477–2487.

Lammert, O; Grunnet, N; Faber, P; Bjornsbo, KS; Dich, J; Larsen, LO; Neese, RA; Hellerstein, MK and Quistorff, B (2000). Effects of isoenergetic overfeeding of either carbohydrate or fat in young men. *British Journal of Nutrition* **84**: 233–245.

Lane, MD Flores-Riveros, JR; Hresko, RC; Kaestner, KH; Liao, K; Janicot, M; Hoffman, RD; McLenithan, JC; Kastelic, T and Christy, RJ (1990). Insulin-receptor tyrosine kinase and glucose transport. *Diabetes Care* **13**: 565-575.

Lane, MD; Tang, Q and Jiang, M (1999). Role of the CCAAT Enhancer Binding Proteins (C/EBPs) in Adipocyte Differentiation. *Biochemical and Biophysical Research Communications* **266**: 677-683.

Langin, D; Portillo, MP; Saulnier-Blache, JS and Lafontan, M (1991). Coexistence of three β - adrenoceptor subtypes in white fat cells of various mammalian species. *European Journal of Pharmacology* **199**: 291–301.

Large, V; Reynisdottir, S; Langin, D; Fredby, K; Klannemark, M; Holm, C and Arner, P (1999). Decreased expression and function of adipocyte hormone-sensitive lipase in subcutaneous fat cells of obese subjects. *The Journal of Lipid Research* **40**: 2059–2066.

Larsson, B; Svardsudd, K; Welin, L; Wilhelmsen, L; Bjorntorp, P; Tibblin, G and Lean, ME (1989). Abdominal adipose tissue distribution, obesity, and risk of cardiovascular disease and death: 13 year follow up of participants in the study of men born in 1913. *British Medical Journal* **288**: 1401-1404.

Larsson, H and Ahren, B (1996). Short-term dexamethasone treatment increases plasma leptin independently of changes in insulin sensitivity in healthy women. *The Clinical Journal of Endocrinology and Metabolism* **81**: 4428–4432.

Lass, A; Zimmermann, R; Haemmerle, G; Riederer, M; Schoiswohl and Schweiger, M (2006). Adipose triglyceride lipase-mediated lipolysis of cellular fat stores is activated by CGI-58 and defective in Chanarin-Dorfman syndrome. *Cell Metabolism* **3**: 309–319.

Laybutt, DR; Sharma, A; Sgroi, DC; Gaudet, J; Bonner-Weir, S and Weir, GC (2002). Genetic regulation of metabolic pathways in beta-cells disrupted by hyperglycemia. *The Journal of Biological Chemistry* **277**: 10912–10921.

Lean, ME (1989). Brown adipose tissue in humans. *Proceedings of the Nutrition Society* **48**:243-256.

Lean, ME; Han, TS and Morrison, CE (1995). Waist circumference as a measure for indicating need for weight management. *British Medical Journal* **311**: 158–161.

Lee, CR; North, KE; Bray, MS; Fornage, M; Seubert, JM; Newman, JW; Hammock, BD; Couper, DJ; Heiss, G and Zeldin, DC (2006). Genetic variation in soluble epoxide hydrolase (EPHX2) and risk of coronary heart disease: The Atherosclerosis risk in Communities (ArIC) study. *Human Molecular Genetics* **15**: 1640–1649.

Lee, GH; Proenca, R; Montez, JM; Carroll, KM; Darvishzadeh, JG; Lee, JI and Friedman, M (1996). Abnormal splicing of the leptin receptor in diabetic mice. *Nature* **379**: 632–635

Lee, SH; Soyoola, E; Chanmugam, P; Hart, S; Sun, W; Zhong, H; Liou, S; Simmons, D and Hwang, D (1992). Selective expression of mitogen-inducible cyclooxygenase in macrophages stimulated with lipopolysaccharide. *The Journal of Biological Chemistry* **267**: 25934–25938.

Lehmmann, V; Benninghoff, B and Droge, W (1988). Tumor necrosis factor a induced activation of peritoneal macrophages is regulated by Prostaglandin-E2 and cAMP.*The Journal of Immunology* **141**: 587–591.

Leibson, HJ; Marrack, P and Kappler, JW (1981). B cell helper factors. I. Requirement for both interleukin 2 and another 40.000 mol wt factor. *The Journal of Experimental Medicine* **154**: 1681-1693.

Lemieux, I; Pascot, A; Couillard, C; Lamarche, B; Tchernof, A; Alméras, N; Bergeron, J; Gaudet, D; Tremblay, G; Prud'homme, D; Nadeau, JA and Després, JP (2000). Hypertriglyceridemic waist: a marker of the atherogenic metabolic triad (hyperinsulinemia; hyperapolipoprotein B; small, dense LDL) in men? *Circulation* **102:** 179–184.

Lemieux, S; Prud'homme, D; Bouchard, C; Tremblav, A and Despres, JP (1996). A single threshold value of waist girth identifies normal weight and overweight subjects with excess visceral adipose tissue. *The American Journal of Clinical Nutrition* **64**: 685-689.

Lepak, NM and Serrero, G (1993). Inhibition of adipose differentiation by 9 alpha, 11 beta-prostaglandin F2 alpha. *Prostaglandins* **46**: 511–517.

Levin, G; Duffin, KL; Obukowicz, MG; Hummert, SL; Fujiwara, H; Needleman, P and Raz, P (2002). Differential metabolism of dihomo-gammalinolenic acid and arachidonic acid by cyclo-oxygenase-1 and cyclo-oxygenase-2: implications for cellular synthesis of prostaglandin E1 and prostaglandin E2. Biochemical Journal 365: 489-496.

Levin, N; Nelson, C; Gurney, A; Vandlen, R and de Sauvage, F (1996). Decreased food intake does not completely account for adiposity reduction after ob protein infusion. *Proceedings of the National Academy of Sciences* **93**: 1726–1730.

Levitsky, KA (1970). Feeding patterns of rats in response to fasts and changes in environmental conditions. *Physiology and Behavior* **5**: 291–300.

Levy, BD; Clish, CB; Schmidt, K; Gronert, K and Serhan, CN (2001). Lipid mediator class switching during acute inflammation: signals in resolution. *Nature Immunology* **2**: 612–619.

Lew, EA (1985). Mortality and weight: insured lives and the American Cancer Study. *Annals of Internal Medicine* **103:** 1024–1029.

Licinio, J; Mantzoros, C; Negrao, AB; Cizza, G; Wong, ML; Bongiorno, PB; Chrousos, GP; Karp, B; Allen, C; Flier, JS and Gold, PW (1997). Human leptin levels are pulsatile and inversely related to pituitary-adrenal function. *Nature Medicine* **3**: 575-579.

Lillie, RD and Ashburn, LL (1943). Supersaturated solutions of fat stains in dilute isopropanol for demonstration of acute fatty degeneration not shown by Herxheimer's technique. *Archives of Pathology and Laboratory Medicine online* **36**: 432.

Lindon, JC; Holmes, E and Nicholson, JK (2003) So what's the deal with metabonomics? *Analytical Chemistry* **75**: 384A–391A.

Livak, KJ and Schmittgen, TD (2001). Analysis of relative gene expression data using real-time quantitative PCR and the 2(-Delta Delta C(T)) Method. *Methods* **25**: 402-408.

Loffreda, S; Yang, SQ; Lin, HZ; Karp, CL; Brengaman, ML; Wang, DJ; Klein, AS; Bulkley, GB; Bao, C; Noble, PW; Lane, MD and Diehl, AM (1998). Leptin regulates proinflammatory immune responses. *The Journal of the Federation o American Societies for Experimental Biology* **12**: 57–65.

Lolmede, K; Durand de Saint Front, V; Galitzky, J; Lafontan, M and Bouloumie, A (2003). Effects of hypoxia on the expression of proangiogenic factors in differentiated 3T3-F442A adipocytes. *International Journal of Obesity* **27**: 1187-1195.

Lonnqvist F; Krief, S; Strosberg, AD; Nyberg, B; Emorine, LJ and Arner, P (1993). Evidence for a functional β3-adrenoceptor in man. *British Journal of Pharmacology* **110**: 929–936.

Louet, JF; Coste, A; Amazit, L; Tannour-Louet, M; Wu, RC; Tsai, SY; Tsai, MJ; Auwerx, J and O'Malley, BW (2006). Oncogenic steroid receptor coactivator-3 is a key regulator of the white adipogenic program. *Proceedings of the National Academy of Sciences USA* **103**: 17868-17873.

Lowell, BB; S-Susulic, V; Hamann, A; Lawitts, JA; Himms-Hagen, J; Boyer, BB; Kozak, LP and Flier, JS (1993). Development of obesity in transgenenic mice after genetic ablation of brown adipose tissue. *Nature* **366**: 740–742

Lu, S; Nishimura, K; Mohammad, AH; Jisaka, M; Nagaya, T and Yokota, K (2003). Regulation and role of arachidonate cascade during changes in life cycle of adipocytes. *Applied Biochemistry and Biotechnology* **118**: 133-153.

Lyngso, D; Simonsen, L and Bulow, J (2002). Metabolic effects of interleukin-6 in human splanchnic and adipose tissue. *The Journal of Physiology* **543**: 379–386.

Ma, K; Nunemaker, CS; Wu, R; Chakrabarti, SK; Taylor-Fishwick, DA and Nadler, JL (2010). 12-Lipoxygenase products reduce Insulin secretion and β-cell viability in human islets. *The Journal of Clinical Endocrinology and Metabolism* **95**: 887–893.

Ma, LJ; Mao, SL; Taylor, KL; Kanjanabuch, T; Guan, Y; Zhang, Y; Brown, NJ; Swift, LL; McGuinness, OP; Wasserman, DH; Vaughan, DE and Fogo, AB (2004). Prevention of obesity and insulin resistance in mice lacking plasminogen activator inhibitor 1. *Diabetes* **53**: 336-346.

MacDougald, OA and Lane, MD (1995). Transcriptional regulation of gene expression during adipocyte differentiation. *Annual Review of Biochemistry* **64**: 345-73.

MacDougald, OA; Hwang, CS; Fan, H and Lane, MD (1995). Regulated expression of the obese gene product (leptin) in white adipose tissue and 3T3-L1 adipocytes. *Proceedings of the National Academy of Sciences USA* **92**: 9034-9037.

Mackall, JC; Student, AK; Efthimios, P and Lane, MD (1976). Induction of lipogenesis during differentiation in a "preadipocyte" cell line. *The Journal of Biological Chemistry* **251**: 6462-6464.

Madsen, L; Petersen, RK; Sorensen, MB; Jorgensen, C; Hallenborg, P; Pridal, L; Fleckners, J; Amri, EZ; Krieg, P; Furstenberger, G; Berge, RK and Kristiansen, K (2003). Adipocyte differentiation of 3T3-L1 preadipocytes is dependent on lipoxygenase activity during the initial stages of the differentiation process. *Biochemical Journal* **375**: 539–549.

Maeda, K; Okubo, K; Shimomura, I; Funahashi, T; Matsuzawa, Y and Matsubara, K (1996). cDNA cloning and expression of a novel adipose specific collagen-like factor, apM1 (AdiPose Most abundant Gene transcript 1). Biochemical and Biophysical Research Communications 221: 286-289.

Maeda, N; Takahashi, M; Funahashi, T; Kihara, S; Nishizawa, H; Kishida, K; Nagaretani, H; Matsuda, M; Komuro, R; Ouchi, N; Kuriyama, H; Hotta, K; Nakamura, T; Shimomura, I and Matsuzawa, Y (2001). PPARgamma ligands increase expression and plasma concentrations of adiponectin, an adipose-derived protein. *Diabetes* **50**: 2094-2099.

Maffei, M; Halaas, J; Ravussin, E; Pratley, RE; Lee, GH; Zhang, Y; Fei, H; Kim, S; Lallone, R; Ranganathan, S; Kern, PA and Friedman, JM (1995). Leptin levels in human and rodent: measurement of plasma leptin and ob RNA in obese and weight-reduced subjects. *Nature Medicine* **1**: 1155-1161.

Maier, JA; Hla, T and Maciag, T (1990). Cyclooxygenase is an immediate-early gene induced by interleukin-1 in human endothelial cells. *The Journal of Biological Chemistry* **265**: 10805–10808.

Makarov, A (2000). Electrostatic axially harmonic orbital trapping: a high-performance technique of mass analysis. *Analytical Chemistry* **72**: 1156–1162.

Makarov, A; Denisov, E; Lange, O and Horning, S (2006). Dynamic range of mass accuracy in LTQ Orbitrap hybrid mass spectrometer. *Journal of the American Society for Mass Spectrometry* **17**: 977-982.

Mantzoros, CS; Qu, D; Frederich, RC; Susulic, VS; Lowell, BB; Maratos-Flier, E and Flier, JS (1996). Activation of beta(3) adrenergic receptors suppresses leptin expression and mediates a leptin-independent inhibition of food intake in mice. *Diabetes* **45**: 909-914.

Maquoi, E; Munaut, C; Colige, A; Collen, D and Lijnen, HR (2002). Modulation of adipose tissue expression of murine matrix metalloproteinases and their tissue inhibitors with obesity. *Diabetes* **51**: 1093–1101.

Masaki, T; Chiba, S; Tatsukawa, H; Yasuda, T; Noguchi, H; Seike, M; et al (2004). Adiponectin protects LPS-induced liver injury through modulation of TNF-alpha in KK-Ay obese mice. *Hepatology* **40**: 177-184.

Mason, EE (1982). Vertical banded gastroplasty for obesity. *Archives of Surgery* **117**: 701-706.

Masuzaki, H; Paterson, J; Shinyama, H; Morton, NM; Mullins, JJ; Seckl, JR and Flier, JS (2001). A transgenic model of visceral obesity and the metabolic syndrome. *Science* **294**: 2166-2170.

Matsubara, M; Maruoka, S and Katayose, S (2002). Decreased plasma adiponectin concentrations in women with dyslipidemia. *The Journal of Clinical Endocrinology and Metabolsim* **87**: 2764–2769.

Matsuzawa, Y; Funahashi, T; Kihara, S and Shimomura, I (2004). Adiponectin and metabolic syndrome. *Arteriosclerosis, Thrombosis, and Vascular Biology* **24**: 29-33.

Matthews, VB; Allen, TL; Risis, S; Chan, MH; Henstridge, DC; Watson, N; Zaffino, LA; Babb, JR; Boon, J; Meikle, PJ; Jowett, JB; Watt, MJ; Jansson, JO; Bruce, CR and Febbraio, MA (2010). Interleukin-6-deficient mice develop hepatic inflammation and systemic insulin resistance. *Diabetologia* **53**: 2431–2441.

McClain, D (1998). Further insights into leptin action. *Endocrinology* **139**: 3679-3680.

McDermott, MF (2001). TNF and TNFR biology in health and disease. *Cellular and Molecular Biology* **47**: 619-635.

McGiff, JC (1991). Cytochrome P-450 metabolism of arachidonic acid. *Annual Review of Pharmacology and Toxicology* **31**: 339-369.

McKeigue, PM. **Metabolic consequences of obesity and body fat pattern: lessons from migrant studies**. In: Chadwick DJ, Cardew OC (eds). The origins and consequences of obesity. Chichester, Wiley, 1996, pp. 54-67 (Ciba Foundation Symposium 2001).

McLuckey, SA and Wells, JM (2001). Mass analysis at the advent of the 21st century. *Chemical Reviews* **101**: 571.

McMinn, JE; Baskin, DG and Schwartz, MW (2000). Neuroendocrine mechanisms regulating food intake and body weight. *Obesity Reviews* **1**: 37-46.

Medhora, M; Daniels, J; Mundey, K; Fisslthaler, B; Busse, R; Jacobs, ER and Harder, DR. Epoxygenase-driven angiogenesis in human lung microvascular endothelial cells. *American Journal of Physiology - Heart and Circulatory Physiology* **284**: H215-H224.

Memon, RA; Feingold, KR; Moser, AH; Fuller, J and Grunfield, C (1998). Regulation of fatty acid transport protein and fatty acid translocase mRNA levels by endotoxin and cytokines.

Miell, JP; Englaro, P and Blum, WF (1996). Dexamethasone induces an acute and sustained rise in circulating leptin levels in normal human subjects. *Hormone and Metabolic Research* **28**: 704-707.

Miles, EA; Allen, E and Calder, PC (2002). *In vitro* effects of eicosanoids derived from different 20-carbon Fatty acids on production of monocyte-derived cytokines in human whole blood cultures. *Cytokine* **20**: 215–223.

Miles, EA; Allen and E; Calder, PC (2002). *In vitro* effects of eicosanoids derived from different 20-carbon Fatty acids on production of monocyte-derived cytokines in human whole blood cultures. *Cytokine* **20**: 215–223.

Miles, PD; Romeo, OM; Higo, K; Cohen, A; Rafaat, K and Olefsky, JM (1997). TNF-alpha-induced insulin resistance *in vivo* and its prevention by troglitazone. *Diabetes* **46**: 1678-1683.

Miller, CW; Casimir, DA and Ntambi, JM (1996). The mechanism of inhibition of 3T3–L1 preadipocyte differentiation by prostaglandin F2alpha. *Endocrinology* **137**: 5641–5650.

Minami, M; Ohno, S; Kawasaki, H; Radmark, O; Samuelsson, B; Jornvall, H; Shimizu, T; Seyama, Y and Suzuki, K (1987). Molecular cloning of a cDNA coding for human leukotriene A4 hydrolase. *The Journal of Biological Chemistry* **262**: 13873–13876.

Miyazawa-Hoshimoto, S; Takahashi, K; Bujo, H; Hashimoto, N; Yagui, K and Saito, Y (2005). Roles of degree of fat deposition and its localization on VEGF expression in adipocytes. *American Journal of Physiology - Endocrinology and Metabolism* **288**: E1128-1136.

Miyoshi, H; Souza, SC; Zhang, HH; Strissel, KJ; Christoffolete, MA; Kovsan, J; Rudich, A; Kraemer, FB; Bianco, AC; Obin, MS; Greenberg and AS (2006). Perilipin Promotes Hormone-sensitive Lipase-mediated Adipocyte Lipolysis via Phosphorylation-dependent and -independent Mechanisms. *The Journal of Biological Chemistry* **281**: 15837–15844.

Mizuno, TM; Kleopoulos, SP; Bergen, HT; Roberts, JL; Priest, CA and Mobbs, CV (1998). Hypothalamic pro-opiomelanocortin mRNA is reduced by fasting and [corrected] in ob/ob and db/db mice, but is stimulated by leptin. *Diabetes* **47** : 294 –297.

Mizuno, TM; Makimura, H; Silverstein, J; Roberts, JL; Lopingco, T and Mobbs, CV (1999). Fasting regulates hypothalamic neuropeptide Y, agouti-related peptide, and proopiomelanocortin in diabetic mice independent of changes in leptin or insulin. *Endocrinology* **140**: 4551–4557.

Mohamed-Ali, V; Goodrick, S; Rawesh, A; Katz, DR; Miles, JM; Yudkin, JS; Klein, S and Coppack, SW (1997). Subcutaneous adipose tissue releases interleukin-6, but not tumor necrosis factor-alpha, *in vivo*. *The Journal of Clinical Endocrinology and Metabolism* **82**: 4196-4200.

Moinat, M; Deng, C; Muzzin, P; Assimacopolulos-Jeannet, J; Seydoux, J; Dulloo, A and Giacobino, J (1995). Modulation of obese gene expression in rat brown and white adipose tissues. *Federation of European Biochemical Societies Letters* **373**: 131–134.

Mokdad, AH; Bowman,A; Ford, ES; Vinicor, F; Marks, JS and Koplan, JP (2001). The continuing epidemics of obesity and diabetes in the United States. *The Journal of the American Medical Association* **286**: 1195-1200.

Moncada, S; Gryglewski, R; Bunting, S and Vane, JR (1976). An enxyme isolated from arteries transforms prostaglandin endoperoxides to an unstable substance that inhibits platelet aggregation. *Nature* **263**: 663-665.

Montague, CT; Prins, JB; Sanders, L; Zhang, J; Sewter, CP; Digby, J; Byrne, CD and O'Rahilly, S (1998). Depot-related gene expression in human subcutaneous and omental adipocytes. *Diabetes* **47**: 1384-1391.

Morham, SG; Langenbach, R; Loftin, CD; Tiano, HF; Vouloumanos, N; Jennette, JC; Mahler, JF; Kluckman, KD; Ledford, A and Lee, CA; Smithies, O. Prostaglandin synthase 2 gene disruption causes severe renal pathology in the mouse. *Cell* **83**: 473-478.

Morita, I; Schindler, M; Regier, MK; Otto, JC; Hori, T; DeWitt, DL and Smith, WL (1995). Different intracellular locations for prostaglandin endoperoxide H synthase-1 and -2. *The Journal of Biological Chemistry* **270**: 10902–10908.

Mukherjee, S and Maxfield, FR (2000). Role of membrane organization and membrane domains in endocytic lipid trafficking. *Traffic* **1**: 203–211.

Mun, EC; Blackburn, GL and Matthews, JB (2001). Current status of medical and surgical therapy for obesity. *Gastroenterology* **120**: 669-681.

Munzenmaier, DH and Harder, DR (2000). Cerebral microvascular endothelial cell tube formation: role of astrocytic poxyeicosatrienoic acid release. *American Journal of Physiology - Heart and Circulatory Physiology* **278**: H1163-H1167.

Murata, T; Ushikubi, F; Matsuoka, T; Hirata, M; Yamasaki, A; Sugimoto, Y; Ichikawa, A; Aze, Y; Tanaka, T; Yoshida, N; Ueno, A; Oh-ishi, S and Narumiya, S (1997). Altered pain perception and inflammatory response in mice lacking prostacyclin receptor. *Nature* **388**: 678–682

Murph, M; Tanaka, T; Pang, J; Felix, E; Liu, S; Trost, R; Godwin, AK; Newman, R and Mills, G (2007). Liquid chromatography mass spectrometry for quantifying plasma lysophospholipids: potential biomarkers for cancer for diagnosis. *Methods in Enzymology* **433**: 1–25.

Murr, MM; Balsiger, BM; Kennedy, FP; Mai, JL and Sarr, MG (1999). Malabsorptive procedures for severe obesity: comparison of pancreaticobiliary bypass and very very long limb Roux-en-Y gastric bypass. *Journal of Gastrointestinal Surgery* **3**: 607– 612.

Nakae, J and Accili, D (1999). The mechanism of insulin action. *Journal of Pediatric Endocrinology and Metabolism* **12**: 721-731.

Napolitano, A; Lowell, BB; Damm, D; Leibel, RL; Ravussin, E; Jimerson, DC; Lesem, MD; Van Dyke, DC; Daly, PA; Chatis, P et al. (1994). Concentrations of adipsin in blood and rates of adipsin secretion by adipose tissue in humans with normal, elevated and diminished adipose tissue mass. *International Journal of Obesity and Related Metabolic Disorders* **18**: 213-218.

Napolitano, L (1963). The differentiation of white adipose cells. An electron microscope study. *The Journal of Cell Biology* **18**: 663-679.

Narumiya, S; Sugimoto, Y and Ushikubi, F (1999). Prostanoid receptors: Structures, properties, and functions. *Physiological Reviews* **79:** 1193–1226.

Natarajan, R and Nadler, JL (2004). Lipid inflammatory mediators in diabetic vascular disease. *Arteriosclerosis, Thrombosis, and Vascular Biology* **24**: 1542–1548.

Nedergaard, J; Bengtsson, T and Cannon, B (2007). Unexpected evidence for active brown adipose tissue in adult humans. *American Journal of Physiology - Endocrinology and Metabolism* **293**: E444-452.

Needleman, P; Moncada, S; Bunting, S; Vane, JR; Hamberg, M and Samuelsson, B (1976). Identification of an enzyme in platelet microsomes which generates thromboxane Aa from prostaglandin endoperoxides. *Nature* **261**: 558-560.

Negishi, M; Sugimoto, Y and Ichikawa, A (1995). Prostaglandin E receptors. *Journal of Lipid Mediators and Cell Signalling* **12**: 379–391.

Negrel, R; Gaillard, D and Ailhaud, G (1989). Prostacyclin as a potent effector of adipose-cell differentiation. *Biochemical Journal* **257**: 399–405.

Netea, MG; joosten, LA; Lewis, E; Jensen, DR; Voshol, PJ; Kullberg, BJ; Tack, CJ; van Krieken, H; Kim, SH; Stalenhoef, AF; van de Loo, FA; Verschueren, I; Pulawa, L; Akira, S; Eckel, RH; Dinarello, CA; van den Berg, W and van der Meer, JW (2006). Deficiency of interleukin-18 in mice leads to hyperphagia, obesity and insulin resistance. *Nature Medicine* **12**: 650–656.

Nicholson, JK; Lindon, JC and Holmes, E (1999). 'Metabonomics': Understanding the metabolic responses of living systems to pathophysiological stimuli via multivariate statistical analysis of biological NMR spectroscopic data. *Xenobiotica* **29**: 1181–1189.

Nishizawa, H; Shimomura, I; Kishida, K; Maeda, N; Kuriyama, H; Nagaretani, H; Matsuda, M; Kondo, H; Furuyama, N; Kihara, S; Nakamura, T; Tochino, Y; Funahashi, T and Matsuzawa, Y (2002). Androgens decrease plasma adiponectin, an insulin-sensitizing adipocyte-derived protein. *Diabetes* **51**: 2734-2741.

Nisoli, E; Briscini, L; Giordano, A; Tonello, C; Weisbrock, SM; Uysal, KT; Cinti, S; Carruba, MO and Hotamisligil, GS (2000). Tumor necrosis factor alpha mediates apoptosis of brown adipocytes and defective brown adipocyte function in obesity. *Proceedings of the National Academy of Sciences USA* **97**: 8033-8038.

Node, K; Huo, Y; Ruan, X; Yang, Y; Spiecker, M; Ley, K; Zeldin, DC and Liao, JK (1999). Anti-inflammatory properties of cytochrome P450 epoxygenase-derived eicosanoids. *Science* **285**: 1276-1279.

Nonogaki, K; Fuller, GM; Fuentes, NL; Moser, AH; Staprans, I; Grunfeld, C and Feingold, KR (1995). Interleukin-6 stimulates hepatic triglyceride secretion in rats. *Endocrinology* **136**: 2143–2149.

Ntambi, JM and Kim, YC (2000). Adipocyte differentiation and gene expression. *Journal of Nutrition* **130**: 3122S-3126S.

Ntambi, JM; Buhrow, SA; Kaestner, KH; Christy, RJ; Sibley, E; Kelly, , Jr TJ and Lane, MD (1988). Differentiation-induced gene expression in 3T3-L1 preadipocytes. Characterization of a differentially expressed gene encoding stearoyl-CoA desaturase. *The Journal of Biological Chemistry* 263: 17291-17300.

Nunemaker, CS; Chen, M; Pei, H; Kimble, SD; Keller, SR; Carter, JD; Yang, Z; Smith, KM; Wu, R; Bevard, MH; Garmey, JC and Nadler, JL (2008). 12-Lipoxygenase-knockout mice are resistant to inflammatory effects of obesity induced by western diet. *American Journal of Physiology - Endocrinology and Metabolism* **295**: E1065–E1075.

Nygren, H; Seppanen-Laakso, T; Castillo, S; Hyotylainen, T and Oresic, M (2011). Chapter 15: Liquid-chromatography-mass spectrometry (LC-MS)-based lipidomics for studies of body fluids and tissues. Metz, TO (Ed.) **Metabolic Profiling: Methods and Protocols** *Methods in Molecular Biology* **208***. New York:* Humana Press pp 247-257.

O'Neill, GP; Mancini, JA; KargmanS; Yergey, J; Kwan, MY; Falgueyret, JP; Abramovitz, M; Kennedy, BP; Ouellet, M and Cromlish, W (1994). Overexpression of human prostaglandin G/H synthase-1 and -2 by recombinant vaccinia virus: Inhibition by nonsteroidal anti-inflammatory drugs and biosynthesis of 15-hydroxyeicosatetraenoic acid. *Molecular Pharmacology* **45**: 245–254.

Ogawa, H; Nielsen, S and Kawakami, M (1989). Cachetin/tumor necrosis factor and interleukin-1 show different modes of combined effect on lipoprotein lipase and intracellular lipolysis. *Biochimica et Biophysica Acta* **1003**: 131-135.

Oh, W; Abu-Elheiga, L; Kordari, P; Gu, Z; Shaikenov, T; Chirala, SS and Wakil, SJ (2005). Glucose and fat metabolism in adipose tissue of acetyl-CoA carboxylase 2 knockout mice. *Proceedings of the National Academy of Science USA* **102**: 1384–1389.

Ohtoshi, K; Kaneto, H; Node, K; Nakamura, Y; Shiraiwa, T; Matsuhisa, M and Yamasaki, Y (2005). Association of soluble epoxide hydrolase gene polymorphism with insulin resistance in type 2 diabetic patients. *Biochemical and Biophysical Research Communications* **331**: 347–350.

Okamoto, H; Obici, S; Accili, D and Rossetti, L (2005). Restoration of liver insulin signaling in Insr knockout mice fails to normalize hepatic insulin action. *The Journal of Clinical Investigation* **115**: 1314–1322.

Okamoto, Y; Kihara, S; Ouchi, N; Nishida, M; Arita, Y; Kumada, M; Ohashi, K; Sakai, N; Shimomura, I; Kobayashi, H; Terasaka, N; Inaba, T; Funahashi, T and Matsuzawa, Y (2002). Adiponectin reduces atherosclerosis in apolipoprotein E-deficient mice. *Circulation* **106**: 2767-2770.

Okazaki, H; Igarashi, M; Nishi, M; Tajima, M; Sekiya, M and Okazaki, S (2006). Identification of a novel member of the carboxylesterase family that hydrolyzes triacylglycerol: a potential role in adipocyte lipolysis. *Diabetes* **55**: 2091–2097.

Olefsky, JM (1975). Effect of dexamethasone on insulin binding, glucose transport, and glucose oxidation of isolated rat adipocytes. *The Journal of Clinical Investigation* **56**: 1499-1508.

Olefsky, JM; Johnson, J; Liu, F; Jen, P and Reaven, G (1975). The effect of acute and chronic dexamethasone administration on insulin binding to isolated rat hepatocytes and adipocytes. *Metabolism* **24**: 517-527.

Oliff, A; Defeo-Jones, D; Boyer, M; Martinez, D; Kiefer, D; Vuocolo, G; Wolfe, A and Socher, SH (1987). Tumors secreting human TNF/ cachectin induce cachexia in mice. *Cell* **50**: 555-563.

Osher, E; Weisinger, G; Limor, R; Tordjman, K and Stern, N (2006). The 5 lipoxygenase system in the vasculature: emerging role in health and disease. *Molecular and Cellular Endocrinology Journal* **27**: 201–206.

Oshima, M; Dinchuk, JE; Kargman, SL; Oshima, H; Hancock, B; Kwong, E; Trzaskos, JM; Evans, JF and Taketo, MM (1996). Suppression of intestinal polyposis in Apc delta716 knockout mice by inhibition of cyclooxygenase 2 (COX-2). *Cell* **87**: 803-809.

Osuga, JI; Ishibashi, S; Oka, T; Yagyu, H; Tozawa, R; Fujimoto, A; Shionoiri, F; Yahagi, N; Kraemer, FB and Tsutsumi, O. Targeted disruption of hormone-sensitive lipase results in male sterility and adipocyte hypertrophy, but not in obesity. *Proceedings of the National Academy of Science USA* **97**: 787–792.

Otero, M; Lago, R; Lago, F; Casanueva, FF; Dieguez, C; Gomez-Reino, JJ and Gualillo, O (2005). Leptin, from fat to inflammation: old questions and new insights. Federation of European Biochemical Societies Letters 579: 295-301.

Ottosson, M; Lonnroth, P; Bjorntorp, P and Eden, S (2000). Effects of cortisol and growth hormone on lipolysis in human adipose tissue. *The Journal of Clinical Endocrinology and Metabolism* **85**: 799–803.

Ouchi, N; Kihara, S; Arita, Y; Maeda, K; Kuriyama, H; Okamoto, Y; Hotta, K; Nishida, M; Takahashi, M; Nakamura, T; Yamashita, S; Funahashi, T and Matsuzawa, Y (1999). Novel modulator for endothelial adhesion molecules: adipocyte-derived plasma protein adiponectin. *Circulation* **100**: 2473-2476.

Ouchi, N; Kihara, S; Arita, Y; Okamoto, Y; Maeda, K; Kuriyama, H; Hotta, K; Nishida, M; Takahashi, M; Muraguchi, M; Ohmoto, Y; Nakamura, T; Yamashita, S; Funahashi, T and Matsuzawa, Y (2000). Adiponectin, an adipocyte-derived plasma protein, inhibits endothelial NF-kappaB signaling through a cAMP-dependent pathway. *Circulation* **102**: 1296-1301.

Ozata, M; Ozdemir, IC and Licinio, J (1999). Human leptin deficiency caused by a missense mutation: multiple endocrine defects, decreased sympathetic tone, and immune system dysfunction indicate new targets for leptin action, greater central than peripheral resistance to the effects of leptin, and spontaneous correction of leptin-mediated defects. *The Journal of Clinical Endocrinology and Metabolism* **84**: 3686–3695.

Ozcan, U; Cao, Q; Yilmaz, E; Lee, AH; Iwakoshi, NN; Ozdelen, E; Tuncman, G; Gorgun, C; Glimcher, LH and Hotamisligil, GS (2004). Endoplasmic reticulum stress links obesity, insulin action, and type 2 diabetes. *Science* **306**: 457-461.

Pantoja, C; Huff, JT and Yamamoto, KR (2008). Glucocorticoid signaling defines a novel commitment state during adipogenesis *In Vitro*. *Molecular Biology of the Cell* **19**: 4032–4041.

Papaspyrou-Rao, S; Schneider, SH; Petersen, RN and Fried, SK (1997). Dexamethasone increases leptin expression in humans *in vivo*. *The Journal of Clinical Endocrinology and Metabolism* **82**: 1635–1637.

Path, G; Bornstein, SR; Gurniak, M; Chrousos, GP; Scherbaum, WA and Hauner, H (2001). Human breast adipocytes express interleukin-6 (IL-6) and its receptor system: increased IL-6 production by beta-adrenergic activation and effects of IL-6 on adipocyte function. *The Journal of Clinical Endocrinology and Metabolism* **86**: 2281-2288.

Paul, W and Steinwedel, H (1953). Ein neues Massenspektrometer ohne Magnetfeld. *RZeitschrift fur Naturforschung A* **8**: 448-450.

Pearson, K (1901). On Lines and Planes of Closest Fit to Systems of Points in Space *Philosophical Magazine* **2**: 559–572.

Peeraully, MR; Jenkins, JR and Trayhurn P (2004). NGF gene expression and secretion in white adipose tissue: regulation in 3T3-L1 adipocytes by hormones and inflammatory cytokines. *American Journal of Physiology - Endocrinology and Metabolism* **287**: E331-339.

Peiris, AN; Sothmann, MS; Hoffmann, RG; Hennes, MI; Wilson, CR; Gustafson, AB and Kissbah, AH (1989). Adiposity, fat distribution, and cardiovascular risk. *Annuals of Internal Medicine* **110**:867–872.

Pelleymounter, MA; Cullen, MJ; Baker, MB; Hecht, R; Winters, D; Boone, T and Collins, F (1995). Effects of the obese gene product on body weight regulation in ob/ob mice. *Science* **269**: 540-543.

Peraldi, P; Xu, M and Spiegelman, BM (1997). Thiazolidinediones block tumor necrosis factor- -induced inhibition of insulin signalling. *Journal of Clinical Investigation* **100**: 1863–1869.

Permana, PA; Menge, C and Reaven, PD (2006). Macrophage-secreted factors induce adipocyte inflammation and insulin resistance. *Biochemical and Biophysical Research Communications* **341**: 507–514.

Petersen, EW; Carey, AL; Sacchetti, M; Steinberg, GR; Macaulay, SL; Febbraio, MA and Pedersen, BK (2005). *American Journal of Physiology - Endocrinology and Metabolism* **288**: E155–E162.

Pietilainen, KH; Sysi-Aho, M; Rissanen, A; Seppanen-Laakso, T; Yki-Jarvinen, H; Kaprio, J and Oresic, M (2007). Acquired obesity is associated with changes in the serum lipidomic profile independent of genetic effects – a monozygotic twin study. *Plos ONE* **2**: e218.

Piomelli, D (1993). Arachidonic acid in cell signalling. *Current opinion in Cell Biology* **5**: 274–280.

Pirro, M; Mauriege, P; Tchernof, A; Cantin, B; Dagenais, GR; Despres, JP and Lamarche, B (2002). Plasma free fatty acid levels and the risk of ischemic heart disease in men: prospective results from the Quebec Cardiovascular Study. *Atherosclerosis* **160**: 377–384.

Poirier, P and Eckel, RH (2002). Obesity and cardiovascular disease. *Current Atherosclerosis Reports***4**: 448-453.

Poitou, C; Viguerie, N; Cancello, R; De Matteis, R; Cinti, S; Stich, V; Coussieu, C; Gauthier, E; Courtine, M; Zucker, JD; Barsh, GS; Saris, W; Bruneval, P; Basdevant, A; Langin, D and Clement, K (2005). Serum amyloid A: production by human white adipocyte and regulation by obesity and nutrition. *Diabetologia* **48**: 519-528.

Pola, R; Gaetani, E; Flex, A; Aprahamian, TR; Bosch-Marce, M; Losordo, DW; Smith, RC and Pola, P (2004). Comparative analysis of the *in vivo* angiogenic properties of stable prostacyclin analogs: a possible role for peroxisome proliferator activated receptors.*Journal of Molecular and Cellular Cardiology* **36**: 363–370.

Postic, C and Girard, J (2008). Contribution of de novo fatty acid synthesis to hepatic steatosis and insulin resistance: lessons from genetically engineered mice. *The Journal of Clinical Investigation* **118**: 829 – 838.

Poulos, SP; Dodson, MV and Hausman, GJ (2010). Cell line models for differentiation: preadipocytes and adipocytes. *Experimental Biology and Medicine* **235**: 1185-1193.

Power, G (1989): Biology of temperature: the mammalian fetus. *Journal of Developmental Physiology* **12**: 295–304.

Poynten, AM; Gan, SK; Kriketos, AD; Campbell, LV and Chisholm, DJ (2005). Circulating fatty acids, non-high density lipoprotein cholesterol, and insulin-infused fat oxidation acutely Iinfluence whole body insulin sensitivity in nondiabetic men. *The Journal of Clinical Endocrinology and Metabolism* **90**: 1035-1040.

Pradhan, AD; Manson, JE; Rifai, N; Buring, JE and Ridker, PM (2001). C-reactive protein, interleukin 6, and risk of developing type 2 diabetes mellitus. *The Journal of the American Medical Association* **286**: 327–334.

Pravenec, M; Kazdova, L; Maxova, M; Zidek, V; Mlejnek, P; Simakova, M and Kurtz, TW (2008). Long-term pioglitazone treatment enhances lipolysis in rat adipose tissue. *International Journal of Obesity* **32**: 1848-1853.

Price, RA and Gottesman, II (1991). Body fat in identical twins reared apart: roles for genes and environment. *Behaviour Genetics* **21**: 1–7.
Prins, JB; Niesler, CU; Winterford, CM; Bright, NA; Siddle, K; O'Rahilly, S; Walker, NI and Cameron, DP (1997). Tumor necrosis factor-alpha induces apoptosis of human adipose cells. *Diabetes* **46**: 1939-1944.

Purnell, JH (1962). **Gas Chromatography**. New York: Wiley.

Radmark, O (2003). 5-lipoxygenase-derived leukotrienes. *Arteriosclerosis, Thrombosis, and Vascular Biology* **23**: 1140–1142.

Radonic, A; Thulke, S; Mackay, IM; Landt, O; Siegert, W and Nitsche, A (2004). Guideline to reference gene selection for quantitative real-time PCR. *Biochemical and Biophysical Research Communications* **313**: 856-862.

Rainville, PD; Stumpf, CL; Shockcor, JP; Plumb, RS and Nicholson, JK (2007). Novel application of reversed-phase UPLC-oaTOF-MS for lipid analysis in complex biological mixtures: a new tool for lipidomics. *Journal of proteome research* **6**: 552–558.

Rajkumar, K; Modric, T and Murphy, LJ (1999). Impaired adipogenesis in insulin-like growth factor binding protein-1 transgenic mice. *Journal of Endocrinology* **162**: 457–465.

Randle, PJ; Garland, PB; Hales, CN and Newsholme, EA (1963). The glucose fatty-acid cycle. Its role in insulin sensitivity and the metabolic disturbances of diabetes mellitus. *Lancet* **1**: 785–789.

Ravussin, E; Lillioja, S; Knowler, WC; Christin, L; Freymond, D; Abbott, WGH: Boyce, V; Howard, BV and Bogardus, C (1988). Reduced rate of energy expenditure as a risk factor for bodyweight gain. *The New England Journal of Medicine* **318**: 467-472.

Rayner, DV and Trayhurn, P (2001). Regulation of leptin production: sympathetic nervous system interactions. *Journal of Molecular Medicine* **79**: 8-20.

Rayner, DV; Simon, E; Duncan, JS and Trayhurn, P (1998). Hyperleptinaemia in mice induced by administration of the tyrosine hydroxylase inhibitor alpha-methyl-p-tyrosine. Federation of European Biochemical Societies Letters 429: 395-398.

Razak, F; Anand, SS; Shannon, H; Vuksan, V; Davis, B; Jacobs, R; Teo, KK; McQueen, M and Yusuf, S (2007). Defining obesity cut points in a multiethnic population. *Circulation* **115**: 2111-2118.

Rea, R and Donnelly, R (2004). Resistin: an adipocyte-derived hormone. Has it a role in diabetes and obesity? D*iabetes Obesity and Metabolism* **6**: 163-170.

Reaven GM and Hoffman, BB (1987). A role for insulin in the aetiology and course of hypertension. *Lancet* **2**: 435–437.

Reaven, GM (1988). Banting lecture 1988: Role of insulin resistance in human disease. *Diabetes* **37**: 1595–1607.

Reaven, GM (2005). The insulin resistance syndrome: definition and dietary approaches to treatment. *Annual Review of Nutrition* **25**: 391-406.

Reilly, KB; Srinivasan, S; Hatley, ME; Patricia, MK; Lannigan, J; Bolick, DT; Vandenhoff, G; Pei, H; Natarajan, R; Nadler, JL and Hedrick, CC (2004). 12/15-Lipoxygenase activity mediates inflammatory monocyte/endothelial interactions and atherosclerosis *in vivo*. *The Journal of Biological Chemistry* **279**: 9440–9450.

Reisner, AH; Nemes, P and Bucholtz, C (1975). The use of Coomassie Brilliant Blue G-250 perchloric acid solution for staining in electrophoresis and isoelectric focusing on polyacrylamide gels. *Analytical Biochemistry* **64:** 509–516.

Ren, T; He, J; Jiang, H; Zu, L; Pu, S; Guo, X and Xu, G (2006). Metformin reduces lipolysis in primary rat adipocytes stimulated by tumor necrosis factor-alpha or isoproterenol. *Journal of Molecular Endocrinology* **37**: 175–183.

Renna, NF; Vazquez, MA; Lama, MC; Gonzalez, ES and Miatello, RM (2009). Effect of chronic aspirin administration on an experimental model of metabolic syndrome. *Clinical and Experimental Pharmacology and Physiology* **36**: 162–168.

Rentsch, J and Chiesi, M (1996). Regulation of ob gene mRNA levels in cultured adipocytes. Federation of European Biochemical Societies Letters 379: 55–59.

Reseland, JE; Haugen, F; Hollung, K; Solvoll, K; Halvorsen, B; Brude, I.R; Nenseter, MS; Christiansen, EN and Drevon, CA (2001). Reduction of leptin gene expression by dietary polyunsaturated fatty acids. *The Journal of Lipid Research* **42**: 743-750.

Reynisdottir, S; Langin, D; Carlstrom, K; Holm, C; Rossner, S and Arner, P (1995). Effects of weight reduction on the regulation of lipolysis in adipocytes of women with upper-body obesity. *Clinical Science* **89**: 421–429.

Ricci, RW; Ditzler, M and Nestor, LP (1994). Discovering the Beer-Lambert Law. *Journal of Chemical Education* **71**: 983-985.

Ricquier, D and Bouillaud, F (2000). Mitochondrial uncoupling proteins: from mitochondria to the regulation of energy balance. *The Journal of Physiology* **529 Pt 1**: 3-10.

Rinaldi-Carmona, M; Barth, F; Heaulme, M; Shire, D; Calandra, B; Congy, C; Martinez, S; Maruani, J; Neliat G; Caput, D; Ferrara, B; Soubrie, P; Breliere, JC and Le Fur, G (1994). SR141716A, a potent and selective antagonist of the brain cannabinoid receptor. *Federation of European Biochemical Societies Letters* **350**: 240–244.

Rivellese, AA; Maffettone, A; Lovine, C; Di Marino, L; Annuzzi, G; Mancini, M and Riccardi, G (1996). Longterm effects of fish oil on insulin resistance and plasma lipoproteins in NIDDM patients with hypertriglyceridemia. *Diabetes Care* **19**: 1207-1213.

Roberts, LD; McCombie, G; Titman, CM and Griffin, JL (2008). A matter of fat: an introduction to lipidomic profiling methods. *Journal of Chromatography B* **871**: 174-181.

Roberts, R; Hodson, L; Dennis, AL; Neville, MJ; Humphreys, SM; Harnden, KE; Micklem, KJ and Frayn, KN (2009). Markers of de novo lipogenesis in adipose tissue: associations with small adipocytes and insulin sensitivity in humans. *Diabetologia* **52**: 882 – 890.

Rodriguez, AM; Elabd, C; Delteil, F; Astier, J; Vernochet, C; Saint-Marc, P; Guesnet, J; Guezennec, A; Amri, EZ; Dani, C and Ailhaud, G (2004). Adipocyte differentiation of multipotent cells established from human adipose tissue. *Biochemical and Biophysical Research Communications* **315**: 255-263.

Rodriguez, AM; Pisani, D; Dechesne, CA; Turc-Carel, C; Kurzenne, JY; Wdziekonski, B; Villageois, A; Bagnis, C; Breittmayer, JP; Groux, H; Ailhaud, G and Dani, C (2005). Transplantation of a multipotent cell population from human adiposetissue induces dystrophin expression in the immunocompetent mdx mouse. *The Journal of Experimental Medicine* **201**: 1397-1405.

Rohana, A; Fadzilah Adibah, AM and Muhammad Roji, MS (2011). Oleate induces apoptosis in 3T3-L1 adipocytes. *World Academy of Science, Engineering and Technology* **57**: 1-4.

Romijn, JA and Fliers, E (2005). Sympathetic and parasympathetic innervation of adipose tissue: metabolic implications. *Current Opinion in Clinical Nutrition and Metabolic Care* **8**: 440-444.

Ronti, T: Lupattelli, G and Mannarino, E (2006). The endocrine function of adipose tissue: an update. *Clinical Endocrinology* **64**: 355-365.
Rose, G (1991). Population distributions of risk and disease. *Nutrition, Metabolism and Cardiovascular Diseases* **1**: 37-40.

Rosen, ED and Spiegelman, BM (2000). Molecular regulation of adipogenesis. *Annual Review of Cell and Developmental Biology* **16**: 145-171.

Rosen, ED and Spigelmann, BM (2006). Adipocytes as regulators of energy balance and glucose homeostasis. *Nature* **444**: 847-853.

Rosen, ED; Sarraf, P; Troy, AE; Bradwin, G; Moore, K; Milstone, DS; Spiegelman, BM and Mortensen, RM (1999). PPAR gamma is required for the differentiation of adipose tissue *in vivo* and *in vitro*. *Molecular Cell* **4**: 611–617.

Rosenbaum, M; Nicolson, M; Hirsh, J; Murphy, E; Chu, F and Leibel, RL (1997). Effects of weight change on plasma leptin concentrations and energy expenditure. *The Journal of Clinical Endocrinology and Metabolism* **82**: 3647–3654.

Rosenbaum, SE and Greenberg, AS (1998). The short- and long-term effects of tumor necrosis factor-a and BRL 49653 on peroxisome proliferator-activated receptor (PPAR)g2 gene expression and other adipocyte genes. *Molecular Endocrinology* **12**: 1150–1160.

Rotter, V; Nagaev, I and Smith, U (2003). Interleukin-6 (IL-6) induces insulin resistance in 3T3-L1 adipocytes and is, like IL-8 and tumor necrosis factor-alpha, overexpressed in human fat cells from insulin-resistant subjects. *The Journal of Biological Chemistry* **278**: 45777-45784.

Ruan, H; Hacohen, N; Golub, TR; Van Parijs, L and Lodish, HF (2002). Tumor necrosis factor-alpha suppresses adipocyte-specific genes and activates expression of preadipocyte genes in 3T3-L1 adipocytes: nuclear factor-kappaB activation by TNF-alpha is obligatory. *Diabetes* **51**: 1319-1336.

Rubin, CS; Hirsch, A; Fung, C and Rosen, OM (1978). Development of hormone receptors and hormonal responsiveness *in vitro*. Insulin receptors and insulin sensitivity in the preadipocyte and adipocyte forms of 3T3-L1 cells. *The Journal of Biological Chemistry* **253**: 7570-7578.

Russell, CD; Petersen, RN; Rao, SP; Ricci, MR; Prasad, A; Zhang, Y; Brolin, RE and Fried, S (1998). Leptin expression in adipose tissue from obese humans: depot-specific regulation by insulin and dexamethasone. *American Journal of Physiology - Endocrinology and Metabolism* **275**: E507–E515.

Ruzickova, J; Rossmeisl, M; Prazak, T; Flachs, P; Sponarova, J; Veck, M; Tvrzicka, E; Bryhn, M and Kopecky, J (2004). Omega-3 PUFA of marine origin limit diet-induced obesity in mice by reducing cellularity of adipose tissue. *Lipids* **39**: 1177-1185.

Ryden, M; Arvidsson, E; Blomqvist, L; Perbeck, L; Dicker, A and Arner, P (2004). Targets for TNF-alpha-induced lipolysis in human adipocytes. *Biochemical and Biophysical Research Communications* **318**: 168–175.

Sabio, G; Das, M; Mora, A; Zhang, Z; Jun, JY; Ko, HJ; Barrett, T; Kim, JK and Davis, RJ (2008). A stress signaling pathway in adipose tissue regulates hepatic insulin resistance. *Science* **322**: 1539–1543.

Saiki, RK; Scharf, S; Faloona, F; Mullis, KB; Horn, GT; Erlich, HA and Arnheim, N (1985). Enzymatic amplification of beta-globin genomic sequences and restriction site analysis for diagnosis of sickle cell anemia. *Science* **230**: 1350-1354.

Saito, M; Okamatsu-Ogura, Y; Matsushita, M; Watanabe, K; Yoneshiro, T; Nio-Kobayashi, J; Iwanaga, T; Miyagawa, M; Kameya, T; Nakada, K; Kawai, Y and Tsujisaki, M (2009). High incidence of metabolically active brown adipose tissue in healthy adult humans: effects of cold exposure and adiposity. *Diabetes* **58**:1526–1531.

Sakoda, H; Ogihara, T; Anai, M; Funaki, M; Inukai, K; Katagiri, H; Fukushima, Y; Onishi, Y; Ono, H; Fujishiro, M; Kikuchi, M; Oka, Y; Asano, T (2000). Dexamethasone-induced insulin resistance in 3T3-L1 adipocytes is due to inhibition of glucose transport rather than insulin signal transduction. Diabetes 49: 1700-1708.

Saladin, R; De Vos, P; Guerre-Millo, M; Leturque, A; Girard, J; Staels, B and Auwerx, J (1995). Transient increase in obese gene expression after food intake or insulin administration. *Nature* **377**: 527–529.

Samad, F; Yamamoto, K; Pandey, M and Loskutoff, DJ (1997). Elevated expression of transforming growth factor-beta in adipose tissue from obese mice. *Molecular Medicine* **3**: 37-48.

Sampath, H; Miyazaki, M; Dobrzyn, A and Ntambi, JM (2007). Stearoyl-CoA desaturase-1 mediates the pro-lipogenic effects of dietry saturated fat. *The Journal of Biological Chemistry* **282**: 2483-2493.

Santos-Alvarez, J; Goberna, R and Sanchez-Margalet, V (1999). Human leptin stimulates proliferation and activation of human circulating monocytes. *Cellular Immunology* **194**: 6–11.

Santry, HP; Gillen, DL and Lauderdale, DS (2005). Trends in bariatric surgical procedures. *Journal of the American Medical Association* **294**: 1909–1917.

Sarraf, P; Frederich, RC; Turner, EM; Ma, G; Jaskowiak, NT; Rivet, DJ III, Flier, JS; Lowell, BB; Fraker, DL and Alexander, HR (1997). Multiple cytokines and acute inflammation raise mouse leptin levels: potential role in inflammatory anorexia. *The Journal of Experimental Medicine* **185**: 171-175.

Sartipy, P and Loskutoff, DJ (2003). Monocyte chemoattractant protein 1 in obesity and insulin resistance. *Proceedings of the National Academy of Sciences USA* **100**: 7265-7270.

Scalbert, A; Brennan, L; Fiehn, O; Hankemeier, T; Kristal, BS; van Ommen, B; Pujos-Guillot, E; Verheij, E; Wishart, D and Wopereis, S (2009). Mass-spectrometry-based metabolomics: limitations and recommendations for future progress with particular focus on nutrition research. Metabolomics 5: 435-458.

Schafer, K; Fujisawa, K; Konstantinides, S and Loskutoff, DJ (2001). Disruption of the plasminogen activator inhibitor 1 gene reduces the adiposity and improves the metabolic profile of genetically obese and diabetic ob/ob mice. *The Journal of the Federation of American Societies for Experimental Biology* **15**: 1840-1842.

Schaffler, A; Neumeier, M; Herfarth, H; Furst, A; Scholmerich, J and Buchler, C (2005). Genomic structure of human omentin, a new adipocytokine expressed in omental adipose tissue. *Biochimica et Biophysica Acta* **1732**: 96–102.

Schmelzer, KR; Inceoglu, B; Kubala, L; Kim, IH; Jinks, SL; Eiserich, JP and Hammock, BD (2006). Enhancement of antinociception by coadministration of nonsteroidal anti-inflammatory drugs and soluble epoxide hydrolase inhibitors. *Proceedings of the National Academy of Science USA* **103**: 13646–13651.

Schmid, H; Cohen, CF; Henger A; Irrgang, D and Kretzler, M (2003). Validation of endogenous controls for gene expression analysis in microdissected human renal biopsies. *Kidney International* **64**: 356–360.

Schneider, WP; Pike, JE and Kupiecki, FP (1966). Determination of the origin of 9-keto-15-hydroxy-10,13-prostadienoic acid by a double-labelling technique. *Biochimica et Biophysica Acta* **125**: 611-613.

Schoeller, DA;Cella,LK; Sinha, MK and Caro, JF (1997). Entrainment of the diurnal rhythm of plasma leptin to meal timing. *The American Society for Clinical Investigation* **100**: 1882–1887.

Schoojans, K; Peinado-Onsurbe, J; Lefebvre, AM; Heyman, RA; Briggs, M; Deeb, S; Staels, B and Auwerx, J (1996). PPARalpha and PPARgamma activators direct a distinct tissue-specific transcriptional response via a PPRE in the lipoprotein lipase gene. *The EMBO Journal* **15**: 5336-5348.

Schoonjans, K; Steals, B and Auwerx, J (1996). Role of the peroxisome proliferator-activated receptor (PPAR) in mediating the effects of fibrates and fatty acids on gene expression. *The Journal of Lipid Research* **37**: 907–925.

Schwartz, MW and Brunzell, JD (1997). Regulation of body adiposity and the problem of obesity. *Arteriosclerosis, Thrombosis, and Vascular Biology* **17**: 233-238.

Schwartz, MW; Prigeon, RL; Kahn, SE; Nicolson, M; Moore, J; Morawiecki, A; Boyko, EJ and Porte D, Jr. (1997). Evidence that plasma leptin and insulin levels are associated with body adiposity via different mechanisms. *Diabetes Care* **20**: 1476-1481.

Schwartz, MW; Woods, SC; Porte, DJ; Seeley, RJ and Baskin, DG (2000). Central nervous system control of food intake. *Nature* **404**: 661-671.

Schwudke, D; Oegema, J; Burton, L; Entchev, E; Hannich, JT; Ejsing, CS; Kurzchalia, T; Shevchenko, A (2006). Lipid profiling by multiple precursor and neutral loss scanning driven by the data-dependent acquisition. *Analytical Chemistry* **78:** 585-595.

Scott, RE; Florine, DL; Wille, JJ, Jr. and Yun, K (1982a). Coupling of growth arrest and differentiation at a distinct state in the G1 phase of the cell cycle:GD. *Proceedings of the National Academy of Sciences* **79**: 845-849.

Scott, RE; Hoerl, BJ; Wille, JJ, Jr.; Florine, DL.; Krawisz, BR and Yun, K (1982b). Coupling of proadipocyte growth arrest and differentiation. II. A cell cycle model for the physiological control of cell proliferation. *The Journal of Cell Biology* **94**: 400-405.

Seagle, HM; Bessesen, DH and Hill, JO (1998). Effects of sibutramine on resting metabolic rate and weight loss in overweight women. *Obesity Research* **6**:115–121.

Sears, DD; Miles, PD; Chapman, J; Ofrecio, JM; Almazan, F; Thapar, D and Miller, YI (2009). 12/15-lipoxygenase is required for the early onset of high fat diet-induced adipose tissue inflammation and insulin resistance in mice. *PloS One* **4**: e7250.

Semb, H; Peterson, J; Tavernier, J and Olivecrona, T (1987). Multiple effects of tumor necrosis factor on lipoprotein lipase *in vivo*. *The Journal of Biochemistry***262**: 8390-8394.

Semenza, GL (2001). HIF-1 and mechanisms of hypoxia sensing. *Current Opinion in Cell Biology* **13**: 167-171.

Senn, JJ; Klover, PJ; Nowak, IA; Zimmers, TA; Koniaris, LG; Furlanetto, RW and Mooney, RA (2003). Suppressor of cytokine signaling-3 (SOCS-3), a potential mediator of interleukin-6-dependent insulin resistance in hepatocytes.*The Journal of Biological Chemistry* **278**: 13740-13746.

Seppanen-Laakso and Oresic, M (2009). How to study lipidomes. *Journal of Molecular Endocrinology* **42**: 185-190.

Serhan, CN; Jain, A; Marleau, S; Clish, C; Kantarci, A; Behbehani, B; Colgan, SP; Stahl, GL; Merched, A; Petasis, NA; Chan, L and Van Dyke, TE (2003). Reduced inflammation and tissue damage in transgenic rabbits overexpressing 15-ilpoxygenase and endogenous anti-inflammatory lipid mediators. *The Journal of Immunology* **171**: 6856–6865.

Serrero, G; Lepak, NM and Goodrich, SP (1992). Prostaglandin F2 alpha inhibits the differentiation of adipocyte precursors in primary culture. *Biochemical and Biophysical Research Communications* **183**: 438–442.

Sethi, JK and Hotamisligil, GS (1999). The role of TNF alpha in adipocyte metabolism. *Seminars in Cell and Developmental Biology* **10**: 19-29.

Sethi, JK; Xu, H; Uysal, KT; Wiesbrock, SM; Scheja, L and Hotamisligil, GS (2000). Characterisation of receptor-specific TNFalpha functions in adipocyte cell lines lacking type 1 and 2 TNF receptors. *Federation of European Biochemical Societies Letters* **469**: 77-82.

Severino, C; Brizzi, P; Solinas, A; Secchi, G; Maioli, M; Tonolo, G (2002). Low-dose dexamethasone in the rat: a model to study insulin resistance. *American Journal of Physiology - Endocrinology and Metabolism* **283**: E367–E373.

Shaw, J; Monticone, V and Paetkan, V (1978). Partial purification and molecular characterization of a lymphokine (co-stimulator) required for the mitogenic response of mouse thymocytes *in vitro*. *Journal of Immunology* **120**: 1967-1973.

Shen, WJ; Sridhar, K; Bernlohr, DA and Kraemer, FB (1999). Interaction of rat hormone-sensitive lipase with adipocyte lipidbinding protein. *Proceedings of the National Academy of Sciences* **96**: 5528–5532.

Shillabeer, G; Kumar, V; Tibbo, E and Lau, DC (1998). Arachidonic acid metabolites of the lipoxygenase as well as the cyclooxygenase pathway may be involved in regulating preadipocyte differentiation. *Metabolism* **47**: 461-466.

Siegel, SA; Shealy, DJ; Nakada, MT; Le, J; Woulfe, DS; Probert, L; Kollias, G; Ghrayeb, J; Vilcek, J and Daddona, PE (1995). The mouse/human chimeric monoclonal antibody cA2 neutralizes TNF *in vitro* and protects transgenic mice from cachexia and TNF lethality *in vivo*. *Cytokine* **7**: 15–25.

Siegrist-Kaiser, CA; Pauli, V; Juge Aubry, CE; Boss, O; Pernin, A; Chin, WW; Cusin, I; Rohner Jeanrenaud, F; Burger, AG; Zapf, J and Meier, CA (1997). Direct effects of leptin on brown and white adipose tissue. *The Journal of Clinical Investigation* **100**: 2858–2864.

Sinal, CJ; Miyata, M; Tohkin, M; Nagata, K; Bend, JR and Gonzalez, FJ (2000). Targeted disruption of soluble epoxide hydrolase reveals a role in blood pressure regulation. *The Journal of Biological Chemistry* **275**: 40504–40510.

Sinha, MK; Ohannesian, JP; Heiman, ML; Kriauciunas, A; Stephens, TW; Magosin, S; Marco, C and Caro, JF (1996). Nocturnal rise of leptin in lean, obese, and non-insulin-dependent diabetes mellitus subjects. *The Journal of Clinical Nutrition* **97**: 1344–1347.

Sjostrom, CD; Lissner, L; Wedelm H and Sjostrom, L (1999). Reduction in incidence of diabetes, hypertension and lipid disturbances after intentional weight loss induced by bariatric surgery: the SOS Intervention Study. *Obesity Research* **7**: 477-484.

Sjostrom, L; Rissanen, A; Andersen, T; Boldrin, M; Golay, A; Koppeschaar, HP and Krempf, M (1998). Randomised placebo-controlled trial of orlistat for weight loss and prevention of weight regain in obese patients. European Multicentre Orlistat Study Group. *The Lancet* **352**:167–172.

Skurk, T; Herder, C; Kraft, I; Muller-Scholze, S; Hauner, H and Kolb, H (2005a). Production and release of macrophage migration inhibitory factor from human adipocytes. *Endocrinology* **146**: 1006-1011.

Skurk, T; Kolb, H; Muller-Scholze, S; Rohrig, K; Hauner, H and Herder, C (2005b). The proatherogenic cytokine interleukin-18 is secreted by human adipocytes. *European Journal of Endocrinology* **152**: 863-868.

Slavin, BG; Ong, JM and Kern, PA (1994). Hormonal regulation of hormones ensitive lipase activity and mRNA levels in isolated rat adipocytes.*The Journal of Lipid Research* **35**: 1535–1541.

Smas, CM and Sul, HS (1993). Pref-1, a protein containing EGF-like repeats, inhibits adipocyte differentiation. *Cell* **73**: 725–734.

Smith, KA; Favata, MF and Oroszlan, S (1983). Production and characterization of monoclonal antibodies to human interleukin 2: strategy and tactics. *Journal of Immunology* **131**: 1808-1815.

Smith, KA; Gilbride, KJ and Favata, MF (1980). Lymphocyte activating factor promotes T-cell growth factor production by cloned marine lymphoma cells. *Nature* **287**: 853-855.

Smith, PJ; Wise, LS; Berkowitz, R; Wan, C and Rubin, CS (1988). Insulin-like growth factor-I is an essential regulator of the differentiation of 3T3-L1 adipocytes. *The Journal of Biological Chemistry* **263**: 9402-9408.

Smith, W (1989). Eicosanoids and their biochemical mechanisms of action. *Biochemical Journal* **259**: 315–324.

Soni, KG; Lehner, R; Metalnikov, P; O'Donnell, P; Semache, M; Gao, W; Ashman, K; Pshezhetsky, AV and Mitchell, GA (2004). Carboxylesterase 3 (EC 3.1.1.1) is a major adipocyte lipase. *The Journal of Biological Chemistry* **279**: 40683–40689.

Souza, SC; de Vargas, LM; Yamamoto, MT; Lien, P; Franciosa, MD; Moss, LG and Greenberg, AS (1998). Overexpression of perilipin A and B blocks the ability of tumor necrosis factor alpha to increase lipolysis in 3T3-L1 adipocytes. *The Journal of Biological Chemistry* **273**: 24665–24669.

Souza, SC; Palmer, HJ; Kang, YH; Yamamoto, MT; Muliro, KV; Paulson, KE and Greenberg, AS (2003). TNF-alpha induction of lipolysis is mediated through activation of the extracellular signal related kinase pathway in 3T3-L1 adipocytes.*Journal of Cellular Biochemistry* **89**: 1077–1086.

Spalding, KL; Arner, E; Westermark, PO; Bernard, S; Buchholz, BA; Bergmann, O; Blomqvist, L; Hoffstedt, J; Naslund, E; Britton, T; Concha, H; Hassan, M; Ryden, M; Frisen, J and Arner, P (2008). Dynamics of fat cell turnover in humans. *Nature* **453**: 783–787.

Spener, F; Lagarde, M; Geloen, A and Record, M (2003). Editorial: What is lipidomics? *European Journal of Lipid Science and Technology* **105**: 481-482.

Spiegelman, BM and Ginty, CA (1983). Fibronectin modulation of cell shape and lipogenic gene expression in 3T3-adipocytes. *Cell* **35**: 657-666.

Spiegelman, BM; Choy, L; Hotamisligil, GS; Graves, RA and Tontonoz, P (1993). Regulation of adipocyte gene expression in differentiation and syndromes of obesity/diabetes. The Journal of Biological Chemistry 268: 6823-6826.

Sporn, MB; Roberts, AB; Wakefield, LM and de Crombrugghe, B (1987). Some recent advances in the chemistry and biology of TGF beta. *The Journal of Cell Biology* **105**: 1039-1045.

Spranger, J; Kroke, A; Mohlig, M; Hoffman, K; Bergmann, MM; Ristow, M; Boeing, H and Pfeiffer, AF (2003). Inflammatory cytokines and the risk to develop type 2 diabetes: results of the prospective population-based European Prospective Investigation into Cancer and Nutrition (EPIC) – Potsdam Study. *Diabetes* **52**: 812-817.

Staiger, H; Kaltenbach, S; Staiger, K; Stefan, N; Fritsche, A; Guirguis, A; Peterfi, C; Weisser, M; Machicao, F; Stumvoll, M and Haring, HU (2004). Expression of adiponectin receptor mRNA in human skeletal muscle cells is related to *in vivo* parameters of glucose and lipid metabolism. *Diabetes* **53**: 2195-2201.

Stanley, S; Wynne, K; McGowan, B and Bloom, S (2005). Hormonal regulation of food intake. *Physiological Reviews* 85: 1131-1158.

Stephens, JM and Pekala PH (1991). Transcriptional repression of the GLUT4 and C/EBP genes in 3T3-L1 adipocytes by tumor necrosis factor-alpha. *The Journal of Biological Chemistry* **266**: 21839-21845.

Stephens, JM and Pekala, PH (1992). Transcriptional repression of the C/EBP-a and GLUT4 genes in 3T3-L1 adipocytes by tumor necrosis factor-a: Regualtion is coordinate and independent of protein synthesis. *The Journal of Biological Chemistry* **267**: 3580-1356.

Stephens, JM; Lee, J and Pilch, PF (1997). Tumour necrosis factor-alpha-induced insulin resistance in 3T3-L1 adipocytes Is accompanied by a loss of insulin receptor substrate-1 and GLUT4 expression without a loss of insulin receptor-mediated signal transduction. *The Journal of Biological Chenistry* **272**: 971-976.

Steppan, CM; Bailey, ST; Bhat, S; Brown, EJ; Banerjee, RR; Wright, CM; Patel, HR; Ahima, RS and Lazar, MA (2001). The hormone resistin links obesity to diabetes. *Nature* 409: 307-312.

Storlien, LH; Kraegen, EW; Chisholm, DJ; Ford, GL; Bruce, DG and Pascoe, WS (1987). Fish oil prevents insulin resistance induced by high-fat feeding in rats. *Science* **237**: 885-888.

Straus, DS and Glass, CK (2001). Cyclopentenone prostaglandins: new insights on biological activities and cellular targets. *Medicinal Research Reviews* **21**: 185-210.

Strong, P; Coleman, RA and Humphrey, Ppa (1992). Prostanoid-induced inhibition of lipolysis in rat isolated adipocytes: probably involvement of EP3 receptors. *Prostaglandins* **43**: 559-566.

Student, AK; Hsu, RY and Lane, MD (1980). Induction of fatty acid synthetase synthesis in differentiating 3T3-L1 preadipocytes. *The Journal of Biological Chemistry* **255**: 4745-4750.

Stunkard, AJ; Foch, TT and Hrubec, Z (1986). A twin study of human obesity. *The Journal of the American Medical Association* **256**: 51–54.

Stunkard, AJ; Harris, JR, Pedersen, NL and McClearn, GE (1990). The body-mass index of twins who have been reared apart. *The New England Journal of Medicine* **322**: 1483-1487.

Su, X; Han, X; Yang, J; Mancuso, DJ; Chen, J; Bickel, PE and Gross, RW (2004). Sequential ordered fatty acid α oxidation and δ9 desaturation are majore determinants of lipid storage and utilization in differentiating adipocytes. *Biochemistry* **43**: 5033-5044.

Subden, RE; Brown, RG and Noble, AC (1978). Determination of histamines in wines and musts by reversed-phase -high-performance liquid chromatography. *Journal of Chromatography* **166**: 310-3 12.

Suganami, T; Nishida, J and Ogawa, Y (2005). A paracrine loop between adipocytes and macrophages aggravates inflammatory changes: role of free fatty acids and tumor necrosis factor alpha. *Arteriosclerosis, Thrombosis, and Vascular Biology* **25**: 2062–2068.

Sumida, M; Shiosaka, T; Nagar, A; Isshikimasuda, M; Okuda, H and Hamada, M (1997). Suppressive effect of tumor necrosis factor-a on adipogenic cell differentiation and on gene expression of hormone-sensitive lipase. *Journal of Clinical Biochemistry and Nutrition* **22**: 1–11.

Sun, J; Sui, X; Bradbury, JA; Zeldin, DC; Conte, MS and Liao, JK (2002). Inhibition of vascular smooth muscle cell migration by cytochrome p450 epoxygenase-derived eicosanoids. *Circulation Research* **90**: 1020–1027.

Swinehart, DF (1962). The Beer-Lambert Law. *Journal of Chemical Education* **9**: 333-335.

Syu, LJ and Saltiel, AR (1999). Lipotransin: a novel docking protein for hormone-sensitive lipase. *Molecular Cell* **4**: 109-115.

Tamori, Y; Masugi, J; Nishino, N and Kasuga, M (2002). Role of peroxisome proliferator-activated receptor gamma in maintenance of the characteristics of mature 3T3-L1 adipocytes. *Diabetes* **51**: 2045–2055.

Tan, BK; Adya, R; Farhatullah, S; Lewandowski, KC; O'Hare, P; Lehnert, H and Randeva, HS (2008). Omentin-1, a novel adipokine, is decreased in overweight insulin-resistant women With polycystic ovary syndrome: ex vivo and *in vivo* regulation of omentin-1 by insulin and glucose. *Diabetes* **57**: 801-808.

Tang, QQ; Gronborg, M; Huang, H; Kim, JW; Otto, TC; Pandey, A and Lane, MD (2005). Sequential phosphorylation of C/EBP b by MAPK and GSK3 b is required for adipogenesis. *Proceedings of the National Academy of Sciences USA* **102**: 9766–9771.

Tartaglia, LA; Dembski, M; Weng, X; Deng, N; Culpepper, J; Devos, R; Richards, GJ; Campfield, LA; Clark, FT; Deeds, J; Muir, C; Sanker, S; Moriarty, A; Moore, KJ; Smutko, JS; Mays, GG; Wool, EA; Monroe, CA and Tepper, RI (1995). Identification and expression cloning of a leptin receptor, OB-R. *Cell* **83**: 1263-1271.

Tatesson, JE; Moncada, S and Vane, JR (1977). Effects of prostacyclin (PGX) on cyclic AMP concentrations in human platelets. *Prostaglandins* **13**: 389-397.

Thornton, JE; Cheung, CC; Clifton, DK and Steiner, RA (1997). Regulation of hypothalamic proopiomelanocortin mRNA by leptin in ob/ob mice. *Endocrinology* **138**: 5063–5067.

Tomas, E; Tsao, TS; Saha, AK; Murrey, HE; Zhang, CC; Itani, SI; Lodish, HF and Ruderman, NB (2002). Enhanced muscle fat oxidation and glucose transport by ACRP30 globular domain: acetyl-CoA carboxylase inhibition and AMP-activated protein kinase activation. *Proceedings of the National Academy of Sciences USA* **99**: 16309–16313.

Tontonoz, P; Hu, E; Graves, RA; Budavari, AI and Spiegelman, BM (1994). mPPARγ2: tissue-specific regulator of an adipocyte enhancer. Genes and Development 8:1224-1234.

Torado, GJ and Green, H (1963). Quantitative studies of the growth of mouse embryo cells in culture and their development into established lines. *The Journal of Cell Biology* **17**: 299.

Tornqvist, H and Belfrage, P (1976). Purification and some properties of a monoacylglycerol-hydrolyzing enzyme of rat adipose tissue. *The Journal of Biological Chemistry* **251**: 813–819.

Torti, F. M., Dieckman, B., Beutler, B., Cerami, A. and Ringold, G. M. (1985). A macrophage factor inhibits adipocyte gene expression: an *in vitro* model of cachexia. Science 229, 867-869.

Trayhurn, P (2005). The biology of obesity. *Proceedings of the Nutrition Society* **64**: 31-38.

Trayhurn, P and Beattie, JH (2001). Physiological role of adipose tissue: white adipose tissue as an endocrine and secretory organ. *Proceedings of the Nutrition Society* **60**: 329-339.

Trayhurn, P and Wood, IS (2004). Adipokines: inflammation and the pleiotropic role of white adipose tissue. *British Journal of Nutrition* **92**: 347-355.

Trayhurn, P; Duncan, JS; Hoggard, N and Rayner, DV (1998). Regulation of leptin production: a dominant role for the sympathetic nervous system? *Proceedings of the Nutrition Society* **57**: 413-419.

Trayhurn, P; Duncan, JS; Rayner, DV and Hardie, LJ (1996). Rapid inhibition of ob gene expression and circulating leptin levels in lean mice by the beta 3-adrenoceptor agonists BRL 35135A and ZD2079. *Biochemical and Biophysical Research Communications* **228**: 605-610.

Trayhurn, P; Duncan, JS; Wood, AM and Beattie, JH (2000). Regulation of metallothionein gene expression and secretion in rat adipocytes differentiated from preadipocytes in primary culture. *Hormone and Metanolic Research* **32**: 542-547.

Trayhurn, P; Hoggard, N; Mercer, JG and Rayner, DV (1999). Leptin: fundamental aspects.*International Journal of Obesity* **23 Suppl 1**: 22-28.

Trayhurn, P; Thomas, ME; Duncan, JS and Rayner, DV (1995). Effects of fasting and refeeding on ob gene expression in white adipose tissue of lean and obese (oblob) mice. Federation of European Biochemical Societies Letters 368: 488-490.

Trujillo, ME; Sullivan, S; Harten, I; Schneider, SH; Greenberg, AS and Fried, SK (2004). Interleukin-6 regulates human adipose tissue lipid metabolism and leptin production *in vitro*. *The Journal of Clinical Endocrinology and Metabolism* **89**: 5577-5582.

Tschop M, Smiley DL, Heiman ML: Ghrelin induces adiposity in rodents. *Nature* **407**: 908–913, 2000.

Tung, CS; Wong, KK and Mok, SC (2008). Biomarker discovery in ovarian cancer. *Womens Health* **4**: 27-40.

Um, JY; Chung, HS; Song, MY; Shin, HD and Kim, HM (2004). Association of interleukin-1beta gene polymorphism with body mass index in women. Clinical Chemistry 50: 647-650.

Ushikubi, F; Segi, E; Sugimoto, Y; Murata, T; Matsuoka, T; Kobayashi, T; Hizaki, H; Tuboi, K; Katsuyama, M; Ichikawa, A; Tanaka, T; Yoshida, N and Narumiya, S (1998). Impaired febrile response in mice lacking the prostaglandin E receptor subtype EP3. *Nature* **395**: 281–284.

Uysal, KT; Wiesbrock, SM; Marino, MW and Hotamisligil, GS (1997). Protection from obesity-induced insulin resistance in mice lacking TNF-alpha function. *Nature* **389**: 610-614.

Vachier, I; Chanez, P; Bonnans, C; Godard, P; Bousquet, J and Chavis, C (2002). Endogenous anti-inflammatory mediators from arachidonate in human neutrophils. *Biochemical and Biophysical Research Communications* **290**: 219–224.

Vague, J (1956). The degree of masculine differentiation of obesities: a factor determining predisposition to diabetes, atherosclerosis, gout, and uric calculous disease. *The American Journal of Clinical Nutrition* **4**: 20 –34.

Vaisse, C; Halaas, JL; Horvath, CM; Darnell, JE Jr.; Stoffel, M and Friedman, JM (1996). Leptin activation of Stat3 in the hypothalamus of wild-type and ob/ob mice but not db/db mice. *Nature Genetics* **14**: 95-97.

van Ginneken, V; Verhey, E; Poelmann, R; Ramakers, R; van Dijk, KW; Ham, L; Voshol, P; Havekes, L; Van Eck, M and van der Greef, J (2007). Metabolomics (liver and blood profiling) in a mouse model in response to fasting: a study of hepatic steatosis. *Biochimica et Biophysica Acta* **1771**: 1263-1270.

van Hall, G; Steensberg, A; Sachetti, M; Fischer, C; Keller, C; Schjerling, P; Hiscock, N; Moller, K; Saltin, B; Febbraio, MA and Pedersen, BK (2003). Interleukin-6 stimulates lipolysis and fat oxidation in humans. *The Journal of Clinical Endocrinology and Metabolism* **88**: 3005–3010.

Van Harmelen, V; Reynisdottir, S; Eriksson, P; Thorne, A; Hoffstedt, J; Lonnqvist, F and Arner, P (1998). Leptin secretion from subcutaneous and visceral adipose tissue in women. *Diabetes* **47**: 913-917.

Van Kerckhoven, R; Kalkman, EA; Saxena, PR and Schoemaker, RG (2000). Altered cardiac collagen and associated changes in diastolic function of infarcted rat hearts. *Cardiovascular Research* **46**: 316–323.

van Weeman, BK and Schuurs, AHWM (1971). Immunoassay using antigen-enzyme conjugates. *Federation of European Biochemical Societies Letters* **15**: 232-236.

Vane, JR (1971). Inhibition of prostaglandin synthesis as a mechanism of action for aspirin-like drug. *Nature* **231**: 232–235.

Vassaux, G; Gaillard, D; Ailhaud, G and Negrel, R (1992a). Prostacyclin is a specific effector of adipose cell differentiation. Its dual role as a cAMP- and Ca(2+)-elevating agent. *The Journal of Biological Chemistry* **267**: 11092-11097.

Vassaux, G; Gaillard, D; Darimont, C; Ailhaud, G and Negrel, R (1992b). Differential response of preadipocytes and adipocytes to prostacyclin and prostaglandin E2: physiological implications. *Endocrinology* **131**: 2393-2398.

Vassaux, G; Negrel, R; Ailhaud, G and Gaillard, D (1994). Proliferation and differentiation of rat adipose precursor cells in chemically defined medium: differential action of anti-adipogenic agents. *Journal of Cellular Physiology* **161**: 249–256.

Vega, JA; Garcia-Suarez, O; Hannestad, J; Perez-Perez, M and Germana, A (2003). Neurotrophins and the immune system. *Journal of Anatomy* **203**: 1-19.

Ventre, J; Doebber, T; Wu, M; MacNaul, K; Stevens, K; Pasparakis, M; Kollias, GK and Moller, DE et al. (1997). Targeted disruption of the tumor necrosis factor-alpha gene: metabolic consequences in obese and nonobese mice. *Diabetes* **46**: 1526-1531.

Vierck, JL; McNamara, JP and Dodson, MV (1996). Proliferation and differentiation of progeny of ovine unilocular fat cells (adipofibroblasts). *In Vitro Cellular and Developmental Biology - Animal* **132**: 564–572.

Villena, JA; Roy, S; Sarkadi-Nagy, E; Kim, KH and Sul, HS (2004). Desnutrin, an adipocyte gene encoding a novel patatin domain-containing protein, is induced by fasting and glucocorticoids: ectopic expression of desnutrin increases triglyceride hydrolysis. *The Journal of Biological Chemistry* **279**: 47066–47075.

Viswanadha, S and Londos, C (2006). Optimized conditions for measuring lipolysis in murine primary adipocytes. *The Journal of Lipid Research* **47**: 1859–1864.

Vozarova, B; Weyer, C; Hanson, K; Taranni, PA; Bogardus, C and Pratley, RE (2001). Circulating interleukin-6 in relation to adiposity, insulin action, and insulin secretion. *Obesity Research* **9**: 414–417.

Wabitsch, M; Brenner, RE; Melzner, I; Braun, M; Moller, P; Heinze, E; Debatin, KM and Hauner, H (2001). Characterization of a human preadipocyte cell strain with high capacity for adipose differentiation. *International Journal of Obesity and Related Metabolic Disorders* **25**: 8–15.

Wabitsch, M; Jensen, PB; Blum, WF; Christoffersen, CT; Englaro, P; Heinze, E; Rascher, W; Teller, W; Tornqvist, H and Hauner, H (1996). Insulin and cortisol promote leptin production in cultured human fat cells. *Diabetes* **45**:1435-1438.

Wada, M; DeLong, CJ; Hong, YH; Reike, CJ; Song, I; Sidhu, RS; Yuan, C; Warnock, M; Schmaier, AH; Yokoyama, C; Smyth, EM; Wilson, SJ; FitzGerald, GA; Garavito, RM; Sui, DX; Regan, JW and Smith, WL (2007). Enzymes and receptors of prostaglandin pathways with arachidonic acid-derived versus eicosapentaenoic acid-derived substrates and products. The Journal of Biological Chemistry 282: 22254–22266.

Wade, AJ; Marbut, MM and Round, JM (1990). Muscle fibre type and aetiology of obesity. *Lancet* **335**: 805–808.

Wagner, H; Rollinghoff M; Pfizenmaier, K; Hardt, C and Johnscher, G (1980) T-T cell interactions during *in vitro* cytotoxic T lymphocyte (CTL) responses. II. Helper factor from activated Lyt 1+ T cells in rate limiting (i) in T cell responses to nonimmunogenic alloantigen, (ii) in thymocyte responses to allogeneic stimulator cells, and (iii) recruits allo- or H-2-restricted CTL precursors from the Lyt 123+ T subset. *Journal of Immunology* **124**: 1058-1067.

Wajchenberg, BL (2000). Subcutaneous and visceral adipose tissue: their relation to the metabolic syndrome. *Endocrine Reviews* **21**: 697-738.

Wallenius, V; Wallenius, K; Ahren, B; Rudling, M; Carlsten, H; Dickson, SL; Ohlsson, C and Jansson, JO (2002). Interleukin-6-deficient mice develop mature-onset obesity. *Nature Medicine* **8**: 75–79.

Wang, B; Jenkins, JR and Trayhurn, P (2005). Expression and secretion of inflammation-related adipokines by human adipocytes differentiated in culture: integrated response to TNF-α. *American Journal of Physiology - Endocrinology Metabolism* **288**: E731-E740.

Wang, DJ; Klein, AS; Bulkley, GB; BaoC; Noble, PW; Lane, MD and Diehl, AM (1998). Leptin regulates proinflammatory immune responses. *The Journal of the Federation of American Socities for Experimental Biology* **12**: 57–65.

Wang, GL; Shi, X; Salisbury, E; Sun, Y; Albrecht, JH; Smith, RG and Timchenko, NA (2006). Cyclin D3 maintains growth-inhibitory activity of C/EBPalpha by stabilizing C/EBPalpha-cdk2 and C/EBPalpha-Brm complexes. Molecular and Cellular Biology 26: 2570-2582.

Wang, MY; Lee, Y and Unger, RH (1999). Novel form of lipolysis induced by leptin. *The Journal of Biological Chemistry* **274**: 19429-19433.

Wang, SP; Laurin, N; Himms-Hagen, J; Rudnicki, MA; Levy, E; Robert, MF; Pan, L; Oligny, L and Mitchell, GA (2001). The adipose tissue phenotype of hormone-sensitive lipase deficiency in mice. *Obesity Research* **9**: 119–128.

Way, JM; Gorgun, CZ; Tong, Q; Uysal, KT; Brown, KK; Harrington, WW; Oliver Jr. WR; Wilson, TM; Kliewer, SA and Hotamisligil, GS (2001). Adipose tissue resistin expression is severely suppressed in obesity and stimulated by PPARγ agonists. The Journal of Biological Chemistry 276: 25651–25653.

Weber, JM and Reidy, SP (2012). Extending food deprivation reverses the short-term lipolytic response to fasting: role of the triacylglycerol/fatty acid cycle. *The Journal of Experimental Biology* **215**: 1484-1490.

Weckwerth, W; Loureiro, ME; Wenzel, K and Fiehn, O (2004). Differential metabolic networks unravel the effects of silent plant phenotypes. *Proceedings of the National Academy of Sciences* **101**: 7809–7814.

Wei, Q; Lu, XY; Liu, L; Schafer, G; Shieh, KR; Burke, S; Robinson, TE; Watson, SJ; Seasholtz, AF and Akil, H (2004). Glucocorticoid receptor overexpression in forebrain: a mouse model of increased emotional lability. *Proceedings of the National Academy of Sciences* **101**: 11851–11856.

Weinstock, PH; Levak-Frank, S ;Hudgins, LC; Radner, H; Friedman, JM; Zechner, R and Jan L. Breslow, JL (1997). Lipoprotein lipase controls fatty acid entry into adipose tissue, but fat mass is preserved by endogenous synthesis in mice deficient in adipose tissue lipoprotein lipase. *Proceedings of the National Academy of Sciences USA* **94**: 10261–10266.

Weisberg, SP; McCann, D; Desai, M; Rosenbaum, M; Leibel, RL and Ferrante, AW, Jr (2003). Obesity is associated with macrophage accumulation in adipose tissue. *The Journal of Clinical Investigation* **112**: 1796–1808.

Wen, Y; Gu, J; Chakrabarti, SK; Aylor, K; Marshall, J; Takahashi, Y; Yoshimoto, T and Nadler, JL (2007). The role of 12/15-lipoxygenase in the expression of interleukin-6 and tumor necrosis factor-alpha in machrophages. *Endocrinology* **148**: 1313–1322.

Wen, Y; Gu, J; Vandenhoff, GE; Liu, X and Nadler, JL (2008). Role of 12/15-lipoxygenase in the expression of MCP-1 in mouse macrophages. *American Journal of Physiology - Heart and Circulatory Physiology* **294**: H1933-H1938.

Wenger, RH (2002). Cellular adaptation to hypoxia: O2-sensing protein hydroxylases, hypoxia-inducible transcription factors, and O2-regulated gene expression. *The Journal of the Federation of American Societies for Experimental Biology* **16**: 1151-1162.

Weyer, C; Funahashi, T; Tanaka, S, Hotta, K; Matsuzaway, Y; Pratley, RE and Tatarnni, PA (2001). Hypoadiponectinemia in obesity and type 2 diabetes: close association with insulin resistance and hyperinsulinemia.The Journal of Clinical Endocrinology and Metabolism 86: 1930-1935.

White, RT; Damm, D; Hancock, N; Rosen, BS; Lowell, BB; Usher, P; Flier, JS and Spiegelman, BM (1992). Human adipsin is identical to complement factor D and is expressed at high levels in adipose tissue. *The Journal of Biological Chemistry* **267**: 9210-9213.

Wide, L and Porath, J (1966). Radioimmunoassay of proteins with the use of Sephadex-coupled antibodies. *Biochimica et Biophysica Acta* **30**: 257-260.

Wilding, JP (2002). Neuropeptides and appetite control. *Diabetic Medicine* **19**: 619-627.

Willoughby, R; Sheehan, E and Mitrovich, S (2002). **A global view of LC/MS**. Pittsburg: Global View Publishing.

Wittamer, V; Franssen, JD; Vulcano, M; Mirjolet, JF; Le Poul, E; Migeotte, I; Brezillon, S; Tyldesley, R; Blanpain, C; Detheux, M; Mantovani, A; Sozzani, S; Vassart, G; Parmentier, M and Communi, D (2003). Specific recruitment of antigen-presenting cells by chemerin, a novel Processed ligand from human inflammatory fluids. The Journal of Experimental Medicine 198: 977-985.

Wolf, AM; Wolf, D; Rumphold, H; Enrich, B and Tilg, H (2004). Adiponectin induces the antiinflammatory cytokines IL-10 and IL-1RA in human leukocytes. *Biochemical and Biophysical Research Communications* **323**: 630-635.

World health report 1998 - Life in the 21st century: A vision for all.

World Health Organization. Definition, diagnosis and classification of diabetes mellitus and its complications. Report of a WHO consultation 1999.

World Health Organization, 2003. Global strategy on diet, physical activity and health.

World Health Organization, Regional Office for the Western Pacific, International Association for the Study of Obesity. International Obesity Task Force. The Asia-Pacific perspective: redefining obesity and its treatment. Melbourne, Health Communications Australia, 2000.

World Health Organization. Obesity: Preventing and managing the global epidemic. Report of a WHO consultation on obesity. Geneva, WHO, 1998.

Wortman, P; Miyazaki, Y; Kalupahana, NS; Kim, S; Hansen-Petrik, M; Saxton, AM; Claycombe, KJ; Voy, BH; Whelan, J and Moustaid-Moussa, N (2009). n3 and n6 polyunsaturated fatty acids differentially modulate prostaglandin E secretion but not markers of lipogenesis in adipocytes. *Nutrition and Metabolism* **6**: 5.

Wu, S; Moomaw, CR; Tomer, KB; Falck, JR and Zeldin, DC (1996). Molecular cloning and expression of CYP2J2, a human cytochrome P450 arachidonic acid epoxygenase highly expressed in heart. *The Journal of Biological Chemistry* **271**: 3460–3468.

Wu, VY; Walz, DA and McCoy, LE (1977). Purification and characterization of human and bovine platelet factor 4. *Preparative Biochemistry* **7**: 479–493.

Wulster-Radcliffe, MC; Ajuwon, KM; Wang, J; Christian, JA and Spurlock, ME (2004). Adiponectin differentially regulate cytokines in porcine macrophages. *Biochemical and Biophysical Research Communications* **316**: 924-929.

Xie, L; Ortega, MT; Mora, S and Chapes, SK (2010). Interactive changes between macrophages and adipocytes. *Clinical and Vaccine Immunology* **17**: 651-659.
Xie, W; Robertson, DL and Simmons, DL (1992). Mitogen-inducible prostaglandin G/H synthase: A new target for nosteroidal anti-inflammatory drugs. *Drug Development Research* **25**: 249–265.

Xu, C; He, J; Jiang, H; Zu, L; Zhai, W; Pu, S and Xu, G (2009). Direct effect of glucocorticoids on lipolysis in adipocytes. *Molecular Endocrinology* **23**: 1161– 1170.

Xu, H; Barnes, GT; Yang, Q; Tan, G; Yang, D; Chou, CJ; Sole, J; Nichols, A; Ross, JS; Tartaglia, LA and Chen, H (2003). Chronic inflammation in fat plays a crucial role in the development of obesity-related insulin resistance. *The Journal of Clinical Investigation* **112**: 1821-1830.

Xu, L; Miyoshi, H; Nishimura, K; Jisaka, M; Nagaya, T and Yokota, K (2007). Gene expression of isoformic enzymes in arachidonate cyclooxygenase pathway and the regulation by tumor necrosis factor α during life cycle of adipocytes. *Prostaglandins and Other Lipid Mediators* **83**: 213-218.

Yach, D; Stuckler, D and Brownell, KD (2006). Epidemiologic and economic consequences of the global epidemics of obesity and diabetes. *Nature Medicine* **12**: 62-66.

Yamaguchi, M; Murakami, T; Tomimatsu, T; Nishio, Y; Mitsuda, N; Kanzaki, T; Kurachi, H; Shima, K; Aono, T and Murata, Y (1998). Autocrine inhibition of leptin production by tumor necrosis factor-alpha (TNF-alpha) through TNF-alpha type-I receptor *in vitro*. *Biochemical and Biophysical Research Communications* **244**: 30–34.

Yamauchi, T; Kamon, J; Ito, Y; Tsuchida, A; Yokomizo, T; Kita, S; Sugiyama, T; Miyagishi, M; Hara, K; Tsunoda, M; Murakami, K; Ohteki, T; Uchida, S; Takekawa, S; Waki, H; Tsuno, NH; Shibata, Y; Terauchi, Y; Froguel, P; Tobe, K; Koyasu, S; Taira, K; Kitamura, T; Shimizu, T; Nagai, R and Kadowaki, T (2003). Cloning of adiponectin receptors that mediate antidiabetic metabolic effects. *Nature* **423**: 762-769.

Yamauchi, T; Kamon, J; Minokoshi, Y; Ito, Y; Waki, H; Uchida, S; Yamashita, S; Noda, M; Kita, S; Ueki, K; Eto, K; Akanuma, Y; Froguel, P; Foufelle, F; Ferre, P; Carling, D; Kimura, S; Nagai, R; Kahn, BB and Kadowaki, T (2002). Adiponectin stimulates glucose utilization and fatty-acid oxidation by activating AMP-activated protein kinase. *Nature Medicine* **8**: 1288-1295.

Yamauchi, T; Kamon, J; Waki, H; Terauchi, Y; Kubota, N; Hara, K; Mori, Y; Ide, T; Murakami, K; Tsuboyama-Kasaoka, N; Ezaki, O; Akanuma, Y; Gavrilova, O; Vinson, C; Reitman, ML; Kagechika, H; Shudo, K; Yoda, M; Nakano, Y; Tobe, K; Nagai, R; Kimura, S; Tomita, M; Froguel, P and Kadowaki, T (2001). The fat-derived hormone adiponectin reverses insulin resistance associated with both lipoatrophy and obesity. *Nature Medicine* **7**: 941-946.

Yan, H; Kermouni, A; Abdel-Hafez, M and Lau, DC (2003). Role of cyclooxygenases COX-1 and COX-2 in modulating adipogenesis in 3T3-L1 cells. *The Journal of Lipid Research* **44**: 424–429.

Yang, Q; Graham, TE; Mody, N; Preitner, F; Peroni, OD; Zabolotny, JM; Kotani, K; Quadro, L and Kahn, BB (2005). Serum retinol binding protein 4 contributes to insulin resistance in obesity and type 2 diabetes. *Nature* **436**: 356-362.

Yang, RZ; Lee, MJ; Hu, H; Pray, J; Wu, HB; Hansen, BC; Shuldiner, AR; Fried, SK; McLenithan, JC and Gong, DW (2006). Identification of omentin as a novel depot specific adipokine in human adipose tissue: possible role in modulating insulin action. *American Journal of Physiology - Endocrinology and Metabolism* **290**: E1253-1261.

Yang, WS; Lee, WJ; Funahashi, T; Tanaka, S; Matsuzawa, Y; Chao, CL; Chen, CL; Tai, TY and Chuang, LM (2001). Weight reduction increases plasma levels of an adiposederived anti-inflammatory protein, adiponectin. *The Journal of Clinical Endocrinology and Metabolism* **86**: 3815-3819.

Yetukuri, L; Katajamaa, M; Medina-Gomez, G; Seppanen-Laakso, T; Vidal- Puig, A and Oresic, A (2007). Bioinformatics strategies for lipidomics analysis: characterization of obesity related hepatic steatosis. *BMC Systems Biology* **1**: 12.

Yin, J; Gao, Z; He, Q; Zhou, D; Guo, Z and Ye, J (2009). Role of hypoxia in obesity-induced disorders of glucose and lipid metabolism in adipose tissue. *American Journal of Physiology* **296**: E333-E342.

Yokota, T; Oritani, K; Takahashi, I; Ishikawa, J; Matsuyama, A; Ouchi, N; Kihara, S; Funahashi, T; Tenner, AJ; Tomiyama, Y and Matsuzawa, Y (2000). Adiponectin, a new member of the family of soluble defense collagens, negatively regulates the growth of myelomonocytic progenitors and the functions of macrophages. *Blood* **96**: 1723–1732.

Yu, Z; Xu, F; Huse, LM; Morisseau, C; Hammock, BD; Draper, AJ; Newman, JW; Parker, C; Graham, L; Engler, MM; Hammock, BD; Zeldin, DC; and Kroetz, DL (2000). Soluble epoxide hydrolase regulates hydrolysis of vasoactive epoxyeicosatrienoic acids. *Circulation Research* **87**: 992-998.

Yuan, JS; Reed, A; Chen, F and Neal Stewart Jr, C (2006). Statistical analysis of real-time PCR data. *BMC Bioinformatics* **7**:85.

Yuan, M; Konstantopoulos, N; Lee, J; Hansen, L; Li, ZW; Karin, M and Shoelson, SE (2001). Reversal of obesity- and diet-induced insulin resistance with salicylates or targeted disruption of Ikkbeta. *Science* **293**: 1673-1677.

Yudkin, JS; Stehouwer, CDA; Emeis, JJ and Coppack, SW (1999). C-reactive protein in healthy subjects: associtaions with obesity, insulin resistance, and endothelial dysfunction. A potential role for cytokines originating from adipose tissue? *Arteriosclerosis, Thrombosis, and Vascular Biology* **19**: 972-978.

Yusuf, S; Hawken, S; Ounpuu, S; Bautista, L; Franzosi, MG; Commerford, P; Lang, CC; Rumboldt, Z; Onen, CL; Lisheng, L; Tanomsup, S; Wangai, P Jr; Razak, F; Sharma, AM; Anand, SS and INTERHEART Study Investigators (2005). Obesity and the risk of myocardial infarction in 27,000 participants from 52 countries: a case-control study. *Lancet* **366**: 1640–1649.

Zabel, BA; Nakae, S; Zuniga, L; Kim, JY; Ohyama, T; Alt, C; Pan, J; Suto, H; Soler, D; Allen, SJ; Handel, TM; Song, CH; Galli, SJ and Butcher, EC (2008). Mast cell-expressed orphan receptor CCRL2 binds chemerin and is required for optimal induction of IgE-mediated passive cutaneous anaphylaxis. *The Journal of Experimental Medicine* **205**: 2207–2220.

Zaagsma, J and Nahorski, SR (1990). Is the adipocyte β-adrenoceptor a prototype for the recently cloned atypical beta 3-adrenoceptor? *Trends in Pharmalogical Sciences* **11**: 3–7.

Zeldin, DC (2001). Epoxygenase pathways of arachidonic acid metabolism. *The Journal of Biological Chemistry* **276**: 36059–36062.

Zhang, B; Berger, J; Hu, E; Szalkowski, D; White-Carrington, S; Spiegelman, BM and Moller, DE (1996). Negative regulation of peroxisome proliferator-activated receptor-gamma gene expression contributes to the antiadipogenic effects of tumor necrosis factor-alpha. *Molecular Endocrinology* **10**: 1457-1466.

Zhang, HH; Kumar, S; Barnett, AH and Eggo, MC (2000). Ceiling culture of mature human adipocytes: use in studies of adipocyte functions. *Journal of Endocrinology* **164**: 119-128.

Zhang, HH; Kumar, S; Barnett, AH; Eggo, MC; (2001). Dexamethasone inhibits tumor necrosis factor-alpha-induced apoptosis and interleukin-1 beta release in human subcutaneous adipocytes and preadipocytes. *Journal of Clinical Endocrinology Metabolism* **86**(6):2817-25.

Zhang, HH; Kumar, S; Barnett, AH and Eggo, MC (1999). Intrinsic site-specific differences in the expression of leptin in human adipocytes and its autocrine effects on glucose uptake. *The Journal of Clinical Endocrinology and Metabolism* **84**: 2550-2556.

Zhang, Y; Matheny, M; Zolotukhin, S; Tumer, N; Scarpace, PJ (2002). Regulation of adiponectin and leptin gene expression in white and brown adipose tissues: influence of β3-adrenergic agonists, retinoic acid, leptin and fasting. *Biochimica et Biophysica Acta* **1584**: 115-122.

Zhang, Y; Proenca, R; Maffei, M; Barone, M; Leopold, L and Friedman, JM (1994). Positional cloning of the mouse obese gene and its human homologue. *Nature* **372**: 425-432.

Zhu, Y; Qi, C; Korenberg, JR; Chen, XN; Noya, D; Rao, MS and Reddy, JK (1995). Structural organization of mouse peroxisome proliferator-activated receptor (mPPAR) gene: alternative promoter use and different splicing yield two m PPAR isoforms. *Proceedings of the National Academy of Sciences USA* **92**: 7921-7925.

Ziccardi, P; Nappo, F; Giugliano, G; Esposito, K; Marfella, R; Cioffi, M; D'Andrea, F; Molinan, AM and Giugliano, D (1992). Reduction of inflammatory cytokine concentrations and improvement of endothelial functions in obese women over one year. *Circulation* **105**: 804-809.

Zimmermann, R; Strauss, JG; Haemmerle, G; Schoiswohl, G; Birner-Gruenberger, R; Riederer, M; Lass, A; Neuberger, G; Eisenhaber, F; Hermetter, A and Zechner, R (2004). Fat mobilization in adipose tissue is promoted by adipose triglyceride lipase. *Science* **306**: 1383–1386.

Zlotnik, A; Morales, J and Hedrick, JA (1999). Recent advances in chemokines and chemokine receptors. *Critical Reviews Immunology* **19**: 1–47.

Zu, L; Jiang, H; He, J; Xu, C; Pu, S; Liu, M and Xu, G (2008). Salicylate blocks lipolytic actions of tumor necrosis factor-alpha in primary rat adipocytes. *Molecular Pharmacology* **73**: 215–223.

Zuk, PA; Zhu, M; Ashjian, P; De Ugarte, DA; Huang, JI; Mizuno, H; Alfonso, ZC; Fraser, JK; Benhaim, P and Hedrick, MH (2002). Human adipose tissue is a source of multipotent stem cells. *Molecular Biology of the Cell* **13**: 4279-4295.

Zurier, RB and Quagliata, F (1971). Effect of prostaglandin E1 on adjuvant arthritis. *Nature* **234**: 304-305.